Computational Intelligence and Neuroscience

Computational Intelligence for Intelligent Information Interpretation

Lead Guest Editor: Yaxiang Fan
Guest Editors: Caifa Zhou and Yan Chai Hum

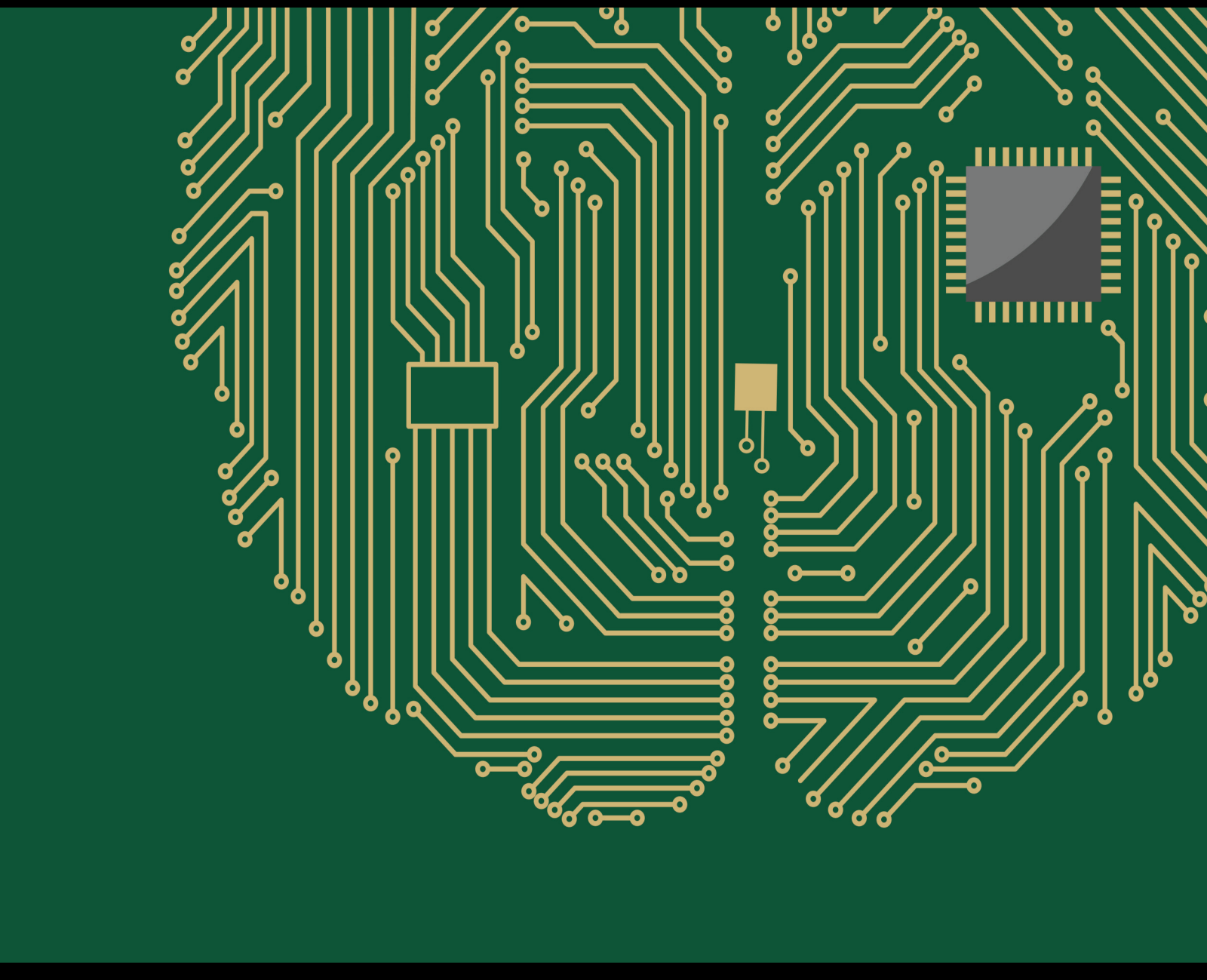

Computational Intelligence for Intelligent Information Interpretation

Computational Intelligence and Neuroscience

Computational Intelligence for Intelligent Information Interpretation

Lead Guest Editor: Yaxiang Fan
Guest Editors: Caifa Zhou and Yan Chai Hum

Copyright © 2023 Hindawi Limited. All rights reserved.

This is a special issue published in “Computational Intelligence and Neuroscience.” All articles are open access articles distributed under the Creative Commons Attribution License, which permits unrestricted use, distribution, and reproduction in any medium, provided the original work is properly cited.

Chief Editor

Andrzej Cichocki, Poland

Associate Editors

Arnaud Delorme, France
Cheng-Jian Lin, Taiwan
Saeid Sanei, United Kingdom

Academic Editors

Mohamed Abd Elaziz, Egypt
Tariq Ahanger, Saudi Arabia
Muhammad Ahmad, Pakistan
Ricardo Aler, Spain
Nouman Ali, Pakistan
Pietro Aricò, Italy
Lerina Aversano, Italy
Ümit Ağbulut, Turkey
Najib Ben Aoun, Saudi Arabia
Surbhi Bhatia, Saudi Arabia
Daniele Bibbo, Italy
Vince D. Calhoun, USA
Francesco Camastra, Italy
Zhicheng Cao, China
Hubert Cecotti, USA
Jyotir Moy Chatterjee, Nepal
Rupesh Chikara, USA
Marta Cimitile, Italy
Silvia Conforto, Italy
Paolo Crippa, Italy
Christian W. Dawson, United Kingdom
Carmen De Maio, Italy
Thomas DeMarse, USA
Maria Jose Del Jesus, Spain
Arnaud Delorme, France
Anastasios D. Doulamis, Greece
António Dourado, Portugal
Sheng Du, China
Said El Kafhali, Morocco
Mohammad Reza Feizi Derakhshi, Iran
Quanxi Feng, China
Zhong-kai Feng, China
Steven L. Fernandes, USA
Agostino Forestiero, Italy
Piotr Franaszczuk, USA
Thippa Reddy Gadekallu, India
Paolo Gastaldo, Italy
Samanwoy Ghosh-Dastidar, USA
Manuel Graña, Spain
Alberto Guillén, Spain
Gaurav Gupta, India
Rodolfo E. Haber, Spain
Usman Habib, Pakistan
Anandakumar Haldorai, India
José Alfredo Hernández-Pérez, Mexico
Luis Javier Herrera, Spain
Alexander Hošovský, Slovakia
Etienne Hugues, USA
Nadeem Iqbal, Pakistan
Sajad Jafari, Iran
Abdul Rehman Javed, Pakistan
Jing Jin, China
Li Jin, United Kingdom
Kanak Kalita, India
Ryotaro Kamimura, Japan
Pasi A. Karjalainen, Finland
Anitha Karthikeyan, Saint Vincent and the Grenadines
Elpida Keravnou, Cyprus
Asif Irshad Khan, Saudi Arabia
Muhammad Adnan Khan, Republic of Korea
Abbas Khosravi, Australia
Tai-hoon Kim, Republic of Korea
Li-Wei Ko, Taiwan
Raşit Köker, Turkey
Deepika Koundal, India
Sunil Kumar, India
Fabio La Foresta, Italy
Kuruva Lakshmanna, India
Maciej Lawrynczuk, Poland
Jianli Liu, China
Giosuè Lo Bosco, Italy
Andrea Loddo, Italy
Kezhi Mao, Singapore
Paolo Massobrio, Italy
Gerard McKee, Nigeria
Mohit Mittal, France
Paulo Moura Oliveira, Portugal
Debajyoti Mukhopadhyay, India
Xin Ning, China
Nasimul Noman, Australia
Fivos Panetsos, Spain

Evgeniya Pankratova, Russia
Rocío Pérez de Prado, Spain
Francesco Pistolesi, Italy
Alessandro Sebastian Podda, Italy
David M Powers, Australia
Radu-Emil Precup, Romania
Lorenzo Putzu, Italy
S P Raja, India
Dr.Anand Singh Rajawat, India
Simone Ranaldi, Italy
Upaka Rathnayake, Sri Lanka
Navid Razmjooy, Iran
Carlo Ricciardi, Italy
Jatinderkumar R. Saini, India
Sandhya Samarasinghe, New Zealand
Friedhelm Schwenker, Germany
Mijanur Rahaman Seikh, India
Tapan Senapati, China
Mohammed Shuaib, Malaysia
Kamran Siddique, USA
Gaurav Singal, India
Akansha Singh, India
Chiranjibi Sitaula, Australia
Neelakandan Subramani, India
Le Sun, China
Rawia Tahrir, Iraq
Binhua Tang, China
Carlos M. Travieso-González, Spain
Vinh Truong Hoang, Vietnam
Fath U Min Ullah, Republic of Korea
Pablo Varona, Spain
Roberto A. Vazquez, Mexico
Mario Versaci, Italy
Gennaro Vessio, Italy
Ivan Volosyak, Germany
Leyi Wei, China
Jianghui Wen, China
Lingwei Xu, China
Cornelio Yáñez-Márquez, Mexico
Zaher Mundher Yaseen, Iraq
Yugen Yi, China
Qiangqiang Yuan, China
Miaolei Zhou, China
Michal Zochowski, USA
Rodolfo Zunino, Italy

Contents

Contents

Hindawi
Computational Intelligence and Neuroscience
Volume 2023, Article ID 9819873, 1 page
https://doi.org/10.1155/2023/9819873

Retraction

Retracted: Improved RRT-Based Moving Path Planning Algorithm for Teaching Reform and Innovation in Western Orchestral Ensemble Classes in Colleges and Universities

Computational Intelligence and Neuroscience

Received 26 September 2023; Accepted 26 September 2023; Published 27 September 2023

Copyright © 2023 Computational Intelligence and Neuroscience. This is an open access article distributed under the Creative Commons Attribution License, which permits unrestricted use, distribution, and reproduction in any medium, provided the original work is properly cited.

This article has been retracted by Hindawi following an investigation undertaken by the publisher [1]. This investigation has uncovered evidence of one or more of the following indicators of systematic manipulation of the publication process:

(1) Discrepancies in scope
(2) Discrepancies in the description of the research reported
(3) Discrepancies between the availability of data and the research described
(4) Inappropriate citations
(5) Incoherent, meaningless and/or irrelevant content included in the article
(6) Peer-review manipulation

The presence of these indicators undermines our confidence in the integrity of the article's content and we cannot, therefore, vouch for its reliability. Please note that this notice is intended solely to alert readers that the content of this article is unreliable. We have not investigated whether authors were aware of or involved in the systematic manipulation of the publication process.

In addition, our investigation has also shown that one or more of the following human-subject reporting requirements has not been met in this article: ethical approval by an Institutional Review Board (IRB) committee or equivalent, patient/participant consent to participate, and/or agreement to publish patient/participant details (where relevant).

Wiley and Hindawi regrets that the usual quality checks did not identify these issues before publication and have since put additional measures in place to safeguard research integrity.

We wish to credit our own Research Integrity and Research Publishing teams and anonymous and named external researchers and research integrity experts for contributing to this investigation.

The corresponding author, as the representative of all authors, has been given the opportunity to register their agreement or disagreement to this retraction. We have kept a record of any response received.

References

[1] W. Zhang, "Improved RRT-Based Moving Path Planning Algorithm for Teaching Reform and Innovation in Western Orchestral Ensemble Classes in Colleges and Universities," *Computational Intelligence and Neuroscience*, vol. 2022, Article ID 4273761, 10 pages, 2022.

Hindawi
Computational Intelligence and Neuroscience
Volume 2023, Article ID 9812159, 1 page
https://doi.org/10.1155/2023/9812159

Retraction

Retracted: Construction of College Chinese Blended Teaching Mode Based on Decision Tree Classification Model in New Media Context

Computational Intelligence and Neuroscience

Received 26 September 2023; Accepted 26 September 2023; Published 27 September 2023

Copyright © 2023 Computational Intelligence and Neuroscience. This is an open access article distributed under the Creative Commons Attribution License, which permits unrestricted use, distribution, and reproduction in any medium, provided the original work is properly cited.

This article has been retracted by Hindawi following an investigation undertaken by the publisher [1]. This investigation has uncovered evidence of one or more of the following indicators of systematic manipulation of the publication process:

(1) Discrepancies in scope
(2) Discrepancies in the description of the research reported
(3) Discrepancies between the availability of data and the research described
(4) Inappropriate citations
(5) Incoherent, meaningless and/or irrelevant content included in the article
(6) Peer-review manipulation

The presence of these indicators undermines our confidence in the integrity of the article's content and we cannot, therefore, vouch for its reliability. Please note that this notice is intended solely to alert readers that the content of this article is unreliable. We have not investigated whether authors were aware of or involved in the systematic manipulation of the publication process.

Wiley and Hindawi regrets that the usual quality checks did not identify these issues before publication and have since put additional measures in place to safeguard research integrity.

We wish to credit our own Research Integrity and Research Publishing teams and anonymous and named external researchers and research integrity experts for contributing to this investigation.

The corresponding author, as the representative of all authors, has been given the opportunity to register their agreement or disagreement to this retraction. We have kept a record of any response received.

References

[1] P. Huang, "Construction of College Chinese Blended Teaching Mode Based on Decision Tree Classification Model in New Media Context," *Computational Intelligence and Neuroscience*, vol. 2022, Article ID 4608631, 10 pages, 2022.

Hindawi
Computational Intelligence and Neuroscience
Volume 2023, Article ID 6257573, 18 pages
https://doi.org/10.1155/2023/6257573

Research Article

Color Image Retrieval Method Using Low Dimensional Salient Visual Feature Descriptors for IoT Applications

Naushad Varish,[1] **Priyanka Singh**,[2] **Prannoy Tugiti**,[2] **Marella Hima Manikanta**,[2] **Bhavana Yedlapalli**,[2] **Abhishree Pappusetty**,[2] **Hiren Kumar Thakkar**,[3] **and Gajendra Sharma**[4]

[1]*Department of Computer Science and Engineering, GITAM (Deemed to be University), Hyderabad 502329, Telangana, India*
[2]*Department of Computer Science and Engineering, SRM University, Guntur 522302, Andhra Pradesh, India*
[3]*Department of Computer Science and Engineering, Pandit Deendayal Energy Univrsity, Gandhinagar 382007, Gujarat, India*
[4]*School of Engineering, Department of Computer Science and Engineering, Kathmandu University, Dhulikhel 45200, Kavre, Nepal*

Correspondence should be addressed to Gajendra Sharma; gajendra.sharma@ku.edu.np

Received 18 June 2022; Revised 19 September 2022; Accepted 11 October 2022; Published 23 February 2023

Academic Editor: Yaxiang Fan

Copyright © 2023 Naushad Varish et al. This is an open access article distributed under the Creative Commons Attribution License, which permits unrestricted use, distribution, and reproduction in any medium, provided the original work is properly cited.

Digital data are rising fast as Internet technology advances through many sources, such as smart phones, social networking sites, IoT, and other communication channels. Therefore, successfully storing, searching, and retrieving desired images from such large-scale databases are critical. Low-dimensional feature descriptors play an essential role in speeding up the retrieval process in such a large-scale dataset. A feature extraction approach based on the integration of color and texture contents has been proposed in the proposed system for the construction of a low-dimensional feature descriptor. In which color contents are quantified from a preprocessed quantized HSV color image and texture contents are retrieved from a Sobel edge detection-based preprocessed V-plane of HSV color image using a block level DCT (discrete cosine transformation) and gray level co-occurrence matrix. On a benchmark image dataset, the suggested image retrieval scheme is validated. The experimental outcomes were compared to ten cutting-edge image retrieval algorithms, which outperformed in the vast majority of cases.

1. Introduction

Due to the advent of diverse devices such as smart phones, tablets, drones, CCTVs, and other image-capturing tools, as well as high-speed Internet, technology and its range of applications are rapidly expanding in the contemporary era. Huge amounts of unstructured image data have been generated in a variety of disciplines, including medical and health insurance, forensics, cars, archaeology, criminal prevention, architecture, and defence [1–4]. As the Covid effect fades across the world, it is anticipated that roughly 1.4 trillion photos will be taken in 2021. In addition, with the apparent rise in relevance of the IoT, edge devices such as smartphones generate a great quantity of photos. Huge amounts of data necessitated an appropriate approach to organise, manage, and retrieve photographs from a vast database, which proved to be a difficult undertaking. Text-based image retrieval (TBIR) techniques were initially used to retrieve images from digital datasets using text-based queries based on their annotations, which could include a range of descriptions or tags. Because human engagement or labour is an important part of the annotation/tagging process, it highlighted numerous errors. Therefore, traditional procedures are ineffective, and their accuracy is questioned. Furthermore, it is a time-consuming, costly, and repetitive operation. As a result, alternative approaches known as content-based image retrieval (CBIR) have been discovered to overcome the shortcomings of traditional methodologies, providing a fresh opportunity to solve the problem of image retrieval

[5]. CBIR is the technique of automatically indexing and retrieving images from big databases based on the contents of the images known as features such as color, texture, and shape. A novel content-based picture retrieval strategy is proposed in the presented work. Unlike previous systems, which rely on a single feature for retrieval, our research uses color and texture content for image retrieval; color and texture are the most important visual features for humans [6]. The color and texture contents of preprocessed photographs were retrieved in this research, and the Laplacian filter was used to remove unnecessary information by sharpening the color images. To extract the image's color instances, the HSV color space quantization approach is being used. The texture contents are obtained with discrete cosine transformation (DCT) and gray level co-occurrence matrix (GLCCM), and the image is then processed with the Sobel edge detection method. The spatial and interblock relationships were determined using GLCCM-based DC and AC coefficients to calculate these contents. Finally, by fruitfully merging color and texture contents, a low-dimensional single feature descriptor is generated, which speeds up retrieval. The Euclidean distance is being used to compute the similarity between the database image feature descriptors and the query image. The accuracy of the proposed scheme was tested using two datasets, the Corel 1K and the UC Merced, in terms of precision rates, recall rates, and F-scores rates.

1.1. Motivation. The retrieval of the desired images from a digital repository with semantically varied categories is a very tedious task for many researchers, especially in cloud assisted IoT [7]. The image retrieval is a searching technique in several real-world applications, such as medical imaging [8], searching individual video frames [9], object retrieval [10], image classification [11], digital libraries [12], and multimedia event detection [13]. In this regard, several CBIR schemes have been proposed based on transformation tools like discrete cosine transformation (DCT) and/or spatial domain techniques like color quantization, color histogram to extract the effective and significant features for image retrieval applications [14–16]. In most of the existing CBIR applications, either transformation tool or color information is applied for feature extraction. It is evident that the combination of the DCT and color-based approaches provide the significant image feature descriptors for image retrieval. The proposed research work is motivated by a simple nonuniform histogram quantization process and block level DCT based interrelated information using statistical analysis. In order to extract image information, the statistical color moments from quantized image have been computed while an image plane is divided into 8×8 fixed-sized blocks, and each block is employed by the DCT transform to get inter-related information. The main advantage of applying DCT is that it has powerful image analysis and discriminative properties. To improve the performance, the color information-based features are fused with DCT-based features for effective and efficient image retrieval.

2. Literature Survey

Numerous CBIR approaches have been presented that are based on the extraction of low-level image features/contents in the transform or spatial domain. Aamer et al. [17] developed a scheme/method for extracting DCT features from images that improves retrieval speed and reduces the amount of storage required during image retrieval. In this study, the researchers separated the input image into 8×8 nonoverlapping chunks and then applied DCT to each one. The image features can be extracted from the histograms of the quantized AC and DC coefficients of each transformed block, and the Euclidian distance between the query image's features and the database images can be calculated, and the closest images from the database can be retrieved using the minimal level quantified similarity measures. Yun et al. [18] suggested a CBIR approach based on the image's color and texture attributes. Color features are taken from distinct normalized GCLMs of the grayscale image, while texture features are extracted from both color and block color histograms. For superior retrieval results, they combined both features using a simple fusion method. Kavitha et al. [19] present another block-based image retrieval approach, in which an image will be first segmented into equal-sized sub-blocks for feature extraction. After that, the color information for each block is recovered by dividing the HSV color space into nonequal periods and representing the color features with a cumulative histogram. To represent the final feature, the texture feature is obtained using GLCM and combined with the color feature. Priyanka et al. [20] conducted a comparison of CBIR systems employing various feature extraction approaches. The texture feature was computed using wavelet and Gabor filters, while the color feature was retrieved using the color moments of the HSV color space. The similarity distance is calculated using the chi-square and Euclidean distances, and the top photos with similar features are retrieved. They found that employing Euclidean distance to combine color moments with Gabor texture gave them the highest precision rates of any known method. Jiquan ma et al. [21] suggested a CBIR scheme for image feature extraction based on HSV color space and discrete wavelet transform (DWT). They used the wavelet transform to breakdown the signal into a number of fundamental functions, and then used the Daubechies-4 wavelet transform to decompose the image. To create an eight-dimensional texture feature, the mean and standard deviation of the four bands are determined. The texture feature based on wavelet transform provides a better performance and stability, according to the testing results. Wang et al. [22] proposed image retrieval based on DCT and DWT with feature extraction utilising grading algorithms in 2015. The color moments, color histogram, and a novel dynamic color space quantization based on color distribution were modified to generate a color feature in the DCT domain, while the texture feature was computed using the DWT domain. In terms of retrieval accuracy, the experimental findings show that two grading image retrieval methods operate efficiently and effectively. Kaipravan et al. [5] propose another CBIR approach based on color and texture features. The color

feature is computed by partitioning an image into three equal horizonal regions and then computing the two color moments from each subimage plane using each color channel separately. Gabor wavelets capture energy at a given frequency and orientation to extract the texture information. Weights are assigned to each feature vector, and the Manhattan distance is used to calculate the similarity measure. They came to the conclusion that a single color or texture feature is insufficient to effectively characterise a picture; therefore, color-texture features are combined for improved retrieval efficiency. Chen et al. [23] constructed a CBIR technique that extracted color-texture features utilising the HSV color space in the year 2020. For feature representation, they first divided the image into 4×4 blocks to split the image into 16 sub-blocks. In order to extract significant features, the proposed method further divides a rectangular overlapping block into nine overlapping sub-block regions based on the sixteen sub-blocks. This overlapping method has advantages such as reducing the storage space and reducing the calculation amount of the similarity measure of the image. This method also does not destroy the information connection between the images because of the sub-blocks, thus ensuring better retrieval accuracy. Our presented work is also compared with some state-of-art schemes; those are described one after another in detail. In year 2015, Shrivastava et al. [24] proposed a new image retrieval technique that retrieves similar images from an image dataset in three stages using primitive low-level image features such as color, texture, and shape. In their proposed scheme, a fixed number of images are first retrieved based on their color feature similarity. The color feature was extracted using quantized color histograms in HSV color space, and the number of pixels in each bin of the histogram was used to form a color feature vector. To improve the retrieved images' relevance, their texture and shape features are matched, respectively. The Gabor wavelet transform was used to compute the texture information of the image, while the shape feature vector was constructed by computing the Fourier descriptor based on centroid distance. This method reduced the computation time and increased the overall accuracy due to the retrieval of images in three different stages. Later in year 2016, Dubey et al. [25] proposed a novel method for image description with multichannel decoded local binary patterns and introduced an adder and decoder-based scheme for combining the local binary patterns (LBPs) from multichannel of image. Two multichannel decoded local binary patterns are introduced-multichannel adder local binary pattern (maLBP) and the multichannel decoder local binary pattern (mdLBP). Both maLBP and mdLBP utilize the local information of multiple channels based on the adder and decoder concepts. The feature descriptor has high dimensionality due to combination of the multi-channel-based LBPs. Mistry et al. [26] proposed a hybrid feature-based efficient CBIR scheme using various distance measures in year 2018. Spatial domain features including color auto-correlogram, color moments, HSV histogram, and frequency domain features like moments using SWT and Gabor wavelet transform were used. Further, color and edge directivity descriptor features were performed to enhance precision binarized statistical image features. They claim that their results are better than all the existing models. Similarly, in 2018, Irtaza et al. [27] proposed an approach that resolves the classification disagreement amongst different classifiers and the class imbalance problem in CBIR. They have used a genetic algorithm (GA)-based classifier comity learning (GCCL) method to generate stable classifiers by combining ANN with SVMs through asymmetric and symmetric bagging. Once the stable classifiers were generated, the query image was presented to the trained model to understand the underlying semantic content of the query image for association with the precise semantic class. Later, they computed the feature similarity within the obtained class to generate the semantic response of the system. Later on, in year 2019, Ahmed et al. [28] proposed a novel technique to fuse the spatial color information with shaped extracted features and object recognition which increases the strength of the image features for the information fusion purpose in retrieval process. They extracted the color features from RGB images and used the gray level image for the pixel intensity-based local features. They combined the local image features, spatial information in BoW architecture and evaluated the results on popular image collection databases. Vimina et al. [29] proposed another CBIR scheme in year 2020 using texture-color descriptor by integrating the multichannel features. For the texture feature, they used a fixed-sized local intensity-based descriptor, MMLBP, integrating the multichannel local intensity information of the image at the pixel level. The dimensionality of the descriptor is fixed irrespective of the number of channels in the image. The resulting histogram of the patterns is used for representing the image texture. The color feature is extracted by quantizing the RGB color space and is represented with a histogram. The color-texture descriptors are further fused to characterise the images. The MMLBP, along with a quantized color descriptor, is used for characterising the images for retrieval purpose. Garg et al. [30] proposed a CBIR scheme in year 2021 to obtain feature descriptor from multilevel image decomposition. They achieved this by extracting approximation and correct coefficients by applying discrete wavelet transformation to the RGB channels. Therefore, both approximation and correct coefficients are applied to the dominant rotated local binary pattern called texture descriptor, which is computationally effective and rotationally invariant. The local descriptors are extracted from the entire image, for which they used methods such as SIFT, SURF, HoD, and LBP. A rotation invariance function image for a local neighbor patch is obtained by measuring the descriptor relative to the reference. It navigated approaches that contained the complete structural information, extracted directly from the local binary patterns, and the additional information like the information of magnitude, which, in turn, achieves extra discriminating power. Then, the GLCM description is used by obtaining the dominantly rotated local binary pattern image to extract. The proposed scheme is trained and tested on the three classifiers: support vector machine, K-nearest neighbor, and decision tree. Varish et al. [31] demonstrates an image retrieval scheme where a fused low-dimensional feature

descriptor is obtained by fusing probability histogram-based HSV color moments and multiresolution-based shape moments. The color moments and shape moments were extracted from the Laplacian filter-based preprocessed image. In addition to the color-shape feature, the texture feature is also included by Sumit et al. [32] for feature representation, where YCbCr color space for the feature extraction process is used and Y, Cb, and Cr color planes are minimally overlapped. A mid-rise quantization scheme preprocesses the images. The texture and shape features are extracted from the Y plane using BDIP and BVLC techniques. Subsequently, they used adaptive tetrolet transform in the output of BDIP and BVLC to extract local textural and geometrical features. At the same time, they selected the Cb and Cr components and applied adaptive tetrolet transform to analyze the regional local color variations of the image. Finally, they combined the nonoverlapping extracted shape, texture, and color features to form the final feature vector for the retrieval process. In order to, reduce image retrieval's search space and computational complexity, Joseph et al. [33] developed a CBIR scheme that investigates various search space reduction techniques and classifies the image collection into a subset of related images. They proposed an image clustering using hybrid K-means moth flame optimization algorithm (KMFO) which enhances the performance of the K-means algorithm by assigning the optimum number of clusters and cluster centroids based on the number of flames and flame values. HSV color histogram, color correlogram, wavelet transform, GLCM, color moments, dominant color, and region-based descriptors are used as feature descriptors. Motivated by the above-discussed works, authors have proposed a novel feature extraction technique using color and texture features based on the spatial domain and transform domain, respectively, where features have been computed from an HSV color image.

2.1. Major Contribution. The main contribution of the proposed image retrieval scheme includes the following:

(i) A low-dimensional feature descriptor using the fusion of spatial domain-based color information and transform domain-based texture information is constructed for image retrieval applications. It reduces the computational overhead for retrieving images from large-scale datasets in a speedy manner.

(ii) To extract the color information, a nonuniform quantized color histogram is used and subsequently the color moments from the preprocessed image have been computed for formation of color feature descriptor.

(iii) The inter-related information between blocks has been extracted using block level DCT tool, where associativity has been determined using the AC and DC coefficients of image blocks.

(iv) The spatial relationship between the preprocessed AC and DC coefficients in the DCT domain has been established using GLCCM, and subsequently, the statistical parameters have been calculated from corresponding GLCCMs for the construction of texture feature descriptors.

(v) The integration of color and texture information is done, and the proposed image retrieval scheme is validated on two Corel 1K and the UC Merced benchmark databases, where the diversified results have been achieved.

2.2. Organization of Paper. The remainders of the paper are laid out as follows: The suggested CBIR image retrieval approach, as well as its feature extraction and retrieval procedure, is discussed in detail in Section 3. The experimental results and comments are detailed in Section 4, and a comparative study with existing retrieval methods is presented to quantify retrieval efficiency. Finally, Section 5 brings the proposed work to a close.

3. Proposed Image Retrieval Methodology

The proposed scheme comprises of preprocessing, color, and texture information, and similarity distance-based image retrieval system. Details of each will be described and discussed in the following subsections.

3.1. Preprocessing. The Laplacian filter [31] is considered in the proposed scheme for sharpening color images. Because it is based on second-order derivatives, this filter produces a considerably enhanced version of the image, whereas other kernels such as Prewitt, Sobel, and others are based on first-order derivatives. Fine thin lines and isolated points are also produced. The 3×3 mask with centre (-8) has been used in the presented work for filtering (L1) images, as shown in equation (1), and it has been implemented in all spots of the image by a convolving operation. This mask is not just for grayscale images; it may also be used on color images.

$$L1 = \begin{bmatrix} 1 & 1 & 1 \\ 1 & -8 & 1 \\ 1 & 1 & 1 \end{bmatrix}. \quad (1)$$

The HSV color image is decomposed into its three color components: H, S, and V. Color visual characteristics are retrieved from the H and S components of the HSV color image, while texture visual features are computed from the V component. In [34], the entire process of preparing an RGB image is detailed with multiple kernels.

3.2. Color Feature Representation. An HSV color image is more intuitive and closer to people's subjective color consciousness than visuals in other color spaces [35]. In this paper, an RGB color image is first converted into the HSV color model, and then some preprocessing processes are performed. This step is important since the RGB color space specifies the image in primary colors, which is less effective than the HSV color space when it comes to describing

objects. Similar to how the HSV color space defines an image, the human eye interprets images based on comparisons such as color, vibrancy, and brightness. The values of H, S, and V must be transformed to a specified range based on the human perception system for easier computation. The hue component has angles ranging from 0 to 360 degrees, while the value and saturation components have values ranging from 0 to 1 percent. The image in HSV color space needs to be quantized according to the human eye's perception characteristics as referenced in [36]. The obtained $H^{'}S^{'}V^{'}$ color image contains only 81 colors which represent original images with lesser numbers of colors as compared to the original HSV color image. The statistical moments-based color information of an image provide the important properties of intensity level distribution like smoothness, uniformity, flatness, contrast, and brightness [37], which improves the retrieval efficiency of system. The proposed color feature representation method computes mean, standard deviation, skewness, and kurtosis from $H^{'}S^{'}V^{'}$ color image for formation of the color feature descriptor [38]. Let μ_{CC} be the mean, σ_{CC} be the standard deviation, γ_{CC} be the skewness, and κ_{CC} be the kurtosis of each CC color component, where $CC \in \{H^{'}, S^{'}, V^{'}\}$. The statistical moments from the quantized color image are computed as

$$\begin{aligned}
\mu_{CC} &= \sum_{i=1}^{T} X_i \mathscr{P}(X_i),\\
\sigma_{CC} &= \sqrt{\sum_{i=1}^{T} (X_i - \mu_{CC})^2 \mathscr{P}(X_i)},\\
\gamma_{CC} &= \frac{1}{\sigma^3} \sum_{i=1}^{T} (X_i - \mu_{CC})^3 \mathscr{P}(X_i),\\
\kappa_{CC} &= \frac{1}{\sigma^4} \sum_{i=1}^{T} (X_i - \mu_{CC})^4 \mathscr{P}(X_i),
\end{aligned} \tag{2}$$

where X_i is the i^{th} pixel value in the CC color component, $\mathscr{P}(X_i)$ is the corresponding probability and T is the total number of pixels in the corresponding component. The μ is the average of intensity values, which describes the brightness of an image while the σ measures the distribution of intensity values about the mean and defines the contrast of an image. The γ the measure of symmetry or more precisely about its mean value and it also determines the lack of symmetry in a set of data points. The kurtosis calculates peak of the distribution of intensity values about the μ and also measures the outliers present in the distribution. An integration of statistical moments from all three color components has constructed the color feature descriptor, which represents the color information of the image effectively. Hence, color feature descriptor is defined as

$$FV_{Color} = \{\mu_{CC}, \sigma_{CC}, \gamma_{CC}, \kappa_{CC}\}, \tag{3}$$

where $CC \in \{H^{'}, S^{'}, V^{'}\}$, since the four moments have been computed from each color component, therefore, the dimension of the color feature descriptor will be 12. The algorithmic 1 steps for color feature representation are as follows:

3.3. Texture Feature Representation. Sobel edge detection ([39]), discrete cosine transformation ([40]), and the gray level co-occurrence matrix (GLCCM) ([41]) are used to extract texture information. It is a derivative-based approximation operator that performs a 2D gradient measurement on an image and accentuates high spatial regions around the edges. As seen in the image in Figure 1, the operator is made up of a pair of 3×3 convolution kernels. One kernel is simply the other one 90^0 rotated. The fundamental goal of edge detection is to reduce the quantity of data in an image while keeping structural qualities that can be used for future image processing. There are several edge detector techniques, and this study concentrates on the Sobel edge detection methodology.

In the proposed method, the Sobel operator is employed on the Laplacian-based preprocessed V-component. The convolved operation is performed image using given template, and the gradient values in each horizontal and vertical directions are computed. These kernels are designed to respond efficiently to the edges running vertically and horizontally relative to the pixel grid. One kernel is considered for each of the two perpendicular orientations noted. These kernels can be used individually on the input image to yield distinct measurements of the gradient component in each orientation as $f_a(a,b) = f_a$ and $f_b(a,b) = f_b$. One can acquire the absolute magnitude of the gradient at each position as well as the gradient's orientation by combining these two. The magnitude of the gradient is calculated as follows:

$$|f| = \sqrt{f_a^2 + f_b^2}, \tag{4}$$

where

$$\begin{aligned}
f_a &= f(a-1, b+1) + 2f(a, b+1) + f(a+1, b+1)\\
&\quad - [f(a-1, b-1) + 2f(a, b-1) + f(x+1, y-1)],\\
f_b &= f(a+1, b-1) + 2f(a+1, b) + f(a+1, b+1)\\
&\quad - [f(a-1, b-1) + 2f(a-1, b) + f(a-1, b+1)].
\end{aligned} \tag{5}$$

The angle of orientation of the edge (relative to the pixel grid) giving rise to the spatial gradient is given by

$$\theta = \arctan\left(\frac{f_b}{f_a}\right), \tag{6}$$

When the orientation is 0, the largest contrast from black to white runs from left to right on the image, and all other angles are measured clockwise from the horizontal direction. The approximate magnitude is determined as follows for easy and quick computation:

$$f = |f_a| + |f_b|. \tag{7}$$

The discrete cosine transform converts an image from the spatial to the frequency domain, and is commonly used

Require: an RGB color image
Ensure: color feature descriptor
(1) Take an RGB color image (I) as an input and use the Laplacian operator to process and analyze it. Transform a preprocessed I I' into an HSV color image. IHSV = HSV(I')
(2) Decompose an HSV color image into its H, S, and V components then quantize each one separately to get H', S' and V' components.
(3) For color feature representation, construct the probability-based histograms of H', S', and V' components, respectively, and accordingly compute the statistical color moments using equation 2.
(4) Finally the color feature descriptor is obtained by integrating all the computed statistical color moments using equation 3 which can be re-written as $FV_{Color} = \{\mu_{CC}, \sigma_{CC}, \gamma_{CC}, \kappa_{CC}\}$.

Algorithm 1: Color information extraction.

+1	+2	+1
0	0	0
-1	-2	-1

-1	0	+1
-2	0	+2
-1	0	+1

Figure 1: Sobel convolution kernels.

in data reduction, feature extraction, and watermarking. The block of size $Y \times Y$ is represented by f(p, q). An image's 2-D DCT transform can be defined as shown in the following equation:

$$\mathfrak{F}(s,t) = \frac{2}{N}\mathfrak{C}(s)\mathfrak{C}(s)\sum_{p=1}^{Y}\sum_{q=1}^{Y} f(p,q)\alpha\beta, \tag{8}$$

where

$$\mathfrak{C}(s) = \mathfrak{C}(t) = \begin{cases} \frac{1}{\sqrt{2}} & \text{if } s = t = 0, \\ 1 & \text{if } s, t > 0, \end{cases} \tag{9}$$

and $\alpha = \cos[((2m+1)u(\pi)/(2N)]$, $\beta = \cos[((2n+1)v(\pi)/(2N)]$.

The function $\mathfrak{F}(s,t)$ represents DCT transformed image corresponding to the given image block $f(p,q)$ with respect to the (p,q) coordinates. The transformed image has DCT coefficients which represents the image information. The most important image information is concentrated in the upper left corner of the transformed image known as the low-frequency band information while the lowest right corner has the insignificant information known as high-frequency band information and it reflects the contour and other unnecessary information of the image. The some coefficients in low-frequency band have been selected by discarding the high-frequency band information completely. The value $\mathfrak{F}(0,0)$ represents DC coefficient or average/energy of image and the remaining DCT coefficients are known as AC coefficients. In order to find the appropriate information, the transformed block is quantized using standard quantization table [42]. Thereafter, the selection of DCT coefficients in zigzag scanning order gives the most appropriate image information, and this order is shown in Figure 2.

Since, the image blocks contains the overlapping or relative information with each other, in order to determine the associativity between the blocks based on the DC and AC coefficients, DC and AC matrices have been established for feature extraction. The process for selection of DCT coefficients and formation of DC and AC matrices are described in the following equation. For two adjacent image blocks,

$$DC_{df\,i} = \left|DC_{b(i+1)} - DC_{b(i)}\right|, \tag{10}$$

where b represents block, $DC_{b(i)}$ is energy of i^{th} block and $DC_{df\,i}$ is absolute difference value between the next block $(i+1)^{th}$ and current block i^{th}. This value has been computed throughout the image. For example, if size of an image size $M \times N$ and block size is 8×8, then total number of blocks will be $bn = M \times N/8 \times 8$. So, all the difference values are collected as follows:

$$DC_{val} = \left\{DC_{df1}, DC_{df2}, \ldots, DC_{df(bn-1)}\right\}. \tag{11}$$

Similarly, eight values have been selected from each block and special kind of coding is performed on selected AC coefficients in zigzag order between two adjacent blocks. The computation process is given as

$$AC^j = \begin{cases} 1 & : \left(AC_{b(i+1)} - AC_{b(i)}\right) > 0, \\ 0 & : Otherwise, \end{cases} \tag{12}$$

where j represents number of selected AC coefficients from each block. For one block AC^j, $j = 1, 2, \ldots, 8$, values are given as for example

$(AC^1, AC^2, AC^3, AC^4, AC^5, AC^6, AC^7, AC^8) = (1,1,1,1,0,1,1,0) = 246$ which is the decimal representation and this decimal value is represented by array $AC_{df\,i}$. Thus, the collected values of an image is given as

$$AC_{val} = \left\{AC_{df1}, AC_{df2}, \ldots, AC_{df(bn-1)}\right\}. \tag{13}$$

Finally, the DC and AC matrices have constructed by using (11) and (13), respectively. These matrices will be used for formation of the texture feature descriptor.

The gray level co-occurrence matrix (GLCCM) is one of the important methods to examining the texture properties

of the image. To obtain the texture feature descriptor, GLCCM is applied on both DC and AC matrices separately and create GLCM eigenvectors from certain parameters. The GLCCM for a given pair of pixels in a specific direction (θ) and particular pixel distance d is defined as the frequency of elements i and j of the matrix, respectively. The value of the GLCCM is denoted by the $P(s,t \mid d,\theta)$ which is computed symmetrically throughout the matrix and the size of GLCCM is depend on gray levels number. In general, the GLCCM method computes four matrices for four directions i.e., $0^0, 45^0, 90^0, 135^0$ and for a constant pixel distance d. For texture feature representation, first GLCCM is normalized to avoid variation among the elements of the matrix. The normalized element $P(i,j)$ of GLCCM is defined as

$$P(s,t) = \frac{P(s,t \mid d,\theta)}{\sum_{s=1}^{G}\sum_{t=1}^{G} P(s,t \mid d,\theta)}, \tag{14}$$

where G is the total number of gray levels. In order to extract the texture features, a number of statistical parameters are obtained from normalized GLCM, however, the computational requirements for considering all these are too high and unrealistic. Therefore, only four parameters are considered for construction of texture feature descriptor in this work. The four parameters are defined as

$$\begin{aligned}
\text{Contrast } F_{con} &= \sum_{i=1}^{G}\sum_{i=1}^{G} (i-j)^2 P(i,j),\\
\text{Energy } F_{asm} &= \sum_{i=1}^{G}\sum_{i=1}^{G} P^2(i,j),\\
\text{Entropy } Fent &= \sum_{i=1}^{G}\sum_{i=1}^{G} P(i,j) log_2 P(i,j),\\
\text{Correlation } Fcor &= \frac{\sum_{i=1}^{G}\sum_{i=1}^{G} ijP(i,j) - u_x u_y}{q_x q_y}.
\end{aligned} \tag{15}$$

In the proposed method, above the texture parameters from the gray level co-occurrence matrices $GLCCM_{DC}$ and $GLCCM_{AC}$ of the DC and AC-based components, respectively, where 4-4 matrices have been constructed using four directions i.e., $0^0, 45^0, 90^0, 135^0$ and corresponding the energy, contrast, entropy and correlation have been constructed. The collective values of the abovementioned four parameters represent the texture feature descriptor of any image.

$$FV = \{F_{con}, F_{asm}, F_{ent}, F_{cor}\}, \tag{16}$$

Let FV_{DC} and FV_{AC} be represent the texture properties of DC and AC-based matrices and calculated by using (16), then the final texture feature descriptor is obtained as

$$FV_{Texture} = \{FV_{DC}, FV_{AC}\}. \tag{17}$$

The speed and retrieval of the system is improved vastly due to the formation of low dimensional texture feature descriptor. The whole process of computing the texture feature descriptor is presented by the following algorithmic 2 steps.

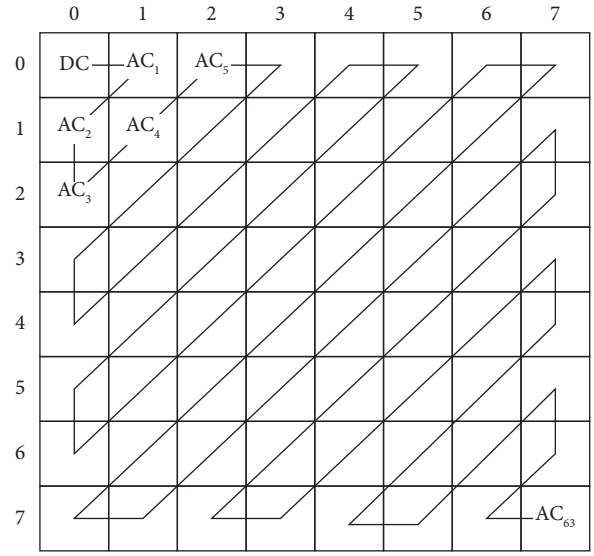

Figure 2: Zigzag scanning order for 8×8 image block [40].

The block diagram of proposed method is shown in Figure 3, where color and texture features are integrated to present final feature descriptor. The final feature descriptor obtained by integrating the (3) and (17) is given as

$$FV_{Final} = \{FV_{Color}, FV_{Texture}\}. \tag{18}$$

Since this feature descriptor is not normalized because the components are already in a proper range and it is not degrading the retrieval accuracy. The final feature descriptors of all images available in the digital repository and that of the query image are constructed. The collection of final feature descriptors is stored in the feature database, and similarity distances are calculated between the given query and digital repository based on the feature descriptors. Corresponding to the first few minimum distances, the top-desired images have returned to the user in relation to the query.

3.4. Similarity Measure. To offer an appropriate response to an image query, a vast number of image databases require both rapid comparison and feature extraction. It can take a long time to look through every image in a huge image library. The appropriate distance between query feature descriptor and database image feature descriptors has been generated to measure the similarity between the query image and the database images. Because of its efficiency and effectiveness, the Euclidean distance is one of the most widely used approaches for retrieval. Therefore, in the proposed system, the Euclidean distance (ED) is used to calculate the similarity measure. It calculates the square root of the total of the squared absolute differences to determine the distance between two image feature descriptors. It is defined as follows:

Require: an RGB color image
Ensure: texture feature descriptor
(1) Consider V-component of the preprocessed HSV color image and apply the Sobel operator to obtain magnitude of gradients (f) in x-and y-directions.
(2) Divide the obtained magnitude of gradients (f) into nonoverlapping blocks of fixed size $bs \times bs$.
(3) Consider FV texture as an empty row vector and p = (Number of rows in f) × (Number of columns in f)/$bs \times bs$.
(4) Collect DC coefficients and select some significant AC coefficients from all blocks. Correspondingly, determine the relation between two adjacent blocks using DC and AC coefficients throughout the image using equation 6 and 8, where two row vectors have been achieved.
(5) Arrange the DC and AC row vectors into the form of matrices and apply the GLCCM approach on them. Then, GLCCM have been constructed for different directions and statistical parameters using equation 10 have been computed and collective integration of them represents the texture feature descriptor FV texture of the image plane.

Algorithm 2: Texture information extraction.

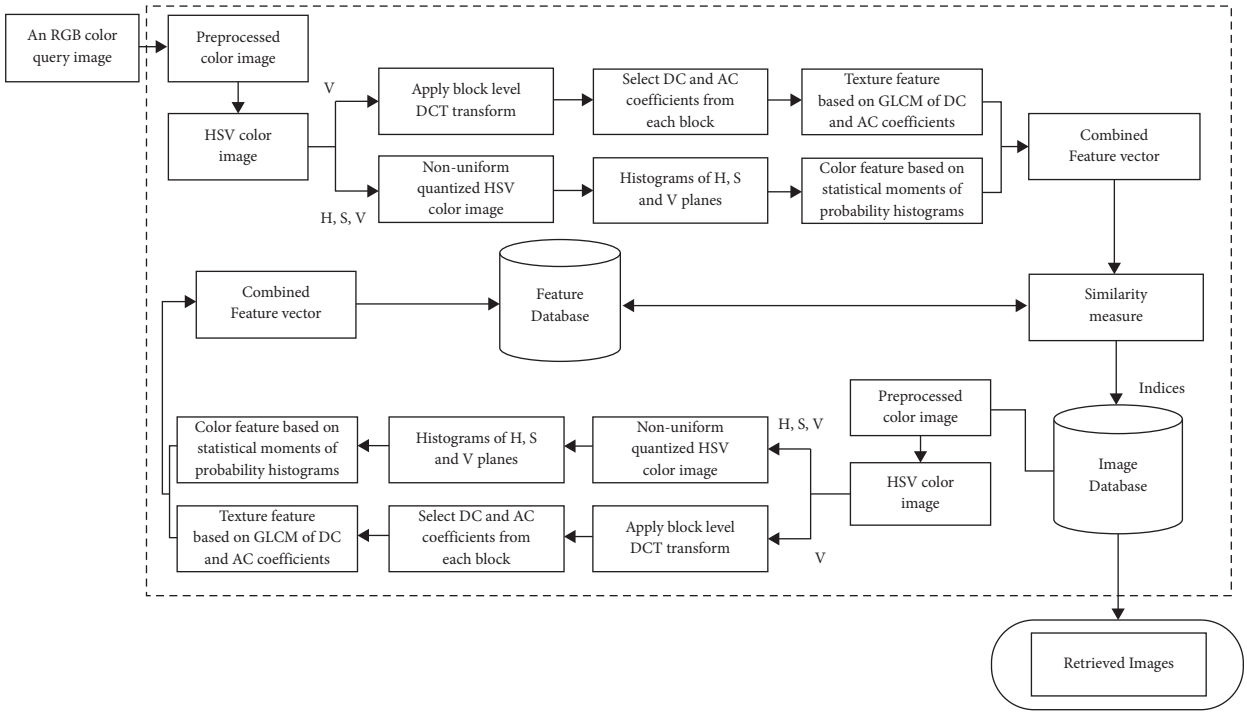

Figure 3: The block diagram of the proposed CBIR scheme.

$$ED = \sqrt{\sum_{i=1}^{d} \left(fd_q^i - fd_t^i \right)^2}, \tag{19}$$

where d is the dimension of the feature descriptor, fd_q and fd_t are feature descriptors of query image and target image of the digital repository.

4. Experimental Results and Analysis

4.1. Database Overview. Two benchmarked datasets were used in the retrieval process to evaluate the efficacy of the proposed CBIR approach. The first is the [43] land-use dataset from UC Merced. It is a typical dataset for image categorization using radar remote sensing that includes 21 different scene types. For the purposes of evaluation, this paper used 900 RGB color photographs divided into nine groups. Agriculture, aviation, roads, grounds, beaches, residential, woodland, chaparral, and harbor are the categories. All of the photos in the collection are 256 × 256 in size, with a resolution of 1 foot. To demonstrate the responsiveness of the retrieval method to changes in image rotation, translation, and size, the image is accessed in JPEG file format. The second is the Corel database [44], which has 1000 RGB color images divided into 10 categories, each with 100 photos of a similar type. People, beaches, buildings, buses, dinosaurs, elephants, roses, horses, mountains, and cuisine are among the image categories. They are in JPEG format and are 256 × 384 and 384 × 256 pixels in size. For both datasets, all of the images were used as query images in the tests. For visualisation, example images of radar and Corel image datasets are shown in Figures 4 and 5, with one image from each category.

Figure 4: Sample images of Corel-1000 dataset.

Figure 5: Sample images of UCML radar image dataset.

In general, any CBIR approach is divided into two parts. In phase I, all of the photos in the dataset are acquired one by one for the extraction of color and texture information. To establish a feature database, the extracted combined features are stored in a database as feature descriptors. In phase II, however, to get comparable types of images from the digital repository using the same way, the user must provide the query as an input image. By computing the similarities using ED, the combined texture and color feature vector is created and compared with the feature descriptors of the database photos. The user gets shown the photographs that are the most comparable to the query image.

4.2. Evaluation Measurements. This section has described the performance assessment methods that not only evaluate the effectiveness of image retrieval but also ensure the stability of findings in order to constructively illustrate the success of the suggested image retrieval system. In the purposed CBIR approach, three significant measurements were employed to evaluate retrieval performance: precision, recall, and f-score. These parameters are described as follows:

$$\begin{aligned} \text{Precision}\,(P) &= \frac{A}{B}, \\ \text{Recall}\,(R) &= \frac{A}{C}, \\ \text{f}-\text{score}\,(F) &= \frac{2P \times R}{(P+R)}, \end{aligned} \tag{20}$$

where A denotes relevant retrieved images, B denotes the total number of retrieved images from the dataset, and C is the total number of relevant images publicly available per category. Consider the following scenario for clearance: a CBIR technique for query image retrieves a total of 10 images, of which 7 are relevant, from a total of 30 similar images in one database category. The precision will be 7/10 = 70%, while the recall rate will be 7/30 = 21%. Therefore, in this observation it can be observed that the recall rate alone is insufficient to establish the success of a CBIR; precision must also be calculated. F-score in the CBIR method designed for it. These parameters are described as follows: precision and recall are two metrics computed to illustrate the effectiveness of image retrieval, and they assess the accuracy of image retrieval with relevance to the database images and query. These two measurements, however, do not represent the total accuracy of effective image retrieval. So they can be combined to produce a single value that measures picture retrieval accuracy, which is known as the F-Score or F-measure. When retrieving images from the Corel-1000 and UCML-2100 datasets based on a query image, the values of B and C are set to 10 or 20 and 100, respectively, in the retrieval. Since each image in the category is used as a query image, the accuracy must be presented in terms of averages/means. The average precision, recall, and F-score can be calculated as follows:

$$\begin{aligned} @P_{avg}\,(M) &= \frac{1}{nc}\sum_{k=1}^{nc} P_k, \\ @R_{avg}\,(M) &= \frac{1}{nc}\sum_{k=1}^{nc} R_k, \\ @F_{avg}\,(M) &= \frac{1}{nc}\sum_{k=1}^{nc} F_k, \end{aligned} \tag{21}$$

where $@P_{avg}\,(M), @R_{avg}\,(M)$ and $@F_{avg}\,(M)$ are the averages for precision, recall, and F-score, respectively, for M image category and nc is the total number of images in each category. In this paper, the Corel and radar image datasets are used so the value of nc = 100 because each image class has 100 images.

4.3. Retrieval Results and Discussion. The proposed method is performed on preprocessed and without pre-processed image in the retrieval process using a simple fusion of color and texture descriptors. For color descriptor, an HSV color model is quantized into nonuniform bins to get a new model color $H^{'}S^{'}V^{'}$ model which consists of 81-colors. Since the four statistical color moments have been computed from each quantized color component, therefore, the dimension of the color descriptor will be $4 \times 3 = 12$-D. For texture descriptor, authors have computed DC and AC matrices (i.e., already discussed in texture feature representation section in detail) of V component and corresponding to each matrix, the GLCM is computed for four directions i.e., $0^0, 45^0, 90^0, 135^0$ and constant pixel distance $(d = 1)$. The four values for DC matrix and four values for AC matrix have been computed, so the dimension of the texture feature descriptor is 8-D. The dimension of the fused feature descriptor will be $12 + 8 = 20$-D. The fused feature descriptors of all database images have been constructed for retrieving process. Table 1 shows the top 10 retrieved images from the

Table 1: $@R_{avg}$, $@P_{avg}$, and $@F_{avg}$ for top 10 retrieved images taken from UC Merced land-use dataset.

Image class name	Top 10 images					
	Without preprocessing			With preprocessing		
	$@R_{avg}$	$@P_{avg}$	$@F_{avg}$	$@R_{avg}$	$@P_{avg}$	$@F_{avg}$
Agricultural	8.46	84.60	15.38	9.10	91.00	16.55
Runway	5.66	56.60	10.29	8.65	86.50	15.73
Roads	7.82	78.20	14.22	9.04	90.40	16.44
Grounds	8.50	85.00	15.45	7.93	79.30	14.42
Beach	6.84	68.40	12.44	7.55	75.50	13.73
Residential	7.75	77.50	14.09	8.17	81.70	14.85
Forest	9.02	90.20	16.40	9.23	92.30	16.78
Chaparral	9.05	90.52	16.46	9.95	99.50	18.09
Harbor	8.59	85.9	15.62	9.29	92.90	16.89
Mean	**7.97**	**79.66**	**14.49**	**8.77**	**87.70**	**14.96**

The bold values concludes the mean representation.

dataset based on preprocessed and without preprocessed images for UC Merced land-use dataset while same is shown in Table 2 for the top 20 retrieved images. In both the cases, the preprocessed method gives the better results as compare to the without preprocessed image method. In case of top 10 images, it is evident that the preprocessed image technique provides the huge improvement in some category images. For example, the best category image i.e., chaparral has increased precision from 90.52% to 99.50%, which is almost 9% hike from without preprocessed to preprocessed image. Similarly, the worst category image i.e., roads have increased precision from 78.20% to 90.40% which is almost 12% hike from nonprocessed to preprocessed technique. In overall, the mean average for precision, recall, and F-score are satisfactory of the proposed CBIR method for top 10 and 20 retrieved images from the digital repository. It is also noticed from the tables that the accuracy is highly increased from top 10 to top 20 retrieved images.

The F-score results indicate that when using statistical texture features with color different quantization gives the highest retrieval performance for the class chaparral.

Similarly, the results for the Corel-1K dataset have been included for the top 10 retrieved images using both the preprocessed techniques. Table 3 shows the retrieval results for the top 10 images using the preprocessed technique for Corel-1K image dataset. In this table, the proposed CBIR method have produced the highest results for dinosaur images while the lowest retrieval results were attained by the mountain category images for the 10 retrieved images. For top 20 images, Table 4 shows the retrieved results, where the most of the category images have good retrieval results but beach and mountains images have the lowest results because the images are complex, structures and their contents are mixed with each other. The overall means for recall, precision, and F-score for top 10 retrieved images without preprocessing are 8.18%, 81.53%, and 14.87%, while it becomes 9.21%, 92.11%, and 16.75% using with pre-processed image. Hence, it is a huge improvement from without preprocessing to with technique. It is also observed from the table that the little bit accuracy has been decreased from top 10 to top 20 images. The retrieval results for top $T - i$, ($i = 10$, 20, 40, 60, 80, and 100) images are shown in Figure 6 for radar remote image dataset in terms of average precision, recall, and F-score rate while it is shown in Figure 7 for Corel-1K image dataset, where $T - i$ represents number of images retrieved from the dataset.For visualisation purposes, we have selected two best and two worst category images from both the radar remote sensing image and Corel-1K image datasets. Figure 8 shows the best retrieval results for retrieving top 20 images from radar remote sensing image dataset for chaparrals and forest image category, where these results are only given query images. For the chaparral query image, values of the precision (P), recall(R), and F-score (F) are 100.00%, 20.00%, and 33.34%, respectively, while the technique gives $P = 80.00\%$, $R = 18.00\%$, and $F = 29.38\%$ for forest image category. For worst-case results, Figure 9 depicts the retrieved images for beach and grounds images, where the first images from top left corner are queries. Figure 10 depicts the top 20 dinosaurs and horses' images from Corel-1K image dataset, where top upper left corner images are the queries. The results may be changes if different query images are selected but in overall categories, dinosaur, and horse images have given the best results. In case of lowest results, the beach and mountain image categories are shown in Figure 11, where blue color cross symbol × represents the nonrelevant images.

4.4. Comparative Study and Analysis. To check the relative efficacy of the proposed CBIR method, the authors have compared the results with ten relative state of art CBIR schemes [24–33]. The discussion and analysis with our proposed scheme is as follows. The most of the above discussed papers have very good retrieval results but they have many limitations such as high dimensional feature, retrieval speed descriptors, and accuracy. However, our proposed method has a high retrieval speed and low dimensional feature descriptors with satisfactory results in terms of average precision, recall, and F-score. The proposed method is compared in terms of average precision ($@P_{avg}$), recall ($@R_{avg}$), and F-score ($@F_{avg}$) with the above-discussed methods and it is shown in Tables 5–7, respectively. In the CBIR schemes [24–27, 29] mountain category images have the minimum retrieval accuracy while beach image category

Table 2: $@R_{avg}$, $@P_{avg}$, and $@F_{avg}$ for top 20 retrieved images taken from UC Merced land-use dataset.

Image class name	Top 20 images					
	Without preprocessing			With preprocessing		
	$@R_{avg}$	$@P_{avg}$	$@F_{avg}$	$@R_{avg}$	$@P_{avg}$	$@F_{avg}$
Agricultural	14.32	71.60	23.87	16.91	84.55	28.18
Runway	11.59	57.95	19.32	15.46	77.30	25.77
Roads	13.57	67.85	22.62	17.07	85.35	28.45
Grounds	12.94	64.70	21.57	14.28	71.40	23.80
Beach	13.86	69.30	23.10	14.71	73.55	24.52
Residential	15.37	76.85	25.62	16.20	81.00	27.00
Forest	16.95	84.75	28.25	18.05	90.25	30.08
Chaparral	18.03	90.15	30.05	19.90	99.50	33.17
Harbor	16.94	84.70	28.23	17.35	86.75	28.92
Mean	**14.84**	**74.21**	**24.74**	**16.66**	**83.29**	**27.76**

The bold value indicates the mean representation.

Table 3: $@R_{avg}$, $@P_{avg}$, and $@F_{avg}$ for top 10 retrieved images taken from Corel-1K dataset using with and without preprocessed technique.

Image class name	Top 10 images					
	Without preprocessing			With preprocessing		
	$@R_{avg}$	$@P_{avg}$	$@F_{avg}$	$@R_{avg}$	$@P_{avg}$	$@F_{avg}$
Beaches	6.45	64.50	11.73	7.91	79.10	14.38
Buses	9.04	90.40	16.44	9.94	99.40	18.07
Dinosaurs	9.86	98.60	17.93	9.98	99.80	18.15
Elephants	7.83	78.30	14.24	8.75	87.50	15.91
Flowers	8.79	87.90	15.98	9.62	96.20	17.49
Foods	8.93	89.30	16.24	9.48	94.80	17.24
Horses	8.86	88.60	16.11	9.96	99.60	18.11
Monuments	7.75	77.50	14.09	8.75	87.50	15.91
Mountains	6.05	60.50	11.00	7.85	78.50	14.27
People	8.21	79.70	14.92	9.87	98.70	17.95
Mean	**8.18**	**81.53**	**14.87**	**9.21**	**92.11**	**16.75**

The bold value indicates the mean representation.

Table 4: $@R_{avg}$, $@P_{avg}$, and $@F_{avg}$ for top 20 retrieved images taken from Corel-1K dataset using with and without preprocessed technique.

Image class name	Top 20 images					
	Without preprocessing			With preprocessing		
	$@R_{avg}$	$@P_{avg}$	$@F_{avg}$	$@R_{avg}$	$@P_{avg}$	$@F_{avg}$
Beaches	12.18	63.30	20.43	15.41	77.05	25.68
Buses	15.80	85.32	26.66	18.71	93.55	31.18
Dinosaurs	18.01	90.05	30.02	19.05	95.25	31.75
Elephants	12.01	69.66	20.49	16.83	84.15	28.05
Flowers	17.40	90.48	29.19	18.98	94.90	31.63
Foods	14.59	77.33	24.55	17.04	85.20	28.40
Horses	16.41	85.33	27.53	18.07	90.35	30.12
Monuments	11.60	58.00	19.33	16.75	83.75	27.92
Mountains	10.82	59.51	18.31	14.54	72.70	24.23
People	15.38	81.51	25.88	18.39	91.95	30.65
Mean	**14.42**	**76.05**	**24.24**	**17.38**	**86.89**	**28.97**

The bold value indicates the mean representation.

in [28, 32] schemes has the minimum accuracy in terms of $@P_{avg}$, $@R_{avg}$, and $@F_{avg}$. The elephant images have the minimum accuracy in CBIR scheme [30] while scheme [31] has the lowest accuracy for monuments image category. Lastly, the foods image category has the lowest accuracy in CBIR scheme [33]. The most of images in mountain, beach, elephant, and monuments categories have blue color contents which are the mixed with each other while the food category images have very complex structures, so it is very difficult to distinguish actual image contents to classify such categories. So, strong feature extraction methods are required. In our proposed method, mountain images have the lowest accuracy i.e., also 72.70% precision which also acceptable. The overall means of $@P_{avg}$, $@R_{avg}$, and $@F_{avg}$ are

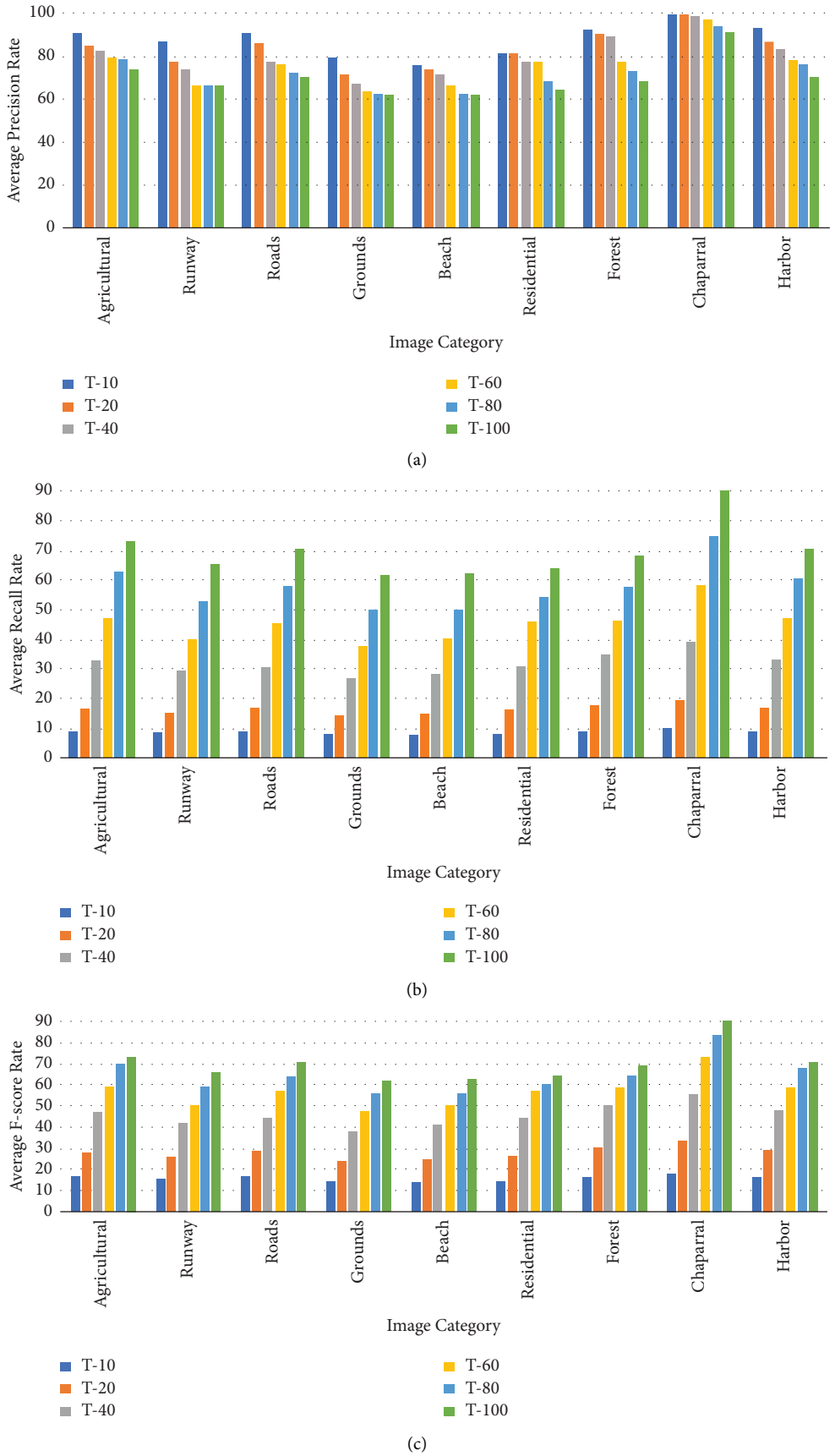

Figure 6: Accuracy in terms of (a) average precision rate (b) average recall rate and (c) average F-score for radar remote sensing image dataset.

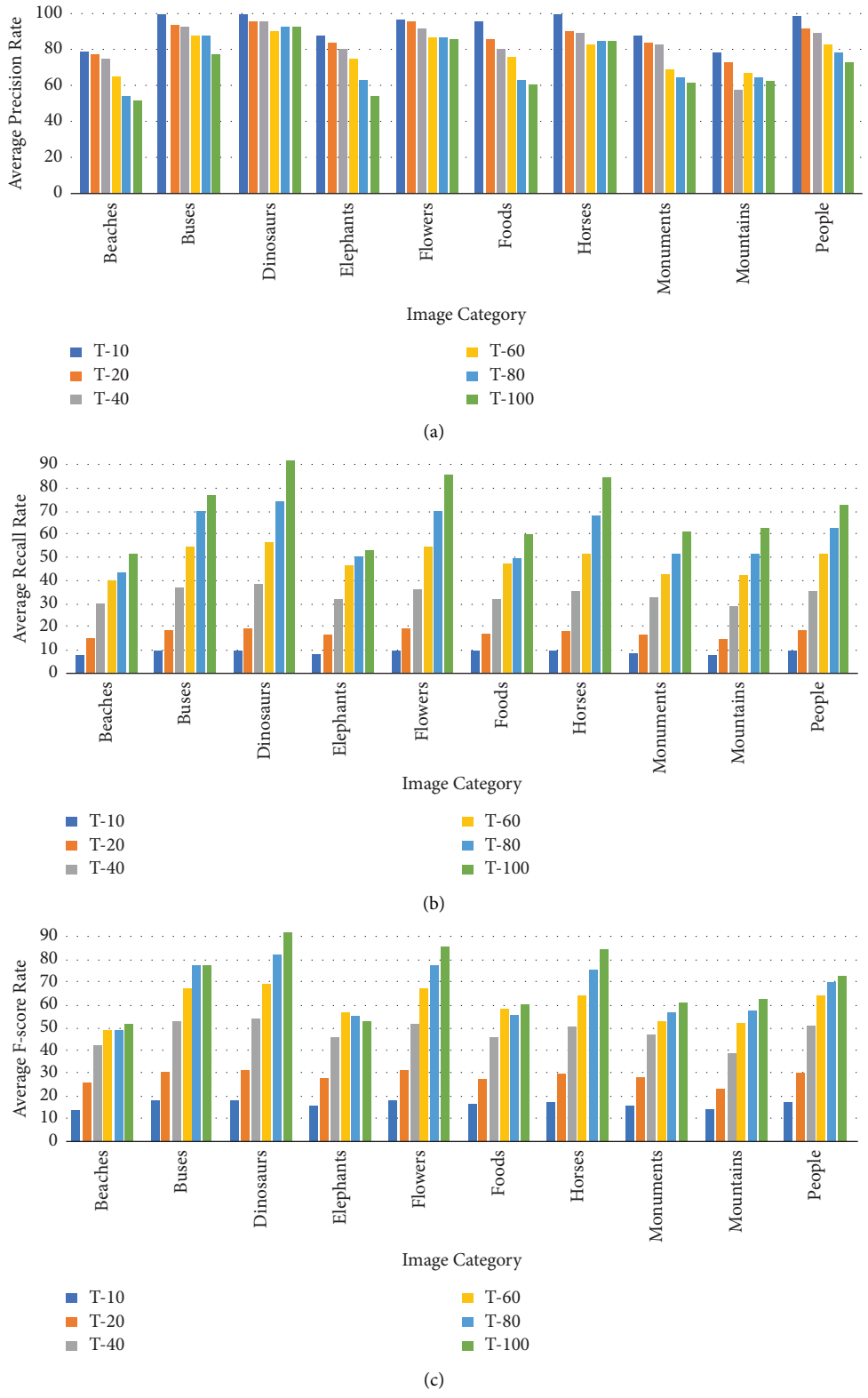

Figure 7: Accuracy in terms of (a) average precision rate (b) average recall rate and (c) average F-score for Corel-1K image dataset.

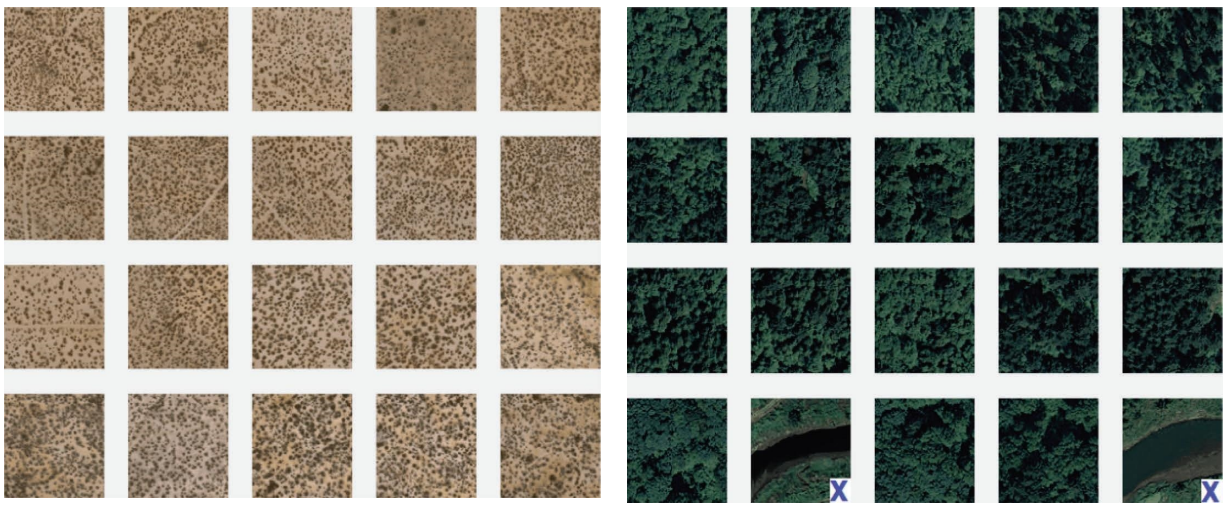

(a) (b)

Figure 8: Top 20 retrieved images from radar remote sensing image Corel-1K image dataset. (a) Chaparrals, $P = 100.00\%$, $R = 20.00\%$, $F = 33.34\%$. (b) Forests, $P = 80.00\%$, $R = 18.00\%$, $F = 29.38\%$.

(a) (b)

Figure 9: Top 20 retrieved images from radar remote sensing image dataset. (a) Beaches, $P = 75.00\%$, $R = 15.00\%$, $F = 25.00\%$. (b) Grounds, $P = 70.00\%$, $R = 14.00\%$, $F = 23.33\%$.

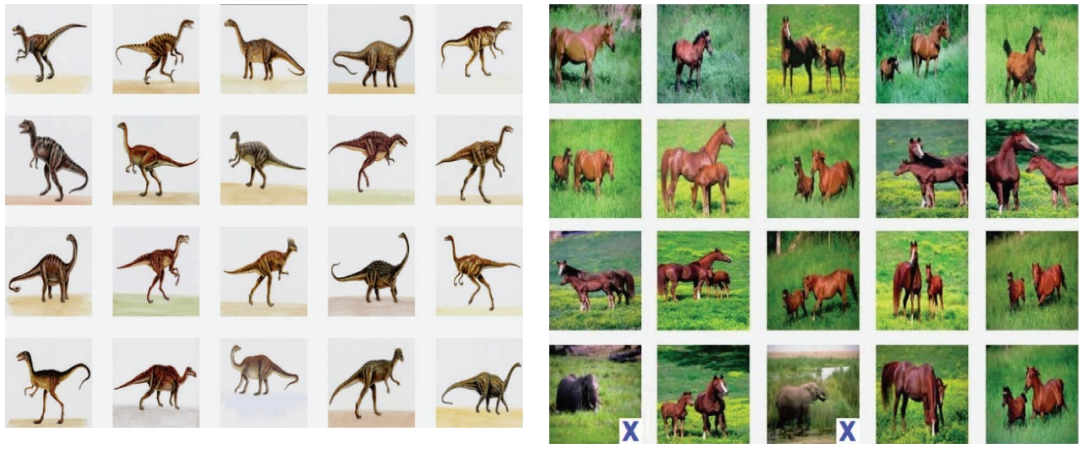

(a) (b)

Figure 10: Top 20 retrieved images from Corel-1K image dataset. (a) Dinosaurs, $P = 100.00\%$, $R = 20.00\%$, $F = 33.34\%$. (b) Horses, $P = 80.00\%$, $R = 18.00\%$, $F = 29.38\%$.

(a) (b)

Figure 11: Top 20 retrieved images from Corel-1K image dataset. (a) Beaches, P = 55.00%, R = 11.00%, F = 18.33%. (b) Mountains, P = 70.00%, R = 14.00%, F = 23.33%.

Table 5: Comparative results in terms of average precision for top 20 retrieved images for Corel-1K dataset with some state of art CBIR schemes.

Image category	Shrivastava and Tyagi [24]	Dubey et al. [25]	Mistry et al. [26]	Irtaza et al. [27]	Ahmed et al. [28]	Garg and Dhiman [30]	Vimina and Divya [29]	Varish and Singh [31]	Kumar et al. [32]	Joseph et al. [33]	Proposed scheme
People	74.80	75.00	62.00	83.00	90.00	81.20	72.50	60.00	80.00	81.00	91.95
Beaches	58.20	55.00	71.00	72.00	60.00	96.56	52.75	55.00	65.00	78.00	77.05
Monuments	62.10	67.00	53.00	86.00	90.00	78.20	52.70	50.00	65.00	80.00	83.75
Buses	80.20	95.00	77.00	100.00	75.00	83.30	93.95	95.00	100.00	81.00	93.55
Dinosaurs	100.00	97.00	89.00	97.00	100.00	82.20	99.45	100.00	100.00	100.00	95.25
Elephants	75.10	63.00	55.00	82.00	70.00	77.50	52.40	45.00	70.00	81.00	84.15
Flowers	92.30	93.00	89.00	86.00	90.00	86.30	86.65	70.00	95.00	89.00	94.90
Horses	89.60	89.00	55.00	82.00	100.00	86.10	83.75	95.00	100.00	95.00	90.35
Mountains	56.10	45.00	52.00	69.00	70.00	86.30	43.15	80.00	70.00	68.00	72.70
Foods	80.30	70.00	55.00	90.00	90.00	90.20	71.05	65.00	90.00	60.00	85.20
Mean	**76.90**	**74.90**	**65.80**	**84.70**	**83.50**	**84.79**	**71.04**	**71.50**	**83.50**	**81.30**	**86.89**

The bold value indicates the mean representation.

Table 6: Comparative results in terms of average recall for top 20 retrieved images for Corel-1K dataset with some state of art CBIR schemes.

Image category	Shrivastava and Tyagi [24]	Dubey et al. [25]	Mistry et al. [26]	Irtaza et al. [27]	Ahmed et al. [28]	Garg and Dhiman [30]	Vimina and Divya [29]	Varish and Singh [31]	Kumar et al. [32]	Joseph et al. [33]	Proposed scheme
People	14.96	15.00	12.40	16.60	18.00	16.24	14.50	12.00	16.00	16.20	18.39
Beaches	11.64	11.00	14.20	14.40	12.00	19.31	10.55	11.00	13.00	15.60	15.41
Monuments	12.42	13.40	10.60	17.20	18.00	15.64	10.54	10.00	13.00	16.00	16.75
Buses	16.04	19.00	15.40	20.00	15.00	16.66	18.79	19.00	20.00	16.20	18.71
Dinosaurs	20.00	19.40	17.80	19.40	20.00	16.44	19.89	20.00	20.00	20.00	19.05
Elephants	15.02	12.60	11.00	16.40	14.00	15.50	10.48	9.00	14.00	16.20	16.83
Flowers	18.46	18.6	17.80	17.20	18.00	17.26	17.33	14.00	19.00	17.80	18.98
Horses	17.92	17.80	11.00	16.40	20.00	17.22	16.75	19.00	20.00	19.00	18.07
Mountains	11.22	9.00	10.40	13.80	14.00	17.26	8.63	16.00	14.00	13.60	14.54
Foods	16.06	14.00	11.00	18.00	18.00	18.04	14.21	13.00	18.00	12.00	17.04
Mean	**15.38**	**14.98**	**13.16**	**16.94**	**16.70**	**16.96**	**14.21**	**14.30**	**16.70**	**16.26**	**17.38**

Table 7: Comparative results in terms of average F-score for top 20 retrieved images for Corel-1K dataset with some state of art CBIR schemes.

Image category	Shrivastava and Tyagi [24]	Dubey et al. [25]	Mistry et al. [26]	Irtaza et al. [27]	Ahmed et al. [28]	Garg and Dhiman [30]	Vimina and Divya [29]	Varish and Singh [31]	Kumar et al. [32]	Joseph et al. [33]	Proposed scheme
People	24.93	25.00	20.67	27.67	30.00	27.07	24.17	20.00	26.67	27.00	30.65
Beaches	19.40	18.33	23.67	24.00	20.00	32.19	17.58	18.33	21.67	26.00	25.68
Monuments	20.70	22.33	17.67	28.67	30.00	26.07	17.57	16.67	21.67	26.67	27.92
Buses	26.73	31.67	25.67	33.33	25.00	27.77	31.32	31.6	33.33	27.00	31.18
Dinosaurs	33.33	32.33	29.67	32.33	33.33	27.40	33.15	33.33	33.33	33.33	31.75
Elephants	25.03	21.00	18.33	27.33	23.33	25.83	17.47	15.00	23.33	27.00	28.05
Flowers	30.77	31.00	29.67	28.67	30.00	28.77	28.88	23.33	31.67	29.67	31.63
Horses	29.87	29.67	18.33	27.33	33.33	28.70	27.92	31.67	33.33	31.67	30.12
Mountains	18.70	15.00	17.33	23.00	23.33	28.77	14.38	26.67	23.33	22.67	24.23
Foods	26.77	23.33	18.33	30.00	30.00	30.07	23.68	21.67	30.00	20.00	28.40
Mean	**25.63**	**24.97**	**21.93**	**28.23**	**27.83**	**28.26**	**23.68**	**23.83**	**27.83**	**27.10**	**28.96**

The bold value indicates the mean representation.

86.89%, 17.38%, and 28.96%, respectively, for the proposed scheme. As compare to the other state of art methods, the proposed scheme has generated the good retrieval results in most of the categories. It is evident that our proposed scheme has better retrieval results than the existing CBIR schemes.

5. Conclusion

A novel content-based image retrieval strategy focusing on key color and texture feature descriptors is presented in this research. Color information has been retrieved from a quantized image using color moments. Using the Sobel edge detection algorithm and the GLCCM approach, texture information based on DCT is calculated. The single feature descriptor has a relatively small dimension, allowing it to represent an original image in a compact format without sacrificing retrieval performance and increasing the system's retrieval speed. The experimental obtained results are [31] compared to certain state-of-the-art algorithms using two benchmark datasets, and it is concluded that the average recall rate [45], precision rate, and F-score rate are extremely efficient. In the future, various deep learning-based features could be used to execute the presented feature extraction technique, which could be useful in a variety of real-world applications.

Data Availability

No data were used to support this study.

Conflicts of Interest

The authors declare that they have no conflicts of interest.

References

[1] X. Li, J. Yang, and J. Ma, "Recent developments of content-based image retrieval (CBIR)," *Neurocomputing*, vol. 452, 2021.

[2] M. Alsaffar and E. M. Jarallah, "Isolation and characterization of lytic bacteriophages infecting *Pseudomonas aeruginosa* from sewage water," *International Journal of PharmTech Research*, vol. 9, pp. 220–230, 2016.

[3] R. Kumar and R. Kumar, "A hybrid feature extraction technique for content based medical image retrieval using segmentation and clustering techniques," *Multimedia Tools and Applications*, vol. 81, no. 6, pp. 8871–8904, 2022.

[4] A. Alzubi, A. Amira, and N. Ramzan, "Semantic content-based image retrieval: a comprehensive study," *Journal of Visual Communication and Image Representation*, vol. 32, pp. 20–54, 2015.

[5] M. Kaipravan and R. Rejiram, "A novel CBIR system based on combination of color moment and Gabor filter," in *Proceedings of the 2016 International Conference on Data Mining and Advanced Computing (SAPIENCE)*, pp. 170–174, Ernakulam, India, March 2016.

[6] U. A. Khan, A. Javed, and R. Ashraf, "An effective hybrid framework for content based image retrieval (CBIR)," *Multimedia Tools and Applications*, vol. 80, no. 17, pp. 26911–26937, 2021.

[7] S. Bhardwaj, G. Pandove, and P. K. Dahiya, "A web application-based secured image retrieval system with an IoT-cloud network," *International Journal of Web Services Research*, vol. 18, pp. 1–20, 2021.

[8] R. S. Bressan, P. H. Bugatti, and P. T. M. Saito, "Breast cancer diagnosis through active learning in content-based image retrieval," *Neurocomputing*, vol. 357, pp. 1–10, 2019.

[9] M. Varges da Silva, A. Nilceu Marana, and M. Marana, "Human action recognition in videos based on spatiotemporal features and bag-of-poses," *Applied Soft Computing*, vol. 95, Article ID 106513, 2020.

[10] Z. Gao, D. Y. Wang, S. H. Wan, H. Zhang, and Y. L. Wang, "Cognitive-inspired class-statistic matching with triple-constrain for camera free 3D object retrieval," *Future Generation Computer Systems*, vol. 94, pp. 641–653, 2019.

[11] A. Shakarami and H. Tarrah, "An efficient image descriptor for image classification and CBIR," *Optik*, vol. 214, Article ID 164833, 2020.

[12] P. S. S. Kumar, N. U. Kumar, A. Ushasree, and G. L. Sumalata, "Key point oriented shape features and SVM classifier for content based image retrieval," *Materials Today Proceedings*, 2020.

[13] X. Chang, Z. Ma, Yi Yang, Z. Zeng, and A. G. Hauptmann, "Bi-level semantic representation analysis for multimedia event detection," *IEEE Transactions on Cybernetics*, vol. 47, no. 5, pp. 1180–1197, 2017.

[14] H. H. Bu, N. C. Kim, K. W. Park, and S. H. Kim, "Content-based image retrieval using combined texture and color features based on multi-resolution multi-direction filtering and color autocorrelogram," *Journal of Ambient Intelligence and Humanized Computing*, vol. 13, no. 3, pp. 1–9, 2019.

[15] S. K. Kanaparthi, U. S. N. Raju, P. Shanmukhi, G. K. Aneesha, and M. E. U. Rahman, "Image retrieval by integrating global correlation of color and intensity histograms with local texture features," *Multimedia Tools and Applications*, vol. 79, no. 47-48, pp. 34875–34911, 2020.

[16] M. Majhi and A. K. Pal, "An image retrieval scheme based on block level hybrid dct-svd fused features," *Multimedia Tools and Applications*, vol. 80, no. 5, pp. 7271–7312, 2021.

[17] A. Mohamed, F. Khellfi, Y. Weng, J. Jiang, and S. Ipson, "An efficient image retrieval through DCT histogram quantization," in *Proceedings of the 2009 International Conference on CyberWorlds*, pp. 237–240, Bradford, UK, September 2009.

[18] J. Yue, Z. Li, Lu Liu, and Z. Fu, "Content-based image retrieval using color and texture fused features," *Mathematical and Computer Modelling*, vol. 54, no. 3-4, pp. 1121–1127, 2011.

[19] Ch Kavitha, B. P. Rao, and A. Govardhan, "Image retrieval based on color and texture features of the image sub-blocks," *International Journal of Computer Application*, vol. 15, no. 7, pp. 33–37, 2011.

[20] P. P. Buch, V. Vaghasia, V. Madhuri, and S. M. Machchhar, "Comparative Analysis of Content Based Image Retrieval Using Both Color and Texture," in *Proceedings of the 2011 Nirma University International Conference on Engineering*, pp. 1–4, Ahmedabad, India, December 2011.

[21] J. Q. Ma, "Content-based image retrieval with HSV color space and texture features," in *Proceedings of the 2009 International Conference on Web Information Systems and Mining*, pp. 61–63, Shanghai, China, November 2009.

[22] C.-Y. Wang, X. Zhang, R. Shan, and X. Zhou, "Grading image retrieval based on DCT and DWT compressed domains using low-level features," *Journal of Communications*, vol. 10, no. 1, pp. 64–73, 2015.

[23] G. Chen, Z. Jiang, and M. M. Kamruzzaman, "Radar remote sensing image retrieval algorithm based on improved Sobel operator," *Journal of Visual Communication and Image Representation*, vol. 71, Article ID 102720, 2020.

[24] N. Shrivastava and V. Tyagi, "An efficient technique for retrieval of color images in large databases," *Computers & Electrical Engineering*, vol. 46, pp. 314–327, 2015.

[25] S. R. Dubey, S. K. Singh, and R. K. Singh, "Multichannel decoded local binary patterns for content-based image retrieval," *IEEE Transactions on Image Processing*, vol. 25, no. 9, pp. 4018–4032, 2016.

[26] Y. Mistry, D. T. Ingole, and M. D. Ingole, "Content based image retrieval using hybrid features and various distance metric," *Journal of Electrical Systems and Information Technology*, vol. 5, no. 3, pp. 874–888, 2018.

[27] A. Irtaza, S. Adnan, K. Ahmed et al., "An ensemble based evolutionary approach to the class imbalance problem with applications in CBIR," *Applied Sciences*, vol. 8, no. 4, p. 495, 2018.

[28] K. T. Ahmed, S. Ummesafi, and A. Iqbal, "Content based image retrieval using image features information fusion," *Information Fusion*, vol. 51, pp. 76–99, 2019.

[29] E. R. Vimina and M. O. Divya, "Maximal multi-channel local binary pattern with colour information for CBIR," *Multimedia Tools and Applications*, vol. 79, no. 35-36, pp. 25357–25377, 2020.

[30] M. Garg and G. Dhiman, "A novel content-based image retrieval approach for classification using GLCM features and texture fused LBP variants," *Neural Computing & Applications*, vol. 33, no. 4, pp. 1311–1328, 2021.

[31] N. Varish and P. Singh, "Image retrieval scheme using efficient fusion of color and shape moments," *Proceedings of International Conference on Big Data, Machine Learning and Applications: BigDML*, Springer, vol. 180, p. 193, Heidelberg, Germany, 2021.

[32] S. Kumar, J. Pradhan, and A. K. Pal, "Adaptive Tetrolet Based Color, Texture and Shape Feature Extraction for Content Based Image Retrieval Application," *Multimedia Tools and Applications*, vol. 80, no. 19, pp. 1–33, 2021.

[33] A. Joseph, E. S. Rex, S. Christopher, and J. Jose, "Content-based image retrieval using hybrid k-means moth flame optimization algorithm," *Arabian Journal of Geosciences*, vol. 14, no. 8, pp. 687–714, 2021.

[34] N. Varish and A. K. Pal, "A content based image retrieval using color and texture features," in *Proceedings of the International Conference on Advances in Information Communication Technology & Computing*, pp. 1–7, New York, NY, USA, August 2016.

[35] Y. Zhang, H. Wang, L. Yang, and J. Li, "Efficient histogram-based range query estimation for dirty data," *Frontiers of Computer Science*, vol. 12, no. 5, pp. 984–999, 2018.

[36] M. D. A. Asif, J. Wang, Y. Gao, and J. Zhou, "Composite description based on color vector quantization and visual primary features for CBIR tasks," *Multimedia Tools and Applications*, vol. 80, no. 24, pp. 33409–33427, 2021.

[37] N. Varish, A. K. Pal, R. Hassan et al., "Image retrieval scheme using quantized bins of color image components and adaptive tetrolet transform," *IEEE Access*, vol. 8, pp. 117639–117665, 2020.

[38] F. Malik and B. Baharudin, "Analysis of distance metrics in content-based image retrieval using statistical quantized histogram texture features in the DCT domain," *Journal of king saud university-computer and information sciences*, vol. 25, no. 2, pp. 207–218, 2013.

[39] N. Kayhan and S. Fekri-Ershad, "Content based image retrieval based on weighted fusion of texture and color features derived from modified local binary patterns and local neighborhood difference patterns," *Multimedia Tools and Applications*, vol. 80, no. 21-23, pp. 32763–32790, 2021.

[40] N. Varish and A. K. Pal, "A novel image retrieval scheme using gray level co-occurrence matrix descriptors of discrete cosine transform based residual image," *Applied Intelligence*, vol. 48, no. 9, pp. 2930–2953, 2018.

[41] M. K. Alsmadi, "Content-based image retrieval using color, shape and texture descriptors and features," *Arabian Journal for Science and Engineering*, vol. 45, no. 4, pp. 3317–3330, 2020.

[42] L. Zhu, X. Luo, C. Yang, Yi Zhang, and F. Liu, "Invariances of JPEG-quantized DCT coefficients and their application in robust image steganography," *Signal Processing*, vol. 183, Article ID 108015, 2021.

[43] Yi Yang and S. Newsam, "Bag-of-visual-words and spatial extensions for land-use classification," in *Proceedings of the 18th SIGSPATIAL International Conference on Advances in*

Geographic Information Systems, pp. 270–279, San Jose California, November 2010.

[44] J. Li and J. Ze Wang, "Automatic linguistic indexing of pictures by a statistical modeling approach," *IEEE Transactions on Pattern Analysis and Machine Intelligence*, vol. 25, no. 9, pp. 1075–1088, 2003.

[45] M. Rahimi and M. Ebrahimi Moghaddam, "A content-based image retrieval system based on Color Ton Distribution descriptors," *Signal, Image and Video Processing*, vol. 9, no. 3, pp. 691–704, 2015.

Hindawi
Computational Intelligence and Neuroscience
Volume 2022, Article ID 2896349, 10 pages
https://doi.org/10.1155/2022/2896349

Research Article

Main Features of Business English Translation and Teaching Model Optimization Based on the Logistic Model

Jingying Huang

Recruitment and Employment Department, Sichuan University of Arts and Science, Dazhou, Sichuan 635000, China

Correspondence should be addressed to Jingying Huang; 10001436@njtc.edu.cn

Received 13 August 2022; Accepted 21 September 2022; Published 11 October 2022

Academic Editor: Yaxiang Fan

Copyright © 2022 Jingying Huang. This is an open access article distributed under the Creative Commons Attribution License, which permits unrestricted use, distribution, and reproduction in any medium, provided the original work is properly cited.

With the continuous development of global trade in recent years, business English has received more and more attention as a medium of communication. Business English is a branch of English, and in order to meet the practical needs in business, business English is involved in various business disciplines from foreign trade to international logistics, to economics, foreign trade correspondence, law, and so on, which need to be translated in a more targeted manner. Therefore, there are many professional tutorials for business English in the market to guide trade personnel in business English translation. Many scholars have also conducted comprehensive studies on business English translation, some starting from its stylistic features and some focusing on translation skills, but fewer scholars have conducted studies on business English translation through models, and there is still a lack of theoretical basis for how to effectively improve the translation of business English. Therefore, in order to reduce the friction between different cultures in trade, promote business English better, and provide convenience for foreign traders, this study will implement the basic principles of "faithfulness, elegance" in English translation, with the aim of improving the practicality and effectiveness of business English, mainly from the main features of business English translation, and then, in the process of analysis, we mainly use the logistic model to analyze the characteristics of business English translation, including timeliness, professionalism, uniqueness, and diversity. The final analysis results show that the influence of professionalism and diversity on the effect of business English translation is more obvious, and we need to carry out a special teaching mode for these two points. The final analysis shows that professionalism and diversity have a significant impact on the effectiveness of business English translation, and special teaching models are needed to optimize these two points.

1. Introduction

The rapid development of business English is inseparable from the globalization of economy and trade. By the end of 2021, there are 73 countries in the world with nearly one billion people using English as their official language, and the importance of English is reflected by the number of countries, nearly 30% of which use English as their primary language. [1] Business English, on the other hand, is a business communication that aimed at adapting to the needs of the market, and it is a business that is specific to business services, forming business English which can penetrate into all aspects of business activities. With the development of the global trade industry, the role of English in the international arena is becoming more and more evident, and many industries are eager for business English translation professionals; so, more and more people are entering the industry. For these talents, business English is a necessary skill, which requires them not only to master professional English translation knowledge but also to understand the relevant processes of the foreign trade industry, understand the differences between different cultures, and understand how to deal with foreigners and talk business. Only in this way can the value of business English be put to good use and promote the continuous development of trade, which has also given rise to a series of teaching activities for business English, dedicated to better promote the development of business English. Based on this, in the modern society with continuous economic transformation and development, we should pay more attention to the relevant features and teaching modes of business English translation [2]. Among them, the number of English speakers and the number of

international business English applicants are shown in Figure 1.

Translation of business English has certain characteristics. Unlike ordinary English, business English has its unique features in style, grammar, and syntax, which need more attention when translating. Some literature suggests that professional foundation is especially important for business English translation; some literature suggest that learning to be flexible and adaptable can accurately translate business English [3]. As can be seen, the findings of domestic and foreign scholars on this research topic are controversial. There are various characteristics of business English translation that have their own bases and have a certain influence on the accuracy and speed of translation, and the attention to any point in the translation process may affect the final result of translation [4]. Some scholars have found that business English is more specialized and some of the vocabulary come from the actual needs in the process of foreign trade. Moreover, the sentence style of business English is mainly for the purpose of understanding and requires more direct communication of information, so the sentence style is compact, logical, and has strong practicality. Gao Limin, a Chinese scholar, believes that linguistic features are very significant in the use of business English, which is more characteristic than the style of everyday English [5], and business English has its distinctive features in the expression of idioms and the transformation of specialized vocabulary [6]. However, there are few studies on the causal relationship between the effect of business English translation and its translation characteristics, among which there is a complex causal relationship between the effect of business English translation and the final translation results due to the large differences in the critique of the effect of business English translation and the lack of obvious embodiment of the characteristics, which makes it very difficult to identify the influence between the two [7]. An overview of the existing literature mostly explores the main features of business English translations from the aspects of comparison and examples, but there is less research on the inference of the degree of influence of these features, such as the study of the degree of influence of professionalism on the accuracy of business English translation results. It may be due to the fact that the most difficult problem to identify the influence of their features on conducting business English translation is the problem of model construction [8]. Therefore, the logistic model can be used as a tool to identify the effect of business English translation. The main differences between business English and ordinary English are shown in Figure 2.

This study uses SPSS 23.0 software to construct a logistic model for analysis. The contribution of this study is as follows: first, using the instrumental variable approach to solve the model construction problem, which makes the research results robust and error-free; second, analyzing the influence of business English translation features on its translation results is helpful to understand the influence of different features on translation effects [9]; third, to analyze the mechanism causes that affect the effectiveness of business English translation; fourth, it provides a reference for China to encourage and support the development of business English, improve the teaching level of related courses, and promote the continuous development of China's foreign trade in the context of economic globalization.

2. Research Background

There are many features of business English, and there is little literature to explore the research on the causal inference between the translation features of business English and the final translation results [10].

The literature review mainly revolves around the following parts: first, regarding the research on the translation characteristics of business English, foreign literature mostly adopts the methods of comparison and example to explore and analyze business English and everyday English. There are four main research results, which argue that the translation of business English has the characteristics of professionalism, timeliness, uniqueness, and diversity. Regarding the definition of professionalism, scholars generally believe that business English belongs to a branch of English, which has many fields, and some of them have special requirements and need to be translated according to the agreed rules in the industry in order to be better understood, such as shipping date, double check, B2B (Business to Business), C2B (Business to Business), and CBS (Business to Business). In addition, scholars also find that the translation of business English is very time-sensitive; because the international economic situation is changing rapidly, the translation of business English cannot be like the translation of ordinary foreign languages that have more ample time for revision and will lose its value in just a few days. Even some emergency messages can become useless in a few hours [11]. While information is changing rapidly, new technologies and products are emerging like a spring, and some relatively new products may not have professional terms to give their meanings, which requires business English to translate them as aptly as possible in the process of translation, showing the uniqueness of business English at the forefront of economic trade and providing reference for subsequent translators. The last is that in business English, a branch of English, many tenses and grammars are executed according to the English standard but need to be combined with the latest laws and regulations and proper nouns, so that business English will be flexible in the process of translation according to the actual situation to better meet the understanding needs of readers and fully reflect its diversity [12]. The main features of business English translation as currently considered by the mainstream are shown in Figure 3.

Second, the research on business English teaching strategies is considered. According to the research of foreign scholars, business English has its special linguistic characteristics, and in the process of trade, different translation needs will arise due to different cultures, which requires targeted teaching and counseling in the process of teaching these characteristics. Therefore, first of all, teachers need to have solid business English translation skills, be able to translate according to certain translation rules, and to summarize these translation strategies. In contrast, Wei Hua, a domestic scholar, discussed the feasibility of targeted

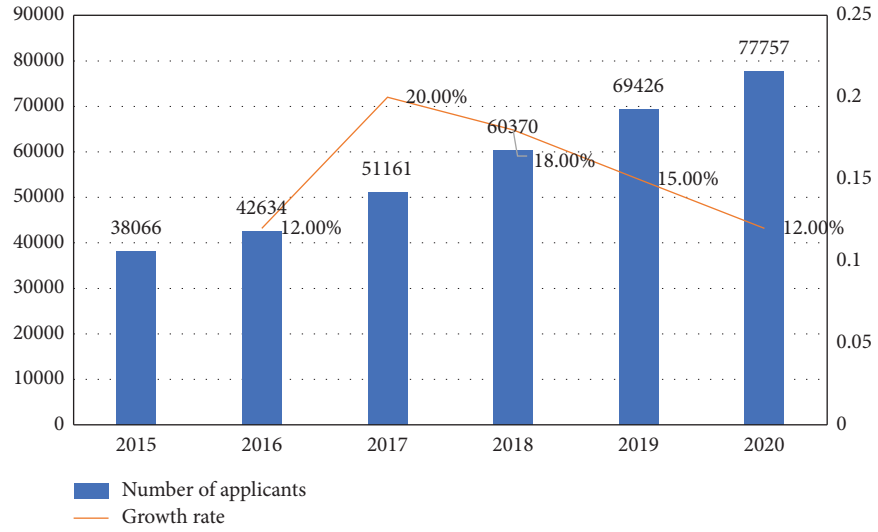

Figure 1: Number of international business English exams and growth rate in China from 2015 to 2020.

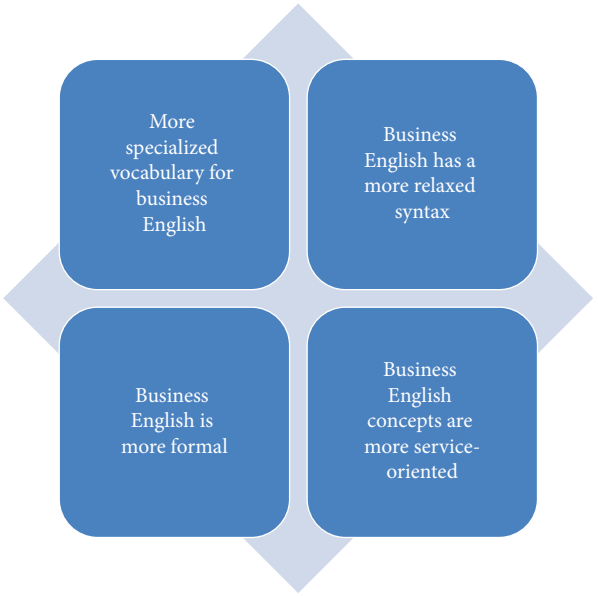

Figure 2: Differences between business English and general English.

teaching in terms of theoretical foundation and practical application of business English from the background of education informatization and verified the effectiveness of the new teaching model in three following aspects: improving students' business English foundation, improving teachers' business English teaching ability, and updating the teaching mode.

Third, scholars' different choices in the selection and use of research methods and research theories of the two can cause certain bias in the research results. In the process of analyzing the characteristics, scholars mostly use simple research methods such as illustration and comparison highlighting; this descriptive analysis is easy, but the analysis perspective is single and limited, and it may not be possible to present the correct and unmistakable result analysis in the complex cause-effect relationship. One of the most important problems faced by choosing a model for inferential analysis is that the model itself has the problem of endogeneity, and if it is not solved, then the inferred results will also be biased [13]. Some other scholars have inferred the relationship between the two through qualitative studies, and this approach has some limitations. In terms of research on the teaching model, most scholars use the 4ES criteria and believe that when translating business English, the effectiveness of translation will be considered in terms of its characteristics, for example, in order to better achieve accurate business English translation, i.e., to accurately complete the communication and delivery of information between different traders, teachers are required to pay attention to the professional basis of explanation [14]. By comparing the characteristics of professionalism, abbreviation, and rhetoric in business English vocabulary, foreign scholars require the popularization of these characteristics in teaching in order to improve the final translation skills [15].

To sum up, the analysis of the features and strategies of business English translation in China still remains in the comparative analysis of theories and examples, and the method of causal inference between various features has not been fully applied to this field. Therefore, this study will make up for the deficiencies of the previous studies by analyzing and studying the features and mechanisms of business English translation, which will help explore the influence of various features on the effect of business English translation and actively improve business English. It will help to explore the influence of various features on the effectiveness of business English translation and actively improve the relevance of business English teaching.

3. Materials and Methods

3.1. Basic Theory

3.1.1. The Logistic Regression Model. The logistic regression model generally belongs to the dichotomous dependent variable model, that is, the dependent variable (generally y)

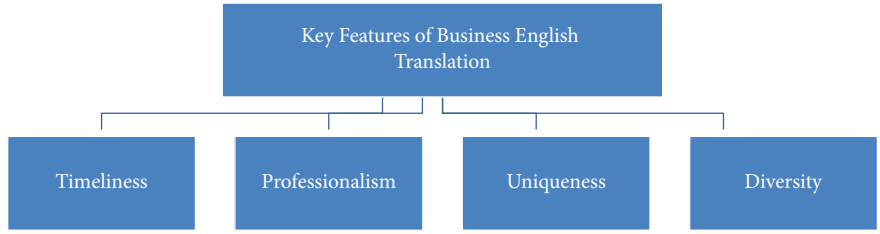

Figure 3: Main characteristics of business English translation.

in the model will be divided into two complementary results for analysis, such as whether it travels and whether the results are reasonable, which is more common in academic research. Its uniqueness lies mainly in its method of parameter treatment; generally, we use linear regression in linear equations, while logistic uses the maximum likelihood estimation method [16]. In the process of data analysis, the maximum likelihood values will have the characteristics of consistency, asymptotics, and asymptotic normality [17]. The business English translation effect of the respondents of this study is expressed by Y under the action of independent variables of several groups of characteristics, and its assignment rule is as follows: 1 = good translation effect and 0 = bad translation effect. Let the probability of the good translation effect be P and the probability of the bad translation effect be Q. $x1$, $x2$, $x3$, and $x4$ denote the four factors that affect the result Y. The evaluation criteria of the four factors are indicated by 1 for satisfied and 0 for unsatisfied, as shown in Figure 4.

3.1.2. The Main Evaluation Method. In this study, we established a logistic regression equation to analyze the translation of business English in real life. However, we cannot analyze and predict the equation directly. In order to more accurately reflect the relationship between the independent and dependent variables, statistical methods are also needed to conduct tests, which are commonly used, namely, the value of the statistic of the regression coefficient test and the standard deviation of the estimated quantity, generally expressed by Wald and S.E. In addition, the Wald test will take into account its probability of significance (Sig), which will be compared by exp (β) [18].

$$S.E. = \sqrt{\text{var}(\beta)}, \tag{1}$$

$$\text{Wald} = \frac{\beta^2}{\text{var}(\beta)}. \tag{2}$$

Generally, we will use 1% or 5% as the test threshold for the significance level, on the basis of which the corresponding value is tested, and less than or equal to the result is considered significant. And some models will use a more precise Sig value to determine the significance. Assuming the premise that the regression coefficient is equal to 0, followed by the calculation of the Sig value, the implication is that the probability that the coefficient estimated by the model will not be smaller than the known coefficient [19]. After calculating the results, even if the original hypothesis has been established, it is still necessary to test whether the Sig value is as expected, and generally, the smaller the Sig value, the less likely the hypothesis will be valid and vice versa, which means that the original hypothesis is valid. Generally, we use SPSS, Excel, and other calculation software to obtain the Sig value [20]. In (1), the size of S.E. reflects the degree of fluctuation of the estimator in the process of taking values, and when the smaller the S.E. is, i.e., the larger the Wald, the higher the importance of the independent variable in the regression equation.

In addition to this, in the regression equation, a one-sample t-test is also conducted to analyze whether there is a significant difference between the mean value of a variable and the specified test value; generally, the null hypothesis for a one-sample t-test is expressed as H0; there is no difference between the mean value and the specified test value. After that, the significance level is compared with the Sig value, which is less than or equal to reject H0, and the opposite is accepted.

Finally, after standardized analysis of the equation, all the relationships between the independent and dependent variables are measured in the same units; although their units may be different in the process of actual measurement, they are also more comparable after substitution into the equation.

3.2. Model Setting and Variable Selection. In order to solve the endogeneity problem in the above study and to perform unbiased estimation, the instrumental variables are chosen to solve the endogeneity problem. Because of the unique advantages of the instrumental variables approach used in this study, compared to the limitations of other research methods, the data in this study have exceptionally good statistical significance.

3.2.1. Model Setting. A model of business English translation effectiveness is first established with the following equations:

$$P = \frac{\left(e^{\beta_0+\beta_1X_1+\beta_2X_2+\beta_3X_3+\beta_4X_4}\right)}{1+e^{\beta_0+\beta_1X_1+\beta_2X_2+\beta_3X_3+\beta_4X_4}}, \tag{3}$$

where P denotes the probability of a good business English translation result. X_i is a series of variables, such as timeliness, professionalism, uniqueness, and diversity. Since $P + Q = 1$, the equation for the probability of a bad business

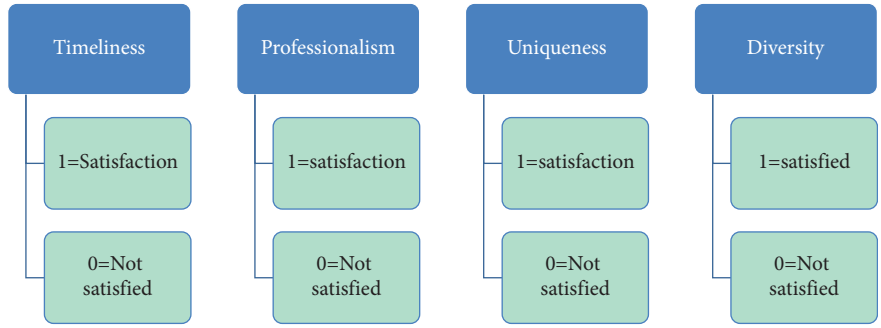

Figure 4: Evaluation criteria of business English translation features.

English translation result can be obtained according to the following equation:

$$Q = \frac{1}{1 + e^{\beta_0+\beta_1 X_1+\beta_2 X_2+\beta_3 X_3+\beta_4 X_4}}. \quad (4)$$

From (4), it can be seen that there is a curvilinear relationship between the effect of business English translation and the variables of interest, and the ratio between the two formulas P and Q is defined as the occurrence ratio odds.

$$\text{Odds} = \frac{P}{Q} e^{\beta_0+\beta_1 X_1+\beta_2 X_2+\beta_3 X_3+\beta_4 X_4} e^{\beta_0} e^{\beta_1 X_1} e^{\beta_2 X_2} e^{\beta_3 X_3} \bullet e^{\beta_4 X_4}. \quad (5)$$

Taking the natural logarithm, there are

$$\text{Ln} = \frac{P}{Q}\beta_0 + \beta_1 X_1 + \beta_2 X_2 + \beta_3 X_3 + \beta_4 X_4. \quad (6)$$

In this equation, β_0, β_1, β_2, β_3, and β_4 are the relevant regression coefficients, where (4) is a nonlinear equation, which is commonly solved by the Newton–Raphson method.

3.2.2. Data Sources. The data used in this study are all survey data, collected through the online release of questionnaires and used for analysis after collation. In the course of the survey, 285 valid questionnaires were obtained.

The number of business English users accounted for 51.25% of the total sample; among the respondents' education, 82.58% of the total sample was bachelor's degree or above, and 75.82% of the total sample aged between 22 and 25. Through the above statistical analysis of the sample, it is clear that most of the respondents are young people in their 20s, with higher education level, and they have a better understanding of the questionnaire content; so, the data of this research activity have high reliability and representativeness. Using SPSS 23.0 software for reliability analysis, the survey used the Cronbach coefficient, which was calculated as 0.815, the best reliability coefficient, indicating that the questionnaire was designed reasonably. In addition, the sample adequacy was assessed by the KMO coefficient, and the calculated result was 0.889, which is a high level, indicating that the number of samples in this survey meets the requirements and the adequacy is good. Finally, the distribution of the data was also analyzed, and the Bartlett value was chosen to measure it, with a value of 1527.942. After performing the calculation, the test value obtained was 0.01, which is less than the hypothesis of 0.05, indicating that the distribution of the survey data obtained is more reasonable.

3.2.3. Definition of Variables and Descriptive Statistics. Dependent variables: timeliness of business English translation, professionalism of business English translation, uniqueness of business English translation, and diversity of business English translation are the dependent variables. This study focuses on the effects of these four characteristics on the effectiveness of business English translation. This study uses a variety of combined data to measure this indicator of the effectiveness of business English translation. The answers to the questions in the original questionnaire are divided into four categories, and this paper reestablishes a dichotomous variable as the dependent variable through the above questions and answers. Any translation result that gets a rating greater than or equal to 75 is recorded as 1, regardless of the specific value; any rating less than 75 is always recorded as 0, indicating a bad translation effect.

Independent variable: the translation effect of business English is the independent variable. In this study, the translation effect of business English is reassigned as a dichotomous variable, and the selected item is assigned a value of 0 for the good translation effect, while the rest of the variables are set as the bad translation effect and assigned a value of 1.

Control variables: English usage, English grammar, and users' English level are the control variables. There are many factors affecting the effect of features on the business English translation effect, which must be controlled in the model as much as possible, and the control variables in this study include three categories.

This work studies the effect of business English translation features on translation results, so the questions used are sample sizes selected from business English exams. Most of the question topics are from the International Business English Qualifying Examination, and a small number of topics are from other teaching and learning materials.

English usage variables including business English, test-taking English, and everyday speaking are not normally distributed.

English grammar variables including whether there are grammatical errors, correct tenses, and spelling errors are generally assigned as dichotomous variables.

User's English level variables including respondents' English level and frequency of exposure to English are generally classified as unfamiliar, beginner's level, mastery level, and proficient level-by-level, and here, the default respondents are all at mastery level to better analyze the influence of translation characteristics on their results. The distribution of respondents' English levels is shown in Figure 5.

4. Results and Discussion

4.1. Analysis of Descriptive Statistical Results. In this survey on the translation characteristics of business English, it involves timeliness, professionalism, uniqueness, and diversity. For better statistical analysis, the questions released will be classified according to these four characteristics, and after the respondents answer the questionnaire, they will then be divided into two following kinds in total: the questionnaire with a good translation effect and the questionnaire with a bad translation effect. These four characteristics are divided into three levels: 0 = no significant characteristics, 1 = average characteristics, and 2 = significant characteristics. First, the statistical results of the questionnaire with a good translation effect are analyzed, as shown in Figure 6.

Next is the analysis of the statistical results of the questionnaire with the poor translation effect, as shown in Figure 7.

This time, the total characteristics of all questionnaires were statistically analyzed, as shown in Figure 8.

In the description of the model variables in this study, first, the explanatory variable is the categorical variable of good and bad business English translation effects, which represents "whether the translation score meets the requirements in the completed business English test," 0 = bad translation effect, and 1 = good translation effect. The next is the explanatory variable, and the four features selected in this study are all categorical variables: (1) timeliness, 0 = features not significant, 1 = features average, 2 = features significant; (2) professionalism, 0 = features not significant, 1 = features average, 2 = features significant; (3) uniqueness, 0 = features not significant, 1 = features average, 2 = features significant; (4) diversity, 0 = features not significant, 1 = features average, 2 = significant.

4.2. The Variable Correlation Test. Among the many methods for identifying causality, SPSS has a more obvious advantage for the comparison between variables. So, in this study, SPSS software is selected for calculation to solve the correlation problem of the model, and the correlation results are given in Table 1.

Among the four translation characteristics of business English, there is a positive correlation between timeliness and the explanatory variables, which indicates that more timeliness for business English will get a better translation effect, which is more in line with the actual needs in trade. Similarly, there is a positive relationship between professionalism, diversity, and the explanatory variables, indicating that the significance of these two characteristics plays a positive role in how well business English is translated. On the other hand, uniqueness is negatively correlated with the explanatory variables, indicating that this feature does not have a positive effect on the translation effectiveness of business English. This is consistent with what was expected at the beginning. In addition, there are positive and negative relationships between different variables, which are consistent with the basic rules of the model, for example, the negative relationship between uniqueness and diversity and the positive relationship between uniqueness and professionalism, which is basically in line with common sense. From the overall data of the table, the absolute values of the correlation coefficients between all variables are less than 0.5, and there is no excessive situation, which is within a reasonable range. It shows that the correlation between these four characteristics is weak, and the variables are more independent from each other, which meets the requirements of the setting of compound variables, and the preliminary judgment is that there is no colinearity between the variables, and the next step of analysis can be conducted.

4.3. Estimation Results of the Logistic Model. The statistical results in this study have good statistical significance, including $^{***}P < 0.01$, $^{**}P < 0.05$, and $^{*}P < 0.1$. Considering the complexity of the operation, the data with 95% confidence interval is selected as the result in this study. According to the above model and related data, after the iterative operation, the final distribution parameters of the logistic probability model are $\beta_0 = 0.062$, $\beta_1 = 0.067$, $\beta_2 = 1.824$, $\beta_3 = 0.526$, and $\beta 4 = 1.241$, so the final derived business English logistic probability distribution function of the effect of translation features on the translation effect is as follows:

$$P = \frac{\left(e^{0.062+0.067X_1+1.824X_2+0.526X_3+1.241X_4}\right)}{1+e^{0.062+0.067X_1+1.824X_2+0.526X_3+1.241X_4}}, \tag{7}$$

where Sig $f = 0.001$, which is less than 0.005, indicating that it passes the validity test within the 95% confidence interval and the statistical results are reliable.

4.4. Analysis of the Mechanism by Which the Main Features of Business English Affect Its Translation Results. This study analyzes four characteristics of business English translation and the first of all is the timeliness of business English. The regression coefficient of the translation effect affected by the timeliness of business English is 0.067 ($t = 2.24$, $P = 0.005 < 0.01$), which is significant at the 5% level, indicating that timeliness has a significant positive effect on the translation effect of business English. It can be said that the stronger the timeliness of English, the better its translation effect and the easier it is to accurately use English to convey information among people of different cultures, especially in the more pragmatic import and export trade, where the

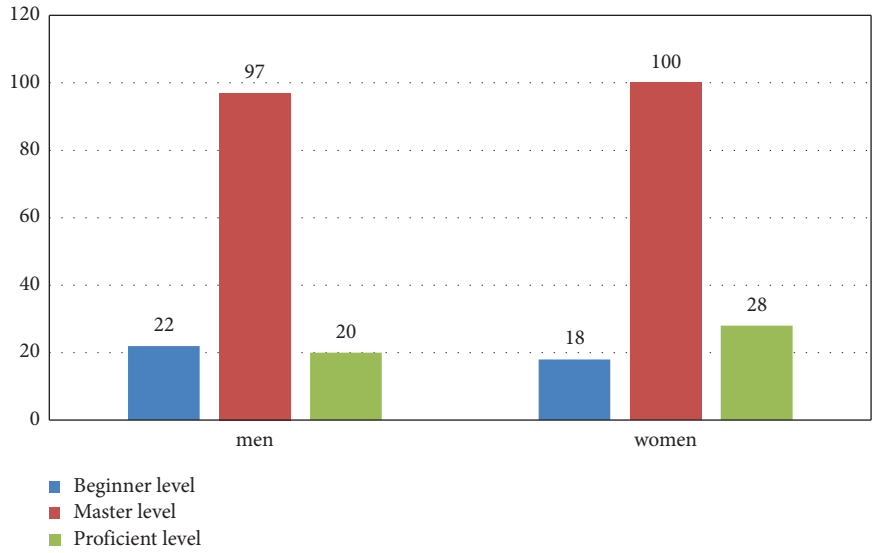

Figure 5: Distribution of the respondents' English proficiency level.

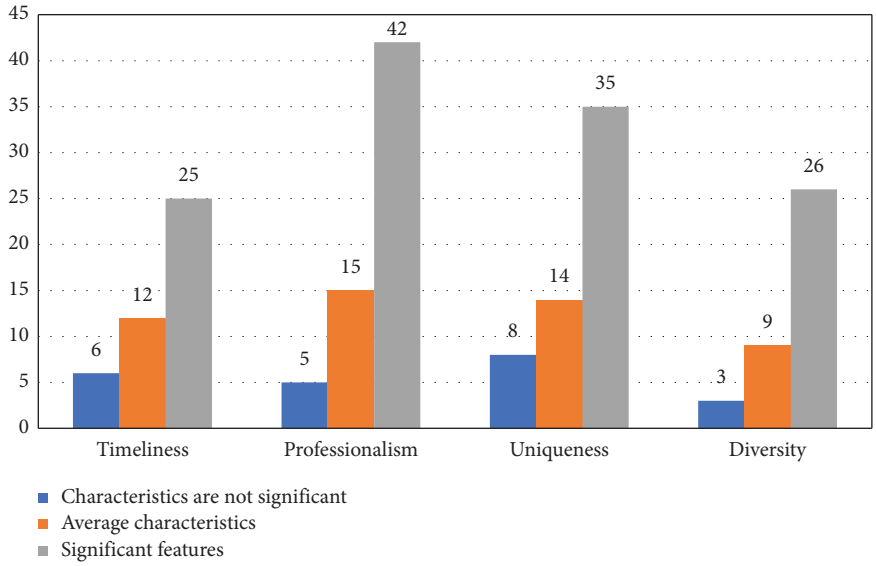

Figure 6: Descriptive statistical analysis of variables with the good translation effect.

timeliness of business English is regarded as very important, and the communication by phone, fax, or e-mail in a short period of time can greatly affect the final translation effect because of the timeliness, which is consistent with the previous expectation.

The second is the professionalism of business English; generally, some fixed words or phrases are used in business English, which are required to be standardized and specialized in certain processes, and are bound by some official documents or rules. In the logistic model of this study, the final estimation result shows that the regression coefficient of professionalism in business English is 1.824 ($t = 1.526$, $P = 0.000 < 0.01$), which is significant at the 5% level, indicating that professionalism has a positive impact on the final translation of business English. In the process of translation, we can better translate the meaning of both parties, use short words or sentences that are easy to understand but professional, and improve the translation effect.

Next is the uniqueness of business English; some common English words will be given special meanings in business English, which can be applied in the original context and adapted to the new business English environment, reflecting a good translation effect. Of course, this is based on the premise that the business English level of the users is still good, which is more conducive to the translation effect of business English. In the logistic equation of this study, the coefficient of business English uniqueness is 0.526 ($t = 4.126$, $P = 0.01 = 0.01$), which seems to have a positive effect on the translation of business English, but the P value

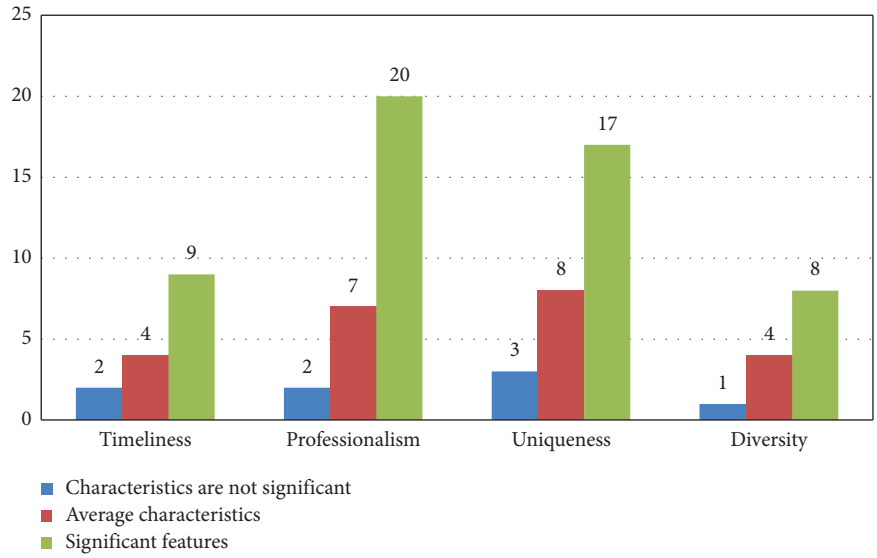

Figure 7: Descriptive statistical analysis of variables with the poor translation effect.

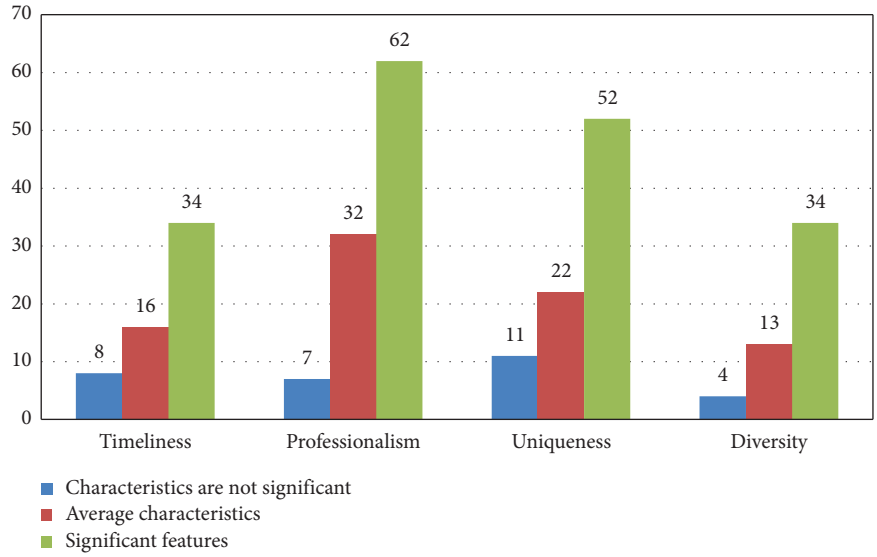

Figure 8: Descriptive statistical analysis of the common variables of good and bad translation results.

Table 1: Correlation test results.

	y	$X1$	$X2$	$X3$	$X4$
y	1				
$X1$	0.023	1			
$X2$	0.032	−0.021	1		
$X3$	−0.014	0.015	0.024	1	
$X4$	0.018	0.036	0.025	−0.021	1

of its test is 0.01, which means that this result is not very significant and does not fully pass the 5% significance test. Combined with the previous respondents' English proficiency, the preliminary analysis is due to the different business English proficiency of the respondents and more deviations in the understanding of particular words.

Finally, the coefficient $X3$ of diversity of business English is 1.241 ($t = 3.51$, $P = 0.001 < 0.01$) from the results of regression analysis, which is significant at the 5% level, indicating that the diversity of business English has a significant positive effect on its translation effect, and the more diverse the meanings of words, the more important they are in the process of translation and the more prominent they are for the overall translation effect. The more diverse the meanings of the words, the more important they are in the translation process and the more prominent they are for the overall translation effect. This indicates that significant diversity in business English can significantly improve the translation effect of business English.

On the whole, the timeliness, professionalism, and diversity of business English have a significant impact on its

translation effect. Especially, professionalism and diversity have a greater impact on achieving good translation effects.

5. Conclusion

This work mainly studies and analyzes the translation characteristics and translation effects of business English, so as to obtain relevant suggestions for the optimization of the teaching mode and solves the correlation problem among variables by SPSS software calculation, so as to achieve the maximum likelihood estimation. The results of the estimation show that, first, the timeliness, professionalism, and diversity of business English translation have an impact on the translation effectiveness of business English. Second, further studies on the influence mechanism show that the professionalism and diversity of business English have more significant effects on the translation effectiveness of business English.

Business English is a professional English and a cross-disciplinary discipline, and its translation is different from traditional British or American English, which only requires learning the corresponding grammar knowledge and mastering a certain amount of vocabulary to complete the translation and achieve better results. In business English, however, due to its timeliness, professionalism, uniqueness, diversity, or other characteristics, translators are significantly affected by these characteristics in the process of translation and need to pay attention to the multiple meanings of words and the timeliness of translation through their accumulated professional knowledge in order to achieve better translation results. In this context, many experts and scholars study about the mode of teaching business English and analyze how to better optimize the existing business English teaching. In summary, based on the results of previous model analysis and mechanism research, this study comes up with the following suggestions for optimizing the business English teaching model.

(a) Choose accurate word meanings: In business English, the same word is likely to have multiple meanings, a phenomenon often encountered in the learning process of general English and even more so in business English, where many words have multiple meanings and are applicable to different contexts. Generally, such words with multiple meanings, such as literal, derived, extended, connotative, and extended meanings, need extra attention in the translation process. Therefore, teachers need to clarify this point when instructing business English translators, remind students of the concept of multiple meanings of words, and strengthen their awareness in this area through repeated practice of typical topics. For example, the most common literal meaning of the word "accident" is "accident," but there are also other meanings such as "traffic accident, accidental event, unpredictable event." Take out accident insurance before you go on your trip. The word "accident" is more in line with the context because there is an "insurance" with it, but if translated as other meanings, it is not very reasonable here. Another example is that talking to others can often help to put your own problems into perspective. In this sentence, the common meaning of "perspective" is "attitude, point of view," which is used as a noun. But considering the overall context, it would be more realistic to translate it as "objective judgment," so that the meaning of this sentence can be more accurately translated and conveyed. The overall point is that business English contains a large number of words that are used in multiple ways, far more complex than ordinary English, reflecting its multidisciplinary character. Instructors are required to pay attention to the distinction when tutoring business English and teach students to choose the exact meaning of words.

(b) Adopting the repetition method of translation: Business English is mostly used by workers in the foreign trade industry, and as China is a major trading country, the number of people using business English is naturally very large. Therefore, educators need to pay extra attention to the instruction of the skills related to business English when translating between Chinese and English. The first thing is to understand the differences between Chinese and English. Chinese often has repetitive words, reflecting the rhythm of Chinese, while English is relatively more concise and clear, focusing on the transmission of the meaning. Therefore, students can be instructed to use the repetition method when translating business English, that is, certain words are repeatedly reflected in the sentence, so as to conform to the expression effect of emphasizing a certain meaning or action in Chinese. For example, during COVID-19, import drivers were required to issue nucleic acid certificates, green travel codes, and freight information. This sentence repeats the translation of the verb "requires," reflecting the strict control of import and export truck drivers during the New Crown epidemic.

(c) Adopt the translation of positive and negative words: Chinese and English expression habits are different, and there are differences between Chinese and English expressions when expressing negative concepts. For example, if "are not agreed" is translated literally as "are not agreed," it is very awkward to read and does not conform to Chinese expression habits. The translator may choose to treat it as an affirmative translation "is against." This kind of translation treatment is called the antithetical translation method, also known as the positive-speaking and negative-speaking translation method. The translation between prospeech and antispeech is a kind of statement conversion. Its basic mechanism of action is the difference of bilingualism in the perspective, emphasis, point of view, and feature selection or copying method in concept naming, topic formulation, mood expression, and emphasis distribution.

For example, the English phrase "self-service bookstand" is in the positive form, which focuses on the subjective behavior process, while the Chinese phrase "no one sells books at the bookstore" is in the negative form, which focuses on the description of the objective status quo. The use of antithetical translation is more common in the translation of business English texts. For example, the government should not hesitate to intervene in the currency market through bold yen-selling and dollar-buying operations. The direct translation of "should not hesitate" as "should promptly" belongs to the opposite translation, which is in line with the Chinese expression habits.

The abovementioned three translation strategies are chosen for the sole purpose of pursuing the equivalence of the meaning of the source language and the target language, which coincides with the viewpoint of the language equivalence translation strategy. The language equivalence translation strategy emphasizes the reciprocity of meaning in the context, with a view to helping the continuous development of China's foreign trade.

Data Availability

The dataset is available upon request.

Conflicts of Interest

The author declares that there are no conflicts of interest.

References

[1] Y. Ren, "Thinking on English translation teaching mode in colleges and universities under network environment," *International Journal of Education and Teaching Research*, vol. 3, no. 4, 2022.

[2] J. Chen, "An exploration of college English translation teaching based on situational cognition theory," *International Journal of Higher Education Teaching Theory*, vol. 3, no. 4, 2022.

[3] J. Teng, T. Yuan, and Yu Qian, "Research on innovation and development of online teaching model of Japanese translation in special period," *International Journal of Higher Education Teaching Theory*, vol. 3, no. 4, 2022.

[4] Y. Liang, J. Guo, and H. Yu, "Research on the reform strategy of college English translation teaching based on POA theory," *International Journal of Educational Management*, vol. 7, no. 3, 2022.

[5] S. Chen, "The current situation and reflections on the teaching mode of translation course for business English majors in general universities," *Education Journal*, vol. 5, no. 3, 2022.

[6] S. Zhang, H. Fan, and Y. Ma, "Strategic innovation of college English translation teaching model for the new-era liberal arts education," *Education Journal*, vol. 5, no. 2, p. 114, 2022.

[7] Li Yang, "Exploring the effectiveness of translation teaching in college English from the perspective of chunks," *Journal of International Education and Development*, vol. 6, no. 4, 2022.

[8] R. Shakina, "Our country has gained independence, but we haven't": collaborative translanguaging to decolonize English language teaching," *Annual Review of Applied Linguistics*, vol. 42, no. 13, 2022.

[9] G. Wang, "Formative assessment system of VR teaching in English translation class," *OALib*, vol. 09, no. 2, pp. 1–7, 2022.

[10] Y. Li, "On teaching English translations in colleges and universities," *Advances in Educational Technology and Psychology*, vol. 6, no. 2, 2022.

[11] Ł. Grabowski, "Provoke or encourage improvements? On semantic prosody in English-to-Polish translation," *Perspectives*, vol. 30, no. 1, pp. 120–136, 2022.

[12] W. Su, "How to use modern teaching methods to improve English Chinese translation ability," *OALib*, vol. 8, no. 12, pp. 1–6, 2021.

[13] Y. Guo, "The introduction of reverse thinking in college English translation rducation," *Advances in Educational Technology and Psychology*, vol. 5, no. 12, 2021.

[14] S. Liu, "Analysis of business English translation teaching from the perspective of the belt and road initiative," *Research on Literary and Art Development*, vol. 2, no. 5, 2021.

[15] J. Wu and Ya Zeng, "Application of functionalist translation theory in the teaching of business English translation," *International Journal of Educational Management*, vol. 6, no. 3, 2021.

[16] X. Guo, "A probe into the cultivation of undergraduates' cross-cultural communication awareness in the business English translation teaching at colleges," *International Journal of Education and Economics*, vol. 3, no. 4, 2020.

[17] L. I. Jing, "The application of CAT tools in business English translation teaching," *JOURNAL OF INTERNATIONAL EDUCATION AND DEVELOPMENT*, vol. 3, no. 1, 2019.

[18] Z. Li, "The construction of the turning classroom of business English translation teaching in higher vocational education under the internet + environment," *Frontiers in Educational Research*, vol. 2, no. 5, 2019.

[19] J. Ying, "Critical thinking oriented teaching reform of business English translation," *Studies in Literature and Language*, vol. 19, no. 1, 2019.

[20] P. Zhou, "Comparative study of traditional teaching method and ISAS teaching method in business English translation teaching in colleges and universities," *Frontiers in Educational Research*, vol. 2, no. 3, 2019.

Hindawi
Computational Intelligence and Neuroscience
Volume 2022, Article ID 8924938, 11 pages
https://doi.org/10.1155/2022/8924938

Research Article

Logistics Path Decision Optimization Method of Fresh Product Export Cold Chain Considering Transportation Risk

Lifu Chen and Zhifeng Shen

Department of International Economy and Trade, Jiangsu University of Technology, Changzhou 213001, China

Correspondence should be addressed to Lifu Chen; chenlifu@jsut.edu.cn

Received 17 August 2022; Accepted 22 September 2022; Published 7 October 2022

Academic Editor: Yaxiang Fan

Copyright © 2022 Lifu Chen and Zhifeng Shen. This is an open access article distributed under the Creative Commons Attribution License, which permits unrestricted use, distribution, and reproduction in any medium, provided the original work is properly cited.

The cold chain logistics route of fresh product export is characterized by large quantity and complexity, which is prone to cause transportation risks of different degrees in the process of fresh product export transportation and affects the decision-making effect of the cold chain logistics route. Therefore, in order to improve the ability of cold chain logistics route planning and shorten the transportation time, an optimization method of fresh product export cold chain logistics route decision considering transportation risk was proposed. This paper analyzes the basic characteristics and classification of cold chain logistics by means of risk quantification and uses the K-nearest neighbor algorithm to predict the risk of traffic congestion, so as to shorten the transportation time. Ahp process is used to construct a risk factor judgment matrix and determine the index weight of risk factors, so as to reduce the error of path planning. A genetic algorithm is introduced to construct the optimal decision function of the cold chain logistics route of new product export and realize the optimization of cold chain logistics route decision of fresh product export. Experimental results show that the method presented in this paper can effectively improve the decision-making effect of cold chain logistics route and select the shortest and most smooth transportation path to complete logistics distribution. The decision-making accuracy of the route decision effect is 90%, and the transportation time is 31.45 min, which has certain feasibility and applicability.

1. Introduction

Cold chain logistics refers to a systematic engineering of refrigerated and frozen food in the production, storage, transportation, sales, and consumption before all the links are always in the specified low-temperature environment, in order to ensure food quality and reduce food loss. Cold chain logistics has higher requirements, and the corresponding investment in management and capital is also larger than ordinary normal temperature logistics. Therefore, in the process of cold chain logistics transportation of fresh product export, costs must be reduced to ensure actual profits [1]. Domestic transport routes are complex, and transport vehicles often fail to choose the shortest route, which reduces distribution efficiency and improves transport costs [2]. With the rapid development of the economy and the improvement of scientific and technological level, people's demand for food has also changed, among which the demand for cold-chain food has been increasing [3]. However, due to low transportation efficiency, backward facilities, backward technology, and other factors, it takes a long time to transport cold-chain food, resulting in food decay and increasing logistics and transportation costs [4]. As export transportation is affected by many factors, the quality of products in export transportation is affected and more economic costs are wasted [5]. Therefore, it is necessary to carry out a lot of planning and research on the cold chain logistics route of fresh product export. Literature [6] proposed a vehicle route optimization method for multivehicle cold chain logistics of fresh agricultural products. By constructing a multivehicle routing optimization model, the adaptive degree of congestion index is considered on the basis of reducing the overall delivery cost and improving customer satisfaction. The genetic simulated annealing

algorithm is used to calculate the total distribution cost of the cold chain logistics path time window to complete the cold chain logistics path planning. The optimization path of this method has some errors and needs to be improved continuously. Literature [7] proposed a method for vehicle routing optimization of cold chain logistics based on the green evaluation. The vehicle path optimization model of cold chain logistics is constructed for the optimization evaluation of total distribution cost. The vehicle evaluation results are considered through the comprehensive method of vehicle evaluation value, so as to obtain the corresponding vehicle path optimization results of cold chain logistics. This method has certain precision, but it ignores the risk interference in transportation and has certain limitations. Literature [8] proposed an optimization method for multitemperature and low-temperature cold chain logistics vehicle distribution route. Considering the interference factors at each stage, the distribution time, distribution cost, and distribution risk of multitemperature cold chain logistics were controlled to optimize the vehicle distribution path of multitemperature cold chain logistics, and the path optimization was realized by the ant colony algorithm. This method can effectively plan the path, but because the ant colony algorithm needs to obtain the optimal value through a large number of calculations, the data results are redundant, which can easily prolong the path optimization time.

In view of the problems in the above methods, this paper proposes an optimization method for cold chain logistics route decision of fresh product export considering transportation risk. Based on the analysis of the basic characteristics and classification of cold chain logistics, a transportation risk factor system of cold chain logistics for new product export considering transportation risks is established based on customs clearance efficiency, vehicle stability, cold chain terminal, traffic congestion, and other factors. The analytic hierarchy process (AHP) is used to obtain the transportation information of the cold chain logistics route of fresh products export, and then the risk factor judgment matrix is constructed to determine the index weight of risk factors. A genetic algorithm is introduced to construct the optimal cold chain logistics route decision function of new product export through encoding, decoding, crossover, and other operations and realize the optimization of cold chain logistics route decision of new product export. The experimental results show that the method proposed in this paper can effectively improve the decision-making effect of the cold chain logistics path. The cold chain logistics path is the shortest, the decision-making accuracy is high, and the transportation time is short, which has certain feasibility and applicability.

2. Cold Chain Logistics System

In order to realize the design of the decision-making optimization method of fresh product export cold chain logistics path, this paper first analyzes the risk factors existing in fresh product export cold chain logistics. Cold chain logistics generally refers to the whole process of refrigerated and frozen products from production and transportation to storage or secondary processing in the warehouse, and finally into the hands of consumers through dealers. And the whole process should be strictly controlled in the low-temperature environment. It is a systematic project to ensure product quality, maintain product freshness, and reduce loss through various refrigeration means [9]. Cold chain logistics is a low-temperature logistics process maintained by refrigeration technology and equipment. The general process of cold chain logistics is shown in Figure 1.

Different cold chain products require different storage temperatures. The classification of cold chain products and their characteristics in China are shown in Table 1.

Cold chain logistics is more demanding and complex than traditional logistics systems. In order to ensure that products will not be corroded and damaged, it is necessary to build a complete cold chain system with investment. It takes the low-temperature environment as the core and meets the timeliness requirements of products through reasonable and effective organization and coordination. In order to ensure the low-temperature environment, the cold chain logistics system is generally accompanied by high costs. Therefore, the reasonable classification of cold chain products and the construction of a cold chain logistics system are of great significance to the development of the cold chain industry [10].

3. Extraction of Transportation Risk Factors of Cold Chain Logistics Based on Risk Quantification

3.1. Establishing the Index System of Cold Chain Logistics Transportation Risk Factors. The risk management of fresh product export cold chain logistics transportation requires to be able to identify the risk, quantify the identified wind direction, and evaluate the risk according to the quantitative results. It also includes the implementation of some risk control methods, decision-making based on risk analysis, and performance evaluation of risk management effect. Risk identification is to collect information such as the possibility of risk occurrence and the number of accidents that have occurred and make probability statistics. There are many methods to identify possible risk factors. Find out the causes of risks according to different links. Generally, experts can identify relevant risks according to their own experience, which is also of great reference significance. In the process of risk identification, many scholars often use a variety of methods together, which can help to identify risk factors as comprehensively as possible. The risk quantification process is mainly based on the analysis of historical basic data, using probability theory and mathematical statistics to quantitatively analyze and describe risk indicators. Reasonable and effective data is the basis of risk quantification because risk quantification must rely on data support. Therefore, this paper analyzes the risk factors of fresh product export cold chain logistics transportation before the decision-making and optimization of the fresh product export cold chain logistics transportation path [11].

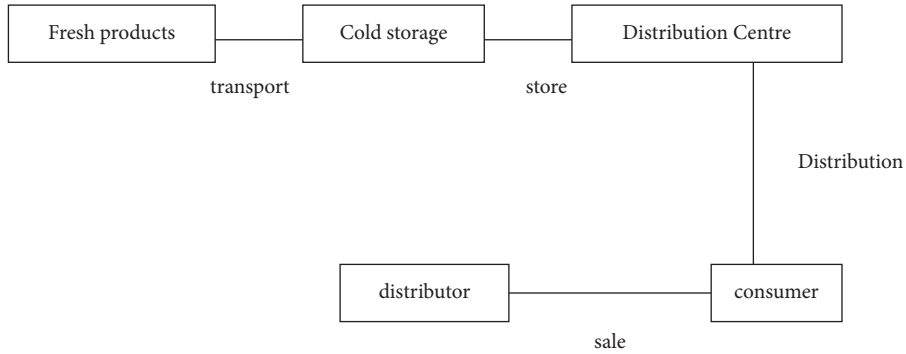

Figure 1: General process diagram of cold chain logistics.

Table 1: Classification of cold chain logistics storage environment.

Storage environment	Temperature (°C)	Product
Ultralow temperature	≤−30	Tuna, reagents, vaccines, etc
Freeze	−23–18	Frozen meat, frozen food
Keep in cold storage	0–8	Cold fresh meat, fresh milk, fruits and vegetables, etc

In the whole cross-border cold chain logistics transportation process, fresh products are faced with various uncontrollable factors, such as many transportation links, complex transportation process, different transportation subjects involved, and different economic, political, and transportation habits at home and abroad. The risk factor index system of fresh product export cold chain logistics transportation constructed in this paper is shown in Figure 2.

In the transportation process of cross-border cold chain logistics of fresh products, transportation cost, time, mode, transportation volume, and transportation path are usually considered. In addition, due to the differences in storage temperature, storage time, storage time limit, and product value of various agricultural products, more suitable transportation methods and more reasonable transportation paths are adopted for different fresh agricultural products in the whole cross-border logistics transportation process. It can maximize transportation efficiency and reduce transportation risks and costs under the conditions of existing infrastructure.

3.2. Extraction of Cold Chain Logistics Transportation Risk Factors. In this paper, considering the customs clearance efficiency, the choice of transportation mode and port will be more objective. Choosing transportation mode and port with higher customs clearance efficiency will make the comprehensive operation efficiency of cross-border cold chain logistics the highest. The customs clearance time per unit cargo volume is used to represent the customs clearance efficiency, but the shorter the time, the higher the customs clearance efficiency [12]. In order to facilitate understanding, the reciprocal is taken in the calculation. At this time, it means that the larger the calculation result is, the higher the customs clearance efficiency is. The calculation formula is

$$A_{in/out} = \frac{N_i}{v_i}. \tag{1}$$

Here, $A_{in/out}$ represents the customs clearance efficiency of import and export, v_i represents the working time of port i, and N_i represents the freight volume exported or imported from port i.

In this paper, the stability of vehicles is mainly based on the transportation stability of different vehicles in the cross-border cold chain transportation of fresh agricultural products, so as to ensure the timely and smooth progress of logistics activities. For high-value and perishable products, each route is weighted according to the punctuality rate of each transportation mode in the selection of different transportation modes. The calculation method is shown in the following formula:

$$B_j = \frac{c_j}{a_j} \times 100\%. \tag{2}$$

Here, B_j represents the punctuality rate of transport, c_j is the number of transport j arriving on time, and a_j is the total number of transport j.

The interruption of the cold chain has a great impact on the quality of fresh products, and the interruption usually occurs at the place of transshipment. Therefore, the probability of interruption is small when the number of loading changes is small. The purpose of selecting this risk index is to replace as little as possible on the basis of considering multiple modes of transportation. Considering the probability of cold chain interruption at each logistics transfer point as the cold chain interruption probability [13] is

$$d_l = D_p^l h_1^l (1 - h_1)^{p-l}. \tag{3}$$

Here, D_p^l represents the probability of cold chain interruption at l transit points, h_1^l represents the probability of

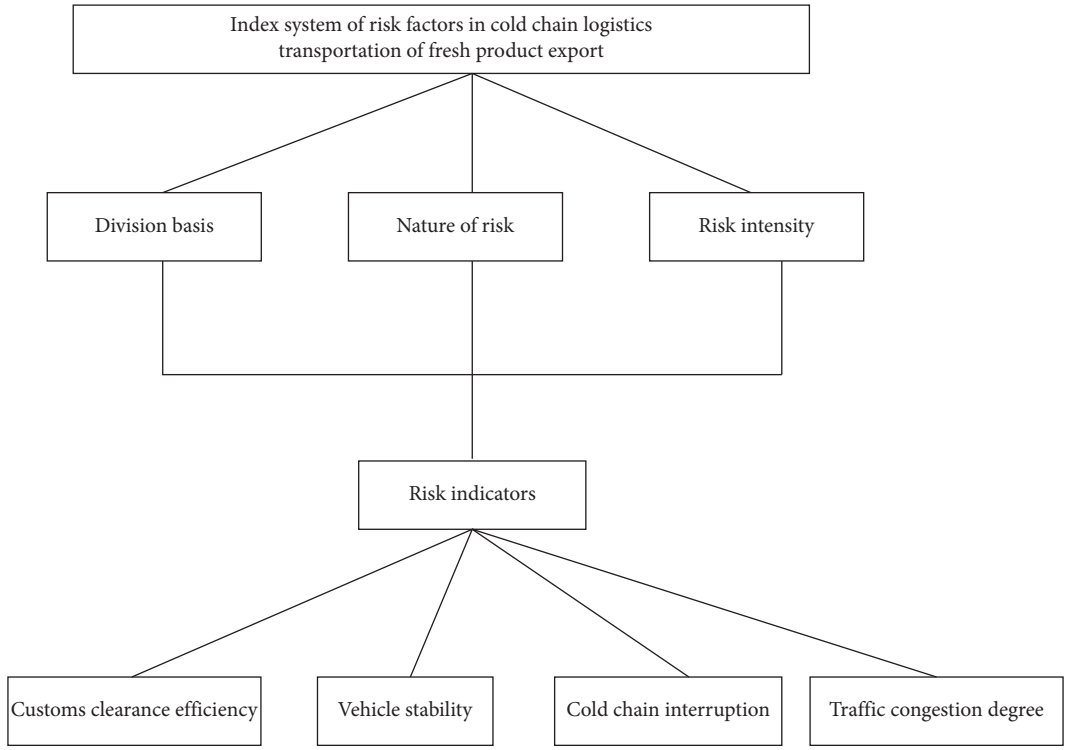

Figure 2: Risk factor index system of cold chain logistics transportation for fresh product export.

cold chain interruption at 1 transit point, and p represents a total of l transit points.

Traffic congestion is also a key factor affecting the cold chain transportation of fresh products. This paper selects the k-nearest neighbor algorithm to predict the risk of traffic congestion. K-nearest neighbor algorithm is one of the simplest methods in data mining classification technology, which means that each sample can be represented by its nearest K neighbors. If most of the k-nearest samples in the feature space belong to a category, then a sample also belongs to that category and has the properties of samples in that category. K-nearest neighbor algorithm only determines the classification of the samples to be divided according to the category of the nearest one or several samples. When making a classification decision, it is only related to a very small number of adjacent samples. New data can be directly added to the data set without retraining. K-nearest neighbor algorithm is simple in theory, easy to implement, high in accuracy, and has a high tolerance to outliers and noise. Therefore, choosing a k-nearest neighbor algorithm to predict the risk of traffic congestion can effectively shorten the transportation time of cold chain logistics.

Through the collection and analysis of related data affecting traffic, build K-nearest neighbor prediction model state vector (x, y, q), according to the collected state vector data, the storage form is (x_i, y_i, q_i), collected historical database should include a variety of possible factors of state vector and congestion index: for traffic congestion index prediction, first build state vector $Q(x, y, q)$ according to the information that can be collected in advance.

Then, calculate the distance between the required state vector and the history vector (x_i, y_i, q_i), search for the first K historical state vector with the shortest distance, and the predicted value is calculated using the TPI corresponding to the K state vectors. The value of the K-nearest neighbor algorithm is shown in Figure 3.

In the k-nearest neighbor algorithm, the distance is the judgment basis of the predicted state vector and the historical state vector. The smaller the distance is, the more similar the historical state vector is. This paper adopts the Euclidean distance calculation method. Euclidean distance is a commonly used definition of distance, which is the true distance between two points in m-dimensional space. The Euclidean distance in two and three dimensions is the distance between two points. Euclidean distance is simple, easy to operate, and widely used. The specific calculation formula is shown in the following formula:

$$dis(x_i, y_i, q_i) = \sqrt{w_i(x_i - y_i)^2} + \sqrt{w_i(x_i - q_i)^2} + \sqrt{w_i(y_i - q_i)^2}. \quad (4)$$

The distance of change trend of congestion index refers to the difference between two time difference series, i.e., numerical difference and change trend difference. The calculation method used in this paper is the variance and correlation coefficient method, in which the greater the variance, the farther the distance between them, the smaller the correlation coefficient, the more uncorrelated, and the greater the distance between them. Assuming that the congestion index sequence of 3 h before the current moment is $F_i[aF_1, aF_2, ...aF_m]$, the congestion index sequence of the same period in the historical library is a, and the number of

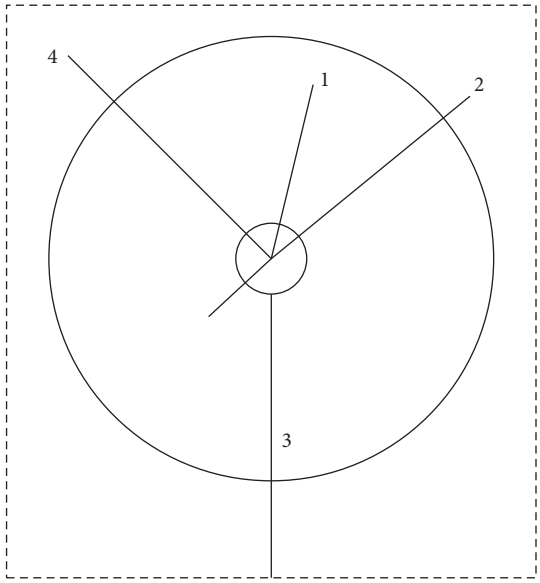

Figure 3: Schematic diagram of k-nearest neighbor algorithm.

elements of f and $a_i[a_{i1}, a_{i2}, \ldots, a_{im}]$ is m, the change trend of the congestion index can be expressed as follows:

$$\alpha_i = \sqrt{\sum_{i=1}^{n} (a_i - F_i)^2}. \tag{5}$$

Among them, α_i indicates the final trend of congestion index change.

4. Weight Calculation of Cold Chain Logistics Risk Factors Based on Analytic Hierarchy Process

According to the above-determined risk factors of fresh product export cold chain logistics transportation, in order to realize the decision-making and optimization of the transportation path, it is necessary to calculate the weight of these influencing factors to determine the key role of different influencing factors. The calculation of the risk factor weight of fresh product export cold chain logistics transportation is an extremely important aspect of risk control management. In enterprise risk management, when the risk evaluation result is a high risk, it is necessary to deal with and strictly control the risk, and the treatment means are relatively complex; When the risk assessment result is low risk, simple and effective risk control measures shall be taken or no risk control measures shall be taken according to the actual situation. The calculation of risk factor weight of fresh product export cold chain logistics transportation provides a theoretical basis for risk intelligent control of fresh product cold chain transportation. In the risk management of fresh product export cold chain logistics transportation, risk accidents are uncertain, the importance of risk factors is different, and the risk intelligent control methods are also different. In this paper, the analytic hierarchy process is used to quantitatively analyze the risk influencing factors of fresh product export cold chain logistics. Combined with the evaluation results, the intelligent control technology is used for risk control. Through the identification and monitoring of transportation risk factors through intelligent control technology, the risk of accident rate is reduced to the lowest; At the same time, it provides research ideas on expected identification, control, and evaluation for the risk management of fresh product export cold chain transportation.

The analytic hierarchy process (AHP) is a method combining qualitative analysis and quantitative analysis. According to the studied target problems, the influencing target factors are divided into different levels and then combined according to the relationship between the factors at different levels to build a multilevel framework model. Therefore, the problems are summarized as the ranking of advantages and disadvantages between the implementation scheme and the overall implementation goal and the measurement of relative importance. When using this method to build the calculation model, there are four steps: (1) establish the hierarchical structure model. 2. Build the judgment (pairwise comparison) matrix. 3. Hierarchical single ranking and its consistency test. 4. Hierarchical total ranking and its consistency test.

4.1. Establish Hierarchy Model. The hierarchical model uses concrete data structure to represent various entities and the relationships among them. Each node represents a record type, and the structure represents the relationships among entity types. The hierarchical model has a clear structure and simple connection between nodes. As long as we know the parent nodes of each node, we can know the whole model structure. Therefore, the establishment of the hierarchical model can effectively optimize the expected identification, control, and evaluation of fresh product export cold chain transportation risk management. The risk evaluation index system of fresh product export cold chain logistics transportation is divided into three hierarchical structures: target layer (layer a), criterion layer (layer B), and index layer (layer C).

4.2. Construction of Judgment Matrix. The value of the judgment matrix element is determined according to the comparison of two factors. The specific value method is expressed by santy's 1–9 scale method. It is more appropriate to compare less than 9 factors. Suppose there are n factors under layer a, and its judgment matrix can be expressed as follows:

$$W = \begin{bmatrix} w_{11} & w_{12} & \ldots & w_{1n} \\ w_{21} & w_{22} & \ldots & w_{2n} \\ & \ldots & & \\ w_{n1} & w_{n2} & \ldots & w_{nm} \end{bmatrix}. \tag{6}$$

Set the judgment matrix as follows:

$$A = \left(w_{ij}\right)_{n*m}. \tag{7}$$

4.3. Level of Single Ranking and Its Consistency Inspection

4.3.1. Level of Single Sorting. Hierarchical single ranking is to obtain the vector M, the feature vector W, and the maximum feature root $\beta_{\max}$ of the judgment matrix. The numerical size of the feature vector W element represents the weight arrangement of the lower layer relative to the upper layer. The specific calculation formula is as follows:

$$M = \left(\prod_{i=1}^{n} w_{ij} \right)^{1/n} (i = 1, 2, \ldots, n), \tag{8}$$

where M represents the normalized vector.

$$w_{ij} = \frac{M}{\sum_{i,j=1} M_j}. \tag{9}$$

4.3.2. Consistency Inspection. The reason for the consistency test is that things have diversity and human cognition has certain limitations. The specific inspection methods are as follows: define the consistency index: CI as follows:

$$CI = \frac{\beta_{\max} - n}{n - 1}, \tag{10}$$

where $\beta_{\max}$ represents the maximum eigenvalue of the judgment matrix; n value is the number of elements.

Hierarchical total rank consistency test, the hierarchical single rank consistency index of factor A in layer B layer is $(b_1, b_2, \ldots b_n)$, then the hierarchical total rank consistency ratio is

$$CR = \frac{\sum_{i=1}^{n} w_{ij} CI}{\sum_{j=1}^{m} RI w_{ij}}. \tag{11}$$

Here, RI represents the relevance Indicator. When the CR is less than 0.1, the total ranking means that the consistency test is passed, otherwise the judgment matrix element with a high single ranking consistency ratio needs to be adjusted.

4.3.3. Calculation of the Weight Result Value. Based on the above-given analysis, the weight of the risk factors of fresh products is calculated, and the calculation formula is

$$P_i = \sum_{i=1}^{n} w_{ij} CI. \tag{12}$$

Among them, P_i indicates the weight results of the cold chain transportation of fresh products.

5. Cold Chain Logistics Route Decision Optimization Based on Genetic Algorithm

The traditional logistics transportation path problem is that without considering its own and external factors, the roads between distribution stations are directly connected. Logistics transportation vehicles start from the central warehouse, transport all distribution stations, and finally return to the central warehouse. All distribution stations are traversed only once. Therefore, this paper adopts a genetic algorithm [14] to realize the decision-making optimization of the cold chain logistics path for fresh product export. Genetic algorithm is famous for its fast search speed, high efficiency, simple structure, and easy control of parameters. So far, it has been studied and applied by the majority of researchers. Therefore, this paper uses a genetic algorithm to solve the logistics transportation path problem, so as to minimize the transportation path and improve the transportation efficiency. At the beginning of the calculation, a certain number of individuals are randomly initialized and the fitness value of each individual is calculated to generate the first generation (initial population). If the optimization criteria are not met, the calculation of a new generation is started, and individuals are selected according to the fitness value to produce the next generation. The parent generation will cross operate according to a certain probability to produce the offspring. All offspring mutate with a certain probability to form a new generation. Calculate the fitness value of the new progeny. This process is repeated until the optimization criteria are met to solve the optimal path problem.

The search object of the genetic algorithm is a group of solutions, not just a single solution. Firstly, all possible solutions of the problem are encoded according to certain rules to obtain the initialization individual, namely, chromosome. Then, according to certain rules and mechanisms, some chromosomes are selected to form the initial population; after the initial population is selected, the fitness of each chromosome in the population should be calculated, and the parent individuals used for heredity should be selected for replication according to the fitness; then select, cross and mutate the individuals according to the algorithm rules, and continuously generate new individuals through iteration to form a new population. The adaptability of these new individuals must be better than that of the previous generation, so as to ensure a stronger ability to adapt to the environment [15]; finally, when the population iterates to the specified algebra or the fitness of the population iterates to a certain algebra, there is no optimization trend. At this time, it can be judged that the individual here is the optimal individual of the population, and the optimal solution of the problem can be obtained by decoding it. The main implementation steps of the genetic algorithm are as follows:

Step 1: the result of solving the cold chain logistics path of fresh product export by the genetic algorithm is greatly affected by the quality of the initial solution, while the quality of the solution obtained by the randomly generated initial solution is usually poor. Based on various performance indicators and personal preferences, the decision-maker proposes to form an initial solution, that is, first divide the value range of each parameter to be optimized into groups and cells, and then randomly generate an initial individual in each cell. In this way, the initial individuals will be evenly distributed in the whole solution space and can

ensure that the initial population contains rich patterns, which increases the possibility of converging to the global optimal solution. In this regard, this paper also proposes a decision-making method of fresh product export cold chain logistics path based on the time processing capacity index. This method first uses the randomly generated location sequence to sort each influencing risk factor and then randomly selects two risk indexes in each region. If the random value between 0 and 1 is less than 0.8, the best index is selected; If the random value between 0 and 1 is less than 0.8.

Step 2: encoding

Whether the coding is completed in the genetic algorithm is the key to successful optimization. The coding based on the process is the most widely used in traditional methods. Each process is represented by the corresponding serial number based on the coding chromosome. When the chromosome is scanned from left to right, the serial number k of the workpiece indicates the k-th machining of the workpiece. The advantage of this method is that the scheduling is feasible, deadlock is avoided, and the representation of solution space is complete. However, logistics path optimization requires not only determining the order of process selection but also selecting the best adapter for each process. Only using a process based coding method can not effectively deal with this problem. Aiming at this problem, an extended process based coding method is proposed. This method is divided into two different parts. The first is based on process coding, which can determine the order of the selection process. The other is based on location coding, which can set the corresponding reasonable location to all processes. The two coding methods are combined. The binary coding method is adopted to make the binary symbol set {0, 1} composed of binary symbols 0 and 1. A binary coding symbol string is an individual genotype, also known as a chromosome. If the value range of a parameter is $[U_{\min}, U_{\max}]$, the code of individual x is $x_l x_{l1} \ldots x_1 x_0$.

Step 3: genetic operator

Genetic operation is basically the same as a traditional genetic algorithm, and its biggest feature is selective operation. The selection of genetic manipulation is generally divided into three parts. Firstly, the best and worst individuals in the current population are found according to the fitness value; secondly, if the fitness value of some individuals in the contemporary population is higher than that of the retained excellent individuals, the existing excellent individuals will be replaced by the contemporary excellent individuals; finally, the retained excellent individuals are used to eliminate the worst individuals in the next generation population. It is assumed that the population can be divided into m layers according to the level of noninferior solution. The smaller the index, the higher the noninferior solution level. For I individuals, if their noninferior solution level is j and individuals at the same noninferior solution level have the same fitness, it is called shared fitness. In order to make the optimization results evenly distributed in the target space, it is necessary to calculate the local crowding distance of individuals on each noninferior solution level. Based on the calculation of shared fitness and local crowding distance, parents were randomly selected. When the sharing fitness is different, individuals with higher sharing fitness can be selected. When the fitness is the same, select the individuals with a large local crowding distance. Repeat the above-given selection until offspring are formed.

Step 4: description of logistics path decision-making problem of fresh product export cold chain

This paper describes the optimization problem of cold chain logistics distribution as follows: when the geographical location of the distribution center and customers is known, according to the customer's demand for products and the arrangement of time, reasonably schedule the cold chain logistics transportation vehicles, and start from the distribution center to provide distribution services for customers in turn; Among them, the customer's demand is known, the customer's requirements for the arrival time window of goods are known, and the vehicle load and the maximum single driving distance are also known. It is required to formulate an efficient and reasonable vehicle distribution scheme on the premise of no repeated distribution, meeting the customer's needs, and meeting the constraints, so as to realize the optimization of the objective function. After the above-given analysis, the cost elements and expressions of each module of cold chain logistics have been established. This paper aims to minimize the total cost of comprehensive logistics distribution, and the final cold chain logistics path optimization model is expressed as follows:

$$\min E = \min\left[\sum_{i=1}^{n} sign(k) + \sum_{j=1}^{n} w_{ij} p_i\right]. \tag{13}$$

The number of refrigerated vehicles, that is, the number of final distribution routes, can be changed and adjusted according to the specific customer demand, so as to meet the demand without waste, as shown in the following formula:

$$T = \operatorname{int}\left[\frac{\sum_{i=1}^{n} r_i}{T}\right] + 1. \tag{14}$$

Here, T represents the number of vehicles, r_i represents the demand of the customer ii, and T represents the maximum carrying capacity of the bicycle. The formula expresses the maximum carrying capacity of the customer with the total demand of the bicycle, and 1 is added as the number of vehicles in the final demand of cold chain logistics.

Fitness is used to evaluate the advantages and disadvantages of the determined distribution scheme. In the path optimization problem, a distribution scheme corresponds to a chromosome. The goal of this paper is that the smaller the

distribution cost, the better. There is a negative correlation between fitness and target value. Therefore, the fitness value can be expressed by the reciprocal of chromosome objective function value.

Fit (i) indicates the fitness, and C_t represents the target function value of the i th chromosome. The relationship expression between the two is

$$Fit(t) = \frac{1}{C_t}. \tag{15}$$

Among them, C_t represents the total cost of the distribution path in Article i, that is, the target function value of this paper, the smaller the total cost, the greater the fitness, the higher the feasibility, so the fitness function is feasible, so the design of the decision optimization method of the export cold chain logistics path of fresh products is completed.

6. Experimental Verification

6.1. Experimental Environment. In this experiment, Matlab is used and implemented in the running environment of the p4cpu program. The main frequency is 3.0 GHz and the memory is 512 MB. This case is divided into two parts. Firstly, the performance of the algorithm is tested and the test results are compared. The running parameters in the experiment include 200 population sizes, selection probability of 0.9, and maximum evolutionary algebra of 80. The area of cold chain transportation in this region is 15 km2. A well-known export company in China is selected to take its primary fresh product export cold chain logistics as the research object to optimize the logistics path. The specific arrival place of the fresh product in the cold chain logistics transportation is shown in Figure 4.

In Figure 4, circle 1 is the starting point of this transportation route. This transportation needs to be transported to circle 13 at the end point, passing through 11 parking spots. In this transportation, it should be driven according to the normal main roads in the map. In the experiment, by optimizing the constructed economic and environmental protection objective function, the values of the objective function are in the same quantitative range, that is, weighted average distribution. The unbalanced weight coefficient can be used to reflect different preference relationships in special cases. By defining the solution, each initial solution has at least one objective function value better than other objectives. The solution at the center of space is an unbiased optimal solution. Under the same conditions of concern, the objective function can choose the unbiased optimal solution as the optimal solution. Under the same conditions of concern, the objective function can choose the unbiased optimal solution as the optimal solution.

In the experiment, the methods of this paper, literature [7] and literature [8] are used to optimize the transportation route decision, and the experimental analysis is carried out with the accuracy of route decision, the time to reach the destination, and the error of route planning as the experimental indicators.

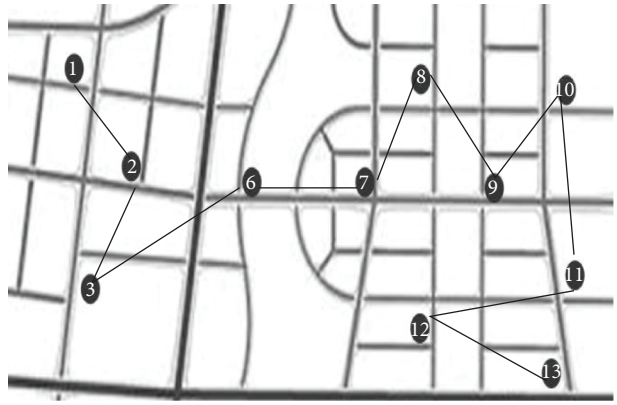

Figure 4: Schematic diagram of export cold chain transportation path of sample fresh products.

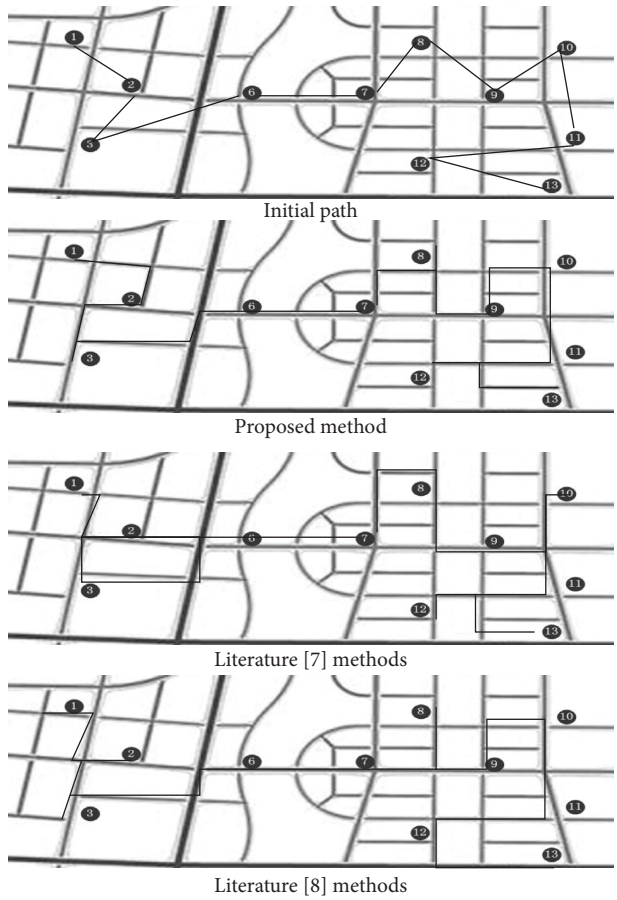

Figure 5: Analysis on the effect of different decision-making methods on transportation route decision-making.

6.2. Experimental Results

6.2.1. Impact Analysis of Traffic Route Decision. In the experiment, the method in this paper, the method in literature [7] and the method in literature [8] are used to optimize the transportation route decision. These three methods are used to make the initial route transportation decision. The effect of route decision is shown in Figure 5.

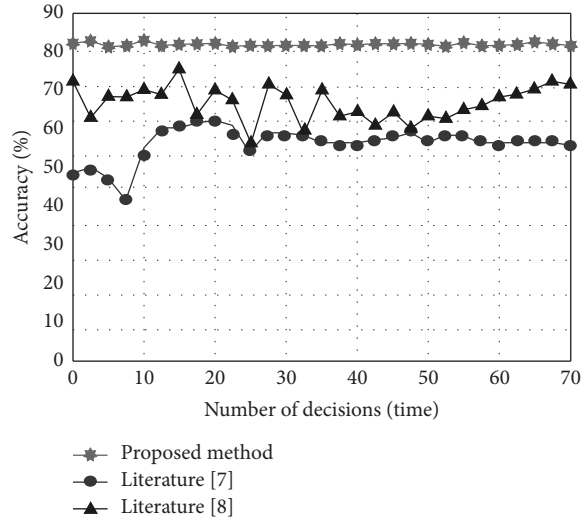

Figure 6: Analysis of decision accuracy of transportation route with different decision-making methods.

Table 2: Time analysis of transportation routes reaching the destination by different decision-making methods (min).

Number of iterations	Paper method	Literature [7] methods	Literature [8] methods
10	30.21	39.41	38.52
20	31.20	40.12	41.20
30	30.85	41.20	41.35
40	30.41	42.13	41.69
50	32.10	42.96	42.10
60	32.14	43.10	42.13
70	31.89	43.21	43.12
80	32.41	44.21	44.15
90	30.41	45.21	45.31
100	31.45	45.32	45.21

By analyzing the experimental results in Figure 5, it can be seen that the methods in this paper, literature [7] and literature [8] are used to optimize the transportation route decision. The routes after the initial route transportation decision are made by these three methods are different. Among them, the path decided by this method is the shortest and smoothest transportation path among the three methods. Compared with the path planned by the other two methods, there are more decisions of repeated sections, so it can be seen that this method is more feasible. This is because a genetic algorithm is used to improve the calculation effect of optimal cold chain logistics route decision function of new product export through encoding, decoding, crossover, and other operations, so as to improve the decision effect of traffic route.

6.2.2. Analysis of Transportation Route Decision Accuracy. In the experiment, the method in this paper, the method in literature [7], and the method in literature [8] are used to optimize the transportation route decision. After using these three methods to make the initial route transportation decision, in order to reflect the data results of the method, the decision accuracy of the obtained route decision effect is quantified. The results are shown in Figure 6.

By analyzing the experimental results in Figure 6, it can be seen that there are some differences in the precision results of transportation route decision optimization by the methods in this paper, literature [7] and literature [8]. It can be seen that the precision of decision optimization using this method is about 90% of the average value, while the precision of decision optimization using the other two traditional methods is low and fluctuates. Therefore, it can be seen that the decision path using this method is more suitable and feasible. This is because the analytic hierarchy process (AHP) is used to take the transportation information of the cold chain logistics route of fresh product export as the value of the risk factor judgment matrix, so as to calculate the accurate index weight of the risk factor and improve the decision-making accuracy of the transportation route.

6.2.3. Transporting Route Arrival Time Analysis. In the experiment, the transportation route decision optimization is carried out according to the methods in this paper, literature [7] and literature [8]. After using these three methods to make the decision of initial route transportation,

the time when the transportation route of the three methods reaches the destination is analyzed. The results are shown in Table 2.

By analyzing the experimental results in Table 2, it can be seen that the method in this paper, the method in literature [7], and the method in literature [8] are used to optimize the transportation route decision. After using these three methods to make the initial route transportation decision, there is a certain difference in the time when the transportation route reaches the destination according to the three methods in the experiment. Among them, the shortest time is the method in this paper. Although the other two methods are within a reasonable range, they are longer than the method in this paper. This is because the transportation risk factor system of cold chain logistics for the export of new products considering the transportation risk is constructed, so as to optimize the customs clearance efficiency, vehicle stability, cold chain terminal, traffic congestion, and other factors of cold chain logistics and shorten the transportation time of cold chain logistics route. Therefore, it can be seen that the method in this paper is more feasible.

7. Conclusion

Based on the analysis of the shortcomings of the traditional cold chain logistics of fresh product export, the optimization method of the cold chain logistics route decision of fresh product export considering the transportation risk factors was proposed, which promoted the vehicle stability of the cold chain distribution link of fresh product export and reduced the traffic congestion. Through the method of risk quantification, the basic characteristics and classification of cold chain logistics are analyzed, and the transportation risk factor index system of cold chain logistics is constructed. The k-nearest neighbor algorithm is used to predict the risk of traffic congestion and extract the transportation risk factors of cold chain logistics, so as to shorten the transportation time. In order to reduce the error of path planning, ahp was used to construct a calculation model, and the index weight of risk factors was calculated by the risk factor matrix. A genetic algorithm is introduced to construct the optimal decision function of the cold chain logistics route of new product export through encoding, decoding, crossover, and other operations and optimize the decision of the cold chain logistics route of fresh product export. Experimental results show that the method proposed in this paper can improve the effect of cold chain logistics route decision, the accuracy of decision optimization is about 90%, and the time to reach the destination is short, reduce the transport time, with a certain transport efficiency.

Data Availability

The dataset can be accessed from the corresponding author upon request.

Conflicts of Interest

The authors declare that they have no conflicts of interest.

Acknowledgments

This work was supported by Jiang Su Social Science Fund: Research on export credit risk avoidance and transfer strategy of Chinese enterprises in Jiangsu under "One Belt And One Road" initiative (Grant no. 18GLD001).

References

[1] C. J. Dai, Y. Li, C. Ma, and H. Chai, "Transportation path optimization for hazardous materials considering characteristics of risk distribution," *Zhongguo Gonglu Xuebao/China Journal of Highway and Transport*, vol. 31, no. 4, pp. 330–342, 2018.

[2] M. Farazmand, M. S. Pishvaee, and R. Ghousi, S. F. Ghannadpour, "Green dynamic multimodal logistics network design problem considering financing decisions: a case study of cement logistics," *Environmental Science and Pollution Research*, vol. 29, no. 3, pp. 4232–4245, 2022.

[3] L. Zhang, M. Fu, and T. Fei, "Research on location of cold chain logistics distribution center with low carbon in beijing-tianjin-hebei area on the basis of RNA-artificial fish swarm algorithm," *Journal of Physics: Conference Series*, vol. 1861, no. 1, Article ID 12005, 2021.

[4] Y. Li, L. Wu, Y. Sun, and M. Lian, "Risk decision-making of multiobjective chaos search in construction projects considering loss level and probability level," *Mathematical Problems in Engineering*, vol. 2022, no. 7, p. 11, 2022.

[5] Y. Zhao, Y. He, D. Zhou, A. Zhang, X. Han, and Y. Li, "Functional risk-oriented integrated preventive maintenance considering product quality loss for multistate manufacturing systems," *International Journal of Production Research*, vol. 59, no. 4, pp. 1–18, 2021.

[6] J. Li, M. Liu, and P. Liu, "Route optimization of multi-vehicle cold chain logistics for fresh agricultural products," *Journal of China Agricultural University*, vol. 26, no. 7, pp. 115–123, 2021.

[7] L. I. Xin, H. Guo, and L. Wang, "Optimization of cold chain logistics vehicle routing based on green evaluation," *Journal of Jiangsu University of Science and Technology*, vol. 35, no. 6, pp. 84–93, 2021.

[8] Y. Ding, "Simulation of vehicle distribution path optimization for multi-temperature co-distribution cold chain logistics," *Journal of Shenyang University of Technology*, vol. 43, no. 3, pp. 311–316, 2021.

[9] Y. Chen, "Location and path optimization of green cold chain logistics based on improved genetic algorithm from the perspective of low carbon and environmental protection," *Fresenius Environmental Bulletin*, vol. 30, no. 6, pp. 5961–5973, 2021.

[10] Y. Zhao, X. Zhang, X. Xu, and S. Zhang, "Research progress of phase change cold storage materials used in cold chain transportation and their different cold storage packaging structures," *Journal of Molecular Liquids*, vol. 31, no. 9, pp. 114–119, 2020.

[11] Y. Lu, X. Xu, C. Yin, and Y. Zhang, "Network optimization of railway cold chain logistics based on freight subsidy,"

Transportation Research Record, vol. 2675, no. 10, pp. 590–603, 2021.

[12] G. Li, "Development of cold chain logistics transportation system based on 5G network and Internet of things system," *Microprocessors and Microsystems*, vol. 80, no. 5, pp. 80–86, Article ID 103565, 2021.

[13] N. Sun, L. I. Yin-Juan, and T. X. Chen, "Analysis of fresh and cold chain logistics transportation service evaluation based on the "internet +" environment," *Logistics Engineering and Management*, vol. 59, no. 2, pp. 1584–1590, 2019.

[14] J. W. Han, M. Zuo, W. Y. Zhu, J. H. Zuo, E. L. Lu, and X. T. Yang, "A comprehensive review of cold chain logistics for fresh agricultural products: current status, challenges, and future trends," *Trends in Food Science & Technology*, vol. 109, no. 19, pp. 536–551, 2021.

[15] M. F. Ibrahim, F. R. Nurhakiki, D. M. Utama, and A. A. Rizaki, "Optimised genetic algorithm crossover and mutation stage for vehicle routing problem pick-up and delivery with time windows," *IOP Conference Series: Materials Science and Engineering*, vol. 1071, no. 1, Article ID 12025, 2021.

Hindawi
Computational Intelligence and Neuroscience
Volume 2022, Article ID 8633955, 5 pages
https://doi.org/10.1155/2022/8633955

Research Article

Detecting Anomaly Event in Video Based on Generative Adversarial Network

Zhaoxian Zhang

Guilin University of Electronic Technology School of Information and Communication, Guangxi, Guilin 541000, China

Correspondence should be addressed to Zhaoxian Zhang; 21022202032@mails.guet.edu.cn

Received 24 August 2022; Accepted 22 September 2022; Published 5 October 2022

Academic Editor: Yaxiang Fan

Copyright © 2022 Zhaoxian Zhang. This is an open access article distributed under the Creative Commons Attribution License, which permits unrestricted use, distribution, and reproduction in any medium, provided the original work is properly cited.

Anomaly detection in videos is a challenging computer vision problem. Existing state-of-the-art video anomaly detection methods mainly focus on the structural design of deep neural networks to obtain performance improvements. Different from the main research trend, this paper focuses on combining ensemble learning and deep neural networks and proposes an approach based on ensemble generative adversarial network (GAN). In the proposed method, a set of generators and a set of discriminators are trained together, so each generator gets feedback from multiple discriminators and vice versa. Compared with a single GAN, the proposed ensemble GAN can better model the distribution of normal data to better detect anomalies. In the experiments, the performance of the proposed method is tested on two public datasets. The results show that ensemble learning significantly improves the performance of a single detection model, which outperforms some existing state-of-the-art methods.

1. Introduction

Anomaly detection in surveillance video is a fundamental computer vision task that plays a crucial role in video analysis. It can be well used in potential applications such as accident prediction, urban traffic analysis, and evidence investigation. Although the problem has attracted intense attention in recent years, video anomaly detection is still a very challenging work due to the severe imbalance between normal and anomalous samples, the lack of detailed anomaly labeled data, and the inconsistent definitions of anomalous behaviors.

To address this problem, researchers have proposed a number of methods. According to the literature review [1], existing anomaly detection methods can be divided into ones based on density estimation and probabilistic models, ones based on single-class classification, and ones based on reconstruction. The methods based on density estimation and probability model [2, 3] mainly calculate the probability density function of the samples at first and then make the judgement by obtaining the distance between the sample and the center of the density function. While the classical nonparametric density estimators perform reasonably well when dealing with low-dimensional problems, the sample size they require to achieve a fixed level of accuracy grows exponentially in the dimension of the feature space. One-class classification-based methods [4, 5] try to avoid full estimation of density as an intermediate step in anomaly detection, and these methods aim to directly learn the decision boundary corresponding to the positive samples, by testing whether the samples under test are within the boundary. Reconstruction-based methods [6, 7] learn a model that is optimized to reconstruct normal data instances well, thereby detecting anomalies by failing to reconstruct them accurately under the learned model.

In recent years, the deep learning models learn efficient representations from the multiple sources of data by training flexible multi-layer deep neural networks, which has achieved breakthroughs in many applications involving complex data types, such as computer vision [8, 9], speech recognition [10, 11], or natural language processing [12, 13]. Methods based on deep neural networks are able to exploit the often inherent hierarchical or latent structure of data through their multi-layer distributed feature representations. Furthermore, advances in parallel computing, stochastic gradient descent optimization, and automatic

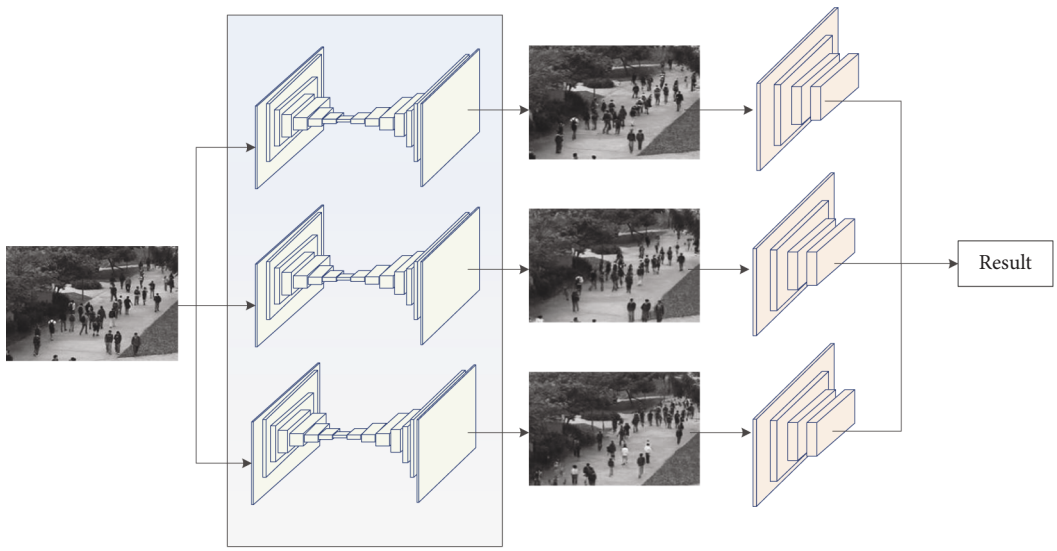

Figure 1: The methodology of abnormal event detection based on GAN ensembles.

differentiation have made it possible to apply deep learning at scale on large datasets. For anomaly detection problems, deep learning methods can optimize the entire anomaly detection model end-to-end and can also learn representations specifically for the anomaly detection problem. In addition, the ability of deep learning methods for large datasets helps to greatly improve the utilization of labeled normal data or some labeled anomalous data.

Under the framework of deep learning, this paper proposes an anomaly detection method based on single-class classification. This approach is an improved form of generative adversarial network (GAN) called GAN ensembles. GAN exploits the competition between the generator and the discriminator, where the generator learns the distribution of samples and the discriminator learns how to detect anomalies. An ensemble GAN consists of multiple encoder-decoders and discriminators that are randomly paired and trained via adversarial training. In this process, the encoder-decoder gets feedback from multiple discriminators, and the discriminator gets "training samples" from multiple generators. Compared with a single GAN, the proposed ensemble GAN can better model the distribution of normal data so it can be better employed to detect anomalies. Finally, the total anomaly score is obtained by taking the average of the calculated anomaly scores from all encoder-decoder discriminator pairs for discrimination. Experimental results on two public benchmark datasets show that the proposed method significantly outperforms some existing methods on a range of anomaly detection tasks.

2. Basic Principle

2.1. Description of Problem. Assuming that the normal sample training set is $\mathbf{X} = \{\mathbf{x}_i \in \mathbb{R}^d : i = 1, \ldots, N\}$, which contains N samples from an unknown distribution $\mathscr{D}$, the sample $\mathbf{x}' \in \mathbb{R}^d$ to be tested may not belong to the unknown distribution $\mathscr{D}$. Then, the problem of anomaly detection is to train the model from $\mathbf{X}$ such that the model can classify $\mathbf{x}'$ as a normal sample if $\mathbf{x}'$ belongs to the unknown distribution $\mathscr{D}$. Conversely, it is anomalous if $\mathbf{x}'$ comes from a different distribution. Typically, the model computes the anomaly score $y' \in \mathbb{R}^d$ of $\mathbf{x}'$ and determines the label of $\mathbf{x}'$ by thresholding y'. Figure 1 shows the general framework of the proposed method.

2.2. GAN. A typical GAN consists of two neural networks, i.e., a generator and a discriminator. Among them, the generator contains an encoder $G_e(\cdot;\phi)$ and a decoder $G_d(\cdot;\psi)$. The encoder encodes the sample x into a vector z, and the decoder reconstructs it into vector $\tilde{x}$. The basic process is as follows:

$$\begin{aligned} \mathbf{z} &= G_e(\mathbf{x};\phi), \\ \tilde{\mathbf{x}} &= G_d(\mathbf{z};\psi). \end{aligned} \tag{1}$$

The discriminator $D(\cdot;\gamma)$ judges the probability that the test sample comes from the dataset $\mathbf{X}$ rather than the generator generated samples. Then, the discriminator should provide higher reconstruction error values for normal samples. Since the model consists of an encoder-decoder and a discriminator, the training process usually takes into account loss functions inherited from both models. The adversarial loss coming from GAN training is defined as follows:

$$L_{a-g}(\mathbf{x}) = \log D(\mathbf{x}) + \log\left(1 - D\left(G_d\left(G_e(\mathbf{x})\right)\right)\right). \tag{2}$$

Another one is the reconstruction loss, which is used to train the encoder and decoder. In fact, the difference between the original sample and the reconstruction result is often calculated by the l-norm as follows:

$$L_r(\mathbf{x}) = \left\|\mathbf{x} - G_d\left(G_e(\mathbf{x})\right)\right\|_l^l. \tag{3}$$

Previous studies have shown that the hidden vector $\mathbf{h}$ of a sample in the last hidden layer of the discriminator $D(\cdot;\gamma)$ is useful for distinguishing normal samples from abnormal

samples. Define $h = D(\mathbf{x}; \gamma)$ as the hidden vector in $D(\cdot; \gamma)$; then, the discriminant loss based on h can be calculated as follows:

$$L_d(\mathbf{x}) = \left\| f_D(\mathbf{x}) - f_D\left(G_d\left(G_e(\mathbf{x})\right)\right)\right\|_l^l. \tag{4}$$

Furthermore, GAN also considers the difference between the encoded vector of a normal sample $\mathbf{x}$ and its reconstruction $\tilde{\mathbf{x}}$. In particular, it encodes the reconstructed $\tilde{\mathbf{x}}$ using a separate encoder $G_e(\cdot; \tilde{\phi})$. Then, the encoding loss is as follows:

$$L_e(\mathbf{x}) = \left\| G_e(\mathbf{x}; \phi) - G_e\left(G_d\left(G_e(\mathbf{x}; \phi); \tilde{\phi}\right)\right)\right\|_l^l. \tag{5}$$

In (5), the encoder parameters ϕ and $\tilde{\phi}$ are distinctly different. To train the discriminator, the GAN model needs to maximize the adversarial loss, which is defined as follows:

$$\max_{\gamma} \sum_{i=1}^{N} L_a(\mathbf{x}_i; \phi, \psi, \gamma). \tag{6}$$

After the GAN parameters are trained, the anomaly score $A(\mathbf{x}')$ needs to be calculated for the test sample $\mathbf{x}'$. Then, the anomaly score is obtained by calculating the weighted sum of the reconstruction loss and the discriminant loss as follows:

$$\mathbf{A}(\mathbf{x}') = L_r(\mathbf{x}') + \beta L_d(\mathbf{x}'). \tag{7}$$

In (7), the weight β is obtained through empirical selection. A higher anomaly score indicates a high anomaly probability.

2.3. Anomaly Detection Based on GAN. This paper proposes an anomaly detection method based on ensemble GANs. The model contains multiple generators and discriminators, with different parameterizations. Assuming that I generators $\{G_e(\cdot; \phi_i), G_d(\cdot; \psi_i)\colon i = 1, \cdots, I\}$ and J discriminators $\{D_e(\cdot; \gamma_i), : j = 1, \cdots, J\}$ are defined, a single generator or discriminator is the same as the base model. During the adversarial training, each generator is matched with each discriminator, which is then evaluated by each discriminator. Also, the discriminator receives synthetic samples from each generator.

For multiple pairs of generators and discriminators, both adversarial and discriminative losses are computed from all generator-discriminator pairs. The loss between each generator-discriminator pair is calculated as follows:

$$\begin{aligned} L_a^{ij} &= L_a\left(\mathbf{x}; \phi_i, \psi_i, \gamma_j\right), \\ L_d^{ij} &= L_d\left(\mathbf{x}; \phi_i, \psi_i, \gamma_j\right). \end{aligned} \tag{8}$$

Similarly, the reconstruction loss and encoding loss for a single generator are calculated as follows:

$$\begin{aligned} L_r^i &= L_r(\mathbf{x}; \phi_i, \psi_i), \\ L_e^i &= L_r(\mathbf{x}; \phi_i, \psi_i). \end{aligned} \tag{9}$$

The discriminator is then trained by maximizing the sum of adversarial losses, while the generator is trained by minimizing the sum of all losses. The objective function is as follows:

$$\begin{aligned} &\max_{\left(\gamma_j\right)_{j=1}^{J}} \sum_{i=1}^{I}\sum_{j=1}^{J} L_a^{ij}, \\ &\max_{\left(\phi_i, \psi_i\right)_{j=1}^{I}} \sum_{i=1}^{I}\sum_{j=1}^{J} \alpha_1 L_a^{ij} + \alpha_2 L_r^i + \alpha_3 L_d^{ij} + \alpha_4 L_e^i. \end{aligned} \tag{10}$$

In one training iteration, only one pair of generator-discriminators is updated rather than all generators and discriminators. In particular, a generator and a discriminator are randomly chosen and the loss is computed with a random batch of training data. Afterwards, for multiple generators and discriminators, the anomaly score of the sample $\mathbf{x}'$ under test is

$$\mathscr{A}(\mathbf{x}') = \frac{1}{IJ} \sum_{i=1}^{I}\sum_{j=1}^{J} A(\mathbf{x}_i; \phi, \psi, \gamma). \tag{11}$$

The average of the outlier scores helps eliminate spurious scores if the model is not well trained on a particular test instance. The threshold θ is set to judge whether the test sample is abnormal as follows:

$$\mathscr{A}(\mathbf{x}') > \theta. \tag{12}$$

3. Experiment

3.1. Experimental Data. In order to evaluate the qualitative and quantitative results of the proposed method and compare it with the state-of-the-art algorithms, this paper selects two public video anomaly detection datasets for experiments, namely, CUHK Avenue [14] and ShanghaiTech [15]. The CUHK Avenue dataset was filmed on the streets of the Chinese University of Hong Kong, which consists of 16 training and 21 testing videos collected from fixed scenes. The training normal data only include pedestrian walking, and there are 47 abnormal events including running and packet loss. Compared to the CUHK Avenue dataset, the ShanghaiTech dataset is very challenging and contains videos from 13 scenes with complex lighting conditions and camera angles. The total number of frames for training and testing reaches 274,000 and 42,000, respectively. The test set includes 130 abnormal events such as chases, quarrels, and sudden movements, which are scattered in 17,000 frames.

3.2. Evaluation Indicators. Based on previous work [14, 15], this paper adopts the area under the ROC curve (AUC) to evaluate the performance. The ROC curve is obtained by calculating the predicted anomaly score at each frame level by varying the threshold.

3.3. Experimental Setup. For both datasets, each frame of video is resized to 286×286, and video blocks of size 256×256 are randomly cropped during each iteration. The structure of the generator adopts C64 × (4 × 4)-C128 × (4 × 4)

Table 1: Comparison of frame-level anomaly detection performance with the state-of-the-art methods (AUC (%)).

Methods	CUHK Avenue	ShanghaiTech
VEC [16]	90.2	74.8
Conv-VRNN [17]	85.8	—
MNAD-P [18]	88.5	70.5
AMDN [19]	84.6	—
Conv2D-AE [6]	70.2	—
StackRNN [16]	80.9	68.0
Proposed	90.6	75.1

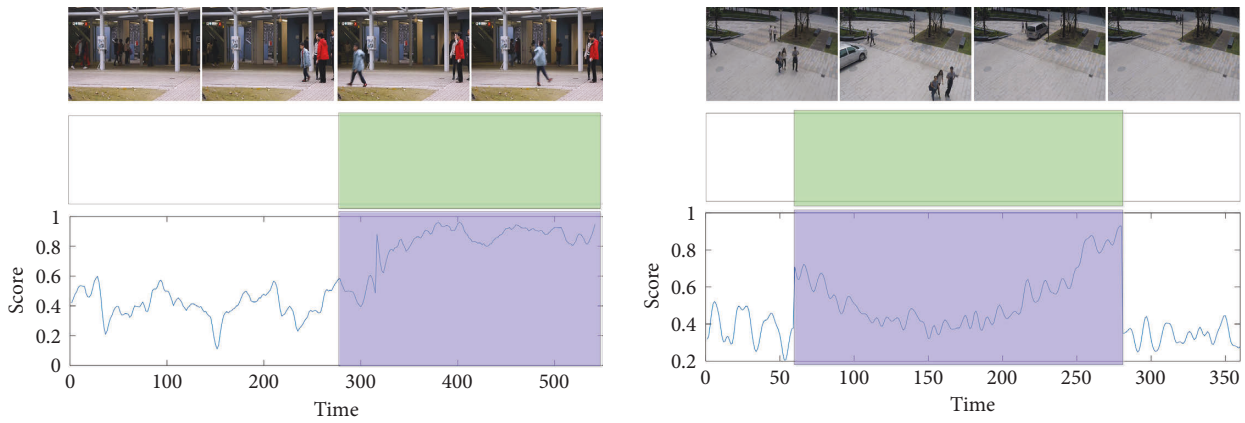

Figure 2: Two examples of anomaly detection comparison on CUHK Avenue dataset and ShanghaiTech dataset.

-C256 × (4 × 4)-C512 × (4 × 4)-C512 × (4 × 4)-DC256 × (4 × 4)-DC128 × (4 × 4)-DC64 × (4 × 4) structure. The first half is the encoder, and the second half is the decoder. The encoder first uses 64 convolutional layers with 4 × 4 convolution kernels and then uses 128 convolutional layers with 4 × 4 convolution kernels. The decoder and encoder structures are completely opposite and contain deconvolutional layers of the same size. The BatchNorm layer and the ReLU activation function are connected after each layer. The discriminator includes a total of 5 convolutional layers, and the size of the convolution kernel is also 4 × 4. The structure adopts C64 × (4 × 4)-Pooling-C128 × (4 × 4)-Pooling-C256 × (4 × 4)-Pooling-C512 × (4 × 4) and finally outputs one-dimensional data. This paper uses TensorFlow2.0 to implement the GAN ensemble method and uses the Adam optimizer ($\rho_1 = 0.9$, $\rho_2 = 0.999$) to optimize it. The initial learning rate is set to 1e−4 and decays by 0.8 after every 50 epochs, for a total of 300 epochs of training.

3.4. Experimental Results. In order to verify the advantages of the method proposed in this paper, it is compared with some existing methods, which are from different types. The first ones are based on density estimation and probability models including VEC [16] and Conv-VRNN [17]. The second ones are single-class classification-based methods including MNAD-P [18] and AMDN [19]. The third ones are reconstruction-based methods including Conv2D-AE [6] and StackRNN [20]. The comparative results are given in Table 1, and the results of other methods are obtained from related papers.

From Table 1, it can be observed that the GAN ensemble model proposed in this paper achieves better results than the state-of-the-art methods on both datasets, which proves the effectiveness of the proposed method. In particular, it achieves an AUC of 91.1% on the CUHK Avenue dataset. It is worth noting that the performance of these methods on CUHK Avenue dataset is better than that on ShanghaiTech dataset, which is due to the fact that ShanghaiTech is a newly proposed dataset with a large number of frames and a large variation in different sample resolutions. In spite of this, the method proposed in this paper achieves 75.1% frame-level AUC on the ShanghaiTech dataset, which also exceeds the best VEC [16] among other methods by 0.3%.

Figure 2 shows anomalous examples of the two test datasets for the proposed method. The anomaly curve shows the anomaly scores for all frames of the video in turn, through which the performance of the method can be observed more intuitively. The green area represents the anomalous part of the ground truth, and the blue area represents the abnormal area detected by the method. It can be seen that the blue area can correspond to the green area. In the normal frame part, the proposed GAN ensembles have low anomaly scores and are very stable. Also, when anomalies occur, such as bicycles and cars on the sidewalk, fights, and pushes, the anomaly score suddenly increases. The scores in the figure correspond exactly to the occurrence of these scenes. All the above results show that the proposed method can achieve superior results on video anomaly detection by comparison with some state-of-the-art methods.

4. Conclusion

This paper introduces ensemble learning into a GAN-based anomaly model for anomaly detection. The discriminator of GAN is very effective for anomaly detection, and ensemble learning can further improve the training of the discriminator. Therefore, the method proposed in this paper is not a simple combination of ensemble learning and GAN. The ensemble learning can effectively affect the prediction quality. Experiments on two datasets demonstrate that the proposed method outperforms some state-of-the-art methods for video anomaly detection. Extensive experiments show that the ensemble approach achieves superior results on both datasets compared to a single model [21, 22].

Data Availability

The datasets used in this paper can be accessed upon request.

Conflicts of Interest

The author declares that there are no conflicts of interest regarding the publication of this paper.

References

[1] R. Lukas, J. Kauffmann, V. Robert et al., "A unifying review of deep and shallow anomaly detection," *Proceedings of the IEEE*, vol. 99, pp. 1–40, 2020.

[2] D. Xu, R. Song, X. Wu, N. Li, W. Feng, and H. Qian, "Video anomaly detection based on a hierarchical activity discovery within spatio-temporal contexts," *Neurocomputing*, vol. 143, no. 2, pp. 144–152, 2014.

[3] M. Ravanbakhsh, E. Sangineto, M. Nabi, and N. Sebe, "Training adversarial discriminators for cross-channel abnormal event detection in crowds," in *Proceedings of the Winter Conference on Applications of Computer Vision*, pp. 1896–1904, Waikoloa, HI, USA, January 2019.

[4] M. G. Narasimhan and S. Sowmya Kamath, "Dynamic video anomaly detection and localization using sparse denoising autoencoders," *Multimedia Tools and Applications*, vol. 77, no. 11, pp. 13173–13195, 2018.

[5] A. Chriki, H. Touati, H. Snoussi, and F. Kamoun, "Deep learning and handcrafted features for one-class anomaly detection in UAV video," *Multimedia Tools and Applications*, vol. 80, no. 2, pp. 2599–2620, 2021.

[6] M. Hasan, J. Choi, and J. Neumanny, "Learning temporal regularity in video sequences," in *Proceedings of the IEEE Conference on Computer Vision and Pattern Recognition*, pp. 770–778, Las Vegas, 2016.

[7] M. Sabokrou, M. Fathy, and M. Hoseini, "Video anomaly detection and localisation based on the sparsity and reconstruction error of auto-encoder," *Electronics Letters*, vol. 52, no. 13, pp. 1122–1124, 2016.

[8] K. He, X. Zhang, S. Ren, and J. Sun, "Deep residual learning for image recognition," in *Proceedings of the IEEE Conference on Computer Vision and Pattern Recognition*, pp. 770–778, Las Vegas, NV, USA, June 2016.

[9] Z. Ma, J. Machado, and J. Tavares, "Weakly supervised video anomaly detection based on 3D convolution and LSTM," *Sensors (Basel, Switzerland)*, vol. 21, no. 22, pp. 2–4, 2021.

[10] D. Amodei, "Deep speech 2: end-to-end speech recognition in English and Mandarin," *International Conference on Machine Learning*, vol. 48, pp. 173–182, 2016.

[11] S. Schneider, A. Baevski, R. Collobert, and M. Auli, "Wav2vec: unsupervised pre-training for speech recognition," pp. 3465–3469, 2019, https://arxiv.org/abs/1904.05862.

[12] J. Pennington, R. Socher, and M. C. Glove, "Global vectors for word representation," in *Proceedings of the Conference on Empirical Methods in Natural Language Processing*, pp. 1532–1543, Honolulu, Hawaii, 2014.

[13] D. Z. Satybaldina, N. S. Glazyrina, and K. A. Kalymova, "Development of an algorithm for abnormal human behavior detection in intelligent video surveillance system," *IOP Conference Series: Materials Science and Engineering*, vol. 1089, no. 1, p. 8, 2021.

[14] C. Lu, J. Shi, and J. Jia, "Abnormal event detection at 150 fps in matlab," *Proceedings of the IEEE international conference on computer vision*, pp. 1–8, ydney, NSW, Australia, December 2013.

[15] Y. Miao, J. Chen, and X. Zhang, "Efficient 3D Object detection of indoor scenes based on RGB-D video stream," *Journal of Computer-Aided Design & Computer Graphics*, vol. 33, no. 7, pp. 1015–1025, 2021.

[16] G. Yu, S. Wang, Z. Cai et al., "Cloze test helps: effective video anomaly detection via learning to complete video events," *Proceedings of the ACM International Conference on Multimedia*, pp. 583–591, WA, Seattle, USA, October 2020.

[17] Y. Lu, K. Mahesh, N. S. shahabeddin, and Y. Wang, "Future frame prediction using convolutional vrnn for anomaly detection," in *Proceedings of the IEEE International Conference on Advanced Video and Signal Based Surveillance*, pp. 1–8, Taipei, Taiwan, September 2019.

[18] Y. Ge, C. Zhang, and K. Wang, "WGI-Net: A weighted group integration network for RGB-D salient object detection," vol. 7, no. 1, pp. 115–125, 2021.

[19] D. Xu, Y. Yan, E. Ricci, and N. Sebe, "Detecting anomalous events in videos by learning deep representations of appearance and motion," *Computer Vision and Image Understanding*, vol. 156, pp. 117–127, 2017.

[20] S. Lin, H. Yang, X. Tang, T. Shi, and L. Chen, "Social mil: interaction-aware for crowd anomaly detection," in *Proceedings of the IEEE International Conference on Advanced Video and Signal Based Surveillance (AVSS)*, pp. 1–8, Taipei, Taiwan, September 2019.

Hindawi
Computational Intelligence and Neuroscience
Volume 2022, Article ID 3083647, 10 pages
https://doi.org/10.1155/2022/3083647

Research Article

Banana Pseudostem Width Detection Based on Kinect V2 Depth Sensor

Jinzhi Wang,[1,2] **Xiuhua Li**,[1] **Yonghua Zhou**,[1] **Huaihai Wang**,[2] **and Minzan Li**[3]

[1]*College of Electrical Engineering, Guangxi University, Nanning 530004, China*
[2]*State Grid Anhui Electric Power Co., Ltd., Feidong County Power Supply Company, Hefei 231600, China*
[3]*Key Laboratory of Modern Precision Agriculture System Integration, Ministry of Education, China Agricultural University, Beijing 100083, China*

Correspondence should be addressed to Jinzhi Wang; wangjz@st.gxu.edu.cn

Received 5 August 2022; Accepted 24 August 2022; Published 27 September 2022

Academic Editor: Yaxiang Fan

Copyright © 2022 Jinzhi Wang et al. This is an open access article distributed under the Creative Commons Attribution License, which permits unrestricted use, distribution, and reproduction in any medium, provided the original work is properly cited.

This study used Kinect V2 sensor to collect the three-dimensional point cloud data of banana pseudostem and developed an automatic measurement method of banana pseudostem width. The banana plant was selected as the research object in a banana plantation in Fusui, Guangxi. The mobile measurement of banana pseudostem was carried out at a distance of 1 m from the banana plant using the field operation platform with Kinect V2 as the collection equipment. To eliminate the background data and improve the processing speed, a cascade classifier was used to recognize banana pseudostems from the depth image, extract the region of interest (ROI), and transform the ROI into a color point cloud combined with the color image; secondly, the point cloud was sparse by down-sampling; then, the point cloud noise was removed according to the classification of large-scale and small-scale noise; finally, the stem point cloud was segmented along the y-axis, and the difference between the maximum and minimum values in the x-axis direction of each segment was calculated as its horizontal width. The center point of each segment point cloud was used to fit the slope of the stem centerline, and the average horizontal width was corrected to the stem diameter. The test results show that the average measurement error is only 2.7 mm, the average relative error was 1.34%, and the measurement time is only about 300 ms. It could provide an effective solution for the automatic and rapid measurement of stem width of banana plants and other similar plants.

1. Introduction

Banana is one of the four largest fruits in the world and occupies an extremely important position in the world [1]. However, the management of banana plantation is still extensive. If the plant phenotype of banana plants can be extracted and applied to farm management, it will be of great significance for banana production efficiency and yield. The main body of banana plant is mainly composed of corms (true stems), pseudostems, leaves, and roots. Pseudostems mainly transport and store nutrients for leaves and fruits. The stem width or diameter of pseudostems largely determines the nutrient transport and supply capacity of the plant, and it is also related to the yield of the plant. Therefore, this study takes the pseudostem of banana plant as the measurement object and studies a rapid, automatic, and accurate method to measure the width of banana pseudostem, so as to guide scientific planting.

For the width measurement of banana pseudostem, the traditional method is generally manual measurement. The tools used include ruler, hand-held laser rangefinder and other tools, or equipment, which not only contains certain subjective factors but also takes time and effort. With the continuous development of technology, binocular vision, depth camera, laser scanning, 2D/3D LIDAR, CT, MRI, and other measurement technologies emerge endlessly. Because these technologies have the advantages of accuracy, speed, and low labor cost, they are widely used in the study of crop phenotypic feature extraction. Although laser scanners, CT, MRI, and other equipment have high advantages in accuracy

or penetrability, they are also expensive; comparatively speaking, low-cost three-dimensional imaging devices such as binocular vision and depth sensor have also attracted more and more attention in agricultural research scenes such as fruit recognition and field plant phenotype measurement [2]. Researchers at home and abroad have also carried out a lot of research on low-cost three-dimensional imaging devices.

In recent 20 years, binocular vision based on stereo matching algorithm has been widely used in fruit recognition [3–5] and agricultural machinery navigation [6–8]. However, binocular vision has the problems of weak anti-interference, low matching accuracy, complex algorithm, and slow processing speed in the complex field environment, and there are some limitations and deficiencies in its application.

Based on the principle of laser ranging, Kinect V2 sensor can quickly obtain the color and three-dimensional point cloud data of the measured object. Compared with binocular vision, the Kinect sensor has low cost and strong resistance to environmental interference. At present, many researchers use it in the agricultural field to obtain plant phenotypic parameters and detect agricultural products [9–11]. Adar et al.[12] compared the current low-cost 3D imaging systems and concluded that the low-cost 3D imaging equipment can replace the laser scanner in many plant phenotype analysis scenes. Yamamoto et al. [13] designed a three-dimensional reconstruction method of apple using the Kinect depth sensor and estimated the fruit volume. Bao et al. [14] developed a noncontact automatic 3D robot blade detection system, which uses Kinect V2 sensor, high-precision 2D laser profiler, and six-axis robot manipulator to realize the automation of blade detection tasks. Hu et al. [15] proposed a nondestructive automatic growth measurement system for leafy vegetables based on Kinect. The system was used to obtain the precise three-dimensional model of the tested plants, and the key phenotypic parameters of the plants were measured according to the acquired model.

Because the banana plant is tall, the pseudostem is similar to the trunk, and the diameter is also large; the required measurement accuracy is not harsh, so it is very suitable to use low-cost Kinect series sensors for measurement. Therefore, in this study, Kinect V2 was used to obtain the three-dimensional point cloud data of banana pseudostems, and a point cloud data analysis and processing method were proposed to quickly calculate the pseudostem stem width, providing support for further prediction of banana crop growth and yield.

2. Materials and Methods

2.1. Experimental Data Collection. The image acquisition site of banana pseudostem point cloud is located in a banana plantation covering an area of 1800 mu in Guangxi subtropical agricultural science new city in Fusui County. During the experiment, it is in the fruit development period of banana. The spacing between each plant is about 0.5 m, and the spacing between rows is about 2 m. Data collection is carried out using the vehicle mounted field operation platform (as shown in Figure 1) composed of Kinect V2 sensor, Dell Precision 7530 Mobile Workstation (Intel-i9 CPU, 32 GB high-speed memory, NVIDIA QuADro P2000 graphics card), 220 V portable emergency energy storage power supply (2 pieces), and Beno KH25 tripod. Main parameters of Kinect V2 sensor are shown in Table 1.

Figure 1: Field operation platform.

The shooting time of the experiment is from 9 a.m. to 5 p.m. By installing Kinect V2 on the vehicle mobile platform through a tripod, and moving at a speed of 8 m/s at a distance of 1.5 m from the ground height and 1 m from the banana pseudostem, the Kinect V2 is always aligned with the center of the banana pseudostem at a distance of 1 m by adjusting the wheel direction of the operation platform, to obtain the depth image and color image of the banana pseudostem. Five rows of banana plants were selected for mobile measurement. Some banana plants were randomly selected, and the resolution was 0 A. 01 mm digital vernier caliper was used to manually measure the diameter of the pseudostem at a height of 1 m. The gray value of each pixel in the depth image (Figure 2(a)) represents the linear distance from the measured point to the sensor. The color image (Figure 2(b)) was captured by the Kinect V2 internal integrated color camera.

2.2. Point Cloud Data Preprocessing. Before banana pseudostem estimation, the original data need to be preprocessed in order to effectively extract the measured banana pseudostem, reduce the measurement error, and improve the measurement speed. Preprocessing mainly includes four steps: ROI recognition, ROI extraction, conversion to point cloud, normal vector correction, voxel down-sampling, and point cloud filtering. The corresponding pretreatment process is shown in Figure 3.

2.2.1. ROI Extraction from Depth Images Based on Cascaded Classifiers. Other background information in the collected original image, such as non-measured banana plants and fallen leaves, will interfere with the measurement. At the same time, the accuracy of the edge region of the depth image is also relatively low. At the same time, if all the information in the original data is transformed into color point cloud, and then the banana pseudostem is extracted by conditional filtering, a large amount of unnecessary

Table 1: Key parameters of Kinect V2 sensor.

Parameter	Value
RGB color image resolution	1920×1080
Depth (infrared) image resolution	512×424
Frame rate (FPS)	30 fps
Horizontal field angle	70 degrees
Vertical field angle	60 degrees
Detection range	0.5~4.5 m

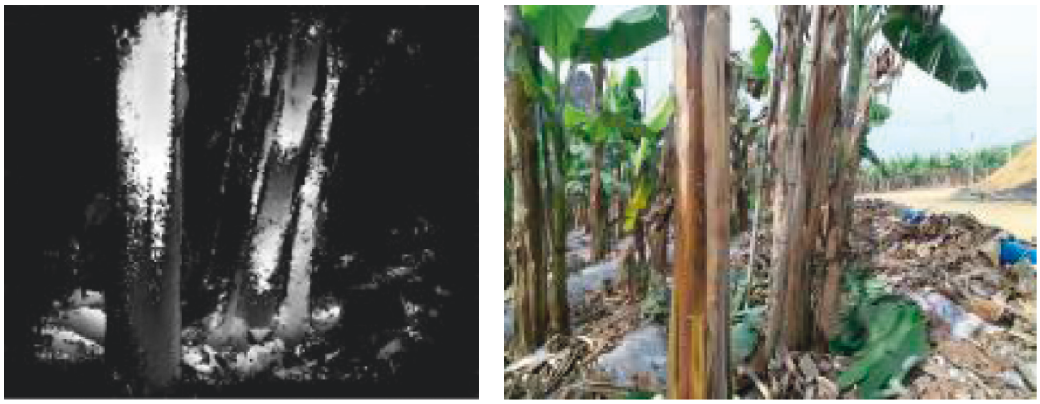

(a) (b)

Figure 2: Images obtained by Kinect V2. (a) Depth image. (b) RGB image.

information will be introduced, resulting in too long processing time and affecting the real-time performance. Therefore, the region of interest (ROI) of banana pseudostem can be extracted from the depth image. Only ROI part is converted to color point cloud, as shown in Figure 4. This method can effectively remove the background information and has good real-time performance with short processing time.

Considering that the angle, orientation, and distance of each shot are not fixed, the range of ROI is not fixed. Therefore, it is necessary to recognize the collected depth image and determine the ROI range containing banana pseudostems. In this study, 500 banana pseudostem depth image samples were randomly classified into training set and test set, including 250 training set and 250 test set samples. In this study, the banana pseudostem model is trained and recognized by cascade classification. The training samples include 250 positive samples and 500 negative samples. The positive samples are the depth images of banana pseudostems obtained by cutting the training and samples, and the negative samples are the depth images with the main body as the background obtained by random cutting. Because the pseudostems of banana crops are cylindrical and tightly wrapped by leaf sheaths, their toughness is poor, and their shape is usually straight. Although they are prone to slight inclination, they rarely bend significantly. Therefore, rectangles can be used to approximate the main body of pseudostems; both positive and negative samples are intercepted by a rectangle with an aspect ratio of 2 : 1. The classifier tool in OpenCV is used to train the positive and negative samples.

In the training process, the classifier will first extract the LBP features of the disparity map of the training samples. LBP is a feature that describes the local texture of an image and has the advantages of rotation invariance and gray invariance [16]. LBP operator is defined in 3×. In the window of 3, the central pixel is compared with the surrounding 8 pixels. The value of the pixel greater than the central pixel is assigned as 1, and the value of the pixel less than the central pixel is assigned as 0, to generate a new 8-bit binary number, and then it is converted it into a decimal number to replace the central pixel value. The training process of strong classifier is shown in Figure 4. First, the data and data weight wi are used to train the weak classifier, and one weak classifier is trained in each iteration. The trained weak classifier continues to participate in the next iteration. The weak classifier can be regarded as a feature trainer of LBP. Each simple feature corresponds to a weak classifier. After n weak classifiers are obtained, a strong classifier can be obtained by taking sign after linear combination through formula (1) [17]. The strong classifier training process schematic diagram is shown in Figure 5.

$$H(x) = \operatorname{sign}\left[\sum_{t=1}^{T} \alpha_t h_t(x)\right], \tag{1}$$

where t is the sequence number of the weak classifier; X is LBP characteristic.

Furthermore, several strong classifiers are concatenated to get the final cascade classifier model. The cascade classifier trained in this study contains 10 strong classifiers, and its model structure is shown in Figure 6. The images to be tested

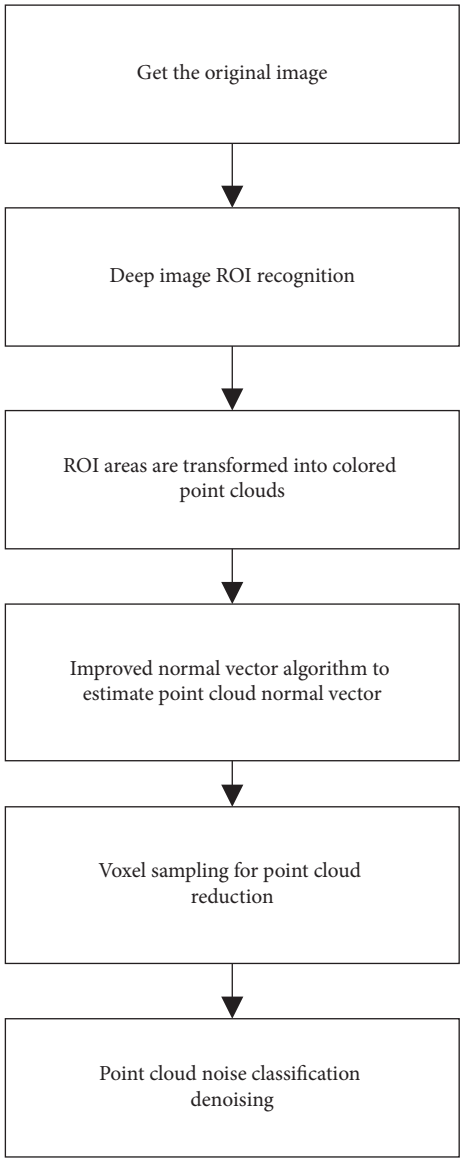

Figure 3: Point cloud pretreatment flow chart.

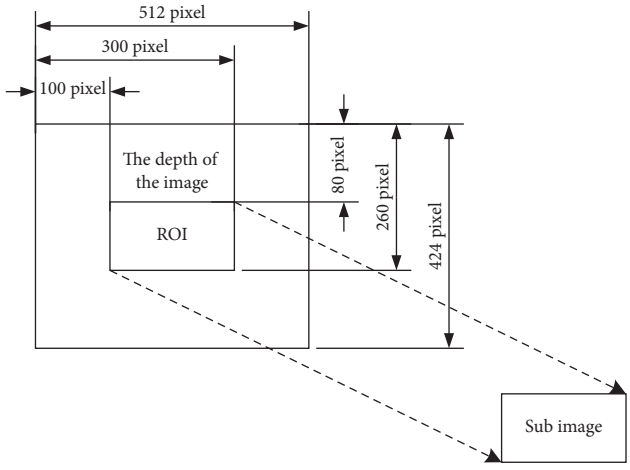

Figure 4: Schematic diagram of depth image ROI extraction.

must all meet the features of 10 strong classifiers in turn before they can be identified as banana pseudostems. The banana pseudostems are marked, and the corresponding ROI boundary is obtained. The identified ROI results are shown in Figure7(a). The recognition rate of banana pseudostem by this method is 92.3%, and the accuracy can be further improved if the number of effective samples is increased in the later stage.

2.2.2. Convert Depth Image to Color Point Cloud. The depth image belongs to the pixel coordinate system, as shown in Figure 8(a). Each point in the image is represented by (Ui, Vi). Since the coordinates in the pixel coordinate system only contain the row and column information of the pixel, it has no physical meaning. Therefore, this study also needs to establish an image coordinate system X-Y with the meaning of actual physical dimensions, as shown in Figure 8(b).

Let the origin coordinate in the image coordinate system be Oi, and the coordinates in the pixel coordinate system be ($U0$, $V0$). dx and dy represent the actual physical size of each pixel. The x- and y -axes are parallel to the u- and v -axes, respectively. The pixel coordinate system is converted to the image coordinate system by the following formula:

$$\begin{bmatrix} x \\ y \\ 1 \end{bmatrix} = \begin{bmatrix} dx & 0 & -u_0 dx \\ 0 & dy & -v_0 dy \\ 0 & 0 & 1 \end{bmatrix} \begin{bmatrix} u \\ v \\ 1 \end{bmatrix}. \tag{2}$$

The image coordinate system is converted to the spatial coordinate system corresponding to Kinect V2, as shown in Figure 8(c).

The midpoint m in the figure is an imaging point in the image coordinate system, and the corresponding coordinates are (x, y). Then, the coordinate point m' in the corresponding spatial coordinate system is (x_c, y_c, z_c), f is the focal length of the camera, and the depth value of point m is d. According to the principle of similar triangles, the following formula can be obtained:

$$\begin{aligned} \frac{f}{z_c} &= \frac{x}{x_c} \\ &= \frac{y}{y_c}. \end{aligned} \tag{3}$$

Then, it can be deduced that

$$\begin{bmatrix} x_c \\ y_c \\ z_c \end{bmatrix} = \begin{bmatrix} \frac{z_c}{f} & 0 & 0 \\ 0 & \frac{z_c}{f} & 0 \\ 0 & 0 & z_c \end{bmatrix} \begin{bmatrix} x \\ y \\ 1 \end{bmatrix}. \tag{4}$$

So far, the conversion relationship between the image coordinate system and the spatial coordinate system has been established. Through equations (2) and (4), the conversion relationship between the pixel coordinate system and the spatial coordinate system can be obtained as follows:

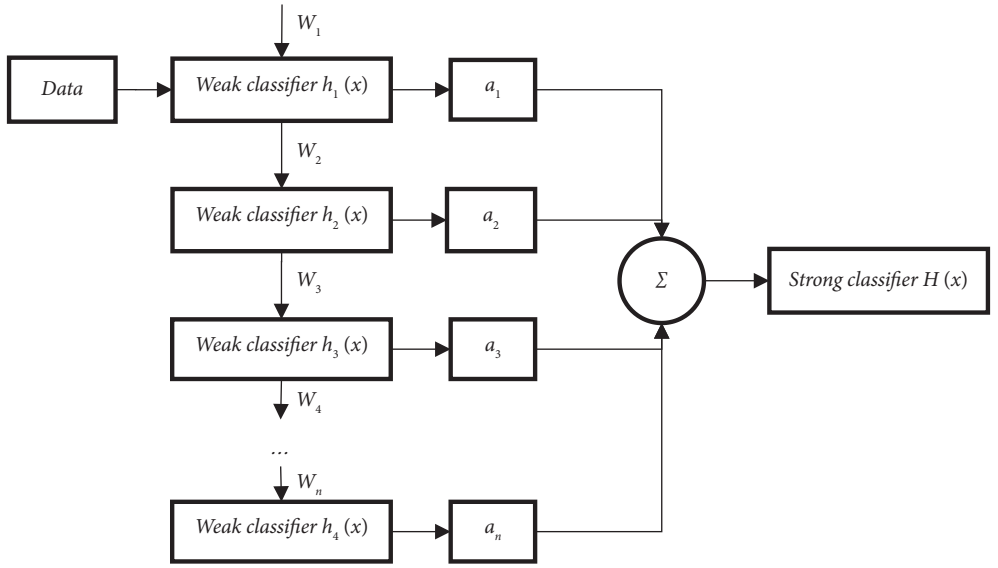

Figure 5: Strong classifier training process.

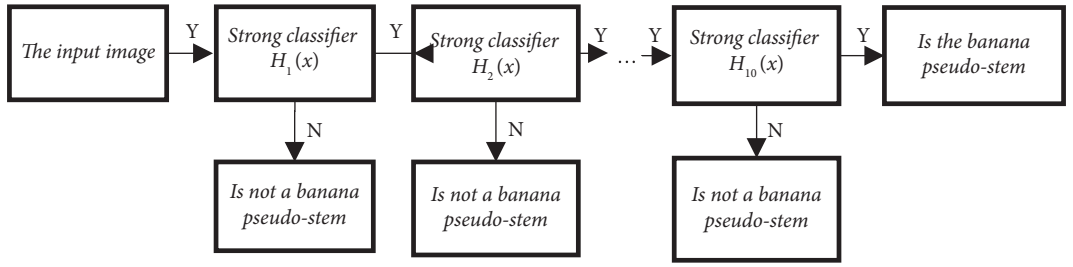

Figure 6: Cascade classifier flowchart.

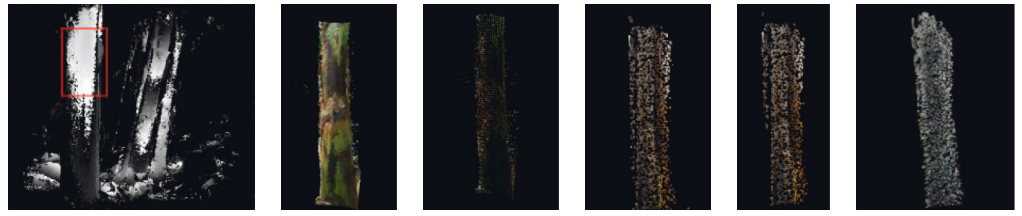

Figure 7: Results of the point cloud for each pretreatment step. (a) ROI recognition. (b) To a point cloud. (c) Voxel down-sampling. (d) Statistical filtering. (e) Radius filtering. (f) Bilateral filtering.

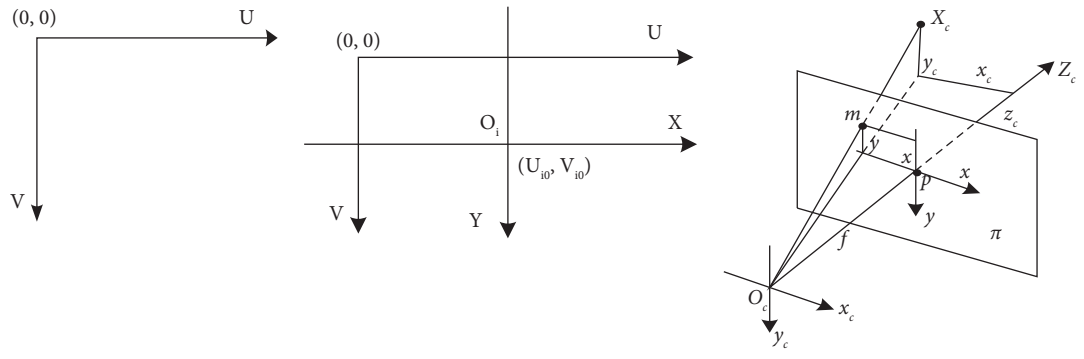

Figure 8: Coordinate transformation relationship. (a) Pixel coordinate system 7. (b) Image coordinate system 7. (c) Spatial coordinate system.

$$\begin{bmatrix} x_c \\ y_c \\ z_c \end{bmatrix} = \begin{bmatrix} \frac{z_c}{f} & 0 & 0 \\ 0 & \frac{z_c}{f} & 0 \\ 0 & 0 & z_c \end{bmatrix} \begin{bmatrix} dx & 0 & -u_0 dx \\ 0 & dy & -v_0 dy \\ 0 & 0 & 1 \end{bmatrix} \begin{bmatrix} u \\ v \\ 1 \end{bmatrix}. \quad (5)$$

Therefore, the ROI extracted from the depth image can be transformed into the spatial coordinate system by equation (5). Since Kinect V2 has been calibrated before leaving the site, internal parameters can be called through API, and color point cloud can be generated through PCL in combination with color information. The result of converting ROI to point cloud is shown in Figure 7(b).

2.2.3. Point Cloud Normal Vector Correction. As a basic morphological feature of point cloud, the quality of normal vector will have a significant impact on the subsequent point cloud dilution, point cloud smoothing, and point cloud computing. At present, the commonly used point cloud normal vector estimation method is the key component analysis method based on point cloud local covariance analysis. V is set as the whole point cloud set, and a point in the point cloud $m_i \in V$ and its set of k nearest neighbors (hereinafter referred to as K neighborhood) $N(m_j)$ are given, and the following covariance matrix C can be constructed:

$$C = \frac{1}{k} \sum_{m_i \in N(m_j)} (m_i - \overline{m})(m_i - \overline{m})^T, \quad (6)$$

where $\overline{m} = 1/k \sum_{i=1}^{k} m_i$ is the centroid of the neighborhood of m_i point K.

Through eigen root decomposition of the covariance matrix C, the eigenvector of the corresponding minimum eigen root is the approximate value of the normal phasor at point MI. Although the covariance analysis method has certain anti-interference ability, its anti-interference ability decreases obviously when the point cloud noise is too complex. Therefore, the Gaussian weight function method is added to the original covariance matrix to smooth the vector, and the following expression is obtained.

$$C = \frac{1}{k} \sum_{m_i \in N(m_j)} e^{-\|m_i - \overline{m}\|^2/\sigma^2} (m_i - \overline{m})(m_i - \overline{m})^T, \quad (7)$$

where $\|\cdot\|$ represents the modulus of a vector and σ is a point cloud density parameter, and the corrected normal vector information can be obtained by eigenvalue decomposition. Normal vectors before and after improvement are shown in Figure 9.

Kinect V2 is used to collect the wall point cloud, and the traditional normal vector estimation method and the improved normal vector estimation method are used to estimate the normal vector, respectively. Through observation, it is found that the improved normal vector becomes more uniform on the point cloud model, and the divergence direction tends to be more consistent, which makes the subsequent down-sampling and bilateral filtering process more efficient and accurate.

2.2.4. Voxel Down-Sampling. Because this study mainly measures the stem width of banana pseudostem, too dense point cloud will reduce the measurement accuracy and real-time performance. Therefore, this study carries out voxel down-sampling on the point cloud to achieve point cloud dilution. Voxel refers to a three-dimensional image with a side length of λ pixel cube, and voxel downsampling is mainly based on the side length λ. Voxel downsampling is mainly to decompose voxels into several small voxel grids with side length λ according to a certain ratio according to the size of side length λ/k. The improved normal vector estimation is carried out for each small voxel cube, and the corresponding center of gravity is estimated. Only the center of gravity and the nearest original point are retained, to approximately represent all points in the whole voxel. While protecting the detailed information of the point cloud, the point cloud is simplified. Through down-sampling, the number of point clouds decreased from 13655 to 3814, a decrease of 72%. The processed results are shown in Figure 7(c).

2.2.5. Point Cloud Filtering. Due to the equipment itself, operator experience, measurement environment, and other factors, a lot of noise will be generated in the process of point cloud data acquisition. Therefore, it is necessary to filter the point cloud before measurement. According to the specific situation of this study, this study proposes a method of noise reduction by classification of large-scale and small-scale noise. Large-scale noise refers to the small and dense point cloud, which is far away from the center of the main point cloud and the sparse points, which are suspended above the main point cloud and deviate from the main point cloud. It has the characteristics of large amplitude and high frequency. Small size noise refers to some irregular data points entangled with the main point cloud. Compared with the single filtering method, the classification noise reduction method used in this study can achieve better noise reduction effect.

(1) Large Size Noise Removal. In this study, the combination of statistical filtering and radius filtering is used to remove large-scale noise. Statistical filtering [16] means that for any point, the average distance between the point and other points in the k field is calculated, and the distribution of the results is assumed to follow the Gaussian distribution. Calculate the mean $\mu$and standard deviation σ of the distance between this point and its points in the neighborhood of K.Keep the points that are within the range of $(\mu - \sigma, \mu + \sigma)$. Radius filtering means that for a certain subject point p in the point cloud data, it is considered that at least M points should exist in the neighborhood with radius r of the subject point; otherwise, it will be determined as discrete points and deleted. The corresponding statistical filtering and radius filtering effects are shown in Figures 7(d) and 7(e).

(2) Small Size Noise Smoothing. Bilateral filtering is a common method in image filtering, which has been extended to 3D point cloud data model filtering. The bilateral

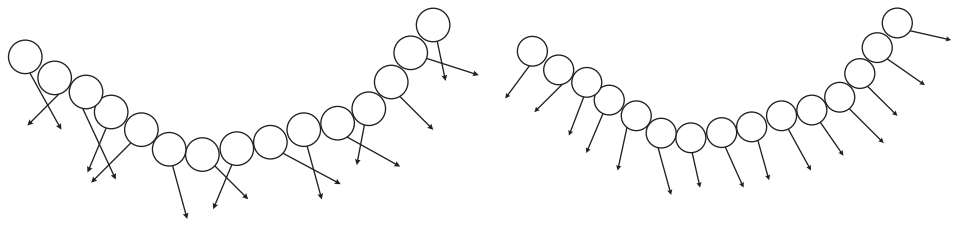

(a) (b)

Figure 9: Schematic diagram of normal vectors before and after improvement. (a) Before improvement. (b) After improvement.

filtering of 3D point cloud data model is to move the noise points along the direction of their normal vector and constantly adjust the position and coordinates of the noise points to smooth the small-scale noise [18].

The expression of bilateral filtering is shown as follows:

$$p_i^{'} = p_i + \alpha \cdot n, \tag{8}$$

where $p_i^{'}$ is the filtered point, p_i is the original data point, α is the bilateral filter factor (as shown in (9)), and n is the normal vector of point p_i.

$$\alpha = \frac{\sum_{p_j \in N(p_i)} W_c\left(\| p_i - p_j \|\right) W_s\left(\| \langle n_i, n_j \rangle - 1 \|\right) \langle p_i - p_j, n_j \rangle}{\sum_{p_j \in N(p_i)} W_c\left(\| p_i - p_j \|\right) W_s\left(\| \langle n_i, n_j \rangle - 1 \|\right)}. \tag{9}$$

In equation (9), p_j is the neighborhood point of the data point p_i; $\| \cdot \|$represents the module of the vector; $\langle \bullet \rangle$ represents the inner product of the vector; n_i is the normal vector of point p_i on the point cloud; and n_j is the normal vector of the adjacent point p. $W_c(x)$ and $W_s(y)$ are smoothing filter weight function (equation (10))and feature preserving weight function (equation (11)), respectively; σ_c and σ_s represent the filtering parameters in the Gaussian weight function, which reflects the influence range of tangent and normal vectors when calculating the bilateral filtering factor of any sampling point.

$$W_c(x) = e^{\left[-x^2/\left(2\sigma_c^2\right)\right]}, \tag{10}$$

$$W_s(\mathrm{y}) = \mathrm{e}^{\left[-y^2/\left(2\sigma_s^2\right)\right]}. \tag{11}$$

The bilateral filtering process is as follows:

(1) For point cloud data points, the k neighborhood is determined by p_i, and the normal vectors corresponding to all points in the neighborhood are solved by the improved normal vector method.

(2) The smoothing filter function $W_c(x)$ parameter $x = \| p_i - p_j \|$ of data point p_i (distance between data point p_i and p_j) and feature retention weight function $W_s(y)$ parameter $y = \| \langle n_i, n_j \rangle - 1 \|$ (the inner product of the angle between the normal vector between point p_i and p_j) are solved. Combined with equations (9)–(11), the improved bilateral filter factor is solved α.

(3) The new coordinate p_i of the data point p_I' is calculated according to equation (8), and the point p_i is moved to p_I' coordinate.

The processed image is shown in Figure 7(f).

2.3. Estimation of Banana Pseudostem Width. Because the banana pseudostem is thick at the bottom and thin at the top, to reduce the measurement error, this study evenly segments the pretreated point cloud from top to bottom, measures the width of each segment of point cloud, sets the condition threshold for judgment and angle correction, and finally takes the average value to obtain the measurement results. The specific algorithm flow is as follows:

(1) The maximum and minimum value points of the pretreated point cloud in the y-axis (height) direction are searched and marked as $Y_{\max}$ and $Y_{\min}$.

(2) The point cloud is divided into n segments from bottom to top along the y-axis.

(3) Each segmented point cloud is queried separately, the maximum value point and minimum value point in the x-axis (width) direction are searched, and they are recorded as $(X_{i\_\max}, Y_{i\_\max})$ and $(X_{i\_\min}, Y_{i\_\min})$. It can be obtained that the width L_i of the point cloud of segment i in the x-axis direction is as follows:

$$L_i = X_{i\_max} - X_{i\_min}. \tag{12}$$

(4) The width of pseudostem is easily affected by withered leaves on the stem, resulting in great changes in the width of some segments. To filter out this effect, the banana pseudostem range thresholds $L_{\max}$ and $L_{\min}$ and the banana pseudostem offset threshold δ are set. Whether L_i satisfies equation (13) at the same time is judged, and if so, it will be recorded as the effective value. This segment of point cloud is called the effective point cloud. By traversing L_i, we get N valid values

$$\begin{cases} L_{\min} \le L_i \le L_{\max} \\ \left|L_i - L_{i-1}\right| \le \delta \\ \left|L_i - L_{i+1}\right| \le \delta \end{cases}. \tag{13}$$

(5) The average value L_{avg} of n effective point cloud widths L_i is found as the average width in the horizontal direction of banana stem.

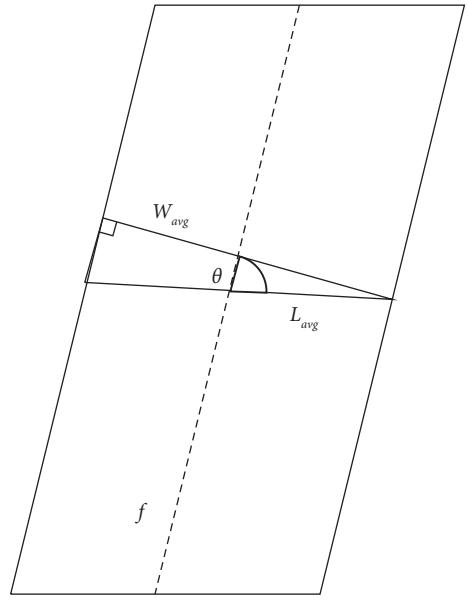

Figure 10: Schematic diagram of angle correction.

Table 2: Measurement results at different distances.

Measuring distance (m)	Measured average value (mm) (average value of manual measurement = 199.8 mm)	Correlation coefficient r between sensor and manual measurement results	Mean absolute error (mm)	Mean value of relative error (%)
0.5	198.9	0.987	2.7	1.34
0.7	196.7	0.949	5.9	2.89
0.9	189.5	0.982	10.3	5.25
1.0	183.8	0.977	16.0	8.35

(6) Since banana pseudostems are inclined to some extent during the growth process, the horizontal span value of each stem point cloud calculated in the previous step is not equal to the diameter of the stem, so the width obtained in step 5 needs to be corrected (see Figure 10 for the schematic diagram). First, the midpoint coordinates (X_{i_mid}, Y_{i_mid}) of each effective point cloud on the X- and Y-axes according to equation (14)are calculated; The center line f of the stem was fitted according to the midpoint coordinates of N effective point clouds, and the inclination Angle θ between the center line f and the X-axis was calculated. The tilt Angle θ of center line f is the tilt of banana pseudostem finally, the vertical section width W_{avg} of the stem is calculated by equation (15).

$$\begin{cases} X_{i\_mid} = \dfrac{(X_{i\_max} + X_{i\_min})}{2} \\ \\ Y_{i\_mid} = \dfrac{(Y_{i\_max} + Y_{i\_min})}{2} \end{cases}. \tag{14}$$

$$W_{avg} = L_{avg} \sin\theta. \tag{15}$$

3. Results and Discussion

The measurement results at different distances are shown in Table 2 and Figure 11. It can be seen that under different distances, the correlation coefficient r between the stem width measured by the sensor and the manual measurement results basically reaches more than 0.95. The lowest error occurs at a distance of 0.5 m, where the mean absolute error is 2.68 mm and the mean relative error is 1.34%; the overall error increases obviously with the increase in the measurement distance, and the average relative error at the distance of 1.0 m is as high as 8.35%. It shows that the measurement accuracy of Kinect V2 sensor is obviously affected by distance. In addition, it can be seen from the measurement results that the average value of the sensor decreases gradually with the increase in the distance; that is, compared with the average value of manual measurement, the farther the distance, the greater the negative measurement error of the sensor. This is mainly due to the thinning of the beam quantity projected by Kinect V2 onto the banana pseudostem, resulting in the measured value of the sensor being gradually lower than the manual measured value.

Through comprehensive analysis, the main causes of measurement errors are as follows: (1) the uneven surface of banana pseudostem leads to inevitable errors in manual measurement; (2) the structure of Kinect V2 sensor causes the measurement accuracy to decrease gradually with the

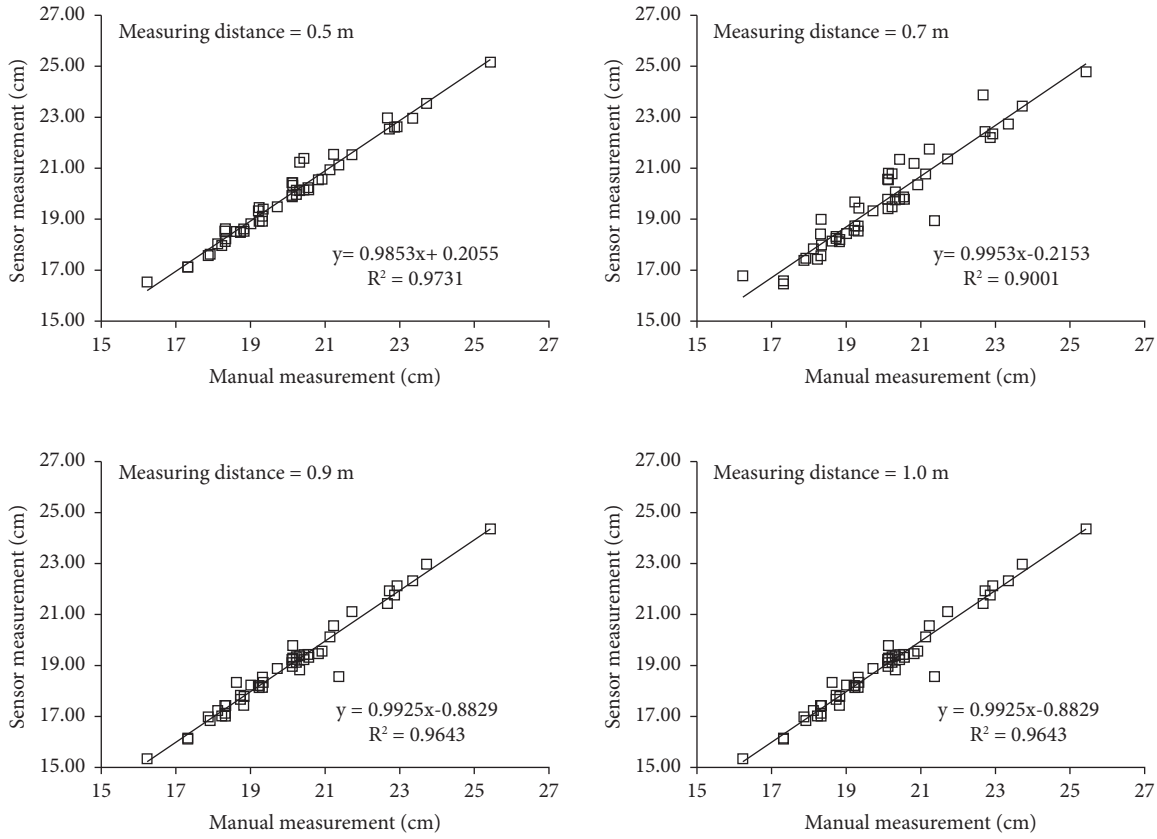

Figure 11: Result comparison between sensor and manual measurement.

increase in distance, resulting in systematic error. In addition, in terms of processing speed, ROI recognition time is 100 ms, point cloud conversion time is about 50 s, downsampling time is about 50 ms, combined filtering time is about 80 ms, measurement time is about 100 ms, and the total measurement time is about 300 ms.

4. Conclusion

(1) Compared with the method of converting the depth image into point cloud and then adjusting the x-, y-, and z-axes, the method of using cascade classifiers to recognize ROI from the depth image and then convert ROI into point cloud greatly shortens the measurement time and improves the measurement accuracy.

(2) By improving the method of point cloud normal vector estimation, the normal vector obtained by estimation is more uniform and smooth, and the measurement accuracy is improved.

(3) According to the difference in the size of point cloud noise, the point cloud is classified into large-scale and small-scale noise. The large-scale noise is removed by statistical filtering and radius filtering, and the small-scale noise is smoothed by bilateral filtering. This method can remove the noise more effectively by differentiating the point cloud noise. Comparing the data before and after the point cloud filtering, the average absolute error is reduced by 35.33 mm and the average relative error is reduced by 17.68% after the point cloud filtering at 0.5 m. The experimental results show that the combined filter has a good effect on noise removal.

(4) According to the characteristics of banana stem, the stem point cloud is divided into n segments from bottom to top, and the span of each segment in the x-axis is obtained and averaged to reduce the measurement error; the stem width was corrected by fitting the stem centerline with the approximate center point to obtain the inclination angle of the stem. The average absolute error is 5.4 mm and the average relative error is 2.70% by comparing the data before the angle correction with the manual measurement data at 0.5 m; the measurement accuracy is improved by 2.7 mm after comparison and correction. At 0.7 m, the average absolute error is 8.8 mm and the average relative error is 8.80% compared with the manual measurement data; the measurement accuracy is improved by 2.9 mm after comparison and correction. It is found that the angle correction is closer to the manual measurement value. The measurement method has high accuracy, can meet the needs of plant stem measurement under a reasonable measurement distance, and can provide technical support for the extraction of key growth parameters of banana plants.

(5) The detection method proposed in this study is not only limited to the detection of banana false stem but also can be applied to the detection of tree stem and other fields. The experimental results show that the method has better measurement speed and accuracy. In the industrial field, the method can also quickly and accurately detect the width and diameter of columnar objects such as telegraph poles. However, the method adopted in this study also has some limitations. This method is not suitable for some small objects and some areas that need accurate measurement, which will lead to excessive relative errors. At the same time, due to the use of active light source to obtain data, it is not suitable for the measurement of transparent, translucent, and reflective objects, which will reduce the measurement accuracy in the strong lighting environment. [19–25].

Data Availability

The dataset can be accessed upon request.

Conflicts of Interest

The authors declare that they have no conflicts of interest.

Acknowledgments

This work received National Natural Science Foundation of China (31760342); Guangxi Science and Technology Major Special Fund Project (guike aa18118037); and Independent Research Project of Guangxi Key Laboratory of Sugarcane Biology.

References

[1] J. Li, X. Li, and Z. Sun, "Analysis of influencing factors of large price fluctuation of bulk fruit in China -- based on price data of apple, pear and banana," *Journal of Hunan Agricultural University*, vol. 19, no. 3, pp. 15–23, 2008.

[2] S. Paulus, J. Behmann, A. K. Mahlein, L. Plumer, and H. Kuhlmann, "Low-cost 3D systems: suitable tools for plant phenotyping," *Sensors*, vol. 14, no. 2, pp. 3001–3018, 2014.

[3] L. Luo, X. Zou, M. Ye et al., "Solution and positioning of anti-collision spatial enveloping body for grape picking based on binocular stereoscopic vision," *Journal of Agricultural Engineering*, vol. 32, no. 8, pp. 41–47, 2016.

[4] B. Li, H. Wang, W. Huang, and C. Zhang, "Construction and field experiment of low-cost binocular vision platform for pineapple harvesting machinery," *Journal of Agricultural Engineering*, vol. 28, no. S2, pp. 188–192, 2012.

[5] M. Ye, X. Zou, L. Luo et al., "Dynamic positioning error analysis of binocular vision of litchi picking robot," *Journal of Agricultural Engineering*, vol. 32, no. 05, pp. 50–56, 2016.

[6] G. Tian, An Qiu, C. Ji, B. Gu, H. Wang, and J. Zhao, "Simultaneous positioning and map creation of intelligent agricultural vehicles based on Gray-EKF algorithm," *Journal of Agricultural Engineering*, vol. 28, no. 19, pp. 17–25, 2012.

[7] F. Xu, L. Zhang, M. Ji, Y.-H. ', X. Zhang, and L. Zhang, "Progress in the realization and application of vision sensing system for agricultural robots," *Journal of Agricultural Engineering*, vol. 04, pp. 180–184, 2002.

[8] Z. Zhai, Z. Zhu, Y. Du, and S. Zhang, "A line recognition method for binocular visual crops based on Census Transformation," *Journal of Agricultural Engineering*, vol. 32, no. 11, pp. 205–213, 2016.

[9] Q. Su, N. Kondo, M. Li, H. Sun, D. F. Al Riza, and H. Habaragamuwa, "Potato quality grading based on machine vision and 3D shape analysis," *Computers and Electronics in Agriculture*, vol. 152, pp. 261–268, 2018.

[10] F. Skerik, J. Volf, and M. Linda, "Methods for detection of objects in agriculture, prague," in *Proceedings of the Conference Proceding-5th International Conference, TAE 2013: Trends in Agricultural Engineering*, pp. 599–601, Czech University of Life Sciences Prague, Prague, Czechia, September 2013.

[11] G. Sun, Y. Li, Y. Zhang et al., "Nondestructive measurement method for greenhouse cucumber parameters based on machine vision," *Engineering in Agriculture, Environment and Food*, vol. 9, no. 1, pp. 70–78, 2016.

[12] A. Vit and G. Shani, "Comparing RGB-D sensors for close range outdoor agricultural phenotyping," *Sensors*, vol. 18, no. 12, p. 4413, 2018.

[13] S. Yamamoto, M. Karkee, Y. Kobayashi et al., "3D reconstruction of apple fruits using consumer-grade RGB-depth sensor," *Engineering in Agriculture, Environment and Food*, vol. 11, no. 4, pp. 159–168, 2018.

[14] Y. Bao, D. S. Shah, and L. Tang, "3D perception-based collision-free robotic leaf probing for automated indoor plant phenotyping," *Transactions of the ASABE*, vol. 61, no. 3, pp. 859–872, 2018.

[15] Y. Hu, L. Wang, L. Xiang, Q. Wu, and H. Jiang, "Automatic non-destructive growth measurement of leafy vegetables based on Kinect," *Sensors*, vol. 18, no. 3, p. 806, 2018.

[16] K. Zhao, Li Guoqiang, and D. He, "Fine segmentation method of cow body region in depth image based on machine learning," *Journal of agricultural machinery*, vol. 48, no. 4, pp. 173–179, 2017.

[17] F. Xiaojian and M. Ma, "Wang Deyu Face detection system based on improved AdaBoost algorithm," *Computer technology and development*, vol. 29, no. 3, pp. 89–92, 2019.

[18] D. Lu and J. Zuo, "Comparative study on noise reduction algorithm of 3D laser point cloud," *Bulletin of Surveying and Mapping*, vol. 2, pp. 102–105, 2019.

[19] Y. Gong and Z. Lv, "Point cloud data preprocessing method based on bilateral filtering," *Mapping and Spatial Geographic Information*, vol. 39, no. 1, pp. 125–127, 2016.

[20] M. Soltani, "Utilization of binary PSO algorithm and DDA method to investigate the plasmonic demultiplexer -based CPA filter," *Optik*, vol. 156, pp. 968–974, 2018.

[21] X. Chen, Y. Chen, K. Gupta, J. Zhou, and H. Najjaran, "SliceNet: a proficient model for real-time 3D shape-based recognition," *Neurocomputing*, vol. 316, pp. 144–155, 2018.

[22] G. Azzari, M. Goulden, and R. Rusu, "Rapid characterization of vegetation structure with a microsoft Kinect sensor," *Sensors*, vol. 13, no. 2, pp. 2384–2398, 2013.

[23] T. T. Nguyen, K. Vandevoorde, N. Wouters, E. Kayacan, J. G. De Baerdemaeker, and W. Saeys, "Detection of red and bicoloured apples on tree with an RGB-D camera," *Biosystems Engineering*, vol. 146, pp. 33–44, 2016.

[24] J. Zhang, X. Wang, Q. Zhang, Y. Chen, J. Du, and Y. Liu, "Integral imaging display for natural scene based on KinectFusion," *Optik*, vol. 127, no. 2, pp. 791–794, 2016.

[25] F. Lu, B. Zhou, F. Lu, Y. Zhang, X. Chen, and Q. Zhao, "Reconstructing non-rigid object with large movement using a single depth camera," *Computer Aided Geometric Design*, vol. 64, pp. 15–26, 2018.

Hindawi
Computational Intelligence and Neuroscience
Volume 2022, Article ID 1848822, 11 pages
https://doi.org/10.1155/2022/1848822

Research Article

Research on the Linkage Mechanism between Migrant Workers Returning Home to Start Businesses and Rural Industry Revitalization Based on the Combination Prediction and Dynamic Simulation Model

Xiaogang Wang

College of Management, Henan University of Technology, Zhengzhou 450052, China

Correspondence should be addressed to Xiaogang Wang; xgwang@haut.edu.cn

Received 23 August 2022; Accepted 7 September 2022; Published 26 September 2022

Academic Editor: Yaxiang Fan

Copyright © 2022 Xiaogang Wang. This is an open access article distributed under the Creative Commons Attribution License, which permits unrestricted use, distribution, and reproduction in any medium, provided the original work is properly cited.

Township and rural migrant workers are returning to the business personnel's main force. Party 18 proposed a rural revitalization strategy, and the central committee of the State Council issued a series of encouraging policy measures to bring them back. The study found that migrant workers' return-home entrepreneurship and the connection between the rural industries on the basis of factor resources flow are related. As a result, this study analyzed the practical situation of migrant workers' return-home entrepreneurship. Next, it used a combination forecast method and dynamic simulation model of the migrant workers' return-home entrepreneurship and revitalization of the relationship with the rural industry. The resuscitation of rural industries can be efficiently facilitated by the return of rural migrant workers to launch firms. Their success can attract more migrant workers to launch businesses. The total regeneration of rural areas and the prosperity of farmers can be achieved by effectively linking the return of migrant workers to launch businesses and the revival of rural industries.

1. Introduction

The rural rejuvenation strategy was presented in the 19th CPC National Congress report. The Strategic Plan for Rural Regeneration (2018–2022) was released by the CPC Central Committee and the State Council. It outlined a strategy for rural revitalization. Farmers play a crucial role and are the central focus of the rural revival strategy. Given the general demographic makeup of rural areas and the rural labor surplus, many agricultural workers migrate to cities yearly. The remaining rural workforce are generally older and less educated mainly because of the more traditional agricultural production and management. Therefore, agricultural modernization needs to rely on the existing rural labor force. Agricultural workers must be moved to towns and villages. In order to strengthen support for the revitalization of rural talents in China, the No. 1 document of the Central Government pointed out that it should be widely used to train new professional farmers, train professional talents, and make full use of scientific and technological talents. In order to promote "returning home," China has taken various measures to greatly increase farmers' enthusiasm to return home. Currently, many farmers participate in home-related entrepreneurial activities, and a new type of professional farmers is growing rapidly. Agricultural production is supported by the input of science and technology, personnel, and capital. In the key stage of building a well-off society in an all-round way, it is of great significance to formulate the rural reconstruction strategy to eliminate poverty and solve some employment problems. Accelerating the process of agricultural modernization, developing and expanding rural agricultural industry and culture, and improving the living conditions of rural residents positively influence the implementation of the agricultural revitalization strategy. The entrepreneurial spirit of migrant workers is more complex. In other words, there are an emotional attachment

to rural areas and a desire to increase family income, self-esteem, and other spiritual sustenance. Migrant workers believe that returning home to start businesses can not only fulfill the responsibility of taking care of the elderly and children, but also save unnecessary travel costs, which is a necessary choice in line with rational economic laws [1].

Combining many distinct forecasting techniques for the same topic is known as combined forecasting. It combines various quantitative and qualitative procedures and several quantitative ones. More significantly, it combines quantity and quality in practice [2]. The combined forecasting method offers certain benefits when looking at the mechanism linking migrant workers who return home to launch their own firms with the rehabilitation of rural industries. This study dynamically simulated the relationship between migrant workers who return home to start their own businesses and industrial revitalization and rejuvenation based on the interpretation of the current situation of migrant workers returning home to start their own businesses, combined with previous research and theoretical knowledge and combination prediction, using linear prediction combination. The study discovered that the link between migrant workers returning home to start businesses and the revitalization of rural industries is based on the flow of resources and is inextricably linked to human, economic, and social resources. Finally, it is concluded that we should lay a good foundation for rural industry revitalization, promote the system's balanced operation, enrich the main body, strengthen the interconnection, improve the mechanism, optimize the interaction of rural migrant workers, integrate high-quality resources, and constantly promote the implementation of the agriculture revitalization strategy. This study systematically analyzes the problems in the linkage process and puts forward some effective solutions and suggestions, which are conducive to the successful entrepreneurship of the returning migrant workers and attract more migrant workers to return to their hometowns to realize the prosperity of rural industry and the common prosperity of farmers.

2. Research Background

2.1. Overview of Combinatorial Prediction Algorithms. Bates and Granger were the first to propose the concept of combinatorial forecasting. Their starting point was an understanding of the challenges involved in creating realistic models. In order to address the issue of a single regression prediction model's weak compatibility, the combined prediction model can present information using a single prediction model and establish a more accurate and stable prediction model using the appropriate combination model *via* the weight coefficient and different methods. Portfolio forecasting is one of the most important forecasting research methods, which is widely used in business, society, and management [3].

When designing a combined prediction model, two aspects should be considered: the selection of the prediction model and the distribution of the model's weight [4]. Select individual forecasting models. Other researchers have analyzed the choice of a single forecasting model from qualitative and quantitative perspectives. From the qualitative point of view, according to the principles of applicability, diversity, and cost, the individual forecast model is considered; the appropriate individual forecast model is selected; and the objective, the nature of the forecast change, and the applicability of the individual forecast model are analyzed. The method of determining the number and weight of a single prediction model is also proposed [5]. The combined prediction model based on the difference algorithm is compared to the prediction model composed of the first prediction algorithm with the most effective prediction effect [6] by studying the difference algorithm and using it to select subprojects. The experimental results show that the model offset algorithm improves the combined model's prediction accuracy and approximate weight distribution. It is proposed to use a combined prediction model based on interval accuracy and the IOWA operator. If the value of the lens function is not differentiable, the weight is changed based on the shape. An example demonstrates the efficacy of combined forecasting. Zhang Yite applied the combined prediction algorithm to the fault prediction of the train control device and proposed a combined prediction method based on the cross-entropy theory [7]. Firstly, the K-nearest neighbor nonparametric regression model and the improved grey Ehrman neural network model are used for prediction analysis. Then, the cross-entropy theory is used for optimization, and the typical equilibrium model is selected for comparative analysis. Chen Yi studied the short-term combination prediction of electric power and wind farm, established the combination prediction model based on the optimal combination prediction model and the nonoptimal combination prediction model using the microselection algorithm model, and made a comparative analysis. Finally, it is concluded that, under the optimal combination, the combination prediction model selected by the algorithm is better than the nonoptimal combination prediction model [8]. Zhou Li used the entropy theory and ant colony algorithm to construct the weight of the combined prediction algorithm. Yu Jin mixed the flow prediction model based on the theory of the intelligent is studied. Based on the introduction of forecasting models based on gray system theory, the advantages of the combined forecasting model are investigated, and a combination of different algorithms to optimize prediction algorithm. On the basis of the combination model, the combination model of the agricultural product recommendation price algorithm is established, which improves the prediction accuracy and makes the algorithm more stable. According to the prediction theory based on reconstruction, a model combining the combined prediction method with the empirical decomposition model, least squares vector mechanism support, and the moving average model of the autoregressive integration was proposed [9].

2.2. Research Review of Migrant Workers Returning Home to Start Businesses and Rural Industry Revitalization. A literature survey on migrant workers returning to start

businesses was conducted in the early 1990s [10]. In 1994, the phrase "migrant workers returning home to start businesses" appeared in a national policy document for the first time. Scientific research shows a general trend from fragmentation to systematization compared to agricultural enterprise practices and policies. Related scientific studies can be divided into three categories: studies show that entrepreneurship has become one of the career choices of agricultural workers at the beginning of this century and the number of migrant workers increases at an annual rate of about 7% [11]. Entrepreneurship is an economic activity, which accurately identifies potential according to industry development, market conditions, and existing equipment and excavates potential to integrate resources and large-scale marketing to create value and achieve greater returns. Due to the idiosyncratic nature of personal devices, the entrepreneurial spirit of agricultural workers is complicated by their decision-making based on economic rationality and emotional attachment, such as emotional attachment to rural areas, desire to increase family income, and self-esteem [12]. Some scholars argue that returning farmers rely on resources and skills acquired through professional experience, a problem facing the countryside in recent years. Under the influence of reason and emotion, the farmers decided to return to their villages to do business. Compared with the past, the Communist Party Central Committee has reached a new level in helping farmers start their own businesses. A series of central documents emphasize that promoting the return of farmers to their hometowns should be one of the priorities. In addition, as a major group, the new generation of migrant workers have broader horizons, more solid knowledge and skill base, and a long-term perspective compared to their parents. They have accumulated sufficient capital, valuable work experience, coordination, and cooperation skills, and the interpersonal network with close ties to the industry forms the real foundation for their entrepreneurship in China. Some scholars define the returning rural workers as those leaving the counties and cities or being laid off due to a variety of measures: lack of knowledge and resources such as prerequisites for entrepreneurship, home, or large-scale development of the small and medium-sized city agriculture. This is the inevitable choice of migrant workers under the law of economic rationality [13]. Some scholars have studied the role of returning rural workers in starting businesses from the macro-level and analyzed the source of returning entrepreneurial elites, the new model of rural reconstruction, and the entrepreneurial management mechanism. The growth of entrepreneurial spirit among returning farmers increases household income, thus stimulating consumption. It stimulates high-quality economic development, promotes the structural transformation of supply chains, and reduces the overall cost of social governance. This will also help in the lagging population's employment rate and quality of life [14]. Other academics believe that migrant workers returning home to start businesses can hasten the accumulation of labor force and production factors in small cities, propel the development of small and medium-sized cities and local economic growth, and play a positive role in the social and economic field. The transfer of the local labor force creates new opportunities for large-scale employment and stable rural income growth. Returning home to start a business can help develop the rural economy and improve the local civilization level, adapt to the structure of the agricultural sector, set an example for the surrounding residents, and solve the problem of abandoned children and shanty towns caused by social problems. Macro and micro factors influence the return of migrant workers to start businesses. Some researchers have examined the macro-level differences in development and living conditions between urban and rural areas and the entrepreneurial decisions made and supported by urban and rural areas. Cao believed that, with the improvement of the business environment, the effective implementation of preferential agricultural policies, the gradual attention paid to social issues such as childcare, and the more comprehensive measures to ensure the success of entrepreneurship, the demonstration effect of agricultural workers is the main motivation for agricultural workers to start new businesses at this stage [15]. In addition, this study focuses on the individual characteristics of agricultural workers, risk factors, capital factors, self-actualization, work experience, and loan facilities and analyzes the behavior and readiness of farmers to return home at the micro level. Other scholars conducted a series of discussions on the practical difficulties faced by returning farmers and identified five bottleneck problems: financing, project selection, land use, recruitment, and work difficulties. In addition, rural and handicrafts industries have low entrepreneurial enthusiasm, weak awareness of cooperatives, low level of entrepreneurial departments, low awareness of preferential policies, and weak ability to obtain resources, which result in a low success rate of operation and a real dilemma in industrial development [16].

3. Research Methods and Materials

3.1. Basic Theory

3.1.1. Combined Forecasting

(1) Concept. A forecasting method based on two or more different forecasting methods for the same problem is known as combined forecasting. It is a combination of several quantitative and qualitative methods. More importantly, it combines both quality and quantity in practice. The primary goal of the combined forecasting methods is to maximize prediction accuracy by combining information from various methods. For example, it is difficult to develop a single forecasting model that is very close to the reality of frequent macroeconomic fluctuations and provide a stable and consistent explanation of their causes during the transition to a market

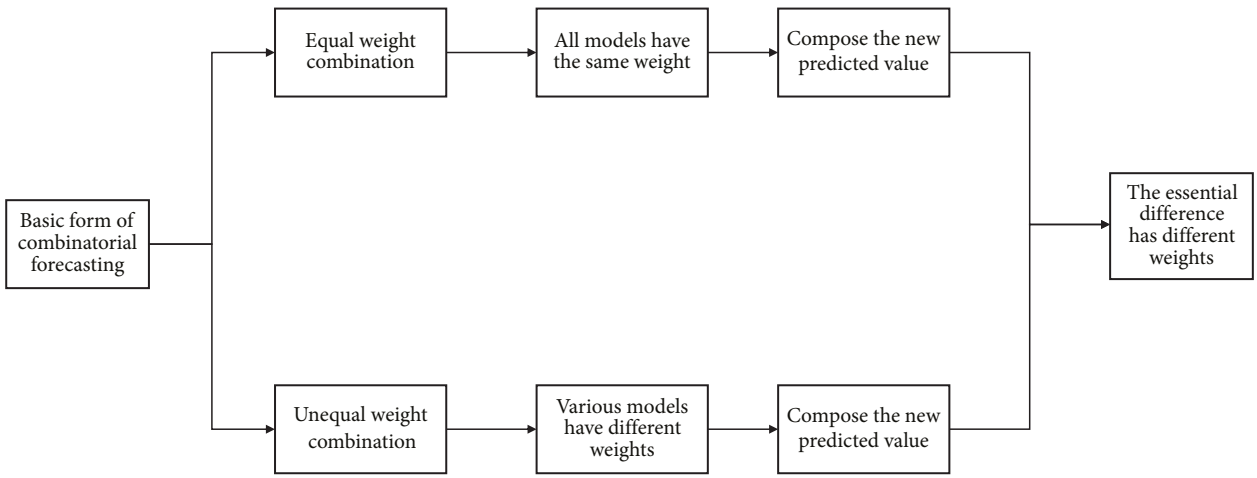

Figure 1: Basic form of combination prediction.

economy. Theoretical and practical studies show that the combined forecasting model can be more predictive than any single predictor for different forecasting models and data sources. The prediction model can reduce systematic errors and increase prediction efficiency [17].

(2) Basic Form. There are two basic forms of combined forecasting: 1) balanced combination refers to combining the prediction results of different forecasting methods into new prediction results according to the same weight array and 2) nonuniform combination is the prediction of a combination based on different weight numbers. Other than that, the principles and methods of application of these two forms are consistent, but there are some differences in the definition of weight. The combined prediction of the nonuniform combination is relatively accurate in terms of prediction [18] as shown in Figure 1.

(3) Application Principles and General Steps. Application principle: the combination of qualitative and quantitative analyses [19].

Steps: take economic forecasting as an example; the general step is to build a separate individual forecasting model based on economic theory and practice. Model similarity was measured by systematic cluster analysis. According to the cluster analysis results, a combined prediction model is established [20]. The steps are shown in Figure 2.

(4) Types of Combination Models. Model 1: linear combination model; model 2: optimal linear combination model; model 3: Bayesian combination model; model 4: transformation function combination model; model 5: combination model of econometrics and system dynamics, as shown in Figure 3.

3.1.2. Migrant Workers Return Home to Start Businesses. The lower cost of living and the desire for a family reunion are motives force of migrant workers to return home. The improvement of urban migrant workers' wages, living

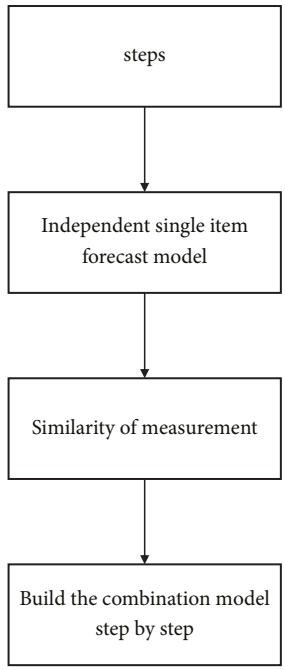

Figure 2: General steps for combination prediction.

conditions, and cultural surroundings is the power to attract agricultural workers into the city, but the unequal social public service system has made migrant workers realize that their living conditions have not improved in a groundbreaking way. As a result, they are encouraged to return home for productive activities that are expected to increase their income. The domestic environment provides policy support for the development of migrant workers returning home, and the rise of the "entrepreneurship boom" has invigorated migrant workers returning home to start businesses.

3.2. Main Formulas and Processes

(1) Building a linear combination model: the linkage approach of migrant workers returning to their hometowns to start their own business and rural

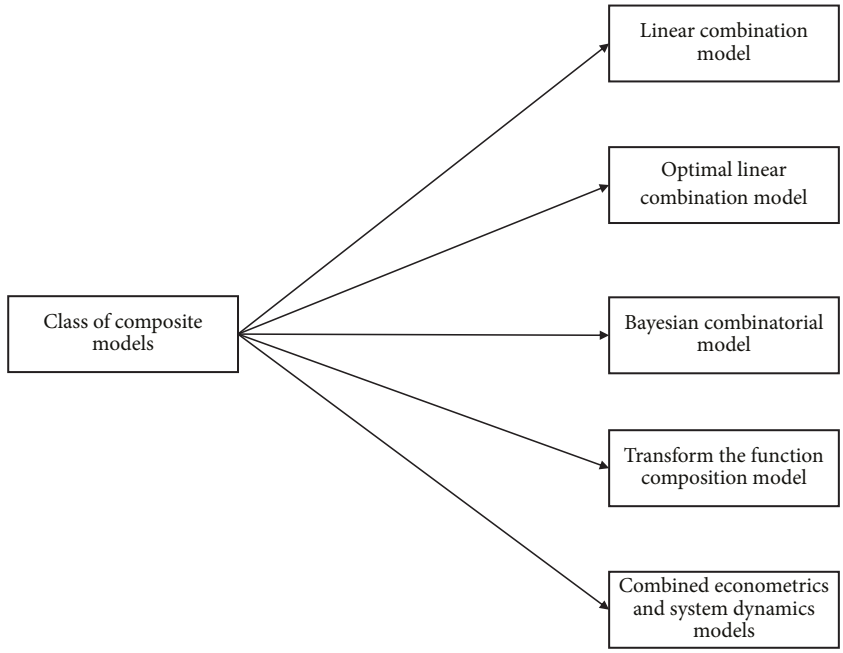

Figure 3: Category of combination prediction.

industrial revitalization is mainly a combination of human resources, economic resources, and social resources, so as to find the best solution:

$$\begin{aligned} Z_1 &= 8.9 + 0.61x_1 + 0.21x_2 + 0.18x_3, \\ Z_2 &= 5.6 + 0.53x_4 + 0.47x_5, \\ Z_3 &= 6.4 + 0.74x_6 + 0.36x_7. \end{aligned} \tag{1}$$

In the above formula, Z denotes rural industry revitalization; x_1, x_2, x_3represent the human resources of migrant workers returning home to start businesses, which are the number, education background, and age of migrant workers; x_4, x_5 represent the economic resources of migrant workers returning home to start businesses, which are their own economic strength and bank loan policy; and x_6, x_7 represent the social resources of migrant workers returning home to start their own businesses, which are respectively the entrepreneurship situation and national macro policies.

(2) Optimization of the combination model:

$$M_i = \frac{\sum_{i=1,2,3}^{n} Z_i - Z_i}{\sum_{i=1,2,3}^{n} Z_i} \quad \frac{1}{n-1}. \tag{2}$$

In the above formula, M_i represents the revitalization of the optimized rural industry.

Based on the above formula, the linkage between migrant workers returning home and rural industry revitalization is based on their human, economic, and social resources.

4. Results and Discussion

4.1. Main Analysis. Based on the human, physical, and social capital of migrant workers returning home to start businesses, this chapter examines their relationship with rural industry revitalization. The human, material, and social capital of migrant workers who return home to start businesses are examined in this study.

4.1.1. Analysis of Human Capital of Migrant Workers Returning Home. The human resources analysis of migrant workers returning home to start businesses includes information such as the number of migrant workers, educational background, age, and other factors. It is clear from the analysis and discussion that (1) year after year, the number of migrant workers returning home to start businesses grows. The key figures are as follows: in 2016, 3.6 million migrant workers returned home to start businesses, 4.1 million in 2018, 5.41 million in 2020, and 6.7 million in 2022. According to data analysis, the number of migrant workers returning home to start businesses is increasing year after year. The primary reason for this is that national policy supports rural industry policy. More migrant workers are willing to join the ranks of the rural industry revitalization, which provides entrepreneurial vitality to the rural industry revitalization, as shown in Figure 4.

(2) Those who have received higher education, such as junior colleges, have the most educational background among migrant workers returning home to start businesses. The key figures are as follows: in 2016, migrant workers returning home to start businesses had an educational background of 200,000 in primary schools, 360,000 in junior middle schools, 520,000 in technical secondary schools, 800,000 in senior high schools, and 1.72 million in junior colleges. In 2018, there are 280,000 in primary schools, 500,000 in middle schools, 620,000 in technical secondary schools, 940,000 in high schools, and 1.76 million in junior colleges. In 2020, there are 360,000 in primary schools, 540,000 in middle schools, 830,000 in technical secondary

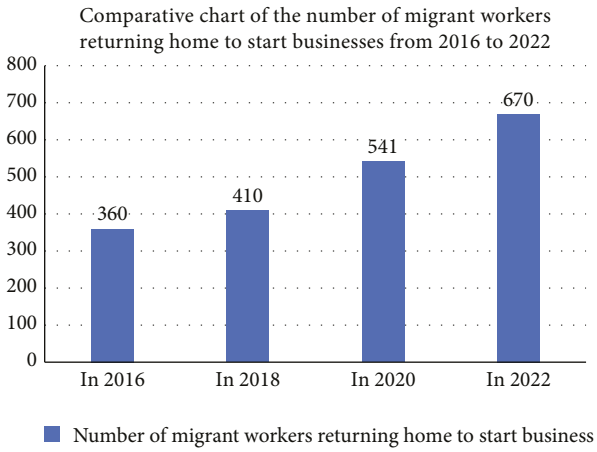

Figure 4: Number of migrant workers returning home to start businesses from 2016 to 2022.

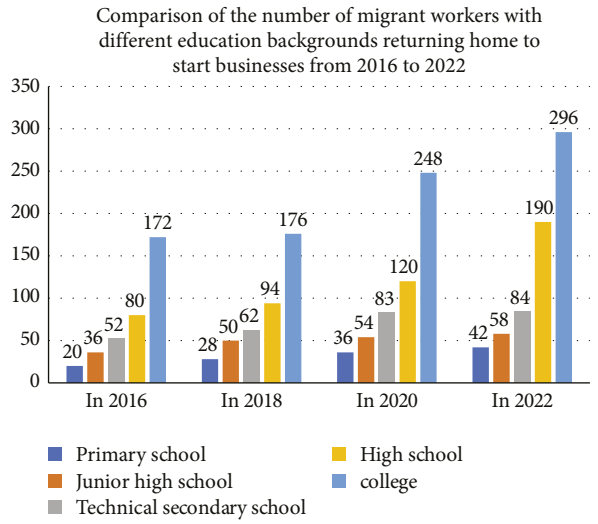

Figure 5: Number of migrant workers with different educational backgrounds returning home to start businesses from 2016 to 2022.

schools, 1.2 million in high schools, and 2.48 million in junior colleges. In 2022, there will be 420,000 primary school graduates, 580,000 junior high school graduates, 840,000 technical secondary school graduates, 1.9 million senior high school graduates, and 2.96 million junior college graduates. According to the data analysis, the following education levels are most common among migrant workers returning home to start businesses: junior college, high school, technical secondary school, junior high school, and primary school. The number of rural migrant workers with various degrees of entrepreneurship is increasing year by year, but with lower degrees, such as elementary and junior high school; compared to high school, college, and other relative degree higher people, the quantity is small. Therefore, better education of migrant workers makes them more willing to start a home business, and the rural industries provide good human resource reserves, as shown in Figure 5.

(3) The age group of migrant workers returning home to start businesses is mainly 30–40 years. The main data are as follows: the age structure under 20 years accounts for 8.2%,

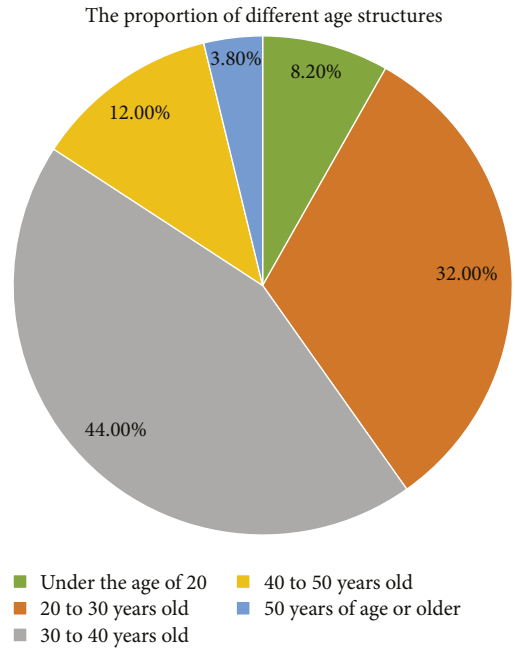

Figure 6: Proportion of migrant workers returning home to start businesses in different age groups.

the age structure of 20–30 years accounts for 32%, the age structure of 30–40 years accounts for 44%, the age structure of 40–50 years accounts for 12%, and the age structure over 50 years accounts for 3.8%. According to the data analysis, most of the age groups of migrant workers returning home are between 20 and 40 years. It has a great advantage in starting a business. It has certain advantages in terms of age, work experience, and relevant experience, so many people of the age group return to their hometown to start a business, as shown in Figure 6.

4.1.2. Analysis of Material Capital of Migrant Workers Returning Home to Start Businesses. The analysis of the economic resources of migrant workers returning home to start businesses includes the economic strength of migrant workers, bank loan policies, and other factors. According to the analysis and discussion, the following can be shown :

(1) The economic strength of migrant workers has a great impact on the return of migrant workers to start businesses, which provides a great economic advantage for migrant workers to start businesses. The specific data are as follows: the probability of success of migrant workers with assets of 200,000 yuan is 80%. With assets of 300,000 yuan, the probability of success is 82.5%. With assets of 400,000 yuan, the probability of entrepreneurship success is 83.5%. However, with assets of 500,000 yuan, the probability of entrepreneurship success is 86%. The success of entrepreneurship is closely related to the economic strength of migrant workers themselves. The higher the economic strength, the easier it is to succeed in entrepreneurship, as shown in Figure 7.

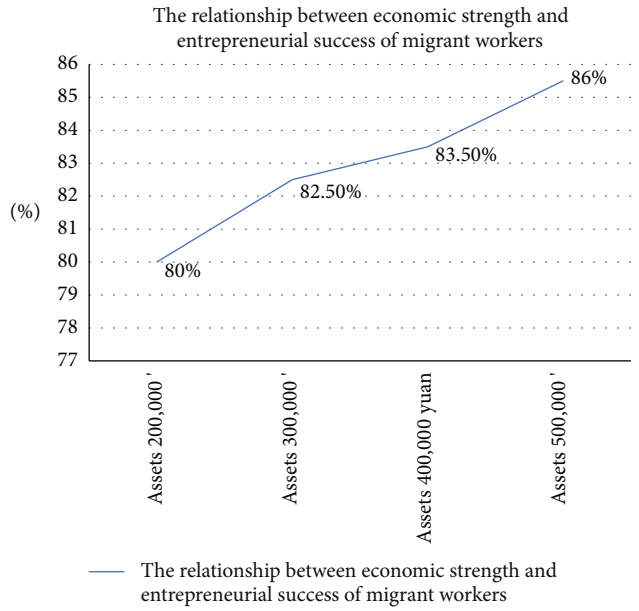

Figure 7: Relationship between economic strength and entrepreneurial success of migrant workers.

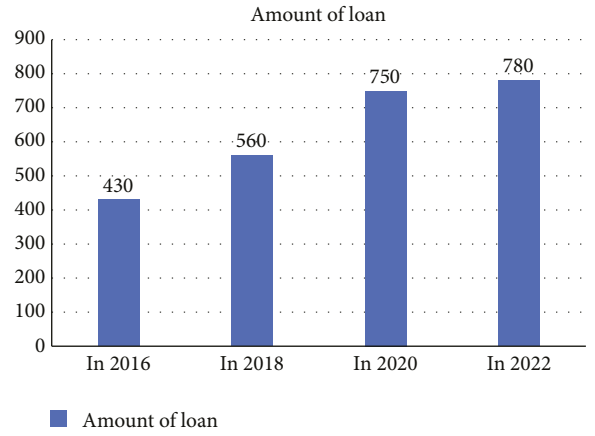

Figure 8: Year-by-year comparison of the amount of bank loans to migrant workers.

(2) The bank loan policy also has a great impact on the entrepreneurship of migrant workers, providing material support. In 2016, the bank lent 4.3 million yuan to the entrepreneurship of migrant workers. In 2018, 2020, and 2022, the bank loaned 5.6, 7.5, and 7.8 million yuan, respectively, to migrant workers to help them start their own businesses. According to the data analysis, banks provided more loans to migrant workers to start their own businesses year after year, which encouraged them to start their own businesses and provided them with strong economic support, as shown in Figure 8.

4.1.3. Analysis of Social Capital of Migrant Workers Returning Home to Start Businesses. The analysis of social resources of migrant workers returning home to start businesses includes factors such as entrepreneurship situation and national macro policies. According to the analysis and discussion, the following can be shown:

(1) Analysis of the entrepreneurial situation: since the 19th National Congress, the National Party Congress has included the rural revitalization strategy into the work plan and has become the master of the work of promoting agricultural and rural modernization and developing "political leaders" in the new era. Although China still faces insufficient regional development, unbalanced development, and insufficient rural development, from the perspective of development, urban and rural immigration has obvious comprehensive. The city began to absorb various factors of production to achieve rapid development. To realize rural revitalization, we need the support of talents, that is, the unidirectional flow of population from rural areas to urban and rural areas. The startup forms from the big environment; however, rural industries are very good but have the following disadvantages: hindered the development of rural industries, migrant workers exist only blind area in the business, will not be able to properly estimate the risk of entrepreneurship, and more and more people join the startup stage, makes the competition increase, etc., caused the startup form.

(2) National macro policy analysis: macro policy proposals and strategic incentives can improve macro policy in the field of migrant workers returning home, initiate a greater incentive effect "from rural to rural," and fully exploit the role of rural "reserve" to solve the problem of surplus labor. When migrant workers return home to start their own businesses, they should adhere to the fundamental background of rural production, life, and ecology; update and create social networks; highlight development achievements in the process of starting their own businesses; and promote overall rural revitalization. It also reveals the linkage relationship and role of migrant workers returning home to start their own businesses and rural revitalization. It serves as a decision-making reference for relevant government departments to promote the development of the national economy, social and economic development, and the building of a harmonious society.

4.2. Results

4.2.1. Linkage Analysis

(1) The goal of farmers returning to their hometowns is to revitalize industry, and their return can effectively increase rural resources. More farmers and workers will be able to return home and start their own businesses as rural industries recover. Farmers returning home to start businesses and revitalize rural industries is an important component of rural revitalization. Farmers can start their own businesses again and realize the effective intensification

of agriculture. Agricultural industrialization can improve the efficiency of resource allocation, promote the scale and industrialization of traditional agriculture, learn modern agriculture-related technologies, drive the development of modern agriculture, make full use of market opportunities, use internal resources for heterogeneity, and more accurately localize entrepreneurial industries and product types. This will help change the pattern of synchronous flow of high-quality resources from rural areas to cities. This part of the highly skilled human capital with substantial physical capital has become an integral part of the rural reconstruction strategy. According to their comparative advantages in diversification, farmers have accumulated a certain amount of entrepreneurial capital, experience, and technology in the activities of urban management. The rehabilitation and integration of agriculture require substantial support for small and medium-sized enterprises scattered in rural areas, most of which are founded by returning farmers. The existence and development of these enterprises are conducive to the stable employment of surplus agricultural labor force, the steady growth of farmers' family income, the strengthening of collective economic strength, the gradual improvement of rural infrastructure, the continuous improvement of rural public services, and the comprehensive recovery of rural areas.

(2) Industrial development and revitalization assist farmers in reestablishing their own businesses, effectively strengthen rural industries, and attract more agricultural workers to establish their own businesses. The revival of rural industries can lay a solid foundation for farmers to return to entrepreneurship. Strengthening basic capacity and sustainable agricultural development can provide incentives and basic support for farmers to return home. Local governments should combine the local social and economic development and the actual allocation of resources and conduct in-depth research on the supply and demand structure of the agricultural products market for those suitable for developing agricultural industries, home to do business. We will strengthen capacity building for sustainable agricultural development and create better business opportunities for returning farmers.

4.2.2. Linkage Analysis. Based on the above analysis of various resources of migrant workers returning home, it is concluded that the development trend of migrant workers returning home to start businesses and rural revitalization is good. However, the linkage mechanism of migrant workers returning home to start businesses and rural revitalization still has the following problems:

(1) Insufficient power of linkage mechanism: different types of entrepreneurial industries have different production needs, and the two-way transmission of information up and down and the mechanism of transmission are not perfect, affecting the entrepreneurial quality of entrepreneurs. The discrepancy between rural industrial development and policy supply, and the asymmetry in the demand of migrant workers returning to their hometowns to start their own businesses, leads to more significant fluctuations in the core agricultural industry.

(2) There are some problems in the construction of linkage mechanisms, such as imperfect organization and leadership and lack of close interaction between groups. First, the lack of unified organizational management, lack of professional and authoritative organizational leadership, and migrant family entrepreneurs having an unclear understanding of their role in rural revitalization, with their sense of efficacy, accomplishment, pride, and belonging being affected, lead to role and communication barriers in the connection between entrepreneurship and rural revitalization. Second, the lack of interaction between organizations and groups; the lack of platforms for communication, dialog, and cooperation; the lack of the formation of entrepreneurial alliances mainly composed of returning migrant workers; and the imperfect interest linkage mechanism are other factors that hinder the entrepreneurial development of migrant workers.

(3) The ability to ensure elements of the linkage mechanism is limited. The most obvious and direct incentive for migrant workers to return home and start a business is capital reward and subsidy. However, the welfare system is limited and only serves a few people. Regional differences in capital reward and subsidy for migrant workers to start a business are due to different financial and development priorities. In addition, the procedure of declaration is complicated and the cycle is long. There is no publicity mechanism around the effect of migrant workers returning home to start businesses. The development of rural industry has strong cyclical characteristics, and migrant workers' land rights and interests are affected to some extent. In comparison to actual needs, the amount, content, and experts of human capital training are insufficient.

(4) There are barriers to communication channels for migrant workers returning to their hometowns to start their own businesses, such as inadequate platforms and poor connections; for example, rural resources information cannot be spread or transmitted in a narrow scope, communication ability is weak, market information cannot spread among them, there is two-way information dissemination. In terms of the actual demand for migrant workers returning home to start their own businesses, entrepreneurs' ability to understand relevant policy information is limited in the absence of established channels. Entrepreneurs have limited understanding

and interpretation of policy documents due to the lack of comprehensive cultural quality and the ability to use the Internet. The meaning and content of policy documents are not timely spread in the business community, and information dissemination has the nature of delay.

5. Conclusion

As the current main body of migrant workers, a new generation of migrant workers has a broader field of vision, a more solid foundation of knowledge and skills of reserves, and a more long-term view. They have accumulated enough capital and valuable work experience and developed the ability of coordination and cooperation. Their industry is closely related to the network. Entrepreneurship provides a realistic basis for them upon return to China. Based on the interpretation of the current situation of migrant workers returning to their hometowns for entrepreneurship, a combination of previous research and theoretical knowledge is used to make predictions, thus dynamically simulating the relationship between migrant workers returning to their hometowns for entrepreneurship and industrial revitalization. The study discovered that the link between migrant workers returning to start businesses and the revitalization of rural industries is based on the flow of resources and is inextricably linked to human, economic, and social resources. Finally, the following findings are reached:

(1) Increasing the driving force foundation for industrial development, promoting equal access to facilities, actively building a driving force mechanism for rural industrial development, and striving to combine rural migrant workers returning to their hometowns to start businesses with rural revitalization strategies: we will increase support for migrant workers returning to their hometowns to start businesses; form an infrastructure construction system of "government, entrepreneurs, agricultural, and industrial support"; achieve breakthroughs; resist core areas and key links; and focus on optimizing the business environment based on the dimension of "industry-ecology-culture-ecology-income growth." We will improve the environment for rural migrant workers in poor counties to return to their hometowns and start businesses. We will fully recognize rural migrant workers in poor counties' positive role in consolidating poverty alleviation achievements and effectively connect them with rural revitalization.

(2) Rural characteristic industries should be developed to set the basis for rural entrepreneurship. First, according to market demand and government policies, in combination with the characteristics of local resources and regional conditions, we should cultivate and develop advantageous industries, focusing on developing entrepreneurial spirit based on business. Second, we should perform well in guiding entrepreneurship, play the role of project engine, optimize the layout of the entrepreneurship industry, and lay the foundation for the entrepreneurship market. Finally, we should do a good job in infrastructure security and promote infrastructure equalization. On the basis of improving the infrastructure service system, we will actively attract logistics, ecological and environmental protection, and intelligent Internet big data facilities and establish and improve a modern infrastructure service system. Simultaneously, we will promote the outsourcing of infrastructure construction and public service projects to qualified migrant workers who return home to start their own businesses. Relevant government departments should regularly provide good management, supervision, and follow-up on project implementation.

(3) Local relationships underpin the development, transformation, and reconstruction of rural resources. The richness and integrity of the relationship network influence migrant workers' return to start businesses. The participation of the government, businesses, scientific research institutions, and industry associations in rural development can promote the accumulation of human, material, and social resources. As a result, we can enrich the main body, strengthen the entrepreneurial relationship network, and improve farmers' ability to return home to start businesses. The formation of agricultural and industrial enterprise clusters, as well as enterprise clusters with local characteristics, can adapt group behavior to individual behavior and promote individual decision-making and collaborative development. It follows the development model of "migrant workers returning to their hometowns to create industrial clusters + enterprises," serves as a feedback collector in the group problem interaction process, and forms the mechanism of imitation, demonstration, and adjustment. We should encourage the formation of strategic alliances, encourage migrant workers' return to start businesses, extend to the front and back ends of the industrial chain, and actively build an all-dimensional industrial chain in rural areas. It follows the development model of "migrant workers returning home to start businesses + industry aggregation + government + banks + scientific research institutions + industry associations" and provides "material resources + financial resources + intelligence" services *via* multisubject participation to improve resource cohesion and integration and effectively promote the core competitive advantage industry aggregation of migrant workers returning home to start businesses. The model of "migrant workers returning home to start businesses" provides timely and real-time professional

knowledge services *via* the cloud platform and strengthens communication between enterprise groups and government departments, thereby broadening information channels and improving policy information efficiency. We will improve mechanisms, optimize services for rural migrant workers returning to their hometowns to start businesses; encourage the establishment of a "city-county- (district-) town (township)," a three-step management system for farmers returning to their hometowns; establish labor unions for farmers returning to their hometowns; and establish a dialog platform with authorities dealing with the issue of farmers returning to their hometowns to improve the efficacy of those farmers. We will improve the service system and mechanisms for encouraging and training rural migrant workers who return home to start businesses.

(4) We will introduce new factors and resources to make entrepreneurship, entrepreneurship bases, and entrepreneurship training bases more inclusive. First, it is necessary to establish an efficient service system for returning rural households and enterprises and improve statistics on entrepreneurship and innovation, multidisciplinary knowledge base, and entrepreneurship consulting platform. We will actively establish the mechanism of party building in colleges and universities and provide various documents, information, and services to farmers returning to their hometowns to start their businesses. Second, we must strengthen financial support, reduce taxes, ensure regulatory accountability, expand credit support, and increase financing channels for returning entrepreneurs. It is necessary to establish a risk prevention mechanism for returning farmers, comprehensively solve the problem of failure in returning to their hometown, and actively investigate the problem of setting up a commercial insurance company for returning farmers. Thirdly, based on the training needs of entrepreneurs, we should improve training coverage, broaden the training content, expand the training form, and improve the quality of the training team. We should actively adopt the "tutorial system" mode to enhance the pertinence of entrepreneurship training for migrant workers. Fourth, we will strengthen the guarantee of water and electricity for rural migrant workers returning home.

(5) In the process of establishing the linkage mechanism between migrant workers returning home to start businesses and rural revitalization, we should give full play to the enthusiasm of returning migrant workers and focus on providing them with statistical data services and communication platform construction services: 1) the statistics of market demand data and the establishment of an entrepreneurial guidance mechanism, 2) policy-oriented statistical information to enhance the universality of policies, 3) statistics of entrepreneurial service information and optimization of the entrepreneurial environment, 4) establishment of multisectoral and multifunctional collaboration mechanisms to facilitate more effective pooling of resources by broadening the range of actors, and 5) a talent pool to enhance the minds of farmers to start businesses back home.

(6) We should build high-quality resources for rural, human resource security, market supervision, and other departments; create a cloud platform for migrant workers to return home and start businesses; improve information exchange between departments; promote the effective integration of all departments' resources; and provide timely feedback to relevant subjects. We will work together to establish an agricultural and industrial enterprise base, mobilize resources for projects in the agricultural and industrial complex's location, and promote business environment structure optimization. The association, comprising scientific research institutions, universities, businesses, and entrepreneurial migrant workers, will be in charge of disseminating information, teaching entrepreneurial skills, and sharing entrepreneurial experiences. We will encourage private capital and government departments to collaborate in establishing angel investment funds for migrant workers returning home to start businesses, expanding channels for entrepreneurs to obtain venture capital, promoting top-level design for migrant workers returning home to start businesses, reducing the blindness of starting businesses, and promoting rural revitalization. Rural migrant workers who return to their hometowns to start businesses are encouraged to collaborate with consumers to establish production bases, and a "community industry" model is adopted, in which consumers take communities as units and subsidize entrepreneurs, and production bases are managed by entrepreneurs to provide final products. We will create a mechanism to connect the interests of migrant workers and local farmers and promote the joint development and sharing of rural industries.

Data Availability

The dataset is available upon request.

Conflicts of Interest

The authors declare that they have no conflicts of interest.

Acknowledgments

This paper is a general project of Humanities and Social Science Research in Colleges and Universities of Henan Province in 2023, "Research on the Linkage Mechanism, Mode Selection and Policy Guarantee of Migrant Workers Returning Home and Entrepreneurship and Rural Industrial

Revitalization" (2023-ZZJH-183), the Soft Science Research project of Henan Province in 2019 "Application Evaluation and Risk Management of PPP Investment and Financing Mode in Urban Rail Transit Construction" (194400410019), and phased results of the National Social Science Fund Project "Research on Mechanism and System Optimization of International Food Resource Utilization Based on Food Security Goals" (20BGJ016) in 2020.

References

[1] L. Wen, Z. Liu, Z. Gao, and S. Khanjari, "Evolutionary path and mechanism of village revitalization: a case study of yvillage, jiangsu, China," *Sustainability*, vol. 14, no. 13, p. 8162, 2022.

[2] H. Li, F. Wang, and X. Tan, "Research on the development of characteristic Food tourism resources in south sichuan under the vision of rural revitalization," *International Journal of Higher Education Teaching Theory*, vol. 3, no. 3, 2022.

[3] Y. Jin, S. Yu, and J. Yang, "The strategic management of yueliangqiao village minsu(bamp;B) brand under the AISAS model," *International Journal of Educational Management*, vol. 7, no. 2, 2022.

[4] L. Huang and Y. Cao, "Review of the integrated development of ecological and cultural forestry," *Sustainability*, vol. 14, no. 11, p. 6818, 2022.

[5] X. Jiang, R. An, G. Zhang, and Y. Zhou, "Research on the coupling and coordinated development of tourism industry and rural revitalization under the new pattern of "double cycle" development," *Scientific Journal of Intelligent Systems Research*, vol. 4, no. 6, 2022.

[6] J. Chen, L. Jiang, J. Luo, L. Tian, Ye Tian, and G. Chen, "Characteristics and influencing factors of spatial differentiation of market service industries in rural areas around metropolises—a case study of wuhan city's new urban districts," *ISPRS International Journal of Geo-Information*, vol. 11, no. 3, p. 170, 2022.

[7] S. Sun, C. Zhang, and Z. He, "Study on the development of ecological sightseeing agriculture from the perspective of rural revitalization—A case study of feng county, xuzhou city," *Scientific Journal of Economics and Management Research*, vol. 4, no. 3, 2022.

[8] Li Jing, "Industrial development in rural areas and the flow of home-coming career-creating talents under the pattern of double circulation economy," *Journal of Innovation and Social Science Research*, vol. 8, no. 11, 2021.

[9] M. Wang, B. He, J. Zhang, and Y. Jin, "Analysis of the effect of cooperatives on increasing farmers' income from the perspective of industry prosperity based on the PSM empirical study in s region," *Sustainability*, vol. 13, no. 23, Article ID 13172, 2021.

[10] Y. Chen, "Research on industrial model under the background of rural revitalization strategy-- taking xiaojialai village, helinger county as an example," *International Journal of Education and Teaching Research*, vol. 2, no. 3, 2021.

[11] Y. Tian, J. Ning, Z. Yang, T. Lu, X. Wu, and S. Zheng, "Research on new media under the background of new consumption-- takes live-streaming marketing as an example," *Scientific Journal Of Humanities and Social Sciences*, vol. 3, no. 9, 2021.

[12] L. Zhang, "Integration and optimization of E-commerce industry cluster and green supply chain network under the background of rural revitalization," *Journal of Sociology and Ethnology*, vol. 3, no. 2, 2021.

[13] D. nbsp, "Rural revitalization boosts meigu's agricultural and rural economic development," *Open Access Library Journal*, vol. 08, no. 7, 2021.

[14] X. Liang, "How to build a model of qilu for rural revitalization," *Scientific Journal of Economics and Management Research*, vol. 3, no. 6, 2021.

[15] H. Fu, "Study on the development of rural tourism in pingdingshan city under the background of rural revitalization strategy," *World Scientific Research Journal*, vol. 6, no. 10, 2020.

[16] W. Fu, "Rural industry and its social foundation in the integrated urban-rural development process: a case study of processing in remote villages under the jurisdiction of city L, zhejiang province," *Social Sciences in China*, vol. 41, no. 3, 2020.

[17] Y. Zhang and Y. Zhang, "Research on guangdong tourism resources development and integration development under the background of rural revitalization strategy," *IOP Conference Series: Earth and Environmental Science*, vol. 546, no. 3, 2020.

[18] H. Guo, J. Sun, and YuS. Zhang, "Difficulties and countermeasures of agricultural products processing industry in rural areas under the background of rural revitalization," *IOP Conference Series: Earth and Environmental Science*, vol. 512, no. 1, Article ID 012100, 2020.

[19] H. Jin, W. Junan, Z. Xuelian, Z. Xiaoxin, W. Weili, and W. Wei, "Study on the evaluation method of operation performance for rural domestic wastewater treatment facilities," *IOP Conference Series: Earth and Environmental Science*, vol. 510, no. 4, Article ID 042032, 2020.

[20] H. Qiu, H. Yuan, and Y. Wang, "Research on the dilemma and countermeasures of migrant workers returning home to start a business," in *Proceedings of the Hohhot : 2022 2nd International Conference on Management Science and Industrial Economy Development (MSIED 2022)*, pp. 38–42, Francis Academic Press, Hohhot, China, March 2022.

Hindawi
Computational Intelligence and Neuroscience
Volume 2023, Article ID 9812159, 1 page
https://doi.org/10.1155/2023/9812159

Retraction

Retracted: Construction of College Chinese Blended Teaching Mode Based on Decision Tree Classification Model in New Media Context

Computational Intelligence and Neuroscience

Received 26 September 2023; Accepted 26 September 2023; Published 27 September 2023

Copyright © 2023 Computational Intelligence and Neuroscience. This is an open access article distributed under the Creative Commons Attribution License, which permits unrestricted use, distribution, and reproduction in any medium, provided the original work is properly cited.

This article has been retracted by Hindawi following an investigation undertaken by the publisher [1]. This investigation has uncovered evidence of one or more of the following indicators of systematic manipulation of the publication process:

(1) Discrepancies in scope
(2) Discrepancies in the description of the research reported
(3) Discrepancies between the availability of data and the research described
(4) Inappropriate citations
(5) Incoherent, meaningless and/or irrelevant content included in the article
(6) Peer-review manipulation

The presence of these indicators undermines our confidence in the integrity of the article's content and we cannot, therefore, vouch for its reliability. Please note that this notice is intended solely to alert readers that the content of this article is unreliable. We have not investigated whether authors were aware of or involved in the systematic manipulation of the publication process.

Wiley and Hindawi regrets that the usual quality checks did not identify these issues before publication and have since put additional measures in place to safeguard research integrity.

We wish to credit our own Research Integrity and Research Publishing teams and anonymous and named external researchers and research integrity experts for contributing to this investigation.

The corresponding author, as the representative of all authors, has been given the opportunity to register their agreement or disagreement to this retraction. We have kept a record of any response received.

References

[1] P. Huang, "Construction of College Chinese Blended Teaching Mode Based on Decision Tree Classification Model in New Media Context," *Computational Intelligence and Neuroscience*, vol. 2022, Article ID 4608631, 10 pages, 2022.

Hindawi
Computational Intelligence and Neuroscience
Volume 2022, Article ID 4608631, 10 pages
https://doi.org/10.1155/2022/4608631

RETRACTED

Research Article

Construction of College Chinese Blended Teaching Mode Based on Decision Tree Classification Model in New Media Context

Pingge Huang

Shangqiu Polytechnic Henan, Shangqiu 476000, China

Correspondence should be addressed to Pingge Huang; 201902012134@stu.zjsru.edu.cn

Received 12 August 2022; Accepted 3 September 2022; Published 26 September 2022

Academic Editor: Yaxiang Fan

Copyright © 2022 Pingge Huang. This is an open access article distributed under the Creative Commons Attribution License, which permits unrestricted use, distribution, and reproduction in any medium, provided the original work is properly cited.

Based on the context of new media and big data, this article uses the decision tree classification model to construct the college Chinese hybrid teaching mode. In order to verify the accuracy of ID3 algorithm prediction, the comparison of the ID3 algorithm, K-means algorithm, and support vector machine classification algorithm was made, and the experimental results show that the ID3 decision tree classification algorithm has better prediction and classification ability, for the construction of college Chinese hybrid teaching mode provides certain practical value and reference basis.

1. Introduction

First of all, what is Chinese? Chinese in many teaching concepts has been defined as a discipline, and it cannot simply be understood as a teaching course; the language is actually built on multidiscipline; almost all of the teaching course is inseparable from the language. Chinese is a comprehensive teaching and is a kind of literary spirit and humanistic concept to all disciplines on the "university." Many students devote themselves to study and life. The influence of Chinese is everywhere. The construction of correct three views and the construction of values of students cannot be separated from the contribution of Chinese, so Chinese is very important for students.

The teaching of Chinese extends from kindergarten to university [1]. With the deepening of the teaching content and the teaching level, Chinese is becoming more and more important to the shaping of students' personality and values [2, 3]. At the same time, due to the arrival of the "Internet +" era and the continuous development of new media technology, the voice of the reform of teaching mode is also rising, and the teaching mode of college Chinese based on the context of new media has been put forward and excavated.

Secondly, what is the context of new media? The main feature of the new media context is multimedia, which can also be understood as the network. The word "context" in English was originally derived from the Greek word "contextre," which can also be literally understood as "interwoven together." It corresponds to college Chinese, which is "network literature." In other words, the knowledge in literature has real-time changes and the ability to be amended at any time compared with traditional college Chinese, whether in terms of interpretation or information sharing [4].

Using the literature analysis method, an online search for the keywords "new media" and "university Chinese" reveals that this study was first conducted from the perspective of building a learning community to reform university Chinese teaching in the context of new media. This paper analyzes the intrinsic connection between media and the concept of Chinese language education in colleges and universities, and proposes a method of teaching Chinese in colleges and universities in the context of new media [5].

With the arrival of the era of big data, the influence of new media technology on the effect of college Chinese teaching has deepened, and the research on the teaching mode of college Chinese in the context of new media has also deepened. From 2014 to 2020, they put forward a series of reflection and research. For example, Rui-Lan Dong in a study put forward the context of the new media college

Chinese teaching reflection, mainly for content that is the reflection of the interaction between teachers and students in the teaching process, and emphasized the importance of interactive language education for the university, and for the context of the new media way of college Chinese teaching provides a new way of thinking and a new direction. In addition, with the deepening of research, the discussion on the teaching methods of college Chinese in the context of new media has risen from a single perspective to a multifaceted and multilevel reform strategy research. In 2020, Li proposed that under the background of the development of new media technology, the trend based on learning community cannot be ignored. Then, he puts forward that the current main teaching goal is to construct the curriculum system of college Chinese in the context of new media and points out the direction and basic principles of college Chinese education reform in the context of new media, which provides a new direction and new thinking for the teaching mode of college Chinese in the new era in the future [6].

2. Background of the Construction of Hybrid Teaching Model in the Context of Big Data and New Media

2.1. The Development Process of College Chinese Blended Teaching. Since entering the 21st century, it is not only a new era of rapid economic and technological development, but also the era of educational reform required by various disciplines [7]. In the course of the development of teaching mode, with the advancement of the trend of The Times, it has moved from a single teaching mode to a mixed and three-dimensional direction. Since the outbreak of COVID-19 in 2020, blended teaching has attracted great attention.

"College Chinese" is not only a subject, but also an important teaching content for contemporary college students to shape correct values, improve humanistic quality, and construct correct three views. It is one of the indispensable open courses in various colleges and universities in China. Blended teaching originated in the United States. According to relevant data, at the current stage of basic education in the United States, more than 75 percent of regions have provided blended education or corresponding teaching resources for students. While blended teaching in China started late compared to foreign countries, after entering the 21st century, blending learning or blended learning was mentioned as a new concept in China, indicating that the new model might become a watershed in teaching reform [8]. Immediately afterwards, Prof. He also pointed out that the significance of the advantages of blended learning lies not only in combining the traditional learning methods in China (i.e. offline learning) with the advantages of making full use of new media for online learning, but also in integrating teachers' guidance and students' motivation into the whole teaching process, reflecting students' autonomy, initiative, enthusiasm, and creativity, as well as giving full play to the teachers' ability to guide, inspire, and supervise.

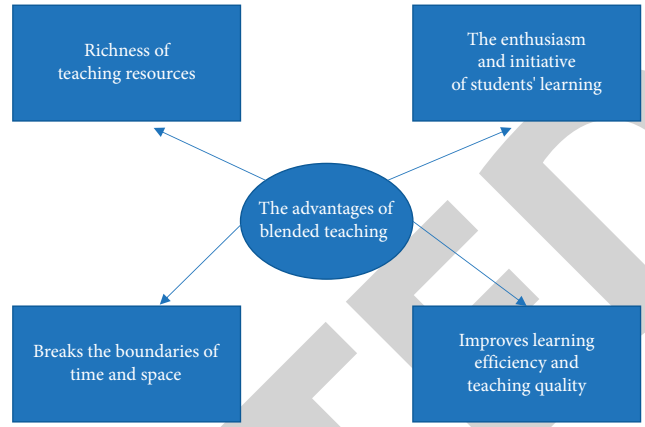

Figure 1: The advantages of adopting the blended teaching mode in university languages.

With the birth of new media context, and the reform of the university language education model, as well as the response to the national policy, the construction of the hybrid teaching model of university language in China has been a hot topic of research; for example, Zhimin Dai proposed to innovate the traditional classroom in terms of content and form, so as to explore the reform of hybrid teaching model of university languages. In addition, other scholars have explored the hybrid teaching model of university languages based on undergraduate teaching providing applied [9]teaching practices, university languages for higher education institutions, university languages based on minority regions in western Yunnan, and learning software, such as SuperStar and MOOC. Thus, it can be seen that the exploration of the blended teaching mode based on the university language classroom in China shows a blossoming state [9].

2.2. The Connotation of Blended Teaching Mode. Blended teaching generally refers to the new teaching mode of online and offline integration, which is similar to the flipped classroom and mobile learning mode, and is a way of teaching through new media technology and network. The two most crucial meanings in the blended teaching mode are the following: firstly, it is based on the learning mode, emphasizing the integration of online and offline learning; and secondly, it is based on the constructivist learning theory, emphasizing the learning task of students as the central goal, for the acquisition of knowledge and the establishment of ability are completed on the basis of students' independent acquisition to complete the construction of the knowledge system [10].

Due to the outbreak of the epidemic, online education is especially important for students in epidemic areas, and the blended education model, which is a teaching method that integrates course resources, online resources, and various teachers that are available both online and offline, will become a major trend in future education reform, and in the teaching mode of university languages, it has the following main advantages, which are shown in Figure 1.

RETRACTED

As shown in Figure 1, there are four main advantages of adopting the blended teaching mode in university language teaching practice [11], which are as follows:

(1) The first is the richness of teaching resources. The "hybrid" of the blended teaching mode refers to the integration of online and offline teaching, and the rich online resources compared with the traditional classroom teaching mode provide rich learning and teaching resources for both students and teachers. For students, if they do not understand a problem, they do not have to wait until they see the teacher to solve it, but can use the Internet to contact the teacher directly or search for related resources to solve it, which improves the students' initiative and enthusiasm for learning. The main reason for this phenomenon is that the traditional teaching model does not put forward higher requirements for teachers, while the blended teaching model requires teachers to be more diverse and grasp the teaching objectives with students as the main focus, and requires the creation of a teaching platform for equal communication, and teachers and students to jointly promote the quality of teaching [12, 13].

(2) Secondly, it enhances students' enthusiasm and initiative. University languages belong to the humanities, which is important for the correct establishment of students' three views and washing their souls. The main reason for this phenomenon is that the atmosphere in the university language classroom is not enough to mobilize, the class content is not compelling enough, and the university language is often used as a public course, some even in the form of an elective course; many students choose it to "get enough credits" or "just pass," so students' motivation and initiative are not high. Ultimately, it is because the teaching mode of the university language cannot keep up with the diversified development of students, and most students' understanding of university language is still on the surface of "rote memorization," while building a hybrid teaching mode of the university language allows students to change their views on the traditional university language classroom. Teachers can enhance students' motivation and enthusiasm for learning university languages by going online and offline, adding videos to watch and explain, and changing the old-fashioned PPT class design [14].

(3) Breaking down spatial and temporal boundaries. Here, the time and space boundaries mainly refer to time and space. The offline teaching activities alone are limited in time and space, while the hybrid teaching mode, which introduces online teaching, allows students to make full use of various hardware resources, such as cell phones and tablets, for language learning anytime and anywhere, which can enhance students' learning efficiency.

(4) Improve the efficiency of learning and the quality of teaching [15]. Why is the traditional university language classroom turned into a "senior language"? A large part of the reason is because the classroom content is relatively deep and abstract, especially for most students in science and technology, this kind of abstract and abstract content is more difficult to understand, so many students cope with the examination; there are a lot of "Beethoven"; this is due to the mismatch between the effectiveness of student learning and the level of teacher teaching in the traditional classroom. The quality of teachers is very poor. The blended teaching mode of the university language, using the advantages of mobile learning and flipped classroom, can fully mobilize students' initiative and combine the new media context and new media technology to assist the teaching practice of university language, which can maximize the learning efficiency of students and the teaching quality of teachers [16].

3. The Significance of Decision Tree Classification Model in Hybrid Teaching Mode

The decision tree classification algorithm is an algorithm in data mining, and the data mining algorithm is based on the theory of big data analysis, so to analyze the significance of the decision tree classification algorithm in blended teaching mode, we must first understand the significance of research in the context of big data in the blended teaching mode [17].

In fact, big data has two meanings: the first meaning refers to big data analysis, which refers to a variety of behaviors generated by people in real life; the computer stores and remembers, thus enabling huge amounts of data, that is, the analysis and processing of a variety of data generated by the behavior of any individual or group. Big data in our study refers to the second level [18].

In today's modern education model, the teaching information platform of many universities generates a huge amount of data and records the behavior of students' learning behavior, students' grades, students' names, students' genders, and learning habits of major categories and online learning [19]. Moreover, the teaching behaviors of different teachers and the teaching interactions between teachers and students, assignment reviews, and evaluation of assignments can be recorded and saved using big data. The purpose of this article is to use big data analysis technology to classify and predict the learning effect of students' learning languages in the blended teaching mode, and to analyze and construct behavioral modules such as teachers' teaching behaviors and students' learning performance and learning habits, to predict future changes in students' learning performance, to help students solve their doubts and difficulties, and to handle and discover difficulties for teachers in the teaching process, and to build a university language. The blended teaching model provides guarantee and strong support.

RETRACTED

In big data analysis, the main use of data mining analysis algorithms to process the massive amount of data, mining its laws and classification or predicting its future development trend, and the visualization of the obtained data results, and finally build the relevant model and apply it to the actual engineering. This is the research significance that exists in data mining. In building a hybrid teaching model of university language, "big data" plays an indispensable role in it and is the source and basis of data based on the decision tree algorithm, which provides a powerful analysis basis for the teaching model and improves the accuracy of scientific decision-making and classification [20].

With the informatization of the teaching platform of universities, it can provide strong support for the construction of today's hybrid teaching model of university languages. At the same time, the development of multimedia technology has created an iterative update of the new media context, which also assists in building a hybrid teaching model based on the decision tree classification model, and big data provides a data basis for teachers to grasp the effect of students' online and offline learning, which is conducive to improving students' learning effect and self-learning ability, and provides a new direction for teaching.

4. Case Design of Hybrid Teaching Model of University Language Based on Decision Tree Classification Model

The decision tree classification algorithm is a class of data mining algorithms. Data mining is a comprehensive and interdisciplinary discipline, and its related fields are shown in Figure 2.

As can be seen from Figure 2, data mining covers a wide range of fields, and the research in this article covers several areas of data mining, such as statistics, information science, visualization, and its algorithms. Data mining is divided into several task types in today's research, which include classification analysis, association analysis, and predictive analysis. The technical areas or algorithmic areas included in the basic data mining system platform are shown in Figure 3 [21].

In this research article, the source of data is mainly the information technology teaching platform of universities; among them, the algorithm used in the data mining process is the decision tree classification algorithm, which finally visualizes the results of model construction and analyzes its data results. The algorithm used in the data mining process is described next [22].

The decision tree classification model used in this article is one of the classification analyses, where classification refers to the algorithmic analysis process of finding the function or model of the concept or data described. Classification analysis is a supervised learning approach, which requires training the data to obtain labels or generate rules for classification, and preprocessing the data to analyze the resulting model, which can be represented in various ways, such as classification rules, decision trees, or neural networks [23]. Prediction is the process of using historical data to

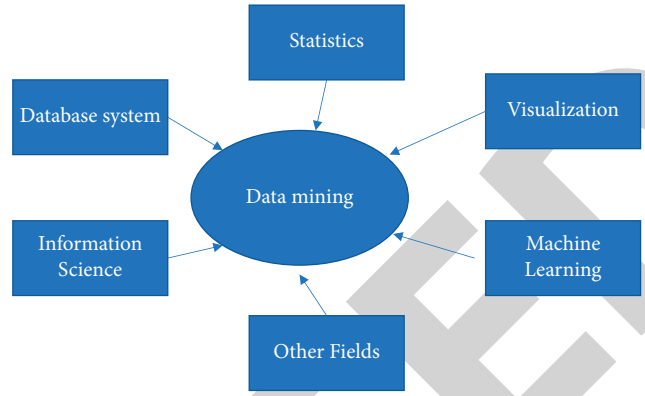

Figure 2: Related fields involved in data mining.

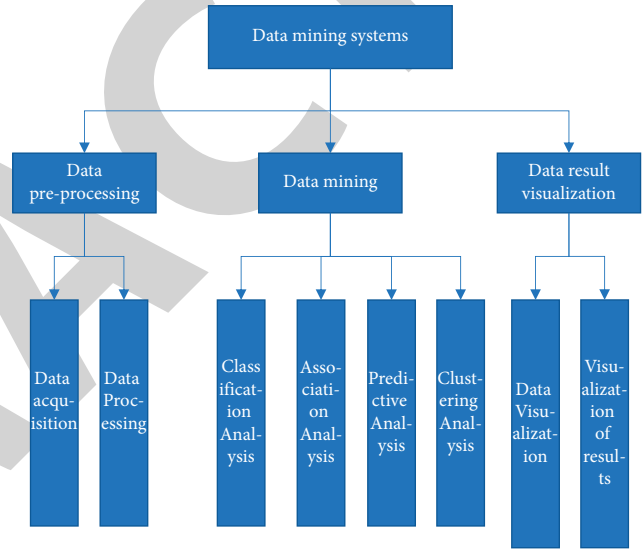

Figure 3: The technical or algorithmic fields involved in data mining.

analyze data to find out the trend or change pattern of current or future data and then using this model to predict the change characteristics of future data by building a relevant model.

As can be seen from Figure 3, there are four types of algorithms for data mining; in addition to the classification and predictive analysis described above, there are also cluster analysis and association analysis. In addition to the decision tree algorithm, there are also Bayesian and neural network methods used for classification, but in terms of practicality, the decision tree algorithm is the best for these three types of classification techniques; in terms of complexity and understanding of the algorithm, the decision tree classification algorithm is also the best; in terms of data preprocessing, decision tree classification is also the best choice for data training [24].

Therefore, in order to explore and build a hybrid teaching model of university language, this article chooses the decision tree algorithm to build a model to analyze and predict the learning behavior and performance of students in a university language classroom in a college, which provides

RETRACTED

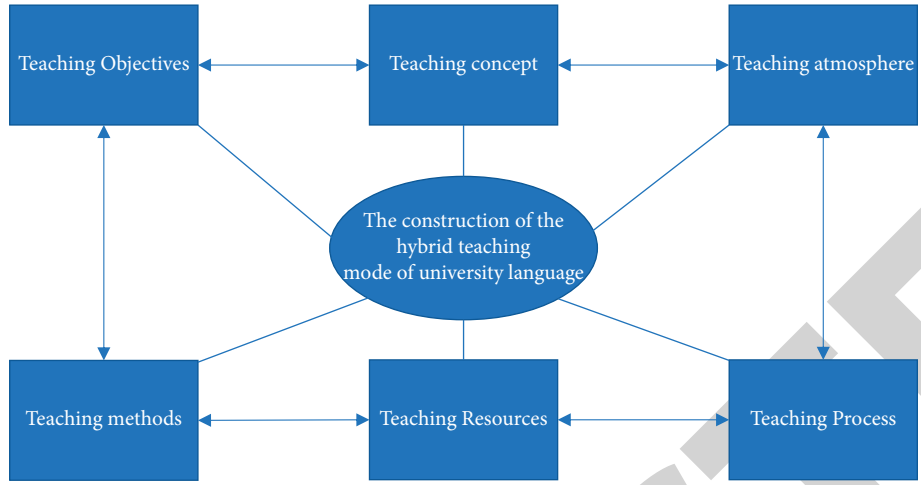

Figure 4: The principles and elements of the construction of the university language blended teaching mode.

new ideas for the teaching mode of modern education, and also improves the subjective motivation and enthusiasm of students' learning.

4.1. Principles of Building a Hybrid Teaching Model Based on Big Data and New Media Context. The basic meaning and the advantages of the of the blended teaching model based on university language are discussed in detail in Section 2.2, but today is the era of Internet and big data, and the economy is still inseparable from the advancement of the trend of the times, let alone education. Since the teaching mode of new media technology-assisted teaching was proposed, the reform about Internet education has never stopped, in order to build a more perfect hybrid teaching mode system for university languages [25], which is shown in Figure 4.

As can be seen from Figure 4, this article will fully consider the learning efficiency of students, the teaching quality of teachers, and the development of the university language teaching mode in the new media context, and combine the six elements of teaching objectives, teaching philosophy, teaching atmosphere, teaching methods, teaching resources, and teaching process to construct the following four principles, and follow the four principles of the completed construction to design the case.

4.1.1. Clarify the Teaching Objectives and Teaching Philosophy. The teaching objectives of the university language should be based on students' ability to learn the language well, build a sound personality, and enhance humanistic connotation and humanistic qualities. The teaching philosophy should also be student-oriented, especially for high-level, deep abstract, and important understanding knowledge like university language, and the teaching objectives and syllabus should be designed in consideration of students' ability to receive, master, and understand. For the university objectives of university languages, on the one hand, the teaching objectives should be converted into learning objectives, and on the other hand, they should [8] have measurable ability; measurable ability refers to the ability to examine students' mastery of classroom knowledge by means of tests, classroom examinations, or midterm assessments, so that the teaching objectives can be changed at any time, so that teachers and students can work together to complete the entire university language course [26].

4.1.2. Create a Relaxed, Interesting, and Diverse Teaching Atmosphere. In building a blended teaching model for university languages, teachers should work with students to create a relaxed and fun atmosphere. A good teaching atmosphere can make students' learning much more efficient, and teachers' teaching quality can be improved, and a relaxed, interesting, and diverse teaching atmosphere for students and teachers is a requirement for a blended teaching model [27]. Blended teaching not only absorbs the advantages of the traditional classroom, but also combines digital education, adding video teaching, group discussion, mutual evaluation of homework, and other more personalized teaching design; these personalized teaching designs can make students feel that the university language is no longer stereotypical, old-fashioned, deep, and difficult to understand, so as to make the atmosphere of the university language class become interesting, as well as full of learning. This is what a university language classroom should be like [28].

4.1.3. Innovative Teaching Methods and Reorganization of Teaching Resources. The online and offline hybrid teaching should not only give full play to the advantages of traditional classroom teaching methods, but also take advantage of multimedia technology, online resources, and live online teaching, so that students can really feel the beauty of Chinese culture and Chinese literature in the university language classroom.

Therefore, in building a hybrid teaching mode of university language, we should abandon the old teaching concept and fully innovate the teaching mode. In the teaching process, we should consider the diverse

RETRACTED

characteristics of modern students and guide them to think and feel the images and feelings of the characters in the text from more angles, while combining them with actual current affairs to trigger students' profound thinking and understanding of today's times and guide them to shape positive and correct socialist core values. Meanwhile, in the construction of the blended teaching mode of university languages, teaching and learning resources can be presented in many aspects, and can respond to the call of national policies and fully rely on China's online learning platforms, such as Chaoxingtong, StudyTong, China University Catechism, and other high-quality online platforms.

Students are encouraged to learn online in [9] a task-driven way, and through the flipped classroom learning mode, students learn online independently and are guided by the offline teacher in a discussion mode, and improve their deep understanding of Chinese culture, and enhance their understanding of the content of the university language classroom by creating scenarios, combining social and livelihood issues, social and political issues, and discussing with each other and completing after-class writing training. We also combine the construction of values education with subject knowledge to meet the individualized teaching needs of today's diverse and pluralistic development characteristics.

4.1.4. Updating Teaching Methods and Rationalizing the Teaching Process with Reality. In the blended teaching model of university languages, teachers should update the teaching methods and change the teaching process according to the actual situation. The teacher should be a supporting presence in the classroom, but the real learning subject is the students, and the teacher should consciously guide students' thinking, inspire them to conduct independent learning discussions, and fully mobilize their enthusiasm and initiative. At the same time, in order to meet students' individual learning needs, teachers should rationalize the teaching process according to the actual situation and adopt more diverse teaching methods to meet the different learning needs of different students. In the blended teaching mode of university language, teachers can adopt online teaching activities, such as teachers' review of homework, students' mutual evaluation of homework, question and answer before and after class, setting group tasks, and guiding students to deepen their understanding of the classroom content of university language while cultivating their cooperative negotiation ability through completing group learning tasks, so as to build a high-quality integrated teaching-learning, learning-teaching, evaluation-learning, and learning-doing system. The classroom is an integrated teaching-learning, teaching-assessment-learning, and learning-doing classroom of high quality.

4.2. Principle of Decision Tree Classification Algorithm. The decision tree algorithm can be classified as a greedy algorithm, which uses a top-to-down recursive relationship to construct a decision tree; that is, the process of classification is based on the attributes to divide the tree branches and the value of the nodes of the tree branches to determine the classification branch process. There are several common decision tree classification algorithms, namely, ID3 algorithm, C4.5 algorithm, C5.0 algorithm, CART algorithm, and so on. The basic principles [14]of ID3 and C4.5 algorithms are explained next, which is shown in Table 1.

4.3. Model Construction Results and Analysis

4.3.1. Data Collection and Preprocessing. In this article, the college language grades and online learning behavior habits of students in two public classes of college language in class 2021 collected from the information-based teaching platform of a university were used as the training sample set, totaling 120 students. The data records of college language grades and online learning habits of three majors, namely, communication engineering, Chinese language, and business English, were randomly selected as a database to analyze the factors influencing students' behavioral habits and make predictions about students' college language grades, and identify the factors that affect student performance and thus respond. In this way, teachers can make real-time changes to the teaching content and lesson plan design in order to better adapt to the students' learning situation and improve their learning efficiency. The percentages of students in each major in the university language classroom and their performance are shown in Figures 5 and 6.

From Figures 5 and 6, we can see that the number of Chinese language majors is the largest, and the number of business English majors is the smallest, at 30, which shows that students of different majors have different interests in learning university languages. This is related to the thinking habits of communication engineering students, who always think about engineering practice in learning languages, which is both the advantage and shortcoming of engineering students. After eliminating the redundancy and other influencing factors, this article formed a table of basic information of online learning with students' names, major categories, grades, and study behaviors, and used it as a data set to build a decision tree model for the blended teaching model of university languages.

4.3.2. Establishment and Analysis of the Decision Tree Classification Model. After the above analysis, this article requires simple training for the dataset, and the setting of relevant rules should not be too complicated, so the ID3 algorithm is chosen to build the decision tree classification model.

Firstly, the basic information table of online learning formed in the above section is calculated as the training dataset S. The sample includes 120 data samples. The total information entropy is

$$I(\mathrm{S1}, S2 \ldots, \mathrm{S}n) = -\sum_{i=1}^{n} p_i \log_2 p_{\mathrm{i}}. \tag{1}$$

where p_i denotes the probability that any sample belongs to the judgment indicator. If all the sample values in the current

RETRACTED

Table 1: Basic principles of the ID3 algorithm and the C4.5 algorithm and advantages of comparison.

Algorithm type	Principle	Advantages
ID3 algorithm	Using a decision tree as a source of information, the root node of the decision tree classification model is obtained by comparing the information gain of each attribute one by one to determine which feature has the most information.	Classification rules are easy to understand, fast, etc.
C4.5 algorithm	Based on the ID3 algorithm, the concept of information gain rate is introduced for attribute selection. The algorithm mainly consists of calculating the expected value, calculating the information entropy of attributes, and calculating the information gain value, that is, information gain rate.	It can handle incomplete data, generate optimal trees by pruning technique, and generate rules with high accuracy.

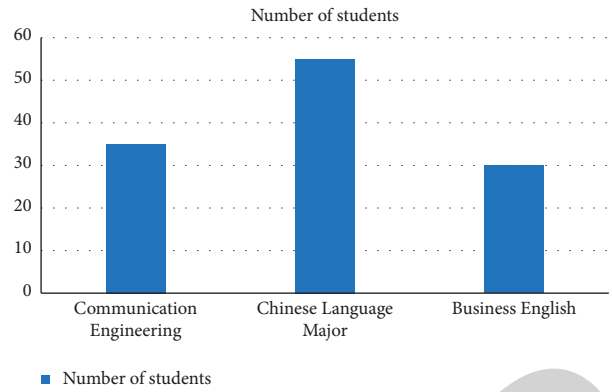

Figure 5: Number of students in each major.

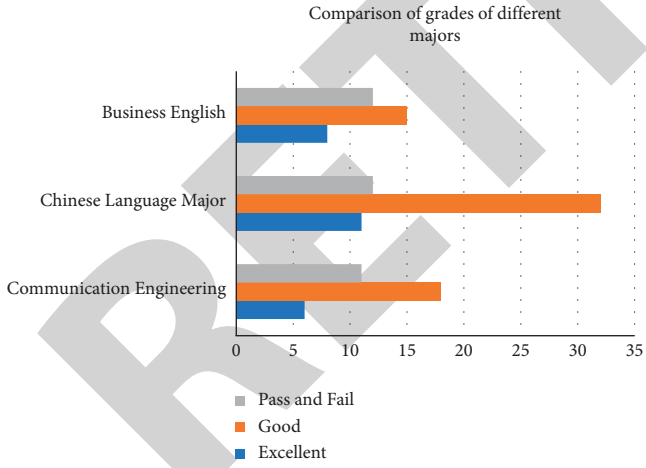

Figure 6: Comparison of the results of different majors.

dataset belong to the same attribute, then I is 0. The training sample set in this article has a total of 120 entries, the number of excellent is 25 in total, the number of good is 65, and the number of passing and failing is 30.

Next, its attribute A is calculated to have K different values {a1, a2, ..., ak}, then the training dataset S is classified as k subsets {S1, S2, ..., Sk} using attribute A. Then, the information entropy of the divided samples according to attribute A is

$$E(A) = \sum_{j=1}^{k} \frac{\{s_{nj}\}}{S} * I\left(\{S_{nj}\}\right). \quad (2)$$

Finally, the information gain obtained by dividing the training dataset S using attribute A is

$$\text{Gain}(A) = I - E(A). \quad (3)$$

Through the above discussion, the simplified decision tree model of the hybrid university language teaching model is derived by computational analysis and combined with the form: IF ... THEN as shown in Figure 7.

By using the above decision tree simplification model, we can analyze the learning effect of students in the hybrid university language classroom by using different attributes, and by combining different attribute nodes by comparing students' gender, major categories, online learning behavior habits, and other multidimensional analyses, we can conclude that high-achieving students like to do their prep work in advance. After the discussion in class, they completed their homework and raised questions online or discussed their questions with their classmates and finally actively participated in answering questions after class. The students with failing or passing grades are related to their major categories. In Chinese language majors, most students are more actively involved in online discussions and completing online assignments, but for communication engineering students, the percentage of students who can actively participate in online discussions and postclass Q&A is still small, which is related to the high intensity of active rational thinking of engineering students, while liberal arts students are more active in online discussions and postclass Q&A compared to engineering students. This is related to the high intensity of rational thinking among engineering students, while students in liberal arts always account for more emotional thinking than engineering students, which is one of the reasons for the difference in students' academic performance.

Therefore, when preparing lessons, university language teachers can take into account the thinking stereotypes of students with different major categories, so that they can better provide targeted guidance for different students' learning situations in classroom teaching or online teaching; if online teaching is more effective, teachers can refer more teaching contents to real life and fully consider students'

RETRACTED

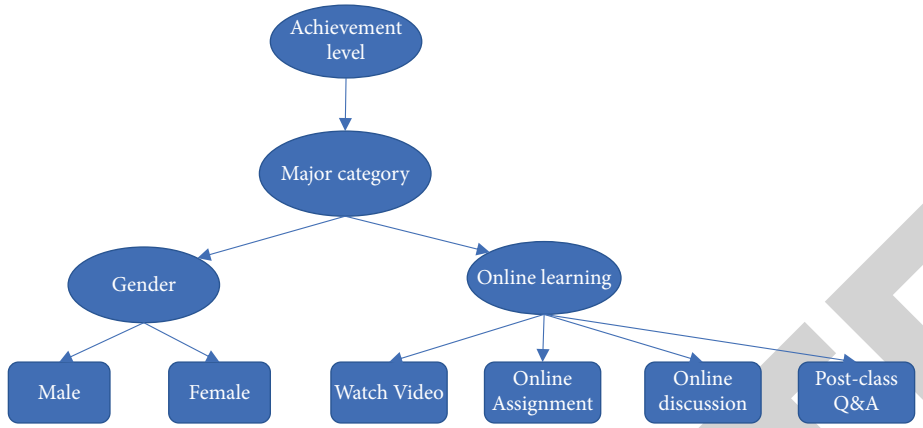

Figure 7: A simplified decision tree classification model for a hybrid university language teaching model.

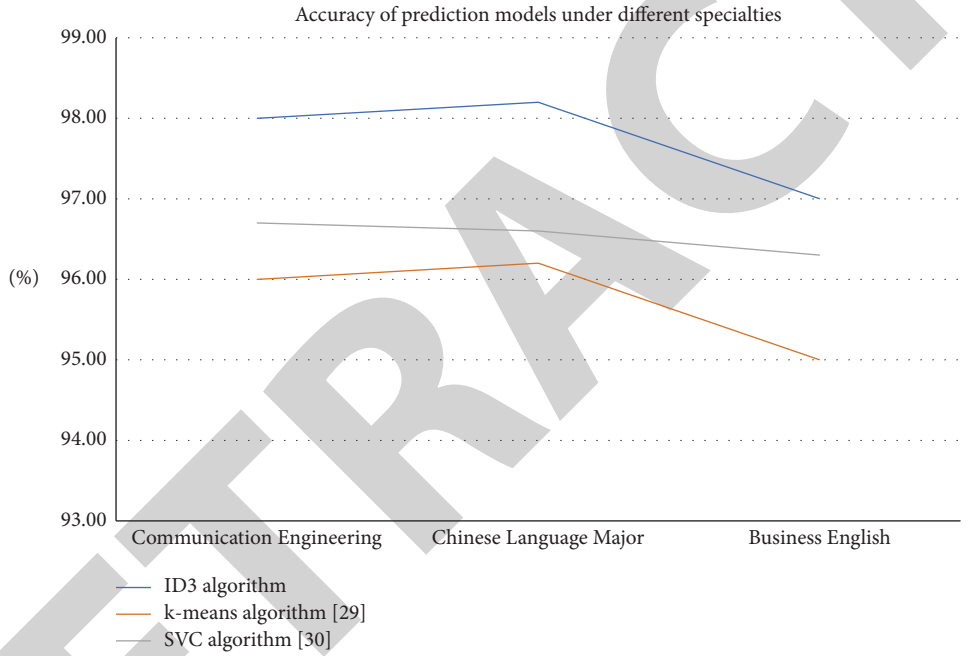

Figure 8: Accuracy comparison curves of prediction models under different majors.

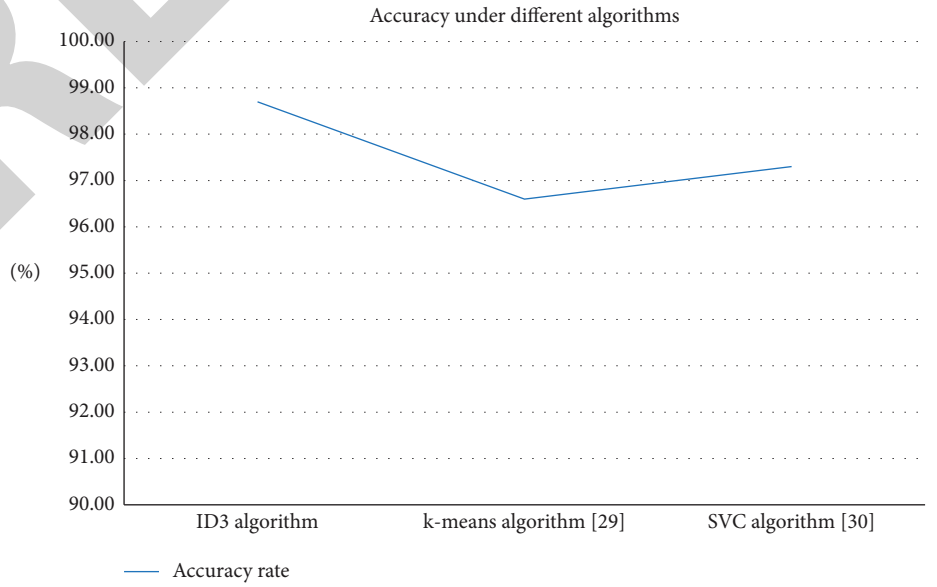

Figure 9: Total accuracy of the classification prediction model with the ID3 algorithm, k-means algorithm, and SVC algorithm.

RETRACTED

diversity, both to let liberal arts. In order to verify the application of the ID3 algorithm to Chinese language learning, the teacher can use the ID3 algorithm to teach the Chinese language [29].

At the same time, in order to verify the correctness of the ID3 algorithm applied to the construction of a hybrid teaching model for university languages, the ID3 algorithm, the cluster analysis classification algorithm, and the support vector machine (SVC) classification algorithm were chosen to construct a prediction model for the grades of students with excellent and passing grades, and the correctness of the final test as shown in Figures 8 and 9.

It can be seen from Figures 8 and 9 that the accuracy rate of the hybrid university language teaching model based on the decision tree classification model constructed by the ID3 algorithm is higher than that of the k-means algorithm (one of the cluster analysis classification algorithms) and the support vector machine classification algorithm (SVC), in terms of both distinguishing professional categories and total categories. It can be seen that the ID3 decision tree algorithm is used to construct a blended teaching model for university languages, which can classify and predict students' learning, and thus can provide some reference significance for teachers' teaching [30].

5. Conclusion

In the decision tree classification model, this is also the design principle under the construction of hybrid teaching model. Under decision analysis, this article constructs decision trees based on the decision tree ID3 algorithm and combines the different attributes of student gender, student achievement, and online learning in the new media context of the times, and analyzes the factors affecting student achievement from the perspective of professional differences and excellent or not, and also constructs prediction models under different algorithms and compares the accuracy of their predictions, so as to provide university language teachers with a hybrid teaching mode for interactive teaching and learning, which provides some reference value and practical significance.

Data Availability

The dataset can be accessed upon request.

Conflicts of Interest

The author declares that there are no conflicts of interest.

Acknowledgments

This work was supported by Project 1: Henan Higher Education Teaching Reform Research and Practice Project (Project no. 2021SJGLX994), Research on the Innovation of Ideological and Dis course System of Political Course in Higher Vocational Colleges in the New Era; and Project 2: "Exploration and Research On Active Classroom Teaching Mode" (Project no.: 2019SJGLX658) is the phased achievement of the key project teaching reform project of the Henan Provincial Department of education.

References

[1] X. Dong and K. Han, "Research on college dance teaching reform in the new media era," *International Journal of Higher Education Teaching Theory*, vol. 3, no. 2, 2022.

[2] Li Ning and M. Ismail, B. Jais and V. Narasimhan, "Application of artificial intelligence technology in the teaching of complex situations of folk music under the vision of new media art," *Wireless Communications and Mobile Computing*, vol. 2022, Article ID 5816067, 2022.

[3] Qi Wang and Y. Jin, "The teaching reform and practice of new media marketing based on the integration of specialty education and innovative and entrepreneurial education[J]," *International Journal of Education and Economics*, vol. 5, no. 1, 2022.

[4] Y. Guo, "Path selection of ideological and political teaching in universities under the new media environment[J]," *International Journal of Computational and Engineering*, vol. 7, no. 1, 2022.

[5] X. Wu, "Research on college English teaching reform under the background of new media," *2022 3rd Annual Conference of Education, Teaching and Learning*, vol. 82, 2022.

[6] S. Yin and X. Yin, "Application of new media technology in education teaching and school management[J]," *International Journal of Social Science and Education Research*, vol. 5, no. 2, 2022.

[7] R. Cinzia, F. Fernanda, and S. C. Anna, "New media literacies and transmedia learning do we really have the conditions to make the leap? An analysis from the context of two Italian licei classici[J]," *Social Sciences*, vol. 11, no. 2, 2022.

[8] W. Kardemark, "New media—new perspectives? "Religion" in Swedish online teaching materials," *Religion Education*, vol. 49, no. 1, pp. 42–60, 2022.

[9] K. T. Berg, "A global perspective on ethics: new resources for teaching and discussing media ethics and journalism ethics," *Journal of Media Ethics*, vol. 37, no. 1, pp. 72–75, 2022.

[10] Z. Wang, "Intersection and integration: interdisciplinary design practice and new media art design teaching," *2021 Conference on Art and Design: Inheritance and Innovation (ADII 2021)*, vol. 643, 2022.

[11] L. Wang, "The skill training of reading music in the teaching of solfeggio and ear training in the new media environment," *Applied Bionics and Biomechanics*, vol. 2022, Article ID 8209861, pp. 1–11, 2022.

[12] Z. Sun, "On strategies for reform of college English teaching in the context of new media[J]," *International Journal of Educational Technology*, vol. 2, no. 1, 2021.

[13] X. Zhu, "The implementation path of ideological and political education in college English teaching based on "new media and integration of online and offline course"--take guangzhou huashang college as an example[J]," *International Journal of Education and Teaching Research*, vol. 2, no. 4, 2021.

[14] M. Kou, "Analysis on the innovative approaches of college English translation teaching based on new media technology," *Learning & Education*, vol. 10, no. 3, p. 44, 2021.

[15] H. Cen, "Research on adult public English teaching based on new media information technology with curriculum

RETRACTED

Hindawi
Computational Intelligence and Neuroscience
Volume 2023, Article ID 9819873, 1 page
https://doi.org/10.1155/2023/9819873

Retraction

Retracted: Improved RRT-Based Moving Path Planning Algorithm for Teaching Reform and Innovation in Western Orchestral Ensemble Classes in Colleges and Universities

Computational Intelligence and Neuroscience

Received 26 September 2023; Accepted 26 September 2023; Published 27 September 2023

Copyright © 2023 Computational Intelligence and Neuroscience. This is an open access article distributed under the Creative Commons Attribution License, which permits unrestricted use, distribution, and reproduction in any medium, provided the original work is properly cited.

This article has been retracted by Hindawi following an investigation undertaken by the publisher [1]. This investigation has uncovered evidence of one or more of the following indicators of systematic manipulation of the publication process:

(1) Discrepancies in scope
(2) Discrepancies in the description of the research reported
(3) Discrepancies between the availability of data and the research described
(4) Inappropriate citations
(5) Incoherent, meaningless and/or irrelevant content included in the article
(6) Peer-review manipulation

The presence of these indicators undermines our confidence in the integrity of the article's content and we cannot, therefore, vouch for its reliability. Please note that this notice is intended solely to alert readers that the content of this article is unreliable. We have not investigated whether authors were aware of or involved in the systematic manipulation of the publication process.

In addition, our investigation has also shown that one or more of the following human-subject reporting requirements has not been met in this article: ethical approval by an Institutional Review Board (IRB) committee or equivalent, patient/participant consent to participate, and/or agreement to publish patient/participant details (where relevant).

Wiley and Hindawi regrets that the usual quality checks did not identify these issues before publication and have since put additional measures in place to safeguard research integrity.

We wish to credit our own Research Integrity and Research Publishing teams and anonymous and named external researchers and research integrity experts for contributing to this investigation.

The corresponding author, as the representative of all authors, has been given the opportunity to register their agreement or disagreement to this retraction. We have kept a record of any response received.

References

[1] W. Zhang, "Improved RRT-Based Moving Path Planning Algorithm for Teaching Reform and Innovation in Western Orchestral Ensemble Classes in Colleges and Universities," *Computational Intelligence and Neuroscience*, vol. 2022, Article ID 4273761, 10 pages, 2022.

Hindawi
Computational Intelligence and Neuroscience
Volume 2022, Article ID 4273761, 10 pages
https://doi.org/10.1155/2022/4273761

RETRACTED

Research Article

Improved RRT-Based Moving Path Planning Algorithm for Teaching Reform and Innovation in Western Orchestral Ensemble Classes in Colleges and Universities

Wang Zhang

Music School of Liaoning Normal University, Dalian 100629, China

Correspondence should be addressed to Wang Zhang; ralvesxqq52445@student.napavalley.edu

Received 22 August 2022; Accepted 13 September 2022; Published 24 September 2022

Academic Editor: Yaxiang Fan

Copyright © 2022 Wang Zhang. This is an open access article distributed under the Creative Commons Attribution License, which permits unrestricted use, distribution, and reproduction in any medium, provided the original work is properly cited.

Western orchestral instruments in colleges and universities, as important instruments, occupy a central place in many bachelor's degree programs in music education. Music teaching reform and innovation are central to the creative wisdom of music teachers, their musical upbringing, and the lived experience of their students. For teachers, the process of pedagogical reform and innovation is the process by which teachers realize their own pedagogical ideals. Teachers must first be motivated; in the absence of motivation, any advanced teaching methods will become pale in comparison and lose their value and usefulness. Therefore, the construction of teaching activities requires teachers to take responsibility for the education and support of students, to align their teaching goals with the development of each student, to make the students' feelings closely connected to them, and to make them feel their value in the learning process. Starting from teaching western orchestral instrument ensembles in colleges and universities, this thesis uses the research method of improving RRT's moving path planning algorithm to explain and analyze some problems that arise in teaching western orchestral instrument ensembles in colleges and universities and puts forward constructive suggestions and recommendations.

1. Introduction

With the development of China's economy and the flourishing of various enterprises, China has more and more musical exchanges with countries all over the world, enabling China to accept more and more Western musical instruments and musical cultures. With the development of the times, Western musical instruments are becoming more and more popular in China. Many people are beginning to understand and learn musical instruments, and professional students are increasingly learning them. However, different instruments have different timbres and difficulties, so learners carefully study their choices. When studying Western music courses in our universities, we find that almost all of them are "one-way." In the study of Western wind instruments, many students study flute and clarinet, but very few students study oboe and bassoon. In the study of Western wind instruments, many choose the cello and violin, significantly more than those who choose the viola. These events clearly indicate a serious imbalance in the scientific study of Western orchestral instruments in colleges and universities. With the booming development of Western orchestral music education in China's colleges and universities, there are college Western orchestral music professionals in higher music institutions [1]. After decades of efforts, the teaching of Western orchestral instruments in colleges and universities have entered a new stage of development. As an important instrument, the college Western orchestral instrument occupies a central place in many music education bachelor's degree programs. As students of Western orchestral instruments in colleges and universities, they should systematically master the basic knowledge of Western orchestral instruments in colleges and universities and know the laws of music education. At the same time, students may choose to teach orchestral music, chamber music, and choreography in the performing arts of music.

While studying Western orchestral instruments, China needs to learn from its study abroad experience in certain areas. The most important approach in choreography programs in foreign schools is to encourage students to adopt a free-form learning model, as well as to encourage them to develop creative and inventive thinking as they understand and play music differently than they initially create it. Overseas schools often organize small recitals at school to allow students to identify and correct performance deficiencies based on their actual academic performance. At the same time, university student competitions are organized in foreign conservatories, and this type of competition can be called a campus singer competition. The purpose is to find new stars in orchestral performance and singing, to strengthen professional exchanges between universities, and to drive the development of universities. According to the situation abroad, the Western orchestral ensembles in our universities should adhere to the principle of freedom, according to the individual wishes of each student, and maximize the students' motivation so that they can organize more friendly games, including intercampus competitions and provide students with more opportunities for activities. Schools should try to encourage students to participate in song competitions held at home and abroad. Regardless of the results of the competitions, hammering and exercising are of utmost importance to the students. Since the music curriculum reform, the new curriculum has been designed and piloted for nearly a decade and subsequently implemented in several pilot provinces across the country. In recent years, the music curriculum reform has been carried out under the overall curriculum reform. Today, the largest basic education reform since the new Chinese education has entered the stage of practical implementation and adaptation. By thinking rationally about and grasping the curriculum reform process, the pace can be further adjusted and forged ahead. Knowing how to implement the curriculum reform is a question that every teacher involved in the curriculum reform must seriously think about. The reform and innovation of the teaching of Western orchestral ensembles in higher education is also a necessary step to meet the requirements of the time and society [2].

This thesis corresponds to the topic of "Music Teaching in Higher Education." Starting from the teaching of Western orchestral ensembles in colleges and universities, this thesis explains and analyzes some problems in the teaching of Western orchestral ensembles in colleges and universities by using the research method of improving the RRT's moving path planning algorithm and puts forward constructive suggestions and recommendations. It is hoped that research and exploration of contemporary musical concepts and modes of upbringing in developed countries, as well as research and exploration of existing teaching models and teaching methods, will make useful and pioneering attempts to bring the overall teaching of Western orchestral ensembles in colleges and universities in China closer to the world trend. Finally, in the teaching and learning of the basic skills in Western orchestral ensembles, the teaching and pedagogy of the basic knowledge of Western orchestral ensemble classes, as well as the elaboration of the inner logic, should be taken into account in the core professional courses in related disciplines such as orchestra, chamber music, and choreography. Learning requires consideration of teacher specificity in the curriculum and special attention to the professional skills of the learner. It is hoped that the exploration of the subject of Western orchestral ensemble in colleges and universities will improve the updating of music pedagogy in Western orchestral ensemble in colleges and universities, the continuous mastery of teaching contents and teaching methods and the cultivation of more highly qualified Western orchestral ensemble students.

2. Research Background

As the cradle of musical talents and the place of musical and cultural exchange, universities have a special role in the development of Chinese music in the West. The teaching of Western orchestral instruments in colleges and universities is both a need for the development of Western music in China and the need for higher art to enter the campus and improve the quality of campus culture, as well as the need for students' era and spiritual struggle. Teachers should view the learning process of instrument composition as a dynamic process that enables teachers and students to learn more deeply from each other. The curriculum for Western orchestral instruments in higher education takes place primarily in the classroom. It is neither a one-way linear influence of the teacher on the students nor a one-way linear influence between the students, but an interaction between the teacher and the students [3]. In particular, music teaching and learning can develop healthily through the constant dynamic interaction between teachers and students in the classroom. Some universities do not have educational institutions that support Western orchestras. Some music teachers of Western orchestral instruments in colleges and universities teach simple methodologies, mainly music and performance, while neglecting the aesthetic skills of their students. The following problems currently occur in Western orchestral ensembles in our colleges and universities: training is inconsistent, the purpose of sound testing is to make each instrument sound almost identical, and rehearsals for musical integrity, unity, and completeness can be better accomplished at the same pitch. The relative instability of intonation still exists in the daily training and rehearsals of the orchestra. In daily orchestra practice and rehearsal, there are often differences between the beginning and the end of the piece. In daily orchestral practice, as the number and complexity of musical performances increases, the potential for complex rhythms, types, or sound types increases. Confronted with multisyllabic patterns, students can become ambivalent, fearful, or even too much bad, so practice is not reinforced. As part of the orchestra's daily curriculum, students need to be familiar with the music, and students are not guaranteed to play at a speed that can be reasonably controlled. Therefore, teachers in universities should currently pay attention to the teaching of music composition courses to develop students' musical aesthetic skills and thus improve their musical abilities [4]. Therefore, this thesis on the reform and innovation of teaching western

RETRACTED

orchestral instrument ensemble class in colleges and universities based on improved RRT's moving path planning algorithm has the following significance and principle requirements.

(1) In the process of building vocal complexes in colleges and universities, teachers should strictly follow the three principles of subjectivity. The teaching of the Western orchestral instrument course in colleges and universities should fully reflect the dominant position of the students in the classroom. Teachers should change the traditional teaching attitude and fully stimulate students to learn practical skills in the teaching course of the Western orchestral instrument in colleges and universities. When constructing the Western orchestral instruments curriculum in colleges and universities, it is important to reflect on the joint harmony between teachers and students and to create a classroom environment where teachers and students have equal status. Teaching in higher education based on orchestras not only stimulates students' personal feelings but also forms their musical taste and aesthetic ability for music. Due to the influence of musical aesthetics on students' personalities, the teaching of the Western orchestral instruments in colleges and universities is receiving more and more attention from teachers [5].

(2) Teachers in current university music teaching need to individualize instrumental-vocal instruction according to students' practical skills and choose appropriate teaching modes to arouse students' interest and motivation in music. In addition, interactive teaching can create a good environment for students to learn music and use music culture to learn music more deeply. In the teaching process, teachers should actively use multimedia to assist students in creating an open environment for teaching Western orchestral instruments in colleges and universities, so that they can focus more on cooperative lessons and take into account the teaching atmosphere created by teachers in the classroom to enrich the ensemble teaching content. Teachers in colleges and universities should not only have professional theoretical knowledge but also have a lot of practical skills. In the context of reforming the curriculum of Western orchestral instruments in colleges and universities, college teachers must break the traditional teaching model, develop new teaching concepts, and dare to use all innovative elements to change the existing curriculum of Western orchestral instruments [6].

3. Research Methods and Materials

3.1. RRT's Moving Path Planning Algorithm

3.1.1. RRT Algorithm Concept and Formula. For the RRT algorithm, it is particularly important to define each expansion step of the moving path planning; if there is no synchronization, then the long time scheduling depends on time and cost. The computation of RRT is terminated when the random tree is expanded with new nodes [7]. The equation is as follows:

$$\mu_X = \mu_M + \frac{\triangle x(\mu_N - \mu_M)}{\|(\mu_N - \mu_M)\|}, \tag{1}$$

where $\triangle x$, $\mu_N - \mu_M$, and $\|(\mu_N - \mu_M)\|$ denote the random tree step size, vector unitization and Euclidean distance, respectively.

Delta-X expansion is a given value which has an important effect on the range of the random tree. If the extension length is small and the tree has many short branches, the path expansion speed can be effectively increased. However, from the beginning to the end, the random tree needs to be expanded step by step, requiring more nodes to find the workspace and find the solution, which reduces the efficiency. However, if the step size is larger, the random tree may have more branches, which will help to reduce the number of nodes required for the path. However, if there are too many obstacles in the room to complete the route planning, a large number of samples are required to obtain the extended nodes. This leads to path degradation too high, resulting in local extremes and even failure to find feasible paths [8]. The RRT algorithm flow is shown in Figure 1 and the RRT algorithm expansion schematic is shown in Figure 2.

3.1.2. Advantages and Disadvantages of the RRT Algorithm. The main advantages of the RRT algorithm are as follows:

(1) RRT algorithm is possible, i.e., it can be found if there exists a path from the start to the destination and the algorithm runs long enough [9].

(2) The RRT algorithm can detect and evaluate obstacles in real time without the need to build a preconfigured spatial model.

(3) The RRT algorithm is efficient and can even meet the requirements of real-time scheduling.

(4) The RRT algorithm still has good performance in high-dimensional space, and it is relatively easy to extend the RRT algorithm from low to high dimensions [10].

(5) The RRT algorithm is well adapted to dynamic environments. Even if the map information changes, it does not affect its effectiveness.

The main disadvantages of the RRT algorithm are as follows:

(1) The study of the RRT algorithm is absolutely random. The RRT algorithm undergoes many invalid studies before an acceptable solution is found, which is an important factor affecting the effectiveness of the RRT algorithm.

(2) The path generated by the RRT algorithm is not guaranteed to be the best solution, which is unlikely to be the optimal solution.

RETRACTED

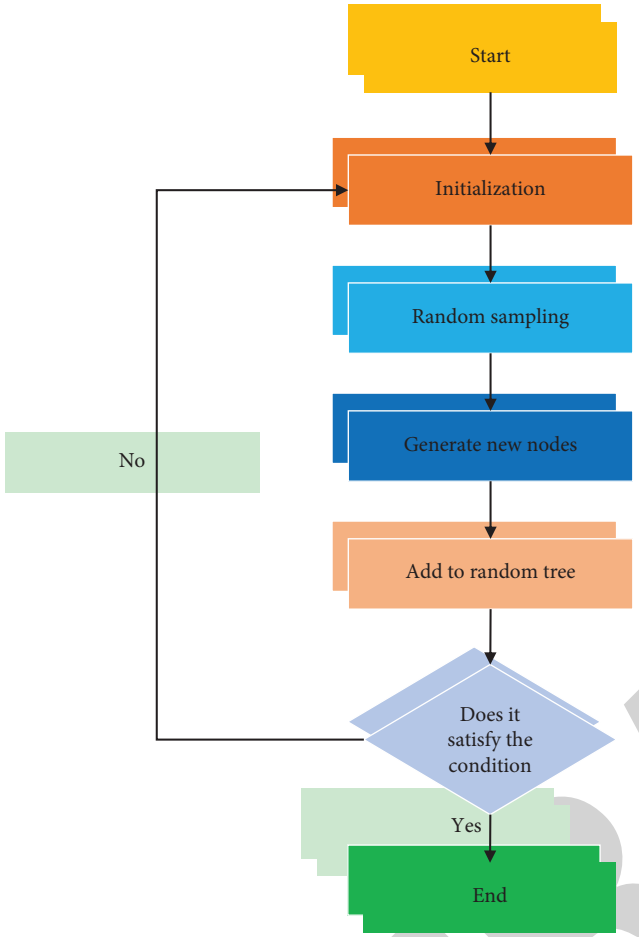

Figure 1: RRT algorithm flow.

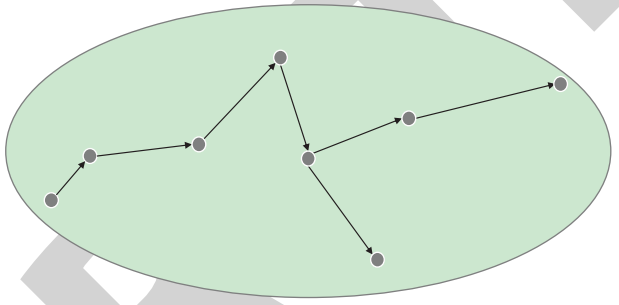

Figure 2: RRT algorithm expansion schematic diagram.

(3) Even under the same laboratory conditions, the RRT algorithm is still unstable, which sometimes causes the RRT algorithm to fall into local minima.

(4) The RRT algorithm must compare the distance between random nodes and extended nodes to determine the location of new nodes, which makes its computational efficiency gradually decrease as the number of nodes increases. Detection at this point has a high probability of redundancy.

(5) In complex conditions such as narrow environments, most RRT calculations are used for obstacle detection, and the overall efficiency of the algorithm will be greatly reduced [11].

A comparison of the advantages and disadvantages of the RRT algorithm is shown in Figure 3.

3.1.3. Path Planning. The route planning process involves obtaining information about the working environment through sensors and reliably determining the best transition path from the starting position to the target position in the working environment based on defined evaluation criteria (e.g., minimum energy consumption, shortest path, and shortest working time) [12]. The path planning equation is as follows.

$$l = \min\{f(\delta) \leftrightarrow S_n, \delta \in [0,1)\}, \quad (2)$$

where l equation represents the optimal path $f(\delta) \leftrightarrow S_n$.

3.2. Reform and Innovation of Music Teaching in Colleges and Universities

3.2.1. Concept Update. In the past, music teachers in China's higher education institutions only focused on the teaching of music knowledge and skills, while neglecting the cultivation of students' practical and application skills. As a result, students' own knowledge and skills often cannot meet the needs of market development. Due to the influence of traditional teaching concepts, music language teachers also ignore students' subjective initiative in the teaching process and the passive learning process affects its effectiveness. To improve the quality of music teaching in colleges and universities, music teachers must carry out reform and innovation in the teaching process and pay due attention to students' initiative in the practical teaching process. They should fully and effectively stimulate students' interest in learning and more active participation in music teaching. Especially in a changing society, college music teachers must change their teaching attitude and clarify the main position of the class to ensure that students can create a more harmonious classroom atmosphere and improve their musical quality [13].

3.2.2. Innovation of Methods. The current traditional music teaching methods do not adapt to the era of rapid economic development. The real needs of our market have limited the development of students. Therefore, it is necessary to reform and update the music teaching methods at this stage. On the one hand, music teachers in colleges and universities should deeply analyze the actual situation and personality characteristics of students in the teaching process, enhance the teaching relevance on the basis of reasonable selection of teaching contents and methods and effectively improve the students' music level. Music, as a unique art form, often puts higher demands on students' practical skills and creative ability. In both cases, teachers should also pay attention to developing students' abilities. At the same time, reform and innovation in teaching methods require teachers to change traditional assessment methods and apply more diverse approaches to improve overall assessment [14].

RETRACTED

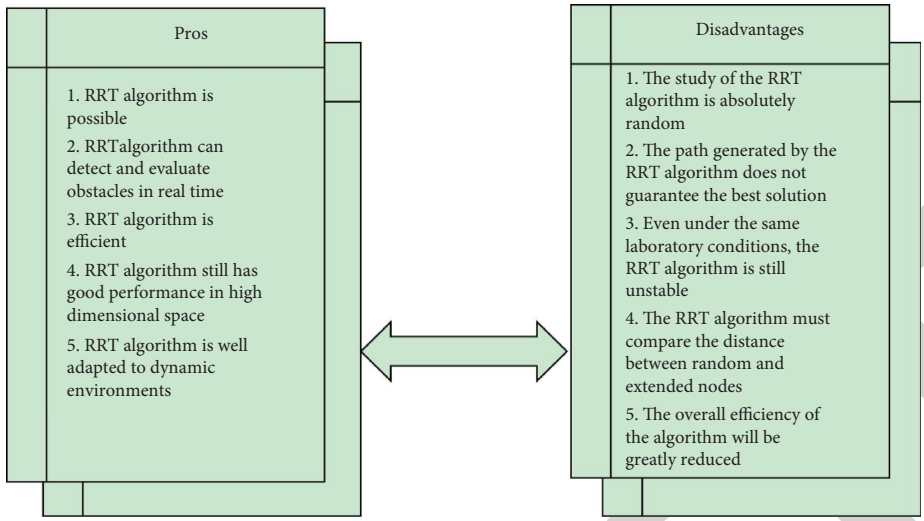

Figure 3: Comparison of advantages and disadvantages of the RRT algorithm.

3.2.3. Improvement of Music Teaching Institutions. The improvement of music teaching institutions is the basis for ensuring the quality of music teaching, so the reform and innovation of music teaching in colleges and universities must be promoted. At present, with the increase of the number of students in higher education institutions, the existing number of music education institutions in China's colleges and universities have not matched the existing number of students, which to a certain extent restricts the quality of music teaching in colleges and universities. Music teaching equipment, as the most important material guarantee for music teaching, not only plays a supporting role for music teaching but also directly affects its effect. In order to effectively improve the quality and level of their music, students need to use their free time outside of class, which usually requires schools to have adequate practice machines. Therefore, our universities need additional funds to improve the equipment and facilities for music teaching [15].

3.2.4. Improvement of Professional Quality and Expertise. The professional quality and professionalism of music teachers in higher education often directly affect the quality of music teaching. Therefore, the reform and innovation of music teaching in colleges and universities also need the optimization and improvement of teachers' team. First of all, in recent years, the number of students in China's universities has been increasing, and the current number of teaching staff cannot meet the needs of the increasing number of students, which not only brings certain pressure to music teachers but also to the overall quality of music teaching. On this basis, our universities should focus on reforming and innovating music teaching, increasing the number of music teachers in schools and ensuring the comprehensive quality of music educators through strict enrollment; in order to improve the teachers' music teaching, our universities should also focus on strengthening the existing education and training of music teachers, improving their professional quality and level, and fundamentally improving their music education [16].

4. Results and Discussion

4.1. Experimental Discussion. In this part, the analysis of the Western orchestral instrument ensemble in China's colleges and universities using the improved RRT's moving path planning algorithm is mainly as follows.

(1) The number of professional learners of the Western orchestral instrument ensemble in China's colleges and universities.

According to the data analysis, it can be seen that the number of people studying the Western orchestral instrument ensemble in China's colleges and universities from 2014 to 2022 has been increasing, mainly because the Western musical instruments are becoming more and more popular in China with the development of the time. Many people are beginning to understand and learn musical instruments and more and more professional students are learning musical instruments, as shown in Figure 4.

(2) Teachers' participation in the teaching of Western orchestral ensemble in China's colleges and universities.

Assuming that the teachers' participation in the teaching of Western orchestral ensemble in China's colleges and universities is 100 points, the analysis of the data shows that the teachers' participation in the teaching of Western orchestral ensemble in China's colleges and universities is above 90 points, which proves that the teachers' participation in the teaching of Western orchestral ensemble in colleges and universities are extremely high, which limits the students' motivation to some extent, as shown in Figure 5.

RETRACTED

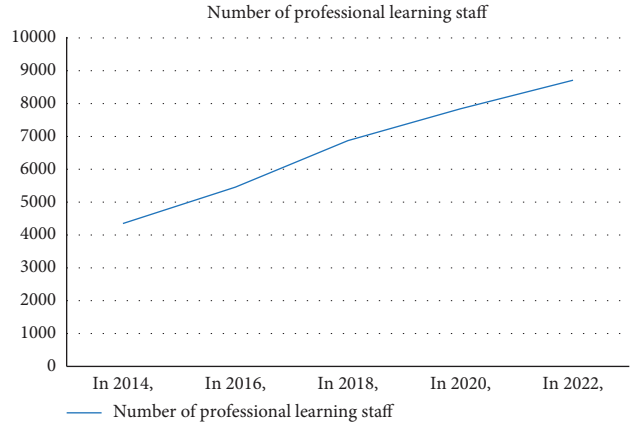

Figure 4: Number of professional learners of the Western orchestral instruments ensemble in China's colleges and universities in the recent years.

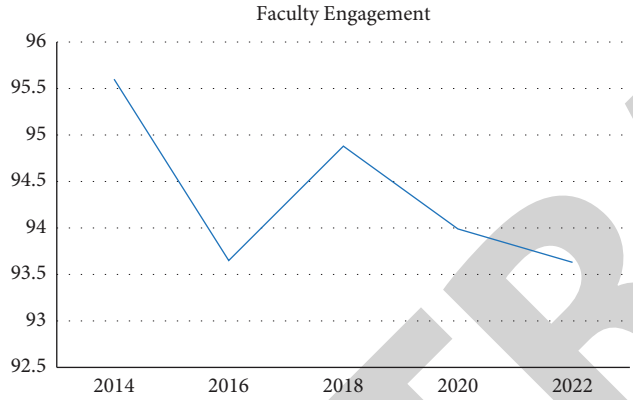

Figure 5: Teacher involvement in the teaching of the Western orchestral instrument ensemble in colleges and universities in China.

(3) Students' initiative in the teaching of the Western orchestral instruments ensemble in Chinese colleges and universities.

Assuming that the initiative of students in the teaching of Western orchestral ensemble in China's colleges and universities is 100 points, the analysis of the data shows that the initiative of students in the teaching of Western orchestral ensemble in China's colleges and universities is above 70 points, and the students' initiative is not enough, as shown in Figure 6.

(4) Relationship between students' initiative and teachers' participation in the teaching of Western orchestral ensemble in colleges and universities in China.

Assuming that students' initiative in the teaching of Western orchestral ensemble in China's colleges and universities is scored 100 out of 100, and the horizontal axis indicates the teacher's participation, it can be seen from the data analysis that students' learning initiative score is getting lower and lower when the teacher's participation is from 10% to 90%. The quality of teaching is as shown in Figure 7.

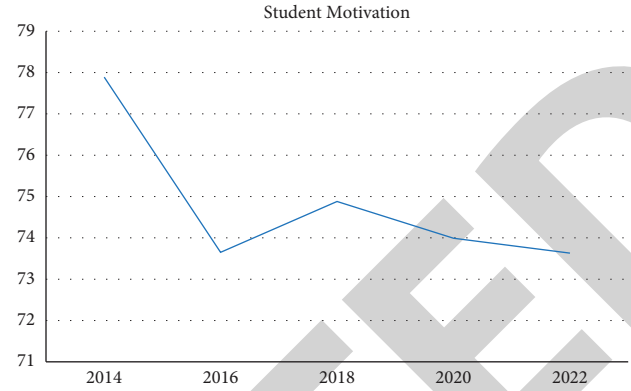

Figure 6: Students' initiative in the teaching of the Western orchestral instrument ensembles in colleges and universities in China.

(5) Satisfaction of teachers and students in the teaching of Western orchestral ensemble in Chinese schools.

Assuming that the satisfaction score of teachers and students in the teaching of Western orchestral ensemble in Chinese schools is 100, the data analysis shows that the satisfaction score of teachers is above 70, and the satisfaction score of students is above 80, which proves that teachers and students are not very satisfied with the teaching of Western orchestral ensemble, so it is necessary to reform and innovate the teaching system of the curriculum, as shown in Figure 8.

4.2. Analysis of Results

4.2.1. Problems of the Western Orchestra Ensemble Courses in Colleges and Universities. Students are not very enthusiastic about Western orchestral ensembles in orchestras. Some university teachers do not understand the importance of the Western orchestra course for training students and some students do not know what professional qualities and skills should be possessed by the Western orchestra ensemble, which leads to a decrease in students' enthusiasm for learning the Western orchestra. For some university teachers, learning the Western orchestra ensembles is an ongoing process. As students become less motivated in the learning process, the learning process is interrupted, which eventually leads them to learn poorly in the orchestra and even affects their future careers.

Some university teachers who teach Western orchestral music not only teach practical training methods for Western orchestral music but also teach courses on instrumental collaboration theory and Western orchestras. However, most students are not interested in the theoretical knowledge of the Western orchestras. Some students have not received specialized and systematic teaching and training, and the Western orchestral ensembles lack intonation and rhythm.

RETRACTED

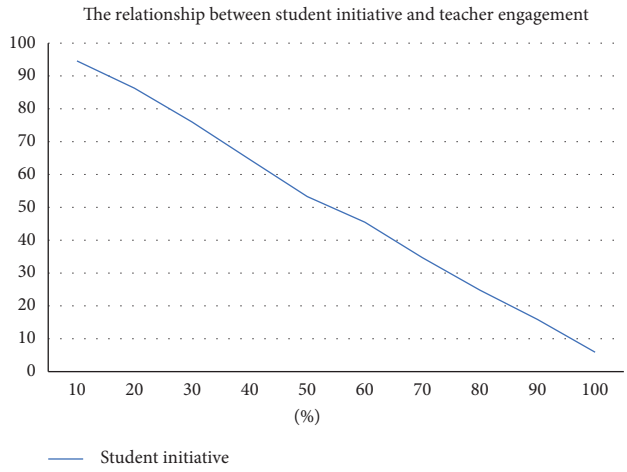

Figure 7: Relationship between students' initiative and teachers' involvement in teaching Western orchestral ensemble in Chinese universities.

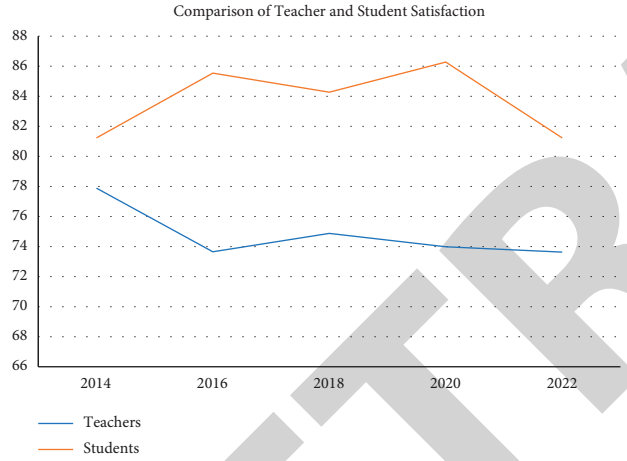

Figure 8: Satisfaction of teachers and students in the teaching of the Western orchestral instrument ensemble in our school.

The lack of awareness of some teachers about the importance of combining theory and practice makes it difficult for some students to give full play to their own initiative and motivation in learning.

In the teaching of vocal instrumental ensemble courses in higher education, some teachers strive only to improve the professionalism and integrity of vocal instrumental ensemble courses, which require different voices to achieve precise division, interaction and balance during performance. However, this requirement can only be achieved with the support of professional training, teamwork, and coordination skills. Any lapses in performance will directly affect the performance of the orchestra. However, some educational professionals in higher education institutions currently exhibit passivity or lack of professional cooperation, resulting in a somewhat unbalanced selection of the Western instruments, thus limiting the balance of string tone.

4.2.2. Requirements for Western Orchestral Ensemble Courses in Colleges and Universities

(1) Requirements for music teachers. In practice, teachers should not only train students to play the instruments but also improve students' independent learning ability. This will enable students to develop good self-learning habits, to become familiar with the music independently before the lesson, to become familiar with the background of the music composition, and to understand the inspiration and meaning of the song composition. The students are taught according to their level of suitability. Different students' perception and understanding of music varies greatly; therefore, their ability to learn the Western orchestral instruments varies as well. In recent years, there has been a wide gap in the level of professional training of string students. These differences do not require teachers to generalize in practice, but rather to reinforce what students already know based on their level of learning. This requires teachers to design different courses and programs for each student. We develop different internship opportunities for different students. For students who have a good professional foundation and lack of practical work, teachers should find more opportunities for them to perform onstage and provide more opportunities for students to perform onstage. This will not only improve students' professionalism but also their adaptability and practical experience. In addition, these students can be encouraged to perform in house concerts, interact with students from other schools, and participate in music competitions. For students with a weak foundation, teachers should encourage them to improve their skills. Teachers will arrange appropriate music and music courses for these students, require them to take specialized subjects carefully when needed and ensure that they do not take exams. Students will be allowed to review the songs carefully after class and play them according to their understanding, giving them new life and meaning. We focus on a comprehensive curriculum. In terms of specialized courses, we should also schedule appropriate orchestra orientation courses. In orchestra orientation classes, students can simulate in the environment and train their reactions to the stage in a playful atmosphere [17].

Teachers need to pay more attention to changes in higher education policy and to the study of Western orchestras. Higher education teachers need to put themselves at the center of their learning, actively learn some theoretical knowledge related to the Western orchestral ensemble courses, and actively participate in artistic practices in and out of school. The traditional method of cooperative learning is reading and games. They neglect choral lessons like other subjects, which cannot be understood solely through collegial learning. Teachers can make full use of multimedia technology for reading, teaching, presenting, and teaching. While playing the Western orchestral instruments, the teacher must take the lead in rehearsing, cooperating, and working closely together in order to play beautiful music under the guidance of the conductor. Therefore, it is necessary to coordinate theoretical teaching, integrate professional masters and teachers, equip students with the ability

RETRACTED

to combine conducting and performance, and integrate the teaching resources of the Western orchestras. In schools that are in a position to attract all relevant professional teachers to form an orchestra, professional teachers can specifically train each voice of the student orchestra in order to improve the students' professionalism within the orchestra and facilitate the integration of the orchestra into the performance process. For some students, it is easy to become distracted and interested in something new in the classroom. Considering the psychological development of the Western orchestra students at this stage, during this time, teachers can recreate instruments, such as string, wind, and other components, and can use the unique sonic characteristics of these instruments to foster active exploration and creative thinking as students learn the instruments. Students are allowed to choose their own notes or substitute original instruments. In addition, as part of teaching western orchestral ensembles, teachers should make full use of various teaching materials and design individualized teaching forms and methods to make teaching Western orchestral ensembles richer and more interesting, thus stimulating students' interest in music more effectively. Teaching Western philharmonic music is an integral part of music teaching in higher education. Accurate rhythm and intonation are the keys to good music. Teachers should understand the difficulties of teaching college orchestras, think deeply about sound teaching methods, apply interdisciplinary, fixed-pitch models to support sound teaching, strengthen students' foresight, and help them develop a sense of proper high level. Teaching evaluation is highly abstract, but most students have a weak sense of abstraction, and disqualification theory often underestimates the meaning and emotional understanding of the work, most often by listening to the music. Combining teaching with comprehension not only allows students to feel the melody of the music more realistically but also reflects the resonance of ideas and emotions, as if they were in the real world, feeling the power of music [18].

(2) Requirements for students. Students are at a stage where they are interested in new subjects. Teachers should take full advantage of these qualities of their students to develop more relevant teaching methods. In Western orchestra instruction, students can only remember the specific rhythms of the notes, not the unique art of the notes. However, if classroom teachers use multimedia technology to represent rhythm in three dimensions in musical performance, they can provide students with a visual and audio-visual three-dimensional musical composition that immerses them in musical appreciation. In evaluating this form of music, students form images and perceptions that are consistent with the notes and have the pedagogical and cognitive potential to enable them to understand the notes in greater depth. Therefore, in the current collaborative teaching, teachers should actively introduce multimedia technology in collaborative teaching so that students can improve their music perception and music perception skills in the learning process [19].

For university teachers, more effective and comprehensive development is inseparable from the university teaching environment and teaching resources. Universities have reformed their teachers at the request of professional associations of education, changing the curriculum of the Western orchestra, and making innovations. The University hires professional faculty members to provide more effective professional advice to young faculty members of higher education institutions, to provide more teaching resources to students, to provide a good learning environment so that they can better develop their acting skills and develop their abilities to express their emotions through instrumental orchestral works, to enable students to combine the theory and practice of the Western orchestra, and to develop their comprehensive skills in order to meet their professional qualities and the higher education in social sphere. In teaching the Western orchestras, teachers should introduce students to the personal emotions that Western music conveys in the teaching process in order to reduce students' tension in collaborative teaching. At the same time, the musical function helps students to establish independent learning patterns. In the teaching process of western orchestral ensembles, teachers can combine the original musical features through interaction and collectivism to encourage students to create their own compositions in daily teaching, so that students can give full play to their creativity and imagination in the sea of music. At the same time, teachers can assess students' creative notes according to their individual characteristics, actively provide tutoring and targeted teaching, and improve students' ability to acquire knowledge and appreciate music. Teacher-student collaboration is an effective way to teach university orchestras. Schools can hire world-class professional artists to serve as sound engineers for the Western orchestras, and students can have them play their instruments, ensuring both the stability and the sonic balance of the core members of the orchestra. However, one will also learn many of the benefits of professional musicians from them, helping the orchestra grow together. In addition, the formation of the strings needs to be relatively stable. It is not enough to rely on students alone, as they are more mobile. After a few years of training, they are just maturing, but they have to leave the orchestra because they are about to graduate. That is why the orchestra is like a cast iron camp and the sailors are like a cycle, one after the other. The people in the orchestra change every year and every year people leave the orchestra. The orchestra was founded in the most difficult period of development, in the middle of a small water period. To solve this problem, professional teachers are required to participate in orchestra rehearsals, and each mainstream music school needs the support of one or two teachers to maintain relative stability [20].

5. Conclusion

With the rapid development of the political and economic life of the country, the level of musical, cultural, and artistic activities of the society is also increasing. According to the demand of the society for musical talents, it is the primary task of the higher music majors to cultivate musical and artistic talents suitable for Chinese conditions. However, the Western orchestral instrument courses in higher education

RETRACTED

institutions are still in the primary stage. Educational philosophy, training objectives, curriculum design, and teaching methods are usually organized according to the pattern of general higher education. The lack of professional experience of teachers, the weakness of students' professional foundation, the lack of understanding of the concept of "qualification standards" in higher education, the lack of "functional and innovative" training, and the development of the Western orchestral instruments in higher education are limited by a number of factors, such as the lack of acceptance of social and professional needs and the lack of talent. The development of the Western orchestral instruments in universities is limited by a number of factors, such as the lack of acceptance of social and professional needs, the characteristics of human resources training, and differences in professional positions. From a macro perspective, this thesis explains and analyzes some problems in the teaching of Western orchestral ensembles in colleges and universities from a practical point of view and puts forward constructive suggestions and recommendations by using the research method of improving RRT's moving path planning algorithm. The reform of talent model in higher music institutions should adapt to the demand of society for music teachers and talents in the new era and to the new changes in the field of basic education reform and basic education. However, considering the new requirements of the new era, the reform of music education in higher music institutions lacks effective means. The reform must be a long-term process, requiring continuous research and experimentation. Therefore, music study programs should be modified and adapted to accommodate the transformations required by the new era in order to produce musicians who may be useful to society. The reform of higher music education should focus on how to maintain the strengths of teaching music skills and fill the gaps in practical courses such as teacher training. Music education should be oriented to the needs of society and clearly oriented to the educational objectives, and in the teaching system, it should be oriented to the training model of music teachers. The concept is based on the talent development model, and the system construction and teaching management should be strengthened to ensure the talent development model. Of course, the road of reform is not smooth, but it will also encounter resistance. The main force of music education professional reform is the first year teachers. They should pay more attention to teaching research. Teachers can only be a permanent source of strength to implement class reforms and to carry out reform measures if they reach a consensus. Unlike general higher education, the goal of higher education talent training is closely related to the social occupation or professional process. Higher music education should go out of the standard basis of music specialization in general higher education system, boldly reform, constantly innovate, fully consider the needs of social music profession, take professional development as the guide, take employment as the guide, clarify the university music career goals, form curriculum model and system, establish corresponding teaching talents and diversified evaluation mechanism, fully reveal the value of music talents, highlight the characteristics of higher education, and improve the social competitiveness of musicians, train musicians, and meet the needs of society. Through studying the Western orchestral ensembles, we have gained a deeper understanding of the Western orchestral instruments. As a cradle of musical talents and a place of musical and cultural exchange, universities have a special role in the development of Chinese music in the West. The teaching of the Western orchestral instruments in colleges and universities is both a need for the development of the Western music in China and a need for higher arts to enter the campus and enhance the cultural quality of the campus, as well as a need for the students' age and spiritual struggle. Given the current situation in China, we must do more to implement effective curriculum reform and development. In terms of training programs, in addition to the basic professional courses, relevant courses such as chorus, band section leadership, and orchestra rehearsal should also be added. We should make the curriculum innovative, based on previous knowledge, more interesting and professional so that students can gain more knowledge and experience in a more favorable environment. It is also worth thinking about the fact that the musicianship courses for the Western orchestral instruments in our universities provide students with good theoretical training and practical orchestral skills, making them more powerful and socially competitive in the future work process.

Data Availability

The dataset is available upon request.

Conflicts of Interest

The authors declare that there are no conflicts of interest.

References

[1] X. Gong, "On the position and function of teaching of musical instruments in national music education," *International Journal of Educational Technology*, vol. 3, no. 2, 2022.

[2] V. Tal, "Teaching musical instruments during COVID-19: teachers assess struggles, relations with students, and leveraging," *Music Education Research*, vol. 24, no. 2, 2022.

[3] J. I. Pozo, M. P. P. Echeverría, A. Casas-Mas et al., "Teaching and learning musical instruments through ICT: the impact of the COVID-19 pandemic lockdown," *Heliyon*, vol. 8, no. 1, 2022.

[4] R. C. Zorzal and J. F. Soares-Quadros Jr, "Taste the value of each note verbal teaching strategies in guitar masterclasses," *Music Education Research*, vol. 23, no. 4, 2021.

[5] S. Melisa, "Monitoring and evaluating body knowledge: metaphors and metonymies of body position in children's music instrument instruction," *Linguistics Vanguard*, vol. 7, no. s4, 2021.

[6] F. A. Simpson, "Inservice music educators' perceived comfort for teaching and performing on secondary band instruments," *UPDATE: Applications of Research in Music Education*, vol. 39, no. 3, 2021.

[7] B. Taylor, "Orchestration and pitch precision in the orchestral music of marc sabat," *Tempo*, vol. 75, no. 295, 2021.

RETRACTED

Hindawi
Computational Intelligence and Neuroscience
Volume 2022, Article ID 4639308, 10 pages
https://doi.org/10.1155/2022/4639308

Research Article

Evaluation Method of Rationality of Creative Genius Cultivation Pattern Based on a BP Neural Network

Yong Li,[1] **Kailing Dong**,[2] **and Qingyuan Wang**[1]

[1]*Chengdu University, Chengdu, Sichuan 610106, China*
[2]*Chengdu Vocational & Technical College of Industry, Sichuan 610213, China*

Correspondence should be addressed to Yong Li; liyong18@cdu.edu.cn

Received 5 July 2022; Revised 9 August 2022; Accepted 17 August 2022; Published 20 September 2022

Academic Editor: Yaxiang Fan

Copyright © 2022 Yong Li et al. This is an open access article distributed under the Creative Commons Attribution License, which permits unrestricted use, distribution, and reproduction in any medium, provided the original work is properly cited.

In order to realize the evaluation of the rationality of an innovative talent training mode, an evaluation model of the rationality of the innovative talent training mode based on a BP neural network is proposed. On the basis of clarifying the principle of the BP neural network model, according to the method of parameter multisource control analysis, the multi-objective characteristic analysis of the rationality of the innovative talent training mode is realized to measure the difference and balance between the two variables of the rationality of the innovative talent training mode. A BP neural network algorithm is designed to find the best feature subset, and a feature sequence sampling and recombination model is constructed. Through reliability evaluation and nonparametric quantitative feature estimation, quantitative analysis and evaluation of the rationality of the innovative talent training mode are realized. The test results show that the confidence level and reliability of the rationality evaluation of the innovative talent training mode using this method are high.

1. Introduction

At present, there is a common problem in talent training in colleges and universities to varying degrees: that is, the problem of "short" and "lack" of elements, such as the talent training mode, follows the old system, and the training objectives and specifications of innovation and entrepreneurship are not clear; or there are various problems in the training process, or the management and evaluation system is imperfect or even lacking; or the way and method are single and lack of incentive mechanism. The limitations of its innovation and entrepreneurship education are as follows: only relying on a small number of lectures on entrepreneurship, relying on entrepreneurship plan competitions, or opening a very limited number of entrepreneurship public elective courses, and there is no systematic framework for the entrepreneurship education curriculum system [1–3].

In the traditional methods, the evaluation algorithms for the rationality of creative genius cultivation pattern mainly include the particle swarm optimization (PSO)-based rationality evaluation algorithm, statistical analysis algorithm, and association rule feature extraction algorithm. Through the statistical analysis of the rationality time series of creative genius cultivation pattern [4–6], the rationality evaluation of creative genius cultivation pattern is realized by the method of correlation feature detection. When the adaptability of the above methods for evaluating the rationality of creative genius cultivation pattern is not good, it is necessary to conduct comprehensive and objective analysis and research on the rationality of creative genius cultivation pattern. As an important research method, computational intelligence and knowledge network pay attention to the network relationship between computational intelligence and network structure [7, 8]. Based on this, this paper attempts to effectively combine the knowledge network with the scale to test the rationality of the innovative talent training mode, and try to find the relationship between the dimensions in the scale in order to better evaluate the innovative talent training mode and solve the problem of the innovative talent training [9].

Therefore, this paper puts forward the rationality evaluation model of innovative talent training mode based on a

BP neural network. The BP neural network algorithm [10] is used for finding the best feature subset. Based on the feature selection method of regular term, a feature sequence sampling and recombination model for the rationality of the innovative talent training mode is constructed. Combined with the BP neural network and the machine learning method, the reliability evaluation and nonparametric quantitative feature estimation of the rationality of the innovative talent training mode are carried out. The sample regression analysis model is constructed to conduct quantitative analysis and evaluation of the rationality of the innovative talent training mode. Finally, the empirical analysis is carried out and the conclusion of effectiveness is drawn.

2. Theoretical Basis of Rationality Evaluation of the Innovative Talent Training Mode

In order to realize the rationality evaluation of the innovative talent training mode based on the BP neural network, it is necessary to first build a statistical analysis model for the rationality evaluation of the innovative talent training mode. The BP neural network is a multilayer feedforward network trained according to error backpropagation (error backpropagation for short). Its algorithm is called the BP algorithm. Its basic idea is the gradient descent method, which uses gradient search technology to minimize the error mean square deviation of the actual output value and expected output value of the network [11, 12]. Figure 1 shows the structure of the BP neural network.

Suppose x_i, y_i, and z_i are the input layer node, hidden layer node, and output layer node of the BP neural network, respectively. The connection weight between x_i and y_i is w_{ij}; the weight between y_i and z_i is v_{ij}. The detailed learning process is as follows:

(1) *Network initialization*. The random value of $[-1, 1]$ interval is defined as the network weight and threshold.

(2) Output calculation of each layer.

(3) Calculate the error of the output layer node.

(4) If the error results meet the expected requirements, this is the end. If not, further correction is required.

(5) Modify the network weight.

(6) Update the network threshold.

If the calculation result is not within the predetermined range, the above process must be repeated until the output error meets the predetermined interval, and the BP neural network training is ended. Thus, the implementation structure of rationality evaluation of the innovative talent training mode based on the BP neural network is shown in Figure 2.

The structure shown in Figure 2 can be summarized into four parts: (1) the data acquisition part of indicator parameters, data management, report management, and visual management; (2) extraction of the training characteristics of innovative talents; (3) rationality evaluation and nonparametric quantity feature estimation; and (4) output of the evaluation results of the innovative talent training mode.

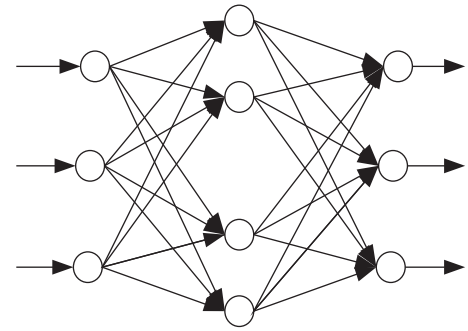

Figure 1: Structure of the BP neural network.

It is necessary to optimize the curriculum structure of creative genius under the background of talent strategy, emphasize the cultivation of methods and abilities, ensure the education quality of creative genius under the background of talent strategy, and promote the teaching reform of creative genius under the background of talent strategy [13–15].

3. Rationality Evaluation Pattern of Creative Talent Cultivation Pattern

3.1. Feature Selection of Rationality Evaluation of Creative Talent Cultivation Pattern. Using traditional statistical methods, the nine dimensions in SCL are divided into four categories, and a statistical analysis model for evaluating the rationality of the innovative talent training mode is established. A figure is calculated by some mathematical method. The calculation methods can be divided into three types: (1) the method of calculating based on the known number or quantity—the calculation method follows a specific relationship; (2) the method of calculating by theoretical reasoning of numbers; and (3) the method of calculating based on the average. In this paper, the second one is selected when constructing the statistical analysis model for the rationality evaluation of the new talent training mode.

According to the Shapiro–Wilk ($n \leq 50$) normality test and variance homogeneity test, we except that the leadership and interpersonal/communication ability dimensions do not meet the normal distribution; the other dimensions meet the normal distribution, and the variance is homogeneous. Therefore, the Mann–Whitney U test in the non parametric test is adopted, and the independent-sample t test is adopted for the rest. The scores of each dimension of the two groups' self-assessment of talents' ability are inconsistent from high to low. The scores of the two groups' interpersonal/communication ability are the highest, and the scores of the teaching/cooperation ability are the lowest. The details are shown in Table 1.

This paper combines the BP neural network with the machine learning method [16–18]. The reliability evaluation and nonparametric quantitative characteristics of the rationality of the innovative talent training mode are

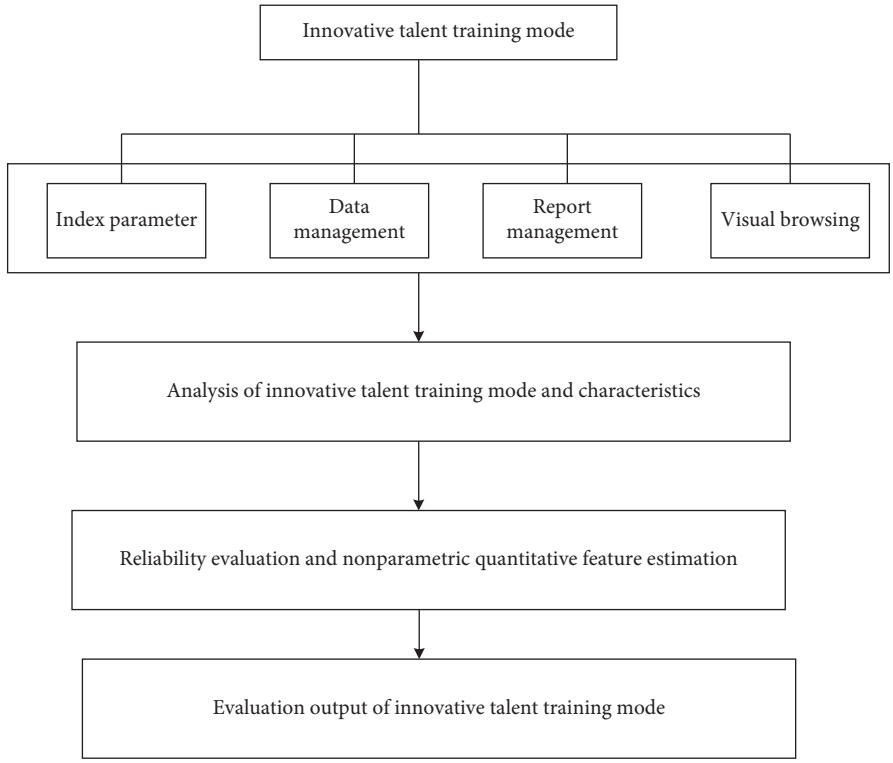

Figure 2: Implementation structure diagram of rationality evaluation of creative genius cultivation pattern based on the BP neural network.

Table 1: Ranking of the average scores of each dimension of the self-assessment of the two groups of students.

Project	Sort/rank	
	Experimental group (36 students)	Control group (40 students)
Leadership	5	4
Interpersonal/ communication skills	8	7
Teaching/cooperation ability	11	10
Professional development ability	6	5

estimated. The correlation gradient function of the rationality of initial creative genius cultivation pattern is expressed as shown in the following formula:

$$x_{ij} = x_{\min,j} + \text{rand}(0,1)\left(x_{\max,j} - x_{\min,j}\right), \tag{1}$$

where $x_{\min,j}$ and $x_{\max,j}$ represent the minimum and maximum interclass distribution feature sets of the rationality distribution of creative genius cultivation pattern, and rand represents random function. According to the mining results of the rationality evaluation information of creative genius cultivation pattern, frequent item sets are reorganized on the rationality evaluation data of creative genius cultivation pattern [19–21], and the statistical analysis pattern of rationality evaluation of creative genius cultivation pattern is constructed by combining quantitative regression analysis method, and the weighted coefficient is expressed as shown in the following formula:

$$\left[\nabla^2 F(x)\right]_{kj} \cong 2J^T(x)J(x), \tag{2}$$

where $J(x)$ and $J^T(x)$, respectively, represent the dynamic detection factor of the rationality distribution factor of creative talent cultivation pattern.

According to the prior data of the rationality results of creative genius cultivation pattern, a multidimensional distributed task set of the rationality of creative genius cultivation pattern is established as $P(n_i) = \left\{p_k | pr_{kj} = 1, k = 1, 2, \cdots, m\right\}$, and the fuzzy iterative equation for evaluating the rationality of creative genius cultivation pattern is obtained by the method of priority attribute scheduling, as shown in the following formula:

$$V_{id}^{t+1} = wV_{id}^{t} + c_1 r_1 \left(p_{id} - x_{id}\right) + c_2 r_2 \left(p_{gd} - x_{gd}\right), \tag{3}$$

where w is the characteristic factor of tree pattern, c_1 and c_2 are dynamic factors for rationality evaluation of creative genius cultivation pattern, x_{gd} and x_{id} are dynamic parameters of differential selection, p_{gd} and p_{id} are clustering parameters of various factors, and hierarchical clustering parameters are used to determine the correlation characteristic quantity of rationality of creative genius cultivation pattern. For each $w \in Z$, a statistical analysis and parameter evaluation pattern of rationality of creative genius cultivation pattern are constructed, and the rationality evaluation of creative genius cultivation pattern is carried out by combining the method of big data

mining. The objective function of rationality evaluation of creative genius cultivation pattern is as shown in the following formula:

$$F = \sum_{j=1}^{n} \sum_{i=1}^{m} C_{ij} X_{ij}, \tag{4}$$

where X_{ij} is the correlation parameter to explain the original variables, C_{ij} is the factor and principal component characteristics, and m, n is the hierarchical structure parameter. The analytic hierarchy process and fuzzy parameter fusion method are used to pattern the rationality evaluation of creative genius cultivation pattern, and the characteristic resolution function of rationality evaluation of creative genius cultivation pattern is obtained, as shown in the following formula:

$$g_k + A_k \Delta x_k = 0, \tag{5}$$

where g_k is the statistical characteristic quantity of the common factor of the rationality evaluation of creative genius cultivation pattern, A_k is the correlation parameter between the original variables explained by the rationality evaluation factor of creative genius cultivation pattern, and Δx_k is the comprehensive variable of the rationality evaluation of creative genius cultivation pattern [22]. The statistical big data analysis pattern is established to evaluate the rationality of creative genius cultivation pattern, and the output statistical characteristic quantity is shown in the following formula:

$$\begin{cases} net_{s1}(k) = r_s(k), \\ net_{s2}(k) = y_s(k), \end{cases} \tag{6}$$

where $r_s(k)$ represents the original variable of factor interpretation, and $y_s(k)$ represents the characteristic quantity of principal component. Combining the BP neural network and the machine learning method, the reliability evaluation and nonparametric quantitative characteristic estimation of the rationality of creative genius cultivation pattern are carried out, and the output statistical characteristic quantity is as shown in the following formula:

$$u_{si}(k) = net_{si}(k), \tag{7}$$

where $net_{si}(k)$ represents the constraint parameters related to principal components. According to the attribute clustering of big data on the rationality of creative genius cultivation pattern, a multi-objective programming is carried out, and the multi-objective programming function is obtained as shown in the following formula:

$$x_{si}(k) = \begin{cases} 1, u_{si}(k) > 1, \\ u_{si}(k), -1 \le u_{si}(k) \le 1, \\ -1, u_{si}(k) < -1, \end{cases} \tag{8}$$

where $u_{si}(k)$ represents the edge node vector of the rational flow load of creative genius cultivation pattern. According to the above analysis, the characteristic sequence sampling and recombination pattern of creative genius cultivation pattern rationality is constructed, and the reliability evaluation of creative genius cultivation pattern rationality is carried out by combining the BP neural network and the machine learning method [23–25].

The entity load of rationality of creative genius cultivation pattern is as follows: fuzzy evaluation and parameter evaluation of rationality of creative genius cultivation pattern are carried out using the method of association regularity detection, and the output migration load of creative genius cultivation pattern is obtained as shown in the following formula:

$$L_t^{eff} = \frac{1}{n_j} \frac{L_0 P_j^{\min} - L_j P_0^{\min}}{P_0^{\min} + P_j^{\min}}. \tag{9}$$

In the above formula, $P_j{}^{\min}$ represents the modified optimal load transfer of the rationality of creative genius cultivation pattern, $P_0{}^{\min}$ represents the decision variable of the rationality evaluation of creative genius cultivation pattern, X_{ij} is the autocorrelation variable of the rationality evaluation of creative genius cultivation pattern, and n_j represents the marginal feature distribution of the rationality evaluation of creative genius cultivation pattern, thus realizing the feature screening of the rationality evaluation of creative genius cultivation pattern.

3.2. Output of Rationality Evaluation of Creative Talent Cultivation Pattern. The characteristic sequence sampling and recombination pattern of the rationality of creative genius cultivation pattern is constructed. Combining the BP neural network and the machine learning method [26], the reliability evaluation and nonparametric quantitative characteristic estimation of the rationality of creative genius cultivation pattern are carried out. The optimization control module of the rationality evaluation of creative genius cultivation pattern is described as shown in the following formula:

$$\begin{aligned} \min(f) &= \sum_{i=1}^{m} \sum_{j=1}^{n} C_{ij} X_{ij}, \\ &= \begin{cases} \sum_{j=1}^{m} X_{ij} = a_i, i = 1, 2 \cdots m, \\ \sum_{i=1}^{m} X_{ij} = b_i, j = 1, 2 \cdots n, \\ X_{ij} \ge 0, i = 1, 2 \cdots m, j = 1, 2 \cdots n, \end{cases} \end{aligned} \tag{10}$$

where C_{ij} and X_{ij} are related. Through the above mathematical pattern construction, a multi-objective programming pattern for evaluating the rationality of creative genius

cultivation pattern is established, which is expressed as shown in the following formula:

$$x_i = \begin{cases} 0, M - \sum_{j=1}^{\lfloor n/2 \rfloor} w_j - \sum_{j=\lfloor n/2 \rfloor + 1}^{i} w_j - \sum_{j=i+1}^{k} w_j < 0, i \le k, \\ f_i(M, n, w, c, r) = \min\{f(M, n, w, c, r)\}, \\ 1, M - \sum_{j=1}^{\lfloor n/2 \rfloor} w_j - \sum_{j=\lfloor n/2 \rfloor + 1}^{i} w_j - \sum_{j=i+1}^{k} w_j > 0, \end{cases} \quad (11)$$

where M is the original variable of factor explanation of creative genius cultivation pattern, w_j is the statistical characteristic quantity of common factor, and $f_i(M, n, w, c, r)$ is the positive correlation parameter between factors. Through the autocorrelation feature matching method, intelligent learning and output control can be achieved, and the statistical characteristic quantity of rationality evaluation of creative genius cultivation pattern meets the multi-objective linear mapping. The mapping relationship between multi-objective programming constraint parameter set R^N and X^N existing correlation is shown in the following formula:

$$p\left(R^N = r_i\right) = p\left(\begin{array}{l} X^N = x_i \,\middle|\, |x_i| = |r_i|, angle(x_i) \\ = \left(angle(r_i) - \varphi_g\right) \bmod (2\pi) \end{array}\right), \quad (12)$$

where X^N is the total score parameter of creative genius cultivation pattern, x_i is the correlation parameter of creative genius cultivation pattern, r_i is the dynamic distribution parameter of creative genius cultivation pattern, and $angle(x_i)$ is the multivariate statistical characteristic parameter of creative genius cultivation pattern. Combining with the artificial intelligence learning method, the self-adaptive learning of rationality evaluation of creative genius cultivation pattern is obtained, and the reliability constraint parameter pattern describing rationality evaluation of creative genius cultivation pattern is as shown in the following formula:

$$H\left(R^N\right) = -\sum_{i=1}^{M} p(r_i) \lg(p(r_i)), \quad (13)$$

where M is the number of elements in the symbol set, the fuzzy characteristic analysis method is adopted, $p(r_i)$ is the correlation parameter between the original variables in the rationality evaluation of creative genius cultivation pattern, $p(x_i)$ is the explanation process parameter of the rationality factor of creative genius cultivation pattern, and X^N is the fuzzy characteristic quantity of the rationality of creative genius cultivation pattern, so as to evaluate the rationality of creative genius cultivation pattern.

Combining the BP neural network with the machine learning method, the reliability evaluation and nonparametric quantitative feature estimation of the rationality of creative genius cultivation pattern are carried out, and the sample regression analysis pattern is constructed to quantitatively analyze and evaluate the rationality of creative genius cultivation pattern; the random distribution concept set of the rationality evaluation of creative genius cultivation pattern is constructed, and the random probability distribution is obtained as shown in the following formula:

$$H = H\left(R^N, \varphi_g | Z^N\right) = H\left(R^N | Z^N\right) + H\left(\varphi_g | Z^N\right) - I\left(R^N; \varphi_g | Z^N\right), \quad (14)$$

where the objective window function of rationality evaluation of creative genius cultivation pattern is $R_2^T R_2 = V_2 \sum_2 V_2^T$, the fuzzy correlation scheduling of rationality evaluation of creative genius cultivation pattern is carried out by the multidimensional hierarchical mining method, the rationality of creative genius cultivation pattern is statistically evaluated by the rough set evaluation and multi-objective programming method, and the optimal learning weight of rationality evaluation of creative genius cultivation pattern is obtained as shown in the following formula:

$$\omega = \omega_{\max} - t \frac{\omega_{\max} - \omega_{\min}}{T_{\max}}, \quad (15)$$

where $\omega_{\max}$ and $\omega_{\min}$, respectively, represent the regulation coefficient of the rationality evaluation of creative genius cultivation pattern, and $T_{\max}$ is the maximum control timescale. Based on the above analysis, a characteristic sequence sampling and recombination pattern of the rationality of creative genius cultivation pattern is constructed. Combining the BP neural network and the machine learning method, the reliability evaluation and nonparametric quantitative feature estimation of the rationality of creative genius cultivation pattern are carried out, and a sample regression analysis pattern is constructed to quantitatively analyze and evaluate the rationality of creative genius cultivation pattern, so as to realize the rationality evaluation of creative genius cultivation pattern. The optimization process is shown in Figure 3.

According to the above optimization process, the rationality evaluation and optimization of the innovative talent training mode are realized. The optimized evaluation model has better evaluation accuracy and efficiency.

4. Simulation Analysis

In order to verify the application performance of this method in evaluating the rationality of creative genius cultivation pattern, a simulation test is conducted, and a simulation analysis is conducted by combining 14.0 Matlab 7 and SPSS14.0. When analyzing the cluster diagram of each factor of SCL-90, hierarchical clustering is adopted, which can also be called systematic clustering. In SPSS, the path is analysis-classification-systematic clustering, and variables are selected in clustering. The cluster ice wall chart and cluster tree chart of each factor are analyzed, as shown in Figures 4 and 5, respectively.

Under the background of talent strategy, the management department of creative genius and 201 creative genius under the background of talent strategy conducted a questionnaire survey (209 valid questionnaires were collected in total). The number of people counted was 2,000,

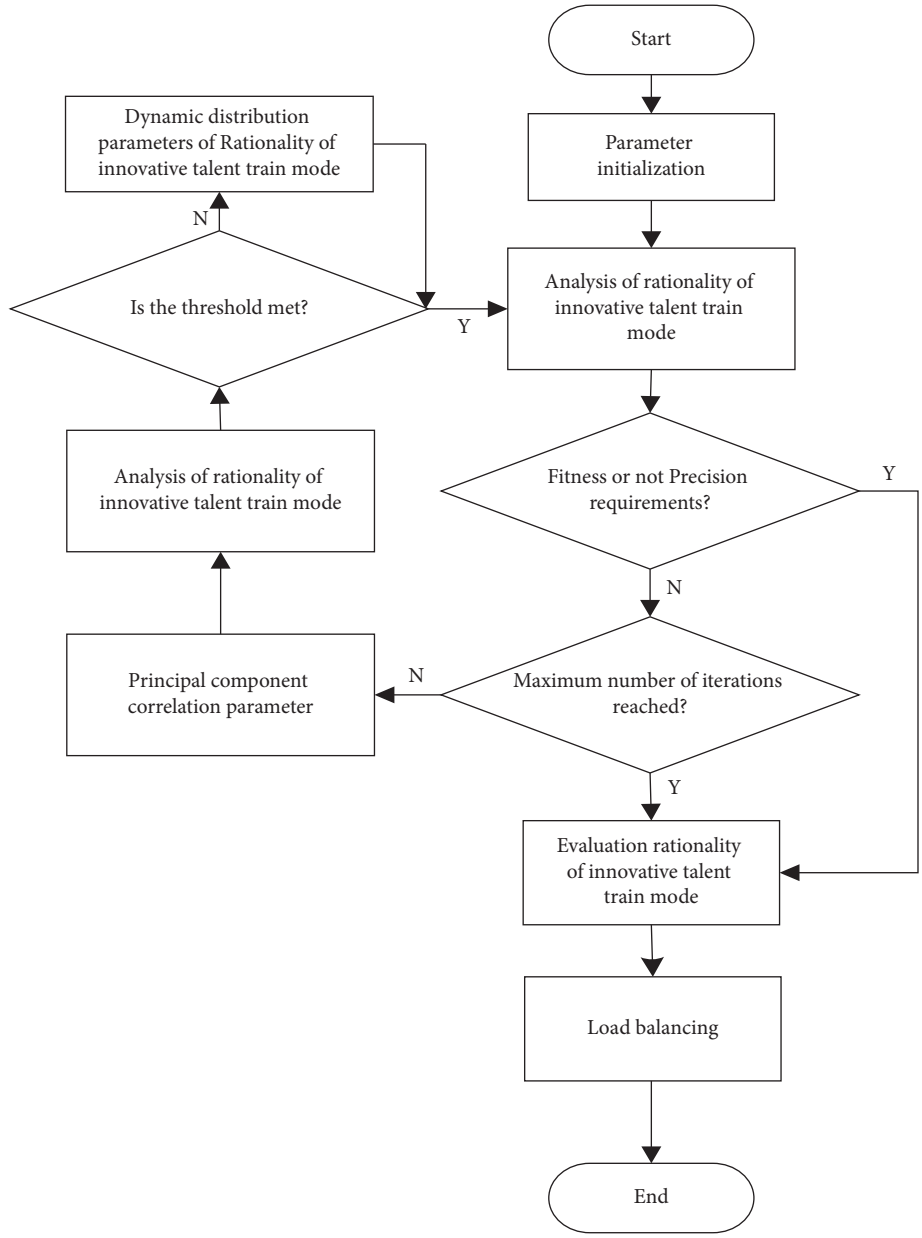

Figure 3: Optimization process of rationality evaluation of creative talent cultivation pattern.

and the number of optimization iterations of multi-objective programming was 400. According to the above simulation parameters, the rationality evaluation simulation analysis of creative genius cultivation pattern was carried out.

Taking the data in Figures 3 and 4 as the research object, the fuzzy correlation big data analysis pattern of the rationality of creative genius cultivation pattern is established, and the fuzzy degree evaluation and parameter evaluation of the rationality of creative genius cultivation pattern are carried out by the method of association regularity detection. The characteristic distribution diagram is shown in Figure 6.

Using the factor analysis method, 748 positive test data were screened, and the results of discipline construction, scientific research, teaching, and achievements were transformed into factors. According to the analysis of Figure 5, this method has good convergence when evaluating the training mode of innovative talents.

The test confidence level is shown in Table 2.

According to the analysis, the rationality evaluation of creative genius cultivation pattern by this method has high confidence level and good reliability, and the evaluation results can accurately reflect the subset of evaluation features related to the rationality of creative genius cultivation pattern. The rationality evaluation parameters obtained by the evaluation all have significant differences ($P < 0.05$), while other factors have no significant differences. The rational distribution of creative talent cultivation pattern is lower than the norm

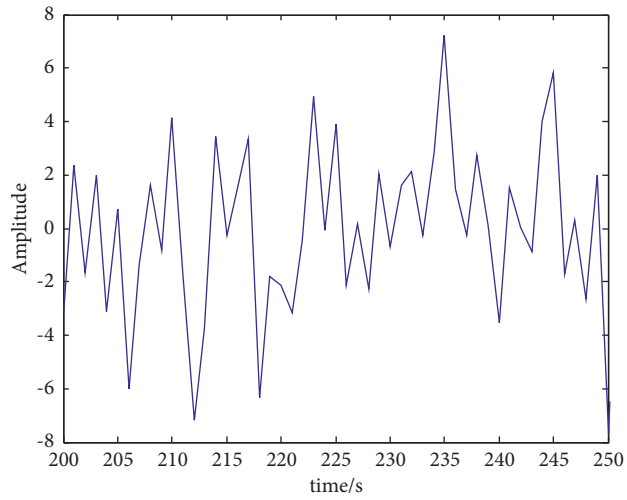

Figure 4: Cluster ice chart of each factor in the rationality evaluation of creative talent cultivation pattern.

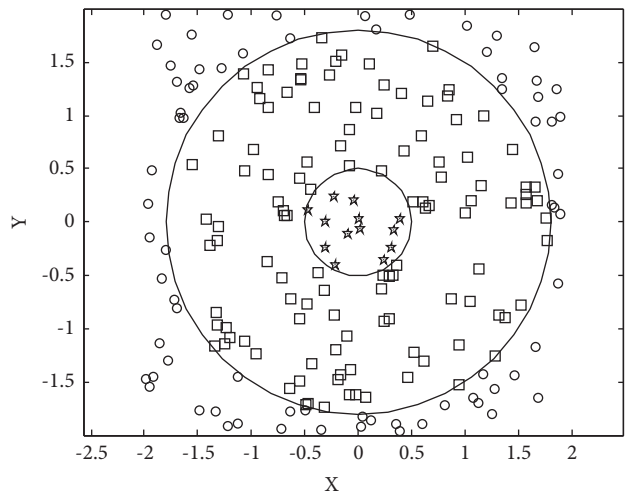

Figure 5: Cluster tree diagram of each factor in the rationality evaluation of creative talent cultivation pattern.

($P < 0.05$), and the talent cultivation is significantly higher than the norm ($P < 0.05$).

In order to further test the reliability of the algorithm in this paper in evaluating the rationality of the innovative talent training mode, statistics are made on the evaluation accuracy of the five universities in the innovative talent training mode using the algorithm in this paper. The statistical results are shown in Figure 7.

It can be seen from the results in Figure 7 that the accuracy rate of evaluating the rationality of the innovative talent training mode using the algorithm in this paper is over 65%, which indicates that the algorithm in this paper can not only effectively evaluate the rationality of the innovative talent training mode, but also has a high evaluation accuracy rate.

On this basis, the computational complexity of the proposed algorithm is calculated by comparing the methods in [4, 5]. The shorter the time of the algorithm, the lower the computational complexity. Therefore, the experiment is

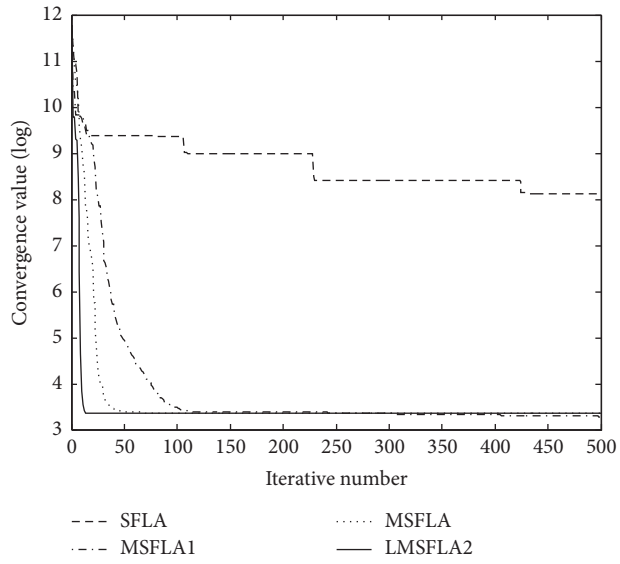

Figure 6: Distribution of features of rationality evaluation of creative talent cultivation pattern.

conducted with the evaluation time as the test index. The experimental results are shown in Figure 8.

As shown in Figure 8, under the same conditions, the time of the proposed method is the shortest and the maximum time is 6S, which indicates that the proposed method has the lowest computational complexity, the strongest operability, and high practical applicability.

5. Discussion

5.1. Deficiency

(1) The cultural atmosphere of innovation needs to be strengthened.

Innovation requires a free, relaxed, and failure-tolerant cultural atmosphere and innovation environment. Although many colleges and universities in China are constantly exploring the innovative talent training mode and formulating the corresponding innovative talent training plans and programs, the cultivation of innovative talents in some colleges and universities is still on the surface, and innovation is not really implemented in teaching.

(2) Lack of innovative teachers.

At present, there is a lack of innovative and double-qualified teachers in colleges and universities in China. Although some college teachers have high academic qualifications, they lack corresponding work experience, social practice, and innovation consciousness. Teachers in colleges and universities still focus on theoretical guidance and adopt a single teacher-based teaching method. They fail to combine theoretical knowledge with social practice in the teaching process, and cannot actively guide students to develop innovative thinking, innovative spirit, and innovative ability. In addition, some teachers are

Table 2: Confidence level test of rationality evaluation of creative talent cultivation pattern.

Test object	Subject	Scientific research	Teaching	Achievement transformation
1	6.914	4.645	76.822	0.574
2	8.164	6.039	43.630	3.956
3	6.834	7.057	42.142	7.798
4	1.755	8.355	34.345	8.470
5	0.826	3.852	58.740	6.270
6	9.928	3.331	91.603	1.912
7	7.342	5.362	77.898	9.333
8	2.739	9.961	13.184	6.011
9	9.794	0.465	67.191	5.985
10	5.407	9.642	32.633	5.679
11	5.505	0.929	12.637	8.074
12	6.771	6.357	77.919	2.099
13	2.308	9.730	66.212	2.991
14	9.493	0.694	81.183	3.316
15	2.804	3.972	14.461	9.432
16	1.151	8.263	12.349	4.159
17	0.663	3.854	58.293	3.454
18	0.254	8.942	3.119	4.646
19	413.211	9.259	96.540	9.152
20	409.572	5.291	20.348	8.138

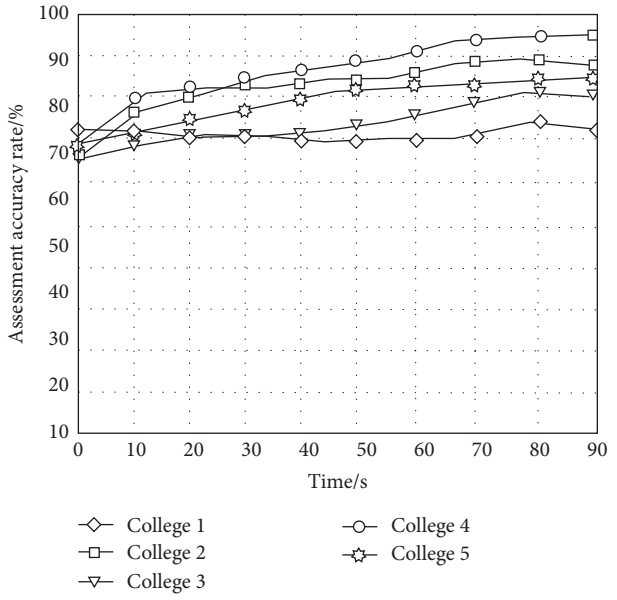

Figure 7: Evaluation accuracy.

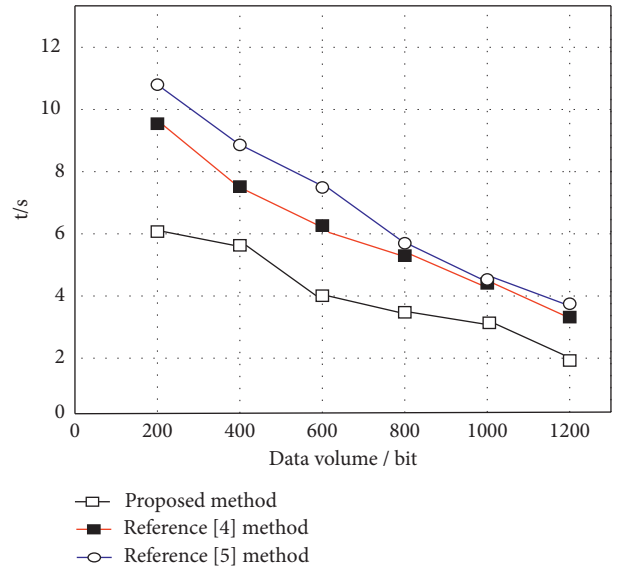

Figure 8: Comparison of evaluation time between different methods.

busy with their own scientific research, pay little attention to the cultivation of students' innovative abilities, and neglect the development of students' innovative potential. The lack of innovative and double-qualified teachers in colleges and universities is far from meeting the needs for cultivating innovative talents in colleges and universities.

(3) The curriculum system of innovative talents training is not perfect.

The imperfection of the curriculum system in colleges and universities is mainly reflected in two aspects: first, undergraduate education lacks courses aimed at cultivating innovative talents. Higher education in China is divided into vocational education and theoretical education. For a long time, higher vocational colleges mainly undertake the task of vocational education, while undergraduate schools mainly undertake theoretical education. Therefore, many undergraduate schools have more theoretical courses, but less or no practical courses for the cultivation of innovative talents; and second, the curriculum system for the cultivation of innovative talents is unreasonable. At present, the practical courses for the cultivation of innovative talents in

many colleges and universities are only case studies in the classroom, which do not allow students to really participate in innovative activities, and fail to enable students to think actively when solving practical problems with theoretical knowledge and cultivate innovative ability. Such a curriculum system is still not separated from theoretical teaching.

(4) The evaluation mechanism of the innovative talent training is not perfect.

At present, the evaluation mechanism of university teachers' talent training does not include the innovative ability in the assessment criteria, which leads to the teachers blindly pursuing the publication of papers, books, and scientific research projects. Therefore, it is difficult to form a long-term innovative cultural atmosphere, and the quality of the innovative talent training cannot be improved.

5.2. Strategy

(1) We should improve classroom teaching efficiency and lay a solid foundation for students' innovation.

We are in the era of knowledge economy and information technology. Compared with their predecessors, today's students need to learn so much and have greater pressure. Therefore, we must teach students the most basic and applicable things, teach them how to learn, how to do things, and how to be a person, and encourage them to be brave in challenges and good at entrepreneurship.

(2) We should reasonably set up practice links to improve students' innovation ability.

attach importance to teaching practice and highlight the creative nature of education. It is an effective way to cultivate students' practical ability and arouse their enthusiasm for innovation to emphasize the link to practical teaching and attach importance to the combination of theory and practice. Social work and social practice play a special role in improving students' comprehensive quality, and cultivating students' practical ability and innovative spirit. According to the requirements of social and economic development, the university pays attention to updating the practice teaching links and contents, advocates the integration of practice activities with production practice, and strengthens the construction of practice. We should make full use of social resources, make students participate in enterprise production and operation activities during school, shorten the distance between school and society, and improve students' practical ability.

(3) We should closely rely on scientific research and training to cultivate students' innovative consciousness.

We should study how to vigorously develop the third class of industry university research cooperation, and adopt various ways to attract students with certain innovation ability to participate in the scientific research work of teachers so that students in school can gain knowledge in practice, increase wisdom in scientific research, and further expand the ways of using educational resources to train application-oriented talents.

(4) We should actively participate in competition activities and induce students' innovative thinking.

The competition is a banner leading modern college students to ignite their passion for innovation, and an important carrier to promote the cultivation of innovative talents in colleges and universities and the construction of an innovative country. Organizing competitions can not only inspire young students' fighting spirit, arouse their innovative consciousness, and cultivate their innovative spirit and ability, but also promote the creation of a positive campus cultural atmosphere and the activation of students' extracurricular scientific and technological activities.

(5) We should carry out the second class extensively and expand students' innovation space.

The second class is an important part of talent training, an important way for students to practice professional theoretical knowledge and cultivate innovative and practical abilities, and an effective means to improve students' employment competitiveness. Through practice and exploration, make full use of the form of students' professional associations, actively organize students to participate in various social practice activities, and gradually form a set of second class implementation plans that are suitable for the training objectives of the major, meet the teaching requirements, and have a relatively perfect system.

6. Conclusions

In this paper, the rationality evaluation model of the innovative talent training mode based on the BP neural network is proposed. A statistical analysis model is built to evaluate the rationality of the innovative talent training mode, and the multiobjective planning and characteristics of the rationality of the innovative talent training mode are analyzed. The fuzzy evaluation and parameter evaluation are carried out using the method of association rule detection to realize the rationality evaluation of the innovative talent training mode. The empirical analysis results show that this method has a high accuracy in evaluating the rationality of creative genius cultivation pattern, and it has a good application value in evaluating and predicting the rationality of creative genius cultivation pattern.

Data Availability

The raw data supporting the conclusions of this article can be obtained from the corresponding author upon request.

Conflicts of Interest

The authors declared that they have no conflicts of interest regarding this work.

Acknowledgments

This work was supported by the Higher Education Talent Cultivation Quality and Teaching Reform Project of Sichuan Province, 2021–2023, "Research and Practice of Sustainable Diversified Collaborative Talent Cultivation Mechanism in Urban Universities" (JG2021-1073), and Talent Cultivation Quality and Teaching Reform Project of Chengdu University "From Emerging to First-class: An Exploration of the Educational Mode of" One Foundation, Three Yuan, Integration of Innovation and Integration "in Urban Universities under the Integrated Development of University and City" (CDJGB2022191).

References

[1] Z. Chen, L. Shi, M. Lin, L. Chen, C. Shen, and X. Wu, "Discussion on model of theory teaching based on nursing clinical thinking training in the course of health assessment," *China Continuing Medical Education*, vol. 13, no. 23, pp. 105–110, 2021.

[2] B. Wang, H. Zhao, and R. Wu, "Exploration and research on the training mechanism of innovative and entrepreneurial talents in universities," *The Theory and Pracice of Innovation And Entreptrneurship*, vol. 5, no. 8, pp. 73–75, 2022.

[3] L. He, Y. Li, K. Zhuang et al., "Network connectivity of the creative brain: current knowledge and future directions," *Chinese Science Bulletin*, vol. 65, no. 1, pp. 25–36, 2020.

[4] J. Sui, Z. Hua, H. Zhu, and S. Shen, "Training mechanism of engineering education and innovation talent based on courses-competitions combination," *Nanotechnology for Environmental Engineering*, vol. 7, no. 3, pp. 833–841, 2022.

[5] R. Mei and J. Zhang, "Mppt algorithm of particle swarm optimization and fuzzy variable step incremental conductance method based on z-source inverter," *Taiyangneng Xuebao/ Acta Energiae Solaris Sinica*, vol. 41, no. 1, pp. 137–145, 2020.

[6] F. Huang and J. H. Wu, "Research on efficient data classification algorithm based on statistical analysis," *Journal of Xi'an University(Natural Science Edition)*, vol. 23, no. 4, pp. 57–61, 2020.

[7] H. Chen, "On the training path of startups and innovation talents in vocational school under school-enterprise cooperation," *International Journal of New Developments in Education*, vol. 40, no. 3, pp. 65–72, 2022.

[8] Y. Zhang and R. Zhang, "Mathematical model and artificial intelligence of multidimensional database and spatial multidimensional data," *Journal of Nanyang Institute of Technology*, vol. 12, no. 4, pp. 121–128, 2020.

[9] Y. Shi, "Research on the cultivation and development of creative talents in colleges and universities," *Scientific Journal Of Humanities and Social Sciences*, vol. 4, no. 1, pp. 49–52, 2022.

[10] W. Wang, Z. Chu, X. Zhang, and Y. Han, "A K-means algorithm for improving BP neural network," *Chinese Journal of Electron Devices*, vol. 43, no. 2, pp. 380–385, 2020.

[11] Y. Zhang, "On mining of frequent item sets of big data based on K-means clustering," *Computer Simulation*, vol. 37, no. 8, pp. 457–461, 2020.

[12] S. Ghosh, D. V. Thang, S. C. Satapathy, and S. N. Mohanty, "Fuzzy rule based cluster analysis to segment consumers' preferences to eco and non-eco friendly products," *International Journal of Knowledge-Based and Intelligent Engineering Systems*, vol. 24, no. 4, pp. 343–351, 2021.

[13] E. Dilworth Mary, "Historically black colleges and universities in teacher education reform," *The Journal of Negro Education*, vol. 81, no. 2, pp. 121–135, 2022.

[14] X. Xu and L. Chen, "Study of student achievement evaluation based on factor Analysis and cluster Analysis on talent cultivation of preventive medicine specialty," *Medical Education Research and Practice*, vol. 29, no. 5, pp. 675–678, 2021.

[15] L. Sun, W. Zhuo, K. Wang, and M. A. Jia, "Study on functional clustering analysis methods," *Applied Mathematics A Journal of Chinese*, vol. 35, no. 2, pp. 127–140, 2020.

[16] Y. Chen and M. Yang, "On the path of law education reform based on mooc environmental analysis," *Curriculum and Teaching Methodology*, vol. 4, no. 6, pp. 62–66, 2021.

[17] Z. Guo and M. Ye, "The development and value of blockchain technology + higher education under the background of China's higher education reform and innovation," *Advances in Educational Technology and Psychology*, vol. 5, no. 8, pp. 45–49, 2021.

[18] Q. Sun, "Exploring the innovation of English education reform in the network environment," *Journal of International Education and Development*, vol. 5, no. 11, pp. 54–59, 2021.

[19] L. Karabassova, "English-medium education reform in Kazakhstan: comparative study of educational change across two contexts in one country," *Current Issues in Language Planning*, vol. 22, no. 5, pp. 553–573, 2021.

[20] H. Zhang, X. Wang, H. B. Yu, and J. F. Douglas, *European Physical Journal E: Soft Matter*, vol. 44, no. 4, pp. 56–60, 2021.

[21] J. Ansorger, "An analysis of education reforms and assessment in the core subjects using an adapted maslow's hierarchy: pre and post COVID-19," *Education Sciences*, vol. 11, no. 8, p. 376, 2021.

[22] C. Cheng, Z. Zhang, and Y. Liu, "Research on innovation and entrepreneurship education reform and university talent cultivation model innovation," *Frontiers in Educational Research*, vol. 4, no. 7, pp. 54–59, 2021.

[23] S. Qu, "Research on innovation and entrepreneurship education reform in vocational colleges," *International Journal of Secondary Education*, vol. 9, no. 2, pp. 51–95, 2021.

[24] Z. Tang, X. Long, and X. Li, "Teaching reform of embedded system under background of artificial intelligence in applied undergraduate," *Industrial Control Computer*, vol. 33, no. 11, pp. 145-146, 2020.

[25] L. Zhang, "Analysis on the employment ability of higher vocational college graduates based on BP neural network——taking jiangsu vocational college of business as an example," *China Computer & Communication*, vol. 32, no. 22, pp. 232–234, 2020.

[26] H. He, H. Yan, and W. Liu, "Intelligent teaching ability of contemporary college talents based on BP neural network and fuzzy mathematical model," *Journal of Intelligent and Fuzzy Systems*, vol. 39, no. 4, pp. 4913–4923, 2020.

Hindawi
Computational Intelligence and Neuroscience
Volume 2022, Article ID 1871315, 11 pages
https://doi.org/10.1155/2022/1871315

Research Article

Financial Management of Listed Companies Based on Convolutional Neural Network Model in the Context of Epidemic

Qian Duan, Xinyu Cao, and Li Xu

The School of Economics and Management, Cangzhou Jiaotong College, Huanghua 061100, Hebei, China

Correspondence should be addressed to Xinyu Cao; xinyuc@czjtu.edu.cn

Received 26 July 2022; Accepted 17 August 2022; Published 17 September 2022

Academic Editor: Yaxiang Fan

Copyright © 2022 Qian Duan et al. This is an open access article distributed under the Creative Commons Attribution License, which permits unrestricted use, distribution, and reproduction in any medium, provided the original work is properly cited.

The goal of financial management is to manage the purchase and sale of assets, the rational financing of funds, the management of cash flow in operations, and finally, the reasonable distribution of company profits in a certain task situation, which is simply the management of the "three statements" of the enterprise. The core issue of the financial mechanism is how to choose a centralized or decentralized management model, which requires the company to consider the internal and external environment, and according to the development of the company, the quality of employees and business characteristics of various factors, in order to make the best choice of the company's financial management model. Therefore, in the context of the epidemic, this article conducts research related to the financial management of listed companies based on convolutional neural network models (radial basis neural network, generalized regression neural network, wavelet neural network, and fuzzy neural network). This article, firstly, discusses the basic theories of macro- and micro-financial management of enterprises and financial management of listed enterprises, secondly, examines the overall financial management model of listed enterprises in China through methods such as the convolutional neural network model research method introduced in this article, and then, after an overall examination and analysis of the financial management situation of X-listed enterprises, finds the macro- and micro-status quo of financial management of listed enterprises in China under the epidemic, and in the sub. On the basis of the status quo, suggestions are made to build a financial management model that combines centralization and decentralization and to build a group financial risk management system.

1. Introduction

The goal of financial management is to manage the purchase and sale of assets, the reasonable financing of funds, the management of cash flow in operation, and finally, the reasonable distribution of company profits in a certain task situation, which is simply the management of the "three statements" of the enterprise. Due to the different methods of allocating financial power within the company, the financial model can be divided into "centralized," "decentralized," and "mixed." At present, the centralized financial management model has been commonly used in the world's major companies, according to statistics, more than 80 percent of the world's top 500 companies have established a centralized financial management model. The core issue of financial mechanism is how to choose a centralized or decentralized management model, which requires the company to consider the internal and external environment, and according to the development of the company, the quality of employees and business characteristics and other factors, in order to make the best choice of the company's financial management model [1].

Regardless of the form of organization, exposure to certain risks is inevitable. In the twenty-first century, changes in the technological and economic environment have made organizations pay more attention than ever to the issue of risk. Among the various types of risks, financial risks are more important in the case of enterprises. After all, generally speaking, the main purpose of a company is to make a profit. Group companies are one of the more advanced forms of corporate organization. Once the financial risk of a group of companies goes wrong, it can have a very

significant impact not only within this enterprise, but also on the stability of society [2]. The collapse of well-known companies such as Arthur Andersen and Kenmore is closely related to financial management, showing that their impact cannot be underestimated, both in China and abroad. The financial risk management of enterprise groups is also attracting more and more attention and many researchers are studying this issue, trying to prevent and reduce the harm caused by financial risks by increasing the importance of the stakeholders of enterprise groups through the study of financial risk management. The constant cases of financial risk leading to corporate bankruptcy have increased the sense of urgency and the need for theoretical research [3].

Group companies are organizations that have evolved from individual companies and naturally have the general characteristics of individual companies' financial risks, such as speculation, objectivity, and fragmentation. However, it also has some more complex characteristics of its own, such as dynamicity, complexity, and comprehensiveness. Due to these characteristics, it is more difficult to identify, assess, and manage the risks of group companies' financial risks. Since the promulgation and implementation of the CE financial management system (COSO-ERM for short), a lot of research has been conducted and discussed by domestic and foreign researchers, trying to make it more operable and effective [4]. However, any program should be used for us, not simply follow the "fetishism," our country's enterprises need to improve the actual political and economic environment in China, and can be based on the CE financial management system to establish a framework system for China's enterprises, to build their own financial risk defense system, and ultimately achieve the enterprise's purpose [5].

2. Research Background

2.1. Research on Enterprise Micro-Financial Risk Management. Chao [6], starting from the analysis of the financial management work mode of corporate enterprises, illustrates that no matter what type of management mode is faced with business risks, the only way to better avoid the occurrence of business risks in enterprise financial management is to follow the management development ideas of flattening hierarchical management, modularization of services, networking of information management, and integration of big data [7]. Professor Gang [8] studied in-depth the basic meaning and principles of risk management of group financial management and gave strategies and measures for prevention and resolution in the face of corporate financial risks [9]. Ouyang [10] studied the main mechanisms of internal financial risk generation in companies and used AVIC as an example to clarify the measures that companies should adopt in their internal financial risk management practices [11]. Professor Pengjie [12] provides an in-depth analysis of the causes of corporate financial risks, while providing a slightly different perspective from other literature research approaches to strengthen corporate risk management, and conducts countermeasures research at various levels such as the strategic financial level, organizational level, internal control level, early warning level, performance level, information and culture of the company, but has not been able to establish a rigorous theoretical framework system [13]. Minhui [14] analyzed the causes of financial risk in a listed company from four major aspects, namely, financing, inputs, capital operation, and profit distribution of the company, and conducted an overall study of its formation characteristics, having specific management policy advice from the perspective of the characteristics of financial risk [15]. Through the above-mentioned literature, we see that most of the studies on corporate financial risks from a microscopic point of view have always been based on theoretical knowledge of the concept, characteristics, and transmission of business risks of corporate financial conditions, and there is a one-sided disadvantage of "treating the head when the head hurts and treating the foot when the foot hurts" in the recommendations for the overall financial management of the enterprise. However, in the context of the company's strategy and development, it is important to consider the overall financial management proposal. However, there are only a few studies that propose specific objectives of enterprise financial risk management based on the company's strategy and development, and the overall objectives of the company according to its financial risk tolerance. It is not in a practical point of view, the establishment of a specific structure of financial enterprise risk management, nor in accordance with the requirements of the enterprise financial risk management objectives, the implementation of the main body of responsibility, improve the procedural approach, improve the protection system, and optimize the management basis [16].

2.2. Research on Enterprise Macro-Financial Risk Management. As a new theory, the application of the CEE financial management system in China has led to some problems, such as the lack of awareness of risk management work by the responsible state and the formal construction of risk mechanisms. It is pointed out in his study that CE financial management system policy must be further adjusted if it is to be successfully implemented in the current market economy, but the adjusted policy framework system is not available in his study [18]. The CE financial management system faces the main problem of fixation, that is, the decision-making implementation contains subjective decisions, and there is still a lack of clear theoretical guidance for the architecture, thus requiring the management of the company to comprehend the meaning of the architecture and the main issues in a comprehensive and in-depth manner. On the basis of an in-depth analysis of the shortcomings of the CE financial management system, an all-round risk management architecture with a "dual core" of internal control and risk management control is proposed. However, the new framework and the CE financial management system also have difficulties such as being too theoretical and obstacles to the translation of the guidance into practice [19, 20]. Zinkewicz [21] explored the current status of ERM implementation in the insurance industry, and the effective implementation of ERM will face challenges from various aspects such as system design and data

acquisition and integration. Similar results were obtained in a related study by Garcia [22]. The results of another study by Beasle et al. [23] also indicate that there are still some financial barriers to the advancement of ERM [24].

Teng [25] explored the suggestion of establishing an overall architecture for enterprise risk management in China by describing the development of enterprise risk management work on internal control architecture and using enterprise risk management work architecture. She also argues that according to the current level of risk in China, the establishment of an effective Chinese system framework is not yet possible overnight. She also emphasized that emphasizing the central role of directors in the construction of corporate structure, defining corporate risk management objectives, actively exploring and establishing a risk assessment system, and creating a corporate management culture are the keys to the successful establishment of an overall corporate framework system [26]. Based on the CE financial management system architecture, Yang [27] proposed that the establishment of a corporate risk management framework that is beneficial to China should establish a corporate risk management committee, an effective corporate regulatory system, and other specific measures [28]. Taking Shaanxi Electric Power Company as an example, Xiaohan [29] attempted to establish a risk management work structure dedicated to the electric power industry and based on the five elements of internal company management. After the summary of these articles, it is seen that on the one hand, CE financial management system as a basic technical theoretical framework system, which is really implemented to the actual enterprise still needs to do the corresponding technical implementation level of conversion and refinement [30]. However, the reality in China is that in the long-term survival and development of Chinese enterprises, it is necessary to establish their own unique characteristics, which means that if the CE financial management system is directly adopted, it will become an unavoidable reality, which will negatively affect the effectiveness of the framework implementation. On the other hand, the summary of the literature on the establishment of financial risk architecture in other companies shows that such articles are more inclined to establish their own new architecture based on the CE financial management system and supplement the original one accordingly. In the strictest sense, the study of such articles must always take the CE financial management system as the basic analytical starting point of the study, without leaving this research framework to provide a unique risk management system [31].

3. Materials and Methods

3.1. Basic Theory

3.1.1. Listed Companies. A listed company is a specific component of a joint stock company, which publicly issues shares, reaches a considerable size, and has its shares approved by law to enter the centralized securities trading market for trading. A joint stock limited company applying for the listing and trading of its shares shall submit relevant documents to the stock exchange. The stock exchange decides whether to accept its shares for listing and trading in accordance with the provisions of this Law and relevant laws and administrative regulations [32].

China's securities law makes strict and detailed regulations for listed enterprises, as specified in Article 50. An enterprise applying for an IPO (initial public offering of shares) needs to meet all of the following conditions: (1) the shares have been examined and determined to have been publicly offered by the CSRC; (2) the registered capital of the company has a share capital of not less than RMB 30 million; (3) the publicly offered shares should account for at least 1/4 of the total amount of shares of the company; in large enterprises with total shares of more than RMB 400 million, this ratio can be reduced to 1; (4) the enterprise cannot have major criminal and civil lawsuits as well as illegal and disorderly acts in the last 3 years, and the accounting report has no false records; and (5) the stock exchange can require the actual standard of the enterprise to be higher than the above terms when applying for listing, and report to the State Council for approval and filing. Our listed enterprises must strictly abide by the relevant accounting standards and legal system in China, and must disclose their financial status within the specified period to the market and shareholders in a timely manner. Accounting reports must be disclosed every 6 months during the accounting year. The above conditions greatly reduce the moral hazard and adverse selection of enterprises, can better protect the rights of shareholders, and are the way for China's listed enterprises to improve their quality, expand their scale, and improve their management [33].

3.1.2. Financial Management. Enterprise financial risk management is to evaluate various financial risks identified in advance in the process of achieving the objectives of the enterprise, to understand the possibility and impact of their occurrence, and to propose corresponding solutions in the context of the enterprise's own situation. It is an objective activity to resolve the events that occur in the objective world. At the same time, the enterprise financial risk management is also a dynamic process, as the environment changes, so does the enterprise risk management.

First, we need to understand the basic concepts involved. Risk is understood in a narrow sense and a broader sense. Risk in a narrow sense refers to the loss caused by uncertain future events, while risk in a broader sense is not only about losses, but also about benefits. The company will always face various uncertainties in the process of achieving its goals, so the company's managers must identify risks, so as to assess the possibility of their occurrence and the severity of their impact, and try to manage them effectively to reduce them to a level that the company can bear, and those that cannot be solved can be solved by transferring them. There are many risks in an enterprise, mainly macroeconomic risks such as socio-political risks and natural environment in China, and also micro-risks of the enterprise itself, such as product

quality risks and solvency risks. We need to classify the risks of enterprises and propose corresponding risk management approaches in a targeted manner.

At the end of the last century, there were many collapses and failures of large companies in the United States, many of which were due to internal control failures. In order to regulate the internal management of companies, the COSO committee in 1992 developed an integrated framework for internal management, which is the first systematic framework on internal control in the world. The framework was not only recognized by theoretical researchers, but also favored by many companies in practice, and indeed helped companies to avoid possible risks. However, 10 years later, it was found that despite the perfect internal control system, there were cases of risky losses, such as the Enron incident. The SO Act of 2002 required comprehensive risk control for companies, and the COSO Committee of September 2004 was keeping pace with the times by incorporating a company's built-in risk management system based on an integrated structure of internal management controls. The official publication of Enterprise Risk Management – An Integrated Framework reminds the theoretical and practical communities to pay comprehensive attention to risk and strengthen risk management. After the severe financial crisis in the USA in 2008, the COSO committee consulted widely and published an exposure draft of the ERM framework in May 2016 in order to reduce the recurrence of financial crises and to find effective prevention methods, and published the finalized "Enterprise Risk Management-Strategy and Performance Alignment" (ERM 2017). This version has added the integration of strategy and performance management inside, which highlights more the effect of the coordination between strategy, performance and risk management, and has stronger guidance for enterprise risk management, putting strategic risk management into a more realistic business environment to be considered.

3.2. Convolutional Neural Network Model Research Method. The following four convolutional neural network models are used in this article: radial basis neural network, generalized regression neural network, wavelet neural network, and fuzzy neural network. Because this aticle involves the financial management of listed enterprises, different research methods are used separately. The models are compared separately and the best model among the four models is simulated.

3.2.1. Radial Basis Neural Network. Radial Basis Function Neural Network (RBFNN) is a most typical three-layer forward neural network structure. In addition to having the information processing of traditional neural networks, its implicit layer uses radial basis functions for nonlinear mapping of input data, which is then passed to the next layer after linear computation. The structure of the radial basis neural network is shown in Figure 1.

In the unsupervised learning part, the data are clustered by using a clustering algorithm such as K-means to obtain

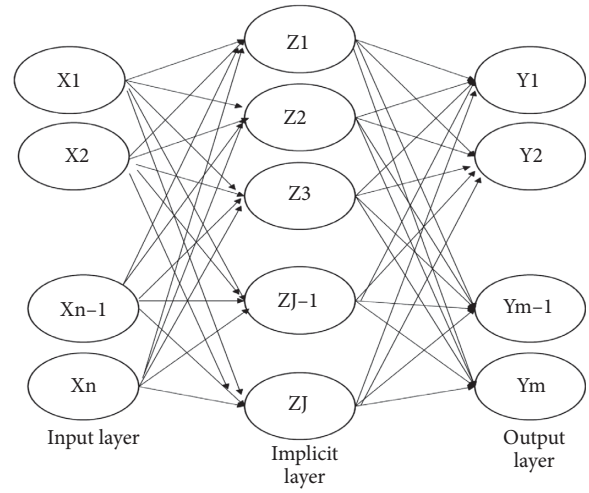

Figure 1: Structure of radial basis neural network.

the centroid of the radial basis function in the hidden layer, and then the width vector of the radial basis function is calculated by using the centroid information, and the width vector is calculated by the following formula (1).

$$\sigma_j = \frac{c_{xy}}{\sqrt{2h}}, \tag{1}$$

where c_{Xy} is the maximum distance before the centroid and h is the number of nodes.

After that, the input data are related to the scattering through the implicit layer and the output layer, respectively, and the output x_i of the first node j of the input sample in the implicit layer is calculated by the following equation (2).

$$\phi(x_i, j) = \exp\left(-\frac{1}{2\sigma_j^2}x_i - c_i\right), \tag{2}$$

where c_j and σ_j are the centroid and width m vector of the first node in the hidden layer, respectively.

The output of x_i the first node of j the input sample in the output layer is calculated by the following equation (3).

$$y_m = \varphi(\phi(x_i, j) * w_m), \tag{3}$$

where w_m is the node weight and φ is the activation function.

In the supervised learning part, it is mainly the process of continuously correcting the parameters in each layer, and this process is mainly calculated by the error function to calculate the gradient value of each parameter, and then the parameters are continuously corrected using traditional gradient descent methods such as stochastic gradient descent (SGD), taking the weights used for linear calculation in the output layer as an example, the update formula is as follows (4).

$$w_t = w_{t-1} - \frac{u * \sigma E}{\sigma w_{t-1}}, \tag{4}$$

where E is the error function and u is the learning rate.

In addition to the above methods, the centroids and width vectors of the hidden layer can be directly generated

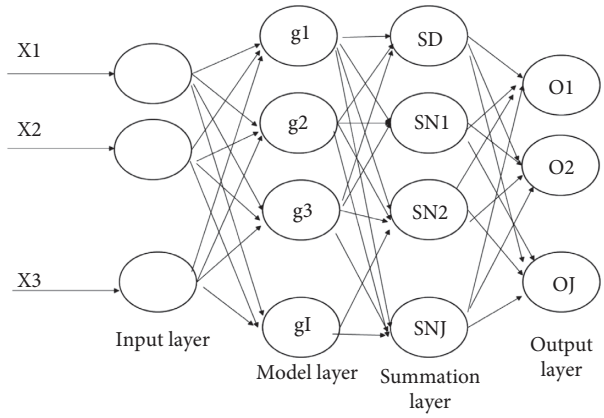

Figure 2: Structure of generalized regression neural network.

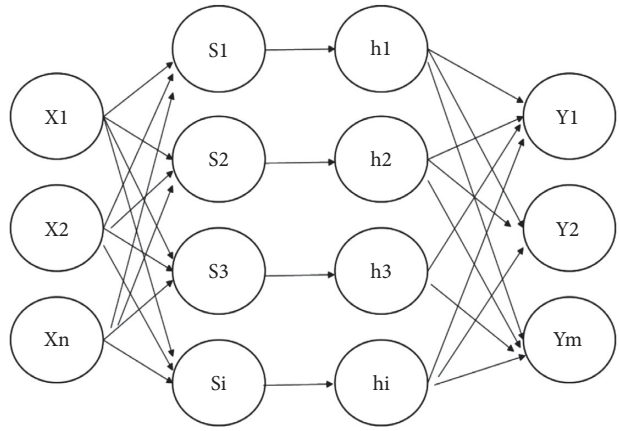

Figure 3: Wavelet neural network structure.

randomly, after which they are updated according to the gradient correction formula of the supervised learning process.

3.2.2. Generalized Regression Neural Network. Generalized Regression Neural Network (GRNN) is a four-layer forward propagation neural network with fewer parameters and better nonlinear mapping capability, and the data are input to the network and then passed through the input layer, pattern layer, summation layer, and output layer to obtain the output results. The network does not have a training process, but mainly optimizes the smoothing factor of the pattern layer to obtain good output results as shown in Figure 2.

The computational process is not shown in detail here, and the specific computational process can be obtained by inversion of radial basis neural network, which is not done in this case. Although GRNN does not require network training, the smoothing factor of the pattern layer has a large impact on the performance of the network, and too large or too small a smoothing factor will lead to underfitting and overfitting of the network, respectively, and it is usually difficult to set the smoothing factor to a better value in the experiment, so if you want to get better network performance, you generally choose an efficient intelligent optimization algorithm to find the optimal smoothing factor.

3.2.3. Wavelet Neural Network. Wavelet Neural Network (WNN) has a three-layer structure, which is characterized by the use of wavelet basis function as the activation function of the neurons in the hidden layer, which makes the network more capable of self-learning when processing data sets with large amounts of data, so it can fit complex relational data faster. Its structure is shown in Figure 3.

The computational process is not shown in detail here, and the specific computational process can be obtained by the radial basis neural network inversion, which will not be done in this example. There are four main parameters in WNN, the size of these four parameter values will directly affect the performance of the network, so the training process of WNN as RBFNN mainly uses the traditional gradient descent method such as stochastic gradient descent (SGD) to continuously correct these four parameters.

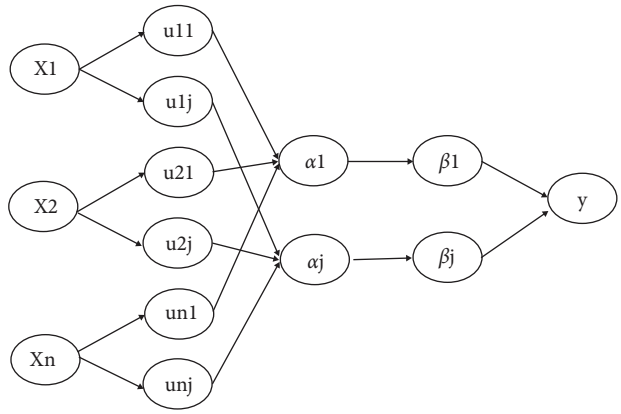

Figure 4: Fuzzy neural network.

3.2.4. Fuzzy Neural Network. Fuzzy Neural Network (FNN) incorporates fuzzy theory into the information transfer process of the network, which can have a larger processing range and faster information processing speed when processing information, so the self-learning ability and mapping of the network is relatively high. The structural diagram of a fuzzy neural network is more commonly used, and can be found in general textbooks as shown in Figure 4.

The data is trained by this neural network in a total of five layers. The first layer is the input layer, where the number of nodes is related to the feature dimension of the data, that is, when the feature dimension of the data is n, the number of nodes in the input layer is n. Then the data is passed from the input layer to the affiliation function calculation layer, where the affiliation function is used to calculate the affiliation of each node, each node represents an affiliation function, and the number of nodes in this layer is the number of possible fuzzy conditions of the input variables. When the dimensionality of the output variables increases, the weights will be adjusted accordingly. In addition, FNN, like the previous RBFNN and WNN, generally uses traditional gradient descent methods such as stochastic gradient descent (SGD) to

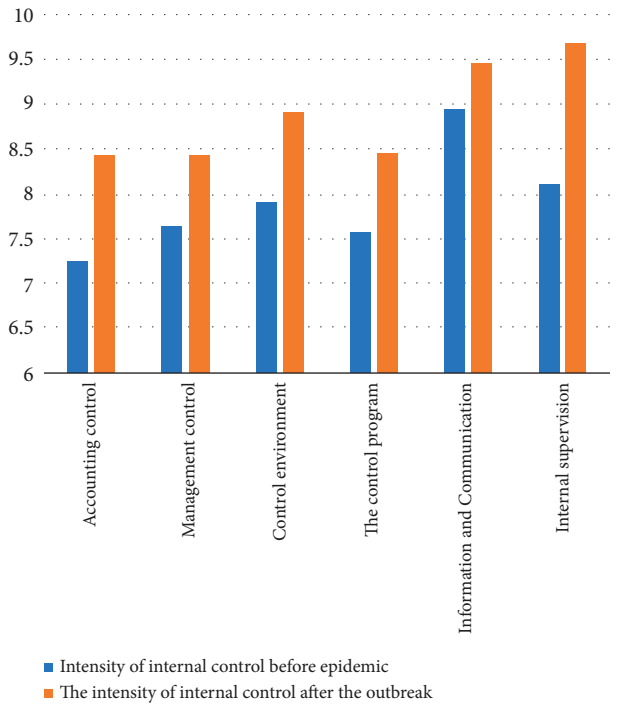

Figure 5: Comparison of the intensity of six major aspects of internal control over financial risk in enterprises before and after the epidemic.

optimize the centroids of the affiliation function, the width vector, and the connection weights of the output layer.

4. Results and Discussion

4.1. Comparison of Financial Management Status Before and After the Epidemic. First, the intensity of each of the six major aspects of a firm's internal controls has been strengthened under the epidemic. The strength of each aspect generally ranged from 7 to 10, with higher indicating a greater intensity of control in that aspect of the enterprise. The history of the development of internal control is seen. Swa [34] first studied the essential attributes of internal control in a company, Swa another Ze pointed out that internal control is an integral part of the accounting system and that the company's requirements for internal control originate from within the company. Domestic research scholars also consider the internal management of a company as an internal control system, in which internal control embodies the relationship of authorization and responsibility, and is the way and means to achieve the goals. Both domestic and foreign scholars have summarized it from the perspective of management science and discussed the essential attributes of internal management from the practical needs of the enterprise, instead of just staying in the internal control practice itself. The Ministry of Finance of the People's Republic of China issued "Understanding the audited entity and its environment and assessing the risk of material misstatement" on April 29, 2016, and emphasized that internal management is the design and implementation of policies and procedures by the management and personnel of the audited entity to reasonably determine the authenticity of the audited entity's financial statements, the efficiency and effectiveness of operations, and to reflect the effective implementation of rules and regulations within the audited entity. Policies and procedures. The change in the intensity of corporate control under the epidemic is shown in Figure 5.

Second, the intensity of each of the 10 secondary aspects of corporate internal control was strengthened under the epidemic. The intensity of each aspect generally ranged from 7 to 10, with higher indicating a greater intensity of control in that aspect of the enterprise. It was only in the late 1990s that scholars began to refer back to the "internal control conclusion theory" and the "three elements." The previous understanding of internal control was rather homogeneous, without effective subdivision, and the role of internal control could not be realized. As the socio-economic environment has changed, the understanding of internal control has deepened, and the basic elements of internal control have changed from three to five: management environment, risk assessment, internal management activities, information dissemination and communication, and internal oversight. Accounting systems are also no longer presented separately and have become information and communication. Control procedures have also been adjusted somewhat, with more refined controls and the formation of risk assessment, control activities, and internal oversight. The changes in these elements are not accidental and reflect the requirements of our new economic environment for companies that can only keep up with the times to help them gain a competitive advantage. The technology-oriented period of internal control changed to management-oriented internal control, several organizations and institutions have not stopped studying the elements of internal control, even if the same organization is constantly developing and improving internal control. As you can see in the chart, we went from 5 elements to 8 elements and later to 5 elements, which is not only a change in numbers, but also a qualitative change in people's understanding of internal control. Exactly what is right and what is wrong is not really conclusive here. We say that the right one is the best one, and the research that can help companies to reduce risks is the most effective one. People's understanding of the nature of internal control varies from era to era; different environments also directly affect the understanding of internal control; and different organizations reach different conclusions about internal control. Different companies will also use different internal control tools and approaches. We can only bring internal control to life by placing it in a specific context as shown in Figure 6.

4.2. Analysis of the Current Situation of Financial Management in a Listed Enterprise. After more than 10 years' development, it has established many production bases at home and abroad and expanded the scale of production and sales of soft plastic materials to 11 times, which is the leading level of the same industry at home and abroad in terms of product technology and equipment level, product production and sales

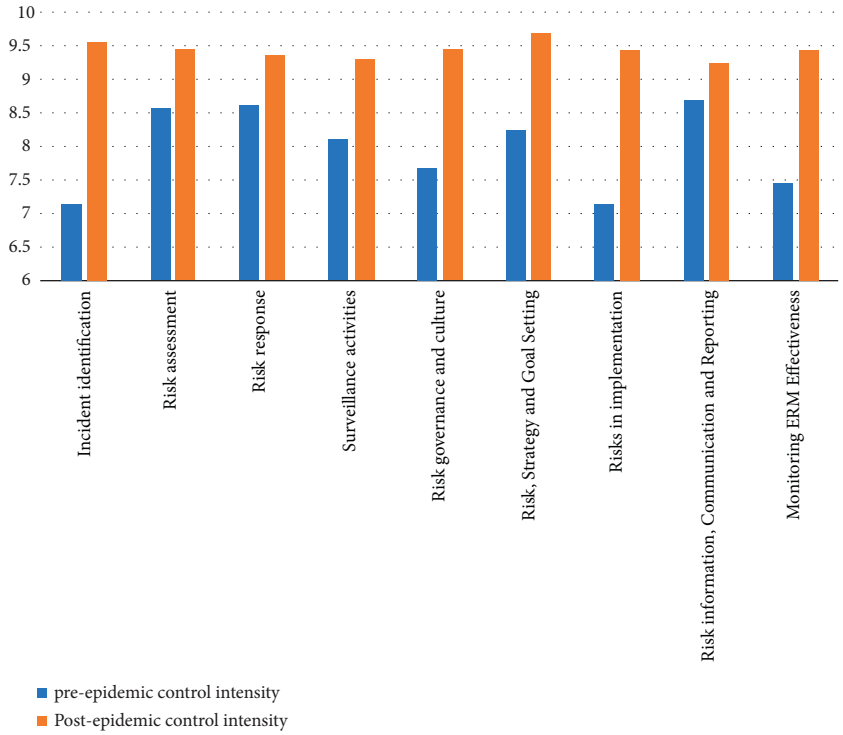

Figure 6: Comparison of the strength of ten secondary aspects of internal control over financial risk in enterprises before and after the epidemic.

scale, and its adaptability to domestic and foreign markets. It is now a leading company of new polymer soft plastic materials and a high-tech company in China. However, the development of a company is not smooth sailing. With the rapid development of the domestic flexible plastic packaging materials industry, as well as the concentration of new production capacity emissions, making the domestic oversupply situation. And as the international crude oil prices continue to soar, driving the company's production of raw materials products rose sharply, product profit margins gradually reduced to the occurrence of losses. At the same time, the downward adjustment of export tax rebate rate and the continuous rise of RMB have gradually reduced the cost advantage of products in the global market. A company's gearing ratio is high and unreasonably composed because of the rapid financing in the early stage. As the interest rate continues to rise under China's macro-tight monetary policy, the company is burdened with risks. Another enterprise's capital chain breaks and the corresponding creditor bank pursues the joint and several guarantee liability of the major shareholder of an enterprise due to the mutual guarantee relationship between the major shareholder of an enterprise and another enterprise, which causes a big panic in the financial industry and will soon spread to an enterprise or the corresponding SMEs with mutual guarantee relationship, making an enterprise's financial risk arise. The main trigger for the explosion of a company's financial risk came from accidental external causes, but it is clear that a company of this size is not just facing financial difficulties due to a several hundred million dollar guarantee crisis. Next, in the future, this article analyzes the causes of a firm's financial risk management failure and its risk treatment measures after the financial risks emerged. In the following, we refer to the research enterprise in this article as this enterprise or enterprise X.

Regarding the choice of financing methods, there are usually debt financing and equity financing, and the company needs to choose the appropriate financing method and financing ratio according to the development stage in which it is located. For this company, the risk in the early stage of development of a new project is high. Choosing a financing method with lower financial risk must keep the overall risk within a certain range. At this time, share-based financing is usually used, and as the project becomes larger and larger, the proportion of debt gradually increases and debt-based financing is used. Now the enterprise is mainly financed by absorbing short-term borrowings and investments from investors. The possession of equity-type capital is large and growing fast, and the enterprise does not need to take big financing risks.

However, as seen in the graph, the growth rate of the total debt of the company in 5 years from 2017 to 2021 has increased by 2.79%. The growth rate of the total share price is 90.27%. The rate of increase in the company's debt and the rate of increase in the share price are the same. The corporate gearing ratio has been below 50% for the last 5 years. It has been very low. The capital structure of the enterprise remains relatively stable and low. By 2021, the ratio of industrial debt capital to equity assets of enterprises has increased by 35% and by 1.61%, still below 50%, but enterprises are still under considerable debt pressure. Most of the main financing for SMEs is the growth of loans and capital investment from investors, and a certain amount of fixed assets of SMEs are supplied to enterprises. There is a

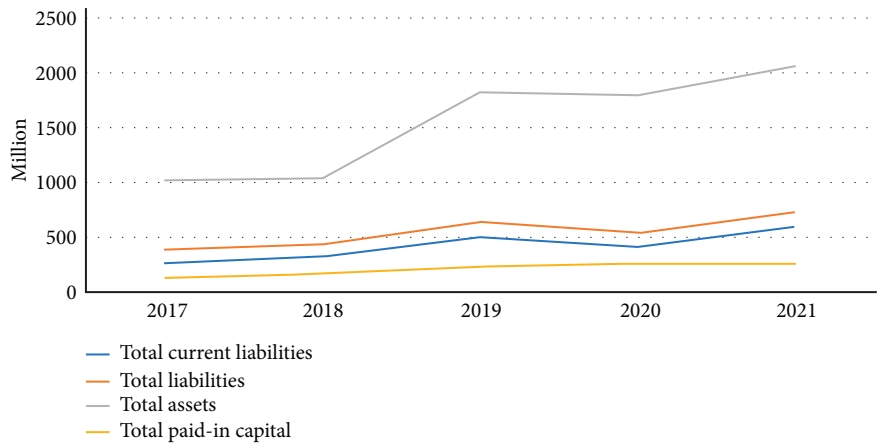

Figure 7: Capital composition of enterprise X from 2017 to 2021.

certain financial leverage effect and the repayment pressure of SMEs increases if the gearing ratio is high. The investor's capital investment is conducive to rapid expansion and development of the enterprise, low repayment pressure, but high financing costs. The enterprise has a large asset ratio and a small proportion of liabilities, so there is no greater repayment pressure, but low long-term debt is not good. Overall the capital structure of this enterprise is not reasonable as shown in Figure 7.

Enterprise X monitors the execution of the project in real time during the financing process and reflects the progress of implementation and problematic points to the company. The company keeps detailed records of where each amount of funds used goes, and management should keep timely records to avoid exceeding the budget and being out of reality and internal improper events confirming these records to ensure the degree of use of funds and smooth project implementation. Company X is still very strict in the process management, but for the outside of the company, the company did not analyze the impact of risk in detail. The amount of the company's long-term equity investments decreases year by year. The year 2017 was the highest value. It was the first loss-making year since the company was founded, in which the company over-invested and the company took a larger financial risk that year. Investments in pursuit of steady growth: in terms of investment income, the company's foreign investment income is considerable, and after reflecting on the investment failure in 2017, the company pays attention to the investment effect, and the company is now in a more stable investment position than before. The external investments are gradually reduced and turned into investments within the company. The ratio of each part of assets is measured to avoid the accumulation of internal assets due to over-investment, which leads to insufficient operating funds as shown in Figure 8.

As can be seen from the Figure, the investment in various assets of enterprise X from 2017 to 2021, by observing the total amount of these three investments will increase from $43325340.80 in 2017 to $4932194595.30 in 2021, with a slow increase every year, in 2019 is the highest value, and in 2020 is

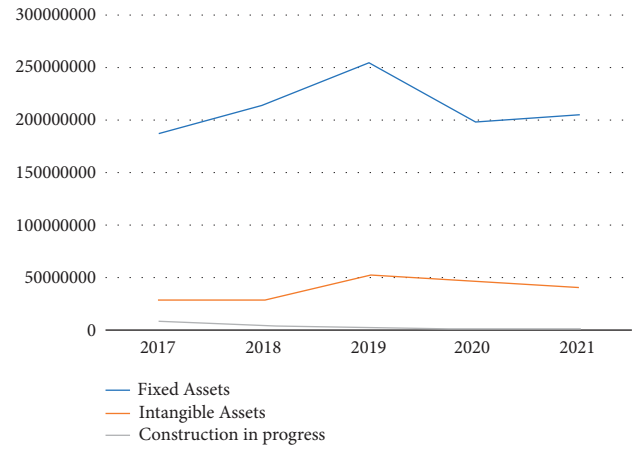

Figure 8: Analysis of investment in each asset of enterprise X from 2017 to 2021.

still slowly increasing after a slight decrease, and in 2018 the highest increase, but relatively low. The increase in the size of fixed assets and intangible assets in construction works of Company X originates from the expansion of subsidiaries, and the enterprise invests a lot of money to purchase network resources in order to network projects with the goal of better development. The level of equipment, backwardness within the enterprise, and equipment and production lines that cannot be replaced by generations are eliminated.

4.3. Countermeasures for Improvement of Enterprise Financial Risk Management

4.3.1. Build a Financial Management Model that Combines Centralization and Decentralization. The relationship between the enterprise and each subgroup is an asset bond relationship, and from the perspective of capital relationship, the key content of the group's management of the subgroup enterprise company is the effective control of capital and financial activities. "Hierarchical management" means that the group company implements first-level management to each subgroup company, while the subgroup company

implements second-level management to the subordinate enterprise group according to the principle of four unified and separate. The core of first-level management is supervision and control, and the core of two-level management is cost management and cash flow. The four unifications, that is, the coordination and unification of information, mechanism, capital and team. Information unification, unified enterprise financial software at all levels, unified financial reporting caliber, and relevant data. It is required to form one account and one set of tables when aggregated within the group to meet the requirements of internal control of enterprises and control of syndicates. The system is unified, and the financial management system, tax policies, accounting methods, and financial software of major enterprise companies are unified and formulated by the group, while local group companies may establish their own implementation rules according to the group's regulations, which must be reported and approved before implementation. The group also conducts inspections on the implementation status of the financial system of each subsidiary. The enterprise capital management is unified, and the entire enterprise company adopts the supervision platform of direct connection between banks and enterprises, and establishes the cash pool system of four subsidiaries to centralize the management and monitoring of all liquid funds of each enterprise company. The centralized monitoring and effective operation of the capital management system, an account to manage the whole enterprise. The team unifies the financial management organization of the small and medium-sized companies under the group as the management organization of the group's business. Each company enterprise has unified the financial setting method and staffing of each enterprise. The financial staff of the group companies and their subordinate enterprise companies are assigned and escorted by the group enterprises, and vertical leadership is implemented. The salaries, rewards, and treatment of the financial and accounting staff are unified and standardized by the enterprises, while the training, recruitment, job transfer, title evaluation, and appointment and removal of the financial staff of the enterprises are unified to the enterprises for arrangement. By the government assigned to the financial organs, in the form of agreements in a variety of personnel management agreements with enterprises or affiliated service companies limited, in order to determine the business content, staff positions, management work standards, and assessment methods. All financial accountants have adopted a job rotation system, in principle, a two-year rotation. "A separation" is the separation of accounting. The products and business results of each enterprise company operate freely in the area of autonomous activities in accordance with the law, with separate cost accounting and self-accounting.

4.3.2. Construction of the Group's Financial Risk Management System

(1) The Principle of Construction. According to the management principle of "centralized control and hierarchical implementation," a capital supervision system with the group's cash asset pool as the core content is established, and the control mode of "hierarchical squeezing, industry segmentation, information system networking and financial data integration" is highlighted in the construction of the group's financial risk control. The control platform should support different forms of financial management control and capital operation within the company in all aspects, and develop and design different levels and modules adapted to the different functions of various forms of financial management institutions, and each level and module can be applied independently of each other, as well as seamlessly integrated and unified.

(2) Optimize the Financial Organization Structure. From the perspective of capital relationship, the focus of the group's enterprise management of subgroups is on the effective control of capital and financial activities. Based on the principle of hierarchy and stratification, risks are set for each group according to the strategic view of risk management. The Management Department has rebuilt the organizational structure by setting up an Early Warning Department and a Crisis Management Department under each department. "Hierarchical management" is implemented by group companies for each subgroup company. Hierarchical management is the second level of management by the subgroup companies over the enterprise groups of the subordinate companies based on the principle of four uniform classifications. The core work of the first level of management is supervision and control. The core work of the second level of management is cost management and capital flow. The products and business results of each enterprise company operate freely in the area of autonomous activities in accordance with the law, with separate cost accounting and self-responsibility for profits.

5. Conclusion

The financial model can be divided into "centralized," "decentralized," and "hybrid" due to the different methods of allocating financial power within the company. The core issue of the financial mechanism is how to choose a centralized or decentralized management model, which requires the company to consider the internal and external environment and to make the best choice of the financial management model based on various factors such as the company's development, staff quality, and business characteristics. Therefore, in the context of the epidemic, this article conducts research related to the financial management of listed companies based on the convolutional neural network model. In this article, firstly, the basic theories of macro- and micro-financial management of enterprises and financial management of listed enterprises are discussed, secondly, the overall financial management model of listed enterprises in China is examined through methods such as the convolutional neural network model research method introduced in this article, and then, after an overall examination and analysis of the financial management situation of X-listed enterprises, the macro- and micro-status quo of

financial management of listed enterprises in China under the epidemic is found, and the following suggestions are made on the sub status quo, the following suggestions are made.

(1) Construct a financial management model that combines centralization and decentralization. The relationship between enterprises and subgroups is asset bond relationship, and from the perspective of capital relationship, the key content of the group's management of subgroup enterprise companies is the effective control of capital, financial and other activities. "Hierarchical management" means that the group company implements first-level management to each subgroup company, while the subgroup company implements second-level management to the subordinate enterprise group according to the principle of four unified and separate. The core of first-level management is supervision and control, and the core of two-level management is cost management and cash flow. The four unifications, namely the coordination and unification of information, mechanism, capital, and team.

(2) Construct the group's financial risk management system. The principles to be followed for the construction. In accordance with the management principle of "centralized control and graded execution," we establish a capital supervision system with the cash asset pool of the group company as the core content, and highlight the control mode of "hierarchical squeezing, industry segmentation, information system networking and financial data integration" in the construction of financial risk control of the group company. The control platform should support different forms of financial management control and capital operation within the company in all aspects, and develop and design different levels and modules adapted to the different functions of various forms of financial management organizations, and each level and module can be applied independently of each other, as well as seamlessly integrated and unified.

Data Availability

The dataset can be accessed upon request.

Conflicts of Interest

The authors declare that there are no conflicts of interest.

Acknowledgments

This work was supported by Cangzhou Federation of Social Sciences, research on the development of Cangzhou city's medical and elderly care service model from the perspective of the government (Project no. 2022249).

References

[1] M. Luo, Y. Zhang, and M. Zhang, "Research on financial risk identification and control of *Y* Energy Co," *Creative Economy*, vol. 6, no. 1, 2022.

[2] X. Wang, "On the enterprise to establish the budget management as the center of financial management mode," *International Journal of Education and Teaching Research*, vol. 3, no. 3, 2022.

[3] Z. Zhu, W. Ting, and Y. Chen, "Research on the strategy of corporate financial distress pre-warning under the new normal of economy," *International Journal of Educational Management*, vol. 7, no. 2, 2022.

[4] X. Zeng, W. Mao, J. Han, and Z. Zhao, "Analysis on the transformation of enterprise financial accounting to management accounting," *Scientific Journal of Intelligent Systems Research*, vol. 4, no. 6, 2022.

[5] K. Owusu Kwateng, C. Amanor, and F. K. Tetteh, "Enterprise risk management and information technology security in the financial sector," *Information & Computer Security*, vol. 30, no. 3, pp. 422–451, 2022.

[6] G. Chao, "New development of internal control framework-enterprise financial risk management framework—new report of COSO Committee," *Enterprise Financial Risk Management Framework*, vol. 6, pp. 11–15, 2004.

[7] S. Marzena and H. Łukasz, "Competency management and the financial results of the foreign subsidiaries of Polish MNCs: the empirical research findings," *Human Systems Management*, vol. 41, no. 3, 2022.

[8] W. Gang, "Internal control evaluation model and application based on enterprise financial risk management framework," *Auditing Research*, vol. 6, pp. 93–101, 2016.

[9] S. A. A. Bokhari and S. Manzoor, "Impact of information security management system on firm financial performance: perspective of corporate reputation and branding," *American Journal of Industrial and Business Management*, vol. 12, no. 05, pp. 934–954, 2022.

[10] H. Ouyang, "Derivatives and corporate financial risk management," *Journal of Xiamen University (Philosophy and Social Sciences Edition)*, vol. 1, pp. 128–137, 2020.

[11] E. Sidorova, Y. Kostyukhin, L. Korshunova et al., "Forming a risk management system based on the process approach in the conditions of economic transformation," *Risks*, vol. 10, no. 5, p. 95, 2022.

[12] N. Pengjie, "New development of COSO risk management framework and its inspiration," *Journal of Xi'an University of Finance and Economics*, vol. 10, pp. 41–47, 2011.

[13] B. Xu and J. Zhu, "Risks and management of international trade financing for small and medium-sized enterprises in my country under the financial turbulent environment," *Scientific Journal of Economics and Management Research*, vol. 4, no. 5, 2022.

[14] Z. Minhui, "Innovation of risk management theory-from enterprise financial risk management to resilient risk management," *Scientific Decision Making*, vol. 9, pp. 1–24, 2019.

[15] D.-D. Wang, "Financial flexibility and commercial credit supply," *Scientific Journal of Economics and Management Research*, vol. 4, no. 5, 2022.

[16] R. Yang, P. Zhang, Y. Fang, and Z. Pan, "Analysis of common risks and control countermeasures of corporate financial investment in the new era," *Scientific Journal of Intelligent Systems Research*, vol. 4, no. 5, 2022.

[17] H. Changhong, "Internal control evaluation model and application based on enterprise financial risk management framework," *Audit Research*, vol. 6, pp. 93–101, 2007.
[18] P. Pronoza, T. Kuzenko, and N. Sablina, "Implementation of strategic tools in the process of financial security management of industrial enterprises in Ukraine," *Eastern-European Journal of Enterprise Technologies*, vol. 2, no. 13 (116), pp. 15–23, 2022.
[19] W. Nonyue, "Group management control and risk management of finance companies-a multi-case analysis based on 10 groups," *Accounting Research*, vol. 5, pp. 35–41, 2018.
[20] N. I. Berzon, M. M. Novikov, E. L. Pozharskaya, and Y. I. Bakhturina, "Monitoring the modern experience of financial risk management in Russia based on corporate social responsibility for sustainable development," *Risks*, vol. 10, no. 5, p. 92, 2022.
[21] Zinkewicz, "Evaluating enterprise risk man-agement(erm); bahrain financial sectors asa case study," *International Business Research*, vol. 3, pp. 83–92, 2014.
[22] V. Garcia, "Enterprise risk management in financial services: from vision to value," *Bank Accounting and Finance*, vol. 12, pp. 3–6, 2015.
[23] Beasleya, "Audit committee quality and internal control: an empirical analysis," *Accounting Review*, vol. 80, no. 2, pp. 649–675, 2020.
[24] K. He, L. Yu, Y. Chen, and F. Xiao, "Research on authority management and risk control of state-owned enterprises based on accounting matters," *Scientific Journal of Economics and Management Research*, vol. 4, no. 4, 2022.
[25] T. Qing, "Internal control, corporate governance, and risk management: relationship and integration," *Accounting Research*, vol. 10, pp. 37–45, 2017.
[26] J. W. Wiśniewski, "Financial liquidity and debt recovery efficiency forecasting in a small industrial enterprise," *Risks*, vol. 10, no. 3, p. 66, 2022.
[27] W. Yang, "Selection and optimization of internal control information disclosure system-an analytical perspective on corporate efficiency," *Audit and Economic Research*, vol. 1, pp. 57–63, 2020.
[28] L. I. Khoruzhy, V. I. Khoruzhy, B. S. Vasyakin, and W. Shen, "Program-targeted approach to managing financial risks of sustainable development based on corporate social responsibility in the decade of action," *Risks*, vol. 10, no. 3, p. 58, 2022.
[29] W. Xiaohan, *An Integrated Framework for Corporate Financial Risk Management*, pp. 80–86, Northeast University of Finance and Economics Press, Dalian, China, 2019.
[30] E. B. Dej, "The ethics of delivering bad news: evaluating impression management strategies in corporate financial reporting," *Journal of Business and Technical Communication*, vol. 36, no. 2, pp. 190–230, 2022.
[31] T. N. Hung and N. T. Thuy Hanh, "Factors impacting on social and corporate governance and corporate financial performance: evidence from listed Vietnamese enterprises," *Journal of Asian Finance, Economics and Business*, vol. 8, no. 6, 2021.
[32] M. Tabash, N. Hamood, A. Ahmad, and E. Al Homaidi, "Factors affecting financial performance of Indian firms: an empirical investigation of firms listed on Mumbai stock exchange (MSE)," *International Journal of Economic Policy in Emerging Economies*, vol. 13, no. 2, p. 1, 2020.
[33] M. H. B. Hidthiir, M. F. Basheer, and S. G. Hassan, "The simultaneity of corporate financial decisions under different levels of managerial ownership: a case of Pakistani listed firms," *Research in World Economy*, vol. 10, no. 2, p. 147, 2019.
[34] J. Swa, *Integrated risk management for the firm: a senior manager's guide*, vol. 80, no. 2, pp. 649–675, 1946.

Hindawi
Computational Intelligence and Neuroscience
Volume 2022, Article ID 4259471, 10 pages
https://doi.org/10.1155/2022/4259471

Research Article

Automatic Segmentation of Lumbar Spine MRI Images Based on Improved Attention U-Net

Shuai Wang,[1] **Zhengwei Jiang**,[1] **Hualin Yang**,[1] **Xiangrong Li**,[1] **and Zhicheng Yang**[2]

[1]*College of Mechanical and Electrical Engineering, Qingdao University of Science and Technology, Qingdao 266061, China*
[2]*Department of Radiology, Qilu Hospital (Qingdao), Cheeloo College of Medicine, Shandong University, Qingdao, China*

Correspondence should be addressed to Zhicheng Yang; 201320145@mail.sdu.edu.cn

Received 23 July 2022; Accepted 25 August 2022; Published 14 September 2022

Academic Editor: Yaxiang Fan

Copyright © 2022 Shuai Wang et al. This is an open access article distributed under the Creative Commons Attribution License, which permits unrestricted use, distribution, and reproduction in any medium, provided the original work is properly cited.

Lumbar spine segmentation is important to help doctors diagnose lumbar disc herniation (LDH) and patients' rehabilitation treatment. In order to accurately segment the lumbar spine, a lumbar spine image segmentation algorithm based on improved Attention U-Net is proposed. The algorithm is based on Attention U-Net, the attention module based on multilevel feature map fusion is adopted, two residual modules are introduced instead of the original convolution blocks. a hybrid loss function is used for prediction during the training process, and finally, the image superposition process is realized. In this experiment, we expanded 420 lumbar MRI images of 180 patients to 1000 images and trained them by different algorithms, respectively, and accuracy, recall, and Dice similarity coefficient metrics were used to analyze these algorithms. The results show that compared with SVM, FCN, R-CNN, U-Net, and Attention U-Net models, the improved model achieved better results in all three evaluations, with 95.50%, 94.53%, and 95.01%, respectively, which proves the better performance of the proposed method for segmentation in lumbar disc and caudal vertebrae.

1. Introduction

In recent years, lumbar spine-related diseases have been affecting people's normal work and lives, and some families are bearing a huge economic burden. Lumbar spine diseases mainly include disc herniation (LDH) and lumbar spinal stenosis [1]. As LDH is mainly caused by disc degeneration or overwork, it has the highest prevalence in the age group of 30–50 years old, with a prevalence ratio of 2 : 1.1 between men and women, and 90% of the elderly over 60 years old worldwide suffer from degenerative disc symptoms [2–5]. Due to the increased pressure in life, more and more young people are also suffering from lumbar spine diseases. Lumbar spine diseases are diagnosed by physicians by examining the relevant parts of the lumbar spine. The imaging modalities mainly include computed tomography (CT) [6], magnetic resonance imaging (MRI) [7], and so on. The images with better imaging are selected from lots of CT or MRI images by physicians, and the possible lesions are diagnosed by physicians. As the number of patients increases, the cumbersome diagnostic approach not only increases the consultation time of patients but also puts tremendous work pressure on physicians. Therefore, lumbar segmentation plays an important part in the whole diagnostic process, which helps doctors to observe medical images quickly and accurately, and it facilitates the patient's further treatment.

Medical image segmentation techniques can be divided into two categories: traditional segmentation techniques and deep learning-based methods. The former includes threshold-based segmentation [8], edge-based segmentation [9], region-based segmentation [10, 11], and active contour model-based techniques [12, 13], and the latter is mainly neural network-based segmentation [14–18]. Earlier studies have been applied to the lumbar spine segmentation by traditional segmentation techniques. Hoad et al. [19] used a traditional threshold segmentation method applied to the spine MRI images to segment lumbar discs from soft tissues, thereby realizing the

computer-aided diagnosis of the spine. Armato et al. [20] demonstrated a random forest based method to extract vertebral height and width, which solved the problem of biomarkers of the lumbar spine. Punarselvam et al. [21] used a watershed method to detect boundaries and edges in the lumbar spine images. Later, this method was added with statistical and spectral texture features by some scholars [22], and they used this method to effectively distinguish the closed area of the intervertebral disc in the image. In recent years, deep learning has shown great advantages in medical image processing. Lee et al. [23] established a reference framework for segmenting lumbar arch roots in CT images, which obtained segmented vertebrae and canal references by using 2D dynamic thresholding and a combined cost based on sparing and finally achieved edge segmentation of the spine. Deng et al. [24] proposed a method based on the combination of contour transform and artificial neural network (ANN). This approach used contour transform to decompose images to obtain contour coefficients and used the ANN to optimize the coefficients of contour transform, thereby improving the performance of lumbar image segmentation. In addition, the method of the deep network with full convolution (FCN) was proposed in some studies [25, 26], which segmented and labeled the lumbar spine at once by using the local lumbar spine environment. FCN combined with the convolutional neural network (CNN) again to improve the segmentation effect, compared the segmentation results with conventional segmentation methods, and the results showed that the segmentation accuracy and efficiency were improved [27]. However, deep convolutional networks are not the only option for medical image segmentation, which requires training with a large amount of data. With the expansion of machine learning, image segmentation has developed different types of models based on full convolutional networks, such as U-Net [28–30], PSPNet [31, 32], and DeepLab [33, 34]. Sunetra et al. [35] showed the LDS U-Net structure to segment ultrasound spine lateral bony features from noisy images, which required only a small number of medical images for training. Saenz-Gamboa et al. [36] used a variant of U-Net for automatic segmentation of lumbar spine MRI images; this model classified labels to each pixel of the image. For the image noise problem of lumbar spine segmentation, Yang et al. [37] showed an automatic initialization level set method based on regional correlation, which introduced the histogram information inside and outside the level set contour, and Tang et al. [38] used a double densely connected U-neural network. This method improved the contrast of vertebral body edges, spinal ducts, and cloudy sacs while reducing image noise.

The lumbar spine can be extracted from the soft tissue by the above lumbar spine segmentation methods, but the accuracy is still slightly low, and the segmentation effect is influenced by the lesion area, as well as the parameter settings, which has some limitations. To solve these problems, this paper proposes a lumbar spine segmentation method with an improved Attention U-Net, which improves the structure of the attention module and residual network. A hybrid loss function is used to improve the detection accuracy. The specific experimental procedure is shown in Figure 1. First, the images are preprocessed by extracting local binary pattern (LBP) features and using contrast limited adaptive histogram equalization (CLAHE). Then, segmentation is performed using a modified Attention U-Net model. Finally, the vertebral blocks and intervertebral discs are extracted by gray threshold, and the images are superimposed by image fusion. MRI is the mainstay of lumbar spine image diagnosis at present. Compared with CT, MRI images have clearer soft tissue contours and have a better effect for imaging intervertebral disc degeneration, so we select MRI images to carry out the experiment of lumbar spine segmentation.

The rest of this article is organized as follows: in Section 2, U-Net and Attention U-Net are introduced, and how to improve Attention U-Net is described in detail. The arrangement of the experiments and the evaluation metrics are described in Section 3. The results of the experiments and postprocessing of the images are described in Section 4. Finally, Section 5 draws conclusions and proposes future research.

2. Methods

2.1. U-Net and Attention U-Net. U-Net is a convolutional neural network architecture with a simple structure and high efficiency. The architecture consists of two parts: an encoder and a decoder. The encoder part uses convolution and pooling to downsample the image, which doubles the number of feature channels and halves the image size. This part consists of two convolutional layers with 3×3 filters and a 2×2 maximum pooling layer with a step size of 2. ReLU is used for the activation function. The decoder part upsamples the feature image by deconvolution, which reduces the number of features channels and increases the image size, and finally outputs an image of the same size as the original image. It mainly consists of a deconvolutional layer with 2×2 filter and two 3×3 convolutional layers and still uses the ReLU activation function. The feature stitching of U-Net has a better processing effect for problems such as the difficulty in distinguishing biological tissue structures and the display of low-level and high-level features [39]. In addition, the experimental data of some medical images are generally so less that they are not suitable for the complex and large networks, while the U-Net with its simple structure can be better processed for these medical images.

Attention U-Net is a network structure based on U-Net with an added attention mechanism [40]. Compared with U-Net, an attention mechanism is added to the feature map in the encoder part before splicing in the decoder part, so that irrelevant background regions are suppressed and target regions are enhanced. In the lumbar segmentation, the vertebral body, intervertebral disk, and sacral regions are enhanced by the attention mechanism, while the soft tissue regions are suppressed [41]. The oversegmentation of images by the network structure can be effectively reduced by the attention mechanism.

2.2. Improved Attention U-Net. In this study, an improved network structure is proposed based on Attention U-Net, as shown in Figure 2. The network is presented as U-shaped,

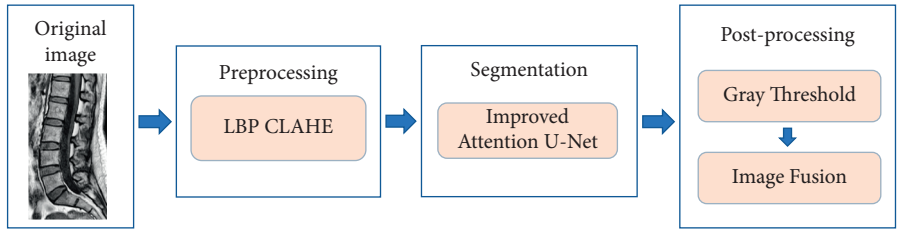

Figure 1: Segmentation process of lumbar spine image.

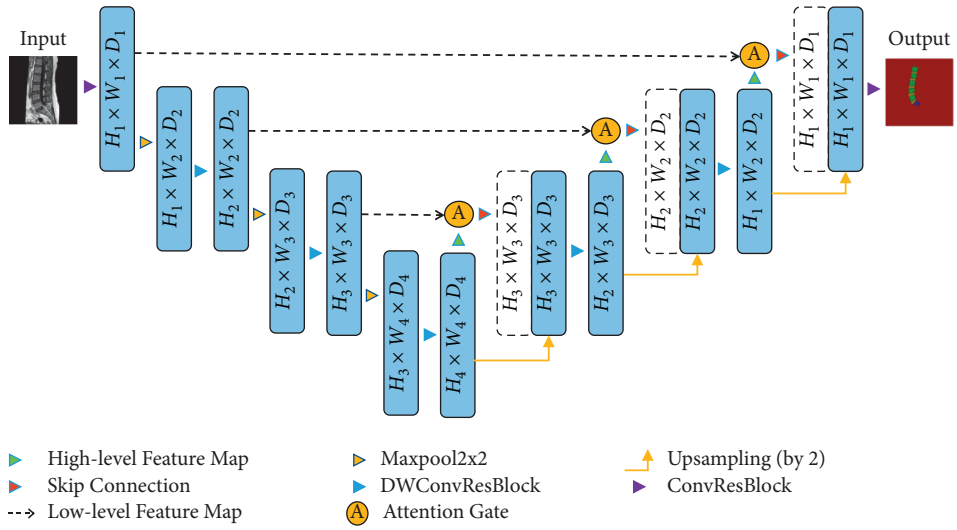

Figure 2: The network structure of improved Attention U-Net.

with the encoder part on the left and the decoder part on the right side. The number of channels, height, and width of the tensor are denoted by D, H, and W, respectively. Compared with the traditional Attention U-Net, the network framework is built by deep convolution in the bottom feature layer and the top feature layer. Improved residual structure is added to the convolution process of each layer to increase the depth and feature fusion ability of the network. Layers 1–3 in the encoding process and layers 6–8 in the decoding process are connected by jump connections, so that the encoder part is used to generate feature information at different scales in the whole network. An improved attention module is introduced for each jump connection that allows the model to acquire local information more accurately. Finally, the structure reduces the number of four downsampling layers in the traditional U-Net to three, which reduces the number of parameters in the network; therefore, the computational complexity is reduced, which facilitates the acquisition of global features.

2.2.1. Improved Multilevel Attention Module. The attention mechanism is generally applied in the dynamic analysis of vision and classification of images and later in segmentation of images. In image segmentation, the attention mechanism is used to remove redundant information from layers to improve the running speed and segmentation performance of matrix algorithms [42, 43]. The expression of this attention mechanism is

$$AG(x, g, g) = \sigma\left(Conv_{2d}^{1\times1}\left(ReLu\left(Conv_{2d}^{1\times1}(Up(g)) \times Conv_{2d}^{1\times1}(x)\right)\right)\right) \times x, \tag{1}$$

where the eigengraphs of the encoder output and the gating signal are represented as x and g, respectively, σ is the sigmoid function, Up represents the upsampling, and $\text{Conv}_{2\text{d}}^{1\times1}$ represents the two-dimensional 1×1 convolution.

According to the characteristics of attention, an attention module based on a multilevel feature map fusion is improved in this study. The improved attention module is shown in Figure 3; in the input phase, the matrix of the encoder part is normalized by conv1×1 and batch normalization (BN) operation in the input stage, combined with the matrix in the upsampling that has undergone convolution and batch normalization, and then, the convergence of the attention parameters is trained by processing the ReLU activation function, the conv1×1, and sigmoid activation functions. The attention coefficients α (i.e., attention weights) are obtained by resampling. Finally, the output α is multiplied with the feature layer of the encoder to obtain the result.

2.2.2. Improved Residual Module. Different from the conventional convolutional neural network, the ResNet [44] residual network deepens the number of network layers through shortcut connections. It still has better running speed and results without adding parameters and data calculations, which can effectively solve the gradient

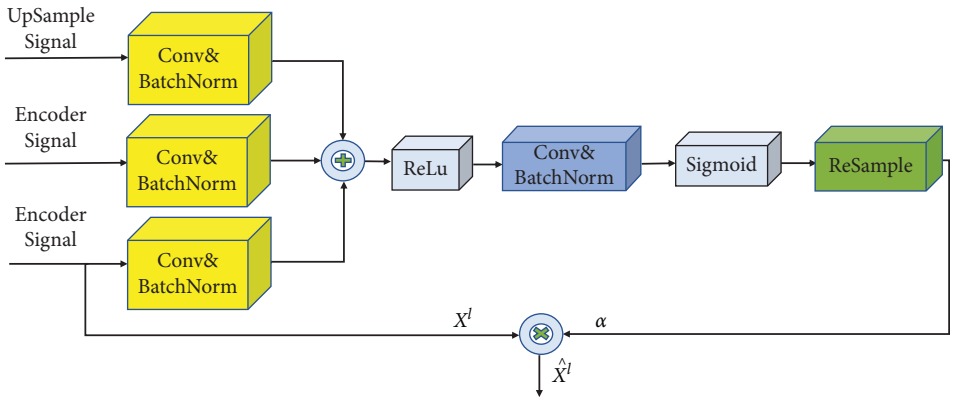

Figure 3: Improved attention module.

dissipation problem caused by too many output features. The residual network is composed of residual modules, which are as follows:

$$y = F(x, \{w_i\}) + w_j x, \tag{2}$$

where y and x are the output and input vectors of the residual module, $F(x, \{w_i\})$ is the residual mapping, and linear projection w_j is used for matching dimensions in shortcut connection.

This study designs two different residual modules based on the ResNet network structure to replace the convolutional blocks in Attention U-Net, and the module structures are shown in Figures 3 and4.

The convolutional module in Figure 4 is used for feature extraction in the first and last layers of Attention U-Net, adding the underlying residual structure to better extract information in large size and shallow-depth feature maps. Its two convolutional layers use a 3×3 convolutional kernel and ReLU function, and the input feature map after 1×1 convolution is subjected to a feature summation operation with the output after 3×3 convolution. In addition, a batch normalization (BN) operation is performed before using ReLU to speed up the convergence of the model.

An improved deep convolutional residual module is shown in Figure 5. It mainly contains two 5×5 convolutional layers, a 3×3 convolution, and some basic operations. For the feature map that is input to the residual module, the feature map after two 5×5 deep convolutional operations is fused to form a new feature map and stitched, at which time the number of channels becomes twice as many as the original one, fusing feature information of different complexity. Then, it is fused with the output feature map after 3×3 convolution, batch normalization, and ReLU operation, and finally, the feature map is input to the next residual model. The residual module introduced in this module enhances the feature extraction capability at different depths; two 5×5 depth convolutional layers are able to extract semantic information at different levels of complexity, which are adopted to the feature extraction stage of the high-level feature map. So, this module is used instead of the convolutional layer in the original Attention U-Net network.

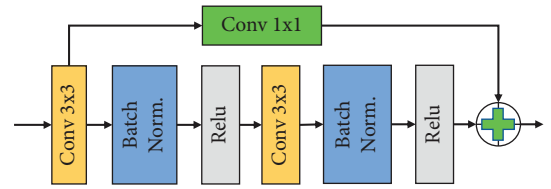

Figure 4: Improved standard convolutional residual blocks.

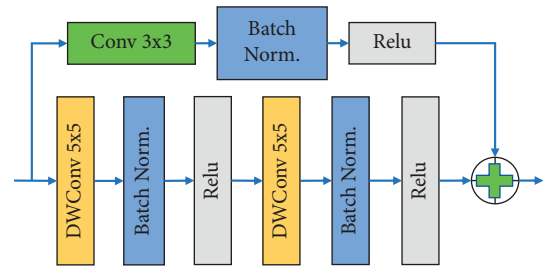

Figure 5: Improved deep convolutional residual blocks.

2.2.3. Hybrid Loss Function. The loss function optimizes the network structure by backpropagating the numerical error of the calculated loss function and continuously updating the weights. In the field of medical image segmentation, the Dice Loss [45] function is commonly used to calculate the degree of differences between the predicted region and the real region. The concepts of Dice Loss are defined by (3). However, the loss function has the problem that the training error curve is very confusing when using the Dice Loss or IOU [46] loss function causes. These situations can be avoided by using the cross-entropy loss (CEL) function, with the expression (4), which makes the gradient form better, but suffers from the problem of class imbalance.

$$D = 1 - 2|X \cap Y| / (|X| + |Y|), \tag{3}$$

$$CL = -\sum_{i=1}^{n} y_i^{c_i} \log\left(\hat{y_i^{c_i}}\right), \tag{4}$$

where $X \cap Y$ denotes the intersection of X and Y; |X| and |Y| denote the number of X and Y, respectively; and $y_i^{c_i}$ and

$\widehat{y_i^{c_i}}$ denote the label value and the predicted value, respectively.

To address the above problems, we use a hybrid loss function based on cross-entropy loss function and Dice loss function, which observes the convergence steadily during the training process and avoids the category of the imbalanced problem. Its formula is as follows:

$$DCL(Q,F) = -\frac{1}{U}\sum_{H=1}^{H}\sum_{U=1}^{U}\left(y_{n,l}\log p_{nl} + \frac{2y_{n,l}p_{nl}}{y_{n,l}^2 p_{n,l}^2}\right), \quad (5)$$

where Q is the actual situation, F is the predicted result from training, $y_{n,l} \in F$ represents the probability of prediction, the $p_{nl} \in Q$ represents the established target, H represents the number of classifications in the dataset, and U represents the number of pixels in the image.

3. Experiment

3.1. Experimental Data and Environment. The experimental dataset used in this study is collected from Qingdao Hospital of Shandong University Qilu Hospital. The collected data contain 420 MRI T1 images of 180 lumbar spine patients, which were expanded to 1000 images by data enhancement. In order to facilitate the later experimental operation, the dcm format of T1 images is changed to jpg format by the SimpleITK toolkit, and the image size is resized to 512×512 by linear interpolation. Finally, the images are classified into training sets, validation sets, and test sets according to the ratio of 7 : 2:1.

Experimental environment: Windows 10 operating system, AMD Ryzen 7 4800H processor, NVIDIA GeForce GTX 1650 GPU with 64 GB of video memory, 8-core CPU, 32 G of memory, PyTorch 1.2.0 is used for the deep learning framework, and Python is used for the programming language.

3.2. Data Preprocessing. The MRI images of the lumbar spine contain tissues such as vertebrae, intervertebral discs, spinal canal, and muscles.

The texture features of tissues reflect different basic feature information. Because the intervertebral disc in the original image is relatively dark and the contrast with the vertebral block is not obvious, it is easy to cause errors in the manual labeling of the intervertebral disc and vertebral block in the later stages, making the labeled image inaccurate and affecting the effect of later deep learning. Therefore, in order to facilitate labeling, the contrast of different tissues in the image needs to be improved. The histogram equalization method can increase the gray value range of the image and uniformize the distribution of pixel gray values, thereby improving the contrast and clarity of the image. The specific steps are as follows: first, the grayscale values are calculated, and the histograms are counted. Then, the cumulative histogram in the statistical histogram is calculated, and finally, the interval conversion is performed on the cumulative histogram. The effect is shown in Figure 6(b). The figure shows that after the histogram transformation of the whole image by the conventional histogram equalization operation, the brightness of the image is improved, the image noise is amplified, and even some parts appear. The effect of excessive brightness is that it eventually leads to a decrease in the sharpness of the image.

In order to effectively solve the problem of the image noise signal being amplified, a method of limiting contrast is added to the adaptive histogram equalization: if the value in a certain range of the histogram exceeds the limited threshold, the exceeding area will be cut out and that area is distributed to the rest of the histogram. As shown in Figure 6, compared with conventional histogram equalization, the method used in this study has a better processing effect and improves the contrast and sharpness of different tissues.

The processed images are labeled and classified by the LabelMe tool; each image is labeled with 3 categories, including 5 vertebral bodies, 5 intervertebral discs, and 1 sacrum, named L, LD, and S. The different tissues labeled are distinguished by different colors, as shown in Figure 7. After the image is annotated, the corresponding JSON format file is obtained, which contains information about the different categories of annotation and the pixel coordinates of the annotation points. The JSON file is transformed into voc data, which contain the segmented mask map, the annotation map combining the mask map with the original map, and the NPY format file.

3.3. Evaluation Indicators. To comprehensively evaluate the effectiveness of the proposed algorithm for lumbar spine segmentation, three metrics are used as evaluation methods, which are accuracy (P), recall (R), and Dice similarity coefficient. As shown in formulas (6) and (7), when the accuracy, P, is high, the recall, R, is low and vice versa. When the two do not conform to this relationship, the Dice similarity coefficient is introduced for comprehensive evaluation. The Dice similarity coefficient is often used to evaluate medical image targets with uneven segmentation size. The obtained formula is (8).

$$P = \frac{\mathrm{TP}}{(\mathrm{TP} + \mathrm{FP})}, \quad (6)$$

$$R = \frac{\mathrm{TP}}{(\mathrm{TP} + \mathrm{FN})}, \quad (7)$$

$$\mathrm{Dice} = \frac{2TP}{(\mathrm{TP} + \mathrm{FP} + \mathrm{TN} + \mathrm{FN})}, \quad (8)$$

where true positive (TP) is the number of lumbar spine images that the model correctly classifies as positive examples, that is, the number of samples that are actually positive examples and are classified as positive examples by the model. False positives (FP), which indicates the number of lumbar spine images that the model incorrectly classifies as positive, that is, the number of samples that are actually negative but are classified as positive by the model. True negative (TN) is the number of lumbar spine images correctly classified as negative by the model, that is, the number of samples that are actually negative and are classified as

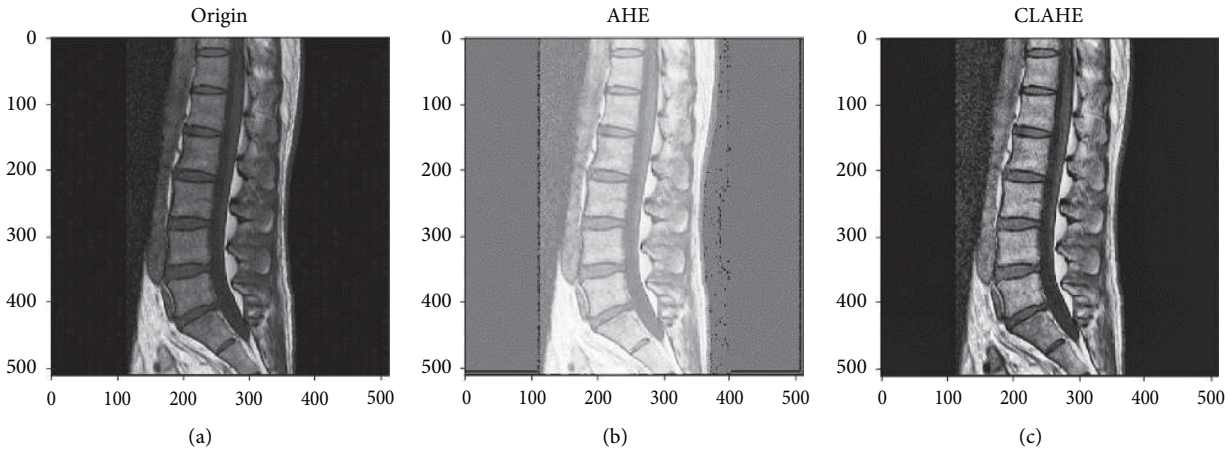

Figure 6: The comparison results of equalization. (a) Original graph. (b) Histogram equalization. (c) Our method.

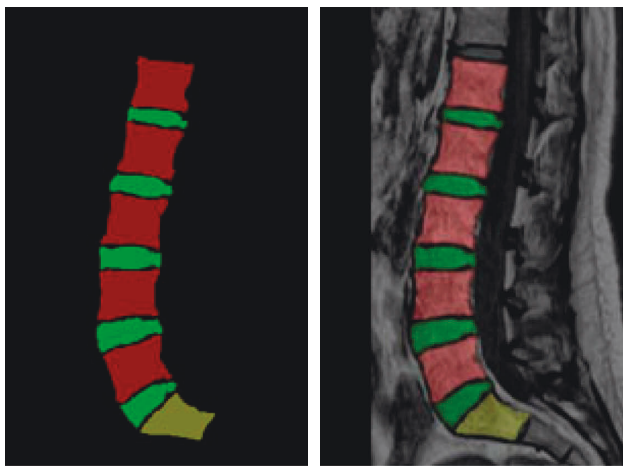

Figure 7: Marked effect.

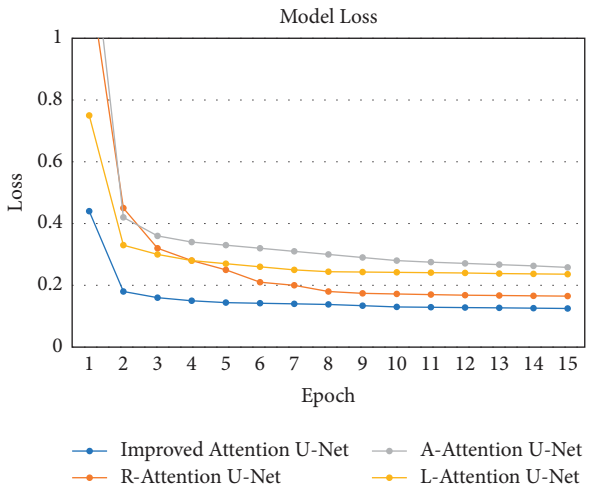

Figure 8: The loss curve.

negative by the model. False negative (FN), which indicates the number of lumbar spine images that the model incorrectly classifies as negative examples, that is, the number of samples that are actually positive examples but are classified as negative examples by the model.

4. Results and Analysis

4.1. Attention U-Net Segmentation Effect. During the training of the algorithm model, the batch size is set to 2, and 15 rounds are trained with one validation per round as well as model preservation. In this paper, the models of the Attention U-Net network with improved residual module, attention mechanism, and hybrid loss function are defined as R-Attention U-Net, A-Attention U-Net, and L-Attention U-Net, respectively. As shown in Figure 8, with the continuous iteration of R-Attention U-Net, A-Attention U-Net, L-Attention U-Net, and the improved model in this study, the loss function gradually decreases. At the beginning of training, after three rounds, the loss function of all models rapidly decreases to below 0.4. After the end of training, the loss functions of all models were stabilized below 0.3, and segmentation models satisfying the requirements were obtained. Table 1 shows the experimental results of different models for lumbar spine detection. The accuracy rates of R-Attention U-Net, A-Attention U-Net, and L-Attention U-Net models are all above 90%, which indicate that the methods for improving a single variable all have better performance. Among them, A-Attention U-Net has the highest recall rate of 95.70%, but the number of incorrectly identified samples is high, resulting in a low accuracy rate. The improved Attention U-Net in this study has a lower recall rate compared with the A-Attention U-Net with the improved attention mechanism only, but the accuracy and Dice similarity coefficient are improved by 2.23% and 0.54%, respectively, i.e., the incorporated residual module and hybrid loss function have a better correction effect for the incorrect identification of the A-Attention U-Net.

Table 2 shows the comparison of experimental results under equal conditions; SVM, FCN, R–CNN, U-Net, Attention U-Net, and improved Attention U-Net are used for samples segmentation, respectively; the improved model in this study achieves the best results in terms of accuracy, recall, and Dice similarity coefficient indexes, which are

Table 1: Comparison of experimental results of different improvement schemes.

Type	TP	FP	FN	P (%)	R (%)	Dice (%)
R-Attention U-Net	728	46	47	94.06	93.94	93.99
A-Attention U-Net	735	53	33	93.27	95.70	94.47
L-Attention U-Net	722	49	50	93.64	93.52	93.58
Improved Attention U-Net	743	35	43	95.50	94.53	95.01

Table 2: Comparison of experimental results of different algorithms.

Type	TP	FP	FN	P (%)	R (%)	Dice (%)
SVM	605	101	115	85.69	84.03	84.85
FCN	644	83	94	88.58	87.27	87.91
R-CNN	712	58	51	92.50	93.32	92.89
U-Net	685	62	74	91.70	90.25	90.10
Attention U-Net	715	49	57	93.59	92.62	93.10
Improved Attention U-Net	743	35	43	95.50	94.53	95.01

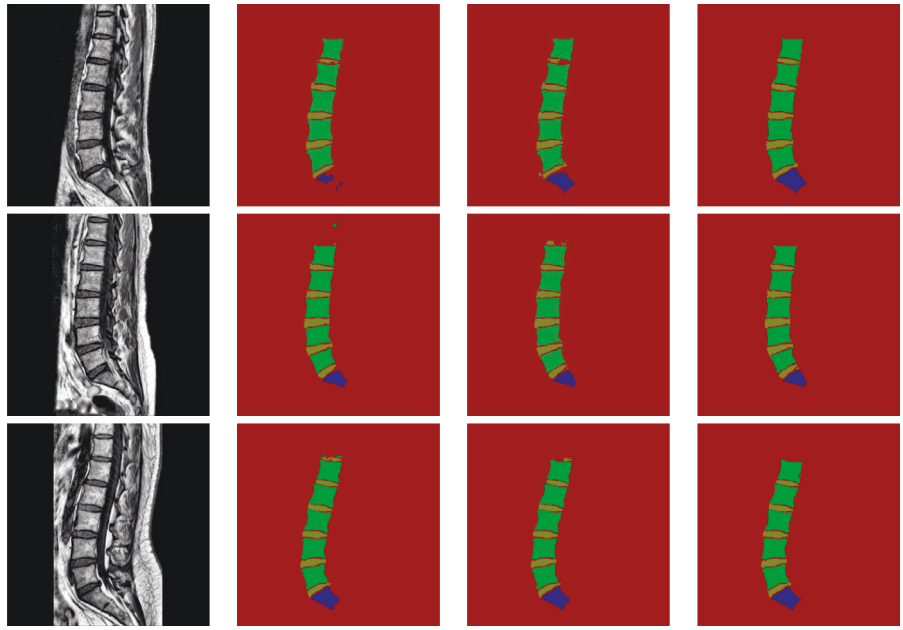

Figure 9: The segmentation effect of different algorithms.

95.50%, 94.53%, and 95.01%, proving that the proposed method meets the requirements of lumbar spine segmentation. Among them, R-CNN and Attention U-Net also have better recognition effects, and by comparing the experimental results of these two models and the method in this study, as shown in Figure 9, the segmentation effect of the algorithm in this study is significantly better than other methods in terms of overall and detail processing. The sacrum and intervertebral disc appear missing and broken by R-CNN and Attention U-Net processing, while the proposed algorithm can segment the feature edges of the target more accurately, reducing the occurrence of problems, such as the mutilation of the intervertebral disc and the missing sacrum, and showing better robustness to targets with poor clarity and different shapes.

4.2. Postprocessing of Segmented Images. Postprocessing of the images is required to observe the different parts of the lumbar spine more clearly. As shown in Figure 10, different categories are represented by different colors, with the vertebral block represented by green, the intervertebral disc represented by yellow, the sacrum represented by blue, and the background represented by red. The extraction of each category is performed according to the different colors of the segmentation object. First, the mask image is converted to a grayscale image, and then, the grayscale value threshold is set by the different grayscale value sizes of the vertebral block and intervertebral disc, so that the vertebral block and intervertebral disc can be extracted. Figure 10 shows the effect of extracting the vertebral block alone.

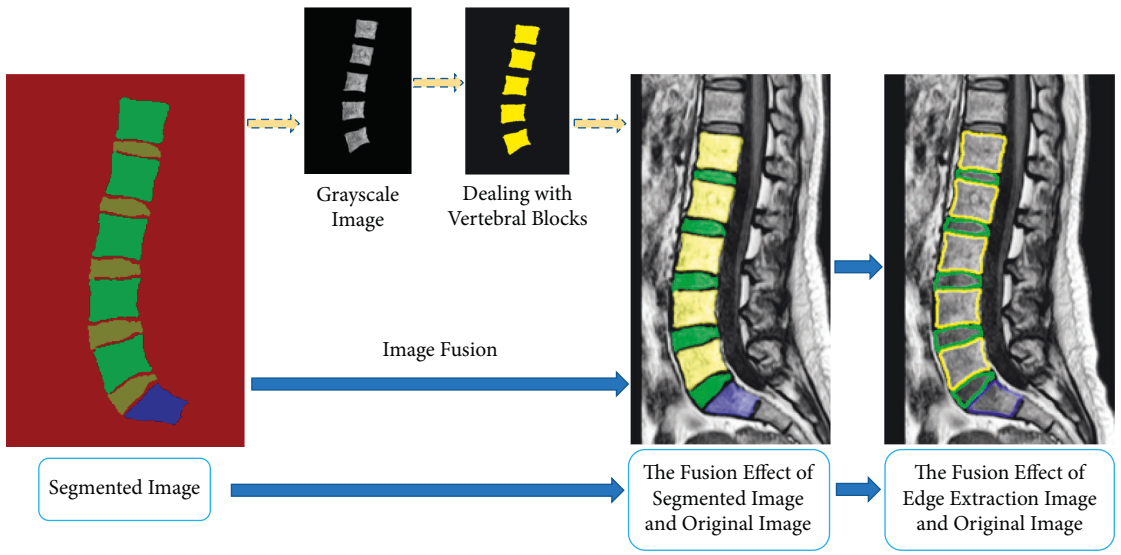

Figure 10: The segmentation effect of different algorithms.

In order to realize the detailed view of different parts, we achieve the superposition of the original lumbar spine image and the mask image by image fusion and add labels to the hybrid map. Figure 10 shows the fusion map of the segmented images and the original image and the fusion map of the edge extraction and the original image, respectively. We can clearly see the various parts of the lumbar spine and lumbar disc from the fusion map, which is beneficial for the doctor to quickly diagnose the lumbar spine MRI images.

5. Conclusions and Future Work

Lumbar spine segmentation is very important for the diagnosis of related diseases. To address the problem of low segmentation accuracy of lumbar spine MRI images, we propose a segmentation method based on improved Attention U-Net. The steps of the study are as follows:

(i) Limiting contrast is added to the adaptive histogram equalization, which reduces the roughness of the image and improves the contrast and sharpness of different tissues, thus facilitating the labeling of experimental data

(ii) By improving Attention U-Net, two residual modules are introduced instead of the original convolutional blocks, an attention module based on a multilevel feature map fusion is used, and a hybrid loss function is used in training for prediction

(iii) Different tissues are extracted according to the different colors of the segmented images. And through image fusion, the superposition of the original lumbar spine image and the segmented image is realized, thus facilitating the physician to observe the lesion of each tissue more intuitively.

According to the comparison experiments of the three models with changing single variable, among them, the recall rate of A-Attention U-Net performs better than the improved method in this paper, reaching 95.70%, but the false recognition rate of A-Attention U-Net is higher, which leads to a decrease in accuracy and Dice similarity coefficient by 2.23% and 0.54%, respectively, proving that the method in this study is better than the improved single-variable method with better equalization ability. In addition, comparison experiments of six different network models were completed, and it was verified that the model in this study has better results in lumbar spine segmentation and outperforms SVM, FCN, R-CNN, U-Net, and Attention U-Net in terms of accuracy, recall, and Dice similarity coefficient, with 95.50%, 94.53%, and 95.01%, respectively. It proves that the method in this study has better performance in the intervertebral disc and more detailed processing of the sacral region with better robustness.

Data Availability

The datasets used to support the findings of this study are available from the corresponding author upon request.

Conflicts of Interest

The authors declare that they have no conflicts of interest.

Acknowledgments

This research was funded by the National Natural Science, China (52101401).

References

[1] D. Hoy, L. March, P. Brooks et al., "The global burden of low back pain: estimates from the Global Burden of Disease 2010 study," *Annals of the Rheumatic Diseases*, vol. 73, no. 6, pp. 968–974, 2014.

[2] D. Hoy, L. March, P. Brooks et al., "Measuring the global burden of low back pain," *Best Practice & Research Clinical Rheumatology*, vol. 24, no. 2, pp. 155–165, 2010.

[3] R. K. Ponnappan, D. Z. Markova, P. J. Antonio et al., "An organ culture system to model early degenerative changes of the intervertebral disc," *Arthritis Research and Therapy*, vol. 13, no. 5, pp. 1711–R212, 2011.

[4] C. W. A. Pfirrmann, A. Metzdorf, M. Zanetti, J. Hodler, and N. Boos, *Spine*, vol. 26, no. 17, pp. 1873–1878, 2001.

[5] T. Yuan, J. Zhang, and Q. Liu, "Treatment of calcified L5S1 lumbar disc herniation with percutaneous endoscopic interlaminar discectomy:A report of 15 cases and literature review," *Journal of Jilin University - Medicine Edition*, vol. 44, pp. 615–619, 2018.

[6] H. J. Bae, H. Hyun, Y. Byeon et al., "Fully automated 3D segmentation and separation of multiple cervical vertebrae in CT images using a 2D convolutional neural network," *Computer Methods and Programs in Biomedicine*, vol. 184, Article ID 105119, 2020.

[7] C. L. Hoad and A. L. Martel, "Segmentation of MR images for computer-assisted surgery of the lumbar spine," *Physics in Medicine and Biology*, vol. 47, no. 19, pp. 3503–3517, 2002.

[8] M. Angulakshmi and M. Deepa, "A review on deep learning architecture and methods for MRI Brain Tumour segmentation," *Current Medical Imaging Formerly Current Medical Imaging Reviews*, vol. 17, pp. 695–706, 2021.

[9] J. Park, S. Park, and W. Cho, "Medical image segmentation using level set method with a new hybrid speed function based on boundary and region segmentation," *IEICE Transactions on Information and Systems*, vol. E95.D, no. 8, pp. 2133–2141, 2012.

[10] G. G. N. Geweid and M. A. Abdallah, "A novel approach for Breast Cancer Investigation and recognition using M-level set-based Optimization functions," *IEEE Access*, vol. 7, pp. 136343–136357, 2019.

[11] Y. Huang, G. Hu, C. Ji, and H. Xiong, "Glass-cutting medical images via a mechanical image segmentation method based on crack propagation," *Nature Communications*, vol. 11, no. 1, p. 5669, 2020.

[12] A. Afifi, T. Nakaguchi, N. Tsumura, and Y. Miyake, "A model Optimization approach to the automatic segmentation of medical images," *IEICE Transactions on Information and Systems*, vol. E93-D, no. 4, pp. 882–890, 2010.

[13] L. Zhang, J. Liu, F. X. Shang, G. Li, J. Zhao, and Y. Zhang, "Robust segmentation method for noisy images based on an unsupervised denosing filter," *Tsinghua Science and Technology*, vol. 26, no. 5, pp. 736–748, 2021.

[14] Y. Ma, X. Li, X. Duan, Y. Peng, and Y. Zhang, "Retinal Vessel segmentation by deep residual learning with Wide activation," *Computational Intelligence and Neuroscience*, vol. 2020, Article ID 8822407, 11 pages, 2020.

[15] M. H. Hesamian, W. Jia, X. He, and P. Kennedy, "Deep learning techniques for medical image segmentation: Achievements and Challenges," *Journal of Digital Imaging*, vol. 32, no. 4, pp. 582–596, 2019.

[16] C. Chen, C. Qin, H. Qiu et al., "Deep learning for Cardiac image segmentation: a review," *Frontiers in Cardiovascular Medicine*, vol. 7, pp. 25–36, 2020.

[17] H. Seo, M. Badiei Khuzani, V. Vasudevan et al., "Machine learning techniques for biomedical image segmentation: an Overview of Technical Aspects and introduction to State-of-Art Applications," *Medical Physics*, vol. 47, no. 5, pp. 148–167, 2020.

[18] S. Asgari Taghanaki, K. Abhishek, J. P. Cohen, J. Cohen-Adad, and G. Hamarneh, "Deep semantic segmentation of natural and medical images: a review," *Artificial Intelligence Review*, vol. 54, no. 1, pp. 137–178, 2020.

[19] F. Eckstein, F. Cicuttini, J. P. Raynauld, J. C. Waterton, and C. Peterfy, "Magnetic resonance imaging (MRI) of articular cartilage in knee osteoarthritis (OA): Morphological assessment," *Osteoarthritis and Cartilage*, vol. 14, pp. 46–75, 2006.

[20] S. G. Armato, N. A. Petrick, A. Kulkarni et al., *Automatic Segmentation of Lumbar Vertebrae in CT Images*, medical Imaging, 2017.

[21] E. Punarselvam, D. P. Suresh, R. Parthasarathy, and M. Suresh, "Segmentation of lumbar spine image using watershed algorithm," *Journal of Engineering Research and Applications*, vol. 3, pp. 1386–1389, 2013.

[22] C. Chevrefils, F. Cheriet, C.-E. Aubin, and G. Grimard, "Texture analysis for automatic segmentation of intervertebral disks of scoliotic spines from MR images," *IEEE Transactions on Information Technology in Biomedicine*, vol. 13, no. 4, pp. 608–620, 2009.

[23] J. Lee, S. Kim, Y. S. Kim, and W. K. Chung, "Automated segmentation of the lumbar Pedicle in CT images for spinal fusion surgery," *IEEE Transactions on Biomedical Engineering*, vol. 58, no. 7, pp. 2051–2063, 2011.

[24] J. M. Deng, H. Y. Li, and H. Wu, "An approach to lumbar Vertebra CT image segmentation using contourlet transform and ANNs," *Advanced Materials Research*, vol. 468-471, pp. 613–618, 2012.

[25] A. Sekuboyina, A. Valentinitsch, J. S. Kirschke, and B. H. Menze, "A Localisation-Segmentation Approach for Multi-Label Annotation of Lumbar Vertebrae Using Deep Nets," 2017, https://arxiv.org/abs/1703.04347.

[26] M. D. Zeiler and R. Fergus, "Visualizing and Understanding convolutional networks," *Anal. Chem. Res.*vol. 12, pp. 818–833, 2014.

[27] M. Vania, D. Mureja, and D. Lee, "Automatic spine segmentation from CT images using Convolutional Neural Network via redundant generation of class labels," *Journal of Computational Design and Engineering*, vol. 6, no. 2, pp. 224–232, 2019.

[28] O. Ronneberger, P. Fischer, and T. Brox, *U-net: Convolutional Networks for Biomedical Image Segmentation*, pp. 234–241, Springer International Publishing, Berlin, Germany, 2015.

[29] O. Ronneberger, P. Fischer, and T. Brox, "U-net: convolutional networks for biomedical image segmentation," *coRR*, vol. 9351, pp. 234–241, 2015.

[30] M. J. Awan, M. S. M. Rahim, N. Salim, A. Rehman, and B. Garcia-Zapirain, "Automated knee MR images segmentation of Anterior Cruciate Ligament Tears," *Sensors*, vol. 22, no. 4, p. 1552, 2022.

[31] H. Zhao, J. Shi, X. Qi, X. Wang, and J. Jia, "Pyramid scene parsing network," in *Proceedings of the IEEE Conference on Computer Vision and Pattern Recognition (CVPR)*, pp. 6230–6623, Honolulu, HI, USA, July 2017.

[32] B. Shi, H. Q. He, and Qi. You, "A method of multi-scale Total convolution network Driven Remote Sensing image Repair," *Journal of Geomatics*, vol. 43, pp. 124–126, 2018.

[33] L. C. Chen, G. Papandreou, I. Kokkinos, K. Murphy, and A. L. Yuille, "Semantic image segmentation with deep convolutional Nets and fully connected CRFs," *Computer Science*, vol. 4, pp. 357–361, 2014.

[34] L.-C. Chen, G. Papandreou, I. Kokkinos, K. Murphy, and A. L. Yuille, "DeepLab: semantic image segmentation with deep convolutional Nets, Atrous convolution, and fully connected CRFs," *IEEE Transactions on Pattern Analysis and Machine Intelligence*, vol. 40, no. 4, pp. 834–848, 2018.

[35] S. Banerjee, J Lyu, Z Huang et al., "Light-convolution Dense selection U-net (LDS U-net) for ultrasound lateral bony

feature segmentation," *Applied Sciences*, vol. 11, no. 21, pp. 10180–10198, 2021.

[36] J. J. Saenz-Gamboa, J. Domenech, A. Alonso-Manjarrez, J. A. Gomez, and I. V. Maria, "Automatic semantic segmentation of the lumbar spine," in *Proceedings of the 25 th International conference Clinical Applicability in a Multi-Parametric and Multi-centre MRI Study*, Milan, Italy, January 2021.

[37] L. Yang, L. Wei, J. Tan, and Y. Zhang, "A novel automatically initialized level set approach based on region correlation for lumbar vertebrae CT image segmentation," in *Proceedings of the IEEE International Symposium on Medical Measurements & Applications*, pp. 291–296, IEEE, Turin, Italy, May 2015.

[38] H. Tang, X. Pei, S. Huang, X. Li, and C. Liu, "Automatic lumbar spinal CT image segmentation with a dual densely connected U-net," *IEEE Access*, vol. 8, pp. 89228–89238, 2020.

[39] K. He, X. Zhang, S. Ren, and J. Sun, "Deep residual learning for image recognition," in *Proceedings of the IEEE Conference on Computer Vision and Pattern Recognition*, pp. 770–778, IEEE, New York, NY, USA, June 2016.

[40] Z. Yin, D. Sun, T. Ren et al., "Research on automatic gallbladder segmentation model based on improved Attention U-Net," *Beijing Biomedicine Engineering*, vol. 40, pp. 346–353+376, 2021.

[41] A. Gupta, S. Upadhyaya, C. M. Yeung et al., "Disk area is a more Reliable Measurement than Anteroposterior Length in the assessment of lumbar disk herniations: a validation study," *Clinical Spine Surgery: A Spine Publication*, vol. 33, no. 8, pp. 381–385, 2020.

[42] L. Itti, C. Koch, and E. Niebur, "A model of saliency-based visual attention for rapid scene analysis," *IEEE Transactions on Pattern Analysis and Machine Intelligence*, vol. 20, no. 11, pp. 1254–1259, 1998.

[43] J. Yin, Z. Zhou, S. Xu, R. Yang, and K. Liu, "A generative Adversarial network fused with Dual-attention mechanism and its Application in Multitarget image fine segmentation," *Computational Intelligence and Neuroscience*, vol. 2021, pp. 1–16, Article ID 2464648, 2021.

[44] P. Liu, L. Sun, and C. Y. Zhang, "Fault Text classification based on Interactive attention mechanism network model," *Computer Integrated Manufacturing System*, vol. 27, pp. 72–89, 2021.

[45] Y. Cai, Q. Li, Y. Fan, L. Zhang, H. Huang, and X. Ding, "An automatic trough line identification method based on improved UNet," *Atmospheric Research*, vol. 264, Article ID 105839, 2021.

[46] Z. Zheng, P. Wang, W. Liu, J. Li, R. Ye, and D. Ren, "Distance-iou Loss: Faster and Better Learning for Bounding Box Regression," pp. 12993–13000, 2020, https://arxiv.org/abs/1911.08287.

Hindawi
Computational Intelligence and Neuroscience
Volume 2022, Article ID 6313161, 7 pages
https://doi.org/10.1155/2022/6313161

Research Article

LawRec: Automatic Recommendation of Legal Provisions Based on Legal Text Analysis

Min Zheng[1], **Bo Liu**[1] and **Le Sun**[2]

[1]*Hubei University of Science and Technology, Xianning, China*
[2]*Nanjing University of Information Science and Technology, Nanjing, China*

Correspondence should be addressed to Bo Liu; lb1@hbust.edu.cn

Received 25 June 2022; Revised 11 August 2022; Accepted 27 August 2022; Published 14 September 2022

Academic Editor: Yaxiang Fan

Copyright © 2022 Min Zheng et al. This is an open access article distributed under the Creative Commons Attribution License, which permits unrestricted use, distribution, and reproduction in any medium, provided the original work is properly cited.

Smart court technologies are making full use of modern science to promote the modernization of the trial system and trial capabilities, for example, artificial intelligence, Internet of things, and cloud computing. The smart court technologies can improve the efficiency of case handling and achieving convenience for the people. Article recommendation is an important part of intelligent trial. For ordinary people without legal background, the traditional information retrieval system that searches laws and regulations based on keywords is not applicable because they do not have the ability to extract professional legal vocabulary from complex case processes. This paper proposes a law recommendation framework, called LawRec, based on Bidirectional Encoder Representation from Transformers (BERT) and Skip-Recurrent Neural Network (Skip-RNN) models. It intends to integrate the knowledge of legal provisions with the case description and uses the BERT model to learn the case description text and legal knowledge, respectively. At last, laws and regulations for cases can be recommended. Experiment results show that the proposed LawRec can achieve better performance than state-of-the-art methods.

1. Introduction

Artificial intelligence technology has flourished in both academy and industry. Face recognition, voice recognition, and other intelligence technologies are developing rapidly [1]. Intelligent products such as smart speakers and sweeping robots have entered thousands of households. Smart court technologies are making full use of modern science such as the artificial intelligence, Internet of things, big data, and cloud computing to promote the modernization of the trial system and trial capabilities, thereby improving the efficiency of case handling and achieving convenience for the people [2].

With the step-by-step advancement of the court's informatization process, the record carrier of case information and adjudication process has been transformed from paper to electronic filing [3]. Relying on the rapid development of the Internet, case records are not limited to a certain court, city, or province, but they have a nationwide network of judgment documents. These conditions have led to the creation of a huge library of judicial documents with standardized formats. The judgment document is the record and summary of the case, the facts of the case, the trial process, and the basis of the trial after the judge completes the trial [4]. It contains a large amount of data information. These accumulated judgment documents have become a powerful data support for legal research, providing a good data foundation for subsequent intelligence.

Article recommendation is an important part of intelligent trial. Because the law is the basis for the outcome of the trial, the judge must handle the case in accordance with the law. Therefore, the statutes represent the direction of the trial of the case to a certain extent. In addition, the value of legal recommendations is also reflected in the help they can provide to various roles involved in legal cases [5]. For judges trying cases, if they can learn from the trial information of similar cases in the past, they can handle cases more efficiently. For lawyers who defend the plaintiff and the defendant, if they can quickly find the applicable laws and regulations from a variety of laws and regulations, they can

better defend their clients with stronger arguments. For plaintiffs and defendants who lack legal knowledge, without the help of professionals, they have no way of knowing whether there are suitable statutes to protect their rights and interests, and a system that can correctly predict statutes can help them save time and money in legal consultation [6].

For ordinary people without legal background, the traditional information retrieval system that searches laws and regulations based on keywords is not applicable because they do not have the ability to extract professional legal vocabulary from complex case processes [7]. The Bidirectional Encoder Representation from Transformers (BERT) model has powerful text representation and text understanding capabilities. This model has been widely used in semantic understanding-based fields, such as entity recognition, text classification, and other fields, but it is rarely used in the field of legal recommendation. This paper proposes a law recommendation framework, called LawRec based on BERT and Skip-Recurrent Neural Network (Skip-RNN) models [8], which intends to integrate the knowledge of legal provisions with the case description and uses the BERT model to learn the case description text and legal knowledge, respectively. At last, laws and regulations for cases can be recommended.

The paper structure is as follows: Section 2 introduced the related work of law recommendation. Section 3 describes the LawRec framework. Section 4 gives the experiment analysis and results. Section 5 makes a summarization.

2. Related Work

At present, the research on judicial intelligence at home and abroad has achieved certain results. Work [9] constructed a dataset of 2.6 million criminal cases for trial prediction, including case facts as input and three predictors of citations, charges, and jail time. Reference [10] proposed a model for predicting whether a court will uphold or overturn a judgment. By analyzing the lawyer's historical case handling and court trial performance, the lawyer is scored, and then the lawyer is recommended according to the current case type. There are also studies conducted on criminal cases. Work [11] used a bidirectional Gated Recurrent Unit (GRU) model to predict criminal charges based on court-finding facts and legal grounds. Work [12] extracted logical basis from case facts through reinforcement learning, which enhanced the interpretability of crime prediction. Work [13] regarded the court opinion as the interpretation of the crime and used the conditional seq2seq model to generate the judge's judgment analysis process according to the criminal facts of the criminal case.

In terms of recommendation algorithms, recommender systems first appeared in the 1990s [14, 15], which provide users with suggestions through historical information analysis and help users quickly find useful information. Collaborative filtering [16] is one of the most widely used algorithms in the field of recommender systems, involving social, shopping, finance, law, and other fields. Work [17] proposed a collaborative filtering-based network news system to help people find favorite articles in a large stream of information. Work [18] proposed content-based collaborative filtering to solve the problem that the workload of traditional methods increases with the increase of system participants.

Considering the recommendations of the law, some scholars have conducted part of the research. Most of them are aimed at expert users such as judges and lawyers and focus on information retrieval or keyword-based classification. How to make computers understand the meaning of natural language correctly has always been a topic of academic research. In recent years, the research of neural network algorithm has made breakthrough progress in this area. Work [19] applied neural network to lexical error correction. Work [20] proposed a neural network combining dynamic pooling and recurrent autoencoders for paraphrase detection. Work [21] used CNN for text classification and achieved better results than other models. Work [22] designed a court judgment evaluation model. The evaluation model is based on BP neural network. Work [23] designed a model based on bidirectional long short-term memory networks. The model can recognize legal text.

3. LawRec: BERT-Based Law Recommendation Framework

The Bidirectional Encoder Representation from Transformers (BERT) model has powerful text representation and text understanding capabilities. This model has been widely used in semantic understanding-based named entity recognition, text classification, and other fields, but it is rarely used in the field of legal recommendation. This paper proposes a law recommendation framework, called LawRec, based on BERT and Skip-RNN models, which intends to integrate the knowledge of legal provisions with the case description and uses the BERT model to learn the case description text and legal knowledge, respectively. At last, laws and regulations for cases can be recommended.

This paper proposes a law recommendation method based on knowledge fusion in the field of judicial law. The overall structure is shown in Figure 1. The proposed model includes rule extraction of laws, BERT training, and rule recommendation of laws. The legal knowledge extraction layer extracts keywords from the legal knowledge in the judicial field to obtain the legal knowledge. The BERT model performs semantic representation of the case description text and legal knowledge based on the Skip-RNN. Therefore, the semantic representation vector can be obtained. The legal rule knowledge integration layer is mainly based on the attention mechanism. The legal rule knowledge integration layer can realize the feature fusion of legal rule knowledge features and case description. And, the case description feature vector fused with legal rule knowledge can be obtained. The legal recommendation layer is like the traditional legal recommendation framework and adopts the idea of text classification to achieve the final legal recommendation.

3.1. Feature Extraction. The legal provisions for specific types of cases are generally long. To accurately locate the core knowledge of legal provisions, this paper extracts the

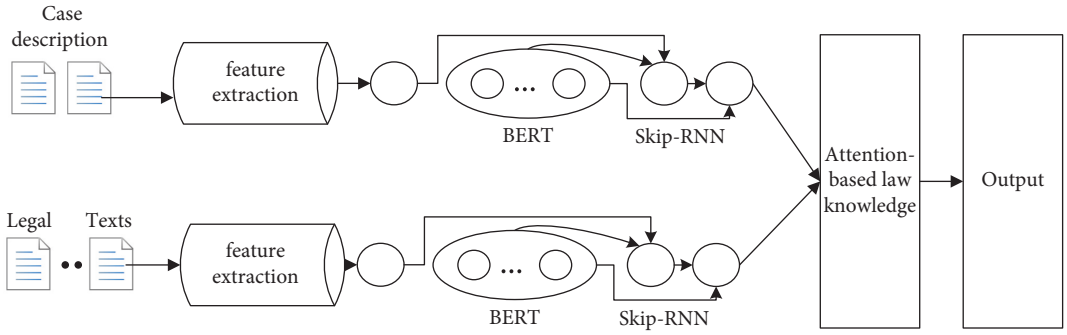

Figure 1: Framework of LawRec based on BERT and Skip-RNN.

keywords of legal provisions and finally obtains the core knowledge of legal provisions, which is convenient for subsequent follow-up.

3.2. BERT Model for Feature Modelling. For the text description $E = [E_1, E_2, \ldots, E_n]$ and legal knowledge $L = [L_1, L_2, \ldots, L_m]$ of a specific case, where n represents the length of the case description text, m is the length of the legal text knowledge, this paper uses the BERT model to characterize them, respectively. Based on the BERT model, we get the specific text description vector which is as follows:

$$\begin{aligned} G_E &= BERT(E) \\ G_L &= BERT(L) \end{aligned}, \tag{1}$$

where G_E and G_L represent the BERT-based case text description vector and legal rule knowledge representation vector, respectively. To improve the continuous representation ability of text sequence information, a Skip-RNN layer is added after the BERT pretraining module. For longer sequences, Skip-RNN adds a skip gate, which outputs the number of steps to be jumped according to the current state, thereby speeding up the training. Skip-RNN can learn forward and backward information, improve the contextual and contextual feature information extraction capabilities of text feature vectors, and solve long-distance dependencies. Specifically,

$$\begin{aligned} G_E &= SkipRNN(G_E, G_{E1}) \\ G_L &= SkipRNN(G_L, G_{L1}) \end{aligned}. \tag{2}$$

Among them, G_E and G_{E1} are the forward and backward outputs of the case description text hidden layer, respectively, and G_L and G_{L1} are the forward and backward outputs of the legal knowledge hidden layer, respectively.

3.3. Legal Knowledge Representation. To enhance the importance of legal article knowledge, attention mechanism is usually used to fuse legal article knowledge and case description. Finally, a case description that integrates legal knowledge can be obtained. The attention calculation formula of case description feature G_E and legal knowledge feature G_L is as follows:

$$f(G_E(i), G_L) = G_E(i) G_L^t, \tag{3}$$

where $G_E(i)$ represents the feature of the i-th text described by the text. Then, normalize the knowledge features of legal articles and the feature attention of each case text, and the specific formula is as follows:

$$t_k = softmax[f(G_E(k), G_L)], \tag{4}$$

where t_k represents the attention vector of the k-th text describing the knowledge features of external legal articles and the facts of the case.

Finally, the case description text features are weighted and summed based on the attention weight to obtain the case description vector G_{EL} fused with legal knowledge. The attention mechanism can focus on useful information and ignore unimportant information. The principle of this mechanism is to calculate the weight corresponding to the information. The greater the weight, the more important the information is.

$$G_{EL} = \sum t_i G_E(i). \tag{5}$$

3.4. Law Recommendation. Like previous legal recommendation methods, the prediction process is still divided into three steps: (1) describe the fusion case features and legal knowledge, (2) perform linear transformation, and (3) use softmax to achieve prediction. g_1 is the prediction result:

$$g_1 = softmax(G_{el}). \tag{6}$$

This paper uses cross-entropy loss to minimize the prediction error between the output result and the label. The cross-entropy loss formula is as follows:

$$loss = -\sum_i l_1 \log l_n + \lambda \|\theta\|^2, \tag{7}$$

where l_n is the label vector predicted by the model in this paper, l_1 is the labeled normal label vector, and l_2 is the regularization term.

4. Experimental Results and Analysis

4.1. Experimental Dataset. In the Fayan Cup dataset, an experiment was conducted on the legal article recommendation task [24]. In order to achieve a relatively balanced dataset, this paper deleted some low-frequency legal articles

in the Fayan Cup dataset and deleted some invalid samples and stop words, and finally, the training set selected in this paper is 800,000, and the validation set and test set are each 50,000. The number of law labels selected in this paper is about 1.1 million. The scale of the data set is shown in Table 1.

Since this article uses the fact description and the law part of the data, the law recommendation data includes the case fact description text and the specific law label. The specific form of the data is shown in Table 2.

Like the traditional law recommendation task, this paper uses the F_1 value as the evaluation index:

$$F_1 = \frac{2PR}{P+R}, \tag{8}$$

where P is the precision rate and R is the recall rate.

4.2. Model Construction and Experimental Parameter Settings. The model used in this paper is built with PyTorch, and the specific parameters are designed as follows: the word vector dimension is 320, the number of Skip-RNN hidden layer units is 440, the learning rate is 0.002, the dropout is set to 0.6 to prevent overfitting, and the batch size is 64.

4.3. Comparative Model and Analysis of Experimental Results. To prove the effectiveness of the method proposed in this paper, we compare and analyze the three aspects of traditional law recommendation method, law knowledge ablation, and BERT pretraining model ablation.

(a) Transformer [25]: it has achieved very good results in the field of machine translation.

(b) SVM [26]: it was first used to solve the two-classification problem in pattern recognition, and it has achieved good classification results in the fields of text classification, handwriting recognition, and image processing.

(c) TextRnn [27]: it is a model that uses RNN for text classification.

(d) FastText [28]: its biggest feature is that the model is simple, the training speed is very fast, and it is widely used in the field of text classification.

(e) BERT [29]: it has strong text representation ability and achieves good results in various tasks of deep learning.

(f) Text CNN [30]: it is a typical model using CNN for text classification.

The specific experimental results are shown in Table 3.

Experimental results show that the LawRec based on BERT significantly outperforms traditional data-driven methods in terms of the accuracy rate P, recall rate R, and F_1 values.

In order to verify the impact of the BERT pretraining model on the experimental performance, this paper uses the BERT pretraining model and the word2vec representation model to conduct a comparison experiment on the legal recommendation task in the Fayan Cup public test data set. The specific experimental results are shown in Table 4.

Table 1: Data set size.

Training set/number	Validation set/number	Test set/number
800,000	50,000	50,000

It can be seen from Table 4 that the model based on BERT characterization can significantly improve the F_1 result of legal recommendation. This is because the BERT pretraining model has strong representation ability for legal knowledge and case description text, so it improves the legal recommendation's performance.

In order to verify the impact of incorporating legal knowledge on the performance of legal recommendation, this paper conducts a comparative experiment of incorporating legal knowledge ablation, and the specific experimental results are shown in Table 5.

It can be seen from Table 5 that adding rule knowledge can greatly improve the $F1$ value of the testing set. This is because the fusion of legal article knowledge can improve the feature extraction performance of case text description to a certain extent, so that the extracted case text features are more inclined to legal article knowledge, so the performance of legal article recommendation is improved. The experimental results demonstrate the effectiveness of incorporating external knowledge of legal articles on the legal article recommendation task.

To further illustrate that the law recommendation model incorporating legal knowledge can effectively solve the problem of recommending confusing laws, here is a specific analysis based on Article 252 of the Criminal Law (crime of intentional injury) and Article 252 of the Criminal Law (crime of intentional homicide). Table 6 is a case of intentional injury that was mispredicted as intentional homicide in a model that did not incorporate legal knowledge. From the description of the case, we can see that there are a large number of keywords that distinguish the crime of intentional injury from the crime of intentional homicide, such as intentional injury, body, negligent death, cruel means, serious injury, serious disability, and other keywords in the crime of intentional injury. Therefore, we conclude that the legal recommendation model incorporating legal knowledge can accurately distinguish the crime of intentional injury and the crime of intentional homicide. This example shows to a certain extent that the legal recommendation model incorporating legal knowledge can effectively solve the problem of confusing legal recommendations.

To more intuitively illustrate the process of legal recommendation, an example analysis of fraud crime is given, as shown in Tables 6 and 7.

Based on the combination of keywords (e.g., "public and private property" and "large amount of money") and the attention mechanism, the attention of fraud crimes can be increased. This paper combines legal knowledge and case description text to achieve targeted feature extraction, thereby achieving accurate legal recommendation.

Table 2: Case description legal data form.

Description of the facts: "After the trial, it was found that at about 20:00 on June 22, 2020, the defendant Zheng Lily, together with Wang and Liu (2 persons were sentenced), drove a red van to the ×× county ×× township × village ×× expressway four-standard project department. There were 60 anchorages on the ×× construction site. During the escape, the project manager Shao found out that Zhang and Zeng got out of the car and threatened Shao, Zhang injured Shao, and the defendant Zhen did not get out of the car or threaten the victim during the process. The last three people drove away from the scene. After identification, the value of the stolen items was 4562 yuan. The above facts, the defendant Liu has no objection during the trial, and there is the confession of the defendant Sun in the public security organs, the testimony of the witnesses Ali, Lily, Wang, Perter, and others, and the appraisal report of the assets involved in the case, criminal judgment, and the evidence of the defendant Liu arrival at the case and his household registration information are sufficient to confirm."

Table 3: Comparative experimental results.

Data set	Model	P	R	F_1	Test set	Model	P	R	F_1
Test	Transformer	0.77	0.76	0.76	Test	Transformer	0.75	0.74	0.74
	SVM	0.84	0.83	0.83		SVM	0.85	0.84	0.84
	TextRnn	0.83	0.82	0.82		TextRnn	0.81	0.80	0.80
	TextRnn	0.81	0.80	0.80		TextRnn	0.82	0.81	0.81
	FastText	0.85	0.84	0.84		FastText	0.85	0.83	0.83
	BERT	0.82	0.80	0.81		BERT	0.82	0.80	0.81
	Text CNN	0.85	0.84	0.84		Text CNN	0.86	0.85	0.85
	LawRec	0.92	0.91	0.91		LawRec	0.93	0.90	0.90

Table 4: Comparison experiment between BERT model and traditional representation model.

Data	Model	F_1
Test set	Traditional model	0.82
Test set	BERT model	0.91

Table 5: Comparative experimental results of external legal knowledge ablation.

Data	Model	F_1
Test set	Models that incorporate legal knowledge	0.92
Test set	Models that do not incorporate legal knowledge	0.80

Table 6: Cases of intentional injury.

Description of the facts: "The XX city procuratorate charged that on the afternoon of July 20, 2020, the defendant, Zhang, learned from his daughter, Zhang, that the victim, Liu, wanted to trouble Liu. Later, Zhang and Liu talked on the phone many times, and the two scolded each other on the phone and agreed to meet at the west bridge in XX town, XX city. At about 12:00 on the same day, Zhang drove Liu and Dan to the west bridge, after which Zhang fought with the victims Liu, Peter, and Lily. During the tussle, Wang took out a crowbar from the trunk of his car and used the crowbar to injure Lily's right thumb and Liu's head and body. It was identified that Lily's injury was a second-level serious injury, and the injury suffered by Peter was minor."
Intentional injury crime: whoever intentionally injures another person's body shall be sentenced to fixed-term imprisonment of not more than three years, criminal detention or public surveillance. Who intentionally murders shall be sentenced to life imprisonment, death, or fixed-term imprisonment of not less than 20 years? If the circumstances are relatively minor, it shall be sentenced to fixed-term imprisonment of not less than 2 years but not more than 20 years.
Intentional homicide: who intentionally murders shall be sentenced to life imprisonment, death, or fixed-term imprisonment of not less than 20 years. If the circumstances are relatively minor, it shall be sentenced to fixed-term imprisonment of not less than 2 years but not more than 20 years.

Table 7: Case analysis on the crime of fraud.

Description of the facts: "The public prosecution alleges that from April 2015 to March 2017, the defendant Ju fabricated the facts of handling work, in the name of the cost of handling the work, successively defrauded Li of RMB 800,000, Peter of USD 35,000, Yang of USD 12,000, Yu of USD 24,000, and Ju of USD 37,000; fraudulently obtained USD 240,000 from Zhang in the name of the cost of handling work, purchasing a house, and treating illnesses by fabricating facts such as working, purchasing a house, and being ill. Defendant Peter also tried to defraud Liu of USD 22,000 by fabricating the fact of handling work and in the name of the cost of handling work."
Fraud crime: refers to the act of defrauding a large amount of public and private property by using fictitious facts or concealing the truth for the purpose of illegal ownership.

5. Conclusion

The traditional information retrieval system based on keyword search for laws and regulations is not suitable for ordinary people without professional legal knowledge. Therefore, it is necessary to propose a legal recommendation framework to help them extract professional legal vocabulary from complex case processes. This paper proposed a law recommendation framework, called LawRec, based on BERT and Skip-RNN models, which intends to integrate the knowledge of legal provisions with the case description and uses the BERT model to learn the case description text and legal knowledge, respectively. At last, laws and regulations for cases can be recommended. Experiment results show that the proposed LawRec can achieve better performance than state-of-the-art methods. The accuracy of LawRec is 92%, which is 12% higher than that of the model that does not incorporate legal knowledge.

Data Availability

The labeled datasets used to support the findings of this study are available from the corresponding author upon request.

Conflicts of Interest

No potential conflicts of interest was reported by the authors.

References

[1] B. L. Sturm, M. Iglesias, O. Ben-Tal, M. Miron, and E. Gómez, "Artificial intelligence and music: open questions of copyright law and engineering praxis," in *Arts*vol. 8, no. 3, p. 115, MDPI, 2019, September.

[2] L. B. Solum, "Legal personhood for artificial intelligences," in *Machine Ethics and Robot Ethics*, pp. 415–471, Routledge, 2020.

[3] M. Veale, "A critical take on the policy recommendations of the EU high-level expert group on artificial intelligence," *European Journal of Risk Regulation*, vol. 11, no. 1, pp. 1–10, 2020.

[4] L. Longo, R. Goebel, F. Lecue, P. Kieseberg, and A. Holzinger, "Explainable artificial intelligence: concepts, applications, research challenges and visions," in *International Cross-Domain Conference for Machine Learning and Knowledge Extraction*, pp. 1–16, Springer, Cham, 2020, August.

[5] W. Tan, P. Huang, X. Li, G. Ren, Y. Chen, and J. Yang, "Analysis of segmentation of lung parenchyma based on deep learning methods," *Journal of X-Ray Science and Technology*, vol. 29, no. 6, pp. 945–959, 2021.

[6] S. Huang and A. Liu, "A novel baseline data based verifiable trust evaluation scheme for smart network systems," *IEEE Transactions on Network Science and Engineering*, p. 6539, 2020.

[7] G. KantShankhdhar, V. K Singh, M. Darbari, D. Yagyasen, and P. Shukla, "Legal semantic web-a recommendation system," *International Journal of Applied Information Systems (IJAIS)*, vol. 7, no. 3, pp. 21–27, 2014.

[8] Y. Zhang, Y. Zhao, and Y. Zhou, "User-centered cooperative-communication strategy for 5G Internet of vehicles," *IEEE Internet of Things Journal*, vol. 9, no. 15, pp. 13486–13497, 2022.

[9] C. Xiao, H. Zhong, Z. Guo et al., *CAIL2018: A Large-Scale Legal Dataset for Judgment Prediction*, Cambridge university, London, 2018.

[10] D. M. Katz, I. Bommarito, J. Michael, and J. Blackman, *A General Approach for Predicting the Behavior of the Supreme Court of the United States*, 2016.

[11] B. Luo, Y. Feng, J. Xu, X. Zhang, and D. Zhao, "Learning to predict charges for criminal cases with legal basis," in *Proceedings of the 2017 Conference on Empirical Methods in Natural Language Processing*, pp. 2727–2736, Copenhagen, Denmark, 2017.

[12] X. Jiang, H. Ye, Z. Luo, W. Chao, and W. Ma, "Interpretable rationale augmented charge prediction system," in *Proceedings of the 27th International Conference on Computational Linguistics: System Demonstrations*, pp. 146–151, Santa Fe, New Mexico, August 2018.

[13] H. Ye, X. Jiang, Z. Luo, and W. Chao, "Interpretable charge predictions for criminal cases: learning to generate court views from fact descriptions," in *Proceedings of the 2018 Conference of the North American Chapter of the Association for Computational Linguistics: Human Language Technologies (NAACLHLT)*, pp. 1854–1864, New Orleans, Louisiana, June 2018.

[14] U. Shardanand and P. Maes, "Social information filtering: algorithms for automating word of mouth," in *proceedings of the 1995 international conference of Human-Computer Interaction (CHI)*, pp. 210–217, Denver, Colorado, July 1995.

[15] W. C. Hill, L. Stead, M. Rosenstein, and G. W. Furnas, "Recommending and evaluating choices in a virtual community of use," in *proceedings of the 1995 international conference of Human-Computer Interaction (CHI)*, pp. 194–201, New York, May -7 1995.

[16] D. Goldberg, D. N. Nichols, and B. M. Oki, "Using collaborative filtering to weave an information tapestry," *Communications of the ACM*, vol. 35, no. 12, pp. 61–70, 1992.

[17] P. Resnick, N. lacovou, M. Suchak, P. Bergstrom, and J. Riedl, "GroupLens: an open architecture for collaborative filtering of netnews," in *proceedings of the 1994 ACM conference on Computer Supported Cooperative Work*, pp. 175–186, North Carolina USA, October 1994.

[18] B. Sarwar, G. Karypis, J. Konstan, and J. Riedl, *Item-Based Collaborative Filtering Recommendation Algorithms*, University of Minnesota, Minneapolis, 2001.

[19] S. Chollampatt, K. Taghipour, and H. T. Ng, *Neural Network Translation Models for Grammatical Error Correction*, National University, Singapore, 2016.

[20] R. Socher, J. Pennington, E. Huang, A. Ng, and C. Manning, "Semi-supervised recursive autoencoders for predicting sentiment distributions," in *Proceedings of the 2011 International Conference on Empirical Methods in Natural Language*, pp. 151–161, Edinburgh, Scotland, UK, July 2011.

[21] Y. Kim, "Convolutional neural networks for sentence classification," in *Proceedings of the 2014 Conference on Empirical Methods in Natural Language Processing (EMNLP)*, pp. 1746–1751, Doha, Qatar, October 2014.

[22] G. Zhao, H. Shi, and J. Wang, "A grey BP neural network-based model for prediction of court decision service rate," *Computational Intelligence and Neuroscience*, p. 2022, 2022.

[23] H. Xu and B. Hu, "Legal text recognition using LSTM-CRF deep learning model," *Computational Intelligence and Neuroscience*, p. 2022, 2022.

[24] S. Zhong and W. Zhang, "Legal supervision mechanism of recommendation algorithm based on intelligent data recognition," *Wireless Communications and Mobile Computing*, vol. 28, p. 23254, 2022.

[25] S. Gerke, T. Minssen, and G. Cohen, "Ethical and legal challenges of artificial intelligence-driven healthcare," in *Artificial Intelligence in Healthcare*, pp. 295–336, Academic Press, 2020.

[26] Z. Huang, C. Low, M. Teng et al., "Context-aware legal citation recommendation using deep learning," in *Proceedings of the Eighteenth International Conference on Artificial Intelligence and Law*, pp. 79–88, 2021, June.

[27] W. Tan, X. Li, S. Xu, Y. Chen, and J. Yang, "Segmentation of lung airways based on deep learning methods," *IET Image Processing*, vol. 16, no. 5, pp. 1444–1456, 2022.

[28] P. Yang, N. Xiong, and J. Ren, "Data security and privacy protection for cloud storage: a survey," *IEEE Access*, vol. 8, pp. 131723–131740, 2020.

[29] R. Wan and N. Xiong, "An energy-efficient sleep scheduling mechanism with similarity measure for wireless sensor networks," *Human-centric Computing and Information Sciences*, vol. 8, no. 1, pp. 18–22, 2018.

[30] A. Deeks, "The judicial demand for explainable artificial intelligence," *Columbia Law Review*, vol. 119, no. 7, pp. 1829–1850, 2019.

Hindawi
Computational Intelligence and Neuroscience
Volume 2022, Article ID 5207178, 9 pages
https://doi.org/10.1155/2022/5207178

Research Article

MRI-Based Medical Image Recognition: Identification and Diagnosis of LDH

Shuai Wang[1], **Zhengwei Jiang**[1], **Hualin Yang**[1], **Xiangrong Li**[1] and **Zhicheng Yang**[2]

[1]*College of Mechanical and Electrical Engineering, Qingdao University of Science and Technology, Qingdao 266061, China*
[2]*Department of Radiology, Qilu Hospital (Qingdao), Cheeloo College of Medicine, Shandong University, Qingdao, China*

Correspondence should be addressed to Zhicheng Yang; 201320145@mail.sdu.edu.cn

Received 23 July 2022; Accepted 23 August 2022; Published 9 September 2022

Academic Editor: Yaxiang Fan

Copyright © 2022 Shuai Wang et al. This is an open access article distributed under the Creative Commons Attribution License, which permits unrestricted use, distribution, and reproduction in any medium, provided the original work is properly cited.

To realize the automatic symptom recognition and classification of MR images and improve the accuracy and efficiency of the diagnosis of lumbar intervertebral disc herniation (LDH), a method for lumbar intervertebral disc recognition and disease classification is proposed in this paper. The method mainly includes three steps: preprocessing, target segmentation, and symptom classification. Preprocessing is performed by noise reduction and interference removal methods for blurred images. The contour poles are used to determine the four points of the tail vertebra in order to reduce the wrong segmentation of the tail vertebra. A classification method based on five judgment indicators is proposed, which effectively improves the stability of disease diagnosis. The example verifies that the algorithm can accurately complete the target segmentation and the accuracy of symptom classification reaches the standard of professional doctors, which proves that the method has good robustness.

1. Introduction

Lumbar disc herniation (LDH) is a very common disease of the lumbar spine, with the main causes being degenerative changes and injuries of the lumbar disc [1]. The diagnosis process of lumbar disc herniation include initial diagnosis and confirmation, and the whole process is cumbersome and time-consuming, and it is difficult to guarantee the real-time application and accuracy for diagnosis with the huge number of patients and the uneven levels of doctors. The efficiency and accuracy of the initial diagnosis have become the bottleneck problem in the diagnosis of LDH. Therefore, the algorithm proposed in this paper for lumbar disc recognition and disease classification could be achieved by three steps including preprocessing, target segmentation and recognition, and symptom classification. With this method, the accurate identification, classification, and diagnosis for LDH are realized to assist doctors.

Target segmentation and recognition is a key step in processing patient image data analysis, which helps in the next step of symptom diagnosis and treatment plan [2–4]. Classical medical image segmentation techniques can be classified as threshold-based segmentation [5], edge or boundary-based segmentation [6], region-based segmentation [7, 8], active contour model-based techniques [9, 10], and neural network-based segmentation [11–15]. To increase the standardization and normality of the diagnosis, the severity of the disease is classified by some scholars. Current classification systems are based on imaging and pathomorphism [16–21], and LDH is classified as bulge, protrusion, and extrusion according to the degree of prominence of the injury. In addition, there are non-ruptured, ruptured, and sequestered types based on surgical pathomorphism. Wiltse et al. described the size of the lesion which can be assessed by normal, mild, moderate, moderately severe, and severe based on the size and location of lesions in the lumbar or thoracic spine [22]. Milette studied the imaging and pathological presentation of lumbar disc herniation and the size of the disc and the location of the herniation to standardize the nomenclature of their types

[23]. Mysliwiec et al. of Michigan State University proposed a simple, objective classification method that expresses the location distribution of herniated discs longitudinally and laterally, respectively, taking into account both the size of the herniated disc and its location in local anatomical conditions [24]. Kaliya-Perumal et al. used the Michigan State University (MSU) lumbar disc herniation (LDH) classification to classify lumbar disc herniations and determined the reliability of this classification system among orthopedic residents at the institute [25]. In 2020, Gupta et al. determined that the cross-sectional area provided a more reliable measurement modality for DiskLDHS compared to linear measurements of anterior and posterior lengths, so the cross-sectional area and its characterization of LDH is superior in its characterization [26]. On the other hand, Hao et al. established new grading and classification criteria for LDH, which combined the patient's clinical manifestations and imageology for LDH which can enable accurate assessment [17]. Divi et al. classified the morphology of disc herniation according to the type, size, and location of the herniated annoyance to determine the predictive factors for surgical intervention of LDH [27]. However, several of the above methods still lack the mode of automatic image recognition followed by automatic classification and diagnosis to give the initial diagnosis and lack the management process from image recognition to classification and diagnosis, which leads to the design of algorithms for each part without considering the application of other parts of the process and thus cannot be effectively applied in practice. In this paper, the features of vertebrae and intervertebral discs including contours based on the improved segmentation and recognition algorithms are extracted, and we also propose five symptom recognition indicators to be applied to the LDH images after automatic recognition and obtain an effective algorithm that can generate the initial diagnosis report. The method optimizes the combination between the steps and achieves better results even for blurred images.

T2-weighted images are used in this paper, and the algorithm model is written and implemented by Python3.0 combined with OpenCV library. The whole diagnostic process is shown in Figure 1.

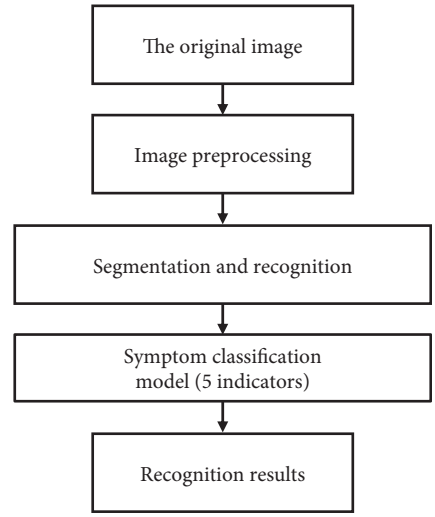

Figure 1: Flow chart of LDH diagnosis.

2. Image Preprocessing

MRI images contain vertebrae, intervertebral discs, spinal canal, muscles, nerves, and other tissues, and accurate recognition for vertebrae and intervertebral discs is the first step for successful diagnosis. Therefore, preprocessing of images to remove noise and interference is essential for better quality segmentation of vertebrae and discs afterwards.

(1) The gray-level open operation was performed on some original images shown in Figure 1(a) on account of the bright noise existing in the right side of the vertebrae. Elliptical structures with a size of 3×3 were selected, and the effect that the noise obviously darkened after filtering is shown in Figure 2(b).

(2) Gamma transform was performed for overall brightness improvement in order to solve the difficulty of the separation between the low grayscale values target and low-light level of the background of the MRI images. The basic formula of gamma transform is

$$s = cr^{\gamma}. \tag{1}$$

In the formula, s is the output of gray level, r is the input of gray level, and the offset c is set to zero.

For Figure 2(b), the gamma transformation was performed by choosing $\gamma = 0.5$ and $c = 1$, and the results are shown in Figure 2(c).

(3) Fuzzy transformation of Figure 2(c), whose results are shown in Figure 2(d), shows the gray value near the middle is separated, increasing the contrast of the image; in some areas, there is an over "exposure" phenomenon, but it did not affect the subsequent binarization process.

(4) Finally, the equalizeHist function in the openCV library is used for histogram equalization, and Figure 2(e) shows the processing results.

3. Segmentation and Recognition of the Vertebrae

Since relative location relationship between the intervertebral discs and vertebrae was the key for LDH diagnosis, the boundary information of each intervertebral disc and vertebra should be extracted separately with the segmentation and recognition of intervertebral discs and vertebrae separately.

3.1. Initial Treatment of Vertebrae. In this paper, the multithresholding method and a grayscale threshold binarization method is used to achieve the segmentation of vertebrae [28, 29].

3.1.1. Initial Treatment of Vertebrae. For blurred images, the contrast of the image is enhanced through the preliminary

(a) (b) (c) (d) (e)

Figure 2: (a) Original image. (b) Image after open operation. (c) Image after gamma transformation. (d) Effect of blurring transformation. (e) Effect of histogram equalization.

processing of grayscale image binarization. The common methods of grayscale threshold binarization include basic global thresholding, the Otsu method, and multithresholding, and the effect is shown in Figure 3 by applying the above three methods to Figure 2(e).

As the result, the segmentation effect of the multithresholding process was better than others. The process of multithresholding is as follows: first, the grayscale histogram of the image was drawn after image preprocessing, and there were two troughs shown by the red and blue arrows in Figure 4 near the grayscale values of 80 and 200. The grayscale value of the second trough was exactly the threshold required for target binarization, while another threshold is obtained by a large number of experiments around 105. For example, the best segmentation results are achieved when 105 and 205 are chosen as thresholds for the MRI of Figure 2(a).

In order to avoid the recognition error caused by the vertebral adhesions, corrosion was used for disconnecting the adhesion region and the same size structural element for the expansion. The interference of adhesions between vertebrae was effectively removed as Figure 5 before and after corrosion.

3.1.2. Screening of Vertebral Contours. The vertebral contours fixed and containing some unique features such as area features, shape features, and so on were screened based on the features. Through statistical analysis of 356 samples obtained from the hospital, the approximate parameter range of the vertebral contour is determined, which is used as a condition to screen the contour.

(1) *Screening of Contours Based on Area Features*

The target contours from the binary image were screened based on the contour area limited from 3000 pixels to 6000 pixels. Then most of the contours such as more than 6000 pixels and less than 3000 pixels were eliminated, and the screening results are shown in Figure 6(a).

(2) *Screening of Contours Based on Shape Features*

The shape feature was more efficient for nontarget contours eliminated with similar size when compared with that of the area feature. As shown in the Figure 6(a), the vertebrae as the target area were similar to a rectangle, while the shape of the nontarget contours was irregular. Through the statistical analysis, the condition with shape features was determined when contour rectangle aspect ratio was set between 0.6 and 1.4.

(3) *Contour Length Was Set Less Than 400*

As an effect after screening, as shown in Figure 6(b), nontarget contours were separated out and eliminated.

3.1.3. Positioning of the Vertebrae. The vertebrae recognized completely need to be positioned as the boundary for determining whether the disc is herniated or not, and since the caudal vertebrae with heeling condition are different from the common lumbar vertebrae, different positioning methods were required.

The characteristic that the ordinary vertebrae were positioned positively while the caudal vertebrae showed an overall inclination, and the best-fitting straight line of the contour is found, and the slope of the straight line from 0.1 to 1 is determined as the range for determining the caudal vertebrae. All the pixel points of each vertebra were acquired with OpenCV, and the coordinate point farthest from the four corners of the picture was found as the target corner point. The caudal vertebrae are tilted in MRI images, so the contour poles were used to determine four points, i.e., the highest, lowest, rightmost, and leftmost points as contour angle points. Each straight line through the vertebrae in Figure 7(a) is the best-fitting straight line, where the blue line is the tail vertebrae fitting straight line.

The results after localization of all vertebrae are shown in Figure 7(b). The locations marked by yellow circles are contour corner points (yellow rectangular boxes are rectangular enclosing boxes), and the pink line segments are the normal demarcation lines of the intervertebral discs.

3.2. Segmentation and Recognition of Intervertebral Discs. Compared to vertebrae, intervertebral discs were segmented better with global thresholding and the separation of the discs from the background which was achieved when pixel points with gray values above 50 are transformed to black by 356 images counted.

(a) (b) (c)

Figure 3: (a) Basic global threshold processing. (b) Otsu method. (c) Multithreshold processing.

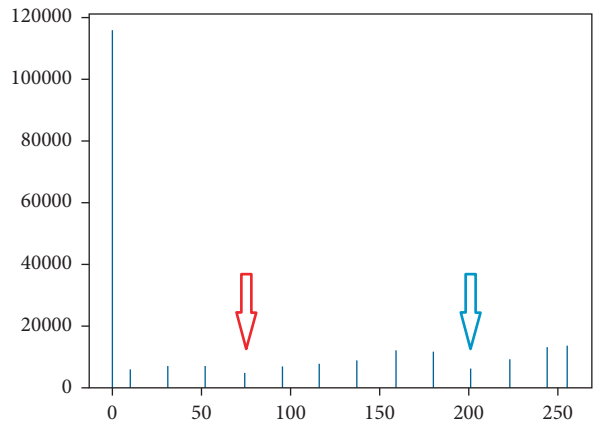

Figure 4: Gray distribution.

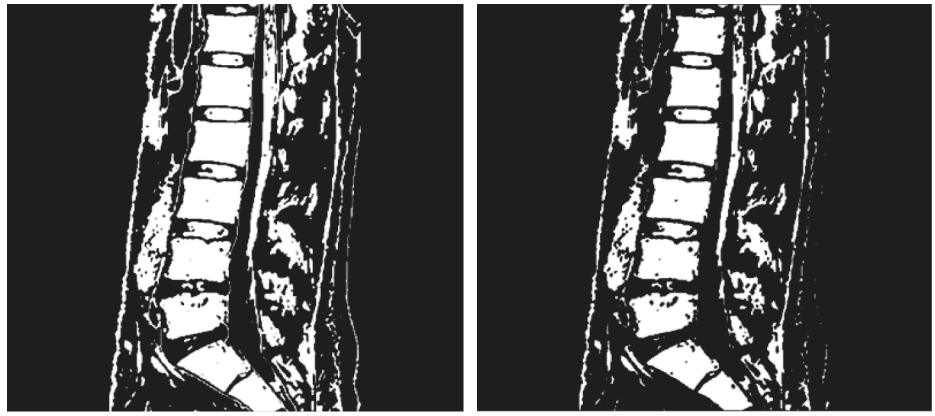

Figure 5: The effect of corrosion operation.

First, the best segmentation results shown in Figure 8(a) were achieved with elliptical structure elements of size 2×2. Then, some nontarget contours, whose area was less than 100 and more than 2000, were removed by the small area removal method. Second, the incidental spine and interspinous ligament on the right side were removed with the rectangular aspect ratio greater than 0.8. Finally, the open operation was performed. The screening effect is shown in Figure 8(b).

4. Initial Diagnosis of Disc Herniation

Preliminary diagnosis can be made after the vertebrae and discs are positioned separately. Following indicators were used for the diagnosis.

4.1. Diagnosis with Protrusion Distance. With the demarcation line acquired in Section 3.1.3, each recognized disc herniation contour was divided into protrusion part and

(a) (b)

Figure 6: (a) Small area removal method. (b) Screening results.

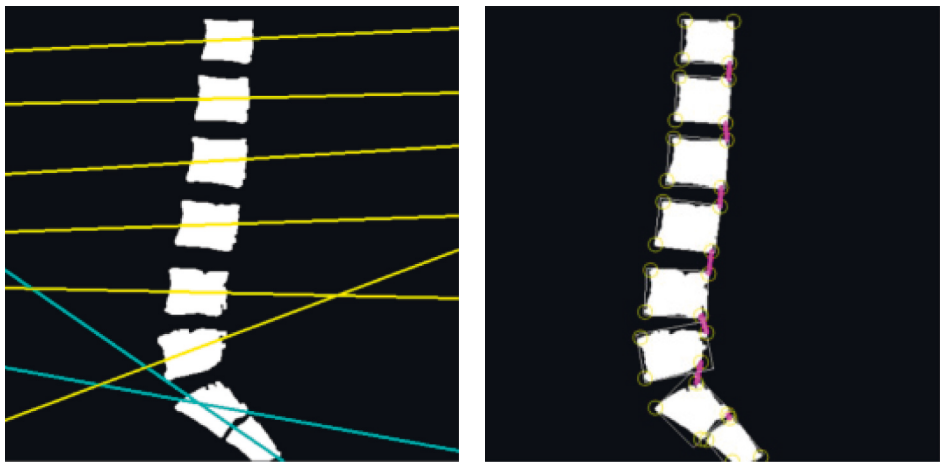

(a) (b)

Figure 7: (a) Optimal fitting line. (b) Optimal fitting line.

(a) (b)

Figure 8: (a) Morphological manipulation. (b) Disc contour.

normal part. As shown in Figure 9, the area on the right was the protrusion part. If the protrusion part is absent or tiny, protrusion had not yet appeared; otherwise, the farthest distance from the point in the area of disc herniation part to the demarcation line was the protrusion distance of this disc for judging the type of disease.

Figure 9: A profile of a disc herniation.

4.2. Diagnosis with the Average Gray Scale. If the area of a disc in MRI was low grayscale, severe degeneration appeared to diagnose the herniation for this disc. For example, 20 was selected as the threshold value of herniation and the average grayscale calculated for each disc in Figure 10(b) is as follows:

[27.06, 50.83, 55.44, 49.95, 47.41, 24.02, 19.42, 24.56].

The results indicate that the severe degeneration appeared on the seventh intervertebral disc with a mean gray level of 19.42.

4.3. Diagnosis with Spinal Canal Recognization. In some cases of extrusion type, the image of spinal canal was disrupted in MRI because of the interruption from the material within the disc moving into the spinal canal. So the presence or absence of disruption in the image of spinal canal acted as an indicator for herniation disc recognition.

The image with binarization was shown as Figure 10(a). Since the vertebrae were close to the spinal canal, an appropriate range was set according to the average X coordinate of the far right of the vertebrae. The spinal canal was identified if the X coordinate of the far left of each contour was within the setting range. The contour in the blue box in Figure 10(b) was the identified spinal canal which is same as the real spinal canal in shape and size.

5. Experimental Results

A preliminary diagnosis can be made by the identification and localization of vertebrae and discs, but this diagnosis is not uniform criteria and not suitable for automatic computerized diagnosis. Therefore, the disease conditions should be classified and the criteria for discriminating each category should be stipulated.

5.1. Indicator Selection. Due to a single index such as protrusion distance, as a basis for judgment can easily lead to misclassification, multiple contour features are considered comprehensively and multiple indexes are used to achieve typing of intervertebral disc disease. In this paper, five judgment indexes based on two-dimensional images were proposed with previous research results including protrusion distance, protrusion area, protrusion length ratio, protrusion area ratio, and average grayness.

(1) Protrusion distance: The farthest distance from the protrusion part to the dividing line AB, as shown in Figure 11

(2) Protrusion area: Protrusion area of part of the outline

(3) Protrusion length ratio: The ratio of the protrusion distance to the length of the entire intervertebral disc in the X-axis direction (CD)

(4) Protrusion area ratio: The ratio of the protrusion part to the whole disc area

(5) Average gray level: Average gray level of the intervertebral disc.

Forty MR images of different patients were selected, and each intervertebral disc in the image was a herniated lesion and a type of herniated lesion to form a labeled MRI. As shown in Table 1, the five indicators of MRI are quantitatively measured, and each indicator accounts for 0.25 of the proportion of symptom assessment. The results show that the five indicators are positively correlated with the three types of protrusion, and each outstanding type of diagnosis satisfies the condition of at least the size of the range containing any three indicators. If in any four of the five indicators, the size of each of the two indicators is within the range of the two types of protrusions;that is, one type of protrusion includes only one indicator, and the other two types of protrusions each include conditions for two different indicators, and it is impossible to determine which type they belong to, and then in accordance with the order of protrusion distance, protrusion area, protrusion length ratio, protrusion area ratio, and average gray scale, the protrusion type corresponding to the top-ranked indicator is the final diagnosed protrusion symptom. According to the above-mentioned conditions, 5 index data are used for disease classification.

5.2. Method Validation and Analysis

5.2.1. Overall Algorithm Validation. The final operation result of the automatic diagnosis is shown in Figure 12. Compared with the results of manual diagnosis, the 7th disc has low brightness and serious degeneration is occurred. The 3rd, 4th, 5th, 6th, and 7th discs in the figure have different degrees of protrusion, and the spinal canal in the images remained continuous and no serious lumbar disc herniation occurred, and the type of herniation of each disc was basically correct, which proved that the algorithm could

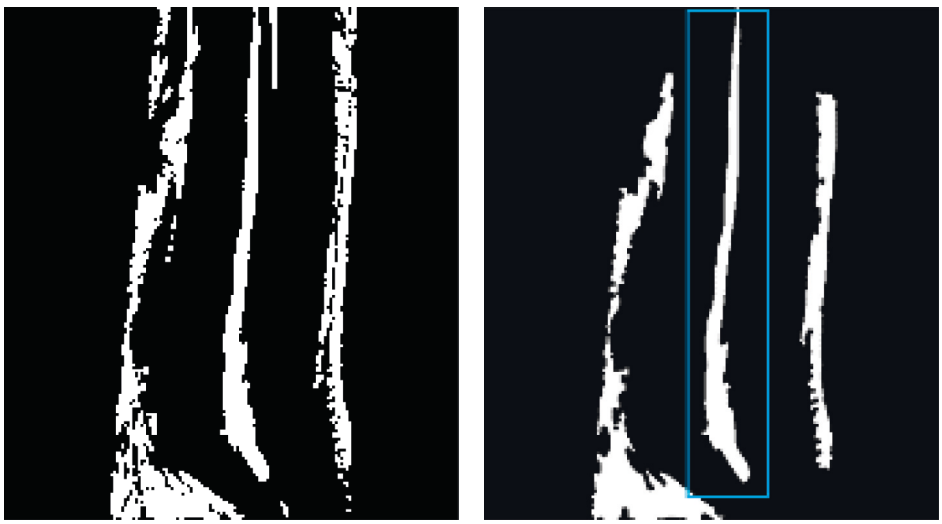

(a) (b)

Figure 10: Spinal canal identification. (a) Binarized image. (b) Disc contour.

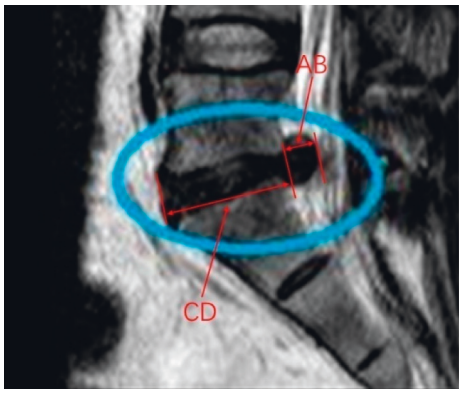

Figure 11: Classification indicators.

Table 1: Mark the prominent type of indicator data statistics.

	Highlight distance (mm)	Highlighted area (mm^2)	Prominent length ratio	Prominent area ratio	Average gray level
Bulge	1~5	10~100	0.01~0.1	0.01~0.1	>35
Protrusion	5~10	100~200	0.1~0.2	0.1~0.2	15~35
Extrusion	>10	>200	>0.2	>0.2	<15

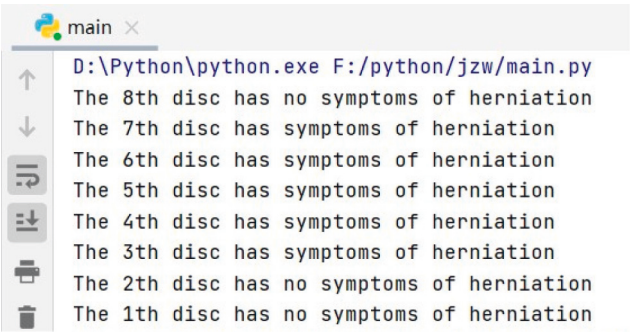

Figure 12: The result of running the program.

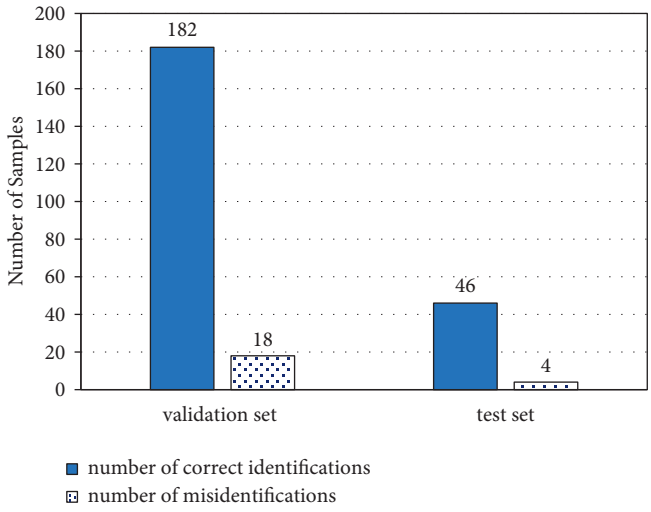

Figure 13: Classification result.

accomplish the research objectives better. The running result is combined with the numerical value of the degree of lumbar disc herniation and showed whether the spinal canal is continuous as the final report result.

5.2.2. Verify the Accuracy of Target Segmentation. Twenty MR images were randomly selected as the initial data set, and those were preprocessed, and then segmented and identified to obtain the vertebral bone and disc contours, and the statistical results were as follows.

There were a total of 169 vertebrae in the 20 images (removing the top incomplete vertebrae). The algorithm could accurately identify 163 vertebrae, with a recognition success rate of 96.45%. There were a total of 153 intervertebral discs (not counting the tail bones) in the 20 images, and 149 discs were identified, with a recognition success rate of 97.38%. It proves that the image processing algorithm in this paper has certain reliability.

5.2.3. Validation of Five Indicators. 200 images in the validation set and 50 images in the test set were used to verify the accuracy of the model. As shown in Figure 13, in the validation set, the number of correct detections is 182, the number of false detections is 18, and the classification accuracy rate is 91%; in the verification set, the number of correct detections is 46, the number of false detections is 4, and the classification accuracy is 92%, which proves that the classification model can meet the requirements of this research and realizes the classification and diagnosis of diseases.

6. Conclusion

In this paper, a new method for LDH automatic diagnosis was proposed to realize the full automation of MR images recognition and diagnosis and provides conclusion of initial diagnosis and forms the basis of final diagnosis for patients and doctors. This method also has a better recognition effect on fuzzy images that are difficult to judge. In addition, five indicators proposed are strongly available for different LDH auxiliary diagnosis. The experimental results show that the classification accuracy of the validation set and test set reached 91% and 92%, respectively, which proves the effectiveness of the method and can provide auxiliary diagnosis for doctors. In the future, we will add other indicators to be used in symptom classification and automatically eliminate unclear MR images to reduce the workload of medical workers.

Data Availability

The data that support the findings of this study are available upon request from the corresponding author.

Conflicts of Interest

The authors declare that there are no conflicts of interest regarding the publication of this paper.

Acknowledgments

This research was funded by the National Natural Science, China (No. 52101401).

References

[1] J. Zhou and M. Yang, "Bone region segmentation in medical images based on improved watershed algorithm," *Computational Intelligence and Neuroscience*, vol. 2022, Article ID 3975853, 1 page, 2022.

[2] C. Li, C. Kao, J. C. Gore, and Z. Ding, "Minimization of region-scalable fitting energy for image segmentation," *IEEE Transactions on Image Processing*, vol. 17, no. 10, pp. 1940–1949, 2008.

[3] N. Paragios and R. Deriche, "Geodesic active regions and level set methods for supervised texture segmentation [J]," *International Journal of Computer Vision*, vol. 46, no. 3, pp. 223–247, 2002.

[4] T. Editor, *Insight into Images: Principles and Practice for Segmentation, Registration, and Image Analysis*, AK Peters Ltd, Natick, MA, USA, 2020.

[5] M. Angulakshmi and M. Deepa, "A review on deep learning architecture and methods for MRI brain tumour segmentation," *Current Medical Imaging Formerly Current Medical Imaging Reviews*, vol. 17, no. 6, pp. 695–706, 2021.

[6] J. Park, S. Park, and W. Cho, "Medical image segmentation using level set method with a new hybrid speed function based on boundary and region segmentation," *IEICE - Transactions on Info and Systems*, vol. E95.D, no. 8, pp. 2133–2141, 2012.

[7] G. Geweid and M. A. Abdallah, "A novel approach for breast cancer investigation and recognition using M-level set-based optimization functions," *IEEE Access*, vol. 12, pp. 6343–136357, 2019.

[8] H. Wu, J. Liu, G. Chen et al., "Automatic semicircular canal segmentation of CT volumes using improved 3D U-net with attention mechanism," *Computational Intelligence and Neuroscience*, vol. 2021, Article ID 9654059, 13 pages, 2021.

[9] A. Afifi, T. Nakaguchi, N. Tsumura, and Y. Miyake, "A model optimization approach to the automatic segmentation of medical images," *IEICE - Transactions on Info and Systems*, vol. E93-D, no. 4, pp. 882–890, 2010.

[10] L. Zhang, J. Liu, F. Shang, G. Li, J. Zhao, and Y. Zhang, "Robust segmentation method for noisy images based on an

unsupervised denosing filter," *Tsinghua Science and Technology*, vol. 26, no. 5, pp. 736–748, 2021.

[11] G. Wang, W. Li, M. A. Zuluaga et al., "Interactive medical image segmentation using deep learning with image-specific fine tuning," *IEEE Transactions on Medical Imaging*, vol. 37, no. 7, pp. 1562–1573, 2018.

[12] M. H. Hesamian, W. Jia, X. He, and P. Kennedy, "Deep learning techniques for medical image segmentation: achievements and challenges," *Journal of Digital Imaging*, vol. 32, pp. 583–596, 2019.

[13] C. Chen, C. Qin, H. Qiu et al., "Deep learning for cardiac image segmentation: a review," *Frontiers in Cardiovascular Medicine*, vol. 7, no. 25, July 2020.

[14] H. Seo, M. B. Khuzani, V. Vasudevan et al., "Machine learning techniques for biomedical image segmentation: an overview of technical aspects and introduction to state-of-art applications," *Medical Physics*, vol. 47, no. 5, pp. 148–167, 2019.

[15] S. A. Taghanaki, K. Abhishek, J. P. Cohen, J. Cohen-Adad, and G. Hamarneh, "Deep semantic segmentation of natural and medical images: a review," *Artificial Intelligence Review*, vol. 54, no. 1, pp. 173–178, 2020.

[16] R. Imaad-ur, R. S. Hamid, W. Akhtar, M. S. Shamim, R. Naqi, and H. I. Siddiq, "Observer variation in MRI evaluation of patients with suspected lumbar disc herniation and nerve root compression: comparison of neuroradiologist and neurosurgeon's interpretations," *Journal of the Pakistan Medical Association*, vol. 62, no. 8, pp. 826–829, 2012.

[17] D. J. Hao, K. Duan, T. J. Liu, J. J. Liu, and W. T. Wang, "Development and clinical application of grading and classification criteria of lumbar disc herniation [J]," vol. 96, pp. 1–7, Medicine, 2017.

[18] F. David, A. L. Williams, E. J. Dohring, F. R. Murtagh, S. L. G. Rothman, and G. K. Sze, "Lumbar disc nomenclature: version 2.0: recommendations of the combined task forces of the North American Spine Society," *The American Society of Spine Radiology, and the American Society of Neuroradiology*, vol. 9, pp. 1448–1465, 2014.

[19] A. P. Janardhana, R. S. Rajagopal, S. Rao, and A. Kamath, "Correlation between clinical features and magnetic resonance imaging findings in lumbar disc prolapse," *Indian Journal of Orthopaedics*, vol. 44, no. 3, pp. 263–269, July 2010.

[20] N. L. Marinelli, V. M. Haughton, and P. A. Anderson, "T2 relaxation times correlated with stage of lumbar intervertebral disk degeneration and patient Age," *American Journal of Neuroradiology*, vol. 31, no. 7, pp. 1278–1282, 2010.

[21] J. S. Ross, "Babel 2.0," *Radiology*, vol. 1, 2010.

[22] L. L. Wiltse, P. E. Berger, and J. A. Mcculloch, "A system for reporting the size and location of lesions in the spine," *Spine*, vol. 22, no. 13, pp. 1534–1537, 1997.

[23] P. C. Milette, "Classification, diagnostic imaging, and imaging characterization of a lumbar herniated disk," *Radiologic Clinics of North America*, vol. 38, no. 6, pp. 1267–1292, 2000.

[24] L. W. Mysliwiec, J. Cholewicki, M. D. Winkelpleck, and G. P. Eis, "MSU Classification for herniated lumbar discs on MRI: toward developing objective criteria for surgical selection," *European Spine Journal*, vol. 19, no. 7, pp. 1087–1093, 2010.

[25] A. K. Kaliya-Perumal, C. A. Luo, Y. C. Yeh, Y. F. Tsai, M. J. W. Chen, and T. T. Tsai, "Reliability of the Michigan state university (MSU) classification of lumbar disc herniation [j]," *Acta Ortopedica Brasileira*, vol. 26, no. 6, pp. 411–414, 2018.

[26] A. Gupta, S. Upadhyaya, C. M. Yeung et al., "Disk area is a more reliable measurement than anteroposterior length in the assessment of lumbar disk herniations: a validation study," *Clinical Spine Surgery: A Spine Publication*, vol. 33, no. 8, pp. 381–385, 2020.

[27] S. N. Divi, H. S. Makanji, C. K. Kepler et al., "Does the size or location of lumbar disc herniation predict the need for operative treatment," *Global Spine Journal*, vol. 12, 2020.

[28] F. Bao, D. Wang, H. Zhao, and B. Xu, "Application of adaptive threshold image segmentation algorithm in orthopedic CT imaging," *Journal of Medical Imaging and Health Informatics*, vol. 9, no. 8, pp. 1736–1740, 2019.

[29] D. Zhao, D. Xin, G. Sun, and T. Lu, "Study on adaptive threshold segmentation method based on brightness," *Przeglad Elektrotechniczny*, vol. 88, no. 9B, pp. 150–152, 2020.

Hindawi
Computational Intelligence and Neuroscience
Volume 2022, Article ID 1265340, 9 pages
https://doi.org/10.1155/2022/1265340

Research Article

Individual Online Learning Behavior Analysis Based on Hadoop

Ning Xiang

School of Journalism and Communication, Hunan Mass Media Vocational and Technical College, Changsha 410100, China

Correspondence should be addressed to Ning Xiang; 9120130138@jxust.edu.cn

Received 24 July 2022; Accepted 13 August 2022; Published 8 September 2022

Academic Editor: Yaxiang Fan

Copyright © 2022 Ning Xiang. This is an open access article distributed under the Creative Commons Attribution License, which permits unrestricted use, distribution, and reproduction in any medium, provided the original work is properly cited.

The online individual behavior analysis is an important means for mining user interests. The user retweeting behavior prediction is typical problem for online individual behavior analysis. In order to make online learning behavior prediction method more suitable for the application of large-scale datasets, the improved condensed K nearest neighbor (ICKNN) method is proposed in this paper. Inspired by the idea of compressing samples in the condensed nearest neighbor (CNN) algorithm, this proposed method has adopted the Hadoop platform to parallelize the traditional CNN algorithm. For the traditional CNN method, as the value of K increases, the compression ratio decreases and so as the efficiency. The proposed ICKNN method can parallelize the traditional CNN method under the Hadoop framework to enhance efficiency. The proposed ICKNN method in this paper is validated by actual Twitter retweeting dataset. It can be seen that the proposed method in this paper has a higher compression rate than the traditional CNN algorithm. In terms of accuracy, the classification accuracy of the proposed ICKNN method has decreased compared with the traditional KNN method. However, the time consumed by the ICKNN method has significantly reduced compared with the traditional KNN method and CNN method, which can greatly improve the efficiency.

1. Introduction

As the access of Internet technology is not limited by time and space, and as it has the feature of low cost and fast information transmission, it has quickly become one part of people's daily lives. Due to the rapid development of the Internet, social network has become ubiquitous. The massive data volume on social media can provide fundamental support for data-related researches, and valuable information can be achieved from data mining, which can be useful for individuals, enterprises, and governments [1, 2]. Under the condition of massive data volume, traditional methods relying only on a single computer have the disadvantages of low efficiency and significant processing latency. Therefore, traditional data mining methods need to be improved to meet the requirements under the condition of big data.

Under current conditions, an important profit model for social networks is to predict the user interests for content promotion according to users' behavior. In order to mine users' interests, it is feasible for online predicting the online learning behavior of individual users. Online learning behavior prediction can enable the study of the transmission mechanism, diffusion mode, and related characteristics of users' tweets, which can provide users with personalized services and enable strategic marketing. Moreover, necessary information from the public social network platform can be obtained for making strategies for the related companies [3, 4]. As a matter of fact, individual online learning behavior analysis and prediction is now a hot research topic.

For the prediction of online learning behavior, the authors in literature [5] have firstly applied the classification algorithm to the area. The content of the microblog is represented by a feature vector and with the number of 0 and 1 to indicate whether a tweet is forwarded. Herein, the retweeting prediction problem can be transformed to a corresponding pattern recognition problem. Current methods for online learning behavior prediction are mainly two folds: (1) the first aspect is to enable more effective establishment of features in the content of the microblog for classification, i.e., the feature-centric methods [6–9]. (2) The second aspect is to build a better classification model to predict whether a tweet is forward or not, i.e., the classifier-centric methods [10–13]. The following will give introductions of the online learning behavior prediction methods

according to the two types of methods mentioned above. In feature-centric methods, it is verified in literature [14] that different features may have a significant impact on the performance. In literature [15], the correlation features between users and their posts are extracted and adopted. It is proved that the correlation features can greatly improve the performance of prediction compared adopting either just user features or just features from the content of the tweets. The authors have added new features to the feature vector, for example, the interaction frequency between the current user and the upstream user, and the feature vector of the upstream user. Thus, the accuracy of online learning behavior can be improved. Similarly, the authors in literature [16] have taken consideration of hot topics and transmission characteristics when establishing the feature vector, which have also improved the accuracy of prediction.

For the classifier-centric methods, in [17], the random walk modeling is applied for the calculation of forwarding probability from the multi-dimensional feature vectors, so as to predict the online learning behavior. In literature [18], the support vector machine (SVM) classifier is adopted. In this literature, SVM is firstly adopted to train an unweighted model, from which the importance of different dimensions of the features is obtained. The importance can be adopted as the feature weights. In this paper, it is proved that blog posts with positive emotions have a greater probability of forwarding than blog posts with negative emotions. The authors in [19] have also adopted SVM for classification, where feature combination method has been applied to verify the importance of different features for online learning behavior prediction. In [20], the forwarding behavior is predicted by adopting a random forest classifier. Specifically, it has adopted the information gain method to make use of three types of features, including user-based, relationship-based, and topic-based features. As a result, the problem of imbalance samples is solved by using the oversampling technology for retweeting prediction. In literature [21], the feature-centric and classifier-centric methods are combined, and the online learning behavior is predicted through multitask learning. The authors in [22] go a step further and take the relationship between different tasks into consideration to improve the prediction accuracy.

Under the background of massive data, traditional data mining methods need to be migrated to such an environment. Hadoop is a big data ecosystem, which can provide an overall solution to large-scale data analysis [23–25]. The core components of Hadoop are the Hadoop Distributed File System (HDFS) and the MapReduce paralleled programming model. The existence of HDFS makes Hadoop capable of storage for large amounts of data in a distributed way. And the existence of MapReduce ensures that Hadoop is efficient for parallel computing. The HDFS is one of the core components of the Hadoop architecture. It can be adopted to store large files. Sometimes, if the size of the file exceeds the capacity of a single computer, HDFS can be used to store the data in a distributed manner on several computers or servers, and the files can then be processed by locating and finding through the directory tree [26–28]. The MapReduce distributed computing framework is suitable for parallel computing in a distributed environment with high availability deployment at multiple servers. It is also one of the core components of the Hadoop system. The core idea is to make use of the distributed large-scale file data in the HDFS system. By dividing the task into multiple MapReduce subtasks for parallel processing, data operations for a large-scale data volume can be reached, even at the TB or PB level [29–31]. Over all, the Hadoop framework has the following advantages: (1) it has better capacity expansion feature; (2) the cost is low, and the framework can meet the computing requirements with only several ordinary computers; (3) the application of HDFS enables the system to have high data reliability; (4) the application of MapReduce makes large-scale data processing more efficient.

In order to make online learning behavior prediction method more suitable for the application of large-scale datasets, the improved condensed K nearest neighbor (ICKNN) method is proposed in this paper, which can be adopted to solve the problem of reduced classification efficiency in the context of big data. In the proposed method, a consistent sample subset from the original sample set is firstly obtained according to a reasonable decision boundary, so as to achieving the goal of compressing sample numbers and improving classification efficiency. Generally speaking, in order to improve the compression ratio of the algorithm, that is, to improve the efficiency of the algorithm, it is necessary to reduce the k value in the algorithm, which is the number of neighbors. However, when $k = 1$, which is the smallest value, the robustness of the classification can be degraded greatly. Therefore, the value of k takes a larger value herein at the cost of a smaller compression ratio. In this paper, in order to further improve the compression ratio of the algorithm and to improve the efficiency, the traditional condensed nearest neighbor (CNN) algorithm is parallelized in the framework of Hadoop. After parallelizing the original CNN algorithm, the proposed method is verified by the actual microblog dataset. The experimental results show that the ICKNN algorithm in this paper implemented on the Hadoop platform has a better compression rate than the traditional CNN algorithm, while the prediction performance is better with a higher classification accuracy.

2. Methods

In the proposed method, after parallelizing the traditional CNN method [32], it can be implemented at the Hadoop big data framework. The results show better retweeting prediction performance with a better algorithm compression ratio, which can effectively improve the computational efficiency. In this section, the basics of the Hadoop framework is introduced at first, then the CNN method is introduced, and at last the descriptions of how to parallelize the CNN method and implement it to the Hadoop framework are introduced.

2.1. Introduction of the Hadoop Framework. Hadoop is an overall solution for processing large-scale data analysis. Traditional databases are only suitable for processing

structured data, such as query using Structured Query Language (SQL) statements, while Hadoop can process structured, semi-structured, and unstructured data from different sources and formats. It has backup in storage and can be dynamically expanded. For processing queries, the Hive statements can be adopted.

The core components of the Hadoop framework are the HDFS and the MapReduce parallel programming model. The existence of HDFS makes Hadoop capable of distributed storage of large amounts of data. The existence of MapReduce ensures that Hadoop is good at efficient parallel computing. The two core components of the Hadoop framework, HDFS and MapReduce, are introduced as follows.

The HDFS supports one-time writing and unlimited reads, and the already written cannot be modified. HDFS is one of the core components of the Hadoop architecture. It can be adopted to store large files. When the size of the stored files exceeds the capacity of a single machine, HDFS can be adopted to store the data in a distributed manner on several computers, and the stored files can be located by the directory tree. The illustrational principle of the mentioned HDFS principle is shown in Figure 1.

HDFS has the following advantages: (1) HDFS supports the storage of large files, with even TB or PB size, and can process tens of thousands of nodes at the same time. (2) The HDFS system is suitable for big data processing. The NameNode is responsible for the management of the file directory tree and the mapping information of data blocks. This can make fast location of the data block [27]. (3) The backup strategy adopted by HDFS is usually twice backup, which are stored in different DataNodes. If a data block is broken, the internal mechanism of HDFS will automatically adopt the backup data to repair it. With this type of data repairing capacity, the HDFS framework can be deployed on relatively cheaper servers. Once the data are lost or interrupted, it can be quickly retrieved.

The MapReduce is also one of the core components of the Hadoop system. It is a distributed computing framework which is suitable for deployment at a distributed environment composed with several servers with high availability. The core idea is to make use of the distributed large-scale file data in the HDFS system. By dividing the task into multiple MapReduce sub-tasks for parallel processing, data operations for a large-scale data volume can be reached, even at the TB or PB level [30]. Similar to the HDFS system, MapReduce has also adopted a master-slave architecture, where the NameNode is responsible for the coordination and control of tasks, including task initialization, assignment, and communication with DataNodes. The DataNode then is responsible for performing the Map and Reduce slicing tasks, and asking the NameNode for the required file information during the processing. The MapReduce can be divided into four stages, including data slicing, mapping stage, shuffle stage, and the combine stage. The processing flowchart of the MapReduce framework is shown in Figure 2.

The MapReduce task is processed with the following stages: (1) at the start of the task, the client sends a Job ID assignment request to the task assignment NameNode. (2) The NameNode returns the Job ID to the client, and the client copies the JAR file package, configuration policy file, and file slice information required for task execution to the job queue of the NameNode node of HDFS. (3) The NameNode schedules the tasks in the job queue, creates a map task for a single job, and assigns it to the DataNode execution node which contains the data blocks processed by the map. (4) After all tasks are executed, NameNode sets the task to "completed state," and the client queries that the NameNode state is "completed," and sends a message to inform the user.

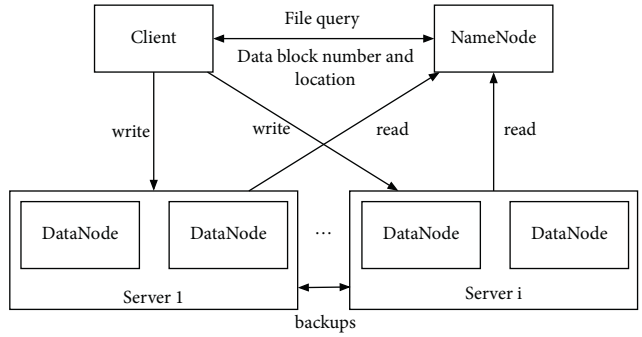

Figure 1: An illustrational principle of how the HDFS works.

MapReduce has the following advantages: (1) nodes are easy to expand. When cluster resources are insufficient, the nodes can be expanded for computing. (2) The resources are easy to coordinate and have strong fault tolerance. When a node failure causes the calculation to fail, other nonfaulty nodes can be adopted for calculation. (3) Parallel computing is adopted, which is suitable for TB or even PB-level data processing.

2.2. The CNN Algorithm. In the traditional K nearest neighbor (KNN) algorithm, each time to determine a sample's type, all samples are traversed. Therefore, the classification efficiency will decrease significantly with an increase of training samples. To solve the problem of reduced efficiency, the condensed nearest neighbor (CNN) algorithm is proposed in [32], which can effectively reduce the number of samples required for classification. In the CNN algorithm, it is believed that the closer a sample is to the decision boundary, the greater the impact it has on the classification results and vice versa. Therefore, the classification problem can be attributed to the problem of obtaining the sample points with the smallest distance from the decision boundary, and at the same time removing the sample points that are far away.

Before the description of the CNN algorithm, a classification model should be established at first. Assuming that S denotes the training set, the number of samples is N, and it should be divided into C classes, the sample set can be expressed as

$$S = \left\{S_1^{N_1}, S_2^{N_2}, \ldots, S_C^{N_C}\right\}. \quad (1)$$

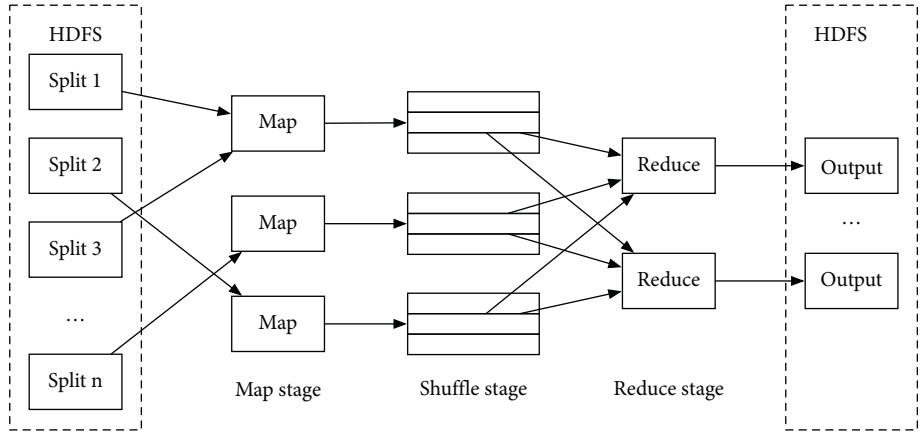

Figure 2: The processing flow of the MapReduce framework.

Among them, $S_i^{N_i}$ represents the sample set from i th class in S, and the number of sample points contained is N_i; then, the sample can be expressed as

$$S_i^{N_i} = \left\{s_i^p\right\}, i = 1, 2, ..., C, p = 1, 2, ..., N_i, \tag{2}$$

where

$$\sum_{i=1}^{C} N_C = N. \tag{3}$$

Then, the set of k nearest neighbors found can be expressed as

$$T_{knn}\left(s_i^q\right)_j = \{x_1, x_2, ..., x_k\}, \tag{4}$$

$T_{knn}(s_i^q)_j$ denotes the sample set of class in i with samples found in class j with k nearest neighbor.

For each sample, a corresponding decision influence factor U_{affect} is assigned, which is determined by the location of the samples. If the decision influence factor is large, it means that the distance between the sample point and the classification decision boundary is closer. The set of decision influence factor can be expressed as

$$U_{\text{affect}} = \left\{u_{\text{affect},1}, u_{\text{affect},2}, ..., u_{\text{affect},c}\right\}, \tag{5}$$

where $u_{\text{affect},n}$ represents the decision influencing factors of all samples in category m, and $u_{\text{affect},1}[i]$ represents the decision influencing factors of sample i within.

The flow of the CNN algorithm is shown as follows.

(1) Iterate over the number of categories C.

(2) In each type c, iterate over the samples in the sample set of $S_c^{N_c}$.

(3) Get the k nearest neighbors for the sample s_i among other types and get $T_{knn}(s_i) = \{x_1, x_2, ..., x_k\}$.

(4) The corresponding decision influence factors are added by 1.

(5) Delete the samples whose decision influence factors are less than 1 and get the consistent subset $S_{\min}^i$.

(6) Perform the normal KNN algorithm over $S_{\min}^i$ and the classification result.

In the CNN algorithm, the value of k is an important factor affecting the compression rate of the CNN algorithm. If k equals to 1, the compression rate of the algorithm is relatively high. After the compression, only the samples which are near to the boundary are remained. In this condition, the classification performance can be degraded if the number of samples has been decreased too much. If the value of k is relatively large, samples which are farther away from the boundary can be remained. In this case, the compression rate will decrease. If all samples are remained in the set, then the compression rate is 0.

2.3. The ICKNN Algorithm Implemented on Hadoop. According to the mentioned CNN algorithm, when k is not equal to 1, its algorithm compression ratio is still unsatisfactory, and when the training dataset is large, there is still a problem of low computational efficiency. In order to improve computing efficiency, a parallel computing method is designed for the CNN algorithm, here noted as IKCNN, and is implemented adopting the MapReduce framework.

It is found that the calculation of k nearest neighbors of each category is independent. As a result, the parallelized calculation can be implemented. If the sample points in the sample set can be divided into C categories, then the number of computing threads can also be set to C. With C threads computing at the same time, the speed can be accelerated significantly.

The MapReduce framework is implemented in this paper for the ICKNN algorithm. The format of data storage is <key, value>, which is key-value paired. As mentioned, it is necessary to allocate the calculation tasks to each sub-nodes and integrate the calculation results from each node to obtain the final result. In the process, Map and Reduce are processed in parallel, which can be independent and efficient. The final output is acquired by the Reduce function. According to the processing flow of by MapReduce, three jobs are formed which can be serially executed. In our paper, the three jobs are named as job A, job B, and job C. Among the jobs, job A is related to the calculation process of nearest neighbors. Job B obtains the k nearest neighbors with their corresponding influence factors based on the results of job

A. If the influence factor is bigger than zero, it is taken out and saved. Job C aggregates the previous results to form the final compressed training set. The three jobs are described as follows, respectively.

In job A, the Mapper class, Combiner class, and Reducer class are included. The functions of each class are different. The Mapper class divides the training sample set into multiple splits and assigns them to different map tasks.

The Mapper class is mainly adopted to calculate the distance between samples in the training set. Then, the Combiner class is adopted to aggregate the obtained results. Both of these two classes are run in a DataNode, which can process the data directly without the need of transmitting data, thus is more efficient. In addition, the Combiner class can also reduce the cost of data transmission from the Mapper class, which will save much time in data transmission. The Reducer class can further process the output of the Combiner class, and after summarizing these results, k global nearest neighbor samples of non-self-category class in the training set can be obtained. The process of job A is shown in Figure 3.

For the Combiner class, the input of the Combiner class is the value list corresponding to the output key of the Mapper class. The Reduce function compares the distances of sample points in the value list and then saves the k values with the smallest distances in the local k nearest neighbor set. It is worth noting that the Combiner class is essentially a Reducer class, and it runs locally. Each Combiner class has a corresponding Mapper class, so the local k nearest neighbor sample point set output by the Combiner class is only the local k nearest neighbors in the block.

For the Reducer class, the execution process of the Reducer class is basically the same as the Combiner class. The value corresponding to the output key of the Combiner class needs to be merged, so as to obtain the input to the Reducer class.

For the work of job B, a new hash table in the Mapper class is built at first, where its key and value should be set. In our implementation, the key is the ID of the samples, and the value is the number of k nearest neighbors (with other categories) of the corresponding sample ID, which is obtained from the results of job A. Here, the output format of job A is shown as follows: Category-id1 to id k. To read the file in this format, the TextInputFormat format is adopted. The input format of the map is <line number, line text>, where the line text has the mentioned format of Category-id1 to id k. The line text can be processed to $k+1$ substrings and is stored in linestr. Then for each id in linestr, the corresponding keys are obtained, which is the ID number plus 1. With the key, it is added to the hash table again. If the key corresponding to the ID cannot be obtained, then the key-value of (id, 1.0) is directly added to the hash table. The above steps have handled the input data. After the processing completed, the k nearest neighbors of all samples belonging to other categories have been stored in the hash table. After the above process, the calculation of the influence factor of each sample is completed. Then after sorting, the IDs of the samples whose influence factors are greater than or equal to 1 can be obtained. The processing flow is shown in Figure 4.

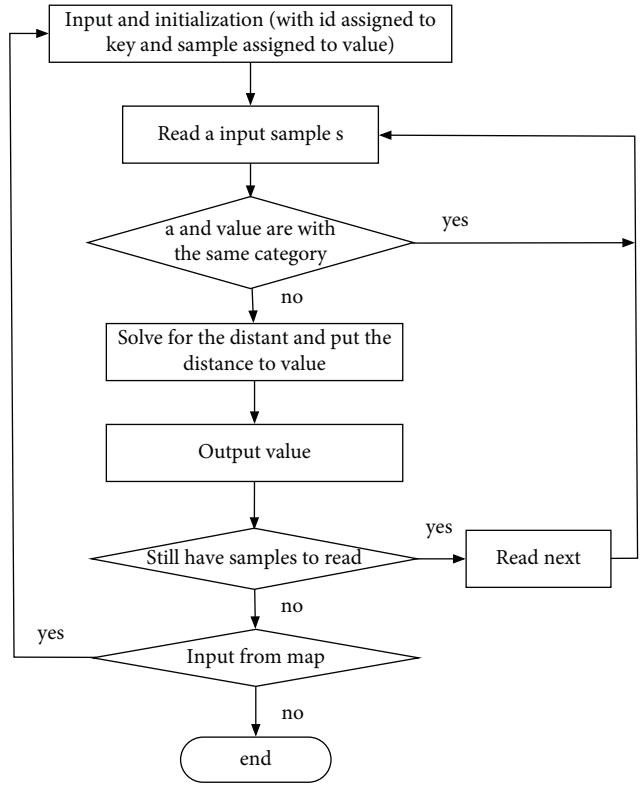

Figure 3: The flowchart of the mapper implementation in job A.

For processing flow of job C, only the Mapper class is included. The initialization is performed by adopting the results of job B as the configuration information. Then, the setup() function of the Mapper class is overloaded and the ID array based on the output of job2 is initialized. Then, the output file from job B is read, and the index array is initialized, which is adopted to store the reserved sample IDs. If the index array includes the input sample ID, it outputs directly.

3. Experimental Results

In this paper, the tweet dataset from [33] is used to evaluate the basic performance of the proposed method. Accordingly, the performance of the proposed method for online learning behavior prediction can be evaluated. In this dataset, there are 436,330 posts that can be forwarded and the attributes of the dataset are shown in Table 1. This part in the dataset can be directly adopted for predict the online learning behavior. Noting that in the dataset, there are some posts which cannot be adopted, including the commenting posts. The construction of a sample is to find out the user's following users based on the user-following relation network constructed by the user_friends table. Then based on the tweet_info table, whether the following users have retweeted the post can be found. The construction of the retweeting information is as follows: (1) build the index list of [userId, (friendsId1,. . ., friendsIdn)] on the user_friend table and the list of [userId, (tweetId1,. . ., tweetIdk)] on the tweet_info table. (2) If a retweeted post is obtained, find user A and the creation time

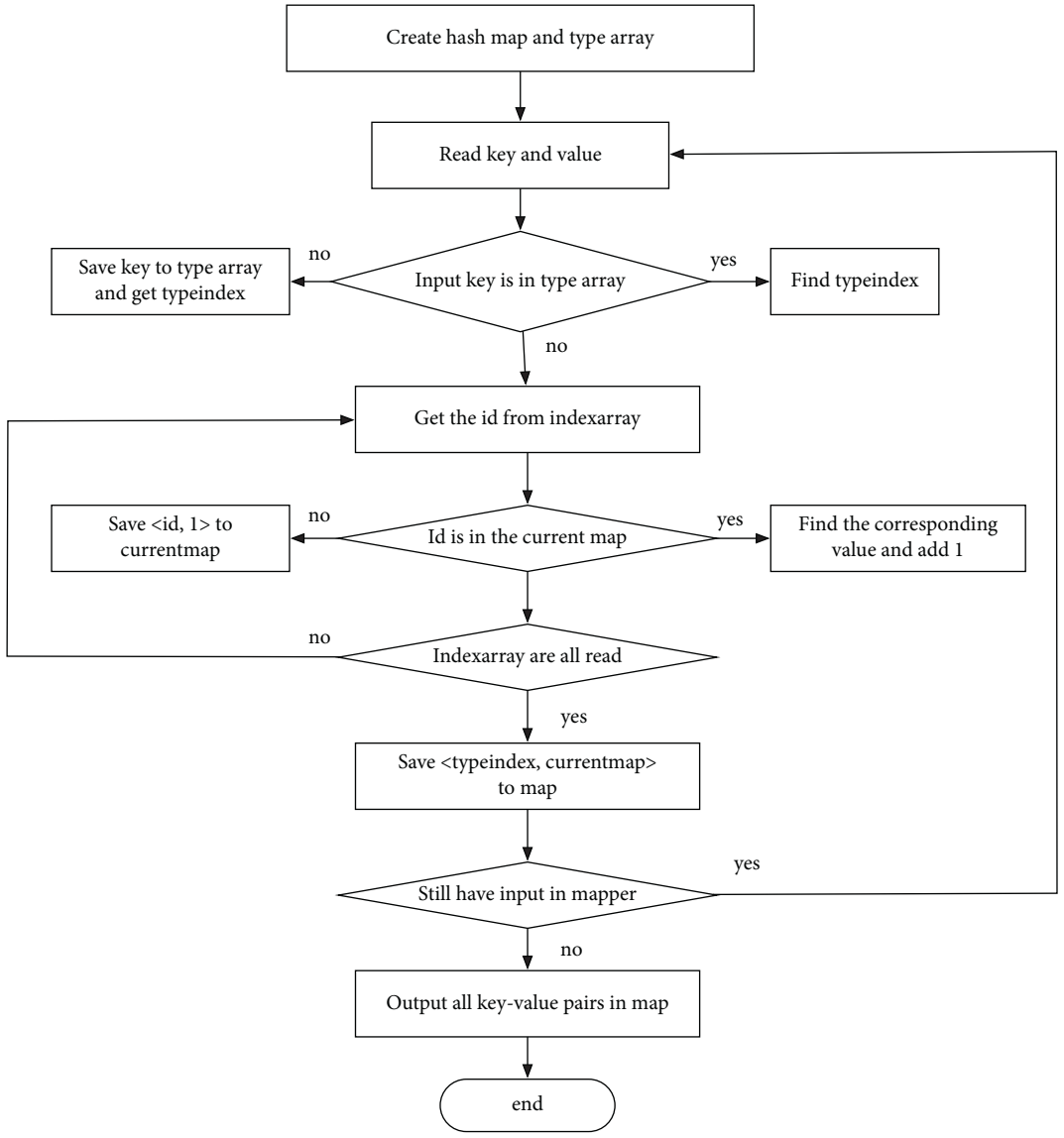

Figure 4: The flowchart of mapper class implementation in job B.

Table 1: Some attributes of the retweeting dataset.

User ID
Creation time T
Post ID
Creation time of the retweeted or un-retweeted post
User ID of the retweeted or un-retweeted post
Post content
Retweeted or un-retweeted

T of the pos. (3) According to user A in [userId, (friendsId1,. . ., friendsId*n*)], find out the corresponding follower user B. (4) According to [userId, (tweetId1,. . ., tweetId*k*)], find out all the blog post IDs of B. (5) Select the non-retweeted post corresponding according to the creation time *T*, and combine user A's own original post at time *T*; the retweeting data samples can be obtained. In addition to the above basic attributes, the number of retweets obtained from tweet_info, the user obtained from user_info, and the user attributes can also be obtained.

After obtaining the relevant data, other procedures are implemented to make the samples more applicable for processing. The data are preprocessed by missing value handling, user cleaning, etc. Then, the relevant features for classification are built. The constructed features can be divided into three categories: user-related feature group, post-related feature group, and context-based feature group. The user-related feature groups are from the perspective of users, including a series of characteristics of the users themselves. The blog-related feature groups are from the perspective of the contents of the tweets. The context-based feature group is a series of feature descriptions of the situations faced by the user.

3.1. Related Metrics of the Method. To better evaluate the proposed method in this paper, proper metrics are needed. The confusion matrix for a common binary classification problem is shown in Table 2.

Table 2: The confusion matrix for the binary classification problem.

	Label 0 (predicted)	Label 1 (predicted)
Label 0 (actual)	True positive	False negative
Label 1 (actual)	False positive	True negative

From the table, the accuracy metric can be derived. The accuracy metric represents the probability that the samples can be accurately classified. It is actually the ratio of the correctly classified samples to the total samples.

$$\text{Acc} = \frac{TP - \text{TN}}{N}. \quad (6)$$

In addition to the metric related to classification, there is also a special indicator in this paper, that is, the algorithm compression ratio. For KNN typed algorithms, the algorithm compression ratio can be expressed as

$$CR = \frac{N - N_c}{N}, \quad (7)$$

where N represents the number of samples in the original sample set and N_c represents the number of samples after compression. According to the evaluation metrics in this section, the proposed prediction method in this paper can be evaluated.

3.2. Comparisons of Different Methods. In order to verify the proposed method in this paper, experiments are carried out adopting the mentioned retweeting dataset. The proposed ICKNN method is compared with the common KNN method and the CNN method. Figure 4 and Table 3 respectively, show the compression ratio, accuracy of the KNN algorithm, and CNN algorithm when the k values are different. According to the results in Figure 5 and Table 3, it can be seen that as K increases, in general, the compression ratio decreases. The blue bar denotes the accuracy, and the yellow bar denotes the compression rate. It can also be seen that the proposed method in this paper has a higher compression ratio than that of the traditional CNN algorithm under the both conditions when $k = 1$ and $k = 2$. In addition, in terms of accuracy, under the conditions of $k = 1$ and $k = 2$, the ICKNN method proposed in this paper has a lower classification accuracy than the traditional KNN method, because in the classification process, only the nearby samples around the classification boundary are remained. However, compared with the traditional CNN algorithm, the accuracy of the ICKNN algorithm has still improved with a higher compression ratio. It can be seen from Table 3 that compared with the traditional CNN algorithm, the proposed method has improved the compression ratio by 3% and the accuracy by 52% under the condition of $k = 1$. Under the condition of $k = 2$, the compression ratio has improved by 8%, and the accuracy has improved by 14%.

Since the proposed ICKNN method in this paper can be run in parallel under the Hadoop platform, in addition to the sample compression ratio, it can still reduce the running time and improve the classification efficiency. The different

Table 3: The method comparisons of accuracy and compression rate.

	Accuracy	Compression ratio
KNN ($k = 1$)	0.754	0
KNN ($k = 2$)	0.863	0
CNN ($k = 1$)	0.712	0.418
CNN ($k = 2$)	0.732	0.397
ICKNN ($k = 1$)	0.734	0.634
ICKNN ($k = 2$)	0.836	0.427

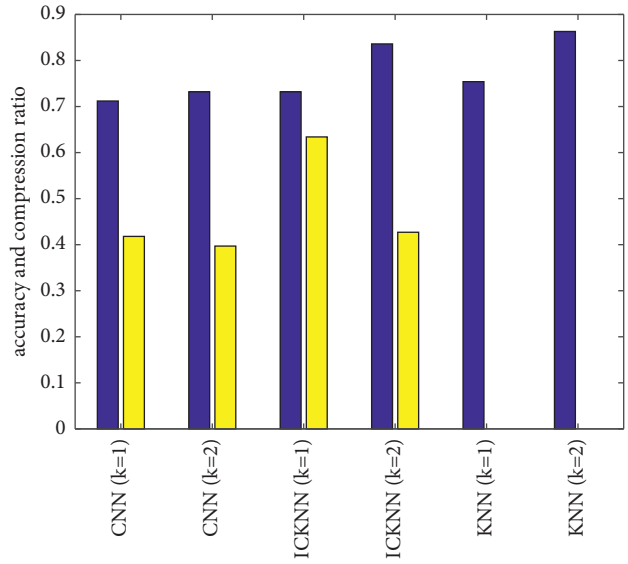

Figure 5: The different accuracy and compression rate of the proposed ICKNN, the KNN, and the CNN method.

Table 4: The method comparisons of time cost for classification.

Method	Time cost (s)	Percentage (decrease)
KNN	429	36%
CNN	420	28%
ICKNN	308	—

time costs of the different methods are shown in Table 4. The time cost of classification by the proposed ICKNN method, CNN method, and KNN method is 420s, 429s and 308s, respectively. Here, the proposed ICKNN method in this paper is run under the Hadoop platform with 4 nodes. It can be seen that compared with the traditional KNN method and CNN method, the time consumed by the ICKNN method has reduced by 36% and 28%, respectively, which can greatly improve the classification efficiency.

4. Conclusions

The online learning behavior prediction is a typical problem for online learning of individual behavior. In order to make online learning behavior prediction method more suitable for the application of large-scale datasets, the ICKNN method is proposed in this paper. The proposed method has adopted the Hadoop platform to parallelize the traditional CNN algorithm to boost classification efficiency. The

proposed ICKNN method in this paper is validated by the actual Twitter retweeting dataset. It can be seen that the proposed method in this paper has increased the compression rate by 3% and 8% than the traditional CNN algorithm under the conditions of $k = 1$ and $k = 2$, respectively. In addition, in terms of accuracy, under the conditions of $k = 1$ and $k = 2$, the classification accuracy of the proposed ICKNN method has decreased compared with the traditional KNN method. Compared with the traditional KNN method and CNN method, the time consumed by the ICKNN method has reduced by 36% and 28%, respectively, which can greatly improve the classification efficiency. The current results are acquired under the condition that the number of nodes of the Hadoop framework is four. For other number of nodes, it will be studied in our future work.

Data Availability

The datasets can be obtained from the author upon request.

Conflicts of Interest

The author declares that there are no conflicts of interest.

References

[1] C. Snijders, M. Uwe, and R. Ulf-Dietrich, "Big Data: big gaps of knowledge in the field of internet science," *International journal of internet science*, vol. 7, pp. 1–5, 2012.

[2] M. Ge, H. Bangui, and B. Buhnova, "Big data for internet of things: a survey," *Future Generation Computer Systems*, vol. 87, pp. 601–614, 2018.

[3] L. Arthur, *Big Data Marketing: Engage Your Customers More Effectively and Drive Value*, John Wiley & Sons, Hoboken, New Jersey, 2013.

[4] C. Strong, *Humanizing Big Data: Marketing at the Meeting of Data, Social Science and Consumer Insight*, Kogan Page Publishers, London, 2015.

[5] S. Petrović, M. Osborne, and V. Lavrenko, "Using paraphrases for improving first story detection in news and Twitter," in *Proceedings of the 2012 conference of the north american chapter of the association for computational linguistics: Human language technologies*, Montreal, Canada, June 2012.

[6] J. O Donovan, B. Kang, G. Meyer, T. Höllerer, and S. Adalii, "Credibility in context: an analysis of feature distributions in twitter," in *Proceedings of the 2012 International Conference on Privacy, Security, Risk and Trust and 2012 International Confernece on Social Computing*, September 2012.

[7] G. Xiang, B. Fan, L. Wang, J. Hong, and C. Rose, "Detecting offensive tweets via topical feature discovery over a large scale twitter corpus," in *Proceedings of the 21st ACM international conference on Information and knowledge management*, Maui, Hawaii, 2012.

[8] S. Wijeratne, A. Sheth, S. Bhatt et al., "Feature engineering for Twitter-based applications," *Feature Engineering for Machine Learning and Data Analytics*, pp. 359–393, CRC Press, 2018.

[9] D. Zimbra, M. Ghiassi, and S. Lee, "Brand-related Twitter sentiment analysis using feature engineering and the dynamic architecture for artificial neural networks," in *Proceedings of the 2016 49th Hawaii International Conference on System Sciences (HICSS)*, January 2016.

[10] S. Vosoughi and D. Roy, "Tweet acts: a speech act classifier for twitter," in *Proceedings of the Tenth International AAAI Conference on Web and Social Media*, Cologne, Germany, 2016.

[11] S. Agarwal and A. Sureka, "Using knn and svm based one-class classifier for detecting online radicalization on twitter," in *Proceedings of the International Conference on Distributed Computing and Internet Technology*, Springer, Cham, 2015.

[12] R. Jose and V. S. Chooralil, "Prediction of election result by enhanced sentiment analysis on twitter data using classifier ensemble Approach," in *Proceedings of the 2016 international conference on data mining and advanced computing (SAPIENCE)*, March 2016.

[13] J. Schnebly and S. Sengupta, "Random forest twitter bot classifier," in *Proceedings of the 2019 IEEE 9th Annual Computing and Communication Workshop and Conference (CCWC)*, January 2019.

[14] Z. Xu and Q. Yang, "Analyzing user retweet behavior on twitter," in *Proceedings of the 2012 IEEE/ACM International Conference on Advances in Social Networks Analysis and Mining*, August 2012.

[15] Y. Ma, "Research on reposting behavior and emotion prediction of Weibo users," Doctor Thesis, 2019.

[16] J. Chen, W. Liu, W. H. Chao, and L. H. Wang, "Microblog forwarding prediction based on hot topics," *Journal of Chinese Information Processing*, vol. 29, no. 6, 2015.

[17] H. Zhang, Q. Zhao, H. Liu, J. He, X. Du, and H. Chen, "Predicting retweet behavior in weibo social network," in *Proceedings of the International Conference on Web Information Systems Engineering*, Springer, Berlin, Heidelberg, 2012.

[18] Y. Zhang, R. Lu, and Q. Yang, "Predicting retweeting in microblogs," *Journal of Chinese Information Processing*, vol. 26, no. 4, 2012.

[19] Y. Z, B. Shao, G. Bian, and D. Song, "Prediction of retweeting behavior for imbalanced dataset in microblogs," *Journal of Computer Applications*, vol. 35, p. 1959, 2015.

[20] J. Yang and C. Scott, "Predicting the speed, scale, and range of information diffusion in twitter," in *Proceedings of the Fourth international AAAI conference on weblogs and social media*, Washington, DC USA, 2010.

[21] W. Galuba, K. Aberer, D. Chakraborty, Z. Despotovic, and W. Kellerer, "Outtweeting the {Twitterers—predicting} information cascades in microblogs," in *Proceedings of the 3rd Workshop on Online Social Networks*, WOSN, Boston, MA, USA, 2010.

[22] J. Yang and J. Leskovec, "Modeling information diffusion in implicit networks," in *Proceedings of the 2010 IEEE International Conference on Data Mining*, December 2010.

[23] T. White, *Hadoop: The Definitive Guide*, O'Reilly Media, Inc, Sebastopol, California, 2012.

[24] A. O'Driscoll, J. Daugelaite, and R. D. Sleator, "Big data, Hadoop and cloud computing in genomics," *Journal of Biomedical Informatics*, vol. 46, pp. 774–781, 2013.

[25] I. Polato, R. Re, A. Goldman, and F. Kon, "A comprehensive view of Hadoop research—a systematic literature review," *Journal of Network and Computer Applications*, vol. 46, pp. 1–25, 2014.

[26] A. K. Karun and K. Chitharanjan, "A review on hadoop—HDFS infrastructure extensions," in *Proceedings of the 2013 IEEE conference on information & communication technologies*, April 2013.

[27] D. Borthakur, "HDFS architecture document on hadoop wiki," 2010, https://hadoop.apache.org/common/docs/r020.

[28] X. Liu, J. Han, Y. Zhong, C. Han, and X. He, "Implementing WebGIS on Hadoop: a case study of improving small file I/O

performance on HDFS," in *Proceedings of the 2009 IEEE International Conference on Cluster Computing and Workshops*, August 2009.

[29] H. Karloff, S. Suri, and S. Vassilvitskii, "A model of computation for mapreduce," in *Proceedings of the twenty-first annual ACM-SIAM symposium on Discrete Algorithms*, Society for Industrial and Applied Mathematics, Austin, TX, USA, 2010.

[30] J. Dean and S. Ghemawat, "MapReduce: a flexible data processing tool," *Communications of the ACM*, vol. 53, pp. 72–77, 2010.

[31] D. Jiang, L. Shi, and S. Wu, "The performance of mapreduce: an in-depth study," *Proceedings of the VLDB Endowment*, vol. 3, no. 1-2, pp. 472–483, 2010.

[32] C.-H. Chou, B. H. Kuo, and F. Chang, "The generalized condensed nearest neighbor rule as a data reduction method," in *Proceedings of the 18th international conference on pattern recognition (ICPR'06)*, 2006.

[33] W. H. L, "Approach for retweet prediction based on user interest," Doctor Thesis, 2017.

Hindawi
Computational Intelligence and Neuroscience
Volume 2022, Article ID 2343181, 11 pages
https://doi.org/10.1155/2022/2343181

Research Article

Risk Constraints in the Context of Big Data and Optimization of a Virtuous Interaction Mechanism for Insurance Management Based on Distorted Risk Metrics

Yuanyuan Zhao

Jiumaojiu International Holdings Limited, Guangzhou 510000, China

Correspondence should be addressed to Yuanyuan Zhao; zhaoyy21@mails.tsinghua.edu.cn

Received 19 July 2022; Accepted 18 August 2022; Published 6 September 2022

Academic Editor: Yaxiang Fan

Copyright © 2022 Yuanyuan Zhao. This is an open access article distributed under the Creative Commons Attribution License, which permits unrestricted use, distribution, and reproduction in any medium, provided the original work is properly cited.

A relevant definition of big data technology has been released by relevant research institutes in China. Big data technology is defined as follows: big data technology is a digitally important productivity factor in the network era; big data technology is based on network technology, statistical technology, and mathematical technology; big data technology, as a carrier of network technology, should be integrated with various industries and technologies other than contemporary ones in order to achieve better informatization and industrialization. In the context of the new crown epidemic in 2020, China's big data technology continues to grow steadily, with a total value of 39.2 trillion yuan, accounting for 38.6% of GDP. This paper investigates the risk constraint in the context of big data and optimizes the benign interaction mechanism of insurance management based on distorted risk metrics in this context. The current situation of insurance risk is investigated through a profound discussion of theories in this paper and through research methods such as distortion risk metrics and SQL Server database management. It is found that the overall situation of insurance industry development in the era of digital economy is not optimistic and so on. And relevant suggestions are made in the conclusion.

1. Introduction

A relevant definition of big data technology has been issued by relevant research institutes in China. It defines big data technology as follows: big data technology is an important productivity factor of digitalization in the network era; big data technology is based on network technology, statistical technology, and mathematical technology; big data technology, as a carrier of network technology, should be integrated with various industries and technologies other than contemporary ones in order to achieve better informatization and industrialization. Accelerate industrial progress and urbanization and transform the economic structure [1]. In the context of the new crown epidemic in 2020, China's big data technology continues to grow steadily, with a scale of 39.2 trillion yuan, accounting for 38.6 percent of GDP [2]. In China, a new five-year plan and long-term plan were released at the same time, and big data technology was included in the development of China's plan to promote the comprehensive development of big data, the development of big data into all walks of life, the process of digitalization in China, and the building of digital power. China's Central Political Bureau has conducted a number of comprehensive big data studies in the process of China's big data. Digital technology has been integrated into the development of all aspects of life in China, and the general secretary has repeatedly emphasized the importance of using big data technology to transform traditional industries all the way through [3]. Insurance has natural digital attributes, and big data and technology empowerment can optimize the insurance business process and inject new momentum into the industry's development; at the same time, the insurance industry's big data transformation can provide strong support for China's digital economic system. Exploring the new characteristics of insurance industry development in the era of big data, finding new opportunities for insurance

industry development in the big data economic system, and studying the dilemmas and challenges facing the development of big data transformation of insurance industry are important in this context for promoting the industrialization of big data economy, accelerating insurance industry reform, and hastening the deep integration of insurance industry [4].

2. Research Background

Domestic research on the development of the insurance industry in the context of big data is as follows: Roland et al. point out that the competition in the insurance industry in the era of big data is based on the degree of understanding of customers and product supply [5]. Serkan and Fatih analyze that the big data transformation of insurance enterprises is mainly reflected in informatization, automation, and scenarioization and point out five issues that are concerned about the big data transformation of insurance enterprises [6]. Asier et al. examine how big data technology drives the changes in consumers' demand for insurance from the perspective of people's consumption behavior and give suggestions on how insurance companies can respond to these changes [7]. Li et al. provide three digital transformation realization paths for insurance companies, including optimizing customer experience, optimizing operation models, and innovating business models, from the essential characteristics of big data technology [8]. By introducing the development experiences of InsurTech enterprises in the United States, Singapore, Germany, and other regions, Lukas et al. put forward the suggestions of government support, social participation, and collaboration among all parties to promote the development of insurance enterprises and InsurTech in China [9].

From the perspective of foreign scholars, Hisako et al. suggest that the entry threshold of the insurance industry will be lowered in the era of big data, more competitive entities will come in, and insurance companies must reposition the value of customers and their core competitiveness in order to occupy a place in the competition [10]. Reimund and Oleksandr believe that insurance companies are providers of risk services and should make full use of the Internet to provide efficient and convenient solutions and risk management for their customers [11]. Sidorova et al. believe that the development of the Internet has influenced the direction of business in the insurance industry [12]. De Lei et al. state that making underwriting and claims online through the Internet can greatly improve efficiency and enhance user experience compared to the traditional model [13]. Muhamat et al. point out that one of the major impacts of the development of online insurance on the insurance industry is that it is more convenient for customers to compare prices, and insurance companies should not see this change as a profit threat but should think about how to change their business model [14].

According to the above analysis, scholars both at home and abroad have focused on the positive aspects of the development of the insurance industry in the context of big data and have suggested that insurance companies should transform in line with the trend, but there has been little research on the specific situation of the development of the insurance industry in China under the macro environment of big data and the dilemma brought about by the emergence of new technologies. However, only by studying the characteristics of digital technologies and analyzing them in combination with the development status and policy background of China's insurance industry today can we better discover how digital technologies should be integrated into various aspects of the insurance industry and give full play to their advantages, as well as digging deeper into the challenges that may be faced to help China's insurance industry ride the wave of change in the new era.

3. Materials and Methods

3.1. Basic Theory

3.1.1. Big Data Collection and Management. This paper's research content is a discussion of the network literacy education system for college students under the big data media management mode. As a result, a big data collection and management system is required, which is used today not only to store a large amount of data and form a large number of data storage network systems but also to analyze and process data extremely quickly [15]. Big data management systems are all about analyzing and processing a wide variety of data with a reasonable use of media such as computers and networks. It is becoming more and more popular in all aspects of life with fast and convenient digital information transmission and processing, bringing a great degree of information convenience to people's future learning life, updating people's traditional view of data management, providing a more innovative and convenient way to store and process complicated data, and greatly improving people's work efficiency [16]. The big data management system has four main features such as large storage volume, rapid information processing, real and effective data results, and a wide variety of data types, as shown in Figure 1.

3.1.2. Insurance Risk Management in the Era of Big Data. The traditional insurance industry has problems such as single type of insurance products, human sea mode marketing, and long underwriting and claims process due to the limitation of technology. Through the introduction of the above 4 major insurance technology technologies, we can see that the drive of insurance technology in the digital economy era has a great impact on various aspects of the insurance industry such as product development, insurance marketing, insurance underwriting, and insurance claims [16]. The impact of different technologies on different aspects of the insurance industry varies, and a new concept and model of the insurance industry has been formed. The application of insurance technology in the digital economy can improve the existing business pain points and expand the social influence and social value of the insurance industry [17], as shown in Figure 2:

Product Development Link. The traditional insurance companies are more production-oriented and product-

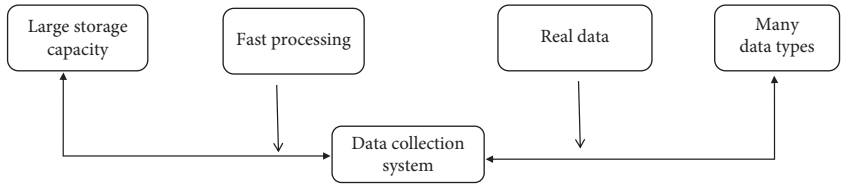

Figure 1: Characteristics of the data collection system.

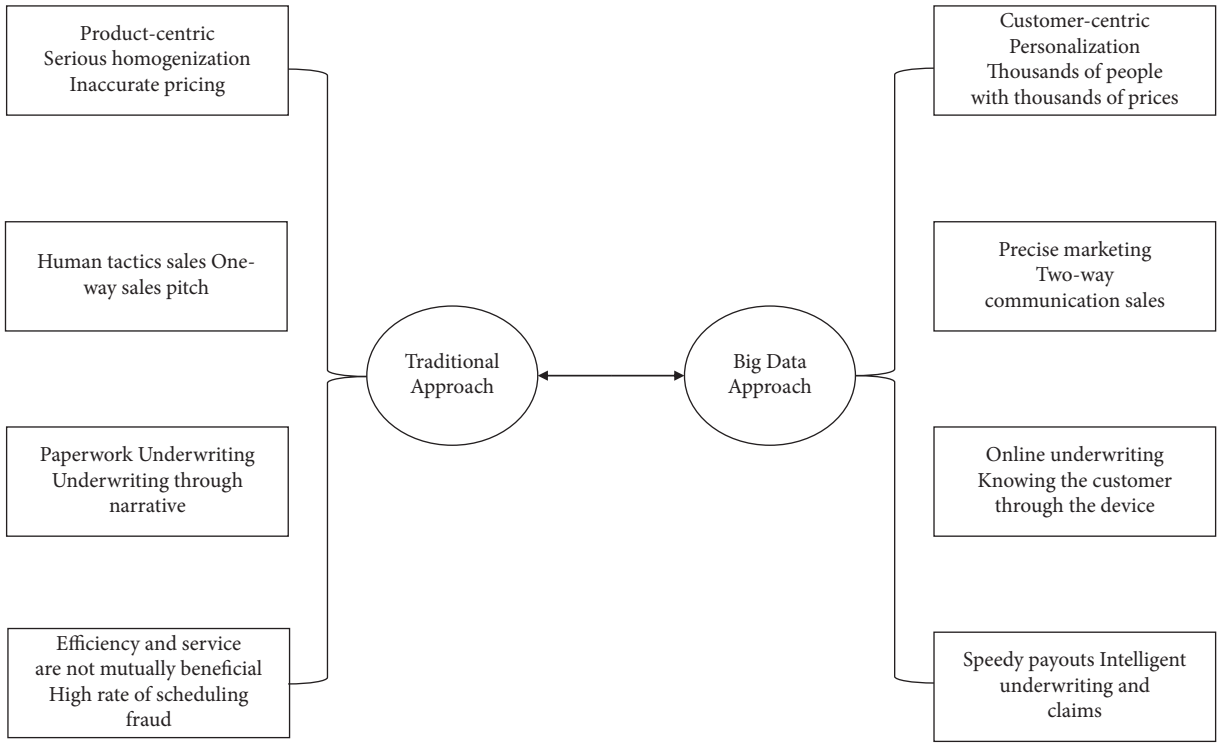

Figure 2: Comparison of the traditional insurance industry and the insurance industry's business development link in the era of big data.

centered in product design, which has problems such as serious product homogenization, small coverage, and inaccurate pricing. The emergence of digital technology will break through the limitations of traditional insurance product design in two aspects: product innovation design and accurate pricing [18]. (1) Product innovation design. From the supply side of the insurance market, although thousands of insurance products have been launched by major insurance companies, only a few dozen of them can really open the market and be favored by consumers. One of the major reasons why insurance companies have difficulty in designing insurance products that are marketable is that the insurance products they design do not have enough depth of integration with customers' daily lives, making it difficult for customers to realize the need for a particular insurance business. For example, Zhong An Insurance uses big data and cloud computing technology to provide return shipping insurance for online shoppers. Ping An General Insurance relies on AI technology to promote the development of pet liability insurance. The "insurance" uses AI and big data technology to provide risk protection for O2O, sharing economy, sports, and other scenarios, increasing the fit between customers' lives and insurance products and insurance needs, and opening up a blue ocean that the traditional insurance market has never ventured into. (2) Accurate pricing of products. Due to information asymmetry, traditional insurance products are unable to make independent risk assessment and product pricing based on customers' personal information, and the emergence and application of digital technology will fundamentally solve this problem. Artificial intelligence devices such as smart watches, smart bracelets, and smart homes enable insurance companies to gain a deeper understanding of consumers' daily behavioral activities. Big data technology categorizes and analyzes the collected data on customers' personal preferences, behavioral habits, and health conditions and can provide differentiated insurance pricing for customers. For example, the "Step Insurance" critical illness insurance jointly launched by Zhong An Insurance and Xiaomi Sports and Le Dynamics APP is based on the number of steps taken by different users as

the basis for premium pricing and implements a dynamic pricing mechanism to motivate customers to exercise while reducing the payout rate of insurance companies, achieving a win-win situation. Digital technology has helped insurance companies shift from "product-centric" to "customer-centric."

Product Marketing. (1) Achieving precision marketing. Traditional marketing in the insurance industry is mainly sales-oriented, where agents or marketers market existing insurance products to customers, and the information channels for customers to understand insurance products are mainly through the introduction of marketers or their own conscious or unconscious exposure to television and Internet publicity, and if they do not spend some time to understand the relevant information, it is difficult for customers to find insurance products that perfectly match their own desires. The use of big data and artificial intelligence has fundamentally altered the traditional marketing model and enabled product personalization [19]. (2) Broadening the contact channels between customers and insurance. The traditional insurance marketing in the insurance industry is more of one-way marketing, which is carried out by marketers or agents who take the initiative to visit or adopt telemarketing, so that customers do not have enough daily contact with insurance and have limited channels to understand insurance products, which makes some customers have doubts when taking out insurance and disputes to be easily caused when claiming. The development of artificial intelligence technology allows insurance sales to be conducted in the form of online interaction, answering customers' doubts and providing corresponding insurance products, turning insurance sales from one-way sales to two-way communication. The outbreak of the new crown epidemic in 2020 accelerated the migration of insurance sales from offline to online, and the Internet interaction will also promote customers' understanding of insurance products.

Insurance Underwriting Link. (1) The policy takes effect after the customer signs with an agent or marketer. After entering the digital economy, insurance companies are more likely to use digital platforms to conduct insurance exhibition business and customers to take out insurance policies online. With the further application of artificial intelligence in the underwriting process, facial recognition can be done only by cell phones to speed up the identification of identity information, calculate scientific and reasonable premiums through the information entered and the relevant data of existing customers in the background, and make the decision of underwriting or not, which is significantly better than the traditional offline cumbersome paperwork mode of insurance underwriting. (2) Reduce the risk of adverse selection. The complexity of underwriting insurance products lies in the need to understand the basic information of customers and minimize the risk of adverse selection, so as to control the payout rate and achieve sustainable operation.

Insurance Claims Processing. (1) Realize efficient underwriting. Insurance underwriting work is an important part of insurance risk control, and meticulous and perfect underwriting work can greatly shorten the claims cycle and reduce the claims complaint rate and also reduce the occurrence of fraudulent insurance incidents and lower the payout rate. The traditional insurance underwriting process in the insurance industry mainly relies on the level of customer integrity and the experience of underwriters, and the tedious and lengthy process of fixing damages and claims reduces the customer experience. For this reason, many insurance companies have made no underwriting, no medical examination, and a very fast claims payment standard for some insurance products, which has led to some fraudulent insurance incidents. Efficiency and service have always been the pain points of the traditional insurance industry in underwriting claims. The emergence of artificial intelligence has led to a shift in this situation. (2) Improving antifraud capabilities. According to the International Association of Insurance Supervisors (IAIS), the lack of data makes it difficult for traditional insurance companies to overcome the problem of insurance fraud caused by information asymmetry, and the restrictive clauses are mainly based on limited fraud models, leading to a series of incidents of malicious insurance fraud. Compared with the tedious manual audit, the two-wheeled platform of "rule audit + big data risk control" built by insurance companies with the help of big data and AI model can accurately capture dozens of typical frauds and abuses of health insurance funds, such as false hospitalization, item cascading, and decomposition of hospitalization, which helps insurance companies reduce medical cost expenses.

3.2. Research Method

3.2.1. Distortion Risk Metric. The set (Ω, ζ, P) is a conceptual space, and x is the set of all wandering variables on the space involved. A risk measure ρ is a mapping x from an x_ρ subset of R to the real numbers, denoted as ρ: $X \in x_\rho \leftrightarrow \rho(X) \in R$.

First, define the g function called the distortion function (distortionfunction) g: $[0,1] \longrightarrow [0,1]$ if it is a monotonically nondecreasing function and satisfies $g(0) = 0, g(1) = 1$.

Next, define the ρ_g: $x \longrightarrow R$ risk measure often called distortionriskmeasure, if $\rho_g(X)$ satisfies

$$\rho_g(X) \coloneqq \int_{-\infty}^{0} \lg\left(S_X(x)\right) - 1dx + \int_0^{\infty} g\left(S_X(x)\right)\mathrm{d}x, X \in x, \tag{1}$$

.

The X assumption is that the total risk faced $f\colon [0,\infty) \longrightarrow [0,\infty)$ by the insurer $f(X)$ is the partition function, representing the insurer transferring part of the risk faced by itself to the reinsurer. The reinsurer charges the insurer for the insurance premium to supplement the risk they bear because they assume a portion of the insurer's risk. In this paper, we assume that the reinsurance cost criterion has the following form:

$$\mu_r(f(X)) = \int_0^{\infty} r\left(S_{f(x)}(x)\right)\mathrm{d}x, \tag{2}$$

. Without loss of generality, we assume that r is not a function that is zero almost everywhere and that the total risk an insurer has to face is the residual risk it will face plus the cost required to transfer the risk. In terms of a formula, this can be expressed as

$$T_f(X) = X - f(X) + \mu_r(f(X)). \tag{3}$$

3.2.2. SQL Server Big Data Management System. Based on today's mainstream Windows and other operating system platforms, SQL Server database as a new generation of database and analysis of the processing platform software is rapidly being widely used and widely accepted by various enterprise customers. Unlike other current database platforms such as FoxPro and smaller databases such as Access, SQL Server has a complete range of powerful and easy-to-use database management and service processing functions. There are engines that support development, standard database languages such as SQL, and extended features such as replication, OLAP, and analytics. It is also significantly ahead of the rest of the market in terms of other key features that only large database software can have access to [20], such as stored procedures and triggers.

Microsoft SQL Server 2010 is based on Microsoft SQL Server 7.0, greatly expanded to increase database performance, reliability, quality management, and ease of use. Microsoft SQL Server 2010 database edition is a high-performance enterprise relational database management system with high reliability, ease of use, and other characteristics. SQL Server 2010 features more comprehensive specific features, as shown in Figure 3.

Therefore, this paper selected SQL Server 2010 for big data analysis; first of all, SQL Server 2010 version has been more mature; secondly, SQL Server is the management of large database use, that is, analysis of big data use; the use of the software is more appropriate; finally, SQL Server is more commonly used to analyze big data software.

3.2.3. Oracle Big Data Analysis Research. Oracle Database Management System is a relational database management system developed by the German company Oracle Software (Oracle in Chinese). It may also be another Microsoft database product that will be designed with distributed database design in mind as its most core feature. It will also be one of the most popular distributed C/S server architecture solutions or distributed B/S database architecture solutions

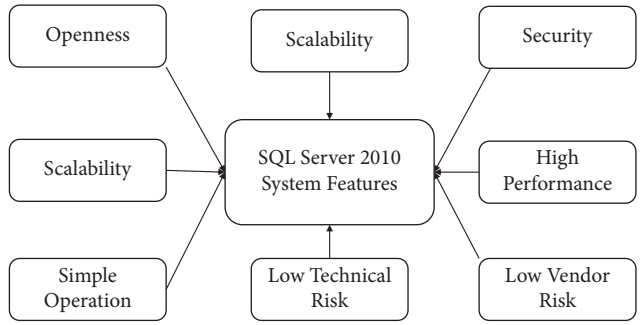

Figure 3: SQL Server 2010 system main features.

used by Microsoft in the world. Compared with SQL Server database, the state of "doubt" is one of the most obvious and attractive performance advantages of the Oracle database parallel server model, which can achieve any one subquery decomposition into any multiple subqueries and then execute subroutines on two different server CPU processors, greatly improving the performance of multiprocessing systems, which should be a data trend with a great potential competitive advantage that is growing rapidly in the coming years. Oracle database also has many other significant advantages over: complete data storage management storage capacity; large data storage capacity, long persistence time, can be shared to ensure reliability. In addition, it has complete distributed management capability and is easy to operate. As shown in Figure 4.

4. Results and Discussion

4.1. Insurance Industry Development in the Era of Digital Economy

4.1.1. The Growth Rate of Original Premium Income of Insurance Industry Returns to the Trend of Steady Growth. According to the statistics of relevant departments, China's premiums show a growth trend, increasing from 2,428.3 billion yuan in 2015 to 4,525.7 billion yuan in 2020. However, the growth rate of original premium income experienced a brief decline from 18.2% to 3.9% from 2017 to 2018, due to the "1 + 4" series of documents issued by the former CIRC in 2017, which clearly defined the requirements of strengthening supervision, managing chaos, preventing risks, and serving the real economy in the insurance market, and various departments also launched relevant systems and measures, initiated special inspections, suspended investment-based risk business pilots, and heavily fined companies for violations. Since then, the business of insurance companies gradually matched the regulatory requirements, risks were released, and the insurance industry redeveloped, as shown in Figure 5.

4.1.2. Policies Promote the Development of Insurance Digitalization. In recent years, China has been paying attention to the digital development of the insurance industry. In 2020, the CIRC pointed out that insurance companies

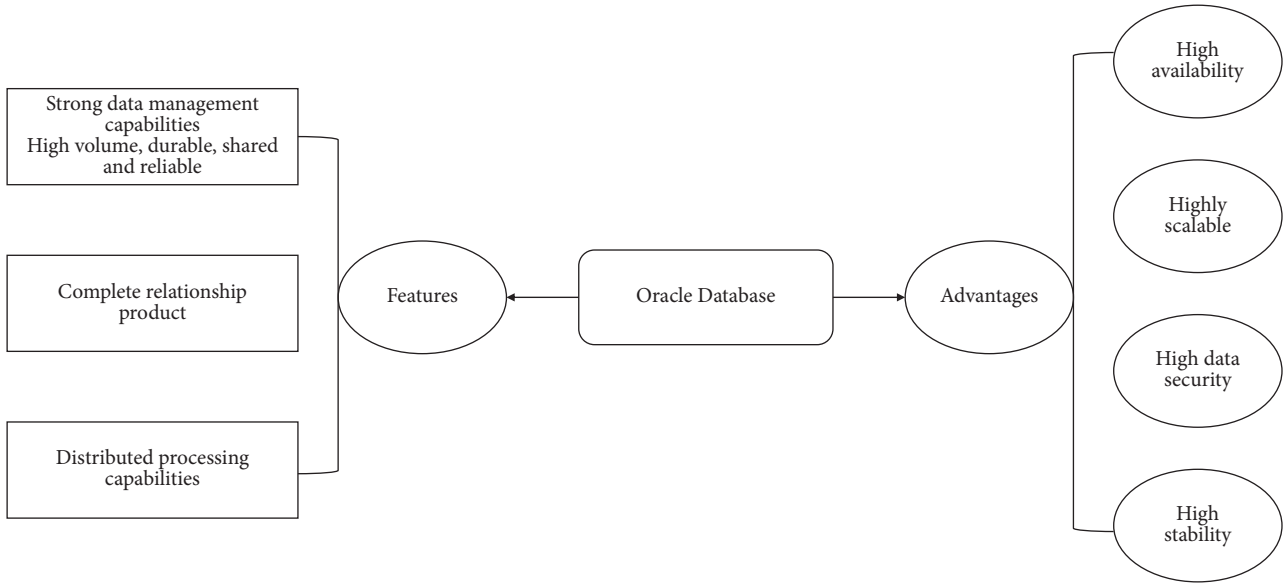

Figure 4: Features and advantages of Oracle database.

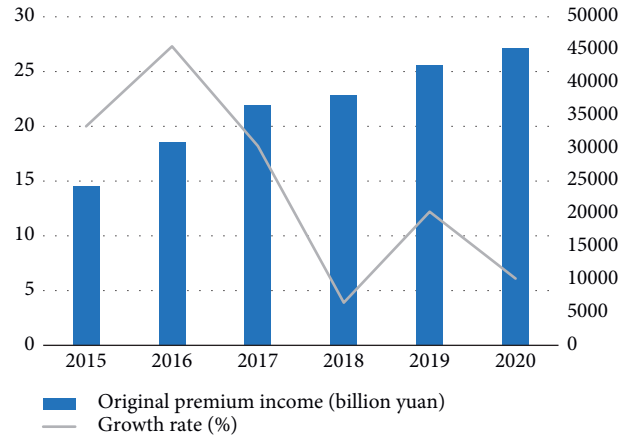

Figure 5: China's insurance original premium income and growth rate from 2015 to 2020.

should explore contactless underwriting and claims under the background of the epidemic and widely use digital technologies such as artificial intelligence and biotechnology to promote off-site investigation, and it is expected that, by 2022, the construction and governance of information security mechanisms and other aspects urge insurance companies to make rectification in data security and information docking; in the "2021 Digital Transformation Development Summit Forum" in April 2021, the CBIRC said it will further promote the digital transformation of insurance companies, clarify the risk bottom line of the transformation process of insurance companies, and formulate corresponding regulatory policies.

By combing through the national policy vein, it can be seen that the state advocates the insurance industry to use artificial intelligence, big data, biotechnology, and other technologies to empower insurance with technology, accelerate the process of digitalization and intelligence of insurance, promote the internal business effectiveness of the insurance industry, and reduce costs and increase efficiency. A major global insurance assessment company released an assessment report stating that the epidemic has accelerated the development of online insurance business. Insurance companies without the support of technology can hardly cope with future challenges. In this context, a series of policies and regulations promulgated by the State Council and CBIRC will provide a good opportunity for business transformation in the insurance industry.

4.1.3. The New Crown Epidemic Catalyzes Insurers' Digital Upgrade. The new crown epidemic outbreak has affected the traditional offline agent model in the insurance industry, and according to McKinsey's "Life Insurance Marketing Transformation and Insurance Agent Workforce Empowerment 2020," the first half of 2021, business growth in insurance types marketed through traditional offline channels, such as life insurance and auto insurance, has been hampered and slowed, while Internet platform insurance, such as health insurance, has continued its 2019 and 2020 growth momentum, climbing up.

All data show that the traditional insurance marketing method has reached a stage where it must be reformed. Influenced by factors such as the receding demographic dividend, the difficulty of offline promotion by insurance marketers leading to a sharp decline in revenue, and the gradual change in customer demand preferences for insurance products in the context of the epidemic, the sea of people tactic that has been going on for years in the insurance industry is destined to be unsustainable. The success of online transformation will be one of the key factors in the growth of premium income of each insurance type. If insurance companies do not carry out digital transformation

in time and actively lay out new online tracks, it will have a great impact on insurance types that rely on traditional marketing models. The comparison of various indicators of insurance companies before and after the epidemic is shown in Figure 6.

4.1.4. Capital Focuses on the Digitalization Process of Insurance. The great prospect of InsurTech development in the digital economy era has attracted a large influx of venture capital. InsurTech ushered in the first wave of financing in 2015, with the number of financing pieces reaching 58 and the financing amount soaring to 8.017 billion yuan from 242 million yuan in 2014. The slowdown in the growth of the original premium income of China's insurance industry under the background of strong regulation in 2017 did not stop capital from enthusiastically chasing the InsurTech industry, and the InsurTech sector still absorbed a financing amount of 4.265 billion yuan in 2017. It is worth noting that although the InsurTech industry maintained a high capital fever from 2017 to 2020, with the financing amount floating above and below 4 billion yuan, the number of financing pieces started to decline from 2017 onwards instead and continued to go down in the following three years, proving that the proportion of small investments is decreasing, while the proportion of large investments is further increasing, and the industry is gradually maturing, as shown in Figure 7.

The use of insurance technology can eventually help the insurance industry to reduce operating costs, enrich product design, improve service experience, and cover a wider customer base with its business. In the context of the trade war between China and the US, the competition between China and the US will eventually turn into a battle of technology, and the only way to occupy a place in the global market is to use technology to promote the development of the industry. There are a lot of opportunities in this process, so the influx of capital is profitable, and it is foreseeable that the insurance technology industry will still be a hot target for capital in the future.

4.2. Challenges Facing the Insurance Industry in the Era of Big Data Economy

4.2.1. Diversified Competition Pattern and Small- and Medium-Sized Insurance Companies Face Challenges. The competition pattern is evolving with the influx of various entities. According to the public data of the Insurance Industry Association, the competition among insurance companies in the same industry has been very intense, and there is also industry competition with banks, securities, and other financial institutions in the insurance industry. As the InsurTech industry continues to expand, more companies with financial strength and technical means will join the competition. Without the support of large companies, small- and medium-sized InsurTech companies will easily face the dilemma of lack of talent, technology, and capital, and even be unable to join the track. Large InsurTech companies actively develop new technologies, undertake industry data collection, and strengthen their own risk control capabilities and pricing levels, which will further aggravate adverse selection, resulting in a situation where the stronger the stronger and the weaker the weaker, which is like a disaster for the submature companies.

Financing winds have changed, and market competition has intensified. In 2015, the finance industry developed rapidly, and the number of transactions reached a new peak; however, the number of seed/angel round financing pieces began to show a downward trend in fluctuation and had dropped to 5% by 2019. The number of Series A rounds accounted for only 19% in 2014 and stabilized at around 40% from 2015 to 2019; the number of Series B rounds declined significantly compared to seed/angel and Series A rounds, accounting for only around 21% in 2017, the year with the largest share; Series C rounds varied widely from year to year, accounting for 18% in 2019 and 0% in 2014 and 2017. These investment evolutions have led to InsurTech companies being more difficult to obtain funding compared to before, with capital acting more cautiously and preferring to invest in projects in their infancy. But even if companies are able to secure Series A funding, moving from Series B to Series C or even Series D is still very challenging, judging by the relatively depleted Series B funding and the unstable Series C funding. Capital for the middle and late failure to achieve "independent blood" of the enterprise will choose to leave the field decisively. Digital technology is an important force in the development of the industry, but this force will intensify the elimination of the best and the worst among enterprises; some submature enterprises must race against time, or may not wait to show the technology in the industry will face a premature death, as shown in Figure 8.

4.2.2. Insufficient Kinetic Energy for Industrial Transformation and Barriers to Technology Upgrade. There are barriers to data acquisition. The development of the insurance industry is to a certain extent constrained by big data. The digital era has accelerated the collection of information by insurers, and major insurers are also paying more and more attention to the collection of data. Large insurers such as Taiping and Taikang are gradually establishing their own independent health care organizations and developing artificial intelligence technologies to get closer to customers' lives and obtain richer data, while small- and medium-sized insurers are also taking this as a long-term development plan. However, at this stage, the collection and use of data by insurance companies is still in its infancy. The accumulation of data of traditional insurance companies mainly comes from the basic information of customers and claims data in their underwriting process, and a considerable part of the data has a large duplication, which can only be used as identity credentials and cannot be used as effective information to portray customer portraits, and cannot be used for in-depth risk mining or developing personalized needs. It is also difficult for traditional insurance companies to collect fragmented information and use it for modeling, which requires external support. Large companies that already have a large amount of user data, such as Meituan, Tencent, and Ali, prefer to improve their financial landscape by acquiring shares in insurance companies with

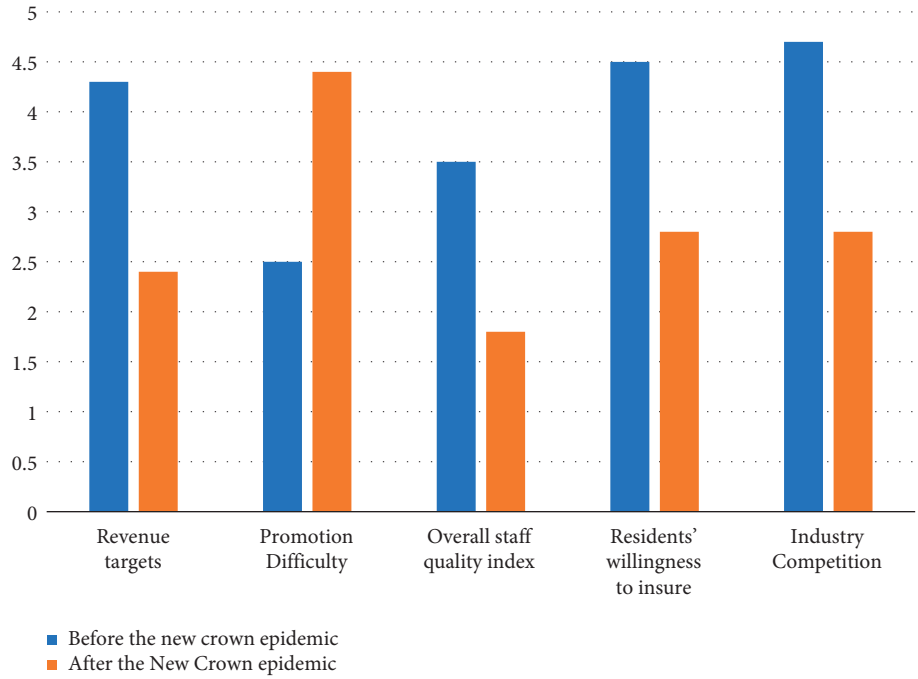

Figure 6: Comparison of various indicators of insurance companies before and after the epidemic.

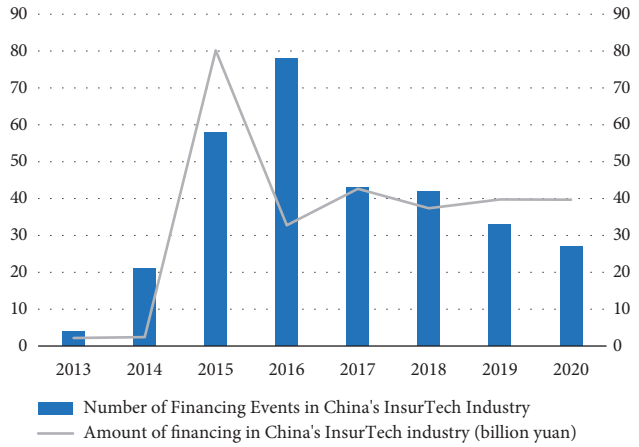

Figure 7: Statistics on the number of financing and amount of financing in China's InsurTech industry from 2013 to 2020.

relevant licenses, rather than serving the insurance industry. Insurance companies have very limited access to public data information from official channels, and data obtained from other nonprofessional third-party organizations may have inconsistent data standards. The existence of data barriers restricts the transformation and upgrading of insurance industry services and hinders the deep integration of insurance and modern information technology:

> *Lack of Composite Talents.* Although, in China, the supply of talent in the financial industry is much greater than the demand for talent, but from the perspective of China's entrepreneurial innovation in the financial sector, most of the innovation and entrepreneurship in the financial sector is still biased towards the sales industry, and there is still relatively little research on specific research and development and computing algorithms. Therefore, the platform of sales, which can better solve the problem of sales, can solve the problem of insurance sales in China and solve the problem of the status quo of online sales, which can make it more convenient for consumers to choose the insurance products they need. According to the data published by the CBIRC, Internet premium income reached 269.63 billion yuan in 2019, up 42.8% year-on-year. The change in the marketing model also means a shift in the demand for talent in the insurance industry. The digital era has made insurance companies more hungry for "insurance + technology" composite talents. In 2019, PwC pointed out in its report that there are a large shortage of financial engineering technical posts and a shortage of more than one million financial technology positions, and talents who can combine technology and finance are the objects of competition for major companies. From the recruitment status of major insurance companies, each insurance company attaches great importance to the development of the field of insurance technology. The chief human resources executive of Ping An Group said in an interview that the technology business segment of Ping An Group has onboarded 6,000 people and will further expand the introduction of talents in the future. From a macro point of view, whether the insurance industry can play the advantages brought by insurance technology in the future depends on the application of talents to new technologies and their adaptation to emerging technologies, while there is still a relative lack of insurance technology talents in China.

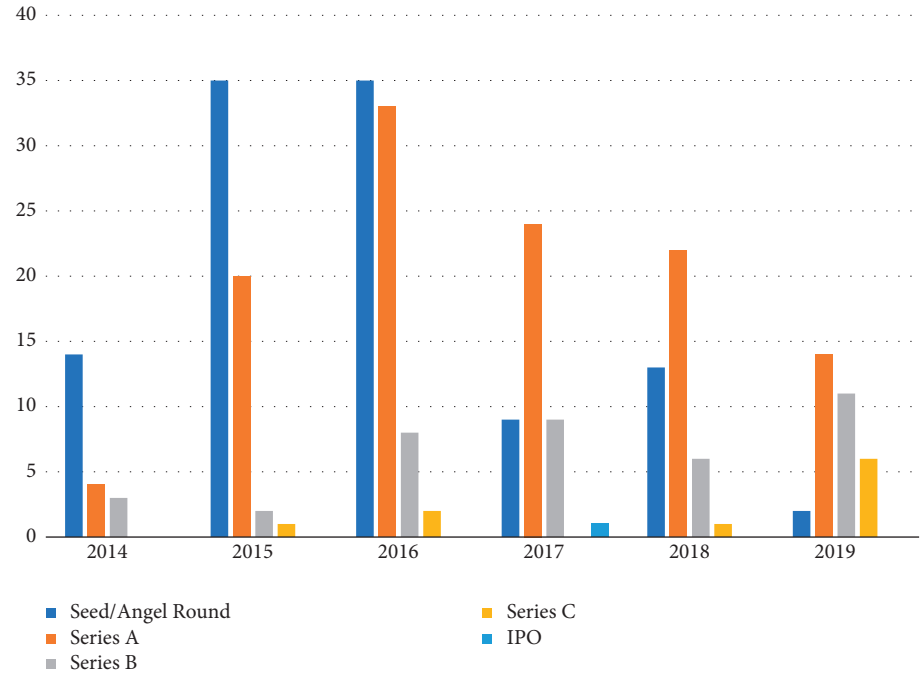

Figure 8: Distribution of InsurTech financing rounds in China, 2014–2019.

Technology Penetration Barrier. The application of digital technology will undoubtedly greatly improve the efficiency of the insurance industry, reduce operating costs, and inject new blood into the development of the insurance industry, but for most insurance companies, the application of digital technology is still in its infancy, and there are certain loopholes in both the technology itself and the technology application environment. As of now, the application of big data technology is the highest in each exhibition environment, followed by artificial intelligence, while blockchain technology, which has the most potential value for application, is still in the stage of pending development. 5G technology, as an auxiliary technology for the above-mentioned technologies, has not yet achieved the full coverage of its base station construction, and the main coverage users are still large city groups. The ultimate goal of digital technology application in the insurance industry is to create an integrated and convergent business development model with omnichannel and omniplatform, which requires joint research and development, investment, and cooperation among major insurance companies, and only a few insurance companies applying related technologies cannot achieve the goal of integrated business development. However, for traditional insurance companies that have already acquired a certain user base and have a model business process, it is still doubtful how much money they are willing to invest in RD and infrastructure construction of new technologies and whether they are willing to share technologies after considering the cost-to-benefit ratio. At present, it is obvious that the technology application status of major insurance companies still cannot meet the requirements of digital technology and insurance industry integration, and there are still some obstacles for digital technology to penetrate the insurance industry.

4.2.3. Changes in the Macro Environment and Increased Business Risks. The regulatory environment is tightening, and policies are gradually being established. In June 2020, China's central bank as well as the CBIRC and other departments jointly issued the latest notice on regulating the insurance industry, the financial industry. It requires that the maintenance of sales records and the regulation of the sales process must be completed by October 2020, further strengthening the regulation of the sales process for back checking when necessary, and specific sales scenarios require audio and video recording, further clarifying the requirements for the sale of Internet products. For some Internet insurance companies or large insurance companies, the capital and RD capabilities enable them to complete the retrospective work rectification earlier, but for other more insurance companies, it is still not a small amount of work. In January 2021, the CBIRC, together with the Central Bank, the Ministry of Finance, and other departments, further improved and issued a further standardized approach for insurance and other intermediaries. This approach requires insurance and other financial institutions to be completed within a year, to be able to complete the relevant records in a timely manner, the relevant sales aspects of the process of tracing, and complete records of the financial business personnel situation of the information technology construction, and to achieve business docking with the insurance company to generate data conditions that meet the

regulatory conditions. However, the current situation, in general, most of the companies still take the offline docking approach, and did not really take the Internet online sales approach to take online docking. From the above-mentioned series of regulatory measures, it can be seen that the insurance regulators are gradually implementing regulatory measures to regulate the process of insurance digitization, maintain market order, and gradually eliminate some "small and messy" business entities.

5. Conclusion

According to the definition of big data technology issued by relevant Chinese research institutes, big data technology is defined as a technology that can be used for digitalization. Big data technology is defined as follows: big data technology is an important productivity factor of digitalization in the network era; big data technology is based on network technology, statistical technology, and mathematical technology; big data technology, as a carrier of network technology, should be integrated with various industries and technologies other than contemporary ones in order to achieve better informatization and industrialization. . In the context of the new crown epidemic in 2020, China's big data technology continues to grow steadily, with a scale of 39.2 trillion yuan, accounting for 38.6% of GDP. At the same time, China's big data technology was included in the development of China's plan to promote the comprehensive development of big data, the development of big data into all walks of life, the process of China's digitalization, and the building of digital power. This paper investigates the risk constraint in the context of big data in the context of rapid information technology development and optimizes the benign interaction mechanism of insurance management based on distorted risk metrics. The current state of insurance risk is investigated through a thorough discussion of theories in this paper and research methods such as distorted risk metrics and SQL Server database management. It has been discovered that the overall situation of the insurance industry's development in the digital economy is not optimistic and so on. The following suggestions are made.

At the level of traditional insurance companies, the first is to accelerate digital transformation and strengthen digital construction. The second is to improve the talent cultivation mechanism and pay attention to the cultivation of composite talents. At the level of new insurance enterprises, the first thing is to maintain the advantages and actively innovate. The second is to be open and inclusive, and mutually beneficial. At the government level, the first is to establish a multilevel subsidy system to support the growth of insurance science and technology companies, and the second is to improve the incentive system to encourage the digital transformation of traditional insurance enterprises.

Data Availability

The dataset is available upon request.

Conflicts of Interest

The author declares no conflicts of interest.

References

[1] T. J. Boonen and W. Jiang, "A marginal indemnity function approach to optimal reinsurance under the Vajda condition," *European Journal of Operational Research*, vol. 303, no. 2, pp. 928–944, 2022.

[2] A. Jordan, Om Dave, N. Kevin, D. Scales Charles, and F. Friedlander David, "Influence of clinical and sociodemographic factors on the management, costs and outcomes of acute urinary retention in the acute care setting," *Urology Practice*, vol. 9, no. 4, 2022.

[3] C. Guo, L. Nozick, J. Kruse, M. Millea, R. Davidson, and J. Trainor, "Dynamic modeling of public and private decision making for hurricane risk management including insurance, acquisition, and mitigation policy," *Risk Management and Insurance Review*, vol. 25, no. 2, pp. 173–199, 2022.

[4] A. De Pin, P. P. Miglietta, B. Coluccia, and F. Capitanio, "Agricultural insurance in the DOCG area of conegliano—valdobbiadene: an assessment of policy measures," *Sustainability*, vol. 14, no. 11, p. 6912, 2022.

[5] H. Roland, P. Matthias, J. Hahn, K. Jang, and I. Rüter, "Financial knowledge of university students in Korea and Germany," *Research in Comparative and International Education*, vol. 17, no. 2, 2022.

[6] T. Serkan and O. Fatih, "A novel framework for extracting knowledge management from business intelligence log files in hospitals," *Applied Sciences*, vol. 12, no. 11, 2022.

[7] G. Asier, De la P. J. Iñaki, and T. Eduardo, "Towards a global solvency model in the insurance market: a qualitative analysis," *Sustainability*, vol. 14, no. 11, 2022.

[8] X. Li, Y. Xie, and J. H. Lin, "Life insurance policy loans, technology choices, and strategic asset-liability matching management," *Emerging Markets Finance and Trade*, vol. 58, no. 7, pp. 1838–1847, 2022.

[9] S. Lukas, P. Carlo, J. Wagner, and R. A. Zeier, "Green insurance: a roadmap for executive management," *Journal of Risk and Financial Management*, vol. 15, no. 5, 2022.

[10] O. Hisako, O. Hiroyuki, and H. Yasunaga, "Oral food challenge management in Japan: a retrospective analysis of health insurance claims data," *Clinical amp; Experimental Allergy*, vol. 52, no. 7, 2022.

[11] S. Reimund and S. Oleksandr, "Climate insurance for agriculture in europe: on the merits of smart contracts and distributed ledger technologies," *Journal of Risk and Financial Management*, vol. 15, no. 5, 2022.

[12] E. Sidorova, Y. Kostyukhin, L. Korshunova et al., "Forming a risk management system based on the process approach in the conditions of economic transformation," *Risks*, vol. 10, no. 5, p. 95, 2022.

[13] S. De Lei, L. Shi, D. Li, and Y. Zhao, "Manage pension deficit with heterogeneous insurance," *Methodology and Computing in Applied Probability*, vol. 24, no. 2, 2022.

[14] A. A. Muhamat, A. F. Zulkifli, M. A. Ibrahim et al., "Realising the corporate social performance (CSP) of takaful (islamic insurance) operators through drone-assisted disaster victim identification (DVI)," *Sustainability*, vol. 14, no. 9, p. 5440, 2022.

[15] C. D. Stafford, F. Keitt, and L. Irvin, "Health disparities in the management of ACL injuries: how socioeconomic status,

insurance, and race influence care," *PM&R*, vol. 14, no. 5, pp. 669–677, 2022.

[16] C. N. Porter, R. Taylor, and A. C. Harvey, "Applying the asymmetric information management technique to insurance claims," *Applied Cognitive Psychology*, vol. 36, no. 3, pp. 602–611, 2022.

[17] U. Vineet, M. Adams, and Y. Jia, "Risk management and the cost of equity: evidence from the United Kingdom's non-life insurance market," *The European Journal of Finance*, vol. 28, no. 6, 2022.

[18] E. R. Finkelstein, M. Ha, P. Hanwright et al., "A review of American insurance coverage and criteria for conservative management of lymphedema," *Journal of Vascular Surgery: Venous and Lymphatic Disorders*, vol. 10, no. 4, pp. 929–936, 2022.

[19] A. Taha, B. Cosgrave, and S. Mckeever, "Using feature selection with machine learning for generation of insurance insights," *Applied Sciences*, vol. 12, no. 6, p. 3209, 2022.

[20] L. Susanna and P. Gabriella, "Mutual peer-to-peer insurance: the allocation of risk," *Journal of Co-operative Organization and Management*, vol. 10, no. 1, 2022.

Hindawi
Computational Intelligence and Neuroscience
Volume 2022, Article ID 9693175, 10 pages
https://doi.org/10.1155/2022/9693175

Research Article

Prediction Model of Soil Heavy Metal Content Based on Particle Swarm Algorithm Optimized Neural Network

Cuiqing Duan,[1,2] Baoqiang Wang ,[3] and Jinxiu Li[3]

[1]*School of Environmental and Municipal Engineering, Lanzhou Jiaotong University, Lanzhou 730070, China*
[2]*Gansu Academy of Social Sciences, Lanzhou 730070, China*
[3]*Gansu Agricultural University, Lanzhou 730070, China*

Correspondence should be addressed to Baoqiang Wang; 201904020932@stu.zjsru.edu.cn

Received 29 July 2022; Accepted 17 August 2022; Published 2 September 2022

Academic Editor: Yaxiang Fan

Copyright © 2022 Cuiqing Duan et al. This is an open access article distributed under the Creative Commons Attribution License, which permits unrestricted use, distribution, and reproduction in any medium, provided the original work is properly cited.

In 2014, the relevant research data from the Ministry of Environmental Protection and the Ministry of Land and Resources showed that the total exceedance rate of soil heavy metal pollution in China had reached 16.1%, and in the construction of ecological civilization in the 13th Five-Year Plan, China has made the prevention and control of soil heavy metal pollution as the focus of prevention and control. Therefore, in this paper, four neural optimization network models, that is, radial basis neural network (RBFNN), generalized regression neural network (GRNN), wavelet neural network (WNN), and fuzzy neural network (FNN), are simulated and created to measure and correlate the soil heavy metal content in a city in northwest China and a city in central China from the actual situation in China. The simulations were conducted. Finally, by analyzing the comparison of predicted and true values of these four models on the test data of two sets of experimental data, the distribution of predicted differences to true values, and the calculation results of three error indicators, we found that WNN has the best prediction performance when using RBFNN, GRNN, WNN, and FNN for soil heavy metal content prediction.

1. Introduction

The current situation of soil heavy metal pollution in China is still in a very serious state, especially with the rapid development of industrialization and urbanization, the emission of heavy metal pollution will continue to grow in the coming period of time, and this pollution will also be absorbed by human body with the material cycle of nature, which directly endangers human health. As early as 2014, the Ministry of Environmental Protection and the Ministry of Land and Resources showed that the total exceedance rate of soil heavy metal pollution in China had reached 16.1%, and in the 13th Five-Year Plan for the construction of ecological civilization, China has made the prevention and control of soil heavy metal pollution a priority [1].

The treatment of soil heavy metal pollution often needs to be tailored to local conditions, and it is necessary to fully understand the information on the content of various heavy metals in the contaminated area, and the main way to obtain this information is through field sampling and testing by researchers [2]. However, in the actual sampling process, due to the large area to be monitored, it is often difficult to collect every area, and because of the tedious process of soil heavy metal content testing and the large number of heavy metal categories to be tested, when the number of sampling points exceeds a certain number, the time and manpower required for testing will also be too high. Therefore, in order to obtain more detailed information about the soil heavy metal content, researchers usually use the soil heavy metal content data from some sampling points to predict the soil heavy metal content in other unknown areas, so as to obtain more abundant data information for decision making.

The traditional data prediction methods can achieve good prediction results when dealing with data with a large number of features, but once the number of features decreases, the prediction performance also decreases. For example, in the source project of this thesis, the soil heavy metal content dataset obtained through the collection only

contains five types of features: longitude, latitude, elevation, functional area, and eight heavy metals, and the number of features is relatively small. Therefore, it is difficult to obtain good prediction results when using traditional data prediction methods. With the continuous development of artificial intelligence in recent years, artificial neural networks have been increasingly used for data prediction in various industries, such as house price prediction, electricity load prediction, and short-time traffic flow prediction [3]. It has been proved to have better mapping ability and self-learning capability when dealing with data sets with complex nonlinear relationships, while the method can still achieve better prediction results when the relevant features in the training data are fewer or less relevant; for example, in the literature, researchers used only three types of feature data, namely, ambient temperature, daily average solar irradiation intensity, and daily average wind speed, as the BP neural network input to predict the output power of PV plants, and the average absolute percentage error of the predicted values is 28.4%, which is a relatively good result [4]. In addition, the application of artificial neural network in soil heavy metal content prediction is relatively small, and conducting related research can further verify the effectiveness of artificial neural network in data prediction, so this study chooses to use artificial neural network as the basic model for soil heavy metal content prediction research [5].

2. Research Background

At present, researchers' research on soil heavy metal content mainly involves several aspects such as pollution analysis of soil heavy metal content, spatial distribution study of soil heavy metal content, and prediction of soil heavy metal content, but when conducting pollution analysis of soil heavy metal content and spatial distribution study, they all involve prediction of soil heavy metal content in unknown areas, so soil heavy metal content prediction study is an, therefore, important part of soil heavy metal content research [6].

In a foreign study on pollution analysis of soil heavy metal content, Susana et al. used geographically weighted principal component analysis to assess the diffuse sources of soil heavy metals and finally identified two major sources, which were geological causes related to mining and atmospheric causes related to vegetation burning [7]. Ha et al. used principal component analysis (PCA) to characterize the distribution of heavy metals in soil, then used kriging interpolation for the creation of regional distribution maps, and finally analyzed the distribution of soil heavy metal content and pollution in the target area using its better linear unbiased estimation; after visualizing the distribution of heavy metal pollution levels in urban soils, Jia et al. established artificial neural networks with reference to knowledge analysis of the causes of pollution as a way to determine the main causes of urban soil heavy metal pollution [8]. Ma et al. applied machine learning algorithm to soil heavy metal pollution analysis and established three prediction models, namely, support vector Machine (SVM), random forest (RF), and extreme learning machine (ELM), respectively, through correlation analysis of heavy metal content. In comparison with the experimental results, it was found that the concentration of soil heavy metal samples had a direct influence on the prediction effect of the model [9].

In the spatial distribution of soil heavy metal content and soil heavy metal content prediction research, Mr. Pandit and others used reflection spectroscopy to measure the reflectivity of different heavy metals, and then, by using partial least squares (PLSR) model to reflect the relationship between the soil heavy metal content and high spectral reflectance, the soil heavy metal content is predicted according to [10]. Aryafar et al. used support vector machine (SVM) to evaluate soil heavy metal pollution in the target river region and compared the prediction results of SUPPORT vector machine with the generalized regression neural network (GRNN). The results showed that the prediction accuracy of heavy metal content of SUPPORT vector machine was higher than that of the generalized regression neural network [11]. Naderi et al. established soil heavy metal distribution models based on stepped-multiple linear regression (MSLR) and genetic algorithm-optimized neural network (ANN-GA), respectively, and then compared soil heavy metal estimation results of the two models. It is proved that the latter method of using intelligent algorithm to optimize artificial neural network parameters has higher prediction accuracy [12].

In the domestic research on pollution analysis of soil heavy metal content, Maimaititurson Aizezi et al. first used geostatistical method to analyze the spatial distribution of soil heavy metal content in the study area and then used two pollution evaluation indexes to evaluate the degree of soil heavy metal pollution in the region. It is determined that the main influencing sources of soil heavy metal content in this region are soil geochemical genesis and human activities [13]. Lin Xiaomei et al. chose least squares support vector machine (LSSVM) and partial least squares method (PLS) as comparative methods and combined them with induction technology, respectively, to conduct comparative experiments on soil heavy metal analysis. The results showed that the least squares support vector machine performed better in model accuracy and stability [14]. Wang Mudong et al. combined BP neural network and principal component analysis when analyzing the content of heavy metals in the soil of oil mining areas. The former was used to supplement the missing data in the experiment, and the latter was used for source analysis. Finally, they learned that the main sources of heavy metals in the soil were nature, agriculture, transportation, and coal burning [15]. In terms of the spatial distribution of soil heavy metal content, Jiang Zhenlan et al., based on geographical weighted regression (GWR) model, applied hyperspectral prediction of soil heavy metal content and compared the prediction results with OLS. The results showed that the geographical weight regression model could well reveal the spatial heterogeneity of the relationship between soil heavy metal content and related variables while having higher prediction accuracy [16]. Bayesian maximum entropy (BME) was applied to the spatial prediction of soil heavy metal content by Fei Xufeng et al. Compared with the ordinary Kriging interpolation method, the prediction error

of this method is smaller, which can effectively help researchers determine the spatial distribution of soil heavy metal content [17]. In terms of the prediction of heavy metal content in soil, Gao Wenwu et al. first used variance analysis to determine the impact of different cultivated land types on heavy metal Mn in soil and then used collaborative Kriging interpolation to predict the content of Mn. Three error indicators, such as the average error, in the experimental results were all at low values. This indicates that the method has a high prediction accuracy for Mn content in soil [18]. Fan Junnan et al. used the applications of BP neural network model to predict soil heavy metal content, using the model of soil spatial location and the nonlinear mapping relationship between different heavy metals, to predict the heavy metal content of the value obtained in the use of simulation efficiency coefficient (NSE) to evaluate reliability prediction results after coming to the conclusion that the NSE value satisfies the requirement of simulation precision of the model, It has a good prediction effect [19]. Qin Xichun used three kinds of neural networks, respectively, to predict soil heavy metal content in his study. Through the comparison of experimental results, it was found that the prediction error of BP neural network was the largest among the three kinds of neural networks, while the errors of wavelet neural network (WNN) and radial basis neural network (RBFNN) were relatively close [20]. Therefore, based on relevant theories, this paper established four models needed in this paper to predict soil heavy metal content, evaluate the advantages and disadvantages of the models, and select the best model.

3. Basic Theories and Research Methods

3.1. Basic Theory

3.1.1. Theory of Soil Heavy Metal Content Measurement. There are many theories about soil heavy metal content measurement at home and abroad, and the measurement methods are abundant and involve a wide range. In metrology, mathematics, statistics, computer, and other disciplines are used to establish a wide range of models, which provides great support for the theoretical research of this paper. Therefore, in this paper, four neural optimization network models including radial basis neural network (RBFNN), generalized regression neural network (GRNN), wavelet neural network (WNN), and fuzzy neural network (FNN) were created to study soil heavy metal measurement methods. This paper focuses on the study and measurement of the following six heavy metals, as shown in Figure 1.

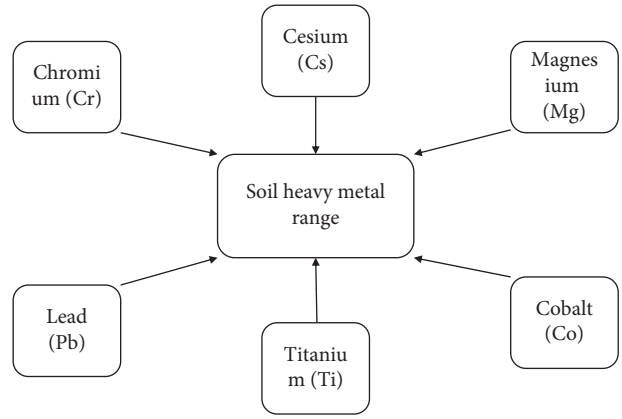

Figure 1: Main types of heavy metals in soil.

3.1.2. Particle Swarm Algorithm Theory. Particle swarm optimization (PSO) algorithm is a new Evolutionary Algorithm (EA) developed in recent years. Dr. Eberhart and Dr. Kennedy were inspired by the regular clustering of birds in 1995 when they studied their predatory behavior. At first, a simplified model was established by using the idea of swarm intelligence, and then particle swarm algorithm was invented. On the basis of swarm intelligence, particle swarm optimization (PSO) makes use of the information exchange and sharing among individuals, so that the movement of the whole group can produce an orderly evolution process in the problem-solving space and then obtain the optimal solution. It has been widely used in the optimization of complex functions, neural network training, and other applications of evolutionary algorithms.

The training process of particle swarm optimization: particle swarm optimization (PSO) randomly starts a set of solutions for each particle and then gradually updates and optimizes them through iterative algorithm. In each iteration, each particle updates its velocity and position by chasing two extremes. An extremum is the optimal solution previously found by the particle, and this extremum is called individual extremum pBest. The other extreme is the optimal solution currently found by the whole population. This extreme is called the global extreme gBest. In addition, gBest can not use the extreme value of the whole population, but only the individual extreme value nBest of the particles in the neighborhood within a certain range of the particle. Such particle swarm is the local version of the particle swarm, and the spatial topological structure of the particle determines the range of the neighborhood.

PSO algorithm is a global search algorithm, which randomly initializes many particles evenly distributed throughout the solution space. These particles carry out iterative search in the global space by combining their own and global information through certain strategies, and it will have a high probability to find a better solution:

(1) *Global Particle Swarm*. If we update gBest each time looking for the best fit of all contemporary particles, then such a particle swarm is a global particle swarm. Global particle swarm is a bit greedy in nature, so its advantage is fast convergence speed, and its disadvantage is being easy to fall into the local optimal solution.

(2) *Local Neighborhood Particle Swarm*. If we update gBest, we can choose a neighborhood K. For each particle, we update gBest according to the particle with the best fitness among the K particles around it. Because the similar particles have more similar properties, the local optimum can be replaced by the

global optimum, so that the whole particle swarm can keep strong searching ability. Therefore, its advantages are having a stronger search range and being easy to jump out of the local optimal, and the disadvantage is also obvious, that is, slow convergence.

(3) *Local Random Particle Swarm*. If K particles can be randomly selected when updating gBest, we will update gBest according to the particle with the best fitness among the K particles. We know that close particles have more similar properties, and if one particle deviates from the optimal solution, then several particles around it may deviate, so that their local optimal may not be very helpful for the whole population to find the optimal solution. Selecting K particles at random (the particles themselves should be kept) gives a certain probability of weeding out the bad ones. Therefore, it is a compromise between maintaining the searching ability and convergence speed of the whole population.

3.1.3. Particle Swarm Optimization Neural Network. With the optimization objective, the parameters of particle swarm optimization algorithm are determined. If the fitness function is known, the particle swarm optimization algorithm can be directly used to replace the BP algorithm to train the convolutional neural network.

The determination of fitness function of particle swarm optimization algorithm: in the process of deriving the parameters of convolutional neural network above, we see that the loss value of a network training loss will be calculated in the last loss layer. SOFTMAX_LOSS is generally used in convolutional neural network. This value is the error of network training. The closer it is to 0, the better the current training model is. This value is directly taken as the adaptive value of PSO, and the adaptive function of PSO can also be used to calculate the forward process of loss by convolutional neural network. After decoding the particle, the corresponding network structure weight can be obtained, and then the input sample is input into the network, and the forward process calculation is carried out with the network weight, and the training error loss value can be obtained.

We have analyzed the codec of convolutional neural network and determined the parameters of particle swarm optimization. The fitness function of particle swarm optimization algorithm is the convolution neural network to calculate the Loss worth process, and the training error loss is the adaptation value of PSO. Given these conditions, we can use particle swarm optimization to train the convolutional neural network.

For small samples, all training can be divided into a group; that is, batch-size is equal to the number of training samples, which is equivalent to full-sample training mode. However, when the sample size increases, the data exchange between layers is also related to batch-size. Generally, the training of convolutional neural networks is run in GPU mode, and all data will be stored in video memory. Too large batch-size will lead to insufficient video memory space for training. Therefore, in the case of large-scale training samples, mini-batch training mode can only be adopted. Since the convolutional neural network is grouped by batch_size for BP training, different training samples with the same network parameters will calculate different loss values, and if our PSO does so, then this loss value has no reference value. Therefore, PSO must go through all groupings to calculate the adaptation value and then find the average loss, which is the final adaptation value. This also means that the PSO algorithm can be very slow in large-scale samples. In addition, we know that BP is a gradient descent algorithm, and the gradient descent algorithm is easy to fall into local optimum; PSO algorithm is a relatively global algorithm, which increases the search range by multiparticle common search, at the cost of its relatively weak local search ability, and it also falls into local optimum solution. Especially in the case of high dimension and high samples, the local optimal solution that PSO falls into may not be as good as BP, and the higher the dimension is, and the more the samples are, the more difficult it is for PSO to jump out of this solution. The optimization performance of the particle swarm algorithm on sample sets of different sizes will be highlighted in the later experimental analysis.

3.2. Research Methods

3.2.1. Radial Basis Neural Network. Radial Basis Function Neural Network (RBFNN) is the most typical three-layer forward neural network structure. In addition to the information processing of traditional neural networks, its implicit layer uses radial basis functions for nonlinear mapping of input data, which is then passed to the next layer after linear computation. The structure of the radial basis neural network is shown in Figure 2.

In the unsupervised learning part, the data are clustered by using a clustering algorithm such as K-means to obtain the centroid of the radial basis function in the hidden layer, and then the width vector of the radial basis function is calculated by using the centroid information, and the width vector is calculated by the following formula:

$$\sigma_j = \frac{c_{xy}}{\sqrt{2h}}, \tag{1}$$

where c_{Xy} is the maximum distance before the centroid and h is the number of nodes.

After that, the input data are related to the scattering through the implicit layer and the output layer, respectively, and the output x_i of the first node j of the input sample in the implicit layer is calculated by the following equation:

$$\phi(x_i, j) = \exp\left(-\frac{1}{2\sigma_j^2} x_i - c_i\right), \tag{2}$$

where c_j and σ_j are the centroid and width m vector of the first node in the hidden layer, respectively.

The output of x_i the first node of j the input sample in the output layer is calculated by the following equation:

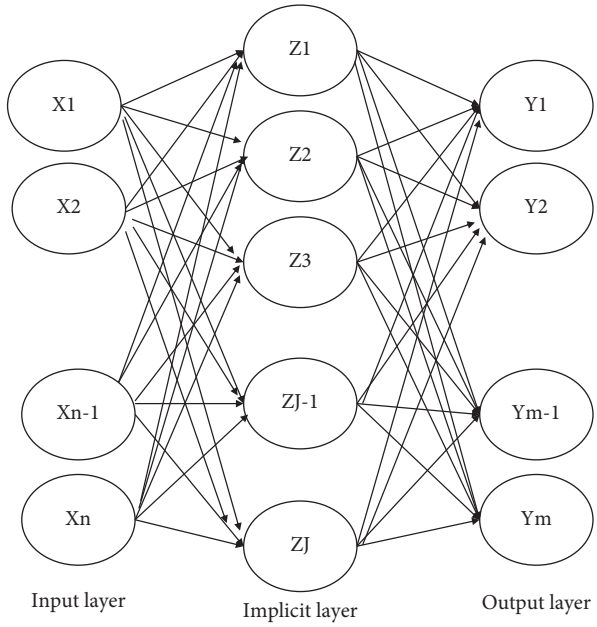

Figure 2: Structure of radial basis neural network.

$$y_m = \varphi\left(\phi\left(x_i, j\right) * w_m\right), \tag{3}$$

where w_m is the node weight and φ is the activation function.

In the supervised learning part, it is mainly the process of continuously correcting the parameters in each layer, and this process is mainly calculated by the error function to calculate the gradient value of each parameter, and then the parameters are continuously corrected using traditional gradient descent methods such as stochastic gradient descent (SGD); taking the weights used for linear calculation in the output layer as an example, the update formula is as follows:

$$w_t = w_{t-1} - u * \frac{\sigma E}{\sigma w_{t-1}}, \tag{4}$$

where E is the error function and u is the learning rate

In addition to the above methods, the centroids and width vectors of the hidden layer can be directly generated randomly, after which they are updated according to the gradient correction formula of the supervised learning process.

3.2.2. Generalized Regression Neural Network. Generalized Regression Neural Network (GRNN) is a four-layer forward propagation neural network with fewer parameters and better nonlinear mapping capability in its network structure [26][27], where the data are input to the network, and the output results are obtained after passing through the input layer, pattern layer, summation layer, and output layer in turn. This network does not have a training process but mainly optimizes the smoothing factor of the pattern layer to obtain good output results as shown in Figure 3.

The computational process is not shown in detail here, and the specific computational process can be obtained by the radial basis neural network inversion, which will not be done in this case. Although GRNN does not require network training, the smoothing factor of the pattern layer has a large impact on the performance of the network, and too large or too small smoothing factor will lead to underfitting and overfitting of the network, respectively, and it is usually difficult to set the smoothing factor to a better value in the experiment, so if you want to get better network performance, you generally choose an efficient intelligent optimization algorithm to find the optimal smoothing factor.

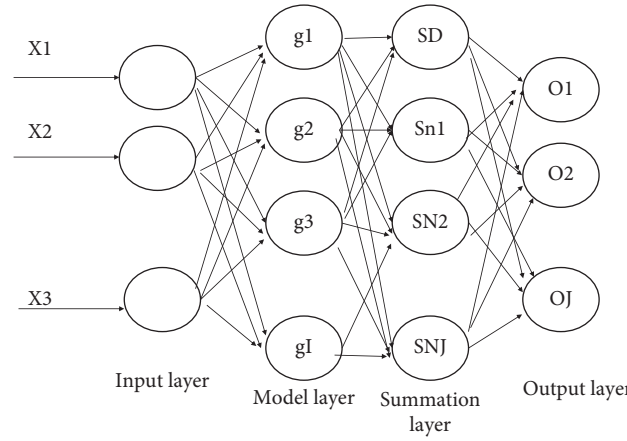

Figure 3: Structure of generalized regression neural network.

3.2.3. Wavelet Neural Network. Wavelet Neural Network (WNN) has a three-layer structure, which is characterized by the use of wavelet basis function as the activation function of the neurons in the hidden layer, which makes the network more capable of self-learning when processing data sets with large amounts of data, so it can fit complex relational data faster. Its structure is shown in Figure 4.

The computational process is not shown in detail here, and the specific computational process can be obtained by the radial basis neural network inversion, which will not be done in this example. There are four main parameters in WNN, and the size of these four parameter values will directly affect the performance of the network, so the training process of WNN as RBFNN mainly uses the traditional gradient descent method such as stochastic gradient descent (SGD) to continuously correct these four parameters.

3.2.4. Fuzzy Neural Network. Fuzzy Neural Network (FNN) incorporates fuzzy theory into the information transfer process of the network, which can have a larger processing range and faster information processing speed when processing information, so the self-learning ability and mapping of the network are relatively high. The structure diagram of fuzzy neural network is commonly used and can be found in general textbooks, so it is not repeated in this paper.

The data is trained by this neural network through a total of five layers: the first is the input layer, and the number of nodes in this layer is related to the feature dimension of the data; that is, when the feature dimension of the data is n, the

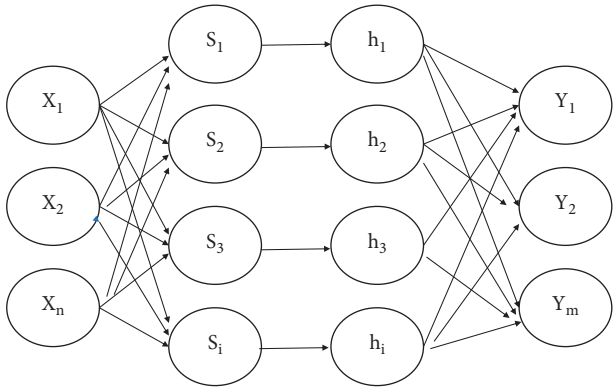

Figure 4: Structure of wavelet neural network.

number of nodes in the input layer is n. Then, the data is passed from the input layer to the affiliation function calculation layer, where the affiliation function is used to calculate the affiliation of each node, each node represents an affiliation function, and the number of nodes in this layer is the number of possible fuzzy conditions of the input variables. When the dimensionality of the output variables increases, the weights will be adjusted accordingly. In addition, FNN, like the previous RBFNN and WNN, generally uses traditional gradient descent methods such as stochastic gradient descent (SGD) to optimize the centroids of the affiliation function, the width vector, and the connection weights of the output layer.

4. Research Results and Discussion

In order to compare the prediction performance of the above four artificial neural networks for soil heavy metal content prediction, the authors will build models for each of the above four artificial neural networks and then choose the same soil heavy metal dataset for prediction experiments under the same experimental environment.

4.1. Selection and Preprocessing of Soil Heavy Metal Data. The first dataset is the surface soil heavy metal content dataset of an urban area in a provincial capital in Northwest China, which was sampled by the School of Resources and Environment of a university and is a publicly available dataset. This dataset contains the contents of a total of six heavy metals, namely, cobalt (Co), chromium (Cr), cesium (Cs), magnesium (Mg), lead (Pb), and titanium (Ti), and the total number of samples is 96 sets of these soil heavy metal content specifics.

Among the specific cases, the minimum value of elemental cobalt (Co) was 16.7 mg per kg of soil; the maximum value was 108.4 mg per kg of soil; the mean value was 37.23 mg per kg of soil; and the standard deviation was 17.43 mg per kg of soil. The minimum value of elemental chromium (Cr) was 66.2 mg per kg of soil; the maximum value was 143.8 mg per kg of soil; the mean value was 109.07 mg per kg of soil; and the standard deviation was 12.79 mg per kg of soil. The minimum value of elemental cesium (Cs) was 0 mg per kg of soil; the maximum value was 42 mg per kg of soil; the mean value was 17.35 mg per kg of soil; and the standard deviation was 9.69 mg per kg of soil. The minimum value of magnesium (Mg) was 0.98 mg per kg of soil; the maximum value was 3.25 mg per kg of soil; the mean value was 2.13 mg per kg of soil; and the standard deviation was 0.4 mg per kg of soil. The minimum value of elemental lead (Pb) was 12.8 mg per kg of soil; the maximum value was 49.1 mg per kg of soil; the mean value was 24.99 mg per kg of soil; and the standard deviation was 5.41 mg per kg of soil. The minimum value of elemental titanium (Ti) was 1189 mg per kg of soil; the maximum value was 2441 mg per kg of soil; the mean value was 2040.23 mg per kg of soil; and the standard deviation was 341.14 mg per kg of soil.

Since this dataset contains a small amount of data, a total of 96 groups of data, no processing such as feature selection was performed on the dataset, and the content of heavy metal Co was selected as the feature to be predicted, and the other five heavy metals were used as the input feature data for the model. After that, 20 sets of data were randomly selected from this data set as the test data, and the rest of the data were used as the training data.

The second data set is the soil heavy metal data set of six new urban areas in a city in central China, which was collected and tested by the Institute of Environmental Safety of the Academy of Agricultural Sciences of a city in central China, one of the contractors of the source project of this study. We use Copper (Cu), Nickel (Ni), Lead (Pb), Zinc (Zn), and Mercury (Hg), giving the relevant situations of these eight heavy metals.

Among the specific cases, the minimum value of elemental chromium (Cr) is 11.13 mg per kg of soil; the maximum value is 171.21 mg per kg of soil; the mean value is 57.49 mg per kg of soil; and the standard deviation is 24.64 mg per kg of soil. The minimum value of elemental arsenic (As) was 0.24 mg per kg of soil; the maximum value was 82.07 mg per kg of soil; the mean value was 10.15 mg per kg of soil; and the standard deviation was 6.00 mg per kg of soil. The minimum value of elemental cadmium (Cd) was 0.01 mg per kg of soil; the maximum value was 4.94 mg per kg of soil; the mean value was 0.21 mg per kg of soil; and the standard deviation was 0.39 mg per kg of soil. The minimum value of elemental copper (Cu) was 2.16 mg per kg of soil; the maximum value was 159.36 mg per kg of soil; the mean value was 26.21 mg per kg of soil; and the standard deviation was 14.06 mg per kg of soil. The minimum value of elemental nickel (Ni) was 3.32 mg per kg of soil; the maximum value was 77.67 mg per kg of soil; the mean value was 28.22 mg per kg of soil; and the standard deviation was 12.04 mg per kg of soil. The minimum value of elemental lead (Pb) was 1.96 mg per kg of soil; the maximum value was 83.30 mg per kg of soil; the mean value was 19.46 mg per kg of soil; and the standard deviation was 8.60 mg per kg of soil. The minimum value of elemental zinc (Zn) was 15.16 mg per kg of soil; the maximum value was 293.73 mg per kg of soil; the mean value was 71.17 mg per kg of soil; and the standard deviation was 29.29 mg per kg of soil. The minimum value of elemental Mercury (Hg) was 0.01 mg per kg of soil; the maximum value was 2.37 mg per kg of soil; the

mean value was 0.14 mg per kg of soil; and the standard deviation was 0.17 mg per kg of soil.

This data set contains a total of 1161 sets of data, and 500 sets of sample data were randomly selected as experimental data. In data prediction experiments, when the correlation between the input features of the model and the features to be predicted is higher, the prediction effect of the model is better, and the correlation between heavy metals and heavy metals is often greater than the correlation between location information such as latitude and longitude and heavy metals. The Pearson coefficients between different heavy metals and heavy metal Cr were calculated, and according to the calculation results, the top five heavy metals with larger Pearson coefficients were As, Cd, Ni, Pb, and Zn selected as the input features of the model. After that, 50 sets of data were randomly selected from 500 sets of sample data as test data, and the remaining data were used as training data, and the prediction results of several models on 50 sets of test data were compared after training of the models. The Pearson coefficients of arsenic (As) were 0.5939; those of cadmium (Cd) were 0.3235; those of copper (Cu) were 0.1475; those of nickel (Ni) were 0.6652; those of lead (Pb) were 0.6356; the Pearson coefficient of zinc (Zn) is 0.4226, and the Pearson coefficient of Mercury (Hg) is 0.0411.

4.2. Experimental Environment and Parameter Settings. In terms of parameter settings, the number of nodes per layer of the four network models needs to be determined first. Since the feature dimension of the input data is 5, and the feature dimension of the output data is 1 for both experimental data sets, the number of nodes and the feature dimension of the input and output layers of these four neural network models are the same, 5 and 1, respectively. The loss values of RBFNN and WNN vary irregularly with the change of the number of nodes in the hidden layer on either dataset, but the loss values of RBFNN and WNN are minimized when the nodes in the hidden layer are 7 and 8, respectively, so the number of nodes in the hidden layer is set to 7 and 8 for both datasets.

The RBFNN loss value and WNN loss value are both lower in a city in Northwest China again on each implied layer node tree, with a total of 11 nodes ranging from 2 to 12, and both loss values are above 2. The results show that the RBFNN loss value and WNN loss value are both lower in this city in Northwest China as shown in Figure 5.

The RBFNN loss value and WNN loss value are both higher for a city in central China than on each implied layer node tree, much higher than the northwest city selected in this paper with a total of 11 nodes from 2 to 12, and both loss values are about 6 or more, and the results show that the RBFNN loss value and WNN loss value are higher for the city in central China, and the contrast with the northwest city is obvious, as shown in Figure 6.

In GRNN, the number of nodes in the mode layer is the number of training dataset samples, then the number of nodes in the mode layer is set to 76 for the experiments on the Ningxia dataset, and the number of nodes in the mode layer is set to 450 for the experiments on the Wuhan dataset,

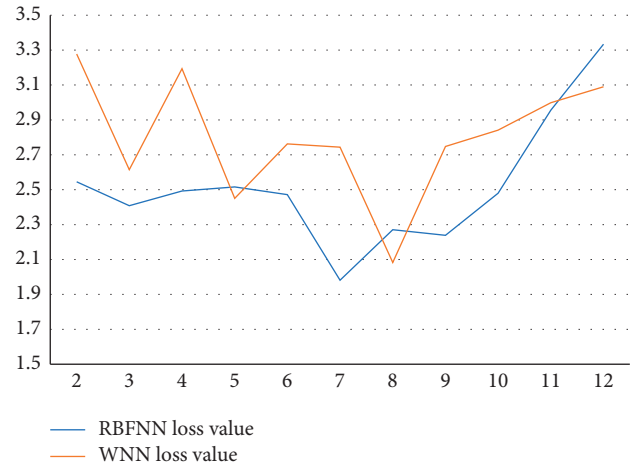

Figure 5: Loss values of RBFNN and WNN on the dataset of this city in Northwest China.

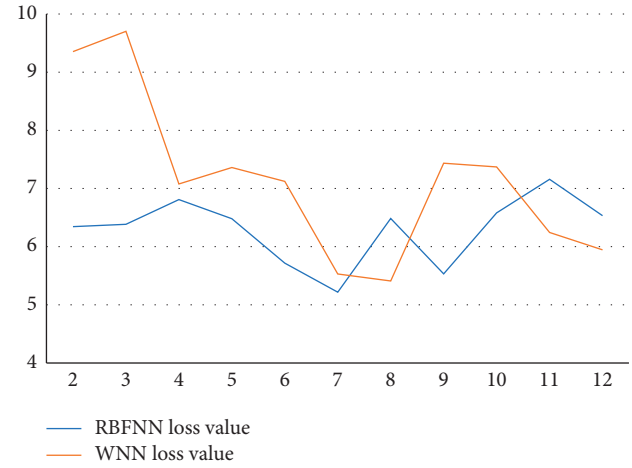

Figure 6: Loss values of RBFNN and WNN on the Han dataset in central China cities.

so their corresponding numbers of nodes in the summation layer are 77 and 451, respectively. Since there is only one index to be predicted, we set the number of fuzzy conditions in FNN to 2. The number of fuzzy gradations for each sample feature in its subordination function calculation layer is 16; that is, the number of nodes in the rule generation layer and normalization layer is 16. GRNN has no training process, so a more appropriate smoothing factor value is selected for it according to the cross-validation method, while the other three neural networks are trained with the parameters of stochastic gradient descent method, and the number of training times of the network is set to 500, and the learning rate is set to the common 0.001.

4.3. Experimental Results. After the training of the four neural network models was completed, their predicted and true values were first compared on the two data sets of the test set, and the graphs in this section show that there are points where the predicted and true values are the same, or the difference is larger for either neural network model,

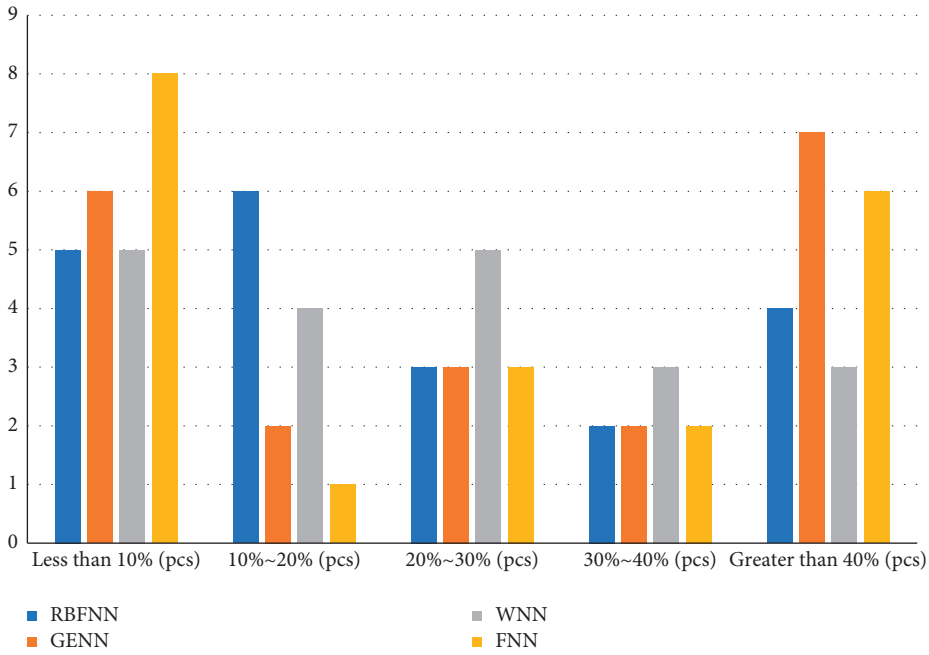

Figure 7: Distribution of the ratio of the difference to the true value of the prediction data of different neural network models on the test dataset of the city in Northwest China.

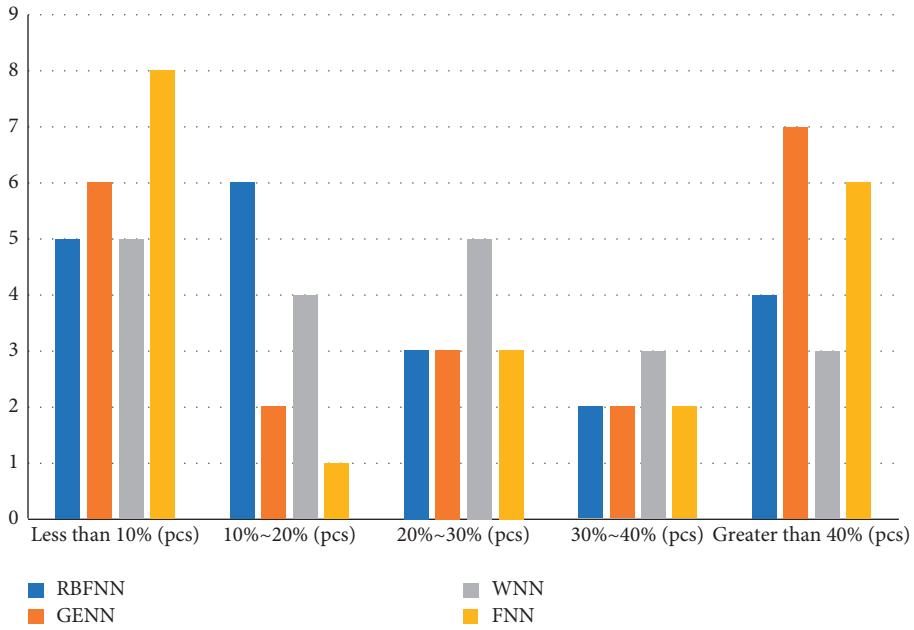

Figure 8: Distribution of the proportion of the difference to the true value of the predicted data of different neural network models on the test dataset of this city in central China.

where the curve representing the predicted value of GRNN has a relatively low agreement with the curve representing the true value, as well as the curves representing the RBFNN, WNN, and FNN. The agreement between the curves representing the predicted values and the curves representing the true values is relatively high. Comparing the curves representing the predicted values of RBFNN, WNN, and FNN, we can see that the trends of these three curves are relatively close to each other. The main difference between a city in Northwest China and a city in Central China is that the curves of RBFNN and GRNN predictions are in relatively low agreement with each other than the curves representing the true values, while the curves representing WNN and FNN predictions are in relatively high agreement with the curves representing the true values. Therefore, it is difficult to see the difference between the prediction performance of these four neural networks from these two comparison graphs alone. In

order to understand more clearly the difference between the predicted and true values of these four neural network models, the prediction difference value of each sample point in the test data set on the two experimental data sets will be calculated separately, and then the ratio situation between this difference value and the true value will be found, and finally the distribution of the 50 test data of the four neural network models in different ratio intervals will be counted. In order to have a clearer understanding of the difference between the predicted and true values of the four neural network models, the predicted difference values of each sample point in the test data sets of the two experimental data sets are calculated, and then, the ratio between the difference value and the true value is calculated, and finally the distribution of the 50 test data of the four neural network models in different ratio intervals is calculated, as shown in Figures 7 and 8.

The distribution of the ratio of the difference to the true value of the prediction data of different neural network models on the test data set of this city in the northwest shows a trend of low in the middle and high in the sides, in which it can be seen more obviously that the prediction model of this city in the northwest has a higher percentage of the true value and a higher accuracy rate as shown in Figure 7.

The distribution of the ratio of the difference to the true value of the prediction data of different neural network models on the test dataset of this city in central China shows a trend of high left and low right, which shows that the prediction model in central China has a lower proportion of true values and a lower accuracy rate as shown in Figure 8.

In Figure 7, the distribution of points of FNN and GRNN is mostly concentrated in the range of less than 10% and more than 40%, and the number of their points greater than 40% is greater than the other two models, while the number of points of RBFNN and WNN in the range of less than 10% is slightly less than the other two models, but overall, the number of points of RBFNN and WNN in the range of difference ratio less than 30% is greater than the other two models. The number of points is more than the other two models. In Figure 8, the distribution of points of RBFNN is significantly smaller than that of the other three models in the interval of less than 10% and larger than that of the other three models in the period of 10% to 20%. The other three models are closer overall, but with 20% as the limit, the number of points of WNN in the interval less than 20% is larger than that of GRNN and FNN, and the number of points in the interval greater than 20% is smaller than them, while the number of points of GRNN and FNN is closer in these two intervals.

In addition to the comparison of the above two experimental results, the mean absolute error (Mean Absolute Error, or MAE), root mean square error (Root Mean Square Error, or RMSE), and symmetric mean absolute percentage error (Symmetric Mean Absolute Percentage Error), the smaller the calculated results of these three error indicators, the better the prediction performance of the model.

From the calculated results, we can understand that the main difference is that the values of the three error metrics of GRNN on the Ningxia test dataset are larger than those of the other three models, while the error metrics of RBFNN on the Wuhan test dataset have the largest values except for the RMSE values. However, the values of the three error indicators of WNN are smaller than those of the other three models in either test dataset, where the calculated results of WNN in the Ningxia test dataset are lower by about 2.8 mg/kg for MAE, 4.5 mg/kg for RMSE, and 7% for SMAPE compared with the maximum values of the three indicators. Compared with the maximum value of these three indexes, the MAE value is reduced by about 1.3 mg/kg, RMSE value is reduced by about 1.7 mg/kg, and SMAPE is reduced by about 2%. Combining the above three experimental results and analysis, it can be concluded that WNN has the best prediction performance when using the four neural networks RBFNN, GRNN, WNN, and FNN for soil heavy metal content prediction.

5. Conclusion

In this paper, we first introduced the basic principles of four common neural networks and then modeled these four neural networks and compared their prediction performance in soil heavy metal content prediction. In this paper, four neural optimization network models, Radial Basis Neural Network (RBFNN), Generalized Regression Neural Network (GRNN), Wavelet Neural Network (WNN), and Fuzzy Neural Network (FNN), are simulated to measure and calculate the soil heavy metal content in a city in Northwest China and a city in Central China, using particle swarm algorithm. Finally, by analyzing the predicted and true values of these four models on the test data of two sets of experimental data, the distribution of the predicted difference to the true value, and the calculation results of three error indicators, we can find the prediction of soil heavy metal content using RBFNN, GRNN, WNN, and FNN neural networks.

This process includes the selection and preprocessing of experimental data, the setting of experimental environment and model parameters, and the training and testing of the four models. Finally, by analyzing the comparison plots between the predicted and true values of these four models on the test data of the two sets of experimental data, the distribution of the predicted difference in proportion to the true value, and the calculation results of the three error indicators, it can be found that the prediction performance of the wavelet neural network is better than that of the other three neural networks when performing soil heavy metal content prediction.

Data Availability

The dataset is available upon request.

Conflicts of Interest

The authors declare no conflicts of interest.

References

[1] P. Mikowiec, "The impact of the mountain barrier on the spread of heavy metal pollution on the example of Gorce Mountains, Southern Poland," *Environmental Monitoring and Assessment*, vol. 194, no. 9, 2022.

[2] N. Čmiková, L. Galovičová, M. Miškeje, P. Borotová, M. Kluz, and M. Kačániová, "Determination of antioxidant, antimicrobial activity, heavy metals and elements content of seaweed extracts," *Plants*, vol. 11, no. 11, p. 1493, 2022.

[3] Z. Liu, Y. Lu, Y. Peng, J. Wang, S. Ding, and S. Liu, "Estimation of soil heavy metal content using hyperspectral data," *Remote Sensing*, vol. 11, no. 12, p. 1464, 2019.

[4] Y. Pirsarandib, M. B. Hassanpouraghdam, F. Rasouli, M. A. Aazami, I. Puglisi, and A. Baglieri, "Phytoremediation of soil contaminated with heavy metals via arbuscular mycorrhiza (funneliformis mosseae) inoculation ameliorates the growth responses and essential oil content in lavender (lavandula angustifolia L.)," *Agronomy*, vol. 12, no. 5, p. 1221, 2022.

[5] L. Hou, Z. Wang, G. Gong et al., "Hydrogen sulfide alleviates manganese stress in arabidopsis," *International Journal of Molecular Sciences*, vol. 23, no. 9, p. 5046, 2022.

[6] M. Li, "Status quo of comprehensive utilization of red mud," *International Core Journal of Engineering*, vol. 8, no. 5, 2022.

[7] F. Alhafizoh, E. L. Widiastuti, Tugiyono, G. N. Susanto, and D. F. Mumtazah, "Heavy metals concentration in green macroalgae spirogyra sp. of way ratai river pesawaran regency lampung," *IOP Conference Series: Earth and Environmental Science*, vol. 1027, no. 1, Article ID 012031, 2022.

[8] S. Birghila, N. Matei, S. Dobrinas, P. Viorica, S. Alina, and N. Anamaria, "Assessment of heavy metal content in soil and Lycopersicon esculentum (Tomato) and their health implications," *Biological Trace Element Research*, pp. 1-2, 2022.

[9] A. A. Bosede and O. Omokaro, "Comparative effect of firewood and automobile tyre flaring on polycyclic aromatic hydrocarbons (PAHs) and heavy metal content of abattoir soils in rivers states," *International Journal of Microbiology and Biotechnology*, vol. 7, no. 2, 2022.

[10] J. Kamil and K. Mirosław, "The toxicological assessment of content and exposure of heavy metals (Pb and Cd) in traditional herbal medicinal products with marshmallow root (althaea officinalis L., radix) from polish pharmacies," *Toxics*, vol. 10, no. 4, 2022.

[11] T. Ali, A. Massimo, A. Giovanna et al., "Heavy metal content and potential ecological risk assessment of sediments from Khnifiss Lagoon National Park (Morocco)," *Environmental Monitoring and Assessment*, vol. 194, no. 5, 2022.

[12] H. M. A. Alhussaini, M. A. Hossain, and S. S. Arputhanantham, "Determination of toxic heavy metal content in a whitening creams by using inductively coupled plasma-optical emission spectrometry," *Arabian Journal of Geosciences*, vol. 15, no. 8, p. 692, 2022.

[13] M. Wyszkowski and N. Kordala, "Role of different material amendments in shaping the content of heavy metals in maize (Zea mays L.) on soil polluted with petrol," *Materials*, vol. 15, no. 7, p. 2623, 2022.

[14] X. Sun, T. Yu, Yi Huang et al., "Effects of different heat treatment methods on organic pollutants and heavy metal content in oil sludge waste and ecotoxicological evaluation," *Applied Sciences*, vol. 12, no. 7, p. 3609, 2022.

[15] D. A. Antonenko, Y. Y. Nikiforenko, O. A. Melnik, D. A. Yurin, and A. A. Danilova, "Organomineral compost and its effects for the content of heavy metals in the top layer leached chernozem," *IOP Conference Series: Earth and Environmental Science*, vol. 1010, no. 1, Article ID 012028, 2022.

[16] A. S. Sheshnev and M. V. Reshetnikov, "Mineral composition and seasonal dynamics of the content of heavy metals in bed loads of ravines and small rivers in the city of Kamyshin (Volgograd oblast, Russia)," *IOP Conference Series: Earth and Environmental Science*, vol. 1010, no. 1, Article ID 012030, 2022.

[17] S. E. Pałka, E. Drąg-Kozak, Ł. Migdał, and M. Kmiecik, "Effect of a diet supplemented with nettle (urtica dioica L.) or fenugreek (trigonella foenum-graecum L.) on the content of selected heavy metals in liver and rabbit meat," *Animals*, vol. 12, no. 7, p. 827, 2022.

[18] H. Yang, H. Xu, and X. Zhong, "Prediction of soil heavy metal concentrations in copper tailings area using hyperspectral reflectance," *Environmental Earth Sciences*, vol. 81, no. 6, p. 183, 2022.

[19] B. K. Mavakala, P. Sivalingam, A. Laffite et al., "Evaluation of heavy metal content and potential ecological risks in soil samples from wild solid waste dumpsites in developing country under tropical conditions," *Environmental Challenges*, vol. 7, Article ID 100461, 2022.

[20] S. Alcides, E. Domínguez-Álvarez, C. Yuan et al., "On the use of metallic nanoparticulated catalysts for in-situ oil upgrading," *Fuel*, vol. 313, 2022.

Hindawi
Computational Intelligence and Neuroscience
Volume 2022, Article ID 3749635, 10 pages
https://doi.org/10.1155/2022/3749635

Research Article

Foreign Object Detection in Railway Images Based on an Efficient Two-Stage Convolutional Neural Network

Weixun Chen, Siming Meng, and Yuelong Jiang

Information Engineering Institute, Guangzhou Railway Polytechnic, Guangzhou 510430, China

Correspondence should be addressed to Weixun Chen; chenweixun@gtxy.edu.cn

Received 21 July 2022; Accepted 12 August 2022; Published 28 August 2022

Academic Editor: Yaxiang Fan

Copyright © 2022 Weixun Chen et al. This is an open access article distributed under the Creative Commons Attribution License, which permits unrestricted use, distribution, and reproduction in any medium, provided the original work is properly cited.

Foreign object intrusion is one of the main causes of train accidents that threaten human life and public property. Thus, the real-time detection of foreign objects intruding on the railway is important to prevent the train from colliding with foreign objects. Currently, the detection of railway foreign objects is mainly performed manually, which is prone to negligence and inefficient. In this study, an efficient two-stage framework is proposed for foreign object detection in railway images. In the first stage, a lightweight railway image classification network is established to classify any input railway images into one of two classes: normal or intruded. To enable real-time and accurate classification, we propose an improved inverted residual unit by introducing two improvements to the original inverted residual unit. First, the selective kernel convolution is used to dynamically select kernel size and learn multiscale features from railway images. Second, we employ a lightweight attention mechanism, called the convolutional block attention module, to exploit both spatial and channel-wise relationships between feature maps. In the second stage of our framework, the intruded image is fed to the foreign object detection network to further detect the location and class of the objects in the image. Experimental results confirm that the performance of our classification network is comparable to the widely used baselines, and it obtains outperforming efficiency. Moreover, the performances of the second-stage object detection are satisfying.

1. Introduction

Railway transport is becoming one of the most popular means of transportation worldwide because of its advantages such as faster speed, higher cost-effectiveness, and better customer comfort [1]. Until the middle of 2021, the national rail operation mileage of China had exceeded 146,300 km. Moreover, according to the latest railway network planning in China, this figure will reach 175,000 km in 2025. However, along with the rapid development of railway transportation, concerns about the accompanying safety issues are also raised, which relate to public property and human life.

Foreign object (obstacle) intrusion is one of the main factors threatening railway safety. In the past, railway safety protection facilities mainly protected the railway from foreign objects by setting up protective nets. However, the protective nets have limited protection against foreign objects with greater mobility, such as pedestrians, large animals, and falling rocks caused by landslides. Collisions of trains with such foreign objects occur from time to time, resulting in large economic loss and casualties. Moreover, railways usually cross remote areas, and if train collisions with foreign objects occur in remote uninhabited places, the rescue will be extremely difficult [2]. Thus, the detection of foreign objects intruding on the railway line is of great significance.

At present, foreign object detection is mainly performed by traditional manual methods [3], which are labor-intensive and time-consuming. Besides, due to the low efficiency of manual methods, it often occurs that foreign objects, such as pedestrians, move to other areas before they are detected. Although the implementation of video monitoring systems greatly improves the detection range and speed, it requires observers to focus on the monitoring video at all times. In

particular, to take timely measures to avoid accidents when the train is running at high speed, the system should respond to foreign object intrusion in real time. However, it is infeasible to achieve reliable real-time and 24-hour monitoring via manual methods. Hence, it is significant to automatically detect foreign objects by monitoring video in real time. Early methods typically employ traditional computer vision algorithms [4, 5] or machine learning techniques [6] to detect foreign objects in railway videos or images. However, these methods failed to balance efficiency and accuracy. In other words, they either suffered from low efficiency or failed to meet the efficiency requirements of the foreign object detection systems or poor robustness when faced with various weather and light conditions. Therefore, research into novel real-time computer vision-based foreign object detection methods that can compensate for the shortcomings of traditional methods is demanded for the safety of railways. In this study, we focus on automatically and efficiently detecting foreign objects in railway images captured by a video monitor.

Deep learning-based methods have demonstrated their superiority in various computer vision tasks in recent years, leading to breakthroughs in various fields, including object detection [7], image classification [8], and image segmentation [9].

By employing deep learning techniques, for example, convolutional neural networks (CNNs), it is possible to develop an efficient and effective foreign object detection system for railways. Early attempts have been made to use CNNs for foreign object detection in railway images [10]. However, the efficiency and accuracy of these methods still have room for improvement.

In this work, a two-stage framework is proposed for efficient foreign object detection in railway images. In the first stage, a railway image classification network is proposed to classify any input railway images into one of two classes: normal and intruded. The "normal" class means the railway image is normal without intrusion, and the "intruded" class means there are foreign objects in the images. Then, if the image is classified into the "intruded" class, it will be fed to the second-stage foreign object detection network to further detect the location and class of the objects in the image. The motivation for setting up the first-stage classification network is to improve the efficiency of the foreign object detection system. In particular, by introducing a lightweight classification network in the first stage, the foreign object detection system can scan the railway scenery at a relatively high speed. The second-stage network that has a slower speed can be called only when objects appear in the image. This way, the overall efficiency of the system is increased, because, in most of the cases, there is no foreign object in the images.

To build the first-stage lightweight classification network, we propose an improved inverted residual unit by implementing the selective kernel convolution [11] and the convolutional block attention module (CBAM) [12] to the inverted residual unit [13]. In the second stage, we directly employ the You Only Look Once v3 (YOLOv3) [14] as our object detector. In Figure 1, we show the overall workflow of our proposed method.

2. Related Works

The recent works of foreign object detection methods for railways are introduced in this section.

2.1. Traditional Computer Vision and Machine Learning-Based Methods. Salman *et al.* [15] proposed a video analysis-based method for railway foreign object detection. Firstly, the system extracts the target area through optical flow segmentation to detect moving objects. Then, based on the center of the rectangular box corresponding to the object, the ideal trajectory of the center of the object is estimated by designing an implicit Markov model. Ruder et al. [16] proposed a method for obstacle detection in front of the train using edge and texture characteristics of images and optical flow method. Then, they used the Kalman filter [17] to track the targets in images. Oh et al. [18] proposed a passenger safety monitoring system for railroad stations. Through an information fusion module, the video input by the camera is analyzed, and the position of the foreign objects within the railway is located by a stereo vision algorithm. Teng et al. [1] proposed a superpixel-based method for railway foreign object detection, which combines a term frequency-inverse document frequency such as transform and machine learning techniques. Mukojima et al. [19] proposed background subtraction for foreign object detection on railway tracks.

Most of the aforementioned methods typically employed handcrafted features or traditional machine learning techniques. Thus, the applicability and robustness of these methods may fail to overcome the challenges of complicated and various railway scenarios. Recently, convolutional neural networks (CNN)-based methods have shown outstanding performances than traditional computer vision-based methods in a variety of fields. CNNs can learn semantic features from sufficient training data, which get rid of the trouble of traditional manual feature construction. In the following, we introduce the recent progresses of CNNs for foreign object detection methods in railways.

2.2. Deep Learning-Based Methods. Ye et al. [20] proposed an end-to-end object detection network, DFF-Net, to detect foreign objects in railways, achieving trade-off between efficiency and accuracy. Cong et al. [21] employed the YOLOv3 [14] model to detect foreign objects on railway tracks. Wang et al. [22] proposed a CNN for foreign object detection by employing residual neural network as main network and a part of single-shot multi-box detection [23] for feature fusion. For vehicle intrusion detection in railway images, Aminmansour et al. [24] designed a region proposal algorithm for generating patches from images and used a CNN to classify the patches. Ye et al. [25] detect foreign objects in front of the train in shunting mode via a feature.

Fusion refine neural network (FR-Net) employed the depthwise-pointwise convolution.

Rail area detection is an important part of a foreign object detection system. For this purpose, Wang et al. [26] proposed a CNN architecture to classify the rail area in pixel-

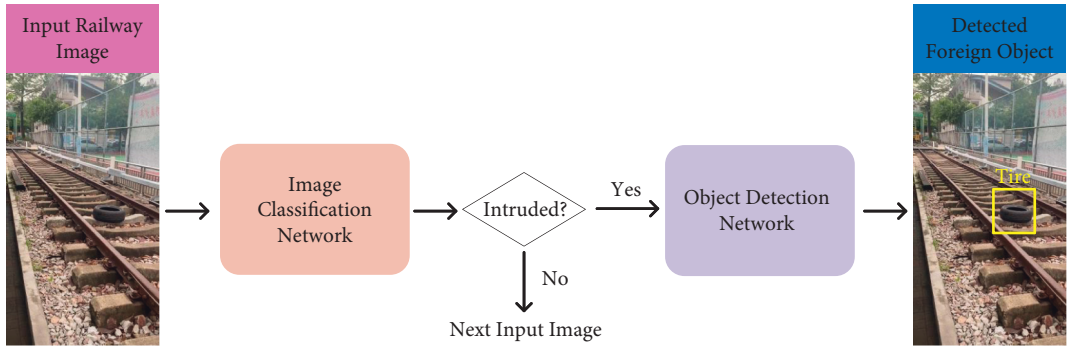

Figure 1: Workflow of the proposed foreign object detection method.

level accuracy, followed by a polygon fitting-based contour optimization method to refine detection results. Wang et al. [27] designed an algorithm for the detection of foreign object intrusion based on adaptive track segmentation. A CNN model was built to classify the track area and the other areas. To overcome the lack of intruding foreign object training samples and provide sufficient training data to the deep learning-based railway foreign object detection methods, Guo et al. [28] developed a C-DCGAN to generate railway images with foreign object intrusion.

Though there are many CNN-based methods for real-time foreign object detection in railway images, the efficiency and accuracy of the existing methods are still required to be further improved to meet the needs of safe railway operation.

3. Lightweight Railway Image Classification Network

To increase the efficiency of our method and achieve real-time processing, we build a lightweight network for railway image classification. Any input railway image will be classified into normal or intruded classes by the proposed classification network. In Figure 2, we show the overall architecture of our network. To achieve higher efficiency without losing much accuracy, we use a similar concept of inverted residual unit (IRU) [13] and make two improvements to build our improved inverted residual unit (IIRU):

(1) We employ the selective kernel convolution [11] in the inverted residual block to dynamically select kernel size and learn multiscale features from railway images, resulting in the IIRU-SK.

(2) To further improve the performance of the proposed network, we employ a lightweight attention mechanism, called the convolutional block attention module (CBAM) [12], to exploit both spatial and channel-wise relationships between feature maps, resulting in the IIRU-CBAM.

In the following, we introduce the modules mentioned above and our IIRU.

3.1. Inverted Residual Unit. A typical inverted residual unit consists of three convolutional layers and uses depthwise separable convolution [29], as shown in Figure 3.

In the first layer of the inverted residual unit, a convolution kernel of size 1×1 is used to expand the input feature maps to a high dimension, followed by ReLU6 as the nonlinearity. Then, the second layer uses a depthwise convolution with kernel size 3×3 to further extract features and also uses ReLU6 as the nonlinearity.

Using depthwise convolution, a single convolutional filter is applied to each input channel. This way, computational costs are effectively reduced, and more convolutional kernels can be applied to this layer. Furthermore, in the third layer, a convolution kernel of size 1×1 is used to reduce the feature dimension. This step is called pointwise convolution. Finally, the output feature maps of the third convolutional layer are directly fed to the next block, which is called a linear bottleneck. A shortcut connection is built directly between the input and output layers. The depthwise separable convolution is composed of the depthwise convolution and the pointwise convolution.

Given an input tensor T_i of size $h_i \times w_i \times d_i$ and output a tensor T_o of size $h_i \times w_i \times d_o$, the computational cost of a depthwise separable convolution with kernel size $k \times k$ is as follows:

$$h_i \cdot w_i \cdot d_i\left(k^2 + d_o\right). \tag{1}$$

Regarding traditional $k \times k$ convolution, this cost becomes the following:

$$h_i \cdot w_i \cdot d_i \cdot k^2 \cdot d_o. \tag{2}$$

Dividing (1) by (2) yields

$$\frac{h_i \cdot w_i \cdot d_i\left(k^2 + d_o\right)}{h_i \cdot w_i \cdot d_i \cdot k^2 \cdot d_o} = \frac{1}{d_o} + \frac{1}{k^2}. \tag{3}$$

This means that compared with traditional convolutional layers depthwise separable convolution reduces computational costs by about k^2 times. This ensures real-time and accurate railway image classification.

3.2. Selective Kernel Convolution. Although the inverted residual unit has high efficiency, it sacrifices some of its accuracies. Thus, to improve the accuracy of our railway image classification network, we improve the inverted residual unit by replacing the depthwise convolution with

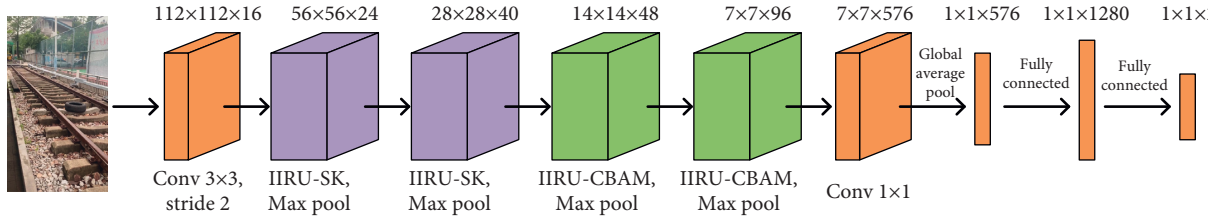

Figure 2: Overall architecture of the proposed railway image classification network. Each rectangle block represents a layer. The operations below the blocks are operations conducted on that layer, and the figures on top of the blocks are the output feature size of that layer. The IIRU-SK is the improved inverted residual unit combined with the selective kernel convolution, and IIRU-CBAM is the improved inverted residual unit combined with the convolutional block attention module.

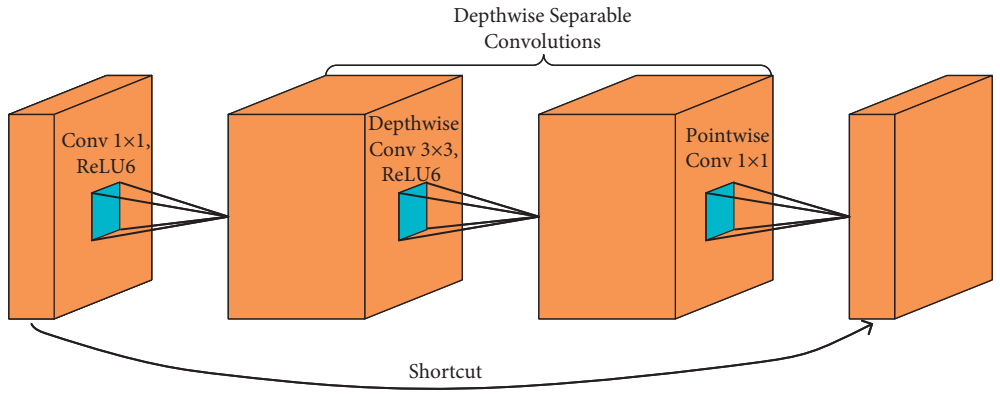

Figure 3: Schematic visualization of the inverted residual unit.

selective kernel (SK) convolution. Using the SK convolution, the network could capture the spatial information of different receptive field sizes in the railway images. Moreover, the SK convolution is computationally lightweight, which only slightly increases the computational burden and parameters of the network. This property is suitable for the efficiency and accuracy requirements of the railway foreign object detection system. In the following, we introduce the SK convolution detailedly.

SK convolution is composed of three main operators: *Split*, *Fuse,* and *Select*, as shown in Figure 4. The *Split* operator generates two paths with different kernel sizes. The *Fuse* operator combines the feature maps produced by the two paths and obtains the global selection weights. Based on the selection weights, the *Select* operator combines the feature maps generated by different paths.

Split: for a given input tensor T of size $h' \times w' \times d'$, two branches with convolution kernels of size 3×3 and 5×5 are used, respectively. Batch normalization and a ReLU nonlinearity are used after the convolutional operations, yielding two distinct feature maps $\widetilde{T}$ and $\widehat{T}$ of size $h \times w \times d$. For efficiency, the convolutional operations are depthwise convolutions and the 5×5 convolution is replaced with the 3×3 dilated convolution using a dilation size of 2. Although the input tensor can be split into multiple branches, in this work, we only use two branches for efficiency.

Fuse: since the two different branches carry information from different receptive fields, an effective fusion operation is required to aggregate the feature maps of the two branches. In particular, $\widetilde{T}$ and $\widehat{T}$ are first fused through an element-wise summation.

$$U = \widetilde{T} + \widehat{T}. \tag{4}$$

Then, a global average pooling F_{gp} is applied to produce $s \in \mathbb{R}^d$ that contains channel-wise information extracted by the *Split* operation. In particular, let s_j denote the jth element of s, and it is calculated as follows:

$$s_j = \frac{1}{h \times w} \sum_{m=1}^{h} \sum_{n=1}^{w} U_j(m, n). \tag{5}$$

Then, the compact features $z \in \mathbb{R}^{c \times 1}$ are generated using a fully connected layer F_{fc} as follows:

$$z = F_{fc}(s), \tag{6}$$

where $c = d/2$. Batch normalization and a ReLU nonlinearity are used after F_{fc}.

Select: the compact features z are then used to guide the information selection process. In particular, to choose information from different branches, a softmax attention is used to obtain the channel-wise weight vectors as follows:

$$a_l = \frac{e^{A_l z}}{e^{A_l z} + e^{B_l z}}, \qquad b_l = \frac{e^{B_l z}}{e^{A_l z} + e^{B_l z}}, \tag{7}$$

where $A, B \in \mathbb{R}^{d \times c}$ are trainable parameters and a, b are the weight vectors for $\widetilde{T}$ and $\widehat{T}$, respectively. A_l is the lth row of A and a_l is the lth element of a, likewise B_l and b_l.

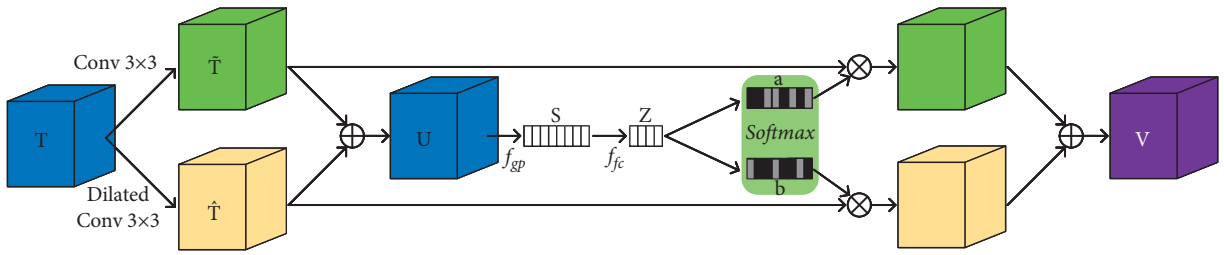

Figure 4: Schematic visualization of the selective kernel convolution.

Finally, the output feature map V is calculated by the weighted sum of the feature maps from the two branches as follows:

$$V_l = a_l \cdot \widetilde{T}_l + b_l \cdot \widehat{T}_l, \quad a_l + b_l = 1, \tag{8}$$

where $V = [V_1, V_2, \ldots, V_d]$ and $V_l \in \mathbb{R}^{h \times w}$.

3.3. Convolutional Block Attention Module (CBAM). Although there are more advanced attention mechanisms, such as the transformer [30], the computational costs of them are too high to fulfill the real-time requirements of the foreign object detection system. Thus, we employ CBAM, a lightweight weight attention module, to improve the performance of our classification network. The input feature maps are adaptively refined by the channel-wise and spatial-wise attention maps through multiplication operation, as shown in Figure 5.

In particular, for a given input tensor T of size $h' \times w' \times d'$, CBAM firstly generates a 1D channel-wise attention map $M_c \in \mathbb{R}^{1 \times 1 \times d'}$ and then produces a 2D spatial-wise attention map $M_s \in \mathbb{R}^{h' \times w' \times 1}$. The feature refinement process can be summarized as follows:

$$\begin{aligned} T' &= M_c(T) \otimes T, \\ T'' &= M_s(T') \otimes T', \end{aligned} \tag{9}$$

where $\otimes$ is element-wise multiplication and T'' is the final refined output feature maps.

Channel-Wise Attention: in this module, the input tensor or feature map T is firstly processed by both average- and max-pooling operations across spatial dimension, resulting in two vectors T^c_{avg} and T^c_{max}, respectively. Then, the channel-wise attention map M_c is generated by feeding the two vectors to a shared multilayer perceptron (MLP) with one hidden layer. For efficiency, the hidden activation size is reduced by a factor r. The two output feature vectors of MLP are then merged via element-wise summation. To conclude, the channel-wise attention can be described as follows:

$$M_c(T) = \sigma\left(\text{MLP}\left(T^c_{\text{avg}}\right)\right) + \sigma\left(\text{MLP}\left(T^c_{\text{max}}\right)\right), \tag{10}$$

where σ is the sigmoid function.

Spatial-Wise Attention: given the output feature maps T' from the channel-wise attention, average pooling and max pooling across channel dimension are conducted to generate two 2D maps T^s_{avg} and T^s_{max}. Then, they are concatenated and convolved by a convolution layer of kernel size 7×7, generating the 2D spatial-wise attention map. In summary, the spatial-wise attention can be represented as follows:

$$M_s(T') = \sigma\left(f^{7\times7}\left(\left[T^s_{\text{avg}}; T^s_{\text{max}}\right]\right)\right), \tag{11}$$

where σ is the sigmoid function and $f^{7\times7}$ is the 7×7 convolutional operation.

3.4. Improved Inverted Residual Unit (IIRU). In Figure 6, we show the architecture of our proposed IIRU. In particular, we replace the depthwise convolution with the SK convolution, aiming at capturing the spatial information of different receptive field sizes in the railway images. Further, the trainable attention mechanism, CBAM, is implemented after the pointwise convolution layer to perform feature recalibration, which adaptively emphasizes important features and suppresses less useful ones. Note that to reduce computational costs, these two modules are optionally added to the inverted residual unit. Thus, we have two modes of the IIRU, which are IIRU-SK and IIRU-CBAM. IIRU-SK means IRU in combination with the SK convolution, and IIRU-CBAM means CBAM is implemented in IIRU.

4. Foreign Object Detection via YOLOv3

After classifying the railway images into normal or intruded classes, we employ the You Only Look Once v3 (YOLOv3) [14] to detect the foreign objects in the intruded images. Different from the two-stage object detection networks [31], YOLOv3 is a one-stage detector. By predicting the locations and classes of the objects in images using one-step regression, the efficiency of YOLOv3 is higher than the two-stage detectors, which is preferable to the foreign object detection system. Moreover, by introducing feature pyramid network (FPN) [32], YOLOv3 is robust to objects at different scales. This makes it suitable to detect foreign objects of different sizes in railway images, such as large objects like vehicles or small objects like boxes. In the following, we briefly introduce YOLOv3.

YOLOv3 uses DarkNet-53 as its backbone feature extractor, which is pretrained on the ImageNet dataset [8]. Its efficiency is about 1.5 to 2 times higher than ResNet-101 and ResNet-152, and the performance is comparable. After the backbone, the concept of FPN is employed to detect targets of different sizes at three different scales. Then, YOLOv3 predicts the locations and classes of the objects by adding several convolutional layers, which output feature maps on

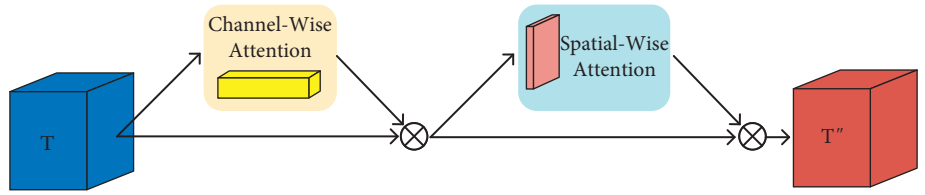

Figure 5: Schematic visualization of the CBAM.

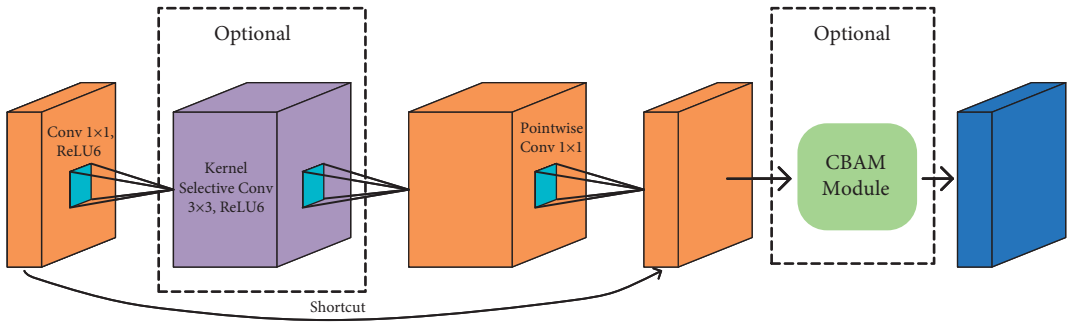

Figure 6: Schematic visualization of the improved inverted residual unit. Compared with the original inverted residual unit, we use SK convolution (purple block) to replace the depthwise convolution. To further improve the performance of the unit, we employ the CBAM mechanism (green box).

three different scales encoding the bounding box, objectness, and class predictions.

Based on the multiscale feature maps, three bounding boxes are predicted by YOLOv3 at each grid cell of the feature maps. Thus, for each scale, the size of the output tensor is $N \times N \times [3 * (4 + 1 + 3)]$, where N can be 13, 26, and 52 for the three different scales, and the numbers 3, 4, 1, and 3 correspond to three bounding boxes, four bounding box offsets, one objectness prediction, and three class predictions (there are three classes of objects in our work), respectively.

To determine the location of the objects, YOLOv3 predicts the center coordinates (b_x, b_y) of the bounding box with respect to the location of the grid cell. Then, it regresses the width b_w and height b_h of the predicted bounding box from a set of predefined reference boxes called anchors, whose width and height are predefined as p_w and p_h, respectively, as shown in Figure 7. Let (c_x, c_y) denote the cell's offsets from the top left corner of the image, and the predictions can be calculated as follows:

$$\begin{aligned} b_x &= \sigma(t_x) + c_x, \\ b_y &= \sigma(t_y) + c_y, \\ b_w &= p_w e^{t_w}, \\ b_h &= p_h e^{t_h}, \end{aligned} \tag{12}$$

where t_x, t_y, t_w, and t_h are the four predicted offsets of each bounding box and σ is the sigmoid function. The objectness score is predicted using logistic regression and the object class is predicted by independent logistic classifiers. More details of YOLOv3 can be found in [14].

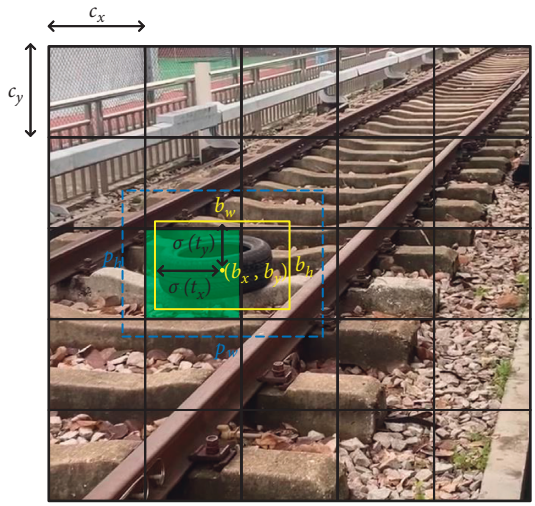

Figure 7: Illustration example of an anchor (blue) and a predicted bounding box (yellow).

5. Experiment and Analysis

5.1. Dataset. For the performance evaluation of our proposed method, we built a railway foreign objects dataset including 3145 railway images. It consists of 1523 normal railway images and 1622 intruded railway images. The size of the images is 720×1280 pixels. The normal railway images were taken from multiple views of a railway scenery that is located at the campus of Guangzhou Railway Polytechnic, Guangzhou, China (Figures 8(a) and 8(b)). To generate the intruded railway images, we placed several foreign objects on the railway and took photographs from multiple views. There are three types of foreign objects in 1622 intruded

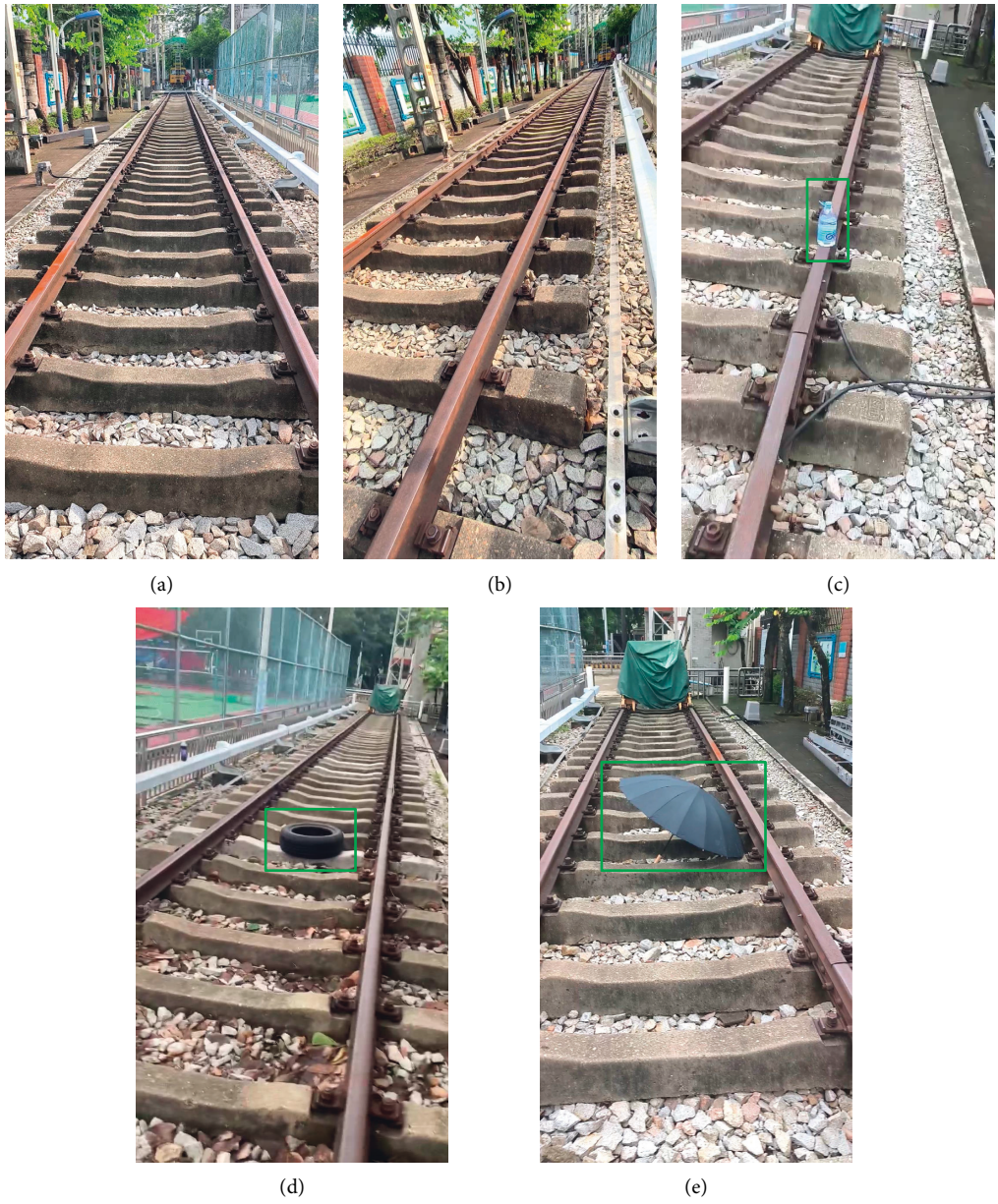

FIGURE 8: Illustration examples of the railway foreign object dataset. (a, b) Normal railway images. (c–e) Intruded railway images with corresponding reference bounding boxes (green) of the objects.

railway images, including 594 bottles, 712 tires, and 316 umbrellas, as shown in Figures 8(c)–8(e). These objects were selected to simulate possible foreign objects of different sizes intruding on the railway

The reference bounding boxes of the foreign objects were labelled manually.

Among 3145 images, we selected 1885 images to train the image classification network. The remaining 1260 images were used to evaluate their performance in the experiments. In particular, the training set consists of 912 normal images and 973 intruded images, and the test set consists of 611 normal images and 649 intruded images. Then, we used 1622 intruded images to evaluate the second-stage foreign object detection. The remaining 1523 normal images were not used in this stage because there is no object to detect in these images. In particular, 1021, 114, and 487 intruded images were split into training, validation, and testing images, respectively. There are 176 bottles, 204 tires, and 107 umbrellas in 487 test intruded images.

5.2. Implementation Details. The railway image classification network was trained using stochastic gradient descent (SGD) optimizer [33]. The momentum was 0.9, the initial

Table 1: Results of comparison with other deep learning-based classification baselines for railway image classification.

	Mean precision (%)	Mean recall (%)	Mean F1 measure (%)	FPS	Model size (M)
Proposed	96.88	96.82	96.85	72.18	0.90
ViT	97.51	97.48	97.49	38.94	85.80
MobileNetV2	96.25	96.19	96.22	59.58	2.23
ResNet-50	96.66	96.24	96.64	52.23	23.51

Figure 9: Illustration examples of the detected railway foreign objects.

learning rate was 0.01, and the weight decay was 0.0005. We set the training batch size to 32. The input images were resized to 224×224 pixels during training.

We also trained the YOLO v3 using the SGD optimizer with the same settings. The training batch size was set to 16, and the input images were resized to 416×416 pixels during training.

All the experiments were carried out on a workstation with a single Titan Xp GPU.

5.3. Evaluation Metrics. We use precision, recall, and F1 measure to evaluate the accuracy of the image classification network, which are calculated as follows:

$$\begin{aligned} \text{Precision} &= \frac{\text{TP}}{\text{TP} + \text{FP}}, \\ \text{Recall} &= \frac{\text{TP}}{\text{TP} + \text{FN}}, \\ F1 - \text{Measure} &= \frac{2\text{TP}}{2\text{TP} + \text{FP} + \text{FN}}, \end{aligned} \tag{13}$$

where TP is true positive, FP is false positive, and FN is false negative.

Moreover, the mean average precision (mAP) [34] was used to evaluate the accuracy of foreign object detection.

Finally, we used frames per second (FPS) to evaluate the efficiency of the compared models.

5.4. Experimental Results of Railway Image Classification. In this part, the performances of the railway image classification network are evaluated, in terms of accuracy and efficiency. Three widely used deep learning-based image classification baselines were compared, including vision transformer (ViT) [35], ResNet-50 [36], and MobileNetV2 [13].

In Table 1, we show the comparison results of our proposed railway image classification network with other deep learning-based image classification baselines. We can see that the performances of all the compared models are close to each other. This confirms the performance of our proposed classification network. Although the latest model, ViT, obtained the best performance among all the compared models, its FPS is the lowest and far from reaching the efficiency requirements of the foreign object detection system. Although the mean F1 measure of our model is 0.64% lower than that of ViT, its FPS is the highest and reaches 72.18. Since the FPS of the video produced by the ordinary monitoring system is 60, the FPS of the classification network should exceed 60 so that it can process the video images in real time. From Table 1, we can see that only the efficiency of our proposed model satisfies the real-time requirement of the ordinary video monitoring system, and the other compared models fail to meet this requirement.

Further, from the model size, we can see that our network is very lightweight. The number of parameters is only about 1% of ViT and 40% of MobileNetV2. Thus, our

network is much more suitable to implement in a foreign object detection system that has limited computational resources. The experimental results demonstrate that our proposed classification network has higher practical value than the compared methods, because of its relatively high accuracy and outperforming efficiency.

5.5. Experimental Results of Foreign Object Detection. Here, the foreign object detection accuracy and efficiency of YOLOv3 in the second stage are demonstrated. Figure 9 illustrates the detection results of the three types of objects. The mAP of YOLOv3 on 487 test images is 85.89%, and the FPS is 32.6. It can be seen that although the accuracy of YOLOv3 is satisfying in our dataset, its efficiency is relatively low. If the foreign object detection system only uses YOLOv3 in all the scenery, it cannot achieve real-time detection. Thus, using our classification network in the first stage, the efficiency of the foreign object detection system is increased.

Further, to simulate the real operation of the foreign object detection system, we test our two-stage framework on all 3145 images in our dataset. In particular, following the workflow illustrated in Figure 1, we feed all these images into our two-stage framework. Then, if there is no foreign object in the current image, the next image will be fed to the framework; otherwise, YOLOv3 will be used to detect foreign objects in the image. Finally, the FPS of our two-stage framework reaches 51.77, which is close to the 60 FPS requirement of the foreign object detection system.

6. Conclusion

This study proposes a two-stage framework for efficient foreign object detection in railway images. The first stage is a railway image classification network that classifies any input railway images into one of two classes: normal and intruded. Then, if the image is classified into the "intruded" class, it will be fed to the second-stage foreign object detection network to further detect the location and class of the objects in the image. By setting the first-stage classification network, we increase the efficiency of the foreign object detection system.

To build the first-stage lightweight classification network, we propose an improved inverted residual unit by implementing the selective kernel convolution and the convolutional block attention module (CBAM) to the inverted residual unit. The experimental results show that the practical value of our proposed classification network is higher than that of the compared methods, because of its relatively high accuracy and outperforming efficiency.

Data Availability

The datasets used and analyzed during this study are available from the corresponding author upon request.

Conflicts of Interest

The authors declare that there are no conflicts of interest.

Acknowledgments

The research was supported by the Innovation Team Project of Guangdong Province General University (Natural Science) under grant 2021KCXTD068.

References

[1] Z. Teng, F. Liu, and B. Zhang, "Visual railway detection by superpixel based intracellular decisions," *Multimedia Tools and Applications*, vol. 75, no. 5, pp. 2473–2486, 2015.

[2] T. Xiao, Y. Xu, and H. Yu, "Research on obstacle detection method of urban rail transit based on multisensor technology," *Journal of Artificial Intelligence and Technology*, vol. 1, no. 1, pp. 61–67, 2021.

[3] D. He, Z. Zou, Y. Chen, B. Liu, and J. Miao, "Rail transit obstacle detection based on improved CNN," *IEEE Transactions on Instrumentation and Measurement*, vol. 70, pp. 1–14, 2021.

[4] C. Wei, Y. Huang, Y. Wang, and M. Shih, "Background recovery in railroad crossing videos via incremental low-rank matrix decomposition," in *Proceedings of the 2013 2nd IAPR Asian Conference on Pattern Recognition*, pp. 702–706, Naha, Japan, November 2013.

[5] Y. R. Pu, L. W. Chen, and S. H. Lee, "Study of moving obstacle detection at railway crossing by machine vision," *Information Technology Journal*, vol. 13, no. 16, pp. 2611–2618, 2014.

[6] P. F. Felzenszwalb, R. B. Girshick, D. McAllester, and D. Ramanan, "Object detection with discriminatively trained part-based models," *IEEE Transactions on Pattern Analysis and Machine Intelligence*, vol. 32, no. 9, pp. 1627–1645, 2010.

[7] Z. Q. Zhao, P. Zheng, S. T. Xu, and X. Wu, "Object detection with deep learning: a review," *IEEE Transactions on Neural Networks and Learning Systems*, vol. 30, no. 11, pp. 3212–3232, 2019.

[8] J. Deng, W. Dong, R. Socher, L. -J. Li, L. Kai, and L. Fei-Fei, "Imagenet: a large-scale hierarchical image database," in *Proceedings of the 2009 IEEE Conference on Computer Vision and Pattern Recognition*, pp. 248–255, Miami, FL, USA, June 2009.

[9] S. Minaee, Y. Boykov, F. Porikli, A. Plaza, N. Kehtarnavaz, and D. Terzopoulos, "Image segmentation using deep learning: a survey," *IEEE Transactions on Pattern Analysis and Machine Intelligence*, vol. 44, no. 7, pp. 3523–3542, 2022.

[10] J. Li, F. Zhou, and T. Ye, "Real-world railway traffic detection based on faster better network," *IEEE Access*, vol. 6, pp. 68730–68739, 2018.

[11] X. Li, W. Wang, X. Hu, and J. Yang, "Selective kernel networks," in *Proceedings of the 2019 the IEEE Conference on Computer Vision and Pattern Recognition*, pp. 510–519, Long Beach, CA, USA, June 2019.

[12] S. Woo, J. Park, J. Lee, and I. Kweon, "Cbam: convolutional block attention module," in *Proceedings of the 2018 The European Conference on Computer Vision*, pp. 3–19, Munich, Germany, September 2018.

[13] M. Sandler, A. Howard, M. Zhu, A. Zhmoginov, and L. Chen, "Mobilenetv2: inverted residuals and linear bottlenecks," in *Proceedings of the 2018 IEEE Conference on Computer Vision and Pattern Recognition*, pp. 4510–4520, Salt Lake City, UT, USA, June 2018.

[14] J. Redmon and A. Farhadi, "Yolov3: an Incremental Improvement," 2018, https://arxiv.org/abs/1804.02767.

[15] H. Salmane, L. Khoudour, and Y. Ruichek, "A video-analysis-based railway–road safety system for detecting hazard

situations at level crossings," *IEEE Transactions on Intelligent Transportation Systems*, vol. 16, no. 2, pp. 1–14, 2015.

[16] M. Ruder, N. Mohler, and F. Ahmed, "An obstacle detection system for automated trains," in *Proceedings of the IEEE 4th 2003 Intelligent Vehicles Symposium*, pp. 180–185, Columbus, OH, USA, July 2003.

[17] F. Auger, M. Hilairet, J. M. Guerrero, E. Monmasson, T. Orlowska-Kowalska, and S. Katsura, "Industrial applications of the Kalman filter: a review," *IEEE Transactions on Industrial Electronics*, vol. 60, no. 12, pp. 5458–5471, 2013.

[18] S. Oh, G. Kim, W. Jeong, and Y. Park, "Vision-based object detection for passenger's safety in railway platform," in *Proceedings of the 2008 International Conference on Control, Automation and Systems*, pp. 2134–2137, Seoul, Korea (South), October 2008.

[19] H. Mukojima, D. Deguchi, Y. Kawanishi et al., "Moving camera background-subtraction for obstacle detection on railway tracks," in *Proceedings of the 2016 IEEE International Conference on Image Processing*, pp. 3967–3971, Phoenix, AZ, USA, September 2016.

[20] T. Ye, X. Zhang, Y. Zhang, and J. Liu, "Railway traffic object detection using differential feature fusion convolution neural network," *IEEE Transactions on Intelligent Transportation Systems*, vol. 22, no. 3, pp. 1375–1387, 2021.

[21] Z. Cong and X. Li, "Track obstacle detection algorithm based on YOLOv3," in *Proceedings of the 2020 13th International Congress on Image and Signal Processing, BioMedical Engineering and Informatics*, pp. 12–17, Chengdu, China, October 2020.

[22] Y. Xu, C. Gao, L. Yuan, S. Tang, and G. Wei, "Real-time obstacle detection over rails using deep convolutional neural network," in *Proceedings of the 2019 IEEE Intelligent Transportation Systems Conference*, pp. 1007–1012, Auckland, New Zealand, October 2019.

[23] W. Liu, D. Anguelov, D. Erhan et al., "Ssd: single shot multibox detector," in *Proceedings of the European Conference on Computer Vision*, pp. 21–37, Amsterdam, the Netherlands, October 2016.

[24] S. Aminmansour, F. Maire, G. Larue, and C. Wullems, "Improving near-miss event detection rate at railway level crossings," in *Proceedings of the 2015 International Conference on Digital Image Computing: Techniques and Applications*, pp. 1–8, Adelaide, Australia, November 2015.

[25] T. Ye, B. Wang, P. Song, and J. Li, "Automatic railway traffic object detection system using feature fusion refine neural network under shunting mode," *Sensors*, vol. 18, no. 6, p. 1916, 2018.

[26] Z. Wang, X. Wu, G. Yu, and M. Li, "Efficient rail area detection using convolutional neural network," *IEEE Access*, vol. 6, pp. 77656–77664, 2018.

[27] Y. Wang, L. Zhu, Z. Yu, and B. Guo, "An adaptive track segmentation algorithm for a railway intrusion detection system," *Sensors*, vol. 19, no. 11, p. 2594, 2019.

[28] B. Guo, G. Geng, L. Zhu, H. Shi, and Z. Yu, "High-speed railway intruding object image generating with generative adversarial networks," *Sensors*, vol. 19, no. 14, p. 3075, 2019.

[29] F. Chollet, "Xception: deep learning with depthwise separable convolutions," in *Proceedings of the 2017The IEEE Conference on Computer Vision and Pattern Recognition*, pp. 1251–1258, Honolulu, HI, USA, July 2017.

[30] A. Vaswani, N. Shazeer, N. Parmar et al., "Attention is all you need," *Advances in Neural Information Processing Systems*, vol. 30, 2017.

[31] S. Ren, K. He, R. Girshick, J. Sun, and R.-C. N. N. Faster, "Faster R-CNN: towards real-time object detection with region proposal networks," *IEEE Transactions on Pattern Analysis and Machine Intelligence*, vol. 39, no. 6, pp. 1137–1149, 2017.

[32] T. Lin, P. Dollár, R. Girshick, K. He, B. Hariharan, and S. Belongie, "Feature pyramid networks for object detection," in *Proceedings of the 2017 IEEE Conference on Computer Vision and Pattern Recognition*, pp. 2117–2125, Honolulu, HI, USA, July 2017.

[33] Y. LeCun, L. Bottou, Y. Bengio, and P. Haffner, "Gradient based learning applied to document recognition," *Proceedings of the IEEE*, vol. 86, no. 11, pp. 2278–2324, 1998.

[34] M. Everingham, L. Van Gool, C. K. I. Williams, J. Winn, and A. Zisserman, "The PASCAL visual object classes (VOC) challenge," *International Journal of Computer Vision*, vol. 88, no. 2, pp. 303–338, 2010.

[35] A. Dosovitskiy, L. Beyer, A. Kolesnikov et al., "An image is 11 worth 16x16 words: transformers for image recognition at scale," in *Proceedings of the 2021 International Conference on Learning Representations*, Vienna, Austria, May 2021.

[36] K. He, X. Zhang, S. Ren, and J. Sun, "Deep residual learning for image recognition," in *Proceedings of the 2016 IEEE Conference on Computer Vision and Pattern Recognition*, pp. 770–778, Las Vegas, NV, USA, June 2016.

Hindawi
Computational Intelligence and Neuroscience
Volume 2022, Article ID 8282854, 5 pages
https://doi.org/10.1155/2022/8282854

Research Article

Intelligent Financial Auditing Model Based on Deep Learning

Xiaofeng Dai[1,2] **and Weidong Zhu**[2]

[1]*Department of Engineering Management, Anhui Audit College, Hefei 230601, China*
[2]*School of Management, Hefei University of Technology, Hefei 230009, China*

Correspondence should be addressed to Xiaofeng Dai; 2008003@ahsjxy.edu.cn

Received 17 July 2022; Accepted 16 August 2022; Published 28 August 2022

Academic Editor: Yaxiang Fan

Copyright © 2022 Xiaofeng Dai and Weidong Zhu. This is an open access article distributed under the Creative Commons Attribution License, which permits unrestricted use, distribution, and reproduction in any medium, provided the original work is properly cited.

The entire auditing process is complicated and tedious and requires a lot of human resources. Therefore, the intelligent development of auditing is the general trend. In order to improve the audit quality, this paper establishes an intelligent financial audit model that can predict the audit opinion of the consolidated financial statements. This paper proposes an audit opinion prediction model based on the fusion of deep belief neural network (DBN) and long-short term memory (LSTM). First, an indicator system is established for audit opinions, and multiple financial parameters are used to describe possible audit opinions. On this basis, a DBN network is designed to complete deep feature extraction and used for LSTM training. According to the prediction model obtained by training, the subsequent audit opinion can be scientifically predicted. In the experiment, the method in this paper is tested based on financial audit related data sets and compared with the prediction results of traditional multilayer perceptron (MLP), convolutional neural network (CNN), and LSTM models. The results verify the validity and reliability of the model in this paper.

1. Introduction

As an external corporate governance mechanism, auditing plays an important role. The governance effect of auditing is directly reflected in the quality of auditing. The overall objective of an audit is to obtain reasonable assurance that the financial statements are free from material misstatement due to fraud or error. It aims to issue an audit report in accordance with auditing standards and to communicate with the client's management [1–3]. To achieve these goals, under the modern risk-oriented audit model, the main line of audit work requires auditors to identify, evaluate, and respond to the risks of material misstatement. Consistent with audit objectives, audit quality refers to the joint probability that auditors detect and report material misstatements. The realization process of audit quality can be summarized as finding, adjusting, and reporting material misstatements to achieve audit quality. How to achieve audit objectives and improve audit quality has always been the focus of audit research.

In the above context, many scholars have established models for predicting audit opinions and used these models to plan audit procedures. It was used as a quality control tool in the commitment review stage and to analyze variables that affect the probability of obtaining a qualified opinion. Reference [4] constructed a multicategory audit opinion prediction model based on the back propagation (BP) neural network method and tested it. Reference [5] used multiple financial indicators as eigenvalues of modeling data for the four types of audit opinions issued by companies and established a multicategory audit opinion prediction model based on error correction output coding and support vector machine (SVM). Reference [6] established a two-category prediction model of bank loan risk level classification authenticity audit based on SVM. However, most models for forecasting audit opinions have only been developed in the context of individual financial statements, and none of the models dealt with consolidated financial statements. In recent years, the rapid development of deep learning algorithms has provided a good tool for data prediction. Deep learning models such as multilayer perceptron (MLP), convolutional neural network (CNN), deep belief neural network (DBN), and long-short term memory (LSTM) have been widely used and verified in various aspects such as

traffic flow, enterprise risk, equipment life, and so on [7–12]. In the field of financial auditing, the continuous application of new models and algorithms to improve forecast accuracy is an important aspect in the future.

Based on the existing literature, this paper designs a model that can predict audit opinions on consolidated financial statements based on a deep learning model. The proposed method combines DBN and LSTM. Among them, DBN is mainly used for deep feature learning to extract discriminative features from massive financial design data. On this basis, the LSTM is trained through the extracted features to build a prediction model. In the experiment, verification is carried out based on real corporate financial data. The samples were divided into the unqualified opinion group and the qualified opinion group during model training and provided a set of initial explanatory variables for the consolidated financial statements. These variables include financial parameters (efficiency, liquidity, profitability, solvency, productivity, and scale), corporate governance measures, and other qualitative parameters. After experimental verification, the method in this paper has performance advantages compared with several existing prediction methods.

2. Deep Learning Models and Prediction Algorithms

2.1. LSTM. LSTM is a variant of the traditional recurrent neural network (RNN). Since RNN is trained by time series gradient descent, the network may experience the problem of gradient disappearance or gradient explosion when the sequence is long and the feedback adjustment is performed. To overcome this problem, researchers proposed to use LSTM gating units to replace RNN units, making the network robust to prevent gradient vanishing (and exploding). So, the modified networks are suitable for training and classifying long time series [13–15].

Figure 1 shows the basic LSTM unit structure. The key to LSTM is the state of the cell C_t. In order to add or delete the information in the cell, 3 gates are used in LSTM to control the training, namely the forgetting gate, the input gate, and the output gate. The gate determines the way the information passes through and protects and controls the cell state.

The forget gate uses a sigmoid layer to determine the information to be deleted in the cell state, which is calculated according to formula (1). For the input x_t and h_{t-1}, the forget gate will output a number in the range [0, 1] and put it into the cell state C_{t-1}. When it is 0, all are deleted; when it is 1, all are retained.

$$f_t = \sigma\left(W_f \cdot \left[h_{t-1}, x_t\right] + b_f\right). \tag{1}$$

In equation (1), x_t is the input at time t; h_t is the hidden layer state at time t; f_t is the output state of the forget gate at time t; σ is the sigmoid activation function; W_f is the weight matrix; b_f is the bias vector. The process of adding new information to a cell can be divided into two steps. First, LSTM uses an input gate containing a sigmoid layer to determine which information should be retained. The calculation process is represented by equation (2). Second, it uses a tanh function to generate a vector for these information, which is used to update the cell state $\widetilde{C}_t$. The calculation process is represented by equation (3).

$$i_t = \sigma\left(W_i \cdot \left[h_{t-1}, x_t\right] + b_i\right), \tag{2}$$

$$\widetilde{C}_t = \tanh\left(W_C \cdot \left[h_{t-1}, x_t\right] + b_C\right). \tag{3}$$

On the basis of the forget gate and the input gate, the cell state can be updated according to the following equation:

$$C_t = f_t \cdot C_{t-1} + i_t \cdot \widetilde{C}_t, \tag{4}$$

where $f_t \cdot C_{t-1}$ indicates the information to be deleted; $i_t \cdot \widetilde{C}_t$ refers to the newly added information.

The output gate determines the output content of LSTM, and the calculation is shown in equations (5) and (6). First, the sigmoid function is used to determine the cell content to be output, and then the tanh function is used to convert the cell state value between −1 and 1 to obtain the final output:

$$O_t = \sigma\left(W_o \cdot \left[h_{t-1}, x_t\right] + b_O\right), \tag{5}$$

$$h_t = O_t \times \tanh C_t. \tag{6}$$

After the forward propagation, the output of the LSTM is connected to the fully connected layer, and the softmax classifier is used for processing to obtain the corresponding prediction result.

2.2. DBN. A multilayer restricted Boltzmann machine (RBM) is a neuroperceptron [16]. It [17] consists of an explicit layer and a hidden layer. The neurons in the two-layer structure are binary units, and the value of each neuron is 0 or 1. The RBM of each layer is through the contrastive divergence (CD) algorithm to achieve fast training. The basic structure of RBM is shown in Figure 2.

In the figure, v represents the visible layer; h represents the hidden layer; w is the connection weight between the visible layer and the hidden layer; a is the bias vector of the visible layer.

The energy function of RBM can be expressed as

$$E(v, h) = -\sum_{i=1}^{n} b_i v_i - \sum_{j=1}^{m} c_j h_j - \sum_{i=1}^{n}\sum_{j=1}^{m} w_{ij} v_i h_j. \tag{7}$$

Accordingly, in a layer of RBM, the probability of the hidden layer neurons being activated is

$$P\left(h_i|v\right) = \sigma\left(b_i + \sum_i w_{ij} v_i\right). \tag{8}$$

The core of DBN is composed of multilayer RBM and one-layer back-propagation neural network [18–20]. Among them, the core function of RBM is to do unsupervised learning. Through recursive RBM, the characteristics of information can be reflected in various types of sample spaces. RBM sets the feature factors that have been trained as the input, uses parameters, adjusts the network layer by

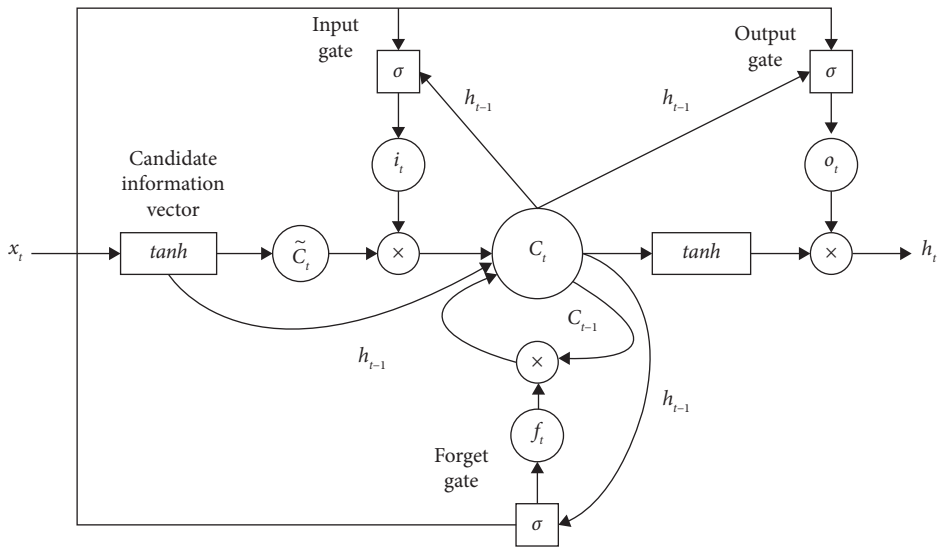

Figure 1: Basic structure of LSTM.

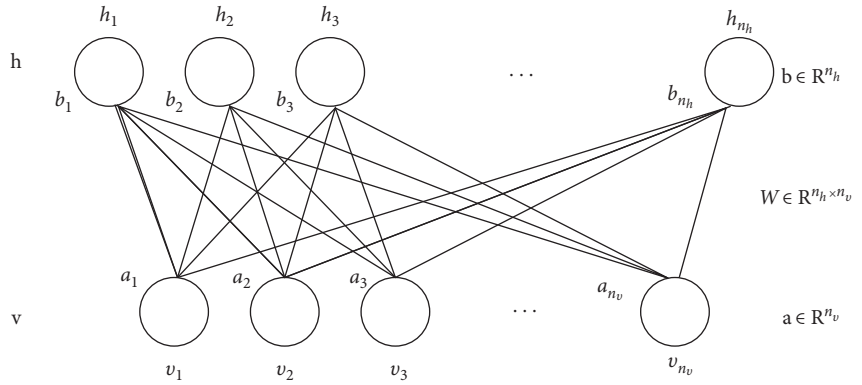

Figure 2: Basic structure of RBM.

layer, and finally realizes the prediction of the model. DBN consists of the input layer, hidden layer, and output layer. When building a DBN model, it is first necessary to determine the number of hidden layers, the number of nodes in each hidden layer, batch size, learning rate, and momentum. The hidden layer of the DBN is composed of several RBM stacks, and the data are extracted layer by layer through the RBM to obtain the abstract high-level features of the input data. Finally, the fault is classified by softmax.

2.3. Financial Audit Forecast Model Construction and Evaluation. In view of the complexity of financial audit data, this paper adopts several representative parameters to characterize, mainly including financial parameters, nonfinancial parameters, and other qualitative parameters including the liquidity, efficiency, solvency, productivity, and scale parameter. On this basis, the deep learning model is used for processing and prediction. In this paper, an audit model based on DBN-LSTM is constructed, which makes full use of the advantages of the DBN multilayer perceptron structure. It can better retain the attributes of the original data and solves the problem of feature extraction of financial audit data, thereby improving the prediction accuracy. Figure 3 shows the basic flow of the model in this paper, and the specific implementation steps are as follows:

Step 1. Data preprocessing. The original financial audit data are preprocessed, and singular value points and invalid data are proposed.

Step 2. Deep feature extraction. The DBN network is trained to extract the deep features of the financial audit data and complete the unsupervised learning training process.

Step 3. Training phase. The deep features extracted by the optimized DBN are input into the LSTM network, and a prediction model is established after training.

Step 4. Testing phase. The divided test set is input into the trained prediction model to obtain the predicted value of the financial audit result.

In order to verify whether the prediction results of the model are true and reliable, this paper defines the evaluation indicators for quantitative calculation. Assuming that the

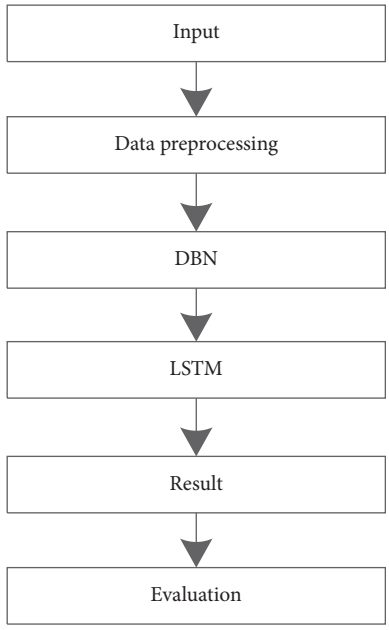

Figure 3: Basic procedure of the proposed method.

predicted value and the actual value are divided by $\hat{y} = \{\hat{y}_1, \hat{y}_2, \ldots, \hat{y}_n\}$ and $y = \{y_1, y_2, \ldots, y_n\}$, the root mean square error (RMSE) and mean absolute percentage error (MAPE) are selected as the evaluation indicators of model accuracy. The expressions of them are as shown in equations (9) and (10):

$$\text{RMSE} = \sqrt{\frac{1}{n}\sum_{i=1}^{n}(\hat{y}_i - y_i)^2}, \tag{9}$$

$$\text{MAPE} = \frac{1}{n}\sum_{i=1}^{n}\left|\frac{(\hat{y}_i - y_i)}{y_i}\right| \times 100\%. \tag{10}$$

Accordingly, the smaller the RMSE and MAPE values are, the closer the predicted value is to the real value, and the higher the prediction accuracy is.

3. Experiment and Analysis

3.1. Dataset. To verify the performance of our method in predicting financial audit opinions, we randomly select 350 companies operating in Beijing in 2021. The audit opinions and group financial information in the sample are obtained from the Internet. Audit opinions are roughly divided into two categories. One is the report with unqualified opinion, that is, the report that fully complies with accounting standards. The other is the report with qualified opinion, that is, the report that does not comply with accounting standards. 125 financial statements received qualified opinions, and 225 financial statements received unqualified opinions. According to the statistical results, compared with the group with unqualified opinions, the group with qualified opinions has poorer results in terms of financial variables, that is, the level of profitability, liquidity, solvency, and productivity of companies with qualified audit opinion is lower. Therefore, the experimental results are in line with the actual situation.

Table 1: Comparison of performance of the different methods using RMSE and MAPE.

Method	RMSE	MAPE (%)
Proposed	201.3	67.2
MLP	256.1	79.3
CNN	221.4	74.3
LSTM	219.3	71.2

Table 2: Comparison of performance of different methods under noises using RMSE.

Method	SNR (dB)			
	−10	−5	0	5
Proposed	302.1	267.3	232.1	211.5
MLP	330.9	312.3	296.4	274.1
CNN	318.1	282.1	261.2	231.4
LSTM	314.7	279.9	243.8	228.1

In order to evaluate the performance of the proposed model, taking into account that the number of samples is not very large, a five-fold cross-validation process repeated 100 times is used in the experiment. For each of these 100 tests, the modes of training, validation, and testing are randomly selected, and all passed the model training and evaluation.

3.2. Results and Analysis. In order to test the pros and cons of the performance of the proposed method, three existing prediction models are selected for simultaneous comparison experiments, i.e., MLP, CNN, and LSTM. Among them, the LSTM method in the comparison method directly trains and predicts, and there is no DBN in this method. Table 1 shows the test results of various methods under the two evaluation indicators. It can be seen that the method in this paper can achieve the best performance under both conditions, showing its effectiveness. In particular, compared with the LSTM method, the performance improvement of our method mainly benefits from the deep feature learning of DBN. Therefore, the DBN-LSTM method proposed in this paper has stronger adaptability to financial audit forecasting.

Considering the influence of noise and interference in the data, this paper adds different degrees of noises to the sample set according to the definition of signal-to-noise ratio (SNR). On this basis, a retest is carried out according to the above ideas, and the statistical results are shown in Table 2 using RMSE as the evaluation index. It can be seen that even in the case of strong noise interference, the method in this paper can still maintain a strong performance advantage, which further reflects its effectiveness.

4. In Conclusion

This paper studies the audit opinion prediction model and consolidated financial statements. On this basis, it introduces the methods, samples, variables, and main results of audit opinion prediction and proposes an audit prediction

model combining DBN and LSTM. The proposed method effectively combines the advantages of DBN in deep feature extraction and the characteristics of LSTM in processing time series, which improves the accuracy of audit opinion prediction. In the experiment, the proposed method is tested based on financial audit-related data and compared with several existing data prediction models. The results reflect the performance advantages of this method. The effective application of the method in this paper can reduce the computational overhead of audit data analysis, thereby improving the accuracy and efficiency of audit analysis.

Data Availability

The dataset can be accessed upon request.

Conflicts of Interest

The authors declare that they have no conflicts of interest.

Acknowledgments

This work was supported by the Natural Science Research Project of Anhui Provincial Department of Education (KJ2021A1550), Key Research Project of Humanities and Social Sciences of Anhui Provincial Department of Education (SK2020A0894), and Natural Science Research Project of Anhui Provincial Department of Education (KJ2020A1129).

References

[1] T. Xie and J. Zhang, "Data-driven intelligent risk system in the process of financial audit," *Mathematical Problems in Engineering*, vol. 2022, p. 9, Article ID 9054209, 2022.

[2] X. Zhang, "Construction and simulation of financial audit model based on convolutional neural network," *Computational Intelligence and Neuroscience*, vol. 2021, no. 1, Article ID 1182557, 11 pages, 2021.

[3] Y. Zhao and Y. Fang, "Financial account audit early warning based on fuzzy comprehensive evaluation and random forest model," *Journal of Mathematics*, vol. 2022, no. 1, Article ID 3090335, 10 pages, 2022.

[4] Y. Lin, H. Yue, H. Liao, D. Li, and L. Chen, "Financial risk assessment of enterprise management accounting based on association rule algorithm under the background of big data," *Journal of Sensors*, vol. 2022, no. 1, Article ID 8041623, 10 pages, 2022.

[5] C. Gu, "Application of data mining technology in financial intervention based on data fusion information entropy," *Journal of Sensors*, vol. 2022, no. 1, Article ID 2192186, 10 pages, 2022.

[6] H. Kusdarwati and S. Handoyo, "System for prediction of non stationary time series based on the wavelet radial bases function neural network model," *International Journal of Electrical and Computer Engineering*, vol. 8, no. 4, pp. 2327–2337, 2018.

[7] R. Li, Z. Zhao, J. Zheng, C. Mei, Y. Cai, and H. Zhang, "The learning and prediction of application-level traffic data in cellular networks," *IEEE Transactions on Wireless Communications*, vol. 16, no. 6, pp. 3899–3912, 2017.

[8] L. Yang, X. Gu, and H. Shi, "A noval satellite network traffic prediction method based on GCN-GRU," in *Proceedings of the International Conference on Wireless Communications and Signal Processing*, Nanjing, China, October 2020.

[9] Y. Lee, H. Jeon, and K. Sohn, "Predicting short-term traffic speed using a deep neural network to accommodate citywide spatio-temporal correlations," *IEEE Transactions on Intelligent Transportation Systems*, vol. 22, no. 3, pp. 1435–1448, 2021.

[10] C. M. Vong, W. F. Ip, P. K. Wong, and J. Y. Yang, "Short-term prediction of air pollution in Macau using support vector machines," *Journal of Control Science and Engineering*, vol. 2012, p. 4, Article ID 518032, 2012.

[11] Y. Liu, H. Zheng, X. Feng, and Z. Chen, "Short-term traffic flow prediction with Conv-LSTM," in *Proceedings of the 9th International Conference on Wireless Communications and Signal Processing*, IEEE, Nanjing, China, December 2017.

[12] W. Jing, J. Tang, Z. Xu et al., "Spatiotemporal modeling and prediction in cellular networks: a big data enabled deep learning approach," in *Proceedings of the IEEE Conference on Computer Communications*, IEEE, Atlanta, GA, USA, May 2017.

[13] P. Hewage, A. Behera, M. Trovati et al., "Temporal convolutional neural (TCN) network for an effective weather forecasting using time-series data from the local weather station," *Soft Computing*, vol. 24, pp. 16453–16482, 2020.

[14] B. Huang, J. Wei, Y. Tang, and C. Liu, "Enterprise risk assessment based on machine learning," *Computational Intelligence and Neuroscience*, vol. 2021, Article ID 6049195, 6 pages, 2021.

[15] T. Chen, Q. Yang, Y. Wang, and S. Wang, "Double-layer network model of bank-enterprise counterparty credit risk contagion," *Complexity*, vol. 2020, no. 1, Article ID 3690848, 25 pages, 2020.

[16] A. Elsheikh, S. Yacout, and M. S. Ouali, "Bidirectional handshaking LSTM for remaining useful life prediction," *Neurocomputing*, vol. 323, pp. 148–156, 2019.

[17] O. Pauplin and J. Jiang, "DBN-based structural learning and optimisation for automated handwritten character recognition," *Pattern Recognition Letters*, vol. 33, no. 6, pp. 685–692, 2012.

[18] D. Jiang, Y. Zhao, H. Sahli, and Y. Zhang, "Speech driven photo realistic facial animation based on an articulatory DBN model and AAM features," *Multimedia Tools and Applications*, vol. 73, no. 1, pp. 397–415, 2014.

[19] V. Campos, B. Jou, and X. Giro-i-Nieto, "From Pixels to Sentiment: Fine-tuning CNNs for Visual Sentiment Prediction," *Image & Visionuting*, vol. 11, 2017.

[20] S. G. Meshram, C. Meshram, F. A. Pourhosseini, M. A. Hasan, and S. Islam, "A multi-layer perceptron (MLP)-Fire fly algorithm (FFA)-based model for sediment prediction," *Soft Computing*, vol. 26, no. 2, pp. 911–920, 2022.

Hindawi
Computational Intelligence and Neuroscience
Volume 2022, Article ID 1366418, 10 pages
https://doi.org/10.1155/2022/1366418

Research Article

Design of Repository and Search Platform for Art Painting Teaching Resources in Universities Based on Model of Decision Tree

Yuling Liu

Solux College of Architecture and Design, University of South China, Hengyang 421001, Hunan, China

Correspondence should be addressed to Yuling Liu; yuling-2018@usc.edu.cn

Received 1 July 2022; Accepted 5 August 2022; Published 25 August 2022

Academic Editor: Yaxiang Fan

Copyright © 2022 Yuling Liu. This is an open access article distributed under the Creative Commons Attribution License, which permits unrestricted use, distribution, and reproduction in any medium, provided the original work is properly cited.

At present, art education curriculum reform is in full swing. Art education in China started late but as an important element of quality education. Art education is particularly important today with rapid economic development and advanced technology. The art subject is the sum of the teaching content of the art subject and the execution of teaching activities expressed through the network, including two components: the teaching content organized according to specific teaching objectives and teaching strategies and the network teaching support environment. Unlike existing multimedia courseware, several features reflect the advantages of online education, unlike online courseware. Each school generates a large amount of student performance data every year, and existing systems only perform simple backups, queries, and statistics on these data, which do not reflect the weaknesses of education in a centralized and comprehensive manner. Data mining can extract valuable information hidden behind the data from a large amount of data and has been applied in more and more fields with good results, which helps people to make correct decisions. In this study, we propose a decision tree model-based repository and search platform for school art and painting education resources, briefly outline the decision tree model, and analyze the architecture and operation of the school art and painting education resources repository and search platform. The experimental results show that the Virginica accuracy of the decision tree model is 0.42 higher than that of C4.5, which greatly improves the accuracy of the preferred class and ensures the overall accuracy remains unchanged. Therefore, this system realizes the art education resource repository system and realizes the needs of college users to share art professional information and resources.

1. Introduction

The rapid development of China's market economy and so the demand for art are growing [1]. Combining the current situation of art education in China with the real problems of art education curriculum reform and proposing new ideas, the field faces continuous, systematic, and in-depth research [2]. The School of Fine Arts drawing resource repository is an important platform to meet the demand for art resources of art majors in schools, and schools can use this platform to play the role of art resource sharing and bring together various resources of art drawing [3]. Since the school drawing resource storage requires high repository and search efficiency, while the picture resource files are large (stored in RDF ternary format) and many process files, system scalability is one of the most noteworthy indicators for this resource [4]. The Internet has a wealth of multimedia information resources, including text, images, sound, video, and other multimedia information resources [5]. However, it also causes problems such as the scattered distribution of resources and disorganization [6].

The ever-increasing amount of information places higher demands on data storage, management, and analysis [7]. This requires new tools that can automatically transform data and convert it into valuable information and knowledge [8]. Starting from the storage capacity problem, information silos and hotspots emerge. This is because information silos and hotspots are independent individuals that do not share information effectively [9]. Therefore, it is necessary to integrate and manage media resources in schools to provide rich

teaching and learning resources for teachers and students to improve teaching and research in high schools and further improve the quality and effectiveness of teaching and learning [10]. However, among the many resource sites in a school or district, system integration differs significantly in the nonstandardization of information transfer protocols and information formats, the establishment of each resource repository on the system platform, database selection, and the way resources are classified. Although regional networks share educational resources, they are unable to share and access resources between different platforms and systems [11].

Data access increases because clients have to specialize in parsing different data structures when accessing data [12]. Concurrent connection time and resource display speed are greatly affected [13]. Decision trees are an important classification and prediction method that can handle both discrete and continuous data and are easy to understand [14]. There have been significant changes in the nature of information retrieval, which can be reflected in more diverse, open, dynamic and widespread deployments, faster update rates, faster change rates, network delivery processes, and network management [15]. However, as the number of components in the component repository increases, users may experience difficulties in finding and selecting components, thus requiring an efficient organization and management of the component repository, which is directly related to the success of reuse cases.

The innovations of this study are as follows:

(1) This study introduces the teaching resources of school art education as an aspect of the art education support system in the whole system and provides a macro and holistic analysis within the framework of the art education support system.

(2) The system design of this study is based on the design requirements of software engineering and uses advanced technology to achieve effective sharing of the networked multimedia network.

(3) Extensive real-world data collection combined with the model of decision tree depicts a more comprehensive and practical development of Chinese school art education and educational resources.

The research framework of this study consists of five parts, which are structured in detail as follows.

The first part of the study introduces the background and significance of the research and describes the main tasks of the study. The second part introduces the work related to the resource repository and search platform and decision tree model of the Department of Fine Arts and Painting. The third part classifies the system operation architecture design and system software architecture so that readers of this study can have a more comprehensive understanding of the resource repository and search platform for picture professors based on the decision tree model. The fourth part is the core of the study, from the analysis of the construction of the decision tree in the resource repository and search platform, and the analysis of the splitting attribute selection of the decision tree in the retrieval process, to complete the description of the application analysis of the model of decision tree in the design of the teaching resource repository and search platform. The final part of the study is a summary of the full work.

2. Related Work

2.1. Fine Art Painting Teaching Resources Repository and Search Platform. The rapid development of China's economy, the significant increase in comprehensive national power, the improvement of people's living standards, and the enrichment of material life inevitably bring a high level of demand for spiritual life, in which more and more people are involved. Art is gradually descending from the top of the pyramid and is no longer the behavior of a few "elites," but is becoming more and more popular. Architectural art education resource storage effectively manages art-related basic data resources and multimedia information resources and provides teacher resources data and platforms for school art professional education and distance art education.

Waldhor proposed a web-based educational technology standard with Chinese characteristics (CELTS). Specifications and standards were mainly developed to describe the attributes of resources, such as media data, courseware, literature data, test papers, question banks, cases, online courseware, and FAQs [16]. From the perspective of resource construction and management, Huizhen classified online teaching resources according to various manifestations. In his opinion, whatever is conducive to the transfer of teaching resources is used as the primary reference for classification and representation [17]. Zheng and Zhou researched and designed a web-based educational resource repository, the main idea of which is to build an educational resource repository through the joint participation of users. The repository provides users with high-quality resources and also encourages them to upload their own resources to build a diverse repository of users and achieve sustainable growth of resources [18]. Starting from real school education, Sharma et al. classified online educational resources according to specific areas of school education and learners of different grades. As resources are presented in different ways on the online platform, the subcategories of their associated metadata must also have different priorities [19]. Mimis et al. introduced Web service technology into the development process of educational resource sharing systems and designed corresponding intermediate application components to access heterogeneous teaching resource databases, thus solving the problem of accessing scattered and isolated heterogeneous resource databases on campus [20].

As China's education system continues to improve and the academic field continues to mature and grow, the long-established field of art is receiving more and more attention. Relevant policies and regulations have been introduced one after another, providing assurance that art education can continue to develop.

2.2. Model of Decision Tree. With the change of the times, Chinese art education has undergone significant changes at all levels, in all dimensions, and in all aspects. Some old

educational concepts of the past need to be changed urgently, and some factors are constrained and affect healthy development. All decisions in human society are inclusive and complex, and in addition to cost factors, other influences and factors can be considered, such as profit-sensitive decision problems need to consider profit factors and preference-sensitive decisions. The causes of the problem need to be considered and taken into account.

Yong and Yan used a decision tree-based classification mining method to analyze the data in the student achievement database and applied the algorithm in the analysis of student achievement to build a decision tree model of professional competence so that teachers and school education decisions conform to those produced by the creators and can gain insight into the problems in education, so they can use the information provided by grades to optimize education and educational planning and decision-making [21]. In order to obtain an ideal decision tree model, Niu et al. conducted an in-depth study of the attribute selection and pruning optimization in the construction process, such as the impact of the decision tree cost model on the actual decision-making process [22]. Lu and Zhou propose the idea of combining data mining techniques with statistical analysis for multi-strategy design. We used a decision tree-based classification mining approach to analyze data in a student grade database to create intuitively displayable decision trees of student grades. In other grade calculation methods, the location of specific grades provides assessment information for the teacher department [23]. Xie et al. used the principles of determining cost-sensitive classification learning and balancing costs to create an objective function with the goal of minimizing costs [24]. Cai and Wu introduced the classical association rule Apriori algorithm and the well-known decision tree algorithm ID3 and used the association rule algorithm to find out the effect of excellence in one course on another course [25].

The decision tree model can obtain various knowledge needed to support decision-making from a large amount of data in the component repository and uses data mining techniques to construct and reuse mining datasets based on historical information and feedback from component reuse. It uses this data mining method to mine some component reuse rules and exclude human factors as much as possible.

3. The Repository and Search Platform of Painting Teaching Resources Based on Model of Decision Tree

3.1. System Operation Architecture Design. There are still many problems in conducting research on the repository and search platform for art painting resources in schools, which makes it difficult for them to bring out their unique advantages under the influence of the traditional model [26]. In traditional art class teaching, students' learning resources mainly consist of learning materials and textbooks prepared by teachers, which are slightly insufficient compared with learning resources on the Internet [27]. Moreover, since most of these materials end with the completion of the teacher's teaching time, students are unable to reorganize their knowledge and rely mainly on the image storage in their minds when completing assignments [28]. In the material management and sharing system, the entities oriented are mainly users and resources. Accordingly, the functional requirements of the system are divided into two modules: user management and material resource storage. The functional requirements of the teaching resource repository platform are shown in Figure 1.

The first is the backend program, which handles the business operations and data processing of the system and realizes the entry of material resource data into the database. The decision tree is constructed by growing the tree several times, specifically by dividing the training samples in a dataset to form a tree structure. It only constructs a decision path to classify each test case:

$$\text{Average Gain}\,(A,T) = \frac{\text{Gain}\,(A,T)}{|A|}, \tag{1}$$

A is the attribute, $|A|$ is the number of nodes, and $\text{Gain}\,(A,T)$ is the reduced misclassification cost.

There are three subcomponents for data generation and pre-processing, the data generator creates data in RDF/XML serialized format and uses the N Triple Converter component to fetch this data and convert it to N-Triples serialized format. And the fuzzy split entropy minimum condition property is selected as an extension property. Where:

$$FE\left(D, A_i\right) = -\sum_{j=1}^{k_i} \frac{m_{i_j}}{m_i} E\left(D \cap A_{ij}\right), \tag{2}$$

D is the leaf node, A_i is the unused conditional attributes, and $FE(D, A_i)$ is the fuzzy partition entropy.

Art education in basic education still belongs to the category of "quality education" [29]. However, art education at higher levels has some characteristics of its own, and the subject matter has increased, and the requirements for teaching resources are relatively high [30]. Therefore, professional art resource teaching websites can provide a relatively wide range of knowledge, and most of them are carefully organized by teachers and provide links to other related online learning resources. Students can find suitable learning resources more easily, which greatly enrich the content of art teaching and provide a new way to cultivate students' creative ability.

Next is the user interaction interface, where users submit business processing requests to the system within their rights, and the control engine controls the order of business processing and coordinates the invocation of functional functions. The component uses the Jena framework to convert data, and a predicate-based file splitter gets the converted data and splits it into predicate files. The splitting attribute selection factor for defining the node attributes is then as follows:

$$\text{ASF}\,(A) = \left(2^{\text{Average Gain}\,(A)} - 1\right) * \text{Incr} - EP\,(A). \tag{3}$$

Average Gain is the average information benefit and Incr – $EP(A)$ is the increment of attribute.

This kind of educational material resources needs to be uploaded in a package in advance before they can be

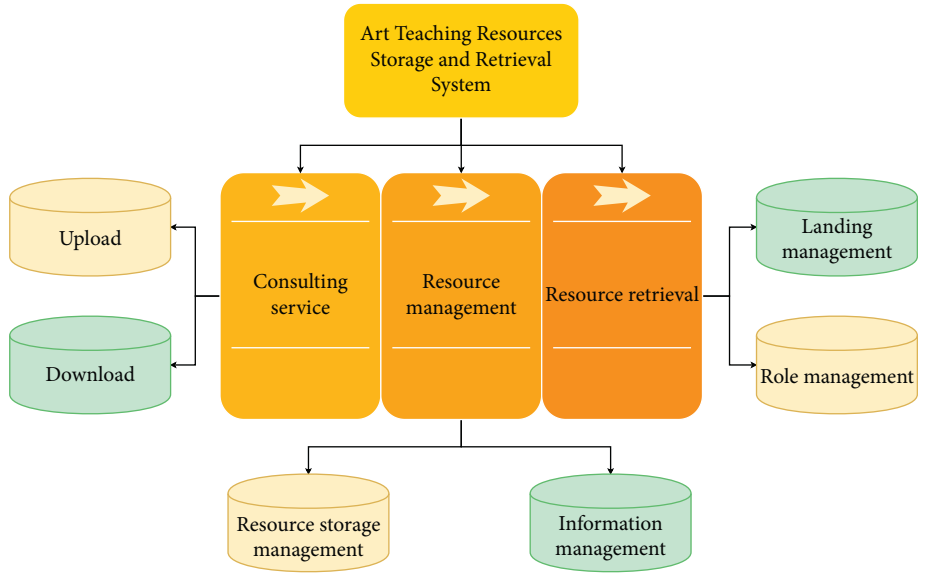

Figure 1: Functional requirements of teaching resource repository platform.

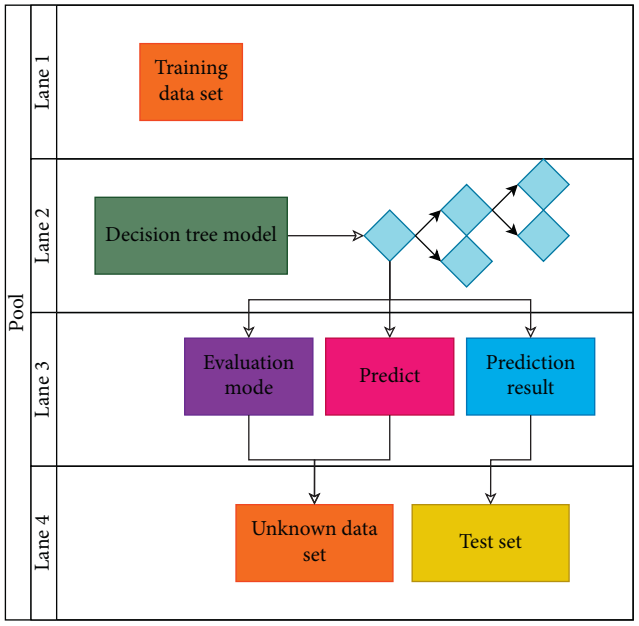

Figure 2: Model of decision tree.

downloaded, and the relevant properties need to be described when submitting the resources. Then even in the case of incomplete training examples, it is possible to learn useful hypotheses from the set of training examples when large to enable the correct classification of unknown examples. The EP increase needs to be defined before giving the formula for the split attribute selection factor:

$$\text{Incr} - EP(A) = \sum_{i=1}^{n} EP(A_i) - EP, \tag{4}$$

$\sum_{i=0}^{n} EP(A_i)$ is the sum of effective preferences of all child nodes split by splitting attribute A and EP is the effective preference of nodes without attribute A as split attribute.

Any non-leaf node of the decision tree represents a partition of the dataset on an attribute, and the dataset corresponding to the corresponding node is split into subsets by the difference in attribute values, and each subset is represented by a branch. The model of the decision tree is shown in Figure 2 below.

When examining the support system of art education, we need to dynamically link and integrate the originally static and independent factors, so that we can grasp the impact of the various "combined forces" on art education from a macro perspective and systematically analyze each link.

Finally, there is a database in which material resource information, user information, etc. are stored. The predicate-based files are then fed into an object type-based file splitter which splits the predicate files into smaller files based on the object type, and then the output of the last component is put into HDFS. the amount of information required for a decision tree to make a correct category judgment, for example, is:

$$I(p,n) = -\frac{p}{p+n}\log_2\frac{p}{p+n} - \frac{n}{p+n}\log_2\frac{p}{p+n}, \tag{5}$$

p, n is the size of positive and negative examples in vector space.

Each split from the root node to the leaf node is unfolded according to some attribute, and each non-leaf node chooses an attribute in the decision process and generates different branches according to different attributes. If a user module adopts the schema, teaching materials are submitted, the directory structure where they are located should be noted, and for the schema, teaching materials submitted online, the same changes in the relative directory structure should be noted. The test attributes of the inner nodes of a decision tree may be univariate, i.e., each inner node contains only one attribute, or multivariate, i.e., there are inner nodes that contain multiple attributes.

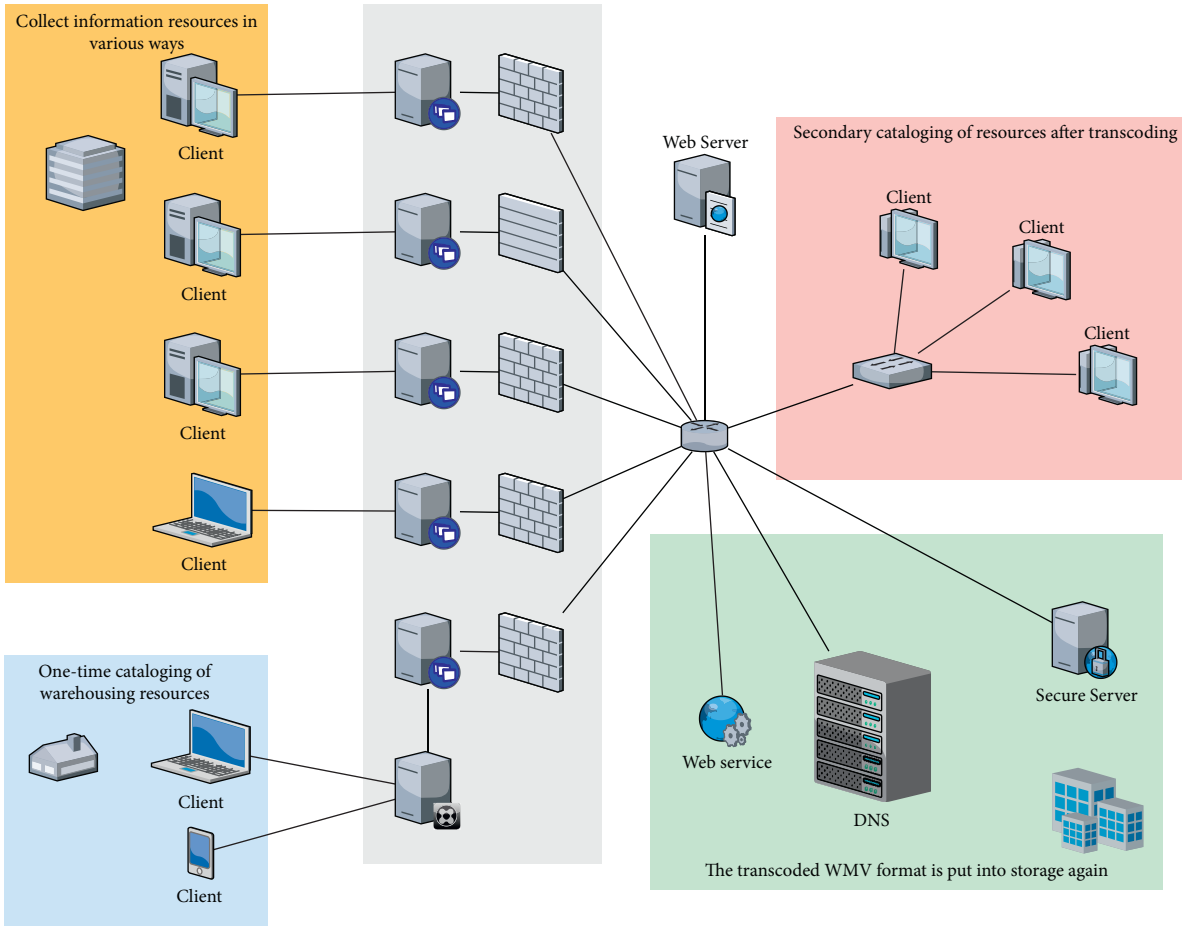

Figure 3: System architecture diagram of front-end resource warehousing and resource storage.

3.2. System Software Architecture. In the whole architecture of the model of decision tree-based painting teaching resource repository and search platform, the control engine is the core of the whole software architecture with other parts interconnected to coordinate and control data processing and business operations and realize communication with users. The system architecture of the front-end resource entry and resource storage part is shown in Figure 3.

The first step is to start the central controller to detect the BUF size of the structure and communication transfer to ensure that the data transfer will not lead to communication errors due to data overflow and other problems. In the model of decision tree, we redefine the split attribute selection factor:

$$ASF(A_i) = \frac{\left(2^{\text{Average gain}(A_i)} - 1\right)}{TC(A_i)_{\text{normal}}} * \text{Incr} - \text{UCB}(A_i), \quad (6)$$

A_i is the i attribute in the set A, Average gain(A_i) is the average information gain, $TC(A_i)_{\text{normal}}$ is the standardized test cost, and Incr − UCB(A_i) is the UCB dosage.

In HDFS, files take up space replication factor size. Since RDF is text data, HDFS needs a lot of space to store the files. The interaction between multiple tasks, which are various "request-response" relationships, is achieved by the client sending a data processing request to the server, requesting the server to complete it, and returning the result to the client. The content of art teaching should reflect the spirit of the times and adapt to the trend of social development. Make full use of the local art resources to enrich the content of art teaching. The content of computer art and pottery can be added in places with conditions. So from the hand of art painting management, we set up electronic files of painting data metadata and digital documents by designing data management system, so as to facilitate the accession and management of digital painting data. It is assumed that the distribution of index words in unrelated documents can be approximated by the distribution of index words in all documents in the information set. That is,

$$\begin{cases} P(t_i|R) = 0.5, \\ \\ P(t_i|\overline{R}) = \dfrac{n_i}{N}, \end{cases} \quad (7)$$

n_i is the number of documents containing index words and N is the total number of documents in information set.

Next is the front-end request processing, the administrator sends the system login request by user name and password, the central controller verifies the user name and password, returns the authentication result, and assigns the

corresponding permission according to the user role. Suppose a decision tree is constructed for a data set with two class attribute values, and there are p positive samples and n negative samples at a node, then the class labeling method for this node is as follows:

$$\begin{cases} P, \text{ifp} \times FN > n \times FP, \\ N, \text{ifp} \times FN < n \times FP, \end{cases} \tag{8}$$

FN is the price to be paid when the positive node is wrongly judged as the negative example, P is the node judged as a positive node, FP is the price to be paid when the counter-example node is wrongly judged as a positive example, and N is the node judged as a counter-example node.

To minimize the amount of space, the public prefix in the URI is replaced with some much smaller prefix string and this prefix string is tracked in a separate prefix file. This greatly reduces the amount of space required for the data, and since there is no cache in Hadoop, each SPARQL query needs to read the file from HDFS. Entropy is a concept of measuring the amount of information, in information theory, it represents the uncertainty of random variables and it focuses on solving the problem of quantifying information. The formula is as follows:

$$P(X = x_i) = p_i, i = 1, 2, \ldots, n, \tag{9}$$

X is the discrete random variable and $P(X = x_i)$ is the probability distribution of discrete random variables.

The school library should be equipped with art books and other art resources, including teachers' reference books, students' reference books, art magazines, art education magazines, slides, CD-ROMs, etc., for teachers to prepare and teach classes, and for students to collect and consult materials and for self-learning or cooperative learning. Out of consideration for the huge amount of school art painting materials, this system will adopt the full-text image retrieval method to store and retrieve digital images of school art paintings.

Finally, after adding, deleting, or updating the resources, the material shared directory will be changed to some extent, and the changed shared directory will be sent to the central server and other node servers for updating the shared directory. The reason for not storing data in a single file is that in Hadoop files are the minimum input unit for MapReduce jobs. If all the data is placed in a single file, then the entire file will be input to the MapReduce job for each query. Model of decision tree always selects the attribute with the largest information gain among all attributes as the split attribute for the current node. The formula to calculate the classification of a given sample is as follows:

$$I(s_1, s_2, \ldots, s_m) = -\sum_{i=1}^{m} p_i \log_2(p_i), \tag{10}$$

S is the collection of sample data, m is the number of distinct values, C_i is the category, S_i is the sample number, and p_i is the probability that any sample belongs to C_i.

Database design is divided into physical database design and logical database design. Logical database design is to design the global logical structure of the database according to the demand of system construction, so as to respond to the business logic. The physical database design is to design and implement the storage structure and access method of the database according to the logical structure of the database. The full-text image search method is used to realize the search of a large number of images of school art and painting resources, so as to improve the efficiency of the system in retrieving images. The RDF type files were also divided into as many files as the number of different objects that the RDF: Type predicate has. This further reduces the amount of space required to store the data.

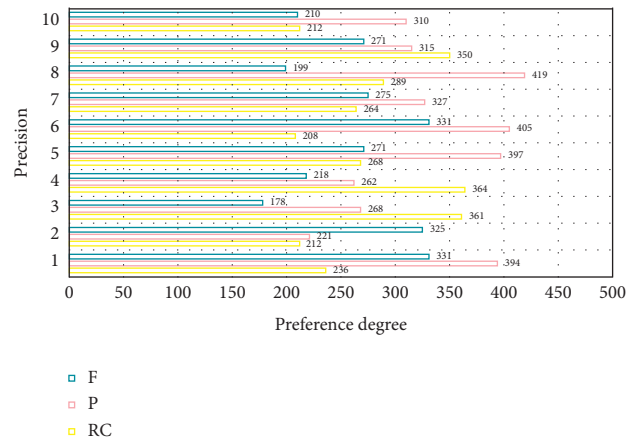

Figure 4: The influence of preference degree on the accuracy of decision tree with preference cost.

4. The Application Analysis of Model Decision Tree in the Design of Teaching Resources Repository and Search Platform

4.1. Construction and Analysis of Decision Tree in Resource Repository and Search Platform. Decision tree-based learning algorithms have the advantages of being fast and accurate, generating understandable rules, being relatively inexpensive, handling continuous and discrete-valued attributes, and showing clearly which attributes are important. In addition, the user does not need to know much background knowledge during the learning process, and the algorithm can be used to learn as long as the training examples can be expressed in an attribute-to-conclusion style. To construct a decision tree, a training sample set with class labels is provided, and then the training sample data space is partitioned by a decision tree classification algorithm, resulting in an inverted tree structure. The cost of predicting versicolo as a preference class is 5, and the cost of predicting setosa as a preference class is 400, the preference cost of the latter is much larger than the former, and the main juggling of the sent sample setting is to tell the algorithm that predicting setosa as a preference class is intolerable behavior. The experimental results are shown in Figure 4.

First, the tree is generated, starting with all data at the root node, and then the data is recursively sliced. The problem of understanding software reuse is a key issue that

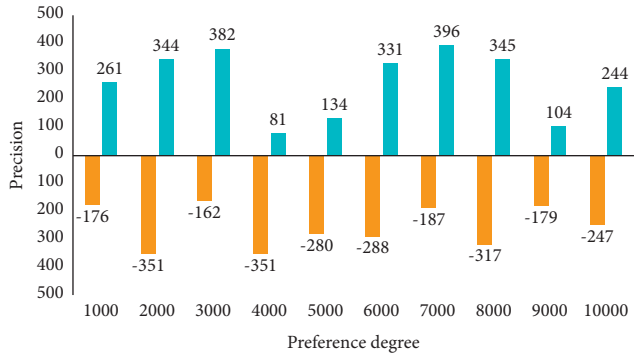

Figure 5: Comparison of F value before and after adding preference cost.

Table 1: Test results based on information gain rate standard.

Data set	Iris	Wine	Glass
Misclassification cost	453	556	768
Profit	16577	21756	32445
UCB	34.25	25.16	19.67
Classification accuracy	97.23	67.45	32.19

affects the success of reuse. In other words, in the actual soft component reuse process, the reusers should not only be able to retrieve the relevant set of components efficiently but also the key is how to make the reusers understand the retrieved components quickly so as to find their real needs in this set of components, which is a complex decision process. Calling the F-value before joining the preference cost as $F1$ and the F-value after joining as $F2$, the comparison of $F1$ and $F2$ is shown in Figure 5.

Data noise elimination, deceptive data, etc., all of which affect the accuracy and practicality of the final generated decision tree and rule extraction, i.e., its application scope is somewhat limited. So the training sample data can reside on disk and only a part of it is loaded into memory. The process of server retrieval is not a process of division of labor, independent search, and processing of one-sided information, and the retrieved information is returned to the server that sent the retrieval request, aggregated, and organized to achieve macro synchronous retrieval.

Next is the tree pruning, which is to remove some data that may be noisy or abnormal. Then the initial training data set is divided into several disjoint subsets according to the selected splitting points or splitting subsets, and these subsets are used to select the training set with splitting attributes by the branching nodes formed after the splitting of the root node. And the generated branching points are split by the same method until the resulting child nodes of the split are all leaf nodes labeled with classes. The test cost for each attribute was randomly assigned between [20, 90], and the cost and gain matrices for each data set were set by reference to manual settings. The test results based on the information gain rate criterion are shown in Table 1.

The samples in the test set are input to the generated decision tree one by one, and then the predicted class number of each sample is compared with the actual class

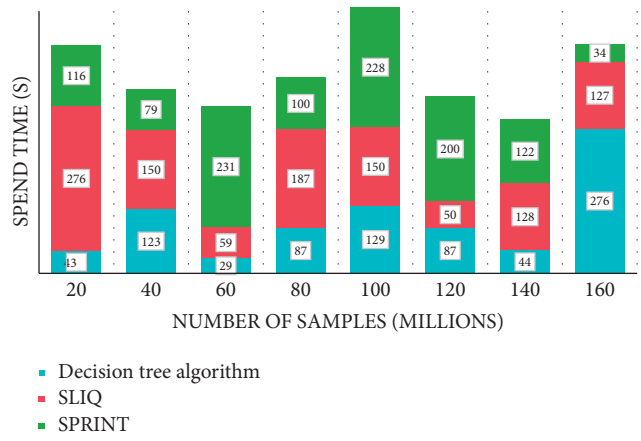

Figure 6: Comparison of running time of decision tree algorithm.

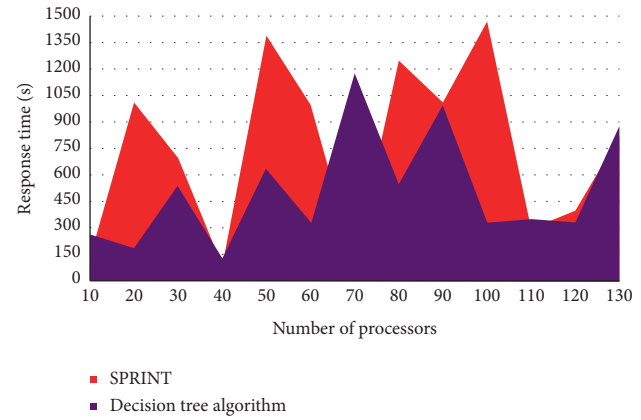

Figure 7: Comparison with SPRINT in parallel environment.

Table 2: Comparison results.

	Decision tree model	C4.5
Virginica accuracy	0.98	0.56
Overall accuracy	0.93	0.67
Variance ratio	0.896	0.453

number, and the results of the comparison are counted to obtain the accuracy of the decision tree classification. Users may not have a clear goal before querying, but just want to search the soft component library to see if there are components that can be utilized and reused, so it is necessary to provide users with a certain degree of help through the reuse history of components and the reuse experience of other users.

Finally, the condition that the decision tree stops partitioning has a node on which the data all belong to the same class no more attributes can be used to partition the data. That is, a certain attribute is selected at a node to divide the construction of different branches according to some rule. Component feedback information can enable the component reusers to get some reuse experience information from previous component reusers, enhance the understanding of the components and reduce the reuse workload. Efforts

Figure 8: Scale up performance of decision tree.

should be made to promote the integration of information technology with the teaching of other subjects, to encourage the application of information technology tools in the teaching of other subjects, and to integrate information technology education into the learning of other subjects. Therefore, the information gain is used as the criterion for attribute selection, so that the largest category information of the tested examples can be obtained when each non-leaf node is tested, and the moisture value of the system is minimized after using this attribute to divide the example set into subsets.

4.2. Analysis of Split Attribute Selection of Decision Tree in Retrieval Process. Educational resources are constantly being added, which makes it difficult to retrieve them. At present, information retrieval technology has been developed to a very mature stage, and has reached the network and intelligence.

First of all, we use average gain instead of traditional information gain to enhance the classification ability of information gain. Information gain or information gain ratio is an important reference data for selecting feature values, and the data classification of the decision tree is to order a large amount of disordered data. The GINI index is used as the criterion for judging the merit of segmentation, and the computation of the GINI index is much smaller than that of the information gain ratio. The decision tree algorithm is compared with the SLIQ algorithm and SPRINT algorithm in a stand-alone environment, i.e., in a serial algorithm. The results are shown in Figure 6.

Search all the internal and external data information related to the business object and select from it the data that is suitable for data mining applications. If the correct rate obtained by classifying the sample data with the features we select is about the same as the correct rate obtained by random classification, then the value of this selected feature is indistinguishable, and not using such a feature for classification does not have the slightest effect on the accuracy of decision tree classification. This metric is called the attribute selection metric or the split merit metric. The attribute with the highest information gain (or maximum decompression) is selected as the test attribute for the current node, which minimizes the amount of information required to classify the samples in the resulting split and reflects the minimum randomness or "impurity" of the split.

Second, the degree of the decision maker's preference for the class is considered in the selection of the splitting attribute, and an assumption exists on the selection of the maximized ASF attribute as the splitting attribute using mutual information as the feature selection amount. That is, the proportion of positive and negative examples in the training example set should be the same as the proportion of positive and negative examples in the actual problem domain. However, in general, the same cannot be guaranteed, so that there is a bias in computing the mutual information of the training set. Thus the optimization of the retrieval method in the real sense can be accomplished only on the basis of a reasonable representation of the resources. To check the performance of this design in a parallel environment, we compare the design of this study with the SPRINT algorithm which has good parallel performance. The SPRINT in a parallel environment is shown in Figure 7.

Convert the data into an analytical model. This analytical model is built for the mining algorithm. Building an analytical model that really fits the mining algorithm is the key to successful data mining. But instead of using information gain to measure the best split, it uses the X-test used in the

column table to determine which category prediction attribute is the most independent from the predicted value. The model of the decision tree is compared with the decision tree built by the C4.5 algorithm on Iris, and the comparison results are shown in Table 2.

As can be seen from Table 2, the Virginica accuracy of the model of decision tree is improved by 0.42 compared to C4.5, which also significantly improves the accuracy of the preference class and ensures the same overall accuracy.

Finally, the number of minimum support terms per branch of the decision tree needs to be predetermined before pruning, and then each subtree is detected from the top down. Then the information gain as the attribute selection benchmark is dropped and replaced by the information gain rate, which is more reasonable for attribute selection. Since the number of samples assigned to each machine is constant, the ideal goal is that the response time of the algorithm remains constant as the number of processors increases. The Scale up performance of the decision tree is shown in Figure 8 below.

That is, some nodes and subtrees are removed by pruning operations to avoid "overfitting" and thus eliminate anomalies and noise from the training set. So a path from the root to the leaf nodes corresponds to a merging rule, and the whole decision tree corresponds to a set of parsing expression rules. Thus, we can see that the information gain from feature improvement is the greatest, and the feature improvement can be selected as the root node or inner node in the feature selection of the decision tree. There were no remaining attributes that could be used to further divide the sample. In this case, majority voting is used. This involves converting a given node into a leaf and labeling it with the class in which the majority of the sample resides, or the class distribution in which the sample of nodes can be stored.

5. Conclusions

In recent years, China's art education reform has made remarkable achievements, and most domestic art educators have invested a lot of energy in both theory and practice. By organizing existing teaching materials and building an art resource room, we can collect and manage a large number of excellent teaching materials, realize the sharing and management of materials, and provide richer and more practical materials for the majority of users. In addition, with the advent of the era of big data, the complexity of the data environment is rapidly increasing as the amount of data accumulated by people is rapidly increasing. Traditional processing methods are facing new challenges, using the rules and laws of decision tree models to provide meaningful information for educational management decisions and help educational administrators allocate educational resources. Coordinating educational programs, reforming teaching practices and curricula, and making relevant educational management decisions. Therefore, this study analyzed and discusses the design of a decision tree model-based repository and search platform for school art and painting materials, aiming to realize the integrated storage and management functions of multimedia data resources. The article proposes a repository and search platform for art painting images and enables the sharing of painting resources among different schools, allows fast retrieval of a large number of RDF files, and describes the algorithm with an example, which also provides a reference for the current development of art painting in schools.

Data Availability

The dataset is available upon request.

Conflicts of Interest

The author declares that there are no conflicts of interest.

References

[1] G. Ma, L. Zhang, G. Cui, and Y. Cheng, "Design of medical examination data mining system based on decision tree model," *Journal of Physics: Conference Series*, vol. 1237, no. 2, Article ID 022022, 2019.

[2] G. Nalinipriya, K. G. Maheswari, and K. Kotteswari, "An enhanced priority scheduling algorithm for multi-server retrieval cloud system," *Journal of Information Science and Engineering*, vol. 33, no. 3, pp. 759–772, 2017.

[3] X. Liu, F. Zhu, Y. Fu, and Q. Liu, "A resource retrieval method of multimedia recommendation system based on deep learning," *International Journal of Autonomous and Adaptive Communications Systems*, vol. 13, no. 4, p. 400, 2020.

[4] M. Kimi, "Storage and retrieval of multimedia resources in multimedia libraries: a study," *IASLIC Bulletin*, vol. 63, no. 2, pp. 105–126, 2018.

[5] E. Chung and H. F. Lee, "A generalised sequencing problem for unit-load automated storage and retrieval systems," *International Journal of Industrial and Systems Engineering*, vol. 2, no. 4, pp. 393–412, 2007.

[6] Z. Mao, T. Zheng, and Z. Lian, "Information system construction and research on preference of model by multi-class decision tree regression," *Journal of Physics: Conference Series*, vol. 1982, no. 1, Article ID 012153, 2021.

[7] U. M. Mokashi, V. Suma, and S. Christa, "Regression and decision tree approaches in predicting the effort in resolving incidents," *International Journal of Business Information Systems*, vol. 1, no. 1, p. 1, 2020.

[8] K. Devasenapathy and S. Duraisamy, "Evaluating the performance of teaching assistant using decision tree ID3 algorithm," *International Journal of Computer Application*, vol. 164, no. 7, pp. 23–27, 2017.

[9] B. V. Tucker, M. C. Kelley, and C. Redmon, "A place to share teaching resources: s," *Journal of the Acoustical Society of America*, vol. 149, no. 4, p. A147, 2021.

[10] O. S. Zav'yalova, "On the relationship between teaching objectives and teaching resources in the electronic course on extensive and intensive reading for foreign students," *Tomsk State Pedagogical University Bulletin*, no. 2, pp. 82–89, 2019.

[11] Z. Cao, "Classification of digital teaching resources based on data mining," *Ingénierie des Systèmes d'Information*, vol. 25, no. 4, pp. 521–526, 2020.

[12] X. Z. Sun, S. Y. Li, X. Y. Tian, Z. Hong, and J. X. Li, *Clinical Hemorheology and Microcirculation*, vol. 71, no. 1, pp. 3–8, 2019.

[13] Y. Du and T. Zhao, "Network teaching technology based on big data mining and information fusion," *Security and*

Communication Networks, vol. 2021, no. 9, Article ID 6629563, 9 pages, 2021.

[14] H. S. Behera, J. Nayak, B. Naik, and A. Ajith, "Advances in Intelligent Systems and Computing," *Computational intelligence in data mining Advances in Intelligent Systems and Computing*, pp. 557–568, Springer, Heidelberg, Germany, 2019.

[15] H. Wei, "Research on the development of ideological and political education resources for college students based on the data mining technology," *International English education research: English version*, vol. 3, no. 3, p. 3, 2019.

[16] K. Waldhor, "Machine learning paradigms: advances in data analytics," *Computing reviews*, vol. 60, no. 4, p. 159, 2019.

[17] J. Huizhen, "Evaluation of british and American literature teaching quality based on data mining," *IPPTA: Quarterly Journal of Indian Pulp and Paper Technical Association*, vol. 30, no. 7, pp. 743–749, 2018.

[18] C. Zheng and W. Zhou, "Research on information construction and management of education management based on data mining," *Journal of Physics: Conference Series*, vol. 1881, no. 4, Article ID 042073, 2021.

[19] S. Sharma, S. Mahajan, and V. Rana, "A semantic framework for ecommerce search engine optimization," *International Journal of Information Technology*, vol. 11, no. 1, pp. 31–36, 2019.

[20] M. Mimis, Y. Es-saady, M. El, and A. Ouled, "Adapted regulation level's flipped classroom using educational data-mining," *International Journal of Computer Application*, vol. 181, no. 24, pp. 28–32, 2018.

[21] N. Yong and Z. Yan, "On-line classroom visual tracking and quality evaluation by an advanced feature mining technique," *Signal Processing: Image Communication*, vol. 84, no. 1–2, Article ID 115817, 2020.

[22] L. Niu, X. Chen, and R. Xu, "Quantitative analysis of the influence of learning resource scheduling in MOOC mode on traditional education and teaching," *International Journal of Continuing Engineering Education and Life Long Learning*, vol. 29, no. 1-2, p. 21, 2019.

[23] L. Lu and J. Zhou, "Research on mining of applied mathematics educational resources based on edge computing and data stream classification," *Mobile Information Systems*, vol. 2021, no. 7, pp. 1–8, Article ID 5542718, 2021.

[24] Y. Xie, P. Wen, W. Hou, and L. Yingdi, "A knowledge image construction method for effective information filtering and mining from education big data," *IEEE Access*, no. 99, p. 1, 2021.

[25] W. Cai and H. Wu, "33.Research on the optimal allocation of intellectual resources based on data mining analysis," *Boletin Tecnico/technical Bulletin*, vol. 55, no. 10, pp. 225–232, 2017.

[26] J. Ai, J. Gao, and P. Du, "Analyse the influence of big data on students' learning behavior," *IOP Conference Series: Earth and Environmental Science*, vol. 234, no. 1, Article ID 012025, 2019.

[27] A. Lino, A. Rocha, L. Macedo, and A. Sizo, "Application of clustering-based decision tree approach in SQL query error database," *Future Generation Computer Systems*, vol. 93, pp. 392–406, 2019.

[28] M. B. López, G. Alor-Hernández, J. L. Sánchez-Cervantes, and M. D. P. Salas-Zárate, "EduRP: an educational resources platform based on opinion mining and semantic web," *Journal of Universal Computer Science*, vol. 24, no. 11, pp. 1515–1535, 2018.

[29] E. Rattanalerdnusorn, "Recbd approach - retrieval of efficient and content based relative data," *International Journal of Computational Intelligence Research*, vol. 14, no. 7, pp. 599–606, 2018.

[30] Q. Xiao, "Resource classification and knowledge aggregation of library and information based on data mining," *Ingénierie des Systèmes d'Information*, vol. 25, no. 5, pp. 645–653, 2020.

Hindawi
Computational Intelligence and Neuroscience
Volume 2022, Article ID 2926669, 9 pages
https://doi.org/10.1155/2022/2926669

Research Article

An Improved Model of Product Classification Feature Extraction and Recognition Based on Intelligent Image Recognition

Baiqiang Gan[1] **and Chi Zhang**[2]

[1]*Guangzhou Nanyang Polytechnic College, Conghua 510925, China*
[2]*Guangzhou Nanfang College, Conghua 510970, China*

Correspondence should be addressed to Chi Zhang; zhangch@nfu.edu.cn

Received 23 June 2022; Accepted 27 July 2022; Published 23 August 2022

Academic Editor: Yaxiang Fan

Copyright © 2022 Baiqiang Gan and Chi Zhang. This is an open access article distributed under the Creative Commons Attribution License, which permits unrestricted use, distribution, and reproduction in any medium, provided the original work is properly cited.

With the development of the new generation of technological revolution, the manufacturing industry has entered the era of intelligent manufacturing, and people have higher and higher requirements for the technology, industry, and application of product manufacturing. At present, some factories have introduced intelligent image recognition technology into the production process in order to meet the needs of customers' personalized customization. However, the current image recognition technology has limited capabilities. When faced with many special customized products or complex types of small batch products in the market, it is still impossible to perfectly analyze the product requirements and put them into production. Therefore, this paper conducts in-depth research on the improved model of product classification feature extraction and recognition based on intelligent image recognition: 3D modeling of the target product is carried out, and various data of the model are analyzed and recorded to facilitate subsequent work. Use the tools and the established 3D model tosimulate the parameters of the product in the real scene, and record them. Atthe same time, various methods such as image detection and edge analysis areused to maximize the accuracy of the obtained parameters, and variousalgorithms are used for cross-validation to obtain the correct rate of the obtaineddata, and the standard is 90% and above. Build a data platform, compare simulated data with display data by software and algorithm, and check by cloud computing force, so that the model data can be as close to the parameters of the real product as possible. Experimental results show that the algorithm has high accuracy and can meet the requirements of different classification prospects in actual production.

1. Introduction

Physical manufacturing has always been the foundation of national economies, so the development of indigenous manufacturing is a top priority for both developed and developing countries.

In recent years, with the continuous development of artificial intelligence technology, the manufacturing industry is also constantly introducing new technologies. The first is the regions represented by developed countries such as Europe and North America. Countries in these regions have vigorously promoted the strategy of returning manufacturing to their own countries in recent years, trying to resist the wave of economic globalization while applying emerging technologies to their own manufacturing industries. At the same time, it can limit the outflow of advanced technology to the greatest extent, so as to improve the competitiveness of its own manufacturing products on a global scale, and try to monopolize technology. Previously, the spillover of manufacturing industry in Europe and the USA was mainly due to the consideration of labor cost. However, the arrival of new manufacturing forms is likely to greatly weaken the position of low-grade cheap labor in manufacturing industry, thus making some labor-oriented countries lose their only advantages in the wave of new industrialization.

After more than 40 years of reform and opening up, China's industrial level has been greatly improved, and China has successfully become one of the world's largest manufacturing countries [1]. However, the new wave of industrialization still has a great impact on China's manufacturing industry. As we all know, due to the implementation of China's reform and opening up strategy

in the 1970s and 1980s, it is since then that a considerable number of manufacturing factories have been introduced in China, but China's advantage has always been a large number of cheap labor market, and the competitiveness in technology is particularly weak. Therefore, although the scale of China's manufacturing industry is in the forefront of the world, the technology of manufacturing industry is always not worthy of today's manufacturing scale. Another problem that cannot be ignored is that most of the foreign-funded manufacturing industries transferred to China are domestic low-end manufacturing industries, which is not conducive to China's technological accumulation. Therefore, China's manufacturing industry is facing the dual challenges of industrial transformation and industrial upgrading. Also to put forward the corresponding strategy in our country, in the information technology in manufacturing practice closer now, again in manufacturing upgrading of key nodes, our country needs to catch up with the pace of the developed countries, break the technical barriers of developed countries, complete its manufacturing technology upgrading, and thus in manufacturing occupy the position of the world.At present, manufacturers who actively follow the trend of the times pay more and more attention to the realization of intelligent manufacturing, and put it into the real production line. The diversity of products makes the classification and identification of products more difficult. In response to this problem, the method proposed in this paper is compared with the analysis method using cloud data to improve the accuracy of recognition between the model and the actual product. Users draw the STL model of the product on the cloud according to their own needs and upload the product data to the manufacturer for production [2]. Industrial cameras are used to collect images of the products and match them with cloud data so as to identify and classify the products. Therefore, in order to solve these problems, this paper makes an in-depth study on the improved model of product classification feature extraction and recognition based on intelligent image recognition.

In addition, a method of image preprocessing is proposed. Finally, the paradigm of contour extraction is determined and the method of contour feature description is studied. Through comparison and analysis, the contour feature description with high recognition accuracy was selected.

2. The Research Background

2.1. Vision and Machine Vision. Vision usually undertakes very important tasks of detection and inspection in the manufacturing industry. Since vision can obtain a large amount of information, vision is often used as a reliable tool in the noninformation age [3]. With the development of manufacturing industry, the accuracy and precision requirements of manufacturing industry are getting higher and higher. The accuracy of information provided by ordinary human vision does not meet the requirements of today's products, while the labor cost is increasing; therefore, machine vision is proposed by scientists and gradually applied in practice. Machine vision recognition was born in the 1950s, and it first uses the camera to record the current state of the machine and then analyzes the speed and direction of the machine's movement based on the captured images. It first used a camera to record the current state of the machine, then analyzed the speed and direction of the machine motion based on the captured images, and then regulated the next machine motion [4]. In the 1960s, the study of machine vision recognition evolved from two-dimensional to three-dimensional. First, American professors believed that, just as polygons can be understood by breaking them into triangles of different sizes, if images of physical objects are taken and processed by a computer program and broken down into more easily understood and analyzed basic three-dimensional structures such as cubes, spheres, cylinders, and vertebrae, and their coordinates and dimensions are described in mathematical language, and if simple regular three-dimensional structures can be extended to more complex three-dimensional structures, machine stereo vision recognition will have a wider application [5]. The above is the theoretical basis for the gradual introduction of machine vision into manufacturing work.

2.2. Research Status. After the 1960s, the research on the three-dimensional effect of machine vision provided objective conditions for future machine recognition and learning of three-dimensional objects in the objective world and also made the application of machine vision possible [6]. Since then, a large number of scientists have joined the research on machine vision, and the related theories have progressed by leaps and bounds. However, since most of the analysis work needs to be done by computers, the upper limit of computer performance determines the upper limit of theoretical analysis of machine vision, and if the current cognitive limit is to be broken, the computing power of computers must be improved first. Until the 1990s, due to the breakthroughs in mathematics, new algorithmic logics were proposed and established that allowed computers to surpass their previous computational power, which meant that computer computing power could finally support the gradual application of machine vision to practice [7].

However, China's machine vision research was influenced by China's national conditions, and the research in this area started late and developed slowly until the 1980s, which was the period when China opened up to the outside world and widely absorbed foreign cultures. In the 21st century, China's machine vision benefited from various "Internet+" policies to develop rapidly [7, 8]. In recent years, with the development of artificial intelligence and the programmatic documents such as "intelligent manufacturing pilot demonstration action implementation plan," the manufacturing industry has been promoted to the direction of intelligence, and the domestic research on machine vision technology has also continued to achieve new results. Although the scale of the domestic intelligent manufacturing industry is developing rapidly, in the actual application of the production line, the scale is small, the degree of automation is low, the effect needs to be improved, and there is still a certain distance abroad, really in the application, such

as workpiece surface quality inspection, electronic device manufacturing, and other fields which still do not completely use intelligent inspection system. In addition, there are many other challenges: a large number of manufacturers have begun to seek new ways to reduce costs and improve efficiency, and this new way is to use machine recognition technology to replace manual quality inspection and product classification [9].

The need to reduce production costs and increase productivity, as well as the expectations of people, has driven the popularity of machine vision technology in practical applications [10]. Nowadays, more and more research institutions, universities, etc., are focusing on machine vision research, investing a lot of time, money, and effort in research, and have made great progress in applications in industry, agriculture, and medicine, which are expected to catch up with foreign research [11]. The first is the application on various electronic components; at present, machine vision is mainly used to check whether the PCB printing is complete, whether the holes are missing, etc. This kind of problem, which is difficult to check precisely under human vision, happens to be the part where machine vision is good at. In addition, our scientists have also used machine vision to measure the density of industrial-grade finished products, etc., and have achieved some results. In agriculture, machine vision is also used to examine the characteristics of plants and analyze their color to screen for quality with a high degree of accuracy in the end. However, at present, the scope of most applications of machine vision in China is still limited to the inspection of appearance, whether the appearance of qualified, uneven, or stained, ultimately based on a simple analysis of the appearance of three-dimensional data, and in a comprehensive view, there are still shortcomings compared with the world's advanced machine vision application technology.

3. Materials and Methods

From the supply side, the transformation and upgrading of this industry of manufacturing have become concerns in various fields at home and abroad in recent years, and at the same time, the current technology can be put into application because of the rapid development of information technology, which also provides the technical basis for the update of manufacturing technology.From the demand side, the current demand for products is increasing, and the manufacturing technology used in the past for a large number of wholesales has been unable to keep up with the development trend of the current era. In order to meet market demand, it is also necessary to match machine vision data with customer demand data to more accurately meet customer needs. Therefore, this paper designs a market demand and technology application implementation framework based on image recognition technology for the common requirements of the supply side and the demand side to meet the supply side and the demand side requirement situation as shown in Figure 1.

The steps on how to compare and analyze the product model with the cloud data for subsequent more detailed processing are as follows: first, preprocessing is performed to reduce the impact caused by the environment, and then contour features are extracted and described. At the same time, the STL model uploaded from the cloud is parsed and the extracted boundaries are extracted for contour features. Then, the similarity between the product image and the contour of the cloud-based STL model is compared and matched. Finally, the results of classification and recognition are output.

3.1. STL-Based Product Matching Template Generation. It mainly refers to parsing the data of STL models uploaded by users. The current method of identifying product types in the actual production line is mainly using identification templates for product matching, and because the process of identification templates is very complicated and the number of templates is limited, this method can only identify a small number of product types in the production process of the same production line, which is difficult to meet user requirements [12]. Therefore, in order to solve the problem of difficulty in manufacturing product matching templates, this section proposes a method to generate matching templates directly using 3D models of products in the cloud. Companies and individuals set the template generation perspective in OpenGL, build a three-dimensional model of the product according to the desired functionality, finally save it as an STL-type file, and then submit the order to the manufacturer for mass production of the product. After receiving the 3D model uploaded by the user, the topological information of the product needs to be completely read, and the read data need to be parsed and processed [13].

3.2. Image Preprocessing and Contour Extraction. Before product classification and recognition, the product images should be preprocessed because in the process of image acquisition, they may be influenced and interfered by the external environment, such as the brightness of the light and the stability of the camera. These interferences may lead to large errors between the acquired images and the actual products, which will inevitably result in overfitting or low accuracy when they are transferred to the system. These disturbances may lead to large errors between the acquired images and the actual products, which may result in overfitting or low accuracy when transmitted to the system, and subsequent image segmentation, recognition, and classification may produce deviations and affect the results of image analysis and processing [14]. In order to solve such problems, the acquired images must be preprocessed with noise removal and enhancement. The contour extraction mainly utilizes the Canny edge detection operator. When performing Canny edge detection, since the input product image is an RGB color image, the range of values for each pixel is too large leading to a very complex calculation, which can be simplified by using a binarized image form in digital image processing, and the input RGB color image is first Gaussian smoothed to convert the color image into a grayscale image [15]. Then, the gradient of the pixels in the grayscale image is calculated; if the gradient between

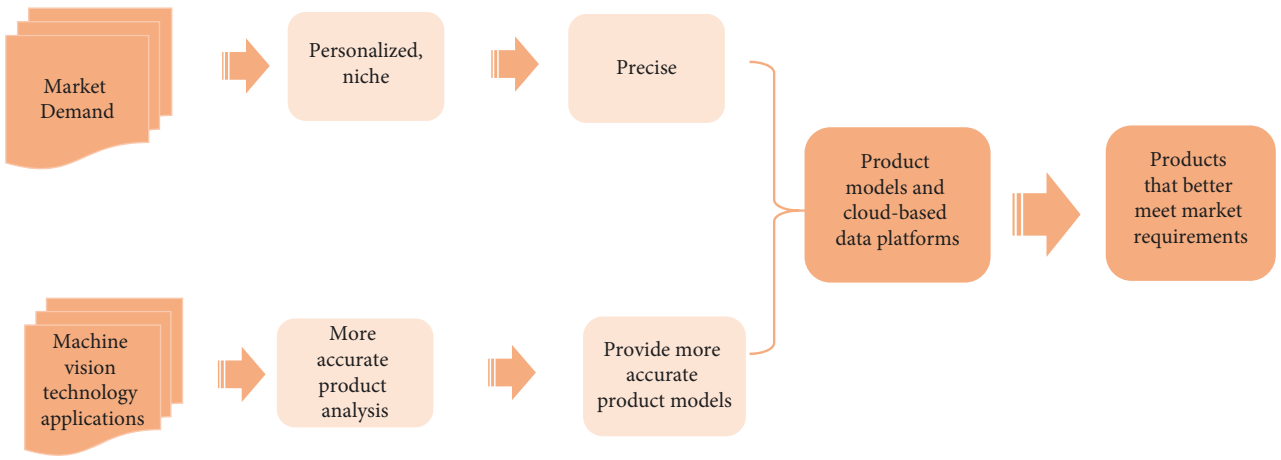

Figure 1: Market demand and technology application implementation framework.

adjacent pixels is zero, these two pixels belong to the same region; if the gradient is not zero, these two pixels belong to different regions. However, the boundary of the region formed in this way is a stepped dash, which needs to be processed in some way using a fitting algorithm, and then two different critical values are used to connect the dividing lines of neighboring pixels; thus, a smooth curve is obtained and the detection results of the grayscale image are finally output and displayed [16]. Meanwhile, the Canny algorithm can be optimized in multiple stages and has good performance in detecting the edges of image pixel regions. After the edge detection of the image using the Canny edge detection operator, the contour extraction of the image is required. In this paper, we choose the contour tracking algorithm to extract the contour features of the image. The algorithm first searches for a point on the image edge as the starting position, and then finds other contour points based on the gradient value of the pixel, tracks the edge, and obtains the complete contour of the image. The gradient of the pixels inside the same contour is the same after the contour tracking is finished [17].

The contour tracking algorithm has the following main steps: first, the preprocessed grayscale image is carpet searched, the gradient of the current pixel point is calculated, it is judged whether the pixel point is a point on the edge, and if this point is judged not to be a point on the edge, the search continues until the point on the edge is searched, which is defined as the starting point and given a tracking label; after the starting point is found, the contour line strip, due to its continuity, it is only necessary to search in the adjacent points of that point. Therefore, the starting point and scanning direction are redefined, the searched contour points are the new starting points, the points are searched one by one in the clockwise direction, and the above judgment method is used to determine whether these points are contour points or not. If there is a point with the same coordinates as the initial point, the search is finished; i.e., all points form a closed and complete contour; otherwise, the search continues according to the above steps until a closed and complete contour is formed. The specific flow is shown in Figure 2.

Although the above algorithm is efficient and simple, in order to make the contour tracking and extraction of the image more effective, the Find Contours function is used in the OpenCV computer vision development library for contour extraction.

3.3. Contour Feature Description. To achieve product-specific recognition and classification, contour features need to be described in a way that is influenced by parameters such as the initial point, size, and orientation of the contour, so Fourier features must be normalized. In this paper, Fourier feature description methods are investigated and the recognition accuracy of SVM-based Fourier transform algorithm, Hu-based Fourier feature description algorithm, and SVM-based elliptic Fourier transform algorithm is compared [18]. The comparison of recognition accuracy data of several types of algorithms is shown in Figure 3.

From Figure 3, it can be seen that the SVM-based elliptic Fourier transform algorithm has the highest recognition accuracy than the SVW-based Fourier transform algorithm and the Hu-based Fourier transform algorithm, so this paper will use the SVM-based elliptic Fourier transform algorithm for contour feature extraction and description to obtain a certain product classification accuracy.

4. Results and Discussion

In this section, experiments are conducted and results are obtained based on the product contour extraction and template matching methods proposed in the previous section. Firstly, the cloud-based STL model uploaded by users is parsed for data, and the contour features are identified and extracted to generate the matching templates for products. Then, the machine vision inspection platform is built, the camera is calibrated according to the accuracy requirements and the size of the product to be inspected, a suitable chip and lens are selected for the camera, and image acquisition is performed. Finally, contour extraction and feature description are performed on the acquired products, and the

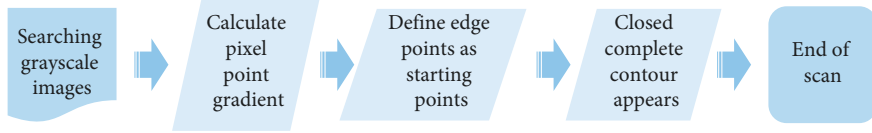

Figure 2: Contour tracking algorithm flow.

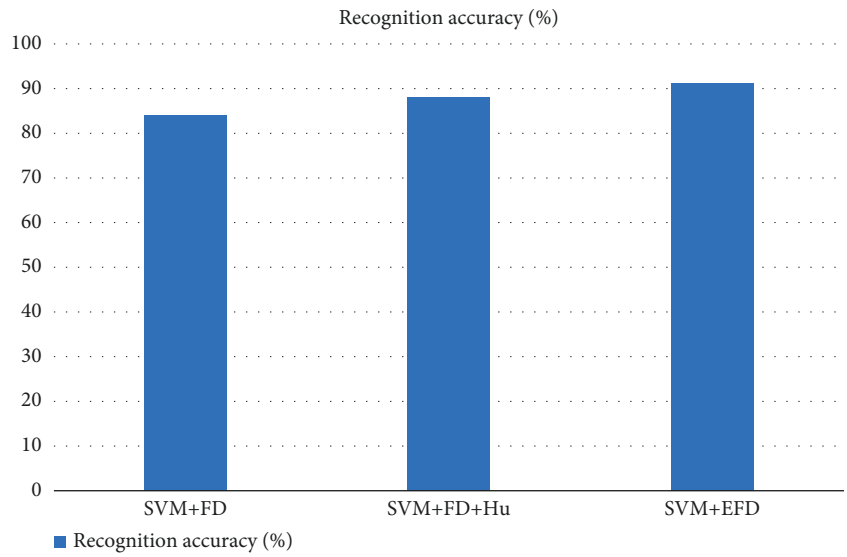

Figure 3: Recognition accuracy of Fourier transform algorithms.

acquired images are matched with the cloud-based STL model to complete the final product identification and classification.

4.1. Selection of Industrial Cameras. The first step of product identification is to acquire images, and it can be said that the camera is the most important instrument in the whole process. Different imaging modes can be formed by matching the camera with the lighting method [19]. The simplest is the reflection mode, which is illuminated by a point light source, and the camera takes pictures directly to the target area, but reflections occur when the target object has a shiny surface. The diffuse mode uses a surface light source, thus providing more uniform illumination and reducing reflections. Transmission method is to place the object between the light source and the camera, the use of shadow imaging. The scattering method uses a shade to scatter the light source. In this experiment, a diffuse reflection approach was used to uniformly illuminate the target object with a white surface light source [20]. Then, the camera uses the lens to focus the light to produce an image. In order to ensure the consistency of the captured image and a certain detection accuracy, there are certain requirements for the parameters of the camera. Among them, the parameters that have the greatest impact on the specific imaging effect are the sensor, the resolution, and the lens of the camera, respectively. This section will analyze specifically from the above three aspects. First is the need to choose the appropriate digital imaging chip as the camera's light sensor. According to the working principle, digital imaging chips can be divided into two types: CMOS and CCD. CMOS cameras have complex transmission paths and are therefore disturbed by more noise, resulting in easy distortion of data and lower accuracy; the CCD camera is very similar to the memory circuit in transmitting data, and the images taken during the transmission process are almost distortion-free and highly accurate. Therefore, the CMOS camera is used in this experiment for subsequent image acquisition. In addition, the resolution of the camera is also an important parameter, which is related to the accuracy of product identification. The higher the resolution of the camera, the higher the accuracy of the product recognition. However, considering the cost, the resolution should not be chosen in pursuit of the detection accuracy, but the actual size of the product to be detected should be considered, and it is enough to accurately record the contour characteristics of the product. It is also necessary to choose the frame rate of the camera and the form of camera scanning imaging. In this experiment, the size of the products to be inspected does not exceed 12 cm, so to ensure that the products to be inspected can be completely photographed, and the camera's photo range is set.

In this experiment, the size of the products to be tested does not exceed 12 cm. The last thing you need to choose is the lens of the camera. The focal length of the lens and other parameters will have an impact on the imaging effect and quality, and the main factors to consider when choosing a lens are contrast, depth of field, and resolution. Therefore, the importance of lens selection is no less than the choice of digital imaging chip. In this experiment, considering the shooting distance and the target object, a fixed-focus lens is selected, whose model is JMSF0618-5A with a focal length of

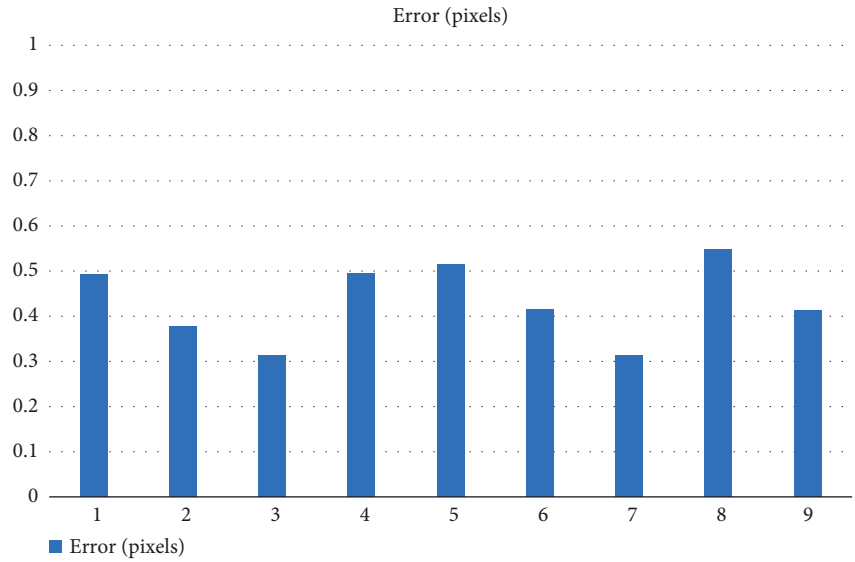

Figure 4: Calibration error.

8 mm. After the camera was selected, a light weight 2036A aluminum plate was used to build the bottom support of the camera on the production line and connect the camera to the computational processing system.

Finally, the internal and external reference matrices of the camera were extracted, then the target object was photographed with the camera, and the parameters of the camera were modified and optimized according to the actual photographs taken. First, the calibration images are taken. The number of calibration images determines the accuracy of camera calibration, and Zhang Zhengyou's calibration method usually requires no less than three images. However, the number of calibration images should not be too many; otherwise, it will affect the calibration efficiency. In order to achieve higher calibration accuracy and ensure the calibration efficiency, the calibration algorithm is written using the OpenCV database and Visual Studio 2016 software, and nine images with different shooting angles are used for calibration. Then, the coordinates of each pixel on the calibrated image need to be calculated, the color of that point is also represented and extracted numerically, and the color values and coordinates are corresponded one by one to generate a two-dimensional matrix. A two-dimensional matrix is likewise generated from the actual photographs taken. A program is written to compare the values of the corresponding positions of the two matrices one by one, and then the parameters of the industrial camera are normatively corrected to determine the final calibration results. The calibration error is shown in Figure 4.

From the calibration errors shown in Figure 4, it can be seen that the calibration errors of the nine calibration images are too large, all of them exceed 30%, and the largest one even reaches 50%. This will lead to excessive distortion and seriously affect the accuracy of product detection, so the calibration camera must be corrected so as to reduce the pixel error. The calibration results were used to correct the selected 9 images, and the corrected errors are shown in Figure 5.

From Figure 5, it can be seen that the calibration error is significantly reduced after the correction of the calibration results, and the calibration error of the nine calibration images is controlled below 30%, which almost does not affect the recognition and classification work of the system. This shows that it is very necessary to correct the calibration results.

4.2. Product Classification Experiment. This paper proposes an experimental validation of the proposed feature extraction and description algorithm on a real production line, and the specific product identification and classification process is shown below.

Uploading STL models of products in the cloud in order to ensure the generality of the experimental results, this experiment uploads five STL models with different structures in the cloud. Then, the data analysis and processing of the STL models in the cloud are performed to generate.

The data from the cloud STL models are then analyzed and processed to generate the matching templates for detection. At the same time, the data of the models were uploaded to the 3D printer to obtain the GCODE files of the models for product production. The parameters of the 3D printer, such as the specific information of the 3D printer, need to be set before 3D printing. Then, we set up a machine vision product recognition and classification platform, set up a camera at a suitable location on the production line, and use the camera to upload images of products to the system for contour extraction and feature description. After getting the matching template of the product, we use Visual Studio 2016 software to write generate descriptor of contour project to extract the features of the matching template, and save the feature data generated by the project in the format of a text document. At the same time, the contours obtained from the product images are also extracted and saved in text file format. Finally, the SVM-based elliptic Fourier algorithm is used to identify and classify the products.

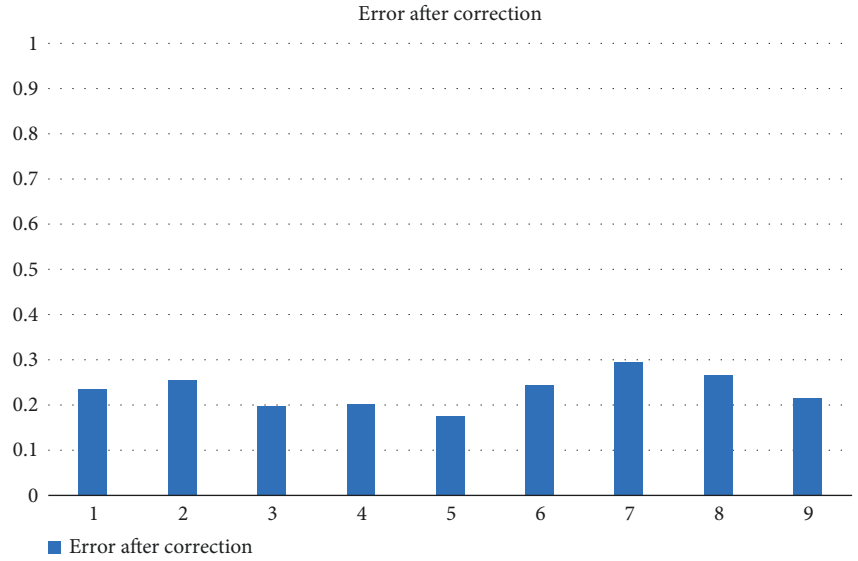

Figure 5: Corrected calibration error.

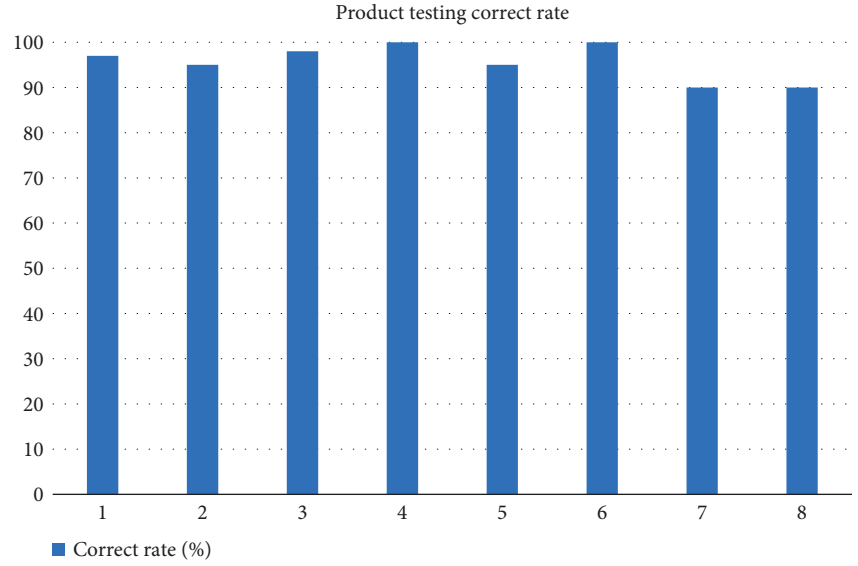

Figure 6: Product detection accuracy rate.

The SVM-based elliptic Fourier algorithm is trained to improve the accuracy of the final product recognition and classification. After obtaining the actual images and matching templates, the MATLAB 2020a software is used to extract features from the sample library and classify the data with similar features into one class. After several training sessions, the parameters of this algorithm will be optimized and the resulting model will be more complete, allowing for more accurate product recognition and classification on the production line. The product recognition and classification system is built on the production line to sort the products. The recognition platform is built on the main conveyor belt, a small section of selected industrial camera is installed above the conveyor belt, and LED backlight with certain light intensity is installed at a suitable location near the camera to fill the light for the products. The product images are sent to the system for feature extraction and description, matching with the target type, and then the product type is detected and sent to the corresponding sub-track. The results of the product detection are shown in Figure 6.

From Figure 6, it can be seen that the accuracy rate of product classification and identification reaches more than 90% each time, and the experimental results fully verify the effectiveness of the proposed algorithm, which can accurately identify and classify products. The product detection time of the eight experiments is shown in Figure 7.

From Figure 7, we can see that the product detection time of each experiment is very short, no more than 2 ms, and the average product classification time is only 1.5 ms. This shows that the proposed algorithm can quickly classify and identify products, which ensures a certain efficiency and can be put into practical application. Therefore, the sequence

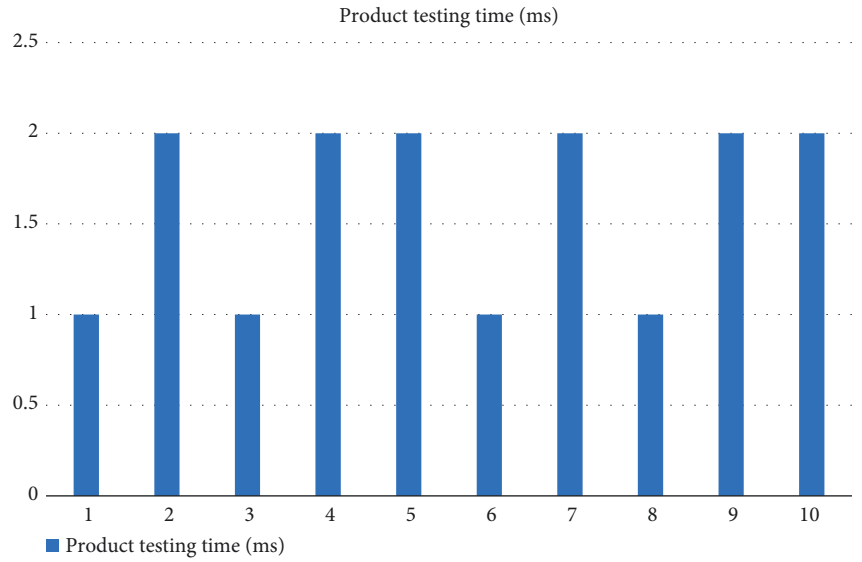

Figure 7: Product detection time.

of this experiment is to collect the required digital chips, lenses, and other hardware, and build a machine vision product recognition and classification platform. Finally, the contour extraction and feature description algorithms were verified, and the product recognition and classification were accurate enough to achieve small-scale production.

5. Conclusion

With the development of artificial intelligence, the manufacturing industry has also entered the era of intelligent manufacturing, and people have higher and higher requirements on the technology, industry, and application of product manufacturing. At present, some factories have introduced intelligent image recognition technology into the production process in order to adapt to the needs of customers' personalization, but the current algorithms have low adaptability to product types. Therefore, to address these problems, this paper conducts an in-depth study on the product classification feature extraction and recognition improvement model based on intelligent image recognition. The first is to propose a more convenient and quicker way to generate matching models, that is, to use the STL models provided by customers for analysis in the cloud: users upload STL models in the cloud according to their needs, and by completely reading the topological information of the 3D graphics such as points, lines, and surfaces of the STL models in the cloud, parsing and processing the read data, and finally generating matching templates. This method of generating matching templates is more concise compared to the traditional method of creating recognition templates. Then, image preprocessing is performed.In the process of image acquisition, it may be affected and interfered by the external environment, such as the brightness of the light, the stability of the camera, etc. These interferences may cause large errors between the acquired image and the actual product. And there are unnecessary noises and other interferences in the collected images, which may cause deviations in subsequent image segmentation, recognition and classification. In order to reduce the error, image preprocessing is required. In this paper, image filtering methods and edge detection algorithms are investigated, and the final decision is made to use the Canny edge detection operator for contour extraction. In addition, the contour feature description method is studied. The current commonly used Fourier transform algorithms are compared and analyzed. Finally, the algorithm with high recognition accuracy is selected for contour characterization of the product.

Data Availability

The labeled dataset used to support the findings of this study is available from the corresponding author upon request.

Conflicts of Interest

The authors declare that there are no conflicts of interest.

Acknowledgments

This study reports the results of the scientific research project of special projects in key project of Guangdong university scientific research platform in 2022(Research and application of model lightweight detection system for small sample image recognition),the Basic and Applied Basic Research Projects of Guangzhou Basic Research Program in 2022 (No. 202201010106),the Special Project of Guangdong Provincial Education Department in Key Areas (No.2021ZDZX1104),the Project of Guangzhou Philosophy and Social Science (No. 2022GZGJ241),and the Scientific Research and practice project of higher vocational education teaching reform in Guangdong Province(construction and practical research of the whole process hybrid teaching mode

based on TPACK theory-Taking the provincial excellent online open course of film and television synthesis as an example),2020 Young Innovative Talents Project of Guangdong Provincial Education Department (No. 2020WQNCX109) ,2020 Education and Teaching Reform Project of Guangdong Province (No. GDJG2004).

References

[1] X. Wang, Z. Vladislav, O. Viktor, Z. Wu, and M. Zhao, "Online recognition and yield estimation of tomato in plant factory based on YOLOv3," *Scientific Reports*, vol. 12, no. 1, p. 8686, 2022.

[2] L. Xiang, D. He, and A. Muhammad, "Image processing and recognition algorithm design in intelligent imaging device system," *Security and Communication Networks*, vol. 2022, Article ID 9669903, 10 pages, 2022.

[3] J. Zhong, Y. Meng, Z. Liu, and F. Zeng, "A novel method for the intelligent recognition of lattice fringes in coal HRTEM images based on semantic segmentation and fuzzy superpixels," *ACS Omega*, vol. 7, no. 17, Article ID 15037, 2022.

[4] P. T. Agne, N. Eimantas, P. Ramunas, L. B. Ingrida, D. Vytautas, and S. Z. Ruta, "An intelligent solution for automatic garment measurement using image recognition technologies," *Applied Sciences*, vol. 12, no. 9, 2022.

[5] L. Bao and K. K. Aruna, "Image energy saving recognition technology of monitoring system based on ant colony algorithm," *Wireless Communications and Mobile Computing*, vol. 2022, Article ID 2178433, 8 pages, 2022.

[6] H. Zhang, Y. Jin, Q. Liu, Y. Zhao, and Q. Gao, "Intelligent monitoring method for tamping times during dynamic compaction construction using machine vision and pattern recognition," *Measurement*, vol. 193, Article ID 110835, 2022.

[7] W. Baojian, C. Li, J. Xu, and T. Yuvaraja, "The relationship between intelligent image simulation and recognition technology and the health literacy and quality of life of the elderly," *Contrast Media amp; Molecular Imaging*, vol. 2022, Article ID 9984873, 9 pages, 2022.

[8] P. He, A. Wu, X. Huang, A. Rangarajan, and S. Ranka, "Machine learning-based highway truck commodity classification using logo data," *Applied Sciences*, vol. 12, no. 4, p. 2075, 2022.

[9] S. Gurram, K. Geetha, S. Neelakandan, A. K. S. Pundir, S. Hemalatha, and V. Kumar, "Intelligent deep learning based ethnicity recognition and classification using facial images," *Image and Vision Computing*, vol. 121, Article ID 104404, 2022.

[10] Z. Yao, T. Jin, B. Mao et al., "Construction and multicenter diagnostic verification of intelligent recognition system for endoscopic images from early gastric cancer based on YOLO-V3 algorithm," *Frontiers in Oncology*, vol. 12, Article ID 815951, 2022.

[11] T. Wang, "Exploring intelligent image recognition technology of football robot using omnidirectional vision of internet of things," *The Journal of Supercomputing*, vol. 78, 2022.

[12] G. Xu, "Design and realization of computer image intelligent recognition system," *Journal of Physics: Conference Series*, vol. 2146, no. 1, 2022.

[13] Z. Guo, Y. Shen, S. Wan, W. Shang, and K. Yu, "Hybrid intelligence-driven medical image recognition for remote patient diagnosis in internet of medical things," *IEEE journal of biomedical and health informatics*, 2021.

[14] Z. Zhang and H. Liu, "Analysis of volleyball video intelligent description technology based on computer memory network and attention mechanism," *Computational Intelligence and Neuroscience*, vol. 2021, Article ID 7976888, 9 pages, 2021.

[15] X. Tang, Y. An, C. Li, and X. Ning, "Intelligent segmentation and recognition method of breast cancer based on digital image processing technology," *Wireless Communications and Mobile Computing*, vol. 2021, Article ID 2256316, 9 pages, 2021.

[16] L. Zhang, "Research on control strategy of multi-source data fusion solar intelligent vehicle based on image recognition," *International Journal of Low Carbon Technologies*, vol. 16, no. 4, pp. 1363–1370, 2021.

[17] Y. Lin, J. Huang, Y. Chen, Q. Chen, Z. Li, and Q. Cao, "Intelligent segmentation of intima-media and plaque recognition in carotid artery ultrasound images," *Ultrasound in Medicine and Biology*, vol. 48, no. 3, pp. 469–479, 2022.

[18] L. Yang, Z. Li, S. Ma, and X. Yang, "Artificial intelligence image recognition based on 5G deep learning edge algorithm of Digestive endoscopy on medical construction," *Alexandria Engineering Journal*, vol. 61, no. 3, pp. 1852–1863, 2022.

[19] H. Chen and M. Chen, "Optimization of an intelligent sorting and recycling system for solid waste based on image recognition technology," *Advances in Mathematical Physics*, vol. 2021, Article ID 4094684, 12 pages, 2021.

[20] H. Li, D. Li, and B. Y. Ding, "Recognition and optimization analysis of urban public sports facilities based on intelligent image processing," *Computational Intelligence and Neuroscience*, vol. 2021, Article ID 8948248, 13 pages, 2021.

Hindawi
Computational Intelligence and Neuroscience
Volume 2022, Article ID 3146488, 13 pages
https://doi.org/10.1155/2022/3146488

Research Article

Color Matching Generation Algorithm for Animation Characters Based on Convolutional Neural Network

Jiali Lyu, Hae Young Lee, and Huwen Liu

Cheongju University, Cheongju 28503, Republic of Korea

Correspondence should be addressed to Huwen Liu; liuhuwen@pdsu.edu.cn

Received 27 June 2022; Accepted 16 July 2022; Published 20 August 2022

Academic Editor: Yaxiang Fan

Copyright © 2022 Jiali Lyu et al. This is an open access article distributed under the Creative Commons Attribution License, which permits unrestricted use, distribution, and reproduction in any medium, provided the original work is properly cited.

In recent years, for China, animation industry is a relatively new and mature emerging national sunrise industry after animation industry, which appears on the world stage more and more frequently and is widely concerned and valued by people from all over the world. Therefore, this paper innovatively uses the convolutional neural network algorithm to innovate the color matching generation of animation characters and improve the traditional technology of color matching for animation characters. In this paper, we mainly use Generative Adversarial Network (GAN), Deep Convolutional Generative Adversarial Network and VGG model, and multiscale discriminator theory and use ACGAN research method. And we study this paper's innovative LMV-ACGAN research method, and we have come to the conclusion that other models have higher collapse rate than this model; this model has higher color matching of anime characters. Color matching improves with the increase of convolutional neural network utilization, etc. Moreover, superior and minor reviews of this study are provided to make later researchers understand this study more rationally and objectively.

1. Introduction

Animation production is another contemporary Chinese specialty that can be completely said to integrate ancient Chinese excellent literature, film, photography, painting, music technology, etc. into one large modern film and television integrated animation production and art field talents [1]. In the early 1960s and 1970s, the animation industry itself was a new high-tech sunrise industry created by another developed country like Japan, and it has been receiving more and more attention from governmental agencies all over the world, and in the future, it will be more and more common and deep and will be used in extensively commercial applications in all walks of life around the world. In today's general trend that the market and competition in the field of animation in China and the world are developing more and more intensively, exploring and summing up such a correct development path, which is suitable for the development of the new mode of China's animation culture industry today and in the future, have become one of the primary issues that we have to pay serious attention to and consider at present, as well as every Chinese animation person who is concerned about China's problems. It has become a primary issue that we have to pay serious attention to and take into consideration. Fortunately, after the release of a series of excellent foreign anime series such as "Mulan" series and "Kung Fu Panda" series, many Japanese anime designers who like Chinese works have slowly started to realize that the traditional Chinese art culture of our ancient times is a rich and profound source of knowledge. The traditional Chinese art culture has created a rich variety of design and creation materials for us [2].

The design of anime character modeling is one of the most fundamental cores of designing all excellent anime works. The design methods of anime character modeling usually include the design of anime character modeling features, character color features, clothing style features, and action modeling features. The color part is another important visual symbol to show the most direct, vivid, and intuitive character effect in anime, and the matching use of color elements and the design and application of color generation and effect have always occupied a significant position in almost all the design methods of anime character modeling [3]. Modern psychological research and

development has long told us that about 80% of children's main cognitive and psychological sources of information and their main social and behavioral power sources are either directly or indirectly from or rely on visuals, so for every normal child like us, a quick glance as a child will, therefore, make it clear what we see, and later, if we look again as we grow up, we may understand how to gradually absorb what is there and imitate what is being created [4]. Academics generally believe that our country should strongly guide and advocate Chinese animation talents in practice to create and design a series of excellent Chinese animation characters with distinctive Chinese national culture, spiritual, and cultural characteristics connotation, and we should take this as an important measure to promote the formation of an animation characteristic cultural strategy for enterprises to actively explore the formation of enterprises with their own individual unique value of the animation market [5].

With the rapid development and popularization of computer technology and technological progress in the information age, algorithms have increasingly become an essential digital technology applied in people's daily work production and practical life [6]. Because this algorithm technology itself has another kind of application scene with strong and highly consistent interactive characteristics and deep learning autonomy, it is more widely and effectively used in many related industry fields such as medical simulation surgery, entertainment game interactive experience, decorative home environment optimization design, animation scene game design, and production process [7]. The scale of digital information technology product application tends to be increasingly popularized and developed at a high speed, which greatly leads to and effectively promotes the smooth and healthy development of the overall pattern of the world domestic film and animation business, which will be regarded as an indispensable and part of the coordinated development of the whole digital culture field industry chain system in China today and has become more and more a part of our promotion of national social and economic and cultural prosperity and global economic and social development, that is, the most important spiritual impetus for the harmonious and simultaneous promotion of national social and cultural prosperity and global economic and social development [8]. In order to further promote the rapid and comprehensive development of the whole and even China's animation industry, through further rationalization and optimization of algorithm technology and application, a set of more perfect and feasible animation character designs and workflows can be quickly formed, which can quickly determine a specific and accurate 3D animation character according to the actual needs of animation character design. It can determine a specific and accurate three-dimensional animation character and can quickly carry out collision trajectory and detection and analysis, so that each animation character can automatically and accurately detect and calculate the most accurate and reasonable collision flight path and can quickly and automatically complete the automatic tracking conversion of target tracking, flight trajectory tracking, and other action mode trajectories, so as to achieve the perfect animation character in the combination of simulation and reality. The perfect roaming in the animation scene system is required [9].

2. Research Background

To match the color of anime characters, let us first understand the definition of manga and animation separately. What is manga? The word "manga" in manga refers to the illustration of the water in the tank beyond the mouth of the tank. This description serves as a representation of the essence of the painting. It means that the character of the painting is the same as the water coming out of the tank. It is a description that goes beyond the description of the current situation. It is also a statement of supernatural expression. Therefore, the character cartoons appearing in the press are representatives of simple and easy-to-understand cartoons. These cartoons usually exaggerate and mutate the drawn objects, magnifying the character's characteristics without losing his nature, depicting life in a simple and exaggerated way, reflecting reality, and generating a sense of fun at the same time. This is how good works usually cause us to have a laugh and resonate with each other [10].

In terms of the development process, animation is the brother of manga, and the creation of animation is usually accompanied by a good manga script. The realization of animation is, in short, the coherent piecing together of a single comic work. Like the animated miniature books that we saw as children, they are composed of many dynamically connected and progressively developing pictures, which are quickly flipped through to obtain a vivid visual effect. It can also be said that animation is a moving comic strip, a combination of film and painting art. Long before digital technology was created, people already began to use simple, crude methods to create animation. Although the effect is far less than nowadays, the brilliant achievements of modern animation industry are inseparable from such exploration [11].

Animation is based on cartoons. As an extension of cartoons, animation automatically inherits the expressive function of cartoons. This means of expression can be used to make up for the lack of performance and expression of real people and objects, especially when it comes to exaggerated and distorted shots or magnificent scenes. From the production method, "animation" is a kind of video technology; that is to say, whether the traditional production of hand-drawn animation, or hand-drawn and computer coloring, and other technical means of combining the new form of animation basically relies on computer animation (including 3D and 2D), it is the use of technical means to achieve the video performance mode. In terms of expression, animation is a mode of running, from the moment of its birth, the way of its picture movement determines that it must be built based on traditional painting, film, music, theater, and other artistic expressions before seeking development. The subversion of live action and traditional theater in animation has also reached new heights with the prevalence of 3D technology today [12].

The specific classification of animation does not have any relatively fixed standard regulations. From the traditional drawing and production of animation, which is mainly classified according to the technical principle and modern art methods, animation art can be roughly divided into most of the traditional mechanical hand-drawn works, which are mainly based on the basic expression technology, and a few works, which are mainly based on the direct use of computer software to draw the basic content form. Mechanical computer animation: according to the closest to its television closest to the natural realistic artistic movement form method of these two kinds of animation of the basic action of the artistic effect expression form method and the basic action expression form method to separate and then according to be relatively comparable to the specific countries and regions, animation television can be divided according to the action of roughly close to the degree of reality and can be roughly divided into the action of the closest to the animation television closest to the natural realistic artistic action expression method of animation TV "perfect animation" (animation TV), and action is relatively more than animation TV to simplify some exaggerated action effect of TV animation TV such as "limited animation" (slide animation), and so on. If we can just move simply from the three-dimensional space plane out of the three-dimensional plane visual effect form and hierarchical relationship to cut, the roughly visual picture can further be cut into three-dimensional and flat animation (such as "cat and mouse") two-dimensional cartoon and three-dimensional animation (such as "monster Shrek"). Making a beautiful and high quality full animated film is a very complex process, while making a semianimated film is relatively simple. But in fact, no matter what kind of animated film it is, it must not be like the old live-action animated film, which first shot a lot of film, and the actors can of course only go to the temporary to play their own style characteristics, in the postediting process to try to cut out the extra parts they do not need to cut and add some relevant sound elements and background music, or even reshoot and cut into the film. The film can even be reshot and reedited into the film. In the process of animation production and implementation, we need to be able to accurately plan and control the specific time and number of images needed to complete each action in advance, and to ensure that there will not be any extra time images during the implementation process, so as to avoid some serious waste of financial resources, energy, and time.

In this paper, based on the above background analysis, we use algorithm technology, especially convolutional network technology, to study anime characters, especially their color matching generation algorithm, thus to innovate the color matching technology of anime characters and contribute to the improvement of our animation technology.

3. Research Method and Basic Theory

3.1. Basic Theory

3.1.1. Generative Adversarial Network (GAN). Generative adversarial network is a generative model proposed by Dellowgeed in 2004. The core idea of the model is "zero-sum game" thinking, and the more important is the optimization objective function, as shown in the following formula:

$$\min_G \max_D V(D,G) = E_{X\sim P_{\text{data}}}(x)[\log D(X)] + E_{Z\sim P_{\text{data}}}(Z)[\log(1-D(X))], \quad (1)$$

where z is the relevant noise value, from the P_z distribution of the collected samples, to generate the G latest required network, and Z according to the G_z formed is thus derived, while giving the color image 0 a label "", meaning that the generated one is a false image. At the same time as that the false image, the true P_{data} image is read from the x relatively correct distribution, and a code "" is given to 1. Subsequently, G_z is fed to the discriminator D together with x for discriminating. For the discriminator D that is used to discriminate, the value of $D_{G(Z)}$ is close to 0, while the value of D_X is close to 1; and with the true and false images, the value of the discriminator is used to reflect D, given G with to update the parameters [13].

3.1.2. Deep Convolutional Generative Adversarial Network with VGG Model. Convolutional neural networks may have been originally designed or developed specifically to deal with supervised object-oriented machine learning problems, but they have also evolved to include a series of unsupervised object-oriented machine learning system paradigms, including Convolutional Auto Encoders (CAE), Convolutional Restricted Boltzmann Machine (CRBM), Deep Convolutional Generative Deep Confidence Adversarial Machine (CRBM), and Deep Convolutional Generative Deep Confidence Adversarial Machine ((CRBM), CAE), Convolutional Restricted Boltzmann Machines (CRBM)/ Deep Convolutional Deep Belief Adversarial Networks (CDBN), and Deep Convolutional Generation Deep Convolutional Generative Adversarial Networks (DCGAN). These hybrid learning algorithms can generally be directly considered as another hybrid learning algorithm constructed by introducing deep convolutional neural networks in another original version of the unsupervised learning algorithm. Therefore, the Deep Convolutional Adversarial Generative Network (DCGAN), which we focus on in this chapter, is one of the core fundamental components of DCGAN.

The deep convolutional adversarial supervised generative network model (DCGAN) was first proposed by Radford et al.'s team in 2016. This network model is also the most effective combination of a deep convolutional neural network system (CNN) network model and a GAN network model and is based on another label-free, nonadversarial supervised generation network model. The two adversarial network models generated by the deep convolutional adversarial network model are actually replaced by the other two adversarial network models, the G model and the D model of the other model generated by the deep convolutional adversarial network model, and at the same time, the work required to do these two network models is replaced by the other two full-depth convolutional neural network

models. The two models are replaced by two other full-depth convolutional neural network models, and at the same time, some specific technical improvements are made to make the whole adversarial network model into another full-depth convolutional neural network.

The VGG model group (Oxford Visual Geometry Group) was originally used as a model for image feature classification systems, but the convolutional neural network part of the model has since been proven by scientists to provide a good technical solution for image feature classification extraction. Technical improvements, which can be used to extract more complete and rich image features with greater visual discrimination [14].

The color matching generation computation and confrontation network formed based on such network structure has been basically realized that it can be directly used in computers for various anime character color matching generation computation and generation, and although there are more problems, it still has the following six characteristics, that is, short generation path, rich diversity, clear type classification, mature automatic color matching system, high degree of completion, and clear color discrimination, as shown in Figure 1.

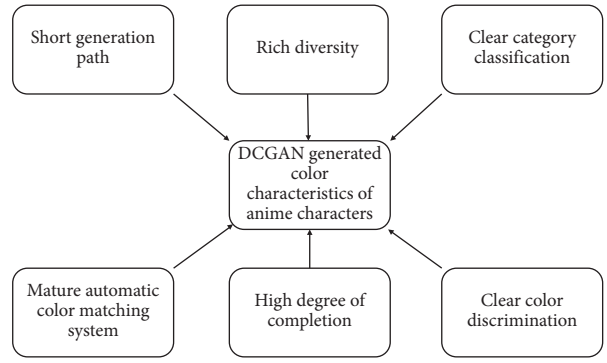

Figure 1: Color characteristics of anime characters generated by using DCGAN.

3.1.3. Multiscale Discriminator. The multisample image scale discriminator technology generally refers to the system that can perform random sampling operation from any one of the images, or at most several times, to obtain one more image of different image sizes and input the image information of all these different image sizes to the corresponding image type of the image information obtained from all these different image sizes that are input to the discriminator system (convolutional neural network) of the corresponding image type to perform the fast extraction and recognition operation of the relevant image feature signals and to complete the operation of various image subsequent recognition related operations. The size feature map of the size feature map of different size images can be built on the base map of the spatial position of each size feature in the range of the size discriminator in the network area map and can be converted into the size feature map of the next feature by convolution, and the size feature map of the size feature map containing a size feature on the base of the area map can be extracted from it. This network approach is also a network approach that fuses the information of scale objects and feature maps to identify and extract information by fusing multiple scale information in the network. The fusion of information is performed, and the final result is to be able to obtain the feature information of the identified object or the identified feature result of the object to be discriminated by the extracted object feature map [15]. This is shown in Figure 2.

3.1.4. Color Matching of Anime Characters. Anime culture refers to a game or a form of entertainment and leisure activity that is currently accepted by the largest masses of human beings and is a product of social reality in a modern and informationized society where human beings are actively seeking to obtain a certain cultural and spiritual value of liberation and a kind of spiritual and aesthetic support characteristics and its realistic spiritual orientation value. The design ability of anime character is one of the most core and key signs to evaluate whether the final form of a domestic original game and animation work can really obtain commercial success. Contemporary Chinese social and cultural life is in a new era of map reading, and symbolized textual information, pictorial information, and dynamic body movement information are undoubtedly among the most popular and easy-to-understand ways accepting new information forms found in the current contemporary environment. The visual image of the animation character is also a visual symbol that reflects its own culture and its aesthetic and cultural appreciation function, which plays an extremely important role in visual culture and aesthetic cognition [16].

The Chinese society in China has a relatively long history and many members and has many excellent cultural traditions and cultural resources that are much better than those of China. Since the development of more than 2.5 centuries, these elements of the world's traditional art have been perfectly integrated into the excellent original cartoon series designed by many famous original cartoon designers in the world today, so that they can be shown in a more unique and vivid form in a more original and unique expression. However, these excellent classic cartoon works are often not really able to fully and skillfully utilize these excellent classic elements. The main drawback of these classic animation works is that they only use a small part of the traditional Chinese costumes and patterns and do not use the traditional Chinese color matching and animation generation methods to use the traditional Chinese elements in a deeper way, animation elements. As a new generation of Chinese animation workers, we need to quietly continue to study, analyze, research, and organize the material culture of the Chinese nation with thousands of years of excellent national history and traditions, so that the most ancient and valuable historical material cultural assets of our nation can be truly preserved and carried forward in a better way. The research results of the project also focus on the in-depth analysis and systematic research to establish the theory of color matching design and the combined color design technology method of our traditional animation characters, which will be of great importance and innovation for the

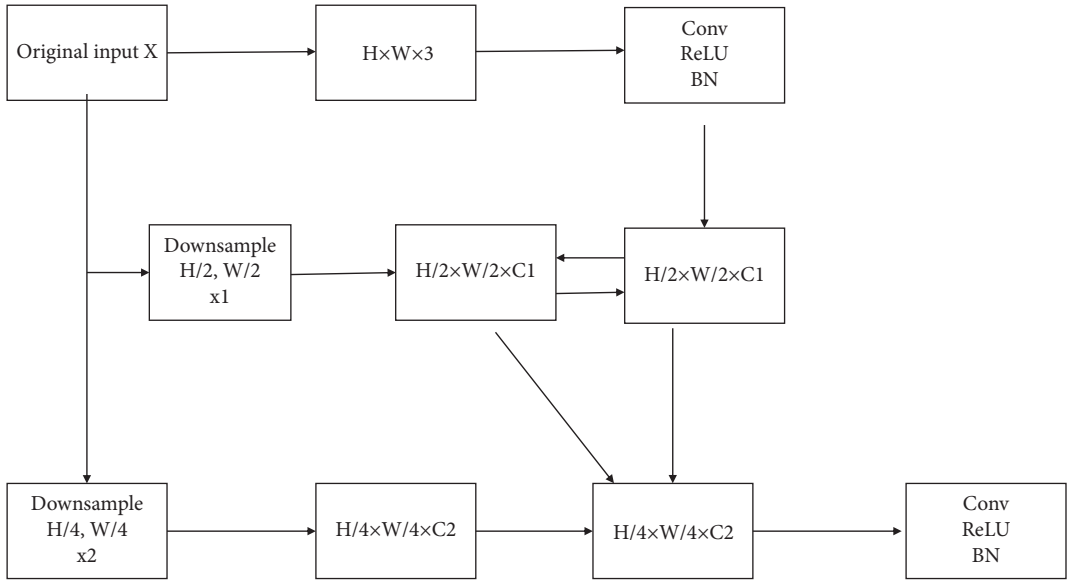

Figure 2: Multiscale feature fusion.

inheritance and continuation of the design of our national and traditional animation national cultural characteristics and for the continued research and development of the modern Chinese traditional color matching technology method of animation characters. This paper uses a variety of research methods to study the significance of this research.

Therefore, this paper uses various research methods to study the generation algorithm of color matching for anime characters, in order to provide reference for anime designers and help the anime industry to add more Chinese traditional cultural factors and promote the development of China's anime industry.

3.2. Research Methods

3.2.1. ACGAN Research Method. ACGAN is an image generation model designed by European computer scientist Odena et al. before 2017 that can autonomously generate images according to the conditions autonomously and, at the same time, improve the quality of automatic image generation. For the training sample set, this model requires not only the sample images, but also the category labels corresponding to each training sample [17].

The loss function simulated by this model mainly consists of the following two parts: one is the loss caused by judging the authenticity of pictures; the other is the loss caused by classifying pictures using discriminators. The specific form of the loss function is shown as follows:

$$L_s = E\left[\log P\left(\frac{S = \text{real}}{X_{\text{real}}}\right)\right] + E\left[\log P\left(\frac{S = \text{real}}{X_{\text{real}}}\right)\right], \quad (2)$$

$$L_s = E\left[\log P\left(\frac{C = c}{X_{\text{real}}}\right)\right] + E\left[\log P\left(\frac{C = c}{X_{\text{real}}}\right)\right]. \quad (3)$$

Among them, L_s is the loss caused by discrimination of true and false L_c images loss caused by map classification, $X_{\text{fake}} = G(z, e)$ are the generated images: training X_{real} images: discrimination of $P(S/X)$ truth and falsehood: $P(C/X)$ classification discrimination.

Because the two loss functions are logarithmic likelihood functions, which are of the same magnitude as $L_c + L_s$ numerically, they will maximize D to $L_c - L_s$ test and maximize G to test.

3.2.2. LMV-ACGAN Method. This article was to create model by using convolution based on neural network part of discriminant by further expanding it into a set of multidimensional scale information, which can help the authors and readers in the process of building model with detailed information and the comprehensive characteristics of some objective feeling, also revised structure of VGG better adapted to the actual task. Finally, the variable tag is applied to add the structure function, and the task of avoiding model collapse is completed well. A huge amount of experimental data proves that the model in this paper plays a good role in animation color matching [17].

LMV-ACGAN model has a good structure. The input variables of this model are mainly composed of z three parts: noise hidden h, parameter variable c, and label. The author uses vector z to h synthesize, and c and z input the G generator to generate the image color through the convolutional neural network to get the $G(z')$ fake image. At the same time, the x true $G(z')$ image and the common image are sent to D_CNN, and the convolution neural network is used for flatten operation to make the feature graph into a one-dimensional feature vector, and the changed feature vector is input to the following three MLP_S, MLP_C, and MLP_H, respectively, to judge the true and false images, classify images, and calculate printing parameter values. The overall structure is shown in Figure 3:

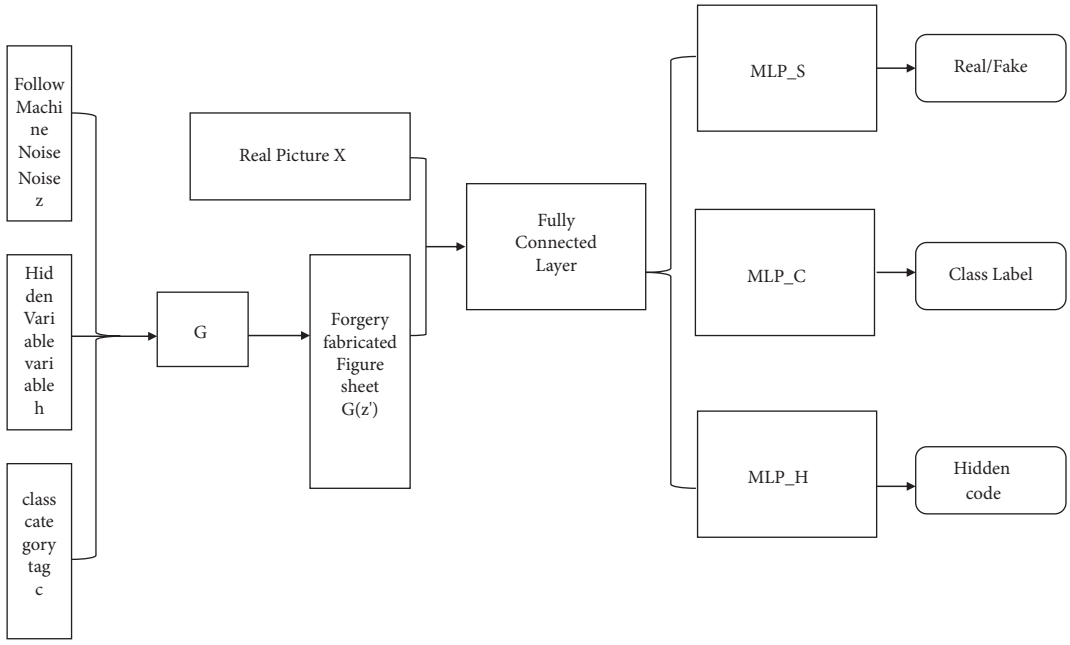

Figure 3: Overall structure of LMV-ACGAN model.

4. Research Results and Discussion

4.1. Discussion on Generator Network Structure. In order to solve the problem of DCGAN mode collapse easily, this paper changes the image generator structure into a new structure. As for the processing of the structural mode of the intermediate layer, the author can directly adopt the structural mode of the inverse VGG network and add it to a deconvolution network mode that contains more layers and smaller center displacement of the convolution kernel to directly conduct the data sampling processing and processing on the data of the structural mode of the characteristic layer. The author also here can directly see the step how to use the deconvolution of the network (convolution kernels center displacement of 2) and the structure of the model to directly complete it instead of using network model to deal with the anti-pooling characteristics of the layer structure model of all kinds of data stored on the network sampling. These data can keep all the different types of network information level data on the connection between as well as to the connection between the various network parameters information layer and network layer, and data exchange of information between data acquisition and transmission way will therefore change and become more simple and highly effective and economically efficient. Compared with the anti-pooling network, information loss is much reduced.

4.2. Discussion on Discriminator Network Structure. For the use of discriminator network, the author uses two criteria to discriminate: the original image: the original image width and half of the height for correlation discrimination. Model of the feature extraction part of the discriminator network, H where: image height, W: image width, DF: number of filters.

First, the first convolution group is fused to form a feature graph, and then the 1/2 feature graph is convolved and fused to the original feature graph and then merged into a feature graph and entered into the next volume group. The second method is to directly replace the mean pooling layer, which is less commonly used in the design of convolutional neural network originally designed by the author, with another convolutional layer with a large number of convolution kernels whose step number is more than 2 times, so as to achieve the purpose of next sampling. In this method, in order to effectively achieve more information retention than the original design of directly replacing with the mean pooling layer or replacing with a maximum pooling layer, the author added the InstanceNormalization layer after the convolution layer to better adapt to how to define the loss function. Solve the problem of bad parameters [18].

The following process can be used to identify the convolutional neural network output. Input three MLP-S without shared parameters, which are, respectively, used to distinguish the authenticity of images, identify network types, and restore implicit function parameters. Although these three networks have the same structure, different input layers can be used to define loss function, and their model structure is shown in Figure 4.

4.3. Discussion on Loss Function. This model is observed from the perspective of network structure. The output of network structure is composed of three parts. The first part is the image "true or false." The second part is image category. The third part is the implicit parameter corresponding to the image. In order to solve the problem of mode collapse and

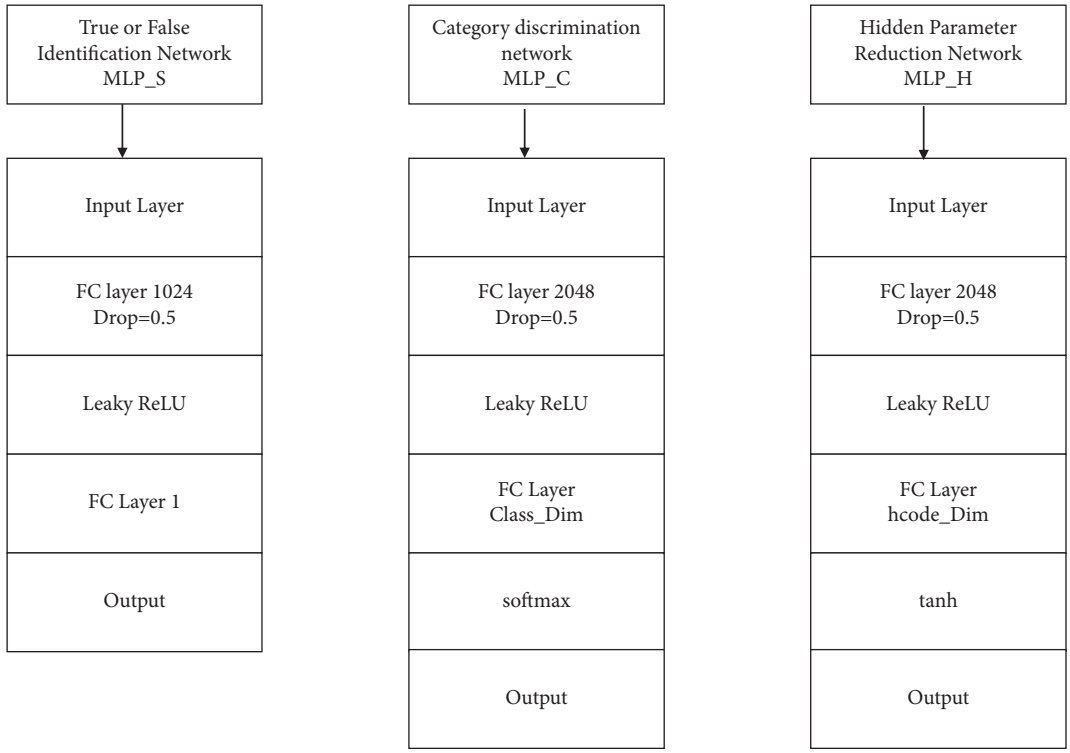

Figure 4: Three fully connected neural networks at the end of the discriminator module.

the defect of divergence used in the original loss function, Wasserstein JS distance was adopted to represent Earth-Mover (EM) distance from the real data set to the generated P_{date} data set. Therefore, P_g the definition of "true and false" loss function is shown in the following formula:

$$L_S = \sup_{//f//_{L\leq 1}} E_{X\sim P_{\text{data}}}[f(x)] - E_{X\sim P_x}[f(x)], \tag{4}$$

where f is a function we hope to find, indicating $//f//_{L\leq 1}$ that the function satisfies Lipschitz-1 continuity; that is, the function is a contraction map [19].

However, since the required function is f not easy to find, the gradient penalty approach is chosen to approximate the implementation [20].

For the category loss of the image, since the category of the image in this model is independent of the "true or false" image, which is equivalent to the convolutional neural network part of the discriminator and the fully connected classifier at the end to complete an independent classification task, the cross-entropy loss is used for the classification loss, and the labels of the input and output are encoded with one-hot, and if the y output of the MLP-C is represented y_i by y the value of each component of y' the representation, the category label corresponding to the input image y_i' is represented by the value of m each component of the total number of categories. The labels of the real image are from the label file (preclassified by chromatic aberration), and the image labels generated by the generator are from the random label vector corresponding to the input generator, and then the classification loss is L_c as shown in the following equation:

$$L_c = \frac{1}{m}\sum_{i=1}^{m}[y_i'\log(y_i) + (1-y_i')\log(1-y_i)]. \tag{5}$$

For the added hidden parameters, we aim to add a continuous set of parameters in addition to the discrete category labels that can provide some independent control over the image generation. According to the theory of mutual information, if this set of parameters can play an independent control role in the generation of images by the generator (i.e., not highly coupled with z the random noise), then the hidden h parameters and the z random noise should be independent of each other.

In this case, if there exists an encoder (input image compressed into a set of vectors), then M for the image from the generator, the output $G(Z')$ is obtained through M the encoder $z\sigma_X^{2,*} = M(G(z'))$, and it should be h possible to separate the individual components. If the hidden parameters of the input generator, $h = (h_1, h_2 \ldots, h_n)$ the solution of the $h = (h_1^*, h_2^* \ldots, h_n^*)$ MLP-H output, then we define the reduction loss of the hidden parameters L_h as in

$$L_h = \sum_{i=1}^{n}(h_i^* - h_i)^2. \tag{6}$$

Also, the optimization of the reduction loss of the hidden parameters can reduce the possibility of pattern collapse. We know that pattern collapse occurs when different random vectors are input, and then extremely similar or identical results are output. That $z_1' \neq z_2'$ is, but $G(z_1') = G(z_2')$ at this time, $G(z_1') = G(z_2')$ due to, so after the discriminator feature extraction, but $D[G(z_1')] = D[G(z_2')]$ the MLP-H

network will try to calculate the part of the reduced random vector according z' to h the extracted features, at this time, because the function has the feature of one input and only one output, so the calculated result will definitely be $h_1^* = h_2^*$, but the initial input into the generator vector is $h_1 \neq h_2$ likely, so the loss of the objective function will be large. Optimization for this part of the objective function will force G the generator to z' generate different results for different inputs. Although ACGAN also has category loss, the problem of too small a difference between images of the same category still occurs because the categories are discrete variables.

For the three losses defined in the above, L_S and, L_c through L_h experimental observation, we can learn that they are often not in the same order of magnitude numerically, and if the total loss is defined by simply adding up the sums often the small magnitude losses are ignored in the optimization, and at the same time, due to the independent branching structure of the total network, it is not very reasonable to update the parameters of the whole network at one time, so the following parameter update is used in training this model.

(i) L_S When optimizing the loss, D update, there are the network parameters of D-CNN and MLP-S. Update L_c for optimization loss, G the network parameters of D-CNN and MLP-S.

(ii) L_h For optimization loss, update G the network parameters of D-CNN and MLP-S.

In this way, the parameters of the generator and the feature extraction network are updated 3 times alternately in one update, and the network parameters of each branch are updated once at the same time. The use of gradient penalty to counteract the loss makes it unnecessary for the L_s loss to go through the Sigmoid function, avoids the unreasonable definition of the distance between the generator distribution and the true distribution due to the use of JS scatter, and solves the problem of updating the parameters of the entire discriminator network at one time in the ACGAN model, which also updates the parameters of the optimized category loss. The unreasonableness of the "true and false" discriminant loss is also solved.

4.4. Analysis of Experimental Results

4.4.1. Data Set and Labels. In order to further train and complete the method of color matching of original anime characters and the generated character models that will be further introduced in this paper, the authors have collected about 25,000 pixels of original anime characters' avatars from the Internet today, which are from different versions of the original anime characters, and all images are labeled with the same color as them. All images are marked with the same pixel resolution as their respective versions for the capture of the original anime character's facial features. The creators will use the lbpcas-cadeanimefcae script from the open source software to capture and analyze the facial information of the original anime characters from the major gallery sites. In order to achieve the final design goal of the author's anime character color model generation, the model will be mainly designed to be applied to the character avatars on personal information pages, etc. Therefore, this paper needs to be able to uniformly scale and convert all these images into a relatively fixed size image to be used as a network for training to generate this model.

Since all the automatic image generation method models that the authors will discuss in the previous paper must first have an automatic image generation method-assisted model classifier, the authors conclude this paper with the need to reconsider and further refine the approach to automatic image generation method models with centralized processing method functionality based on real image data reclassification. After careful observation, the authors soon found that when the model designers used some relatively new and original versions of WGAN, LSGAN, DCGAN, etc. for image color model generation and postproduction design, the head hair tones often formed a serious degree of color crossover and mingling with the image background color, and the boundaries were not clear. Therefore, in this paper, we will use the head hair color as one of the main categories of the image color expression, so that the modelers can try to learn how to apply the hair color to the "drawing" image by this method to increase the success rate of hair color matching in images.

Based on the large number of basic color data sets that the authors have personally measured in practice and the basic color theory based on CIEDE2000 color difference theory calculations, we are hopeful that we can determine, in practice, the 8 basic color categories that were calculated, which can be referred to as black, red and white, red, green, blue, brown, purple, and yellow, respectively. Through the application of CIEDE2000 color difference theory to analyze through the calculation of the hair color measured by the most should belong to which kind of what type of hair color class to analyze further analysis to further determine the hair image color category, so that we can finally, directly get the hair label.

4.4.2. Generating Model Evaluation. The collapse of the model will mean that the image will look like the real one, but in reality, it is likely to be a real one that looks very much like the impossible one. The model in this paper is a good solution to the problem of model collapse in practice. The generated model solves the problem of collapse better, and the number of collapses decreases significantly. The collapse rates of the models used in this paper have all decreased significantly. The authors have not been able to find out that although these models are generally easy to generate images accurately and quickly but normally and effectively in the early stages of the development of the training generation models; in fact, after the models have reached the level of 100th generation of the training generation (epoch), the DCGAN models and WGAN models are very likely or effective. However, in fact, after the training generation (epoch) of the model has reached the level of 100th generation, the DCGAN model and the WGAN model are very likely or easy to have a serious error result of image pattern

collapse. In contrast, the model in this paper has completely solved the problem of model collapse and improved the image realism and color matching of anime characters only at a certain level of theoretical foundation [20] as shown in Figure 5.

The higher the value, the higher the color matching of the anime character, and the better the color matching of the anime character designed in this paper. This index is an indirect index. After comparison, it is found that the color matching degree is significantly improved in this design model, as shown in Figure 6.

This algorithm study also investigated the relationship between the color matching degree of the anime character and the utilization rate of the convolutional neural network algorithm, and the horizontal coordinate of Figure 7 is the utilization rate of the convolutional neural network algorithm, and the vertical axis is the color matching degree. The results show that as the utilization rate of convolutional neural network algorithm keeps improving, the level of color matching of anime characters also keeps improving. Although this study investigated the relationship between the color matching degree of anime characters and the utilization of convolutional neural network algorithm, there is a significant effect between the two. However, this study is an indirect study and does not directly prove a correlation. Even if there is a regression relationship, it is necessary to include other variables for comparison and to consider the influence of disturbing factors, to consider the statistical relationship comprehensively, and to consider the range of p-values as well as the range of u-values as shown in Figure 7.

4.5. Discussion of Image Generation by Category. In this paper, the model design only supports the automatic image generation under the specified category conditions. In order to make the analysis and comparison between the further model design and the modification of the original ACGAN model, the authors have recently modified the system and optimized the design and improved the system by using the same method as the original ACGAN model. The authors have recently redesigned and optimized the system to use the automatic image generator and the automatic image performance discriminator and analyzer that may be used in the modification of the original ACGAN model.

For CGAN, in addition to the above-mentioned differences between the same type of ACGAN tags, one of the most important features of CGAN tags is that they can be used as part of the network image feature extraction by direct input, together with the network image tag part and the final discriminator part of the direct input method. The final discriminator part is generally responsible for inputting the network image features as true or false, but not for outputting the network image features to be extracted from the input, and can then perform a new network image classification based on the additional network image features provided in the network input information to obtain another classification of the network label, which can be used to compare with the input network label features. The network labels are then used for analysis and comparison with the network label features of the input information. The authors have now trained and tested these three models for automatic image generation by category after completing about 300 epochs. After further careful study and analysis, the authors further found that the three original models mentioned above have been or can be fully implemented to identify and generate each category of image errors in the input images and to separately identify and generate each category of image errors in the input images according to the requirements. For the original model of CGAN, similar to the original model of ACGAN, there are several phenomena that may occur at the same time when there are errors in recognition or when recognition fails to generate when there are errors in individual input images or multiple image categories. In the process of recognizing the color of multiple input image categories, there are several common situations in which the color discrimination may be wrong (e.g., the color discrimination of white and brown categories of CGAN is wrong or cannot be generated, the blue category of ACGAN cannot be generated correctly, and the green and brown categories are wrongly judged by the model), and special optimization processes are carried out for such special situations.

4.6. The Role of the Implicit Function in Generating the Model. In this section, the noise parameter vector z and the image class parameter vector c are introduced for the special treatment of the images, and the process requires special attention in the next steps to make them as stable as possible when observing all the images in the image dimension and any values in the other or in any other range of image dimensions and to keep the maximum value at or equal to or less than to 0. In this experimental and research process model, the authors will also be able to observe and obtain, at the same time, that the continuous variation of each image dimension value parameter will be such that one image parameter in the image generated by the authors' research will be able to produce a continuous variation in each or several image dimensions, while it will also vary continuously with each other, such that it will be able to produce a continuous variation in each image dimension parameter. The continuous changes of the image parameters in each dimension are also independent of each other, and the continuous changes of the image parameters in each dimension can affect the continuous generation process of the whole image parameters. The main feature of the 1st dimensional parameter that can be used to control the change and transition of the image is simply the relative value of the length of the hair, which is obviously a transition from a medium-length image with a value of -1 or so to a medium-length image with a value of 1 or less that can be directly observed. The transition from a medium-length image with a value of about -1 or less to a medium-length image with a value of about 1 or less and the whole process of the transition in this mutual continuous change will be a mutual continuous change in the transition process; observing the 2nd dimensional hair data, it is already obvious that the hair parameter here is mainly used to control another hair

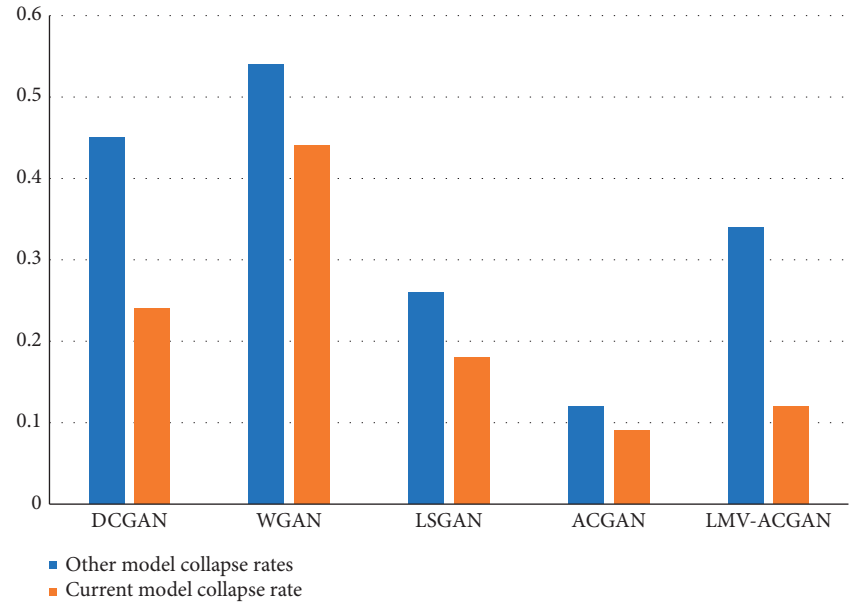

Figure 5: Comparison between other models and the present model collapse rate.

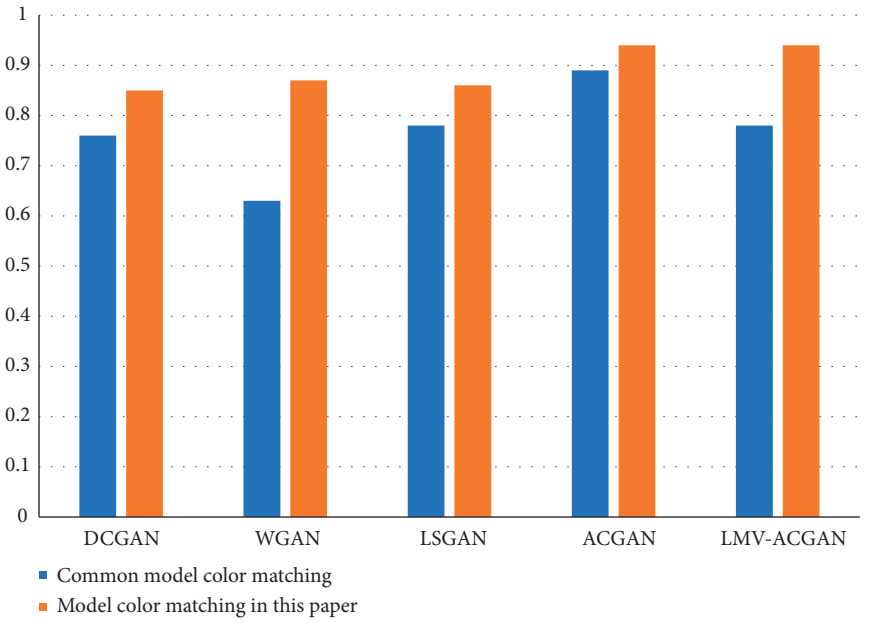

Figure 6: Comparison of color matching degree of anime characters.

parameter that can be used to control the facial features of the hair, that is, the shade value of the hair color, from a value of less than -1 or an absolute value greater than 1 when the overall color of the hair is light dark red. When the value is 0 or the value is equal to 1, the overall color of the hair is dark. By comparing the 3rd and 4th dimensional observations, it is possible to obtain the intuitive result that these two data have the property of being transformed into each other; comparing the observation data in the 5th dimension, the author will also be able to see a more intuitive and clearer comparison of the observation data and will find that the color matching effect is very good. In the process of controlling the generation of the actual parameters of the image, the authors may also or may not be able to simultaneously consider how the generation of the "detail" parameters of the image can be controlled by modifying some of the hidden actual parameters.

4.7. The Role of Hidden Parameters and Multiscale Discriminations in Training and the Impact on the Auxiliary Discriminators. A comparative analysis and illustration are presented to show how the ACGAN model is used in the original early version and the LMV-ACGAN model presented in this paper and how the loss values of the auxiliary classifier parameters change during the actual

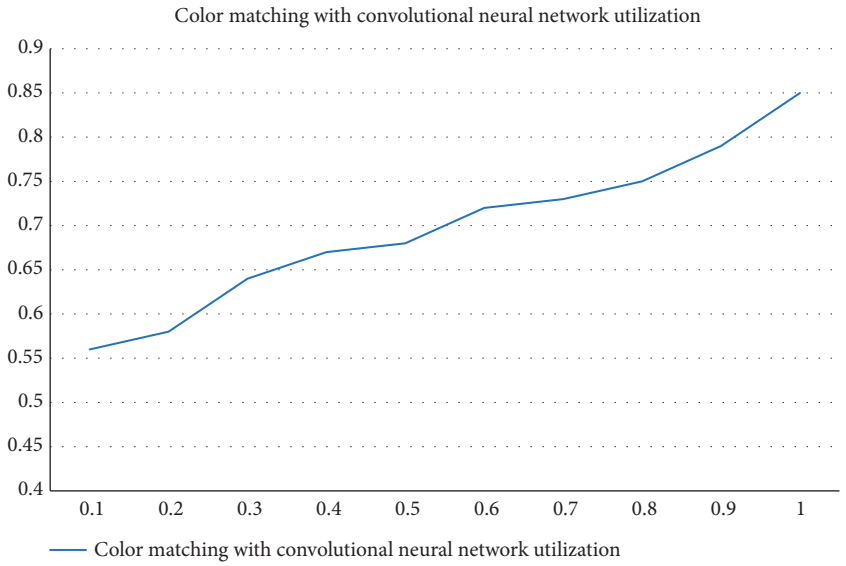

Figure 7: Color matching with convolutional neural network utilization.

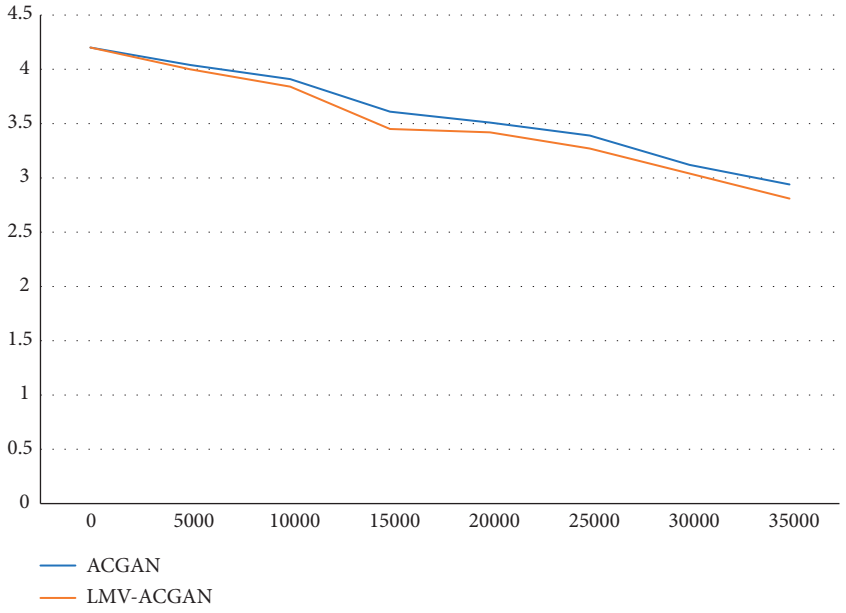

Figure 8: Comparison of classification loss of ACGAN and LMV-ACGAN.

training process. From the comparison of the graphical results, it is clear to the authors that the number of losses of the implicit parameters in the model is increasing gradually and rapidly and that the discrimination and errors that may arise in the multi-implicit parameter scale model are clearly likely to develop further, leading to an increase in the number of losses in the parameters of the scale model. However, I have not seen any direct impact on the convergence rate of the model parameters due to the continuous and rapid increase in the amount of hidden parameter losses. At the same time, the weighted mean value of the classification loss information is obtained after increasing the number of iterations to about 35,000 per second; that is, the authors can directly see that the weighted mean value of the classification loss information obtained after increasing the number of iterations to about 35,000 per second has been significantly reduced from the original 2.94 to nearly half of the current value and has now significantly exceeded the original 2.81, by a certain degree. This is undoubtedly a significant increase in the accuracy of the image classification function and the image judgment ability of the auxiliary image generator when generating auxiliary images by category. At the same time, this model can ensure faster and more effective image classification and discrimination results at the performance level with fewer iterations and generation times than the model that can be applied to ACGAN independently as shown in Figure 8.

5. Conclusion

Animation media language refers to a kind of audio-visual combined with a comprehensive use of audio-visual effect of the animation language, rapid and convenient mode of transmission, and young and old children of both sexes, which also often contains the performance of the integration of a variety of traditional human values, outlook on life, and world view, reflecting a profound and rich variety of national cultural significance and ideological tendencies enough to affect deeply the daily work of people in contemporary society. It is a correct choice of various social ways of thinking and behavior concepts and various social life path patterns. Anime media is one of the most important media that the author has vigorously inherited and developed under the essence of our long-standing Chinese traditional animation culture. Anime character modeling design is one of the most fundamental cores of the author's styling creativity for all traditional animation works. The content of anime character modeling design usually also includes traditional anime character image modeling design, character color modeling design, costume style design, and action modeling design content. The color part is also one of the main visual symbols to show the most direct and vivid and intuitive character effect in anime, and the design techniques of color element matching and color generation have been occupying an extremely important position in almost all the visual design methods of anime character modeling.

In this paper, we innovatively used convolutional neural network algorithm to innovate the color matching generation of anime characters and improve the traditional technology of color matching of anime characters. This paper mainly utilizes Generative Adversarial Network (GAN), Deep Convolutional Generative Adversarial Network and VGG model, and multiscale discriminator theory, uses ACGAN research method and this paper's innovative LMV-ACGAN research method for study, and concludes that other models have higher collapse rate than this model; this model has higher color matching of anime characters, and color matching improves with the utilization of convolutional neural network improved with the increase of convolutional neural network utilization and other conclusions. Moreover, the advantages and disadvantages of this study are reviewed, so that later researchers can have a more rational and objective understanding of this study. In general, this model has advantages over the traditional model, but there are problems such as pseudoregression that needs the attention of later researchers.

Data Availability

The dataset can be accessed upon request.

Conflicts of Interest

The authors declare no conflicts of interest.

References

[1] H. Yuan, J. H. Lee, and S. Zhang, "Research on simulation of 3D human animation vision technology based on an enhanced machine learning algorithm," *Neural Computing and Applications*, 2022.

[2] Z. Xu and Z. Mu, "Evaluation and analysis of animation multimedia 3D lip synchronization considering the comprehensive weighted algorithm," *Advances in Multimedia*, vol. 2021, Article ID 8189082, 7 pages, 2021.

[3] R. Zhang and H. Lv, "Computer vision-based art color in the animation film performance characteristics and techniques," *Journal of Sensors*, vol. 2021, Article ID 5445940, 12 pages, 2021.

[4] Q. Ahmad, T. Salah, H. Aljammal Ashraf, H. Nabhan, B. Mustafa, and K. Mohammad, "Parallelism exploration in sequential algorithms via animation tool," *Multiagent and Grid Systems*, vol. 17, no. 2, 2021.

[5] Z. Lin, "Research on film animation design based on inertial motion capture algorithm," *Soft Computing*, vol. 25, 2021.

[6] D. Shen and Y. Dong, "The ideographic function of color language in animated film works," in *Proceedings of the 2021 4th International Conference on Arts, Linguistics, Literature and Humanities*, Tokyo, Japan, June 2021.

[7] X. Liu, "The ideographic function of color language in film and television animation works," *International Journal of Education and Economics*, vol. 4, no. 2, 2021.

[8] L. Xu, "Fast modelling algorithm for realistic three-dimensional human face for film and television animation," *Complexity*, vol. 2021, Article ID 3346136, 10 pages, 2021.

[9] D. Cheng, J. Peng, Y. Di, and S. Wu, "3D face modeling algorithm for film and t elevision animation based on lightweight convolutional neural network," *Complexity*, vol. 2021, Article ID 6752120, 10 pages, 2021.

[10] J. Liang, "Design and realization of animation composition and tone space conversion algorithm," *Complexity*, vol. 2021, Article ID 5579547, 11 pages, 2021.

[11] X. Fan, "Application of style transfer algorithm in the design of animation pattern special effect," *Journal of Physics: Conference Series*, vol. 1852, no. 2, 2021.

[12] W. Bao, "The application of intelligent algorithms in the animation design of 3D graphics engines," *International Journal of Gaming and Computer-Mediated Simulations*, vol. 13, no. 2, pp. 26–37, 2021.

[13] Y. Zhu, Q. Chen, J. Liu, and X. Tian, "Fast Adaptive Character Animation Synthesis Based on Greedy Algorithm," *Complexity*, vol. 2021, Article ID 6685861, 11 pages, 2021.

[14] H. Zheng and K. Wang, "Psychological display of color VISION IN flash animation making course," *Psychiatria Danubina*, vol. 33, no. 5, 2021.

[15] H. Ren, "Study on aesthetic value of color art in movie and TV Animation," in *Proceedings of the 7th International Conference on Arts, Design and Contemporary Education (ICADCE 2021)*, August 2021.

[16] D. Roy, G. Fragulis, H. A. Cantu Campos, A. Sugiyama, and M. Cohen, "Animated Color Cube," *SHS Web of Conferences*, vol. 102, 2021.

[17] L. Dai, "The influence of traditional Chinese art color on animation creation," *International Journal of Social Science and Education Research*, vol. 4, no. 1, 2021.

[18] L. Zhu and L. Zhu, "Research on color design in interactive animation design software," *Journal of Physics: Conference Series*, vol. 1648, no. 2, Article ID 022159, 2020.

[19] X. S. Zhang and D. H. Choi, "Color analysis of the skeleton images in animation - focused on coco," *Cartoon and Animation Studies*, vol. 59, pp. 155–175, 2020.

[20] D. Dey, A. Habibovic, P. Bastian, M. Martens, and J. Terken, "Color and Animation Preferences for a Light Band eHMI in Interactions between Automated Vehicles and Pedestrians," in *Proceedings of the Human Factors in Computing Systems*, April 2020.

Hindawi
Computational Intelligence and Neuroscience
Volume 2022, Article ID 3781750, 10 pages
https://doi.org/10.1155/2022/3781750

Research Article

Application of Artificial Intelligence within Virtual Reality for Production of Digital Media Art

Yunxuan Wu [1,2]

[1]*College of Culture and Communication, Liming Vocational University, Quanzhou, Fujian 362000, China*
[2]*Graduate University of Mongolia, Ulaanbaatar 14192, Mongolia*

Correspondence should be addressed to Yunxuan Wu; 20022313@lmu.edu.cn

Received 20 June 2022; Revised 16 July 2022; Accepted 19 July 2022; Published 10 August 2022

Academic Editor: Yaxiang Fan

Copyright © 2022 Yunxuan Wu. This is an open access article distributed under the Creative Commons Attribution License, which permits unrestricted use, distribution, and reproduction in any medium, provided the original work is properly cited.

As technology changes, virtual reality generates realistic images through computer graphics and provides users with an immersive experience through various interactive means. In the context of digitalization, the application of VR for digital media art creation becomes a normalized method. Today's digital media art creation is closely related to vigorous technological innovation behind it, so the influence of modern technology is inevitable. Virtual reality and artificial intelligence have gradually become the main technical means in line with the development aim for digital media art creation. This work proposes an art object detection method AODNET in virtual reality digital media art creation with AI. Aiming at the particularity of object detection in this direction, an art object detection strategy based on residual network and clustering idea is proposed. First of all, it uses ResNet50 as backbone, which deepens network depth and improves the model feature extraction ability. Second, it uses the K-means++ algorithm to perform clustering statistics on the size of the real annotated boxes in the dataset to obtain appropriate hyperparameters for preset candidate boxes, which enhances the tolerance of the algorithm to the target size. Third, it replaces the ROI pooling algorithm with ROI align to eliminate the error caused by the quantization operation on the characteristics of the candidate region. Fourth, to reduce the missed detection rate of overlapping targets, soft-NMS algorithm is used instead of the NMS algorithm to post-process the candidate boxes. Finally, this work conducts extensive experiments to verify the superiority of AODNET for object detection in virtual reality digital media art creation.

1. Introduction

VR technology is to create virtual environment through the application of computer operation and image technology. This virtual environment is a dynamic and perceptible simulation environment, in which users can perceive and obtain relevant information through physical senses. Since the simulation environment constructed by VR technology adopts 3D modeling technology, the rendered scene is relatively realistic. Coupled with the application of some other technologies, users can perceive information in the VR environment through vision, hearing, touch, and even smell and taste, so that users are immersed in it, and the transmission of information becomes more direct and specific. Artificial intelligence technology refers to a technology that imitates the consciousness and thinking cognition of the human brain through computer technology and on the basis of big data. As an interdisciplinary frontier discipline, artificial intelligence covers a series of disciplines such as mathematics, computer science, psychology, statistics, and biology and integrates knowledge. This enables it to perform simple self-learning and achieve intelligence. At present, although artificial intelligence technology has not been fully applied to life, the prototype of aAI applications has been seen in many industries. It will become the main technical support for various industries in the future [1–5].

The traditional approach of creating digital media art is straightforward, but it also necessitates a high level of imagination and perception on the part of the artist. Because of this, creating a work of digital media art requires a significant investment of time, energy, and materials. The advent and development of AI and VR technologies, however, have given rise to new idea for digital media art in the current social context. To a certain extent, this lessens the

difficulty of digital media art creation and improves producers' job efficiency and their work quality. Work in diverse forms and unique creation processes are continually appearing as a result of involvement of virtual reality in digital media art. As the VR and AI have grown, it has range of digital media art forms and content available [6–10].

With VR, the makers of digital media art can not only experience a virtual world, but they can also keep their biological perceptions as well. As a result, it might provide a sense of immersion, which is extremely advantageous to the creative process of the creator. To provide a pleasant experience from start to finish, virtual reality's artificial intelligence may adapt to the preferences of the user. To the designers of digital media art, virtual reality technology can provide a unique experience because it is a front-end technology that includes a wide range of functionalities. It is possible to create a more lifelike virtual reality experience by utilizing artificial intelligence in conjunction with the enhanced three-dimensional perception provided by human vision. The artificial intelligence of VR technology can also help digital media artists gather a large amount of data, giving them a better understanding of how their methods of information transmission differ from others. VR can be used to create three-dimensional sensation of immersion in the virtual environment by digital media artists. Because of the great capabilities of virtual reality's artificial intelligence application, it is possible to immerse oneself in the virtual world and improve one's effectiveness and breadth in receiving information from it. When seeing digital media artworks in the past, people relied solely on view. All the senses can be activated when appreciating these works under influence of science, resulting in greater realism and a more authentic experience. With the help of artificial intelligence, virtual reality may be used to its greatest potential, allowing users to gain a deeper understanding of creators and goals for their works. VR's artificial intelligence challenges and expands the creative possibilities of digital media artists, according to their perspective. Because virtual reality art is created using artificial intelligence and relies on digital media, it is safe to assume that digital media has played a significant role in shaping its organizational structure and aesthetic attributes. Although digital media art is still a form of art, its unique characteristics need a shift in the way people view and appreciate it [11–15].

Aiming at the particularity of object detection in digital media art creation of virtual reality, this work proposes an art object detection algorithm based on residual network and clustering idea. First of all, it uses ResNet50 as the feature extraction network, which deepens the network depth and improves the model feature extraction ability. Second, it uses the K-means++ algorithm to perform clustering statistics on the size of the real annotated boxes in the dataset to obtain appropriate hyperparameters for preset candidate boxes, which enhances the tolerance of the algorithm to the target size. Third, it replaces the ROI pooling algorithm with ROI align to eliminate the error caused by the quantization operation on the characteristics of the candidate region. Fourth, to reduce missed detection rate of overlapping targets, soft-NMS algorithm is used instead of the NMS algorithm to post-process the candidate boxes. Finally, this work conducts extensive experiments to verify the superiority of AODNET for object detection in virtual reality digital media art creation.

2. Related Work

Reference [16] analyzed some basic characteristics and development of virtual reality technology and made a general analysis of future applications. However, the writing time of the article was relatively early, the analysis process was brief, and the examples cited in the article were also the artist's own vision, and at that time, there was no suitable case to prove it. Literature [17] not only systematically introduced the technology, application, history, and development issues involved in VR virtual technology but also introduced how to use virtual technology in art. This was a large-scale introduction to some big concepts, and the author also explained it from the perspective of a virtual reality technology researcher. Literature [18] made clear expectations for the combination of virtual reality and art and analyzed several important factors for the combination of the two: the development of art in the computer age, the subjective exploration of artists, and the needs of audiences. Literature [19] compared VR technology with the current Internet and genetic engineering. At the same time, it introduced many artists who used virtual reality technology as a means to create and also introduced various types of virtual art. Literature [20] roughly talked about the impact of virtual reality technology on artistic creation, teaching, and the application of installation art, conceptual art, and urban public art. It briefly introduced that virtual reality technology would be used in this area, but there was no specific and in-depth analysis, and the research was not detailed and rigorous enough. Literature [21] proposed that with the development of virtual reality technology, new conditions and requirements were provided for the application of art in teaching, and a lot of practice had proved that virtual reality technology was very effective in art teaching. An in-depth look at the existing and potential future effects of virtual reality on our daily lives may be found in the literature [22]. It considered how virtual reality could be used in a wide range of industries, as well as its creative and entertainment applications. It argued idealists' enthusiasm for computerized life that must be balanced with the need for a deeper understanding of basic reality. Reference [23] analyzed the virtual reality in the past few years, the new hardware had been entering the market, and the price was reasonable. The driving force of virtual reality was not only in the scientific community, but more and more enthusiasts were also expanding with new technologies. The situation of virtual reality in the field of commodities was becoming more and more important, and it was said that the current technology was already very powerful.

Reference [24] proposed R-CNN, a classic work that applied deep learning technology to target detection. Its main steps were divided into two parts: target candidate region generation and accurate classification and regression, which were called two-stage target detection. Reference [25]

proposed the SPPNet algorithm, which used full-image convolution as feature extraction, and proposed a spatial pyramid pooling network structure. Reference [26] proposed Fast-RCNN, performed ROI pooling on the feature map to obtain the sampled feature map, and used the multitask loss to realize the end-to-end network training process. Reference [27] proposed faster R-CNN, which uses RPN to realize target candidate region screening with a convolutional neural network and proposed to encode and assign targets in the way of anchor. It defined the network position output as the relative relationship with the anchor box, so that the whole process task was completed by the neural network structure. Reference [28] proposed feature FPN, which developed a top-down horizontal connection structure to form a feature pyramid for the problem that the low resolution of deep networks was not conducive to accurate regression. Reference [29] pioneered the use of a single-stage network structure to complete the target detection task and proposed the YOLO algorithm. It did not use the RPN structure to perform coarse-grained estimation of the target existence area, but directly regarded target detection as a regression problem and predicted that the target position represented by each pixel position on the feature map was in the target category. Reference [30] assigned different scale targets to feature maps of different resolutions as output, which improved the detection ability of the algorithm for small-scale targets. Reference [31] analyzed the reasons why the performance of the single-stage detection lagged behind the two-stage detection algorithm. The conclusion was that the single-stage detection algorithm had a process similar to dense sampling, which led to extremely serious sample imbalance in the process of positive and negative sample assignment. Therefore, the focal loss was proposed, which enabled network to obtain a higher loss for the allocation of few samples and difficult samples during the training process, so as to control the bias of the algorithm. Reference [32] proposed CornerNet, which defined the object detection task as a key point regression task. It defined the supervision signal of the key point as a Gaussian patch whose variance was determined by the target scale, proposed a corner pooling structure, and assigned the network output as the heat map composed of upper left and lower right corners of bounding box as key points to be regressed. The CenterNet proposed in the literature [33] inherited the idea of key point detection, took the center position of the target as the key point to be returned, and could be extended to tasks such as monocular 3D detection and pose estimation. This kind of target detection algorithm based on Gaussian spot detection as a key point used the positive sample representation of the target at the maximum value position in the heat map, thereby replacing the non-NMS process in other detection algorithms.

3. Method

Aiming at the particularity of object detection in digital media art creation of VR, this work proposes an art object detection algorithm AODNET based on residual network and clustering idea. First of all, it uses ResNet50 as the feature extraction network, which deepens the network depth and improves the model feature extraction ability. Second, it uses the K-means++ algorithm to perform clustering statistics on the size of the real annotated boxes in the dataset to obtain appropriate hyperparameters for preset candidate boxes, which enhances the tolerance of the algorithm to the target size. Third, it replaces the ROI pooling algorithm with ROI align to eliminate the error caused by the quantization operation on the characteristics of the candidate region. Fourth, to reduce the missed detection rate of overlapping targets, soft-NMS algorithm is used instead of the NMS algorithm to post-process the candidate boxes.

3.1. Convolutional Neural Network. CNN is a kind of feedforward network whose function is similar to that of multilayer perceptron. Convolutional neural networks are mainly composed of multilayer convolutional layers and the convolution kernels they contain. To ensure nonlinear transformation between convolutional layers and efficient computing process, its network components also include activation layers and pooling layers. Finally, the final output is obtained through the fully connected layer, the loss value is calculated in the objective function, and the partial derivative of the objective function to each layer is calculated through backpropagation, to update the weight parameters of the network, so that the network can learn from the data.

The convolutional layer is composed of multiple convolution kernels and is the basic structure of CNN. The main function is extracting local features. The essence of convolution is many multidimensional matrices responsible for saving the parameters learned by the network. Each convolution kernel has the characteristics of local receptive field and weight sharing for the input image, which can reduce the computational complexity and parameters compared with traditional ANN. In a convolutional neural network, the convolution kernel of each layer is only connected to some of the convolution kernels of the previous layer, the low-level convolution kernel is responsible for extracting local features, and a high-level convolution kernel is responsible for integrating feature information to obtain global feature map. Compared with fully connected layer, the partial connection method can better alleviate the problem of overfitting, reduce parameters, and speed up the convergence speed of network. The weight-sharing feature of the convolution kernel is that the convolution kernel shares the same set of parameter operations in all regions of the input feature map. However, since the convolution kernel extracts the local features of the input image, each convolution kernel can only extract fixed features. Therefore, by increasing convolution kernels, image attributes that can be extracted by the convolution layer can be increased. Convolutional layers of different depths can extract different features, and feature maps extracted by low-level convolutions learn local features due to the small receptive field. A high-level feature map is composed of low-level feature maps, so the convolution kernel can extract more complex and comprehensive features. The convolution is calculated as follows:

$$\mathrm{Conv}(x) = \sum_i w_i x_i, \tag{1}$$

where w is weight and x is feature.

The pooling layer is usually connected after a single or multiple convolutional layers, and its main function is to simplify the total amount of parameters and computation of the entire model by reducing feature map size. This can also increase the receptive field of convolution kernel, ensure the invariance of the network, and prevent overfitting during network training. Average pooling is to calculate the average value, and max pooling selects the maximum value. Both of these operations can increase the nonlinearity of the feature and reduce the error caused by feature extraction. The error mainly comes from two aspects. Average pooling can reduce the increase in error due to the limited field size and can retain more background information of the input image. Maximum pooling can reduce the estimated value shift caused by the error of the convolution kernel parameters and can retain more texture information of the input image. The main function of global pooling is to replace the FC layer and convert the feature map into a one-dimensional feature and pass it into the classifier for classification. The fully connected layer has the disadvantage of limited input dimension. The input feature map needs to be converted and spliced into a one-dimensional vector before it can be calculated, and the number of parameters is very large. Therefore, global pooling can directly calculate a one-dimensional feature vector.

The activation layer mimics the reflex function of neurons by modeling its design after the human neural network. The classifier cannot discriminate between the abovementioned convolutional and pooling layer operations on the image because they are linear transformations. Therefore, the extracted feature map can be nonlinearly mapped through the nonlinear activation function, thereby enhancing the expressive ability of the feature. The commonly used activation functions are as follows:

$$\begin{aligned} \mathrm{Sigmoid}(x) &= \frac{1}{\left(1 + e^{-x}\right)}, \\ \mathrm{Tanh}(x) &= \frac{\left(e^{x} - e^{-x}\right)}{\left(e^{x} + e^{-x}\right)}, \\ \mathrm{ReLU}(x) &= \max(0, x), \end{aligned} \tag{2}$$

where x is feature.

FC layer basically corresponds to a convolutional layer of 1×1. The fully connected layer takes input features from the previous layer and performs a global analysis on the output features of all previous layers. Then, a nonlinear combination is performed, so it is generally used at the end of the network for classification tasks.

3.2. Combination of ResNet and Faster R-CNN. The shallow network can extract the simple outline information of the target, and the deep network can extract complex semantic information. However, with the deepening of the number of network layers, the model training process is difficult to converge, and classification accuracy is hard to improve. The special residual structure in ResNet subtly alleviates the problems of gradient dispersion, gradient explosion, and insignificant network performance improvement when the network depth is deepened. The idea of residual network draws on the definition of residual in statistics, and the residual is the difference between actual observed value and fitted value. Suppose one of the residual units in the residual network has to learn a mapping, but this mapping is difficult to learn directly. The residual network then transforms the original complex mapping into a simple summation operation.

Figure 1 is a schematic diagram of the residual unit. There are two branches when the feature is input into the network. One is the direct identity mapping branch without any processing. The other is the mapping branch obtained after the feature is convolutional, normalized, and activated. Then, at the confluence of the two branches, a linear superposition operation is performed on them to obtain output for the residual unit.

$$x_{l+1} = \mathrm{ReLU}(x + F(x)), \tag{3}$$

where x is feature and F is residual function.

The residual unit realizes the identity mapping of the deep network without increasing the computational cost by using a shortcut connection, which ensures the smooth transfer of the gradient and the continuous increase in the network depth. Compared with the original feature extraction layers ZF and VGG, ResNet has a deeper network layer and can extract deeper and more abstract target features. Moreover, the residual structure in ResNet is beneficial to solve the problems of gradient dispersion, gradient explosion, and insignificant network performance improvement when the network depth is deepened. In this study, ResNet50 is selected as the basic backbone. ResNet50 structure is demonstrated in Table 1.

The original faster R-CNN algorithm uses VGG and ZF as the feature extraction network. If conv 1 to conv 5 of the residual network are directly combined with faster R-CNN as a new feature extraction network, although the depth is increased, model accuracy has not been effectively improved. To solve this issue, feature extraction layer is deepened and the target detection accuracy is not improved significantly, and this study adopts the networks on convolutional feature map structure (NoCs), and the specific structure is illustrated in Figure 2.

The NoCs uses conv 1 to conv 4 in ResNet50 as feature extraction layers and conv 5 and fully connected layers as the final detection subnetwork. Moving conv 5 to the detection subnetwork improves the classifier performance and thus the overall detection accuracy.

3.3. Cluster-Based Optimization for Preset Candidate Box. In the target detection and regression task based on a regional convolutional neural network, the degree of agreement between the size of the anchor and the real candidate box size of the target in the experimental dataset is one of the

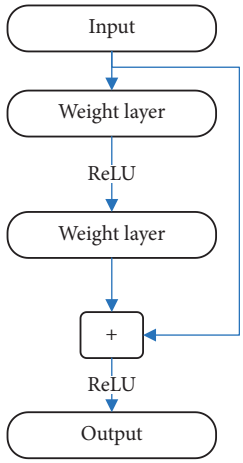

Figure 1: Residual unit.

Table 1: ResNet50 structure.

Layer	Parameter
Conv 1	7×7, 3×3, Maxpooling
Conv 2	$[1\times1, 3\times3, 1\times1]\times3$
Conv 3	$[1\times1, 3\times3, 1\times1]\times4$
Conv 4	$[1\times1, 3\times3, 1\times1]\times6$
Conv 5	$[1\times1, 3\times3, 1\times1]\times3$
Average pooling	14×14
FC	1000
Softmax	1000

important reasons that affect the detection results. During the model training process, iterative learning will be performed according to the preset anchors, and the width and height are adjusted in time. If the size and scale of the initial proposal box of the prediction layer are properly selected, the model will soon be close to the real sample, saving training time and improving detection accuracy. The original faster R-CNN presets three sizes and three scales of boxes.

To improve the detection effect, this study uses the K-means clustering idea in the YOLO algorithm to perform clustering statistics on the real proposal boxes in the dataset and can obtain more scientific preset candidate box size and proportional hyperparameters. K-Means is a classic unsupervised learning clustering algorithm. The idea of K-means is to assign all points in the dataset to K clusters by distance division, ensuring that the distance between each sample data point and centroid of cluster to which it belongs is the closest among all cluster distances. K-Means algorithm first randomly selects K objects as the initial cluster centers according to the expected number of clusters K. Second, it calculates the distance from the remaining sample points to each cluster center and assigns it to cluster center with the smallest distance to form K clusters. Third, the average distance of all sample points is recalculated in each cluster center to the centroid. It is compared with the average distance of other sample points in the cluster, and the sample point with the smallest average distance in the cluster is selected as the new centroid. Fourth, new clusters are formed based on the new centroids, and the error sum of squares for the new clusters is recorded. Fifth, steps 2 and 3 are repeated until the end condition is reached.

The K-means algorithm used in the YOLO algorithm cannot completely converge to the global optimal value due to the random determination of the initial centroid and K value. It can only converge to the local optimum and is greatly disturbed by abnormal data. Therefore, this work adopts K-means++ strategy, which improves clustering accuracy and speed by improving the method of initializing cluster centers. The biggest difference between K-means++ and K-means is the selection of initial clustering center. First, a data point is randomly selected from the dataset as the first cluster center. Second, the distance between the remaining points in dataset and existing cluster centers is calculated, and the shortest distance is selected among them. Third, the probability that each data point is utilized as the next cluster center according to (4) is calculated, and the point with the highest probability is utilized as the new cluster center. Fourth, the first to third steps are repeated until K initial cluster center points are selected, and the remaining steps are the same as the K-means algorithm.

$$p = \frac{D^2}{\sum D^2}, \tag{4}$$

where D is distance.

The commonly used K-means++ clustering algorithm is aimed at scattered data points, and it is very appropriate to use Euclidean distance as a metric for data point classification. However, in the target detection task, the dataset to be divided is not a scattered data point, but a set of length and width values of candidate boxes. When detecting objects, the higher the overlap between the two candidate boxes, the more likely they contain the same object, and the more they should be classified into the same class. Therefore, the metric in this study does not use Euclidean distance but uses the following index to extract the size of the preset frame in the experiment.

$$\begin{aligned} d(\text{box}, \text{centroid}) &= 1 - \text{IOU}(\text{ox}, \text{centroid}), \\ \text{IOU}(\text{box}, \text{centroid}) &= \frac{(S_{\text{box}} \cap S_{\text{centroid}})}{(S_{\text{box}} \cup S_{\text{centroid}})}, \end{aligned} \tag{5}$$

where box represents the real labeled box sample, centroid represents the existing cluster center, IOU represents the intersection ratio between the sample box and the cluster center box, S_{box} represents the area of sample box, and S_{centroid} is area of cluster center box.

When the K-means++ algorithm selects a new cluster center point, the farther the distance is, the greater the probability of being selected and the greater the possibility of becoming the next cluster center, and finally, the preset cluster center is obtained.

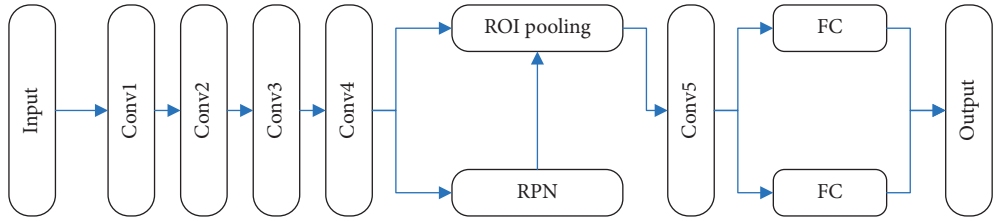

Figure 2: Combination of ResNet and faster R-CNN.

Table 2: Experimental environment details.

Name	Parameter
GPU	GTX 1080Ti 16 GB
CPU	Intel Core i5-9300H
System	Ubuntu 18.04
Language	Python
Framework	PyTorch

3.4. ROI Align Algorithm. The ROI pooling layer undergoes two quantization operations during training. One time is to convert the coordinates of the candidate frame on the original image to the coordinates on the downsampled feature layer. The other time is when the feature map corresponding to the candidate box is divided into a grid of fixed size. Both quantization operations are rounded, so the position of the candidate box cannot be accurately expressed. Mask R-CNN proposes the ROI align method, which no longer performs rounding operations, but retains the floating point coordinates of the corresponding candidate boxes on the feature layer. It adopts the bilinear interpolation method to determine the pixel value in the grid to obtain a fixed-scale feature map. The pixel value is generated with bilinear interpolation from the four nearest pixels on the feature map of the candidate region. After obtaining the pixel value for the sampling point, the maximum pooling operation is performed on each subregion to obtain the feature map. The ROI align algorithm avoids the position error caused by the two quantization operations in ROI pooling without adding new parameters, which is beneficial to the refined positioning of dense targets in the creation of virtual reality digital media art.

3.5. Soft-NMS Algorithm. In target detection, the NMS algorithm is usually used as a post-processing step to delete redundant detections and retain the detection frame with the highest target score, and the NMS algorithm contains the following steps. First, coordinate information and category score probability value of all candidate boxes are selected under one of the categories, the candidate boxes are sorted in descending order with confidence, and the sequence number of the candidate box is obtained with the highest confidence. Second, all remaining candidate boxes are traversed and the IOU value between them and the candidate box is calculated with the highest confidence. IOU represents the ratio of the overlapping area of the two candidate frames to the combined area, which reflects the overlap between two candidate frames. The larger value, the higher degree of overlap. If the IOU value is greater than threshold, the candidate box is discarded. Third, the candidate frame with the highest confidence in the remaining candidate frames is selected, then other candidate frames and their IOU values are judged, and then the second candidate frame is retained. Fourth, the above process is iterated repeatedly, the candidate boxes are rough screened, and a certain number of candidate boxes are retained until all the candidate boxes meet the IOU threshold and the confidence score threshold, and the processing methods for other categories of candidate boxes are the same. NMS is calculated as follows:

$$s_i = \begin{cases} s_i, & \text{IOU} < T, \\ 0, & \text{IOU} \geq T, \end{cases} \tag{6}$$

where s is score and T is threshold.

NMS algorithm is simple, fast, and has excellent performance, but NMS sets a hard threshold, and the selection of this threshold will directly affect the quality of the screening results. In the densely distributed area of targets, the distances between different targets are very close, so their bounding rectangles inevitably have overlapping areas. If the IOU threshold set by the NMS algorithm is too small, many suggestion boxes containing detection objects will be deleted by mistake, increasing the missed detection rate. On the contrary, if the IOU threshold set by the NMS algorithm is too large, the same detection target will be reserved for multiple proposal boxes, which will reduce the average detection accuracy. Therefore, the NMS algorithm is too absolute, and it is difficult to accurately retain the correct candidate boxes in different situations. To improve detection accuracy, this work adopts the soft-NMS algorithm for post-processing.

$$s_i = \begin{cases} s_i, & IOU < T, \\ s_i(1 - IOU), & IOU \geq T, \end{cases} \tag{7}$$

where s is score and T is threshold.

The difference between the soft-NMS algorithm and the NMS algorithm is that it does not directly delete the candidate boxes whose IOU is higher than a given threshold, but attenuates their confidence, so that the proposed boxes of adjacent targets will not be missed. The larger IOU for two candidate boxes, the greater attenuation degree, because the greater the overlap rate, the more likely it is the proposed box of the same detection target. If the IOU value of the two

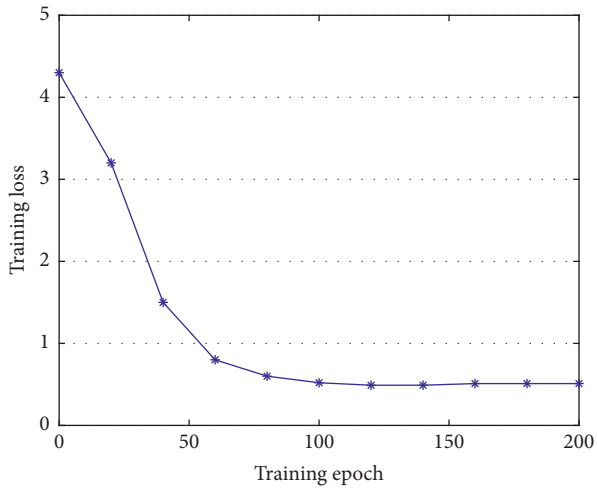

Figure 3: AODNET training loss.

candidate boxes is very small, the confidence score is not affected. The soft-NMS algorithm has a simple idea, does not increase the amount of new parameters, and does not increase the additional computational cost.

4. Experiment and Discussion

4.1. Dataset and Environment. This work uses images collected from virtual reality digital media art creations as a dataset, including 90,837 training images and 30,871 test images, and it contains 103 types of targets. The experimental environment of this work is illustrated in Table 2.

The training process uses stochastic gradient descent, based on experience, the initial learning rate is 0.0001, and training iterations are 200 epochs. This work uses mAP and accuracy as evaluation indicators for target detection, and the calculation method is as follows:

$$\text{mAP} = \frac{1}{N}\sum_{i=1}^{N} AP_i,$$
$$\text{Accuracy} = \frac{(TP + TN)}{(TP + TN + FP + FN)}. \tag{8}$$

4.2. AODNET Training Loss. In the target detection task with deep learning, network training is necessary. This work evaluates the training process for AODNET and shows training loss, as demonstrated in Figure 3.

As the training iteration grows, the loss gradually decreases and finally stabilizes at around 0.5, at which point the network has converged.

4.3. Comparison with Other Detection Methods. To effectively prove the reliability of AODNET, it is compared with other detection methods, such as faster R-CNN, YOLO, and SSD. The comparison results of mAP and accuracy are demonstrated in Table 3.

Table 3: Comparison with other detection methods.

Method	mAP	Accuracy
Faster R-CNN	83.8	86.4
YOLO	86.1	89.5
SSD	87.9	91.4
AONET	90.3	93.6

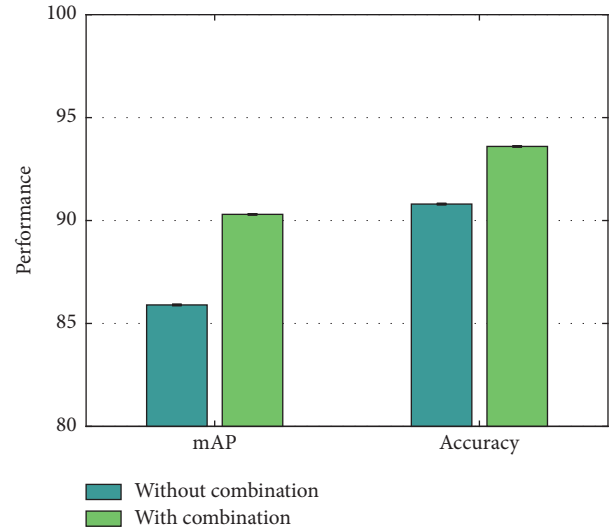

Figure 4: Analysis on combination of Faster R-CNN and ResNet.

Compared with other detection methods listed in the table, AODNET achieves the highest mAP and accuracy, 90.3% and 93.6%. Compared with the SSD method, these two performance indicators are improved by 2.4% and 2.2%, respectively.

4.4. Analysis on Combination of Faster R-CNN and ResNet. AODNET combines faster R-CNN and ResNet networks. To verify the superiority of this combined strategy, mAP and accuracy are compared between uncombined and combined. To ensure the reliability of the experiment, the rest of the network parameter settings remain unchanged, and the results are demonstrated in Figure 4.

As can be seen from the data comparison in the figure, when faster R-CNN and ResNet are combined, the mAP is increased by 4.4% and the accuracy rate is increased by 2.8% compared with performance when they are not combined. This shows that the combination of faster R-CNN and ResNet can mine deep features more effectively.

4.5. Analysis on Candidate Box Optimization. AODNET utilizes K-means++ for size optimization of candidate box. To verify the superiority of this method, it is compared with the original candidate frame selection strategy and the K-means optimization strategy. The mAP and accuracy corresponding to the three methods are demonstrated in Figure 5.

Compared with the original candidate box selection strategy, using the clustering algorithm for optimization can achieve a certain degree of performance improvement. However, the mAP

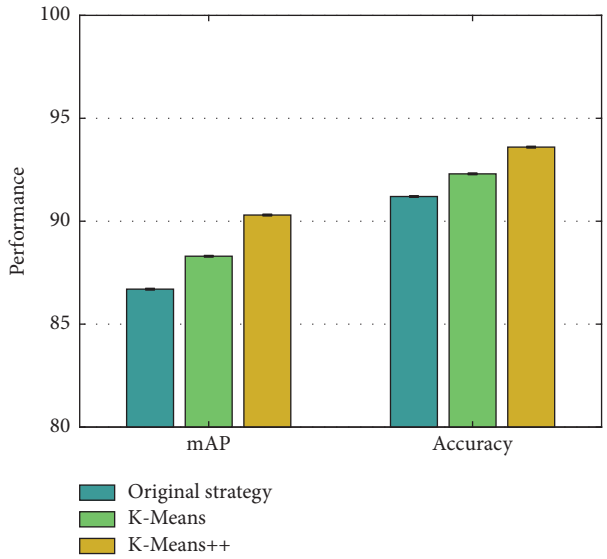

Figure 5: Analysis on candidate box optimization.

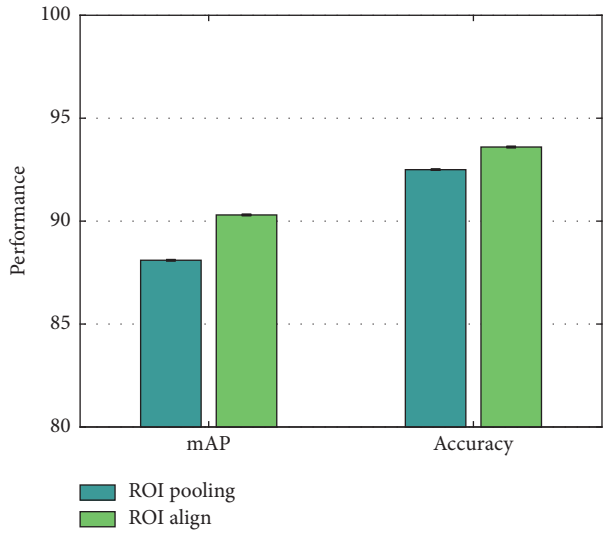

Figure 6: Analysis on ROI align.

and accuracy corresponding to the K-means++ algorithm are the highest. Compared with K-means optimization, index improvement of 2% and 1.3% is obtained.

4.6. Analysis on ROI Align. AODNET replaces the ROI pooling in the original faster R-CNN with ROI align. To verify the superiority of this replacement strategy, the performance of using ROI pooling and using ROI align is compared, respectively. The mAP and accuracy of the two are compared in Figure 6.

Compared with using ROI pooling, after using ROI align, the mAP and accuracy of AODNET are improved by 2.2% and 1.1%, respectively. This is mainly because ROI align reduces the error caused by two quantizations, thereby improving the robustness and discrimination of features.

4.7. Analysis on Soft-NMS. AODNET uses soft-NMS to process the detection frame. To verify its superiority compared with traditional NMS, this work compares the mAP and accuracy when using NMS and soft-NMS, respectively, as demonstrated in Figure 7.

As can be seen from the data comparison in the figure, when using soft-NMS, the mAP is increased by 1.6% and accuracy rate is increased by 0.7% compared with performance when using traditional NMS.

4.8. Analysis on Training Batch. In deep neural network training, the training batch is variable. To verify the impact of different batches on the detection performance, this work compares the mAP and accuracy rates corresponding to different batch sizes, as demonstrated in Table 4.

When batch changes, the mAP and accuracy of AODNET will also change dynamically, and the overall change shows a trend of rising first and then falling. When the batch size is set to 32, the highest mAP and accuracy can be obtained.

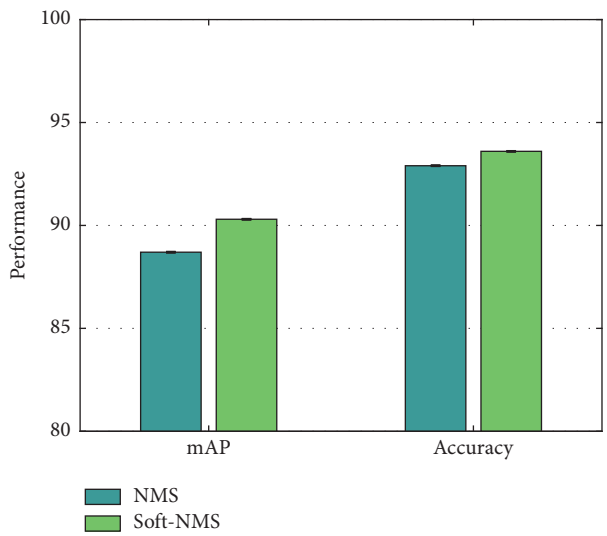

Figure 7: Analysis on soft-NMS.

Table 4: Analysis on training batch.

Batch size	8	16	32	64	128
mAP	85.3	88.9	90.3	89.5	87.5
Accuracy	90.9	92.6	93.6	93.1	91.2

5. Conclusion

Industry and academics have paid increasing attention to virtual reality technology in recent years. Users can interact with virtual items using numerous interactive methods thanks to virtual reality technology, which generates realistic visuals, sounds, and other sensory experiences using computer technology. Artificial intelligence has advanced rapidly in tandem with computer technology. As digital media art continues to evolve, virtual reality and artificial intelligence

have become the primary tools for creating new works of art. Aiming at particularity for object detection in digital media art creation of VR, this work proposes an art object detection algorithm based on residual network and clustering idea. First of all, it uses ResNet50 as the feature extraction network, which deepens the network depth and improves the model feature extraction ability. Second, it uses the K-means++ algorithm to perform clustering statistics on the size of the real annotated boxes in the dataset to obtain appropriate hyperparameters for preset candidate boxes, which enhances the tolerance of the algorithm to the target size. Third, it replaces the ROI pooling algorithm with ROI align to eliminate the error caused by the quantization operation on the characteristics of the candidate region. Fourth, to reduce missed detection rate of overlapping targets, soft-NMS algorithm is used instead of the NMS algorithm to post-process the candidate boxes. Finally, this work conducts extensive experiments to verify the superiority of AODNET for object detection in virtual reality digital media art creation.

Data Availability

The datasets used during this study are available from the corresponding author on reasonable request.

Conflicts of Interest

The author declares that he has no conflicts of interest.

References

[1] A. H. Sadeghi, A. P. W. M. Maat, Y. J. H. J. Taverne et al., "Virtual reality and artificial intelligence for 3-dimensional planning of lung segmentectomies," *JTCVS techniques*, vol. 7, pp. 309–321, 2021.

[2] S. K. Bakshi, S. R. Lin, D. S. W. Ting et al., "The era of artificial intelligence and virtual reality: transforming surgical education in ophthalmology," *British Journal of Ophthalmology*, vol. 105, no. 10, pp. 1325–1328, 2021.

[3] R. Antel, S. Abbasgholizadeh-Rahimi, E. Guadagno et al., "The use of artificial intelligence and virtual reality in doctor-patient risk communication: a scoping review," *Patient Education and Counseling*, p. 1, 2022.

[4] S. Lin, B. Zheng, G. C. Alexandropoulos, M. Wen, F. Chen, and S. Mumtaz, "Adaptive transmission for reconfigurable intelligent surface-assisted OFDM wireless communications," *IEEE Journal on Selected Areas in Communications*, vol. 38, no. 11, pp. 2653–2665, 2020.

[5] N. Mirchi, V. Bissonnette, R. Yilmaz, N. Ledwos, A. Winkler-Schwartz, and R. F. Del Maestro, "The Virtual Operative Assistant: an explainable artificial intelligence tool for simulation-based training in surgery and medicine," *PLoS One*, vol. 15, no. 2, Article ID e0229596, 2020.

[6] Y. Gong, "Application of virtual reality teaching method and artificial intelligence technology in digital media art creation," *Ecological Informatics*, vol. 63, Article ID 101304, 2021.

[7] I. Hacmun, D. Regev, and R. Salomon, "Artistic creation in virtual reality for art therapy: a qualitative study with expert art therapists," *The Arts in Psychotherapy*, vol. 72, Article ID 101745, 2021.

[8] K. A. Mills and A. Brown, "Immersive virtual reality (VR) for digital media making: transmediation is key," *Learning, Media and Technology*, vol. 47, no. 2, pp. 179–200, 2022.

[9] K. Z. Ghafoor, L. Kong, S. Zeadally et al., "Millimeter-wave communication for internet of vehicles: status, challenges, and perspectives," *IEEE Internet of Things Journal*, vol. 7, no. 9, pp. 8525–8546, 2020.

[10] G. Kaimal, K. Carroll-Haskins, M. Berberian, A. Dougherty, N. Carlton, and A. Ramakrishnan, "Virtual reality in art therapy: a pilot qualitative study of the novel medium and implications for practice," *Art Therapy*, vol. 37, no. 1, pp. 16–24, 2020.

[11] X. Zhao and S. Ye, "Space reconstruction of audiovisual media based on artificial intelligence and virtual reality," *Journal of Intelligent and Fuzzy Systems*, vol. 40, no. 4, pp. 7285–7296, 2021.

[12] L. Shamri Zeevi, "Making art therapy virtual: integrating virtual reality into art therapy with adolescents," *Frontiers in Psychology*, vol. 12, Article ID 584943, 2021.

[13] C. I. Park, "A study on the development direction of new media art using virtual reality," *Journal of the Korea Academia-Industrial Cooperation Society*, vol. 21, no. 1, pp. 97–102, 2020.

[14] A. Kargas, N. Karitsioti, and G. Loumos, "Reinventing museums in 21st century: implementing augmented reality and virtual reality technologies alongside social Media's logics," *Virtual and Augmented Reality in Education, Art, and Museums*, pp. 117–138, IGI Global, Pennsylvania, USA, 2020.

[15] I. Pioaru, "Virtual reality holography—a new art form," *Technology, Design and the Arts-Opportunities and Challenges*, pp. 317–333, Springer, Cham, 2020.

[16] M. Cavazza, J. L. Lugrin, S. Hartley et al., "Intelligent virtual environments for virtual reality art," *Computers & Graphics*, vol. 29, no. 6, pp. 852–861, 2005.

[17] J. L. Rubio-Tamayo, M. Gertrudix Barrio, and F. García García, "Immersive environments and virtual reality: systematic review and advances in communication, interaction and simulation," *Multimodal Technologies and Interaction*, vol. 1, no. 4, p. 21, 2017.

[18] G. Riva, F. Mantovani, C. S. Capideville et al., "Affective interactions using virtual reality: the link between presence and emotions," *CyberPsychology and Behavior*, vol. 10, no. 1, pp. 45–56, 2007.

[19] T. Flint, L. Hall, F. Stewart, and D. Hagan, "Virtualizing the real: a virtual reality contemporary sculpture park for children," *Digital Creativity*, vol. 29, no. 2-3, pp. 191–207, 2018.

[20] I. Hacmun, D. Regev, and R. Salomon, "The principles of art therapy in virtual reality," *Frontiers in Psychology*, vol. 9, p. 2082, 2018.

[21] S. DeLahunta, "Virtual reality and performance," *PAJ: A Journal of Performance and Art*, vol. 24, no. 1, pp. 105–114, 2002.

[22] K. Mack, "Blortasia: a virtual reality art experience," in *Proceedings of the ACM SIGGRAPH 2017 VR Village*, pp. 1-2, Los Angeles CA, USA, July 2017.

[23] W. Zhanjun, "Application research of virtual reality technology in environmental art design," *Acta Technica CSAV (Ceskoslovensk Akademie Ved)*, vol. 62, no. 1, pp. 215–224, 2017.

[24] R. Girshick, J. Donahue, T. Darrell et al., "Rich feature hierarchies for accurate object detection and semantic segmentation," in *Proceedings of the IEEE Conference on Computer Vision and Pattern Recognition*, pp. 580–587, Columbus, OH, USA, June 2014.

[25] K. He, X. Zhang, S. Ren, and J. Sun, "Spatial pyramid pooling in deep convolutional networks for visual recognition," *IEEE Transactions on Pattern Analysis and Machine Intelligence*, vol. 37, no. 9, pp. 1904–1916, 2015.

[26] R. Girshick, "Fast r-cnn," in *Proceedings of the IEEE International Conference on Computer Vision*, pp. 1440–1448, Santiago, Chile, June 2015.

[27] S. Ren, K. He, R. Girshick et al., "Faster R-CNN: towards real-time object detection with region proposal networks," *IEEE Transactions on Pattern Analysis and Machine Intelligence*, vol. 39, no. 6, pp. 1137–1149, 2016.

[28] T.-Y. Lin, P. Dollár, R. Girshick et al., "Feature pyramid networks for object detection," in *Proceedings of the IEEE Conference on Computer Vision and Pattern Recognition*, pp. 2117–2125, Honolulu, HI, USA, July 2017.

[29] J. Redmon, S. Divvala, R. Girshick et al., "You only look once: unified, real-time object detection," in *Proceedings of the IEEE Conference on Computer Vision and Pattern Recognition*, pp. 779–788, Las Vegas, NV, USA, June 2016.

[30] W. Liu, D. Anguelov, D. Erhan et al., "SSD: Single Shot MultiBox detector," in *Proceedings of the European Conference On Computer Vision*, pp. 21–37, Amsterdam, Netherland, October 2016.

[31] T. Lin, P. Goyal, R. Girshick et al., "Focal loss for dense object detection," in *Proceedings of the IEEE International Conference on Computer Vision*, pp. 2980–2988, Venice, 2017.

[32] H. Law and J. Deng, "Cornernet: detecting objects as paired keypoints," in *Proceedings of the European conference on computer vision*, pp. 734–750, Munich, Germany, September 2018.

[33] X. Zhou, D. Wang, and P. Krähenbühl, "Objects as points," 2019, https://arxiv.org/abs/1904.07850.

Hindawi
Computational Intelligence and Neuroscience
Volume 2022, Article ID 4841387, 12 pages
https://doi.org/10.1155/2022/4841387

Research Article

A Study on Exploring the Path of Psychology and Civics Teaching Reform in Universities Based on Artificial Intelligence

Liang Han[1] **and Jijuan Gong**[2]

[1]*School of Marxism, Chongqing College of Humanities, Science and Technology, Hechuan, Chongqing 401520, China*
[2]*School of Politics and Law, Chongqing College of Humanities, Science and Technology, Hechuan, Chongqing 401520, China*

Correspondence should be addressed to Liang Han; tw@cqrk.edu.cn

Received 20 June 2022; Revised 16 July 2022; Accepted 18 July 2022; Published 8 August 2022

Academic Editor: Yaxiang Fan

Copyright © 2022 Liang Han and Jijuan Gong. This is an open access article distributed under the Creative Commons Attribution License, which permits unrestricted use, distribution, and reproduction in any medium, provided the original work is properly cited.

The development of precise teaching of civics with artificial intelligence not only is the realistic need of the development of the times and technological innovation but also provides a new picture to solve the problem of the relevance of civics, so it is the inevitable requirement for the quality and efficiency of civics teaching. Curriculum Civics is an important support for the cultivation of innovation ability of college students. To effectively identify the state categories of college students' psychology and civics and to fully consider the emotional factors between teachers and college students, this paper proposes a psychological civics teaching model based on graphical convolutional neural network. First, the dialog texts of psychology and civics teaching between teachers and students are coded in sequence context using Bi-GRU to obtain discourse text representations; then, a directed graph is constructed based on the order of the dialog between teachers and students in psychology and civics teaching, and a new text representation vector for each discourse text is obtained using graph convolutional neural network; finally, the two discourse representation vectors obtained are connected, and a similarity-based attention mechanism is used. Finally, the final discourse text representation is obtained using an attention-based mechanism to perform psychological and ideological state. The proposed method is conducive to the implementation of the teaching practice exploration of organic integration of ideals and beliefs with the cultivation of innovation ability in colleges and universities.

1. Introduction

In the National Conference on Ideological and Political Work in Colleges and Universities, General Secretary put forward the concept of "Curriculum Civics," emphasizing that teachers should integrate socialist core values into the whole process of teaching and educating people, so that all courses can play the role of ideological and political education, and realize the same direction of professional courses, public courses, and ideological and political theories, thus resonating and forming a synergistic effect [1–3]. To implement this teaching concept, all universities actively explore the teaching reform of curriculum thinking and politics, trying to educate people through "all courses, all aspects, all staff"; effectively respond to the development needs of "big thinking and politics" in the new era; realize the goal of curriculum thinking and politics; and achieve the goal of "establishing moral education." During the period of accelerated social transformation, the impact of multiple cultures and trends and the collision of money worship, universal values, Buddhist culture, etc., intertwined with the dregs of traditional culture, have a huge impact on young people. For example, lack of faith and moral decline are no longer uncommon; the proportion of psychological problems and mental illnesses increased; and even frequent psychological crisis events like "depression," "confusion," and "anxiety" have become the buzzwords in college campuses, so it is urgent to strengthen the psychological construction, ideological guidance, and value shaping for college students [4–7]. Mental health education and ideological and political education are closely related, the former is an important part of the latter, and the effectiveness of the latter

cannot be achieved without the promotion of the positive results of the former. Therefore, from the perspective of integration, it is important to deeply understand the rich connotation of the mental health education curriculum of college students' ideology and politics and reform the curriculum design and teaching practice by setting clear integration teaching objectives, following certain implementation principles, reasonably planning teaching contents, choosing appropriate teaching methods, improving assessment methods, giving full play to the role of the main channel of classroom teaching, and realizing the organic role of psychological education and core values leadership. The integration of psychological education and core values is of great practical significance for both internal and external talent cultivation and for comprehensive development of morality and talent. It not only promotes the realization of the "three comprehensive" education requirements, but also accelerates the development of "greater thinking and politics."

The schematic diagram of psychology and civics teaching in higher education is shown in Figure 1. Theoretically, it solves the contradiction of "two skins" between civic theory and professional education, clarifies the orientation of education in practice, and unifies the direction of socialist talent training. Reflecting the essence of higher education, the 18th National Congress of the Party has made it clear that "establishing morality and educating people" is the fundamental task of education, establishing morality is the prerequisite and requirement of educating people, and educating people is the goal and value of establishing morality [7, 8]. Moral education is the foundation of colleges and universities, and it is the way to inherit the spirit of Chinese nation and to run a good socialist education with Chinese characteristics. Curriculum Civics requires the role of the main channel in the classroom to urge students to make the core socialist values a guideline to lead their external behavior. By establishing a correct outlook on life, worldview, and values, students can realize a higher sense of value effectiveness and eventually become socialist builders and successors with equal emphasis on competence and moral conduct. The implementation of the concept of "three comprehensive education" is the key to building a system of thinking and education. The Ministry of Education has promoted the construction of two batches of pilot units of comprehensive reform, and although there has been great progress, there are still some problems [9]. The phenomenon of emphasizing the teaching of professional knowledge and skills while neglecting the cultivation of personality and the guidance of values in the teaching of different disciplines still cannot be ignored. The introduction of Curriculum Civics has clarified the mission of professional teachers to educate people and the responsibility of leading values in the classroom, prompting teachers of each course to "guard a section of the canal and plant a responsible field," to do their duty and work together to realize the essence of education, and further highlight the systematic and holistic nature of ideological and political education. Setting clear teaching objectives is the direction of classroom teaching; the course should be able to effectively support the training objectives, in line with the school's positioning, and talent training objectives. The main contributions of this paper are as follows: (1) Firstly, we assume that the objectives of the civics course should be integrated with the original teaching objectives of the course, and the teaching objectives of the chapter should also be reflected specifically, so as to maximize the civics education function of the mental health education course. In this way, the mental health education course can serve to improve the psychological quality of college students to the greatest extent, and help them to form good psychological quality, so as to realize the education concept of "establishing morality and educating people." (2) In order to effectively identify the state categories of college students' psychology and civics and fully consider the emotional factors between teachers and college students, this paper proposes a psychological civics teaching model based on graph convolutional neural network. This paper uses Bi-GRU to extract text feature vectors and proposes to use graph convolutional neural network (GCN) for text emotion recognition in psychology and civics teacher-student dialogs, fully considering the emotional interactions between the people involved in psychology and civics teacher-student dialogs, combining two kinds of contextual information to obtain better text representations, and finally for text emotion classification. (3) The obtained experimental results prove that, compared with current classification methods, Bi-GRU combined with GCN model has better performance in sentiment classification.

2. Related Work

2.1. Teaching Psychology and Civics in Higher Education. Only through the mutual integration of knowledge and value can we realize the comprehensive development of individuals and the sustainable progress of society. In education and teaching, we should not only pay attention to the implicit value leadership in knowledge dissemination, but also emphasize the cohesion of knowledge underpinning in value dissemination, which is also the essence of curriculum thinking and government. Some teachers at college students' mental health education come from the counseling team, are easily influenced by the value neutrality of counseling, and are even confused. However, it should be clear that Curriculum Civics is not psychological counseling; "moral education" itself has ideological attributes; adhering to the correct political direction is necessary; cultivating socialist builders and successors with firm ideals and beliefs is the purpose, so the value leadership here is to serve the goal of talent training; there is a difference between right and wrong [10]. In conclusion, the integration of subject knowledge, competence, and correct value leadership is one of the basic principles that needs to be followed in Curriculum Civics.

Combining explicit teaching and implicit transmission in the classroom helps individuals unknowingly gain experience and influence subsequent behavior in contact with the environment. This requires teachers to pay attention to their own speech and behavior and to infect students with their personality and cultivation. Assisting in problem solving and promoting psychological experience combined with the vigor

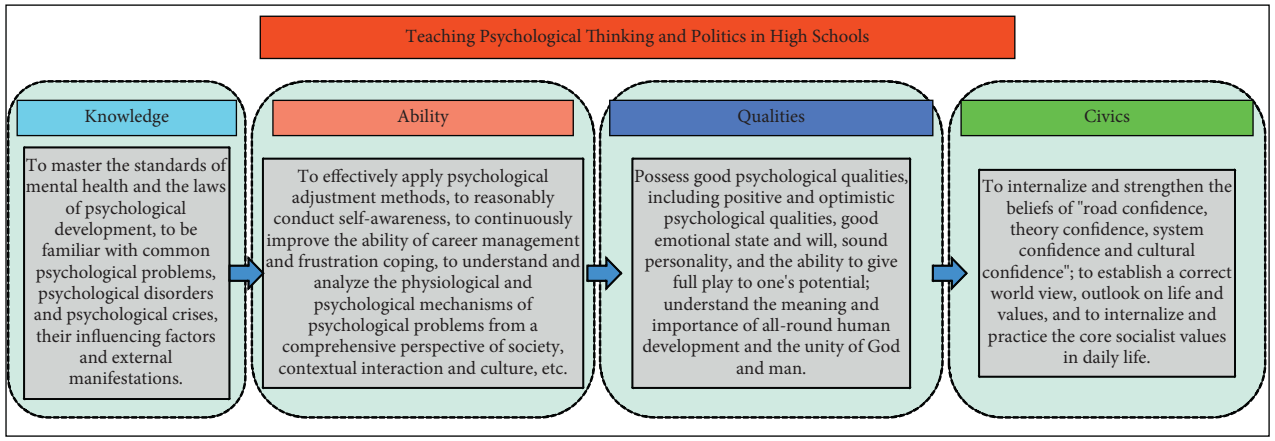

Figure 1: Schematic diagram of psychological and political teaching in colleges and universities.

of college students, in addition to a lot of problems, such as academic delays, information selection difficulties, Internet addiction, interpersonal tension, and out-of-control emotions, to help students solve problems are also part of good ideological and political education. Problem solving is the process of solving a problem through various thinking operations caused by a certain situation and according to a certain goal [11]. Experience is a fusion of emotion-centered sensibility and rationality, and strengthening the psychological experience of successful problem solving can effectively raise the level of individual self-esteem. The formation of virtue is the fusion of the subject and object of the individual's external "situation-event" and internal "experience-experience." Therefore, the combination of helping individuals to solve problems and promoting psychological experiences can not only achieve the unification of perceptual awareness and rational discernment, but also balance the observational and experiential selves and effectively promote the formation of individual virtues [12–14].

Integration is the most significant feature of the curriculum, which refers to the effective integration and logical post-contraction of the curriculum with other disciplines to achieve its political direction, values, and methodological leadership. Therefore, finding the right point of integration is the key to the construction of the content of Curriculum Civics. The generation of psychological problems among college students is since individual worldview and values are not mature and definite enough. Mental health education in colleges and universities should realize the autonomy of students in understanding and value judgment and the development of individual mind and give proper guidance on personality and moral development while keeping some space for students to think and solve problems, so that students can realize their personality and moral refinement in the process of self-examination. The process of self-examination allows students to achieve character and moral refinement. Full media is gradually penetrating our education system; has a certain positive impact on the civic education in colleges and universities, providing a full-media environment for the innovation of modern education technology; and can effectively promote the reform and innovation of teaching strategies, enhance the effectiveness of civic education in colleges and universities, give a positive role to the whole media, break through the limitations of the obsolete education concept, and achieve the ideal effect of education reform [15–18].

Omni-media refers to the role of information dissemination of multimedia such as animation, images, sound, and web pages; with the help of diversified media forms, like TV, radio, audio and video content, magazines, and other communication paths, business integration of multimedia and media forms, and integration of three networks (broadcasting, telecommunication, and Internet) through information network, users receive the integrated information with the help of communication terminals such as TV and computer, breaking through the time and place. Omni-media has the following four characteristics and plays its value with its own characteristics. First, full media achieves maximum information flow integration. The current existence of the Internet has been updated to 5G; in addition, there are a variety of technical support platforms such as WAP, GSM, CDMA, GPRS, and streaming technology and a rich variety of communication tools, in addition to the traditional newspapers and magazines; there are also the network, telecommunications, satellite communications and other carrier tools to achieve the integration of information flow. Second, full media is compatible with traditional media [19–21]. Full media will improve and innovate traditional media, integrate and use diversified forms of media expression, pay attention to the single form of traditional media, and realize the "full" aspect in the "full" media. Third, omni-media focuses on all-round integration; based on traditional media, omni-media realizes the integration with network media, comprehensive interaction, complementarity, mutual dissolution, and full coverage of omni-media in the information age. This mainly involves the media carrier and audience dissemination of the whole media. Fourth, in addition to the "full" characteristic, it also has the "large" characteristic and provides segmentation services for a wide range of audiences. In the media market, with the help of the omni-media platform, rich forms of information are expressed, and information media are

screened according to the different needs of the audience, so that information interaction can be achieved. Full media is built based on "cross-media," and with the use of media streams, more economical information delivery is achieved, with the outstanding advantages of low investment and good results. Establish the thinking of "Internet + psychological education + curriculum thinking," break the time and space limitations of the classroom, and build a mixed teaching mode online and offline. The use of online multimedia with images, sound effects, and animations can stimulate students' interest in learning and expand the integration path of learning resources; the equality and interactivity of online communication can effectively stimulate the role of educated subjects and provide a new teaching ecology. In addition, the flipped classroom changes the status of teachers and students in teaching activities and improves the enthusiasm and initiative of students' participation.

2.2. Exploring Educational Reform Paths. The classroom is designed to enhance the development of independent thinking and creative thinking by increasing the proportion of discussion and practice among students. The value orientation of the curriculum of "seeing things but not people" will aggravate the dichotomy of knowledge transfer and value guidance and deviate from the fundamental task of "cultivating people" [22]. It is crucial to choose appropriate classroom teaching methods based on the psychological rules of students, the realities of classroom teaching, and the achievement of course objectives. To increase the proportion of student discussion and practice, to enhance the development of independent thinking and creative thinking, and to appropriately reduce the proportion of traditional lectures are an important part of the curriculum reform. Schools that are in a position to do so can conduct small classes where students hold group discussions and become course participants along with the instructor, which can greatly stimulate students' interest in learning. Throughout the process, students are guided to comprehend, practice, and internalize socialist core values at all times through online submission of ideas, classroom group discussions, off-class practical assignments, social research, and other activities, so that individual understanding and practice are mutually evidenced and promoted to achieve unity and recognition of the 3 aspects of socialist core values: rationality, emotion, and behavior. The dual interactive learning path of online knowledge transfer, psychological test, knowledge quiz, group discussion, teacher feedback and expansion, offline case and video sharing, practical activities, teacher and student sharing, value leadership is realized. In addition, the recent emergence of virtual reality technology has enabled the completion of operations that were not possible in teaching in the past. The use of virtual technology can be explored in future course construction, for example, a chapter on emotion management can have different simulation scenarios for students to choose from, that is, public speaking, group discussions, and interviews, to promote the practice of managing students' anxiety in special situations, so that theory and practice can be seamlessly integrated in a relatively short period of time to enhance the effectiveness of the course. This requires teachers to set up new educational thinking, to enrich and update the teaching content as necessary, to introduce content that is in line with the spirit of the times and has a cutting-edge atmosphere, so that students can fully understand and master the essence of the subject. In the process of education and teaching, we can delete the old and outdated contents from the textbooks and introduce the contents that are in line with the spirit of the times and the cutting-edge contents, and we should evaluate the textbooks together with students. At the same time, it is necessary to teach students multiple types and aspects of knowledge in order to facilitate the cultivation of innovative talents. In the process of teaching, teachers need to conduct in-depth research on different versions and different content systems and also need to fully understand the frontier topics of subject development, which should be compared, optimized, analyzed, and organized to reflect the development trend. In terms of teaching content, it is necessary to achieve vigorous reform, innovative teaching content, and dynamic integration with the development of the discipline. Teachers need to teach students not only theoretical and fundamental knowledge, but also to reveal the laws of the discipline, to integrate the theoretical system of the discipline with the social reality, and to keep pace with the development of the times. At present, a big part of the problem is not only the outdated content, but also the repetition and fragmentation of course content, and there is a divergence between knowledge generation processes and knowledge research methods. Teachers need to introduce students to the appropriate background knowledge and always provide the necessary penetration of the scientific method and scientific thinking based on subject knowledge [23]. In addition, it is necessary to ensure that education and teaching are close to real life and reflect the latest achievements of current scientific and technological development. In the process of teaching content innovation and reform, the relevant staff is required to start from the following aspects: First, the staff needs to fully grasp the combination point between major disciplines and also needs to achieve mutual integration, crossover, and communication between disciplines, to achieve the necessary penetration between disciplines, to guarantee students' complete mastery of knowledg. Second, necessary measures need to be taken to enhance students' independent thinking ability and also to further enhance their learning ability. Third, students' scientific thinking should be cultivated. Education is not only about teaching students to apply knowledge, but also about making students investigate knowledge, making them understand the process of knowledge formation, and cultivating their creative spirit and innovative consciousness. In addition, in the process of teaching exercises, teachers are required to dig deeper into the scientific methods embedded in them and to train students in the necessary thinking methods. The whole teaching process needs to penetrate and integrate innovative ideas, pay attention to the cultivation of students' innovative consciousness, guide students to make the necessary discoveries for classroom problems, let students learn to think independently about the problems, and also let students master professional knowledge and then contact scientific research experiments. The key is to cultivate

students' innovative thinking, humanistic quality, and practical hands-on ability and guide students to achieve all-round development. In addition, teachers are required to create appropriate teaching situations, cultivate students' innovative spirit, carry out inquiry-based teaching, organize and purposeful teaching activities, guide students to think deeply, cultivate students' interest in innovation, stimulate students' passion for independent inquiry and independent learning, and make students more active and positive in the process of knowledge construction. At the same time, teachers should pass on to students the spirit of rigor and good governance, which is of great value and significance to the cultivation of students. Against the background of innovative talent cultivation, the reform of university education should change the teaching concept, reform the teaching content, and enrich the teaching mode, so that the students' innovative thinking ability and innovative consciousness can be improved. In addition, always adhere to the concept of tolerance, equality, and democracy; encourage students to actively participate in teaching discussions and teaching research; allow students to be different, make mistakes, and say wrong things; and fully respect and understand students. The key is to guide students, not just to instill knowledge into them or adopt a fill-in-the-bag teaching style that is not qualitatively effective and does not improve students' creative thinking and innovative abilities.

3. Methods

3.1. Model Architecture. The main results of the model are as follows: Bi-GRU is used to extract the sequential contextual features of the psychological and civics teacher-student communication texts; then, a directed graph is constructed with the psychological and civics teacher-student dialog utterances in sequence, and GCN extracts the speaker-level contextual encoding features by aggregating the information of local neighbor nodes; finally, the two different feature vectors are combined for sentiment classification [24–26]. The key to modeling inter-speaker dependencies is the speaker information, which enables the model to understand how speakers affect the emotional states of other speakers. In addition, speaker's own or self-dependence helps to understand the emotional inertia of individual speakers, due to which speakers resist the influence of external factors on their own emotions. Moreover, the relative position of the target discourse and the contextual discourse determines how previously spoken words influence future discourse. The framework of the sentiment recognition method for psychological and Catholic teacher-student dialogs in this paper is broadly divided into 3 parts, as shown in Figure 2, which are a sequence context encoder, whose role is to extract sequence contextual information from the text of dialogs; a speaker-level context encoder, which is used to extract speaker-related contextual features from the dialogs; and a sentiment classifier, which is used to extract speaker-related contextual features from the dialogs by combining the two contextual feature representations and using a similarity-based attention mechanism to obtain the final utterance feature representation, which is input to the fully connected layer for sentiment classification.

3.2. Sequential Context Encoder. Suppose we construct a dialog between teachers and students of psychological and ideological teaching, and count the number of people involved in the dialog as X, denoted as $e_1, e_2, \ldots, e_X$, and these X people say a total of Y statements in the dialog, denoted as $u_1, u_2, \ldots, u_Y$. $u_t \in R_Y^D$ is the initial feature vector representation, u_t corresponding to the speaker is es, and s is a mapping between the discourse and its corresponding speaker index. The goal of text sentiment analysis of psychological and ideological teacher-student dialogs is to predict the psychological and ideological teaching status category corresponding to each discourse in the dialogs. In this paper, we use Bi-GRU to extract the textual information features of psychological and civics teacher-student dialogs to obtain the sequential contextual representations of the dialog sentences, and the process is shown in the following equation:

$$\begin{aligned} \overrightarrow{g_t} &= \overrightarrow{\mathrm{GRU}}(\overrightarrow{g_{t-1}}, u_t), \\ \overleftarrow{g_t} &= \overleftarrow{\mathrm{GRU}}(\overrightarrow{g_{t+1}}, u_t), \\ g_t &= \left[\overrightarrow{g_t}, \overleftarrow{g_t}\right], \quad t = 1, 2, \ldots, Y, \end{aligned} \tag{1}$$

where u_t is the initial context-independent discourse representation; g_t are the outputs of positive GRU and negative GRU, respectively; and g_t is the discourse representation containing the sequence context information. Two unidirectional and opposite directional GRUs form the Bi-GRU network model, and the outputs are jointly determined by the states of the two different GRUs. The specific structure of Bi-GRU is shown in Figure 3.

3.3. Speaker-Level Context Encoder. In order to effectively obtain the speaker-level contextual information in the dialog sequences of psychology and civics teachers and students, this paper constructs a directed graph to portray the emotional interactions between psychology and civics teachers and students and uses a spatial domain-based graph convolutional neural network model to obtain a textual representation containing speaker-level contextual information, and the specific structure of the speaker-level context encoder is shown in Figure 4.

A directed graph $G = \{V, E, R, W\}$ is constructed to represent the dialog between teachers and students in psychology and civics teaching, where V denotes the set of nodes; E denotes the set of edges; each discourse is represented as a node $V_t \in V, t = 1, 2, \ldots, YV_t \in V, t = 1, 2, \ldots, Y$; the initialized feature vector representation is noted as g; the edges in node v and node v are denoted as $r_{ts} \in E; r \in R$ denotes the edge relationship type; and the relationship type of the edge depends on two aspects of speaker category and discourse temporal order, i.e., the speaker es corresponding to v and the sequence of node utterances v. Suppose a dialog between teachers and students of psychology and civics teaching contains only two speakers e_1 and e_2 and a total of five utterances; then, the entire psychology and civics teacher-student dialog constitutes a directed graph as shown in Figure 4. The edge weights w_{ts} are set using the

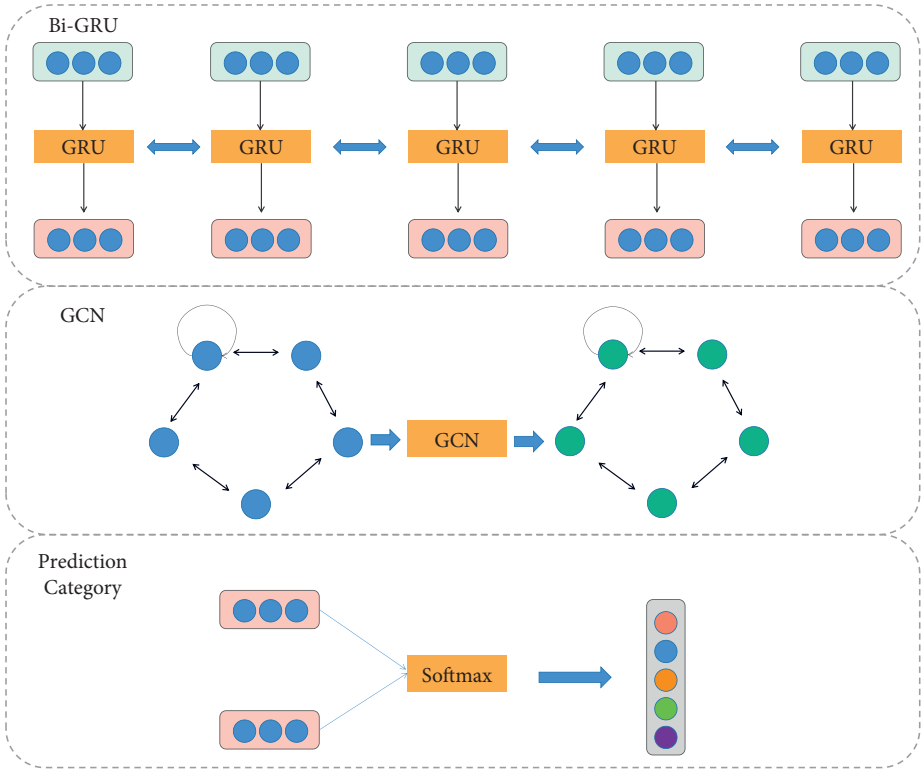

Figure 2: Model structure.

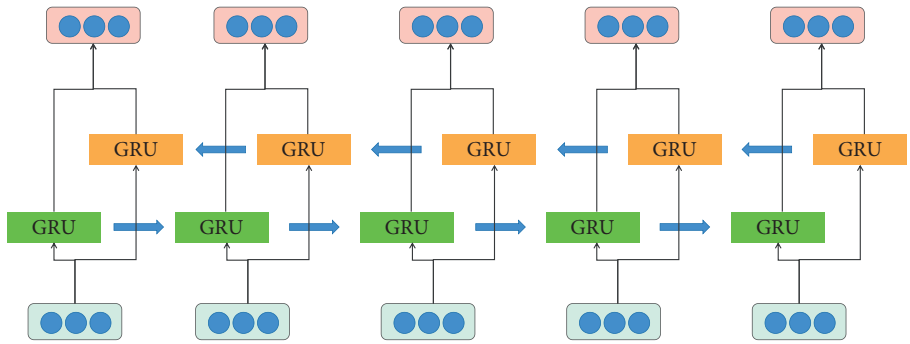

Figure 3: Bi-GRU structure.

attention model based on text similarity; i.e., for each node, the weights of the input edges all add up to 1. Considering the m sentences before and the n sentences after each node statement, the weights of the edges between nodes v are specifically calculated in the following equation:

$$w_{ts} = \text{softmax}\left(g_t^T W\left[g_{t-m}, \ldots, g_{t+n}\right]\right), s = t-m, \ldots, t+n. \tag{2}$$

In the equation, the softmax function ensures that the sum of the total weights of the input edges in node v is 1. The graph convolutional neural network model (GCN) uses a two-step graph convolution operation to convert the speaker-independent node by aggregating the local neighbor node feature information of each node feature vector g_t into a new feature vector representation h_t related to speaker information using a two-step graph convolution operation, which is calculated as shown in the following equations. The sum of the total weights of the input edges innode v is 1.

$$\begin{aligned} h_t^{(1)} &= \sigma\left(\sum_{r\in R_s, s\in Y_i'} \frac{w_{ts}}{c_{t,r}} W_r^{(1)} g_s + w_t W_0^{(1)} g_t\right), i = 1, 2, \ldots, Y, \\ h_t^{(2)} &= \sigma\left(\sum_{s\in Y_i'} W^{(2)} h_s^{(1)} + W_0^{(2)} h_t^{(1)}\right), t = 1, 2, \ldots, Y. \end{aligned} \tag{3}$$

3.4. Emotion Classifier. The structure of the sentiment classifier is as follows: firstly, the feature vector g_t containing the sequence contextual information and the feature vector h_t related to the speaker information are connected; then,

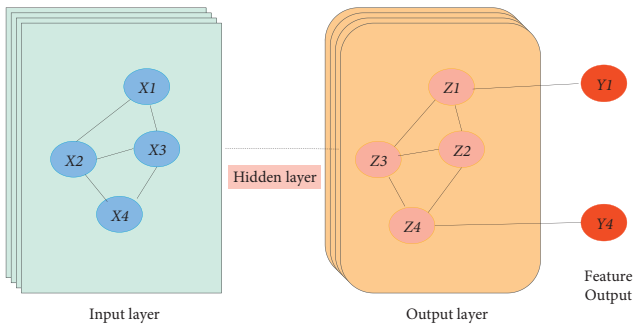

Figure 4: Graph convolution structure.

the new psychological and civics teacher-student dialog text feature representation is obtained by the similarity-based attention mechanism; and finally the sentiment classification of the discourse is performed using the fully connected layer psychological and civics teacher-student to get the text corresponding to the psychological and civics teaching state category labels. The connected text vector representations are converted into the final psychological and civics teacher-student dialog text feature representations h_t using a similarity-based attention mechanism.

$$\begin{aligned} h_t &= \left[g_t, h_t^{(2)}\right], \\ \beta_t &= \text{softmax}\left(h_t^T W_\beta [h_1, \ldots, h_Y]\right), \\ \widetilde{h}_t &= \beta_t [h_1, \ldots, h_Y]^T. \end{aligned} \tag{4}$$

Finally, the new utterance feature representation h_t is input to the fully connected layer, and the softmax layer performs multi-categorization of the sentiment of text utterances to obtain the maximum probability sentiment label x_t.

$$\begin{aligned} l_t &= \text{ReLU}\left(W_1 \widetilde{h}_t + b_l\right), \\ X_t &= \text{softmax}\left(W l_t + b\right), \\ x_t &= \underset{m}{\text{argmax}}\left(X_t[m]\right). \end{aligned} \tag{5}$$

4. Experiments and Results

4.1. Experiment Setup. The specific configuration is shown in Table 1. The experimental dataset selected for this paper's experiments is a crawl through a large number of learning websites of psychology and civics teacher-student dialog. The original data contains about 11318 psychology and civics teacher-student dialogs. The selected part of the corpus was translated into Chinese and used for Chinese psychology and civics teacher-student dialog sentiment analysis research. The excerpted Chinese corpus contains about 600 dialogs between teachers and students in psychology and thinking and political science teaching, with an average of 10 rounds, about 6000 sentences, and 7 categories of psychology and thinking and political science teaching states, namely, neutrality, anger, disgust, fear, happiness, sadness, and surprise. The corpus selected in this paper mainly consists of multiple rounds of psychological and civic studies teacher-student dialogs between two people in daily chat scenes, which involve many relatively rich life topics and extremely rich emotional information, being suitable for psychological and civic studies. The text data are classified, and the corresponding psychological and civics teaching status category labels are obtained. The model hyperparameters are set as shown in Table 2.

In text data preprocessing, in general, symbols do not have great significance to the algorithm. In order to reduce noise interference, we first use regular expressions to filter out useless punctuation marks in the text; then use the stuttering word separation library in *Python* to sub-phrase the text in the experimental dataset; and finally, based on the pretrained word vectors, use the Doc2vec tool to vectorize the text and obtain the text utterance. The obtained input sentence vectors will be used for model training in this paper. The training process loss convergence curve and performance improvement are shown in Figures 5 and 6.

4.2. Experimental Results. In order to better carry out the algorithm experiments, the length of the input samples is analyzed in this paper. Suppose the maximum value of the sample length of the selected data set is maxL; then, when the sample length is less than maxL, the sample needs to be filled with zero vector operation to make the sample length reach the maximum value, and when the sample length is greater than maxL, the excess part of the sample needs to be discarded and the overlength sample truncated. The selection of the maximum value of the sample length maxL is related to the good or bad experimental results. When maxL is set larger, the sample data zero vector is overfilled, while when maxL is set smaller, the sample data discard too much information; therefore, setting the maxL size may have some influence on the model performance. In this paper, by setting different maxL, we observe and compare the effect caused by the size of maxL on the model performance, the variation of F1 value with sample length is shown in Figure 7, and the differences of experimental results are shown in Table 3.

Observing Figure 7 and Table 3, we can find that when maxL is set less than 100, the F1 value is relatively low, which is due to too much information discarded from the sample data; when maxL is taken as 100, the F1 value reaches the highest point of 79.54%; when maxL is greater than 100, the F1 value is reduced and the model performance decreases; and the F1 value achieves the lowest value when maxL is 175, which is only 63.66%, because when maxL is set too large, the sample data are filled with too many zero vectors, causing interference with the data features.

In constructing the directed graph of contextual statements, there is a constructed edge relationship between the statement node and several statement nodes before and after it. The experiments in this paper show that the size of F1 value varies with the size of the context window on the dataset as shown in Figure 8; the model performance is poor when the window setting is less than 2; and when the window setting value is larger than 2, the performance rises steadily. For the sake of the number of rounds of dialogue between teachers and students in psychology and Civics

Table 1: Experimental environment configuration.

Python	3.8
Operating system	Windows 10
CPU	i5 6200U
PyTorch	1.0
Matplotlib	3.4.2
SciPy	1.6.3
Tushare	1.2.62
TA-Lib	0.4.24
yfinance	0.1.59

Table 2: Model parameter setting.

Hyperparameter name	Hyperparameter value
Word vector dimension	300
Bi-GRU coding layer dimension	300
Number of Bi-GRU coding layers	1
Number of GCN layers	1
GRU decoding layer dimension	600
Number of GRU decoding layers	1
Batch size	20
Learning rate	0.0008
Optimization algorithm	Adam
Weight decay rate	0.0001

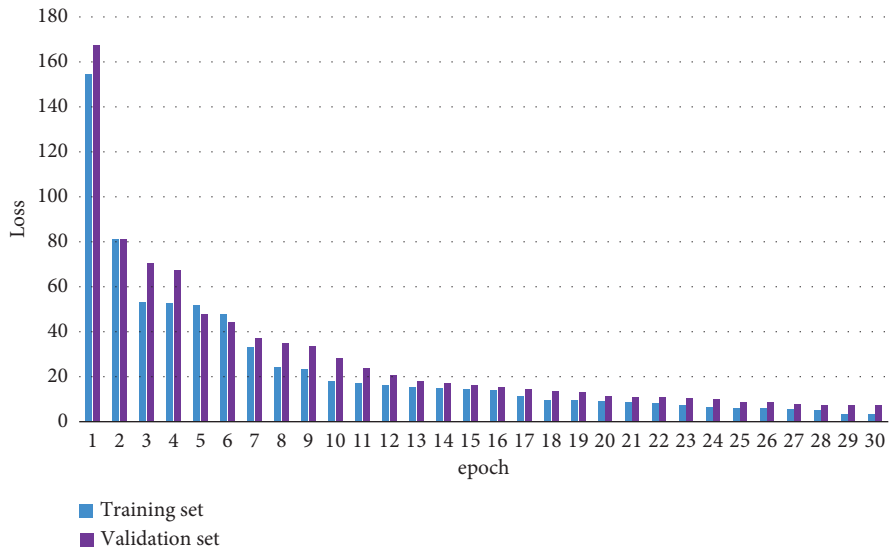

Figure 5: Training process loss convergence curve.

teaching in the experiment, this paper sets the window size to 5, and the experimental setting window size of 5 is sufficient in this paper.

In this paper, Bi-GRU + GCN is compared and analyzed with CNN, BiLSTM, Bi-GRU, and other models, and the experimental results of sentiment analysis on Chinese corpus are shown in Figures 9 and 10.

Observing the experimental results of each model, we can see that on the dataset, the F1 value is increased by 15.69% compared with the BiLSTM model and 14.87% compared with the Bi-GRU model. Compared with CNN and BiLSTM models, the hybrid model of Bi-GRU combined with GCN has significantly improved the accuracy of text emotion recognition in dialogs between teachers and

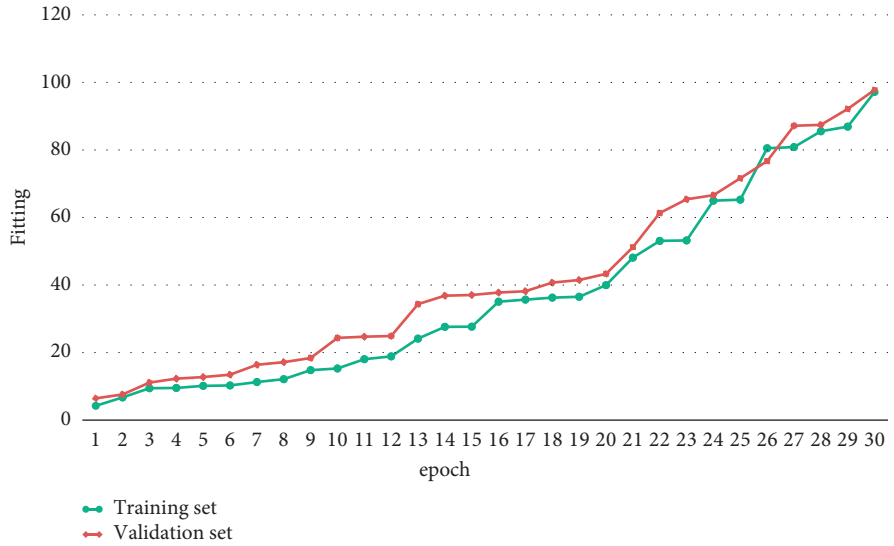

Figure 6: Training process performance improvement diagram.

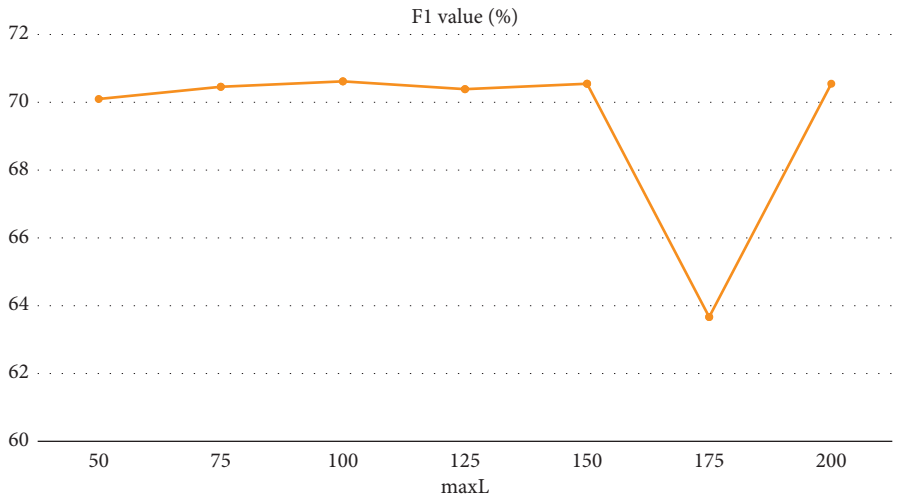

Figure 7: Effect of maxL value size on F1 value.

Table 3: Effect of sample length on experimental results.

maxL	Accuracy (%)	*F*1 value (%)
50	70.71	70.09
75	79.05	70.45
100	79.54	70.61
125	78.93	70.38
150	79.39	70.54
175	72.41	63.66
200	79.39	70.54

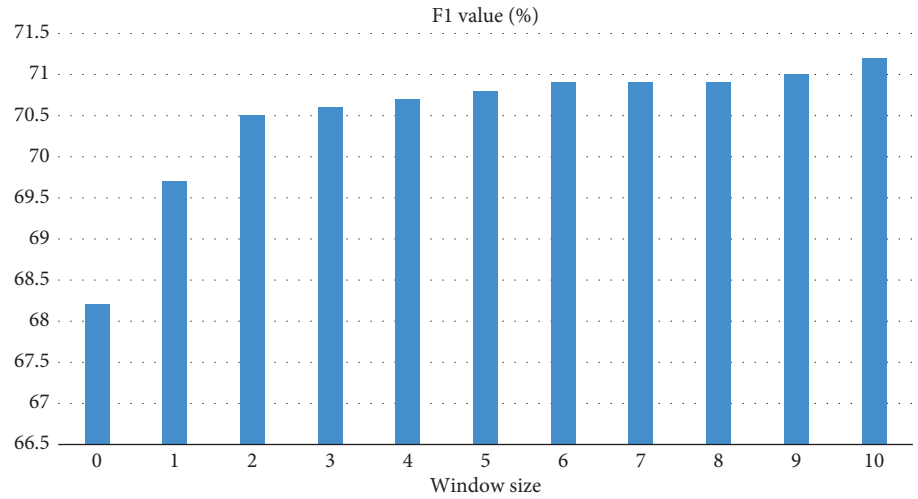

Figure 8: Effect of window size on F1.

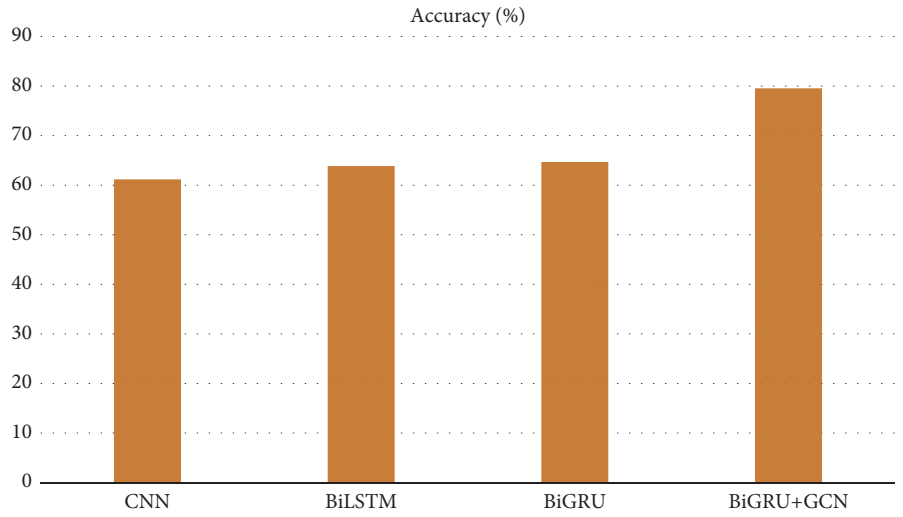

Figure 9: Experimental results on the accuracy of different models.

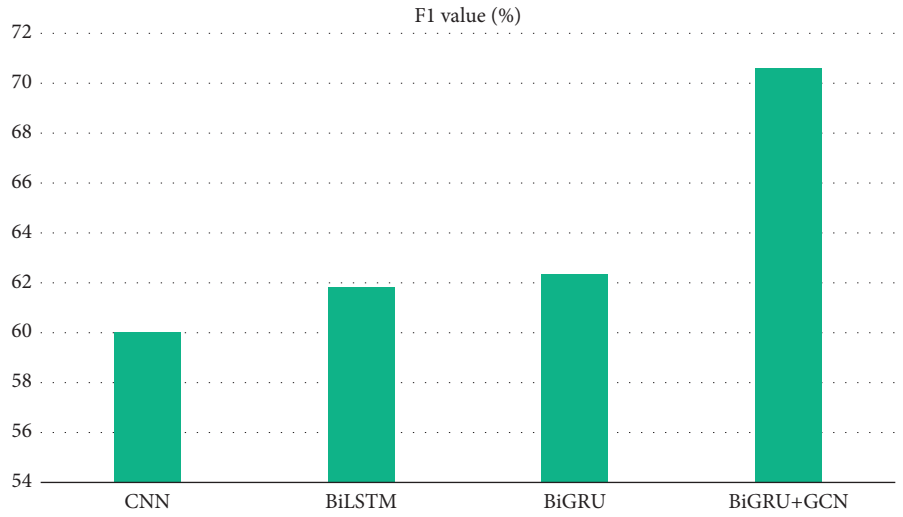

Figure 10: Experimental results of F1 for different models.

students in psychology and civics teaching, and the F1 value is as high as 70.61%, so the overall classification performance is better.

5. Conclusion

The addition of artificial intelligence provides a powerful boost to the content dissemination and scene application of civics and political science teaching, which makes civics and political science teaching develop in a more accurate direction in many aspects such as portrait, supply, leadership, and evaluation, directly driving the revolutionary changes in the internal elements and external forms of civics and political science teaching and providing powerful kinetic energy for the governance of major real-life problems in ideological and political education. Therefore, the teaching of civics and political science class should embrace new technologies such as artificial intelligence with open arms. At the same time, we also need to maintain sober awareness; even with the infinite empowerment of technology and powerful help, the ideological attributes of the civics class cannot change; its political guidance and ideological leadership of the basic functions must not be weakened by technology; the logical starting point for the use of technology is the human scale; the purpose is to stimulate the teaching of civics class itself to educate people; technology always has to serve the content, to be adapted to the content. The present is better. In this paper, we fully consider the emotional interaction between speakers, use graph convolutional neural network (GCN) to extract text features related to speakers, then use Bi-GRU model to extract text sequence features to connect the two in order to improve the contextual understanding in the emotional analysis of dialog utterances between teachers and students of psychology and civics teaching, and effectively identify the psychology and civics teaching states in the dialog texts of teachers and students of psychology and civics teaching categories. The experimental results prove the effectiveness of the model, which shows good classification effect in the sentiment analysis of psychological and civics teacher-student dialogs compared with other methods. In this paper, the graph convolutional neural network is used for text sentiment classification of psychological teacher-student dialogs, so only the textual information in the experimental dataset is focused on, and the multimodal sentiment recognition needs to be further studied. The accuracy in sentiment recognition was significantly improved, the F1 value was as high as 70.61%, and the overall classification performance was better. In the future, we plan to use convolutional neural networks for state recognition and reform analysis of psychological and civic teaching.

Data Availability

The datasets used during the current study are available from the corresponding author on reasonable request.

Conflicts of Interest

The authors declare that they have no conflicts of interest.

References

[1] S. Ding, S. Qu, Y. Xi, and S. Wan, "A long video caption generation algorithm for big video data retrieval," *Future Generation Computer Systems*, vol. 93, pp. 583–595, 2019.

[2] Z. Gao, Y. Li, and S. Wan, "Exploring deep learning for view-based 3D model retrieval," *ACM Transactions on Multimedia Computing, Communications, and Applications*, vol. 16, no. 1, pp. 1–21, 2020.

[3] Z. Gao, H. Xue, and S. Wan, "Multiple discrimination and pairwise CNN for view-based 3D object retrieval," *Neural Networks*, vol. 125, pp. 290–302, 2020.

[4] S. Ding, S. Qu, Y. Xi, and S. Wan, "Stimulus-driven and concept-driven analysis for image caption generation," *Neurocomputing*, vol. 398, pp. 520–530, 2020.

[5] J. Pei, Z. Yu, J. Li, M. A. Jan, and K. Lakshmanna, "TKAGFL: a federated communication framework under data heterogeneity," *IEEE Transactions on Network Science and Engineering*, 2022.

[6] A. V. Selezneva and A. A. Azarnova, "Birth of a citizen": political and psychological analysis of Russian high school students' civic consciousness," *Polis. Political Studies*, vol. 5, no. 5, pp. 101–113, 2020.

[7] M. Barrett and D. Pachi, "Psychological factors linked to youth civic and political engagement," *Youth Civic and Political Engagement*, 2019.

[8] M. Eimanzadeh, N. Farrokhi, and H. Bahrami, "Structural relationship pattern between psychological capital and national identity mediated by self-efficacy, social competence and civic culture of female students," *Journal of School Psychology*, vol. 7, no. 3, pp. 46–68, 2018.

[9] R. C. H. Chan and W. W. S. Mak, "Empowerment for civic engagement and well-being in emerging adulthood: evidence from cross-regional and cross-lagged analyses," *Social Science & Medicine*, vol. 244, Article ID 112703, 2020.

[10] H. Bang, N. P. Smith, S. E. Park, and C. Lee, "Perceived quality and organizational support for enhancing volunteers' leisure satisfaction and civic engagement: a case of the 2020 super bowl," *Leisure Sciences*, pp. 1–22, 2022.

[11] D. T. Lardier, P. Garcia-Reid, and R. J. Reid, "The examination of cognitive empowerment dimensions on intrapersonal psychological empowerment, psychological sense of community, and ethnic identity among urban youth of color," *The Urban Review*, vol. 51, no. 5, pp. 768–788, 2019.

[12] M. Balkaya-Ince, C. S. L. Cheah, L. Kiang, and M. Tahseen, "Exploring daily mediating pathways of religious identity in the associations between maternal religious socialization and Muslim American adolescents' civic engagement," *Developmental Psychology*, vol. 56, no. 8, p. 1446, 2020.

[13] S. I. Belentsov, V. A. Gribanova, and N. V. Tarasova, "Conditions and factors of the development of creative civic engagement of students," *European Journal of Contemporary Education*, vol. 8, no. 2, pp. 409–417, 2019.

[14] E. A. Sorokoumova and E. I. Cherdymova, "Developing structural components of ecological consciousness to promote civic identity formation," *Psychological Science and Education*, vol. 26, no. 1, pp. 102–112, 2021.

[15] E. S. White, "Parent values, civic participation, and children's volunteering," *Children and Youth Services Review*, vol. 127, Article ID 106115, 2021.

[16] E. E. McGinty, R. Presskreischer, K. E. Anderson, H. Han, and C. L. Barry, "Psychological distress and COVID-19–related stressors reported in a longitudinal cohort of US adults in

April and July 2020," *JAMA*, vol. 324, no. 24, pp. 2555–2557, 2020.

[17] E. E. McGinty, R. Presskreischer, H. Han, and C. L. Barry, "Psychological distress and loneliness reported by US adults in 2018 and April 2020," *JAMA*, vol. 324, no. 1, pp. 93-94, 2020.

[18] S. N. Blok, H. J. M. Fenger, and M. W. van Buuren, "Stimulating civic behavior? The paradoxes of incentivising self-organization," *Local Government Studies*, pp. 1–20, 2022.

[19] W. G. Weber, C. Unterrainer, and T. Höge, "Psychological research on organisational democracy: a meta-analysis of individual, organisational, and societal outcomes," *Applied Psychology*, vol. 69, no. 3, pp. 1009–1071, 2020.

[20] S. Sunil and S. K. Verma, "Moral identity and its links to ethical ideology and civic engagement," *Journal of Human Values*, vol. 24, no. 2, pp. 73–82, 2018.

[21] H. Yildiz, "The interactive effect of positive psychological capital and organizational trust on organizational citizenship behavior," *Sage Open*, vol. 9, no. 3, Article ID 2158244019862661, 2019.

[22] C. A. Merza, P. C. N. Baga, and P. S. Bautista, "Pakikipagkapwa: pathways in developing civic engagement among student leaders," *Philippine Social Science Journal*, vol. 5, no. 2, pp. 61–72, 2022.

[23] R. Hoefer, "Applications of theory to social policy: civic engagement theory," *Journal of Policy Practice and Research*, vol. 2, no. 2, pp. 67–70, 2021.

[24] S. Zhang, H. Tong, J. Xu, and R. Maciejewski, "Graph convolutional networks: a comprehensive review," *Computational Social Networks*, vol. 6, no. 1, pp. 1–23, 2019.

[25] M. Sun, S. Zhao, C. Gilvary, O. Elemento, J. Zhou, and F. Wang, "Graph convolutional networks for computational drug development and discovery," *Briefings in Bioinformatics*, vol. 21, no. 3, pp. 919–935, 2020.

[26] W. Cai and Z. Wei, "Remote sensing image classification based on a cross-attention mechanism and graph convolution," *IEEE Geoscience and Remote Sensing Letters*, vol. 19, 2020.

Hindawi
Computational Intelligence and Neuroscience
Volume 2022, Article ID 6374988, 13 pages
https://doi.org/10.1155/2022/6374988

Research Article

Research on Named Entity Recognition Method of Metro On-Board Equipment Based on Multiheaded Self-Attention Mechanism and CNN-BiLSTM-CRF

Junting Lin and Endong Liu

School of Automation & Electrical Engineering, Lanzhou Jiaotong University, Lanzhou 730000, China

Correspondence should be addressed to Junting Lin; linjt@lzjtu.edu.cn

Received 8 May 2022; Accepted 12 June 2022; Published 6 July 2022

Academic Editor: Yaxiang Fan

Copyright © 2022 Junting Lin and Endong Liu. This is an open access article distributed under the Creative Commons Attribution License, which permits unrestricted use, distribution, and reproduction in any medium, provided the original work is properly cited.

Massive and complex unstructured fault text data will be generated during the operation of subway trains. A named entity recognition model of subway on-board equipment based on Multiheaded Self-attention mechanism and CNN-BiLSTM-CRF is proposed to address the issue of low recognition accuracy and incomplete recognition features of unstructured fault data named entity recognition task of subway on-board equipment: BiLSTM-CNN parallel network extracts context feature information and local attention information, respectively; In the MHA layer, the features learned from different dimensions are fused through the Multiheaded Self-attention mechanism, and the dependencies of various ranges in the sequence are captured to yield the internal structure information of the features. The conditional random field CRF is used to learn the internal relationship between tags to ensure their sequence. This model is tested with other named entity recognition models on the marked subway on-board fault data. The experimental results demonstrate that this model is able to recognize 10 kinds of labels in the dataset. Moreover, the recognition effect of each label has a good performance in the three evaluation indexes of P, R, and $F1$ score. Moreover, the weighted average evaluation indexes Avg − P, Avg − R, and Avg − F_1 of 10 labels in this model reach the highest 95.39%, 95.48%, and 95.37%, which has high evaluation indexes and can be applied to the named entity recognition of Metro on-board equipment.

1. Introduction

Subway on-board equipment is the basic piece of equipment guaranteeing the safe operation of the subway train. On-board equipment is also constantly upgraded owing to the rapid development of China's urban rail transit. With the accumulation of subway operation mileage and operation time, a consequential amount of fault data about on-board equipment has been generated. These data record the detailed fault information in the form of text, containing useful knowledge of fault diagnosis and processing. However, given that it is stored in the form of unstructured text, it is not conducive for computer processing and understanding. It has long been delved into by field engineers and technicians who suggest that the fault knowledge cannot be reused efficiently. Therefore, for these large amounts of unstructured subway fault knowledge, knowledge entities should be efficiently identified and integrated, the fault cases and treatment methods in the fault knowledge should be identified, the subway knowledge map should be built, and field personnel should be provided with accurate subway fault information. The human-computer interaction platform provides field personnel with three kinds of information: subway fault information, fault causes, and other knowledge information. Moreover, the named entity recognition task related to subway on-board equipment also establishes a knowledge base to serve subway fault diagnosis, subway train information service, and subway information intelligent recommendation [1].

Named entity recognition (NER) [2] is an essential component of natural language processing (NLP) [3]. It aims to identify various named entities from the original text,

such as name, location, and organization. It can subsequently extract the concerned information in the fault text data as named entities [4]. The extracted entities can subsequently pave the way for other NLP tasks. The methods of named entity recognition mainly include rule-based methods, statistics-based methods, and deep learning-based methods: Pan [5, 6] constructed the rule base of named entity recognition and used the method of rule matching to identify named entities. However, the rule writing based on rules and dictionary methods requires the involvement of domain experts, thereby requiring high language knowledge and poor portability. Therefore, statistical machine learning was employed to deal with the NER problem. In statistical machine learning, the main algorithms suitable for sequence annotation tasks are: Hidden Markov models (HMM) [7, 8], Maximum Entropy Markov models (MEMM) [9], conditional random field (CRF) [10], etc. However, the method based on machine learning requires a substantial amount of labeled data to train the model, requiring significant manpower, thereby leaving much room for improvement in recognition accuracy. In recent years, deep neural network has been used to realize the key tasks in the knowledge map due to the advent of deep learning technology [11], garnering extensive attention. The use of named entity recognition technology to identify entities in subway operation and maintenance logs is a basic step in the conversion of subway fault text into structured data, thereby laying a foundation for mining and developing the rich knowledge contained in a large amount of fault data recorded during subway operation [12]. The current mainstream deep learning solutions tend to embed layer and Bidirectional long short-term memory (BiLSTM) layer, allowing the machine to directly learn the features. It subsequently directly inputs the learned features into CRF, thereby circumventing the tedious task of manually formulating the feature function [13]. Literature [14, 15] uses the neural network model to learn the internal representation of text on a large number of unmarked datasets, which does not require the setting of artificial features. Literature [16] adopts the long short-term memory (LSTM) neural network model, boosting the performance of word segmentation. However, this method cannot yield the semantic information behind the sentence. Literature [17, 18] proposes that CRF is used as the processing mode of output processing layer on the basis of bidirectional LSTM, effectively improving the performance of the model. Furthermore, convolutional neural network (CNN) [19] has also achieved desirable results in solving NER problems; literature [20] uses CNN to obtain multilevel features, thereby yielding local attention information and improving the sensitivity of entity boundary information; literature [21] adopts the serial strategy of CNN and LSTM-CRF to recognize the named entity of the conll2003 English dataset, and obtains a higher F1 value. However, LSTM network cannot capture text information in both directions. Document [22] uses the Bidirectional gate recurrent unit (BiGRU) and CRF combined with CNN for named entity recognition, and uses the connection vector including affix vector, part of speech vector, and word vector as input. It ultimately outputs through the CRF layer, which can address the issue of automatic named entity recognition and exert a desirable effect on entity recognition. Document [18] proposed a method to fuse character and word vectors. It adopted the Chinese named entity recognition method of BiLSTM-CRF to effectively extract two features at character and word level, thereby effectively improving the accuracy of named entity recognition. Literature [23] adopts the BERT-CRF model, extracts the global features of the input sequence through the Bert pretraining model, adds the CRF layer at the end of the model, introduces hard constraints, and constructs the model framework of named entity recognition. However, the Bert model has a lengthy pretraining time, and it is only used as a transfer learning model, which is hindered by insufficient information recognition ability for small areas. Much research has been conducted in the field of railway text data analysis. In terms of named entity recognition, Yang [24] used word2vec to represent the characteristics of railway accident faults, and used BiLSTM-CRF to realize the named entity recognition of railway electrical service accident faults. Literature [17] uses BiLSTM-CRF to realize the named entity recognition of high-speed railway signal equipment and puts forward the entity relationship representation method of multidimensional word segmentation features, thereby achieving high evaluation indexes for the task of named entity recognition of high-speed railway signal equipment.

Based on the above literature research, this paper proposes a named entity recognition method for Metro on-board equipment based on multiheaded self-attention (MHA) and BiLSTM-CNN- CRF. The core idea of the method is as follows:

(1) YMDAA is used to complete the sequence annotation [25], and the location, phenomenon, and measure of the fault in the subway on-board fault text are marked and exported in an Ann format file. The file is subsequently read through Python and added to the BMEO label to complete the pre-annotation of fault text data.

(2) The tag and word sequence of the prelabeled fault text are input into the word2vec model and transformed into feature vectors. The strategy of CNN and BiLSTM working in parallel is adopted, whereby CNN and BiLSTM work simultaneously, extract the context and local attention features in the fault text, respectively, and ultimately fuse the two kinds of information.

(3) The multihead self-attention mechanism is adopted to give higher weight to the more important information in the input word sequence and label sequence. This mechanism can boost the sensitivity of the machine towards important information, mining the association between different input features to extract the feature vector containing other word information. The recognition ability of the machine to feature information can be more comprehensive by defining the number of heads of multiple groups of attention mechanisms, extracting important features from different dimensions, and splicing and linear processing these features [26].

2. Design of Named Entity Recognition Model Based on Multihead Self-Attention Mechanism and BiLSTM-CNN-CRF

Based on the multiheaded self-attention mechanism and BiLSTM-CNN-CRF, the named entity recognition model architecture of Metro on-board equipment is illustrated in Figure 1. It includes four main layers: word embedding layer, BiLSTM-CNN layer, MHA layer, and CRF layer.

In the word embedding layer, the subway on-board fault database is first loaded, the fault text records in the database are marked with BMEO through YMMDA, the word vector of large-scale marked text is subsequently trained in the same field as word2vec. The generated word vector is then input into the BiLSTM module and CNN module in the BiLSTM-CNN layer, respectively. The BiLSTM module is used to learn the time characteristics and context information of the text sequence, The CNN module is used to extract the local features in the text. The outputs of BiLSTM and CNN are then spliced and fed to the MHA layer to yield the global features of the text sequence and the correlation strength between words. Finally, the CRF layer marks the output sequence from the MHA layer according to the importance of the features and outputs the entity prediction label.

2.1. Word Embedding Layer. Data preprocessing is first performed on the prelabeled subway on-board fault text, which is subsequently segmented. Stop words and low-frequency words are then discarded. The accuracy of word segmentation exerts a direct impact on the training effect of the model, while the Jieba word segmentation tool may fail to identify some proper nouns in this field. Therefore, a dictionary of proper nouns in the subway on-board field should be defined according to relevant data and existing knowledge, to improve the reliability of word segmentation task and lay a foundation for the vectorization of text [27].

In this paper, word2vec model is used to train word vectors, transforming large-scale subway vehicle fault text and label data into low dimensional and dense word vectors. This model can reflect the relationship between words but does not necessarily ensure sufficient training of proper nouns. To address this issue, word2vec is used to train word vectors on the training set data and other corpora in the field. Word2vec trains the word vector through the skip gram model, whereby the central word predicts the words around it and solves the context word vector through the conditional probability value of the intermediate word vector, to fully learn the semantic vector representation [28]. Suppose the sample S is composed of n sentences, input the text sequence $S = [s_1, s_2, \cdots, s_n]$, the i sentence in the text sequence is represented as $s_i = [w_{i1}, w_{i2}, \cdots, w_{ik}]$, whereby k represents the number of words contained in the sentence s_i, and $\mathrm{w_{ik}}$ represents the k word in the i sentence. The skip gram model converts the input text sequence into word vector, and further generates the corresponding word vector matrix. $\mathbf{W}_{ij}$ represents the j word vector in the i sentence, and the word vector matrix of the sentence s_i with the length of k is represented as $\mathbf{W}_{i1:\,im} = [\mathbf{W}_{i1}, \mathbf{W}_{i2}, \mathbf{W}_{i3}, \cdots, \mathbf{W}_{ik}]$. Finally, $\mathbf{E} = [\mathbf{W}_{11:\,2k}, \mathbf{W}_{21:\,2k}, \mathbf{W}_{31:\,3k}, \cdots, \mathbf{W}_{n1:\,nk}]$, the word vector matrix spliced by n sentences in the sample S, is used as the output of the word embedding layer.

2.2. BiLSTM-CNN Layer. This layer adopts the strategy of BiLSTM and CNN working in parallel, whereby the feature vectors generated by word2vec are input to BiLSTM and CNN networks, respectively; the context features and local attention features are extracted respectively; and the two fusion features are subsequently input to the MHA layer.

2.2.1. BiLSTM. LSTM effectively calculates and controls the input and output of information by designing gating units in neurons. The design of this gating unit addresses the problem of text sequence length dependence. Its structure is illustrated in Figure 2.

The information of cell state C_{t-1} is transmitted through the top straight line. The hidden layer state h_t and input x_t at t time will modify C_t appropriately and then output to the next time. Moreover, C_{t-1} will participate in the calculation of h_t output at t time, and alter the cell state through the gate structure of LSTM. After connecting h_{t-1} and x_t, calculate with different weight matrices $(\mathbf{W}_f, \mathbf{W}_i, \mathbf{W}_i)$ and offset (b_f, b_i, b_o) through the sigmoid function, and output f_t, i_t, and o_t respectively. The calculation formula is shown in (1)–(3). The amount of information needed to be forgotten from the previous hidden layer h_{t-1} is controlled by multiplying f_t and C_{t-1}; the content is planned to (–1, 1) through the function, so that the updated cell $\widetilde{C}_t$ is multiplied with i_t to control which information needs to be retained. The calculation is shown in formula (4), where $\mathbf{W}_C$ denotes the weight matrix. When the information in the cell state C_t is completely updated, as shown in formula (5), it is scaled by tanh and multiplied by o_t to output h_t as the next LSTM hidden layer state. The calculation is shown in formula (6).

$$f_t = \sigma\left(\mathrm{W}_f \cdot \left[h_{t-1}, x_t\right] + b_f\right), \tag{1}$$

$$i_t = \sigma\left(\mathrm{W}_i \cdot \left[h_{t-1}, x_t\right] + b_i\right), \tag{2}$$

$$o_t = \sigma\left(\mathrm{W}_o \cdot \left[h_{t-1}, x_t\right] + b_o\right), \tag{3}$$

$$\widetilde{C}_t = \tanh\left(\mathrm{W}_C \cdot \left[h_{t-1}, x_t\right] + b_C\right), \tag{4}$$

$$C_t = f_t * C_{t-1} + i_t * \widetilde{C}_t, \tag{5}$$

$$h_t = o_t * \ \tanh\left(C_t\right). \tag{6}$$

However, given that the unidirectional LSTM model can only capture the information before the sequence and cannot capture the context semantics, Li et al. [27] improved the RNN model to yield the LSTM, which can solve the problems of gradient disappearance and gradient explosion that could occur in the process of long sequence training. BiLSTM is composed of forward propagating LSTM and back propagating LSTM. It captures the above and below

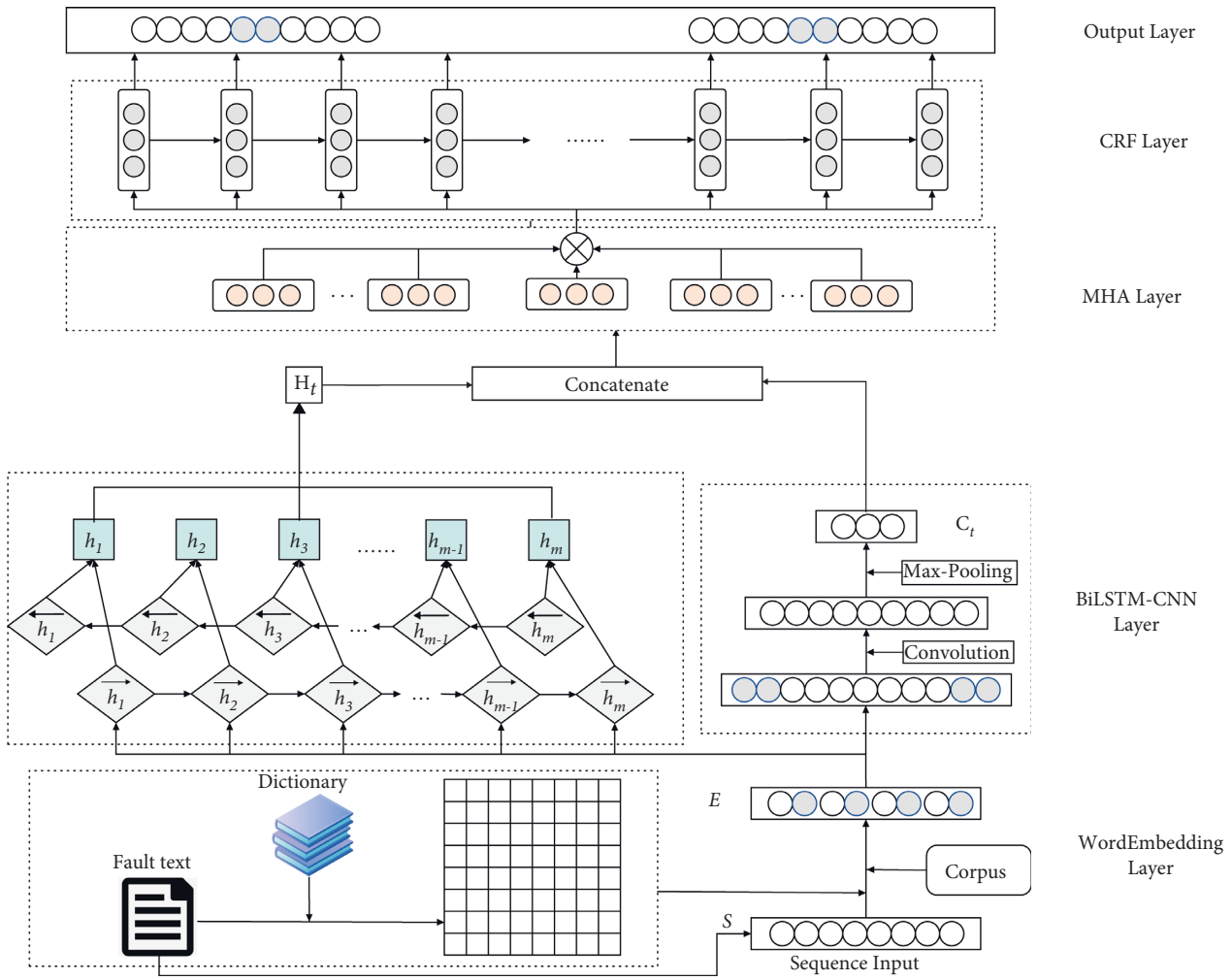

Figure 1: The overall model architecture of NER.

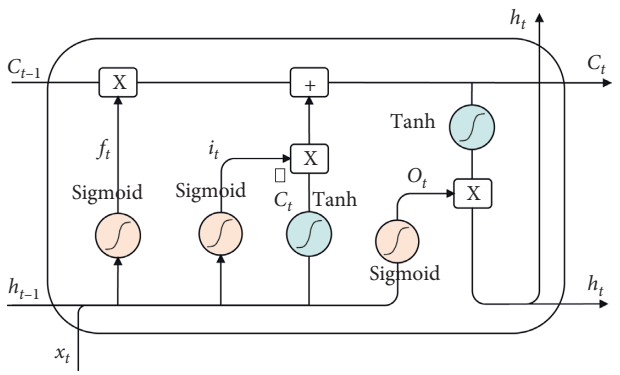

Figure 2: The structure of LSTM.

information of the current text, respectively, and then combines the feature information extracted from the two directions to yield the text features of remembering the past and the future. The word vector matrix E obtained through the word embedding layer is input to the BiLSTM part in the BiLSTM CNN layer as illustrated in Figure 1. The LSTM forward propagation generates the forward hidden layer state sequence: $\mathbf{H}_1 = [\overrightarrow{h_1}, \overrightarrow{h_2}, \ldots, \overrightarrow{h_m}]$, and the reverse hidden layer state sequence: $\mathbf{H}_2 = [\overleftarrow{h_1}, \overleftarrow{h_2}, \ldots, \overleftarrow{h_m}]$. The forward hidden layer state sequence H_1 is spliced with the reverse hidden layer state sequence H_2 to obtain the complete hidden layer state sequence $\mathbf{H}_t = [\overrightarrow{h_m}, \overleftarrow{h_m}]$, where m represents the dimension of the BiLSTM input word vector. This combination of forward and reverse states gives full play to the advantages of BiLSTM and addresses the issue whereby the traditional one-way LSTM model fails to capture the context information. It fully combines the context and extracts the features through the overall environment, which can substantially mitigate feature loss. The hidden layer state sequence $\mathbf{H}_t = [h_1, h_2, \ldots, h_m]$ is the final output of the BiLSTM layer and is input to the MHA layer.

2.2.2. CNN. The word vector matrix set generated by the word embedding layer is input to the CNN layer. The CNN layer includes two steps: convolution and max pooling. Its working process is depicted in Figure 3. Convolution is the

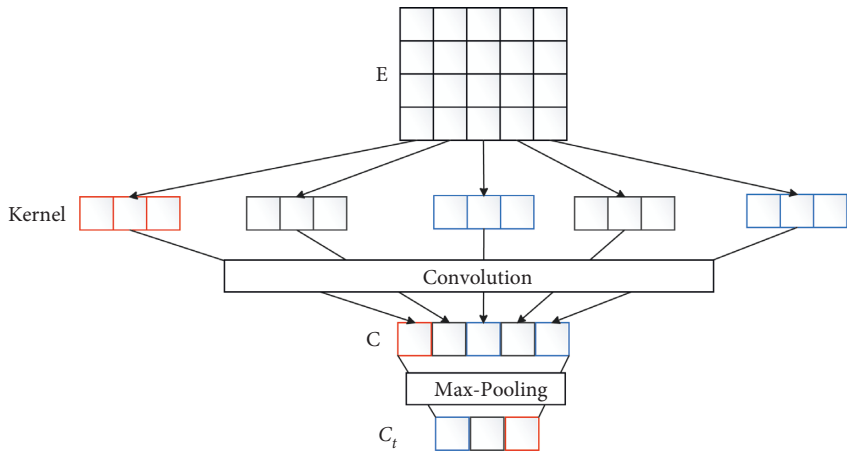

Figure 3: Working principle of the CNN layer.

use of different sizes of convolution to check the input eigenvector matrix for feature calculation, and then extracting the local feature information of the text. The operation process of convolution can be expressed as follows:

$$c_i = f\left(\mathbf{F} \cdot \mathbf{W}_{i:j} + b\right), \tag{7}$$

where c_i denotes the ith eigenvalue of the text output through convolution operation; F represents the matrix corresponding to the convolution kernel; f is a nonlinear activation function; $\cdot$ indicates that the two matrices are multiplied by points; $\mathbf{W}_{i:\ j}$ represents the word vector matrix from i word to j word; and b is the offset term. Convolution operation on the characteristic matrix of each word vector is carried out in the input, and the characteristic graph $\mathbf{c}$ is calculated through formula (8).

$$\mathbf{c} = (c_1, c_2, \cdots, c_n). \tag{8}$$

The pooling layer samples the text features by setting a fixed step stripe. In this paper, the maximum pooling strategy max pooling is used for pooling processing. This process aims to effectively extract the local key information in the sequence, compress the input feature map, reduce the size of the feature map $\mathbf{c}$, to simplify the network calculation, and finally calculate the output fixed length vector $\mathbf{C}_t$ through formula (9).

$$\mathbf{C_t} = \text{Max} - \text{pooling}(\mathbf{c}). \tag{9}$$

2.3. MHA Layer. The output $\mathbf{H}_t$ of BiLSTM network and the output $\mathbf{C}_t$ of CNN network are spliced into a feature vector $\mathbf{X}_t$ with a dimension of 320 (the dimension of feature vector $\mathbf{H}_t$ is 256 and the dimension of feature vector $\mathbf{C}_t$ is 64). However, this feature vector cannot display the importance of key information in the context, which could entail the loss of important information in the named entity recognition task. Therefore, the introduction of the multiheaded self-attention mechanism is essential to learn the dependence between any two words in the sentence, obtain the internal structure information, and distinguish the significance of each word. The calculation principle of self-attention mechanism is illustrated in Figure 4.

Taking the feature x_1 in $\mathbf{X}_t$ as an instance, the self-attention mechanism initializes the $\mathbf{W}^Q$, $\mathbf{W}^K$, and $\mathbf{W}^V$ matrices, and obtains $\mathbf{Q}_n$, $\mathbf{K}_n$, and $\mathbf{V}_n$ matrices, respectively, by multiplying with the input feature x_1 points, as shown in formula (10). It then calculates the attention a_{1n} from formula (12) to represent the correlation degree between the feature x_1 and the feature x_n.

$$x_1 \cdot \mathbf{W}^Q = \mathbf{Q}_n x_1 \cdot \mathbf{W}^K = \mathbf{K}_n x_1 \cdot \mathbf{W}^V = \mathbf{V}_n, \tag{10}$$

$$a_{1n} = \text{softmax}\left(\frac{\mathbf{Q}_1 \mathbf{K}_n^T}{\sqrt{d_k}}\right). \tag{11}$$

Among them, $\mathbf{Q}_n$ represents the query matrix, $\mathbf{K}_n$ represents the key value matrix, $\mathbf{V}_n$ represents the score matrix, and n is the serial number corresponding to other input features. Through the combination of a_{1n} and $\mathbf{V}_n$, the association $\mathbf{head}_{1n}$ between x_1 and other different features is obtained. The calculation is shown in formula (12). All the feature vectors $\mathbf{head}_{1n}$ are added and the Z_{11} vector is calculated and can represent the connection between the first word and other words through formula (12).

$$\mathbf{head}_{1n} = a_{1n}\mathbf{V}_n, \tag{12}$$

$$\mathbf{Z}_{11} = \mathbf{Concat}\left(\mathbf{head}_{11}, \mathbf{head}_{12}, \ldots, \mathbf{head}_{1n}\right). \tag{13}$$

The MHA calculation principle is depicted in Figure 5, whereby the multiple groups of $\mathbf{W}^Q$, $\mathbf{W}^K$, and $\mathbf{W}^V$ matrices are initialized, multiple groups of $\mathbf{Q}$, $\mathbf{K}$, and $\mathbf{V}$ characteristic matrices are generated through point multiplication, thereby yielding multiple groups of Z_{1t}. After completing the splicing of multiple groups of Z_{1t}, the dimension is reduced through linear transformation, whereby t denotes the number of self-attention heads, to obtain $\mathbf{Z}_1$ containing other feature information. MHA linearly maps the input features to different information subspaces through different weight matrices, and calculates the same attention function

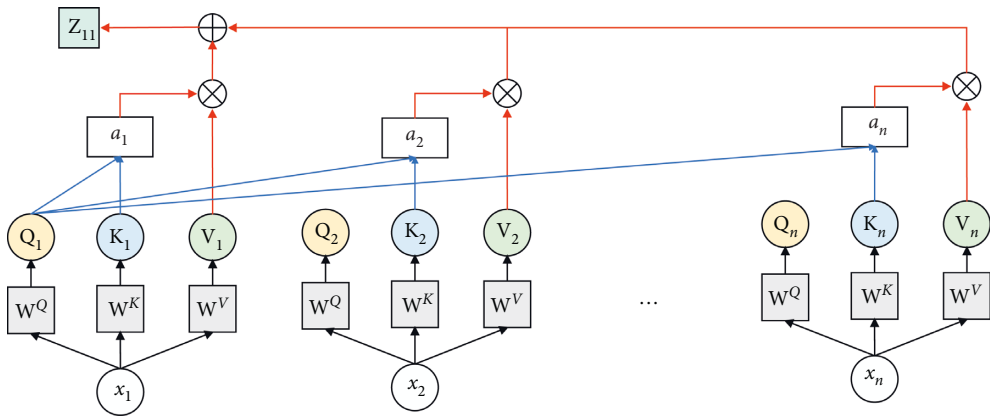

Figure 4: Calculation schematic diagram of self-attention mechanism.

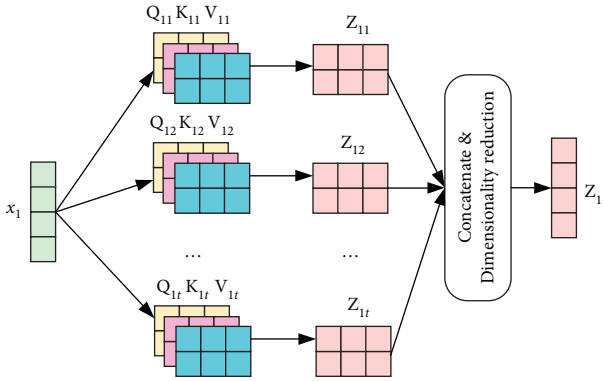

Figure 5: MHA calculation schematic diagram.

in each subspace, thereby expanding the ability of the model to consider different positions, to fully understand the structure and semantics of sentences. The output x_1' of the final MHA is calculated by the tanh function from $\mathbf{Z}_1$ and the input characteristic x_1, as shown in formula (14). The MHA value of other features x_n in X_t is calculated as above.

$$\mathbf{Z}_1 = \tanh\left(x_1 \oplus \mathbf{Z}_1\right). \tag{14}$$

2.4. CRF Layer. BiLSTM only considers the long-term dependency information of sentences but overlooks the dependency between tags. For instance, in the entity tags defined in this paper, b-phenomenon cannot appear after the m-phenomenon. Therefore, CRF needs to be introduced to learn the internal relationship between tags to ensure the sequence of tags. The conceptual diagram of CRF conditional random field is depicted in Figure 6.

The conditional random field model, CRF, is based on the calculation of a given random variable sequence $\mathbf{X} = (x_1, x_2, \cdots, x_n)$. The conditional probability distribution of the random variable sequence $\mathbf{Y} = (y_1, y_2, \cdots, y_n)$ is $P(\mathbf{X}|\mathbf{Y})$, and n denotes the sequence length. The model assumes that the random variable sequence satisfies the Markov property:

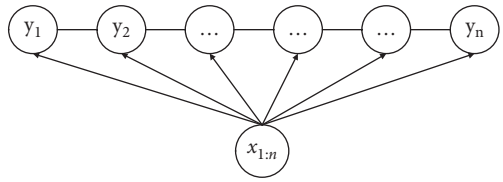

Figure 6: Conceptual diagram of CRF.

$$P\left(y_i|\mathbf{X}, y_i, \cdots, y_n\right) = P\left(y_i|\mathbf{X}, y_{i-1}, y_{i+1}\right). \tag{15}$$

$P(\mathbf{X}|\mathbf{Y})$ can subsequently represent the linear chain conditional random field. In the labeling problem, $\mathbf{X}$ represents the input observation sequence, $\mathbf{Y}$ represents the corresponding output mark sequence or state sequence, and the evaluation score $\text{Score}(\mathbf{X}, \mathbf{Y})$ can be obtained through formula (16).

$$\text{Score}\left(\mathbf{X}, \mathbf{Y}\right) = \sum_{i=1}^{n} \mathbf{P}_{i,y_i} + \sum_{i=0}^{n} \mathbf{W}_{y_i,y_{i+1}}, \tag{16}$$

whereby $\mathbf{W}$ represents the transition matrix, and $\mathbf{W}_{i,j}$ represents the state transition score from the i character to the j character. $\mathbf{P}$ denotes the weight matrix output by the decoding layer, $\mathbf{P}_{i,y_i}$ represents the probability that the ith word is marked as y_i, and exp represents the exponential function of the natural constant e. Assuming that the input sentence feature is $\mathbf{X}$, the probability distribution of the output sequence y' is $P(y'|\mathbf{X})$. Finally, the maximum probability is yielded by the maximum likelihood estimation in the process of fitting the model. The calculation process is shown in formula (17).

$$\begin{aligned}\log P\left(y'|\mathbf{X}\right) &= \log \frac{\exp\left(\text{score}\left(\mathbf{X}, y'\right)\right)}{\sum_{i=0}^{n} \exp\left(score\left(\mathbf{X}, y\right)\right)} \\ &= \text{score}\left(\mathbf{X}, y'\right) - \log\left(\sum_{i=0}^{n} \exp\left(score\left(\mathbf{X}, y\right)\right)\right).\end{aligned} \tag{17}$$

3. Data Set and Experimental Evaluation Index

3.1. CRF Layer. The named entity recognition method of subway on-board equipment requires the deep learning method of supervised learning. Therefore, the sample data labeling is required before training. According to the fault knowledge structure, the fault text data of each Metro on-board equipment define three types of named entities: fault location, fault phenomenon, and fault solution. The named entity identification sequence is represented by BMEO, where B (begin) represents the starting position of the entity, *M* (middle) represents the middle part of the entity, and *E* (end) represents the end character of the entity, O (other) represents a nonentity character, and "–" is used to connect the sequence annotation symbol with the defined entity type. Therefore, this paper selects the fault text data recorded in the depot of a subway company from 2016 to 2021 according to the functions and fault characteristics of each equipment. After preprocessing these fault text data, the total amount of data is 51652 marked data, divided into the training set, development set, and test set; 41526 pieces of data are selected as the training set data as the data samples of model fitting; 5035 pieces of data are development set data, which are used to adjust parameters, select features, and make other decisions on learning algorithms; 5091 pieces of data are test set data, used in model evaluation. The knowledge annotation of some data in this paper and the process of input to the model in this paper are illustrated in Figure 7.

3.2. Experimental Evaluation Index. In this paper, the Precision, Recall, and F_1 – Score are used as the evaluation indexes of this experiment, whereby TP represents the number of samples classified and divided correctly; FP represents the number of samples classified and divided incorrectly; FN indicates the number of unclassified samples, which are wrong.

3.2.1. Precision. The accuracy rate is only for the positive samples with correct prediction, as opposed to all samples with correct prediction. It is calculated by dividing the number of positive samples with correct prediction by the ratio of the number of positive samples predicted by the model. It shows that the predicted positive samples are really positive, as shown in formula (8):

$$\text{Precision} = \frac{TP}{TP + FP} \times 100\%. \tag{18}$$

3.2.2. Recall. It is calculated by dividing the predicted correct number of positive samples by the actual number of positive samples in the test set; it shows that the number of samples that are really positive can be recalled by using the classifier, as shown in formula (9):

$$\text{Recall} = \frac{TP}{TP + FN} \times 100\%. \tag{19}$$

3.2.3. F1-Score. F_1 – Score is the harmonic average of accuracy rate and recall rate. Both Precision and Recall are expected to be higher; however, both these indicators are contradictory and cannot both be high. Therefore, F_1 – Score should be introduced as an appropriate threshold point to maximize the ability of the classifier, as shown in formula (10):

$$\text{F}_1 - \text{Score} = \frac{2}{1/\text{Precision} + 1/\text{Recall}} \times 100\%. \tag{20}$$

3.2.4. Weighted Average. In this paper, the evaluation indexes Avg – P, Avg – R, and Avg – F_1 are defined as the weighted average values of 10 entity labels' Precision, Recall, and ,F_1 – Score respectively. The calculation process is shown in formula (21).

$$Avg - P = \frac{\sum_{i=1}^{10} N_i \cdot P_i}{\sum_{i=1}^{10} N_i} \; Avg - R = \frac{\sum_{i=1}^{10} N_i \cdot R_i}{\sum_{i=1}^{10} N_i} \; Avg - F_1 = \frac{\sum_{i=1}^{10} N_i \cdot F_i}{\sum_{i=1}^{10} N_i}. \tag{21}$$

Where i denotes the value corresponding to the entity category (there are 10 named entity categories in this paper), N_i represents the number of entities in this category, and P_i, R_i, and F_i represent Precision, Recall, and F_1 – Score corresponding to class i entities, respectively.

4. Experimental Verification

4.1. Experimental Environment. The experimental hardware includes a i7-6700HQ CPU, a GTX960M graphics card, a video memory of 8G, a Win10 64bit operating system, a 3.60 python version, a Spider 5.0.5 development tool, and a 1.11.1GPU Pytorch version.

4.2. Experimental Super Parameter Optimization

4.2.1. MHA Attention Heads Number Selection and Other Parameter Settings. The number of attention heads is set to t in the MHA layer. During the operation of the MHA layer, the input features need to be divided into t parts, and the dimension of the feature vector X_t input to the MHA layer is 320. It is necessary to ensure that the set number of attention heads' t value is divisible by 320. Therefore, this paper selects MHA with the number of attention heads of 2, 4, 5, 8, and 10 to test the model in this paper, and the experiment uses all the parameters in Table 1 except attention_heads, and the optimizer chosen is Adam.

It can be inferred from Figure 8 that after the addition of the multihead self-attention mechanism, the prediction results of the model gradually improves with the increase of the number of self-attention heads; when the head is 8, the Avg – P, Avg – R, and Avg – F_1 of the model reach the optimum, and the $Avg - F_1$ of the model is increased by 0.52%, 0.46%, and 0.34%, respectively, compared to the number of self-attention heads of 2, 4, and 5. By further increasing the number of heads, the accuracy of the model decreases. This finding arises because an excessive number of attention heads will lead to overfitting of the model. The

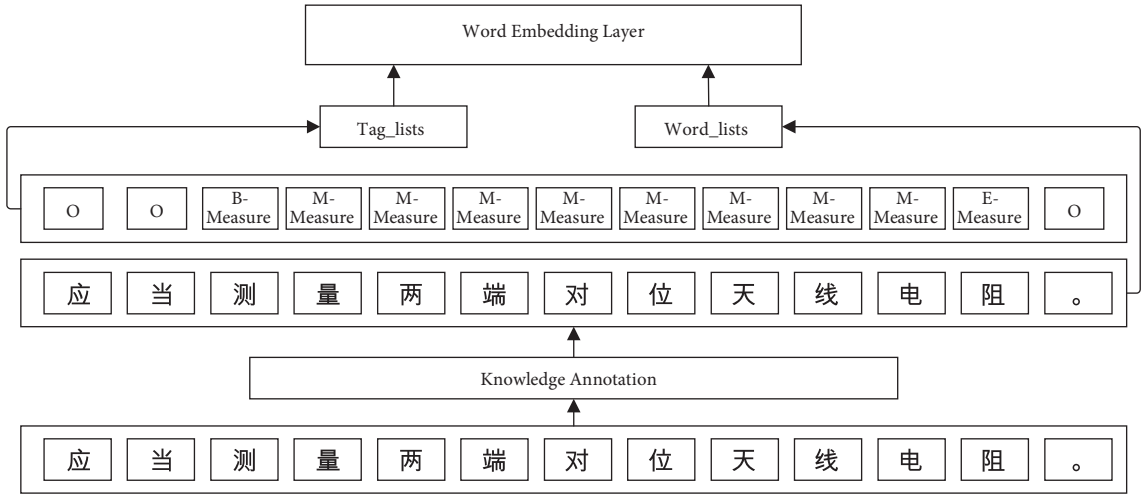

Figure 7: Knowledge annotation and input process of fault text of metro on-board equipment.

Table 1: Parameter setting.

Parameter	Value
Batch_size	64
Learning rate	$8e-4$
Hidden layer dimension	128
Epoch	25
LSTM_dim	128
cnn_size	64
attention_heads	8
kernel_size	(3, 4, 5)
Activation function	Relu
Max_seq_len	128
Dropout	0.5
Loss function	Cross entropy

number of MHA attention heads is set to 8, and the parameter settings are shown in Table 1.

4.2.2. Optimizer Selection. In the deep learning task, the optimizer is used to update and calculate the network parameters affecting the model training and model output, to approximate or reach the optimal value, and to minimize (or maximize) the loss function. In this experiment, five commonly used optimizers are selected: SGD (stochastic gradient descent), momentum optimization method, adaptive learning rate optimization algorithm Adagrad, RMSprop, and Adam. SGD selects a mini batch each time and uses the gradient descent to update the model parameters; Momentum optimization method adds the momentum optimization mechanism based on SGD. The Adagrad algorithm automatically attenuates the learning rate by using the number of iterations and cumulative gradient; RMSprop adds iterative attenuation; The Adam optimizer dynamically adjusts the learning rate of each parameter by using the first-order moment estimation and second-order moment estimation of the gradient [28]. In this experiment, the five optimizers are applied to the named entity recognition training task of this model. The parameter values set in

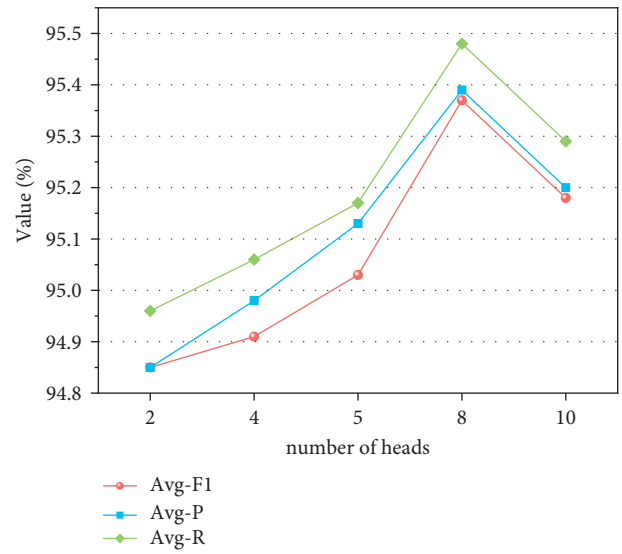

Figure 8: Effects of different attention heads on model performance.

Table 1 are used as the parameter values of this experiment, and The alpha of RMSprop is 0.99 and eps is $1e-08$; the beta1 of Adam is 0.9, beta2 is 0.999, and eps is $1e-08$, and the rest of the optimizers are the system default parameters. In the process of model training, the variation of loss function value loss with iteration step in the 5th, 10th, 15th, 20th, and 25th epoch rounds is shown in Figures 9(a) to 9(e), respectively.

Adam and RMSprop have the smallest loss function value and stable iterative waveform, while Adam showcases better performance in these two aspects. Therefore, Adam is selected for subsequent experiments in this paper. Moreover, it can be inferred that with the increase of training rounds epoch and training samples in each round, the loss function value loss constantly declines, and finally tends towards

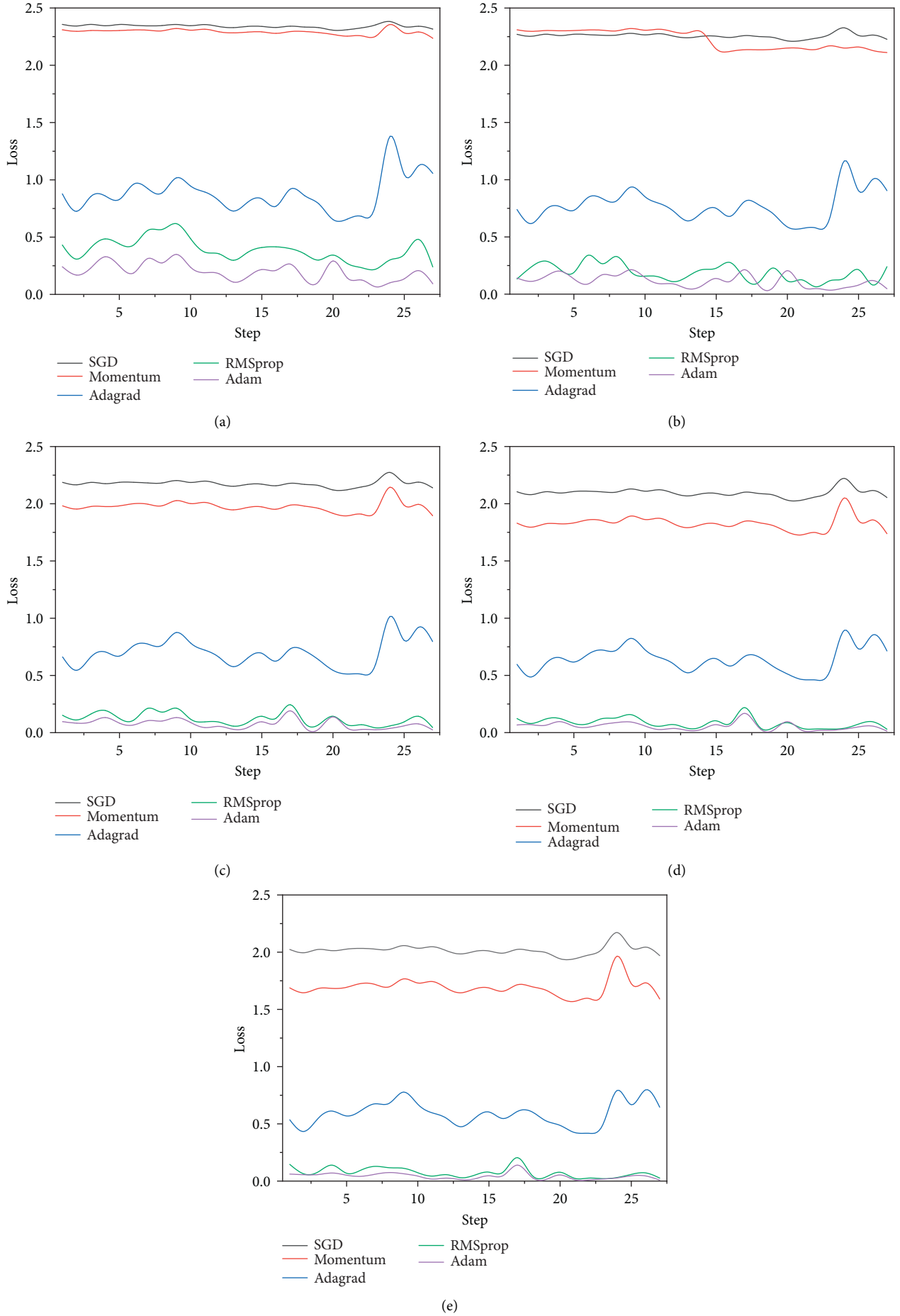

Figure 9: The loss function value of different optimizers varies with the number of iteration steps in different epochs: (a) 5th Epoch; (b) 10th Epoch; (c) 15th Epoch; (d) 20th Epoch; (e) 25th Epoch.

stability and 0, indicating that the parameter values in Table 1 optimizes the network training of this model.

4.3. Overall Comparison

4.3.1. Experimental Super Parameter Optimization. Several common named entity recognition models in NLP field are used to train the dataset in this paper. After 25 rounds of epoch, the recognition results of 10 entity labels in this paper are generated, as listed in Table 2 respectively. The following comparative analysis is carried out:

The recognition results of phenomenon are shown in Table 2. The *F*1 values of HMM model for BME of phenomenon are 65.52%, 80.33%, and 71.93%, respectively. Compared with (Table 3) CRF model, the F1 value of HMM model for entity (Table 4) label b-phenomenon is 4.81% lower, the F1 value of m-phenomenon is 2.01% lower, and the F1 value of e-phenomenon label is 4.99% lower. These findings arise as the limitation of HMM model is that it uses the trained local model to make a global prediction. The independent BiLSTM model is slightly better than the CRF model for the recognition of these three named entities, and the *F*1 value of Table 5 phenomenon's BME is increased by 2.61%, 2.87%, and 0.97%, respectively, because the single CRF model can only capture the internal relationship between named entities within a certain range. It fails to capture long-distance previous and subsequent information. However, the disadvantage of BiLSTM is that it has a general learning effect on the internal relationship between tags, which can be compensated by combining it with the CRF model. Therefore, the *F*1 value of BiLSTM CRF for entity tag b-phenomenon and e-phenomenon is increased by 0.33% and 1.87%, respectively, compared with BiLSTM, and the *p* value of entity tag m-phenomenon is increased by 3.75%. BiLSTM-CNN-CRF adds a CNN network based on BiLSTM-CRF. The output results of CNN and BiLSTM are fused into the CRF network to complete the named entity work and boost the extraction ability of local features. Therefore, the *F*1 value of BME named entities of phenomenon is increased by 1.4%, 1.63%, and 3.45%, respectively, compared with BiLSTM-CRF, and 1.73%, 0.9%, and 5.23%, respectively, compared with BiLSTM. Moreover, the *P* and *R* values are also improved to varying degrees. BiLSTM-CNN-MHA-CRF adds MHA based on BiLSTM-CNN-CRF to learn the dependency between any two words in the sentence and yields the internal structure information. The *F*1 value of BME three named entities has increased by 0.33%, 1.46%, and 0.83%, respectively. Although the *p* value has decreased slightly, the *R* value has increased by about 4–5 percentage points compared with BiLSTM-CNN-CRF, with a more balanced recognition effect of phenomenon entities.

Most location type named entities correspond to station names, place names, or section names, with relatively fixed names. Therefore, the six models have good recognition effects on location type named entities. The *P*, *R*, and *F*1 of BiLSTM-CNN-MHA-CRF have reached over 90%. Compared with the other five models, the *p* values for BME tag recognition of location are 97.37%, 94.27%, and 94.87%, respectively, which are the highest values. Also, the *F*1 values have reached the highest at 93.67%, 92.79%, and 92.50%, respectively. The recognition effect on the next three BME entity tags is relatively balanced.

The recognition effect of three named entity labels of BME of measure is shown in Table 4. The *F*1 value of b-measure in this paper is only second to BiLSTM-CNN-CRF and BiLSTM-CRF, at 86.73%. The recognition effect of E-MEASURE is general, with *P*, *R*, and *F*1 values of 89.58, 81.69, and 85.45%, respectively. The reason is that the number of these two entity labels is the least, resulting in insufficient learning of these two types of labels in the main model and the inability to play the role in MHA mechanism. However, for the largest number of entity tags with a complex structure, the *P* recognized by the m-measure is 96.23%, which is 4–19 percentage points higher than other models. The *F*1 value reached 91.07%, which is also the highest value among the six models, which is 5–13 percentage points higher than other models.

The recognition effect of other nonentity tags *o* is shown in Table 5. Tag O indicates a type of the label o, as the largest number of 10 tag types, the P, R and F1 values of the proposed six models exceed 94%, while the recognition effect of this model is slightly better. The *P*, *R*, and *F*1 values reach 96.37%, 98.87%, and 97.60%, respectively, and the *F*1 value is 0.6–2 percentage points higher than that of other models.

To sum up, for the identification of the above 10 Tags, the other five models except the model in this paper have relatively good recognition effects on BME entity tag and nonentity tag *o* in location. Also, the model in this paper has better recognition effects on these types of tags. The recognition effect of phenomenon's BME entity label is relatively poor, as the description of fault phenomenon will be detailed to each component. Given the numerous components of subway on-board equipment, the description of fault phenomenon is relatively complex, and the model fitting is more complex. Using the model proposed in this paper, the *F*1 value recognized by BME tag and m-measure tag of phenomenon is substantially improved, and the *F*1 value recognized by b-phenomenon is about 0.4–10 percentage points higher than that of other models. The *F*1 value of m-phenomenon increased by about 1.4–7 percentage points; the *F*1 value of e-phenomenon increased by about 2–4 percentage points; the *F*1 value of m-measure increased by about 5–13 percentage points. Due to the insufficient number of b-measure and E-MEASURE entity labels, the recognition effect of this model on b-measure and E-MEASURE entity labels is general; however, this model improves the recognition effect of 8 entity labels except for b-measure and E-MEASURE.

4.3.2. Overall Recognition Effect. Further comparison of the weighted average evaluation indexes Avg – *P*, Avg – *R*, and Avg – F_1 of the six models on the recognition results of 10 labels. As depicted in Figure 10 and Table 6, in terms of Avg – *P*, Avg – *R*, and Avg – F_1, the combined model IV–VIII outperforms I, II, and III. Compared with IV, V, and VI, Avg – *P*, Avg – *R*, and Avg – F_1 of V are increased

Table 2: Recognition effect of different named entity recognition models on phenomenon.

Models	B-phenomenon			M-phenomenon			E-phenomenon		
	P (%)	*R* (%)	*F*1 (%)	*P* (%)	*R* (%)	*F*1 (%)	*P* (%)	*R* (%)	*F*1 (%)
HMM	55.58	79.17	65.52	74.90	86.61	80.33	62.12	85.42	71.93
CRF	74.42	66.67	70.33	86.49	78.57	82.34	81.40	72.92	76.92
BiLSTM	83.78	64.58	72.94	84.92	85.49	85.21	78.72	77.08	77.89
BiLSTM-CRF	81.25	66.72	73.27	88.67	80.67	84.48	84.85	75.09	79.67
BiLSTM-CNN-CRF	84.85	66.67	74.67	95.59	78.33	86.11	91.43	76.19	83.12
BiLSTM-CNN-MHA-CRF	78.95	71.43	75.00	93.67	82.22	87.57	87.18	80.95	83.95

Table 3: Recognition effect of different named entity recognition models on location.

Models	B-location			M-location			E-location		
	P (%)	*R* (%)	*F*1 (%)	*P* (%)	*R* (%)	*F*1 (%)	*P* (%)	*R* (%)	*F*1 (%)
HMM	92.92	91.67	92.29	91.26	92.57	91.91	91.18	86.11	88.57
CRF	96.88	86.11	91.18	95.28	86.43	90.64	93.75	83.33	88.24
BiLSTM	96.43	75.00	84.37	92.81	92.14	92.47	91.43	88.89	90.14
BiLSTM-CRF	94.87	90.24	92.50	91.30	90.74	91.02	92.31	87.80	90.00
BiLSTM-CNN-CRF	97.30	87.80	92.31	92.31	87.80	90.00	93.67	91.36	92.50
BiLSTM-CNN-MHA-CRF	97.37	90.24	93.67	94.27	91.36	92.79	94.87	90.24	92.50

Table 4: Recognition effect of different named entity recognition models on measure.

Models	B-measure			M-measure			E-measure		
	P (%)	*R* (%)	*F*1 (%)	*P* (%)	*R* (%)	*F*1 (%)	*P* (%)	*R* (%)	*F*1 (%)
HMM	67.14	85.42	75.20	77.99	94.88	85.61	75.71	96.36	84.80
CRF	84.62	80.00	82.24	89.40	76.38	82.38	90.38	85.45	87.85
BiLSTM	86.00	78.18	81.90	92.11	68.90	78.83	91.67	80.00	85.44
BiLSTM-CRF	92.59	84.75	88.50	91.37	82.04	86.46	89.29	84.75	86.96
BiLSTM-CNN-CRF	92.41	84.94	88.52	90.76	79.58	84.80	94.34	84.75	89.29
BiLSTM-CNN-MHA-CRF	90.74	83.50	86.73	96.23	86.44	91.07	89.58	81.69	85.45

Table 5: Recognition effect of different named entity recognition models on other nonentity tags *O*.

Models	*O*		
	P (%)	*R* (%)	*F*1 (%)
HMM	97.70	92.76	95.17
CRF	94.99	97.91	96.43
BiLSTM	95.20	97.63	96.40
BiLSTM-CRF	95.26	98.64	96.92
BiLSTM-CNN-CRF	96.59	98.79	97.01
BiLSTM-CNN-MHA-CRF	96.37	98.87	97.60

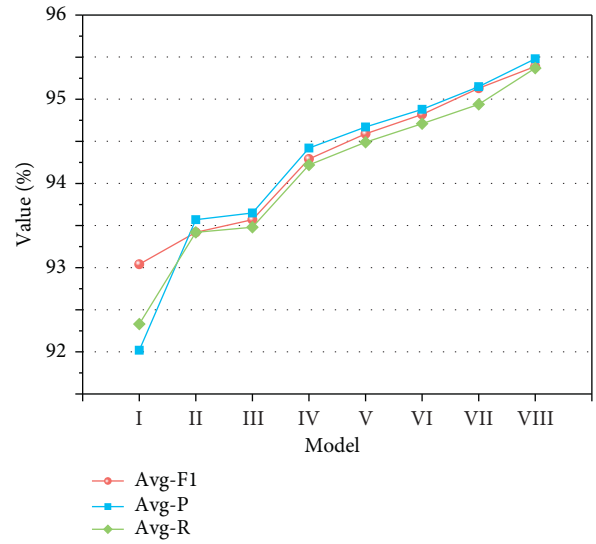

Figure 10: Weighted average of different named entity recognition models.

by 0.3%, 0.25%, and 0.27%, respectively, compared with and those of VI is increased by 0.53%, 0.46%, and 0.49%, respectively, compared with IV, indicating that adding CNN can improve the ability of extracting local features. The introduction of MHA largely makes up for the lack of BiLSTM's ability to capture the association relationship between words when processing long sequences and can capture various semantic features and highlight the key information of characters, the level of words and sentences. Therefore, the Avg – *P*, Avg – *R*, and Avg – F_1 of VIII are 0.57%, 0.6%, and 0.66% higher than those of VI, respectively, and the Avg – *P*, Avg – *R*, and Avg – F_1 of VIII are the highest among the six models, 95.39%, 95.48%, and 95.37%, respectively. Both V and VII models connect BiLSTM and CNN in series, whereby the word vector generated by

Table 6: Weighted average of different named entity recognition models.

No	Models	Avg – P (%)	Avg – R (%)	Avg – F_1 (%)
I	HMM	93.04	92.02	92.33
II	CRF	93.42	93.57	93.42
III	BiLSTM	93.57	93.65	93.48
IV	BiLSTM-CRF	94.29	94.42	94.22
V	$(\text{BiLSTM-CNN})_{\text{SPI}}$-CRF	94.59	94.67	94.49
VI	BiLSTM-CNN-CRF	94.82	94.88	94.71
VII	$(\text{BiLSTM-CNN})_{\text{SPI}}$-MHA-CRF	95.13	95.15	94.94
VIII	BiLSTM-CNN-MHA-CRF	95.39	95.48	95.37

Word2Vec is first input to BiLSTM. The output of BiLSTM is subsequently used as the input of CNN. Compared with V, VI, VII, and VIII, VI has increased by 0.23%, 0.21%, and 0.22%, respectively, in three indexes compared with V; VIII compared with VII, the three indexes are increased by 0.26%, 0.33%, and 0.43%, respectively, indicating that the effect of parallel work of BiLSTM and CNN outperforms serial work.

Therefore, adopting the strategy of BiLSTM and CNN working in parallel and effectively combining MHA and BiLSTM-CNN-CRF can improve the recognition effect compared with other named entity recognition models, which is of great significance to improve the overall performance of the named entity recognition model of Metro on-board equipment.

5. Conclusion

Based on unified labeling of Metro on-board equipment fault text data, aimed at solving the problem of low accuracy of naming entity recognition task of unstructured Metro on-board fault data, this paper proposes a Metro on-board equipment naming entity recognition model based on multihead self-attention mechanism and CNN BiLSTM CRF. Compared with the traditional naming entity recognition model BiLSTM CRF, this model adds a CNN network with parallel processing characteristics with BiLSTM. The two extracted features are combined and sent to MHA, which extract the context information and local feature information, and mine the internal relationship between different features through MHA. This paper defines the entity tag BME and other nonentity tags o corresponding to the three types, through the named entity recognition experiment of Metro on-board equipment fault text data with this model and other common named entity recognition models, and the experiment results show that:

(1) The proposed named entity recognition model has conspicuous advantages in the three indexes of P, R, and $F1$ for the recognition results of all tags except entity tag b-measure and E-MEASURE, which is higher than HMM, CRF, BiLSTM, BiLSTM-CRF, and BiLSTM-CNN-CRF.

(2) The model in this paper has a good performance in the weighted average evaluation indexes Avg – P, Avg – R, and Avg – F_1, reaching 95.39%, 95.48%, and 95.37%, respectively. It is the highest value when compared with the other five named entity recognition models. Moreover, the strategy of parallel work of BiLSTM and CNN outperforms serial work.

Therefore, it can meet the performance requirements of high accuracy of subway on-board equipment fault text named entity recognition, provide theoretical basis and application value for subway on-board equipment fault named entity recognition, and establish a good foundation for the subsequent establishment of subway on-board knowledge map and the subway on-board knowledge base.

Data Availability

The dataset can be obtained from the corresponding author upon request.

Conflicts of Interest

The authors declare that they have no conflicts of interest.

Acknowledgments

The authors gratefully acknowledge the valuable cooperation of Dr. Lin and other members of the laboratory in collecting data, debugging programs, and writing papers, as well as the National Natural Science Foundation of China (Grant no. 52162050) and the Natural Science Foundation of Gansu Province (Grant no. 20JR5RA375).

References

[1] C.-H. Gao, *A Communication Based on Train Control system*, China Railway Publishing House, Beijing.

[2] J. Lei, B. Tang, X. Lu, K. Gao, M. Jiang, and H. Xu, "A comprehensive study of named entity recognition in Chinese clinical text," *Journal of the American Medical Informatics Association*, vol. 21, no. 5, pp. 808–814, 2014.

[3] R. C. Wasserman, "Electronic medical records (EMRs), epidemiology, and epistemology: reflections on EMRs and future pediatric clinical research," *Academic pediatrics*, vol. 11, no. 4, pp. 280–287, 2011.

[4] C.-Q. Zong, X. Rui, and J.-J. Zhang, *Text Data Mining*, Tsinghua University Press, Beijing, 2019.

[5] C.-G. Pan, "Research on Chinese named entity recognition based on rule and statistics," *Information Science*, vol. 30, no. 5, p. 6, 2012.

[6] J.-H. Zheng, X. Li, and H.-Y. Tan, "Research on Chinese name recognition method based on corpus," *Chinese Journal of information*, vol. 14, no. 1, pp. 7–12, 2000.

[7] D. Bikel, "Nymble: a high-performance learning name-finder," in *Proceedings of the Fifth Conference on Applied Natural Language Processing*, pp. 194–201, ACM, Washington, USA, March 1997.

[8] D. M. Bikel, R. Schwartz, and R. M. Weischedel, "An algorithm that learns what's in a name," *Machine Learning*, vol. 34, no. 1/3, pp. 211–231, 1999.

[9] Y.-J. Zhang, Z.-T. Xu, and X.-Y. Xue, "Maximum entropy Chinese named entity recognition model based on multi feature fusion," *J], Computer research and development*, vol. 45, no. 6, 2008.

[10] A. McCallum and W. Li, "Early results for named entity recognition with conditional random fields, feature induction and web—enhanced lexicons [C/proceedings of the seventh conference on natural language learning at HLT — NAACL. Stroudsburg, USA," *ACLPPinforma*, no. 4, pp. 188–191, 2003.

[11] Z. Y. Ji, D. Y. Kong, L. W. D. W, and Y. J. Sang, "Research on named entity recognition based on deep learning [J/OL]," *Computer integrated manufacturing system*.

[12] K. Chen, *Research on Fault Diagnosis Method of Urban Rail Transit CBTC System Based on Text Mining*, Beijing Jiaotong University, Beijing china, 2020.

[13] P. Liu, Y.-P. Guo, F.-L. Wang, and G.-H. Li, "Chinese Named Entity Recognition: The State of the art," *Neurocomputing*, p. 473, 2022.

[14] R. Collobert, J. Weston, L. Bottou, L. Karlen, M. Kavukcuoglu, and P. Kuksa, "Natural language processing (almost) from scratch," *Journal of Machine Learning Research*, vol. 12, no. Aug, pp. 2493–2537, 2011.

[15] Y. L. Miao, W.-F. Cheng, Y.-C. Ji, S. Zhang, and Y. L. Kong, "Aspect-based sentiment analysis in Chinese based on mobile reviews for BiLSTM-CRF," *Journal of Intelligent and Fuzzy Systems*, vol. 40, no. 7, pp. 1–11, 2021.

[16] X. Chen, X. Qiu, C. Zhu, P. Liu, and X. J. Huang, "Long short-term memory neural networks for Chinese word segmentation," in *Proceedings of the 2015 Conference on Empirical Methods in Natural Language Processing*, pp. 1197–1206, Beijing china, Oct2015.

[17] Q.-H. Zhou and X.-L. Li, "Research on fault short text classification method of railway signal equipment based on MCNN," *Journal of Railway Science and Engineering*, vol. 2, no. 16, pp. 2859–2865.

[18] N. Ye, X. Qin, L. Dong, X. Zhang, and K. Sun, "Chinese named entity recognition based on character-word vector fusion," *Wireless Communications and Mobile Computing*, vol. 2020, no. 3, pp. 1–7, 2020.

[19] Y. Kim, *Convolutional Neural Networks for Sentence Classification*, https://arxiv.org/abs/1408.5882, 2014.

[20] J. Gao, Z.-P. Zhang, P. Cao, W. Huang, and F.-F. Li, "Citation entity recognition method using multi-feature semantic fusion based on deep learning," *Concurrency and Computation: Practice and Experience*, vol. 34, no. 6, 2021.

[21] X. Ma and E. Hovy, "End-to-end Sequence Labeling via Bi-directional LSTM-CNNs-CRF," in *Proceedings of the 54th Annual Meeting of the Association for Computational Linguistics*, 2016.

[22] M. Ayifu, S. Wushouer, and M. Palidan, "Multilingual named entity recognition based on the BiGRU-CNN-CRF hybrid model," *International Journal of Information and Communication Technology*, vol. 15, no. 3, p. 223, 2019.

[23] X.-L. Liu, M.-Q. Zhang, Q. Gu, Y.-Z. Ren, D.-B. He, and W.-L. Gao, "Named entity recognition of fresh egg supply chain based on BERT-CRF model," *Journal of agricultural machinery*, vol. 52, no. S1, pp. 519–525, 2021.

[24] L.-B. Yang, *Research and Application of Key Technologies of Railway Accident Fault Text Big Data Analysis*, China Academy of Railway Sciences, Beijing, 2018.

[25] J. Yang, Y. Zhang, L. Li, and X. Li, "YEDDA: A Lightweight Collaborative Text Span Annotation Tool," in *Proceedings of ACL 2018, System Demonstrations*, 2018.

[26] K. Dheeraj and T. Ramakrishnudu, "Negative emotions detection on online mental-health related patients texts using the deep learning with MHA-BCNN model," *Expert Systems with Applications*, vol. 182, Article ID 115265, 2021.

[27] C.-F. Li and K. Ma, "Entity recognition of Chinese medical text based on multi-head self-attention combined with BILSTM-CRF," *Mathematical Biosciences and Engineering*, vol. 19, no. 3, pp. p2206–2218, 2022.

[28] T. P. Adewumi, F. Liwicki, and M. Liwicki, "Word2Vec: Optimal Hyper-Parameters and Their Impact on NLP Downstream Tasks," *Open Computer Scienc*, vol. 12, pp. 134–141, 2020.

[29] A. Graves, *Supervised Sequence Labelling*, Springer Berlin Heidelberg, Berlin, Germany, 2012.

[30] R. Sun, "Optimization for Deep Learning: Theory and algorithms," 2019, https://arxiv.org/abs/1912.08957.

Hindawi
Computational Intelligence and Neuroscience
Volume 2022, Article ID 6069881, 11 pages
https://doi.org/10.1155/2022/6069881

Research Article

Analysis of the Effect of Urban Residents' Sports Consumption on GDP Growth Based on Deep Learning

Heng Gao,[1] Yawen Zhang,[2] Yinhong Zhao,[1] Junjie Ma,[1] and XinGuo Yuan[1]

[1]*College of Education and Sports Sciences, Yangtze University, Jingzhou, China*
[2]*School of Physical Education and Health, Guangxi Normal University, Guilin, China*

Correspondence should be addressed to XinGuo Yuan; yuanxinguo@yangtzeu.edu.cn

Heng Gao and Yawen Zhang contributed equally to this work.

Received 12 May 2022; Accepted 23 May 2022; Published 29 June 2022

Academic Editor: Yaxiang Fan

Copyright © 2022 Heng Gao et al. This is an open access article distributed under the Creative Commons Attribution License, which permits unrestricted use, distribution, and reproduction in any medium, provided the original work is properly cited.

Nowadays, emerging industries are emerging, and the sports industry has become a remarkable new economic growth point. Vigorously tapping the potential of residents' sports consumption has important theoretical and practical significance for promoting the development of the sports industry, improving people's living standards, and stimulating economic growth. In this paper, a deep learning model is constructed, and the random forest and random network models in the deep learning network are used to analyze the pulling effect of urban residents' sports consumption on economic growth. Since the consumption level of urban residents is much higher than that of rural residents, urban residents are in a dominant position in sports consumption, so this paper takes urban residents' sports consumption as the core to explore the pulling effect of urban residents' sports consumption on economic growth. The research theme of this paper is the pulling effect of urban residents' sports consumption on economic growth, so this paper sets the explanatory variable as the added value of GDP, expressed by GDP. Sports consumption has the characteristics of inevitability, gradualness, and diversity. With the continuous change of people's living standards, sports consumption also presents several stages of relative consumption pattern changes. Research shows that sports consumption has a positive role in promoting economic growth and the transformation and upgrading of economic development mode. Every one percentage point change in sports consumption leads to an economic growth of 0.186 percentage points, and with the increase of the lag period, urban residents' sports consumption will gradually increase the driving effect of economic growth. This effect can be analyzed at the micro- and macrolevels and enhanced by a causal cumulative cycle mechanism.

1. Introduction

The needs in social production and life are people's desire to obtain something to satisfy their own desires under certain conditions, and it is the driving force for a series of human behaviors. Demand, defined in GDPs, is the quantity of goods that consumers are willing and able to buy in a certain period of time and at a certain price level. Then, people's demand for sports can be defined as the number of sports consumers who are willing and able to buy sports commodities at a certain market price level within a certain period of time [1]. Demand is the driving force for people to generate consumption behavior, and similarly, sports demand is the driving force for sports consumption. Sports consumption will be generated when there is a demand for sports. Sports consumption is not only affected by GDP, social, political, cultural, and environmental factors but also by people's values, lifestyles, living habits, consumption characteristics, etc. From the perspective of GDPs, the motivation of sports demand can be roughly classified into two aspects. On the one hand, it is the pursuit of immediate consumption utility. When people participate in sports activities and buy sports goods and services, they can obtain satisfaction directly from psychological or physical to varying degrees [2]. For example, participating in sports such as swimming, skiing, and yoga can relax and delight the body and mind, watching synchronized swimming and rhythmic gymnastics can bring beauty to people, and

watching NBA basketball and World Cup football can make people excited and stimulated. What sports brings to consumers is an immediate benefit, which can directly enter the consumer's utility function. In addition, most participatory sports can also give people a healthy body, and health itself can be regarded as a consumption utility, and sports consumers are satisfied because of their physical comfort. On the other hand is the pursuit of future investment returns. Physical exercise can form healthy capital in human capital, and it can prolong the working hours of workers, improve work efficiency and quality, and gain an advantage in the labor market, thereby obtaining higher income [3].

Sports brings a future benefit to consumers. People are willing to take time to participate in sports activities to exercise because they expect that the effectiveness of physical exercise will be enough to make up for the monetary expenditure and opportunity cost of taking up time to participate in sports activities. Different people have different motivations to participate in physical activities, which may be related to factors such as age and experience. In general, young people may want more direct pleasure from physical activity, but as they get older, they tend to turn more interested in healthy forms of physical activity. Since the consumption level of urban residents is much higher than that of rural residents, urban residents are in a dominant position in sports consumption. This paper uses the method of deep learning to multiply the per capita sports consumption of urban residents by the annual number of urban residents to obtain the total sports consumption data of urban residents. Therefore, this paper takes urban residents' sports consumption as the core to explore the driving effect of urban residents' sports consumption on GDP growth. It has a certain reference value [4].

The research theme of this paper is the pulling effect of urban residents' sports consumption on GDP growth, so this paper sets the explanatory variable as the added value of GDP. Consumer behavior analysis is driven by data. It is necessary to filter out main factors and design features from various information such as consumers, commodities, and consumption behaviors and use machine learning algorithms to train models on the selected data to predict consumers with the trained models and buy the most likely item. The prediction method based on consumer behavior is one of the important ways to accurately recommend the Internet and improve the purchase rate of goods. At present, this method has become a research hotspot in many disciplines such as machine learning and recommender systems [5]. The core of the consumer behavior analysis and prediction problem is to construct potential data features and build a prediction model with low cost so as to achieve the purpose of increasing the transaction scale.

The chapter arrangement of this paper: the first chapter introduces the relevant scholars' research on the consumption adjustment effect of urban residents; the second chapter introduces the basic probability of deep learning and applies the random forest and deep network in deep learning to sports consumption behavior data The third chapter makes an experiment and analyzes the relationship between urban residents' sports consumption and GDP effects based on deep learning; the fourth chapter summarizes the full text.

The innovation of this paper: Relevant scholars have now fully realized the importance of sports consumption to GDP growth, but from the perspective of existing related research progress, there is a lack of research on the regional structure of sports consumption, and it is not possible to analyze sports from the perspective of regional differences the relationship between consumption and the coordinated development of regional economy. Based on this, the research content of this paper mainly studies the significance of sports consumption to GDP growth from a macroperspective and makes a specific analysis of the relationship between sports consumption and GDP effects from the perspective of deep learning.

2. Related Work

In view of the special significance of sports consumption to GDP growth, the research of foreign scholars mainly focuses on the following aspects: the definition of sports consumption behavior, the demand of sports consumption market and residents' expenditure, and the motivation and behavior of sports consumption.

Zhao et al., according to the contemporary sports consumption's pride that comes from favorable marketing prospects, pointed out that in the research of marketing and sports consumer behavior, the feeling and process of pride has been achieved, and although they have been very important to sports consumers and operators, marketers have a significant impact. In this article, the findings are qualitatively analyzed through a multidimensional process view, with fan capital providing pride as a factor. Targeting four types of pride, introspective, alternative, contagious, and compelling, their research experiences and results are always in development, and a range of theoretical and managerial outcomes influence the final recommendations, making sports consumer pride in a brand or company may lead to stronger commitment and loyalty, combined with increased consumption, word-of-mouth industry and collaboration to create value [6]. Xiangqian conducted a study on the 1992 Barcelona Olympics and concluded that the total GDP impact of the Barcelona Olympics between 1987 and 1992 was US$26.048 billion. The number of employment opportunities brought by the Olympic Games was 59,328 [7]. Ding and Kong summed up the qualitative and quantitative investigations of consumer behavior in their published paper. They proposed that the investigation of consumer behavior should clarify the consumer's living background, consumption motives, and consumption patterns; fully understand consumers; and then analyze consumption behavior. In the qualitative investigation, the method of group discussion is used to explore the consumer's brand cognition, purchasing habits, usage habits, and brand evaluation [8]. Ahmad and Hall used the improved behavior tree model to analyze and predict consumer behavior and compared the models before and after the improvement. The experimental results show that the improved model has improved the effect of analyzing and predicting consumer behavior, which further proves that the decision tree model is very effective and has improvement value and potential

[9]. Peng and Zeng, through the analysis of impulse response function, pointed out that GDP growth has a greater impact on urban residents' sports consumption, while the impact of urban residents' sports consumption on GDP growth is relatively low in the initial stage but gradually increases with time [10]. Ali et al. work to explore the determinants of household spending when participating in sports. Due to the huge amount of data, taking a simple regression method is not suitable. Specifically, they looked at whether factors involved in decision-making (spending money) influenced parental participation in sports, household income, education, sports club membership, and frequency of exercise. These determinants (spending large amounts of money on sports participation) included household income, participation in sports when parents were young, sports club membership, frequency of exercise, youngest child, and family size. In addition, the results suggest that a two-stage approach is necessary because it provides a more in-depth look at household spending behavior. For example, highly educated families often participate in sports and invest a lot of money [11]. Zhang et al. pointed out that GDP development should be driven from investment demand to consumption demand in a timely manner, and gradually from external to internal, to cultivate consumption power, thereby driving the timely consumption of residents [12]. Jafarzadeh and He pointed out that consumption has a long-term and stable role in promoting GDP growth, and consumption should be vigorously stimulated. In particular, consumption by residents, which accounts for a large proportion of consumption, is an effective means to promote GDP development [13]. Chen and Yan-Li believe that in the short term, the role of rural residents' consumption on GDP growth is more obvious, while urban residents' consumption has a long-term and stable role in promoting GDP growth [14]. Zhang pointed out that the consumption rate has remained at a low level for many years, but the speed of GDP growth has been fast and stable, which mainly depends on exports and investment, but it is difficult to maintain GDP growth by relying on exports and investment for a long time without the strong support of consumption, and the quality of GDP growth cannot be improved [15]. Zhou established the basic model of cross-domain sports consumption and pointed out that the development space of cross-domain sports consumption is huge, which can stimulate the development of the sports industry and related GDP growth [16]. Peng et al. discussed the relationship between sports consumption and the structure of the sports industry and proposed that the current development of the sports industry should be based on the sports goods industry, and the sports fitness and entertainment industry should be the leading realistic choice [17].

To sum up, relevant scholars have now fully realized the importance of sports consumption to economic growth, but from the relevant research progress, the research content mainly studies the significance of sports consumption to economic growth from a macroperspective. Most of them focus on theoretical research and questionnaire research, and the research depth and intensity are insufficient, neglecting to examine the economic growth effect of sports consumption from a dynamic perspective, especially the research on the impact of sports consumption on economic growth from a quantitative perspective has not yet been seen. There is a lack of research on the regional structure of sports consumption and failure to analyze the relationship between sports consumption and the coordinated development of regional economy from the perspective of regional differences, and the analysis of the relevant transmission mechanism and its action mechanism is almost blank. Policy research on GDP growth needs to be improved urgently. Based on this, from the perspective of deep learning, this paper makes a specific analysis of the relationship between sports consumption and GDP effects.

3. Data Processing of Sports Consumption Behavior Based on Deep Learning

3.1. Build the Overall Framework of the Model. In this section, before exploring the traditional forecasting model, we first design the basic process of building a forecasting model as shown in Figure 1.

Building the model is done on the basis of data processing and feature engineering. Different algorithms are used for model training, and a unified evaluation standard is used to evaluate the effectiveness of the model, and then, the optimal model is selected to recommend and predict the sports consumption behavior in the sports consumption behavior subset so as to improve the accuracy of the recommendation. Logistic regression is one of the most widely used algorithms [18]. It can not only do regression analysis but also perform classification tasks. In dealing with classification problems, it adds $g(z)$ transformation on the basis of linear regression model, and its function form is given in the following equation:

$$g(z) = \frac{1}{1 + e^{-z}}. \tag{1}$$

Since the logistic regression classification model is essentially a linear classification model, it has high requirements for input, requiring the target object to be linearly separable, the features are independent of each other, there are fewer default values in the features, and the continuous numerical features can be more efficient. It is suitable for use, but the features proposed in sports consumption and economic effects are not strongly correlated, and there is a complex nonlinear relationship. Therefore, this model is not used in this paper.

3.2. Random Forests and Neural Networks. In classification algorithms, decision tree is a very commonly used model, but the decision tree is prone to overfitting during training, and ensemble algorithms can often effectively solve the overfitting problem and improve model efficiency. Bagging is a representative of parallel ensemble learning algorithms [19]. Random forest is an extension of Bagging. It builds Bagging ensemble based on the decision tree as the basic learner and adds random attribute selection to decision tree training as shown in Figure 2.

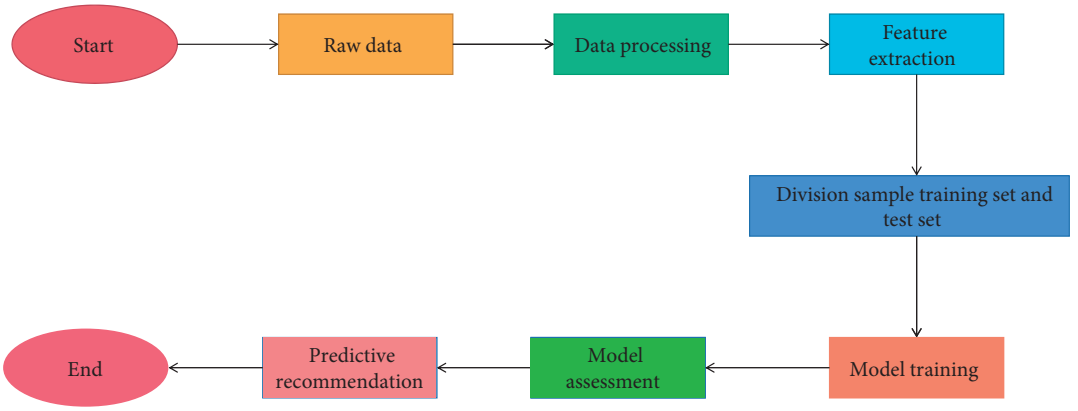

Figure 1: Flow chart of building a prediction model.

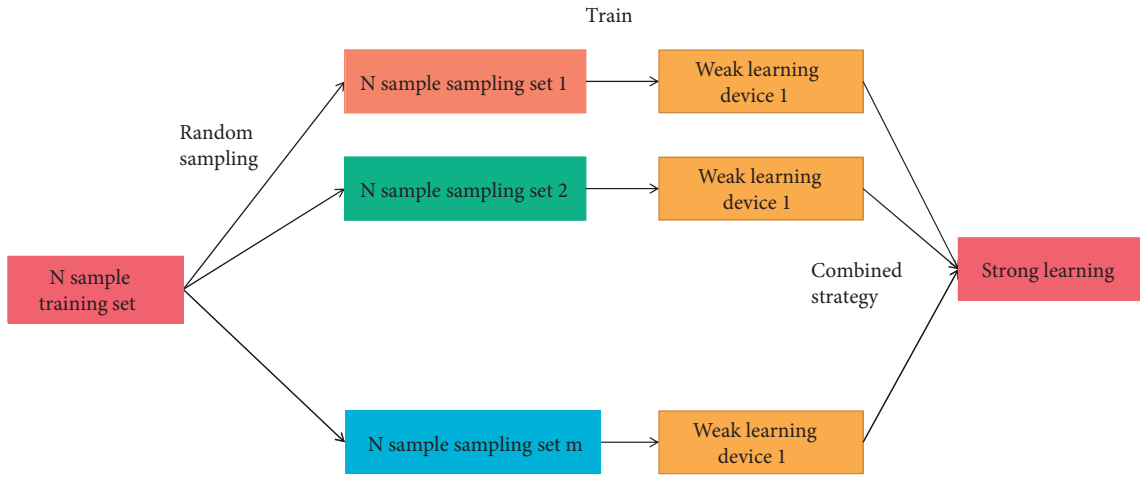

Figure 2: Principle of random forest algorithm.

Random forest is an improvement of Bagging in two aspects. One is to use CART decision tree as a weak learner. The other is to randomly select some sample features of nodes, and select the best feature among the random sample features to divide the left and right sub-numbers of the decision tree. Each branch in a random forest is a weak classifier. A label is predicted from the class label set and the output on the class label [20]. In the research of consumer behavior analysis and prediction random forest randomly solves the problem of overfitting of a single decision tree in the research of analysis and prediction of consumption behavior, and multiple decision trees improve the generalization ability. The feature of high parallelism is widely used in classification problems..

Training the neural network model essentially makes the predicted value approach the actual value, and the difference between the two is defined as a loss function. Assuming that the training set is the sample size, the overall loss function of the neural network model is given in the following equation:

$$h^{(l)} = \sigma\left(w^{(l)}h^{(l-1)} + b^{(l)}\right). \tag{2}$$

The first term is the mean square error cost function, which aims to control the error between the model output and the target, and the second term is the weight decay term, which prevents the model from overfitting by the weight decay magnitude. When training a neural network, gradient descent is used to update the weights. The residual between the predicted value and the true value is shown in the following equation:

$$\delta^{L} = \frac{\partial}{\partial Z_z^L}\frac{1}{2}|y - h(x)| = -\left(y_i - a_i^L\right)f\left(z_i^L\right). \tag{3}$$

Hidden layer residual is given in the following equation:

$$\delta^{l} = \left(\left(w^{(i)}\right)^{T}\delta^{(l+1)}\right)\cdot f\left(z_i^L\right). \tag{4}$$

Updating Weight Parameters Using Gradient Descent as shown in the following equation:

$$w^{l} = w^{l} - \eta\nabla_{w(l)}J(w,b). \tag{5}$$

Neural network has the characteristics of self-learning and nonlinear mapping and has been widely used in pattern recognition, classification processing, and nonlinear prediction [21]. The wide application of neural networks has also found some problems. When the number of neurons is

too large, overfitting is easy to occur; and with the increase of network derivatives, gradient disappearance is easy to occur, and the effect of learning will also be affected. *Problem*. In this paper, the gradient descent method is used to easily make the model fall into local minimization, which reduces the number of neurons in the hidden layer and is used to solve the problem that the feature information cannot be fully learned.

3.3. Model Construction. After the data preprocessing in the previous section, the training set and the test set are divided, and then, the model is built on this basis as shown in Figure 3.

The training set features are used as the input of random forest and neural network, respectively, and the corresponding samples are used as the output to train the model. Input the sample into the trained model, calculate the output value, evaluate the quality of the model prediction result, compare the performance of the model in the consumption behavior prediction problem, and analyze the reasons.

3.4. The Inevitability of Urban Residents' Sports Consumption and the Analysis of Consumption Structure. Urban residents are generally satisfied with the quality of life, which provides favorable conditions for the development of sports consumption. The premise of people's spontaneous sports consumption is that they have a lot of free time, a high proportion of disposable income, the awareness of obtaining health through reasonable exercise, and a strong interest in sports-related products. Only when the quality of life reaches a corresponding level, people will actively participate in sports consumption [22]. According to Maslow's Hierarchy of Needs theory, human beings live in a social environment and will generate five needs from their hearts. From the lowest to the highest, they are physiological needs, safety needs, love and belonging, respect, and self-actualization. After people have solved the problem of food and clothing, the social environment is relatively stable; the family, friendship, love, and other social interpersonal relationships are satisfied, and after obtaining a certain social status, they are respected by others, and finally, they will seek self-worth, through different ways to experience oneself, because sports is an industry that can constantly challenge the limits of human beings, so the birth of sports consumption has its inevitability and fully conforms to the laws of social development [23].

In this paper, the deep learning model is used to require the variables in the system to be stable, and then, the unit root test needs to be performed on the selected variable data first. The unit root test generally uses the Dick–Fuller test. According to the calculation process proposed in this paper, the ADF test results of urban residents' sports consumption and GDP growth variables are obtained as shown in Figure 4.

Although some nonstationary time series have a trend of showing common changes, there is not necessarily a direct causal relationship between these series, and the regression results do not actually contain practical significance, so in order to ensure the validity of the estimated results and avoid

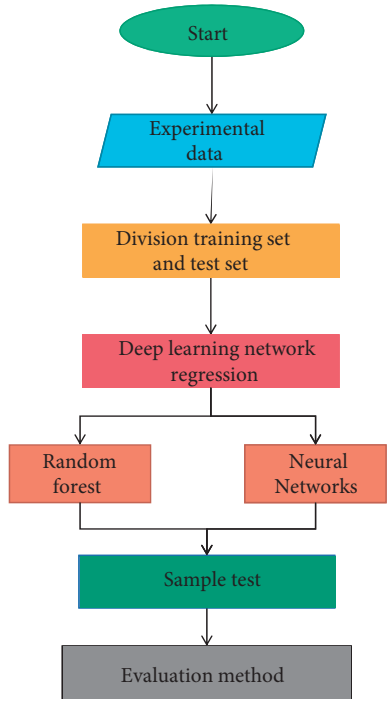

Figure 3: Model construction flow chart.

the appearance of pseudo-regression, the model data need to be tested for stationarity before regression. Stationarity means that the basic characteristics of the current sample time series and the fitted curve may remain continuous and stable for a period of time in the future. For other sample time series that can continue to be obtained in the future, we are also able to determine with certainty that its basic characteristics must be the same as the time series of the currently obtained samples. It can be seen that the stationarity of the time series is the most basic assumption for the classical regression analysis to continue. Predictions based on stationary time series may be ultimately valid. To test the stationarity of the data, firstly, it is necessary to draw a time series diagram of the data and observe the time series diagram and analyze the trend items and intercept items contained in the fitting curves described by each observed variable in the time series diagram. This is also necessary for the next step and prepare for the unit root test.

4. Quantitative Measurement of the Effect of Total Sports Consumption of Urban Residents on GDP Growth

4.1. The Causality Test of GDP Effects Based on Deep Learning. This paper uses economic effect causality to test the causal relationship between two variables. In the stationarity test in this paper, each variable is stable after one difference, so this paper uses a deep learning model composed of two variables and their lag variables to test the causal relationship between the economic effects of the four variables. If one is accepted and the other is rejected, there is a one-way causality. In this paper, the selection of the causal lag period of the GDP effect

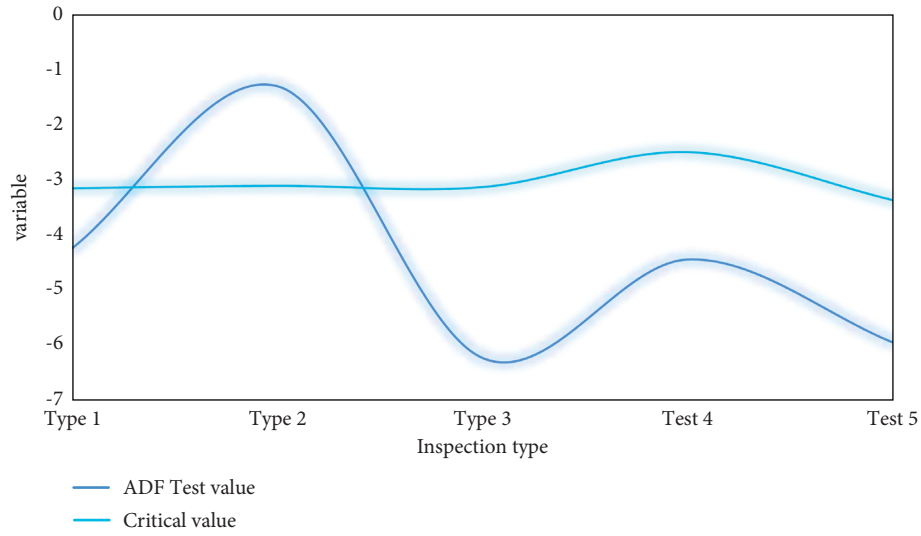

Figure 4: ADF test results of urban residents' sports consumption and GDP growth variables.

is selected by the selection criteria of the lag period of the two-variable deep learning model.

As can be seen from Figure 5, the relationship between GDP growth and sports consumption expenditure is somewhat in conflict with the theoretical analysis that sports consumption should significantly promote GDP growth. There is no deep learning causal relationship between different consumption behaviors and GDP, indicating that the correlation between rural residents' consumption and GDP growth is small. In the relationship between GDP growth effect and GDP, the GDP growth effect is the cause of the GDP effect of GDP at the 10% confidence level, that is, changes in urban residents' consumption can cause changes in GDP growth, but GDP is not the cause of GDP effect changes in GDP growth effects. There is a causal relationship between the GDP growth effect and sports consumption, indicating that there is a strong correlation between changes in urban residents' consumption expenditures and changes in sports consumption expenditures. There is no deep learning causal relationship between different sports consumption behaviors, economic growth effects, and different consumption behaviors, and there is little interaction between changes in rural residents' consumption expenditures, changes in sports consumption expenditures, and urban residents' consumption expenditures.

4.2. Cointegration Relationship Test of Deep Learning Model. According to the viewpoint of GDP theory, cointegration can be understood as the existence of an equilibrium force between GDP time series variables, that is, there is a mechanism to make nonstationary different variables move together in the long run, that is, if there is long-term stability between the variables' relationship (cointegration relationship), the growth rate of variables shows a common growth trend. Conversely, if these two or more variables are not cointegrated, there is no long-term equilibrium relationship between them. Cointegration theory selects the variables of the model based on whether there is a cointegration relationship between the variables, which makes the data foundation more stable and the statistical properties better. In order to examine whether there is a long-term stable relationship between urban residents' sports consumption and GDP growth, it is necessary to conduct a cointegration test, assuming a deterministic trend in the data, an intercept term in the cointegration equation, and a lag of 12, as shown in Figures 6 and 7.

As shown in Figures 6 and 7, at the 5% significant level, the null hypothesis is rejected, and there is no unit root in the residual of the equation. It shows that there is a long-term stable cointegration relationship between GDP and sports consumption. Sports consumption of urban residents is the GDP effect of GDP growth. Therefore, when external investment is impacted, GDP growth can be stimulated by stimulating domestic demand. The elasticity of this positive effect is 0.353, that is, every one percentage point change in sports consumption leads to a GDP growth of 0.353 percentage points, which proves that sports consumption of urban residents is an influential factor driving GDP growth. A lag order that is too small may not fully reflect the dynamics of the model, as potentially useful information contained in more distant lag values may be missed. When the lag order is too large, the number of parameters to be estimated in the model will increase, and the degrees of freedom will be reduced, which is more prominent in the case of small samples, and a too large lag order may bring additional estimation errors into the in the predicted value.

In econometrics, dependencies between time series variables in particular are rarely instantaneous. A common situation is that there is a time delay in the response of the dependent variable to the explanatory variable, and this time delay is called a lag. Lags play an important role in time series econometrics, and in practice, choosing an appropriate lag order requires a trade-off between the benefits of including more lags and the cost of additional estimation uncertainty. The traditional concept of sports consumption restricts consumers. The reason why most residents are reluctant to

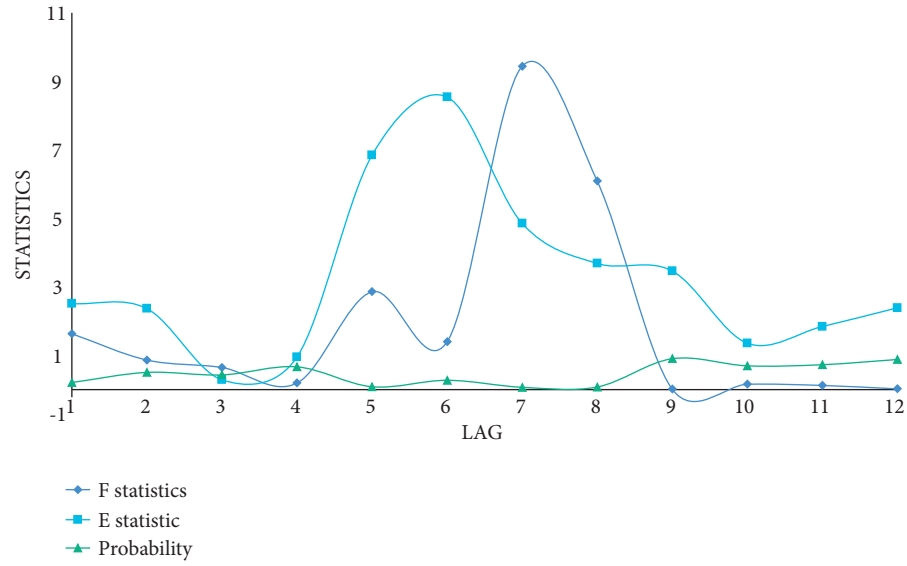

Figure 5: The causality test results of the GDP effects of each series.

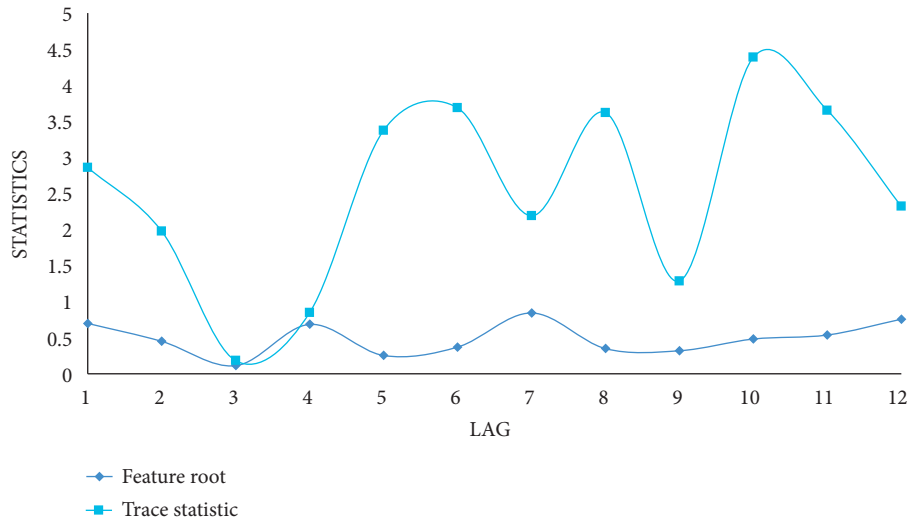

Figure 6: Trace statistics test results.

engage in sports consumption is because they have many uncertainties about their future life. Residents spend far less time on participatory sports consumption than on viewing sports consumption. It also shows that the overall sports consumption level of urban residents is moderately low. The formation of sports consumption concept is based on sports consumption demand as the premise and guides the generation of sports consumption motivation to promote the implementation of sports consumption behavior. This is a step-by-step mechanism process.

4.3. Analysis of Impulse Response Function of Deep Learning Model. Impulse response function describes the response of one endogenous variable to another endogenous variable, and the impact of a unit change on its future value in a specific period, and provides information such as the positive and negative directions, adjustment time delay, and stabilization process of the system response to the impact. Figure 8 reflects the fluctuation of the impulse response function generated by the impact of one standard deviation new interest rate on the total GDP of urban residents.

It can be seen that when the total sports consumption of urban residents in this period has a positive standard deviation impact on the total GDP, GDP development immediately responds, showing a positive impact effect. The period from the first period to the fourth period increased steadily. As the income of urban residents continued to increase, relevant consumption policies were successively introduced to vigorously stimulate residents' consumption. Urban residents' sports consumption responded strongly to GDP growth. After the sixth period, it remained stable. It shows that urban residents' sports consumption has a significant impact on GDP development and is sustainable. The

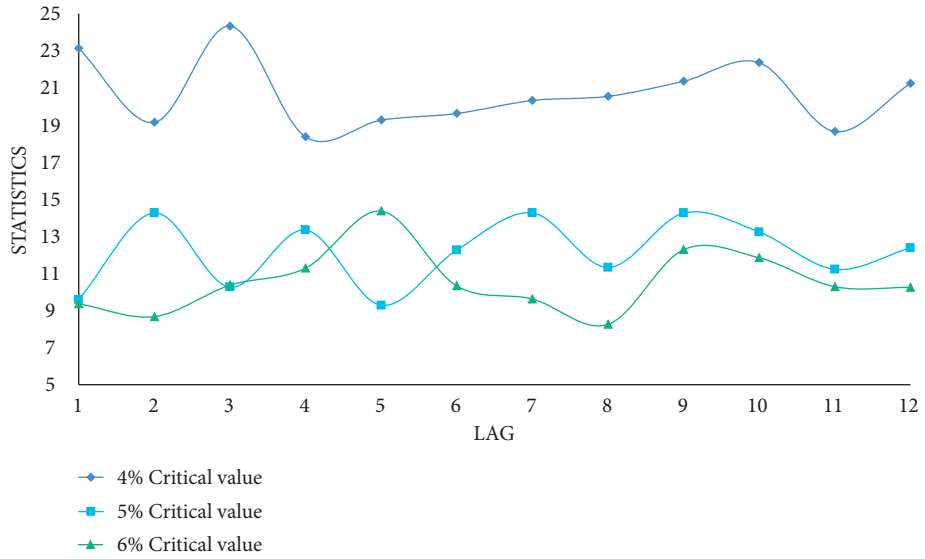

Figure 7: The results of the largest eigenvalue statistic test.

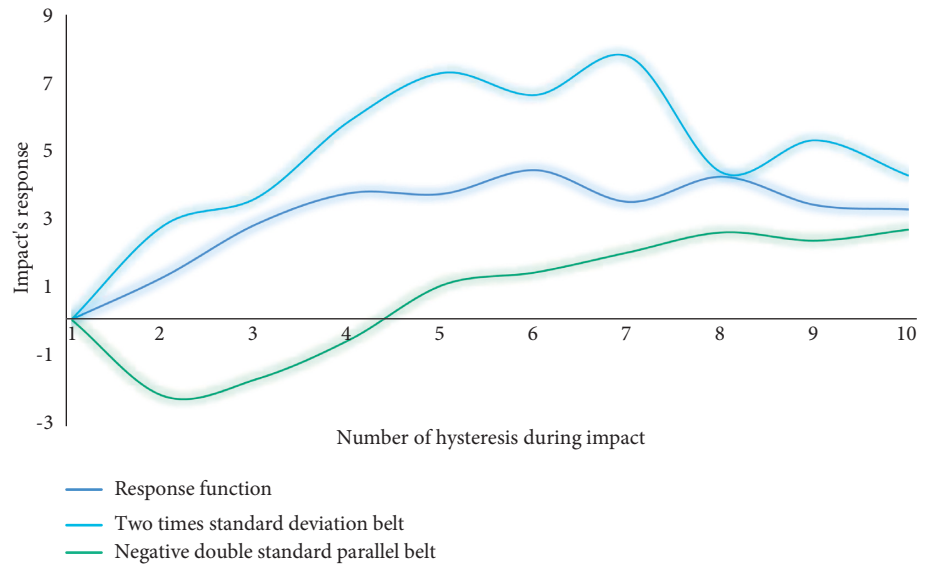

Figure 8: Fluctuation of the response function.

responses of sports consumption to various shocks are shown in Figure 9.

Response of sports consumption to shocks from GDP. The response of sports consumption to the shock from GDP starts to be positive, will be negative around the third period, and turn positive after the sixth period, and the impact will gradually weaken. As a part of GDP, sports consumption naturally increases with the growth of GDP, but in the long run, the impact of GDP growth shocks on government consumption expenditure alternates and gradually declines.

4.4. Analysis of Vector Error Correction Deep Learning Model. The vector error correction model (VEC) is an empirical test method that reflects the short-term dynamic relationship between variables. According to Granger's theorem, if there is a cointegration relationship among several first-order nonstationary variables, then these variables must have an error correction model expression. The error correction model is a special form of difference equation model between first-order single-integrated time series with cointegration relationship. It can not only preserve the long-term dynamic information of variable relationships but also ensure the validity of regression analysis. Vector error correction model is divided into bivariate bivariate vector error correction model and multivariate vector error correction model. In view of the analysis of two vectors of economic growth effect and sports consumption in this paper, bivariate vector error correction model is used to empirically test the short-term dynamic relationship between the total consumption of urban residents and economic growth. Because

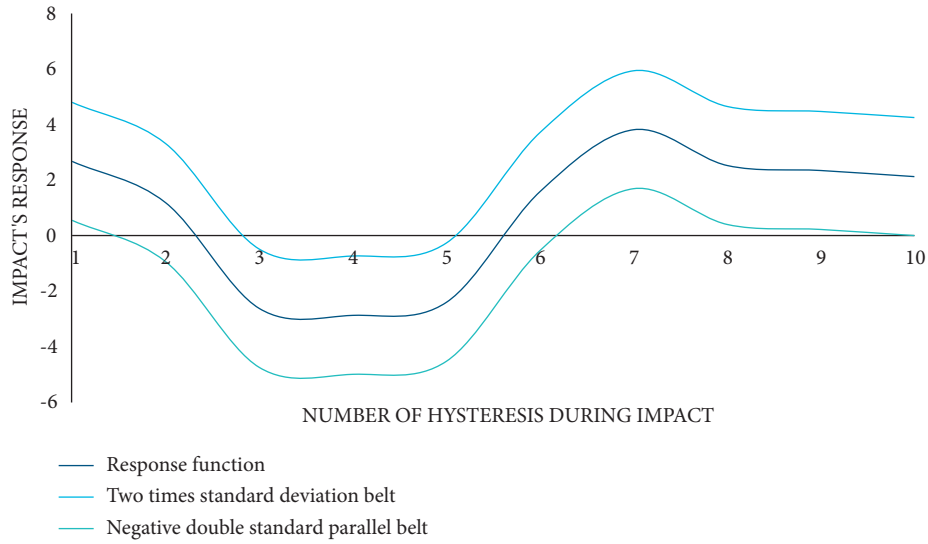

Figure 9: Impulse response diagram of sports consumption to shock.

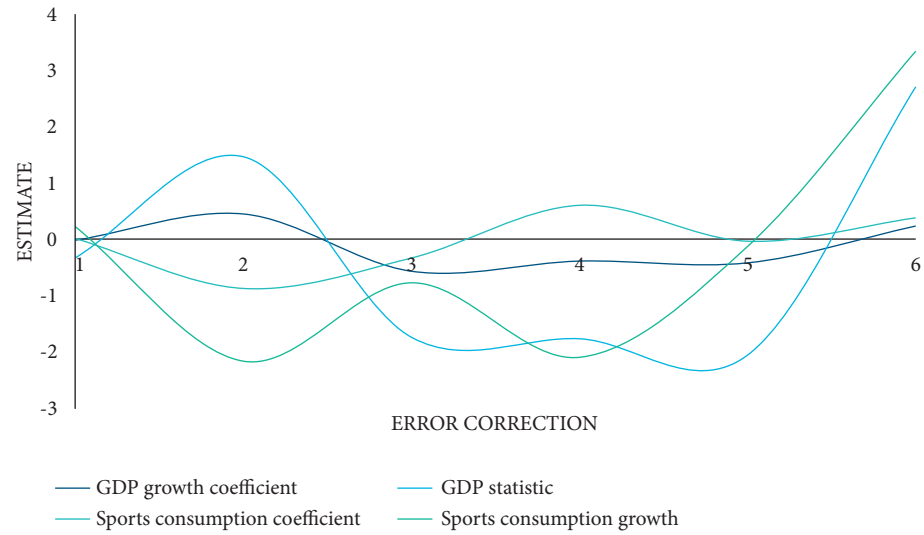

Figure 10: Estimation results of vector error correction model.

the long-term relationship between urban residents' sports consumption and economic growth effect has been determined, but whether there is short-term fluctuation between the two has been established, and a bivariate vector error correction model is established as shown in Figure 10.

The constant term is 0.5513, AIC and SC are both negative and small, the error correction value is 34.4980, and each equation in the model has a good fit. From the overall inspection of the model, AIC and SC are small and negative numbers, the error correction is too large, and the goodness of fit of the deep learning model is good. According to the evaluation statistics of the equation, for GDP growth in the short term, the coefficient of the first lag period of GDP is positive, the coefficient of the second lag period is negative, and the coefficient of the error correction term is negative. When the economy grows, the error correction mechanism will weaken the economy. The strength of growth, every one percentage point change in sports consumption, leads to a GDP growth of 0.186 percentage points. Through the above empirical analysis on the relationship between urban residents' sports consumption and GDP growth effect, it can be concluded that there is a stable correlation between urban residents' sports consumption and GDP development.

On the whole, urban residents' sports consumption has just been active. During this period, people's needs for sports consumption are still in the basic stage, or some people have just entered the demand for a comfortable environment, and fewer people have reached a higher level of demand. The needs of some consumers remain on meeting the general conditions of consumption, and the residents' awareness of sports consumption is reflected in the degree of dependence on the existing environment and the urgency to transform the environment. As far as the overall level of urban residents' sports consumption is concerned, there should be a demand for a higher level of sports consumption

environment. Therefore, strengthening and guiding residents' awareness of environmental needs is an important way to promote the improvement of sports consumption. The news media plays an important role in improving residents' awareness of sports consumption. The combination of publicity and guidance will effectively change residents' demand concept. Starting from the demand, timely guidance can promote the development of residents' sports consumption demand to a high level. Residents should also take the initiative to integrate their awareness of consumer demand with their own consumption activities to coordinate with their own consumption levels.

5. Conclusions

The main purpose of this study is to study the relationship between sports consumption and GDP growth. The reason for the analysis is that through the analysis of the GDP effect mechanism of sports consumption, this paper summarizes the mechanism of sports consumption's role in regional development as GDP growth effect, industrial structure effect, regional agglomeration effect, and regional innovation effect. Every one percentage point change in sports consumption leads to a GDP growth of 0.186 percentage points, and with the increase of the lag period, urban residents' sports consumption will gradually increase the driving effect of GDP growth. Through the analysis of impulse response function, it can be seen that my country's GDP growth has a greater impact on urban residents' sports consumption, while the impact of urban residents' sports consumption on GDP growth is relatively low in the initial stage but gradually increases with time. The GDP growth effect of sports consumption is the display basis and dominant indicator of regional GDP development. The industrial structure effect of sports consumption is the resource converter of regional GDP development. The regional agglomeration effect and regional innovation effect of sports consumption are the strong driving force of regional GDP development. The GDP growth effect of sports consumption is mainly manifested in demand-driven GDP growth, and factors such as labor quality and technological level will also play a role. The development of sports consumption is accompanied by the construction of stadium facilities and supporting infrastructure, and the influx of event tourists will expand the total demand and stimulate GDP growth. Sports consumption will promote the development of the urban entertainment and fitness industry, improve the quality of laborers, and ultimately affect the long-term regional impact. Now we see a huge consumer market and development space for the sports industry, abandoning those resistance factors that are not suitable for the development of the sports economy, and gradually establishing a sports GDP system. With GDP development and people's living standards increasing, the socialization of sports is getting higher and higher, and the level of sports consumption will also increase, eventually forming a benign process of production, consumption, and reproduction, making sports consumption a new growth that promotes GDP growth.

As the economy has entered a new normal, the industrial structure has been optimized and upgraded, from investment-driven and factor-driven to innovation-driven, emerging industries have sprung up, and the sports industry has become an eye-catching new economic growth point. Because the consumption level of urban residents is much higher than that of township residents, and the sports consumption of urban residents is still dominant, the sports consumption level of urban residents is the core content of this study. Vigorously tapping the potential of residents' sports consumption has important theoretical and practical significance for promoting the development of the sports industry, improving people's living standards, and stimulating economic growth.

Data Availability

The data set can be accessed upon request from the corresponding author.

Conflicts of Interest

The authors declare no conflicts of interest.

Authors' Contributions

Heng Gao and Yawen Zhang contributed equally to this paper.

References

[1] F. Li, "Research on sports Consumption level of urban residents in Lanzhou city based on data analysis," *IOP Conference Series: Earth and Environmental Science*, vol. 692, no. 4, Article ID 042125, 2021.

[2] L. Wang and H. Deng, "A ELES Model-based quantitative analysis of the consumption structure of the Chinese urban residents," *Journal of Physics: Conference Series*, vol. 1774, no. 1, Article ID 012029, 2021.

[3] Y. Jiang and F. Chang, "Influnce of aging trend on consumption rate of rural residents - empirical analysis based on provivial panel data," *Asian Agricultural Research*, vol. 10, no. 4, p. 7, 2018.

[4] X. Zhang and L. Guo, "Research on the impacts of real estate on GDP Growth: a theoretical model-based analysis," *Chinese Journal of Urban and Environmental Studies (CJues)*, vol. 06, 2018.

[5] L. I. Jing, S. A. Zhang, and L. W. Liu, "Environmental costs and determinants of urban residents' consumption in China——based on the input-output analysis in thirty provincial-level administrative areas," *East China GDP Management*, vol. 396, no. 2, pp. 53–65, 2018.

[6] S. Zhao, K. Wang, C. Tai, and J. Cai, "Research on the characteristics of urban residents' views on sports consumption based on social stratification," *Cien Sport Science*, vol. 51, no. 2, pp. 25–29, 2019.

[7] L. I. Xiangqian, Z. Wang, and X. Mao, "Analysis of influencing factors on urban resident low-carbon consumption behaviour based on quantification method: taking beijing as an esample," *Ecological Economy*, vol. 20, no. 02, p. 336, 2019.

[8] Z. F. Ding and C. Y. Kong, "The welfare comparison of consumption growth and consumption equality - based ON

numeric simulation analysis of urban group consumption data," *Consumer GDPs*, vol. 57, no. 8, pp. 35–47, 2019.

[9] M. Ahmad and S. G. Hall, "Trust-based social capital, economic growth and property rights: explaining the relationship," *International Journal of Social Economics*, vol. 44, no. 1, pp. 21–52, 2017.

[10] X. Peng and G. Zeng, "An empirical analysis on the diffusion and lagging effects of information technology," *Journal of Information Hiding and MultiMedia Signal Processing*, vol. 9, no. 3, pp. 733–742, 2018.

[11] M. h Ali, R. A. Ali, and a Farooq, "The effect of tourism, GDP growth and environment in developing countries," *IRASD Journal of Energy and Environment*, vol. 2, pp. 82–87, 2021.

[12] B. Zhang, H. Xiao, and H. Chen, "Empirical research on the "GDP growth effect" of the openness of service sector - based on the analysis of the provincial panel data of China," *International Business*, vol. 17, no. 6, pp. 43–49, 2017.

[13] E. Jafarzadeh and S. He, "The effect of internal and external conflicts on the country trade and GDP growth: case from emerging and developed countries," *International Journal of GDPs and Finance*, vol. 13, 2021.

[14] B. J. Chen and L. V. Yan-Li, "Study on the relationship between GDP growth and urban-rural income gap in deep poverty-stricken areas——taking linxia hui autonomous prefecture of gansu province as an example," *Journal of Lanzhou University of Arts and Science (Social Science Edition)*, vol. 34, no. 49, p. 36, 2019.

[15] S. Zhang, "StudyOn information consumption level dynamic comprehensive evaluation of urban residents in China," *Journal of Applied Sport Management*, vol. 15, no. 1, pp. 63–71, 2018.

[16] X. Y. Zhou, "An empirical study of the stock market wealth effect of the InfluUnce of the urban residents consumption level in China," *Advances in Social Sciences*, vol. 06, no. 2, pp. 203–210, 2017.

[17] S. Peng, X. Jiang, C. Yang, T. Wang, and X. Feng, "Insufficient consumption demand of Chinese urban residents: an explanation of the consumption structure effect from income distribution change," *Sustainability*, vol. 11, no. 8, pp. 6–18, 2019.

[18] M. Y. Shang and L. Zhang, "Empirical study on sports consumption structure of urban residents in wuhan," *Hubei Sports Science*, vol. 12, no. 37, p. 65, 2018.

[19] L. Yi, "The development of leisure sports consumption of urban residents under the view of marine EcoLogical environment," *Journal of Coastal Research*, vol. 104, no. SP1, 2020.

[20] P. X. Li, "Factors of the urban residents' sports consumption intension on the logistic regression model," *Journal of Qiqihar University (Philosophy & Social Science Edition)*, vol. 11, pp. 25–37, 2018.

[21] X. Xiao, "An empirical study ON agritainment consumption behavior of urban residents - a case study of huangpi district of wuhan city," *Asian Agricultural Research*, vol. 10, no. 03, pp. 92–99, 2018.

[22] X. Huang, A. O. Xiang, and X. J. University, "OBSTACLES and transcendendenece residents sports consumption in China under the background of promoting consumption," *Journal of Guangzhou Sport University*, vol. 74, no. 02, pp. 21–29, 2018.

[23] C. Fang and P. Chen, "An empirical study on the relationship between development level of urbanization in China and consumption demand of residents' sports lottery," *Journal of Xi'an Physical Education University*, vol. 23, no. 2, pp. 23–30, 2019.

Hindawi
Computational Intelligence and Neuroscience
Volume 2022, Article ID 1359730, 11 pages
https://doi.org/10.1155/2022/1359730

Research Article

The Design of Personalized Education Resource Recommendation System under Big Data

Rong Fu, Mijuan Tian, and Qianjun Tang

School of Educational Sciences, Leshan Normal University, Leshan, Sichuan 614000, China

Correspondence should be addressed to Rong Fu; furong@lsnu.edu.cn

Received 12 May 2022; Accepted 7 June 2022; Published 28 June 2022

Academic Editor: Yaxiang Fan

Copyright © 2022 Rong Fu et al. This is an open access article distributed under the Creative Commons Attribution License, which permits unrestricted use, distribution, and reproduction in any medium, provided the original work is properly cited.

With the advent of the Internet and the era of big data, education is increasingly dependent on data resources to support product and business innovation, and the lack of data resources has severely limited the areas involved. As a general information filtering method, personalized recommendation systems analyze the historical interaction data between users and items to build user interest models in an environment of "information overload", allowing users to discover and recommend information that interests them. However, the explosive growth of information in the network makes users wander in the sea of information, and it is increasingly difficult to find the information they really need, i.e., information overload. This has given rise to personalized recommendation systems, which currently have more mature applications in industries such as e-commerce, music services, and movie services. To this end, this paper studies and implements a customized educational resource recommendation system that can handle big data. The results show that the values of different similarity calculations all fluctuate with the gradual increase of the number of nearest neighbors, and the algorithm in this paper is maximum at the number of neighbors around 60; then, it is inferred that applying the calculation method to the recommendation algorithm will improve the recommendation accuracy. Therefore, education uses the concept of big data to process the huge amount of education data and find some correlations and laws in education, so as to realize "teaching according to the material, teaching according to the material".

1. Introduction

With the continuous progress of China's education reform, the education informatization has made positive progress, especially since the introduction of education planning programs, the importance of education informatization has been widely recognized by the whole society [1]. The development and maturity of educational big data, especially learning analytics and data mining technologies, have provided a scientific basis for carrying out personalized and accurate learning support services [2]. In particular, the current boom in personalized education and quality education has made people more eager to access educational resources at a specific individual level [3]. It is hoped that learning contents and learning orientations suitable for the development of different learners can be provided accordingly, thus promoting their individual development and thus realizing personalized education in the true sense [4]. Recommendation systems have been successfully used in many applications and recommendation algorithms have achieved great success [5]. The amount of data entered in public curriculum resources and social discourse resources in universities will grow at a faster rate. How to maximize the academic value of so many electronic educational resources has become a critical issue that needs to be addressed [6].

The continuous development of education informatization has led to a dramatic increase in the volume of educational resources, and users need to spend a lot of time searching for educational resources in this huge amount of educational data, which leads to the phenomenon of "information overload" [7]. Digitization transforms complex and constantly changing educational information into digital or measurable data [8]. Multimedia provides more ways to exchange information in the teaching and learning process [9]. Compared to traditional data, such big data (complete data) has a huge volume of distributed

unstructured data, and data analysis is shifted from the expert level to the user level [10]. Search engines, as a new method of information filtering, filter out a large amount of irrelevant information by keywords and present the query result information to the user [11]. The strategic significance of big data does not lie in the mastery of big data information, but in how to process this data professionally and efficiently through algorithms [12]. As a result, big data alliances have been formed to support big data organization management and value discovery, driven by big data.

Recommender systems are a new way of discovering information. Historical user behavior information is analyzed, user interests are modeled, and user education is recommended based on user preferences [13]. In this process, the user does not need to provide any information about the needs and the recommendation system actively sends information to the user [14]. Big data in education focuses more on the micro and individual level, which requires information collection at all times, comprehensive and objective recording of information, and the use of a large number of visualizations to help information collectors obtain accurate material [15]. The use of digital educational resource platforms provides students with high-quality and rich educational resources, creating more learning opportunities and a better learning environment, in addition to overcoming the time and space limitations of traditional education methods and providing flexible learning methods. In the recommendation system, considering the scale of user data on the Internet and the overall process of machine service, the distributed computing power of Hadoop can be used to find the optimal combination of algorithms to analyze the characteristics of users based on traditional machines.

The innovations of this paper are as follows:

(1) According to the characteristics of a big data alliance, a recommendation system is designed to identify target users, process alliance data according to user needs, and recommend data resources for different types of users. The learning platform established by ontology records a large number of student data, which are analyzed by data mining tools. These data produce some rules and have a positive impact on teaching.

(2) Make use of the characteristics of ontology clarity, objectivity, and scalability to construct the ontology of educational resources, as well as the ontology of student users.

(3) According to the characteristics of a big data alliance, a recommendation system is designed to identify target users, process alliance data according to user needs, and recommend data resources for different types of users.

The research framework of this paper consists of five parts, and the specific arrangements are as follows.

The first part of this paper introduces the research background and significance and then introduces the main work of this paper. The second part introduces the work related to personalized educational resource recommendation systems and personalized recommendations under big data. The third part combs the recommendation methods based on similarity and the data storage methods of the recommendation algorithm so that readers of this paper can have a more comprehensive understanding of the main methods of constructing a personalized educational resource recommendation system. The fourth part is the core of the paper, which describes the analysis of personalized recommendation algorithms based on big data from two aspects: collaborative filtering recommendation algorithm analysis and personalized recommendation system test analysis. The last part of the paper is a summary of the whole work.

2. Related Work

2.1. Personalized Educational Resource Recommendation System. Social informatization and educational informatization are becoming more and more mature, social networks are gradually rising, sensor devices and mobile terminals are more and more connected to the network, and various statistical data, transaction data, interactive data, and sensor data are generated and exist. The era we live in seems to be an era of information explosion, but the emergence of massive information has overwhelmed the Internet people. There is more and more useless information, and it is difficult for users to really pay attention to themselves. A large amount of useful information is covered up and cannot be obtained by the target audience. Therefore, personalized education resource recommendation is expected to provide users with higher precision and faster recommendation services.

Gan and Zhang [16] proposed properly processing these complex and diverse structured, semistructured, and unstructured educational data to form an integrated solution covering business, technology, and IT infrastructure to process, store, manage, and analyze educational big data [16]. Zheng [17] constructs a model based on the user's past behavioral history (previous purchases, choices, item ratings) and other users' decisions and then uses the model to predict or evaluate items and then recommend a high recommendation value to the user [17]. Saito and Watanobe [18] present educational application areas and cases of big data in the United States and the challenges they face with big data application to self-learning systems as an example of educational applications of big data [18]. Ying and Boqin [19] argued that recommendation systems based on content filtering algorithms typically use a set of individual characteristics of items to calculate similar items [19]. Wu [20] argued that analyzing recorded data and discovering potential rules based on big data techniques can guide teacher education and personalized learning for teachers and students [20].

Therefore, with the increase in educational resources, building a personalized recommendation system for educational resources is a necessary link to promote students' online learning mode. How to track students' learning progress and recommend truly useful educational resources to students is a real need.

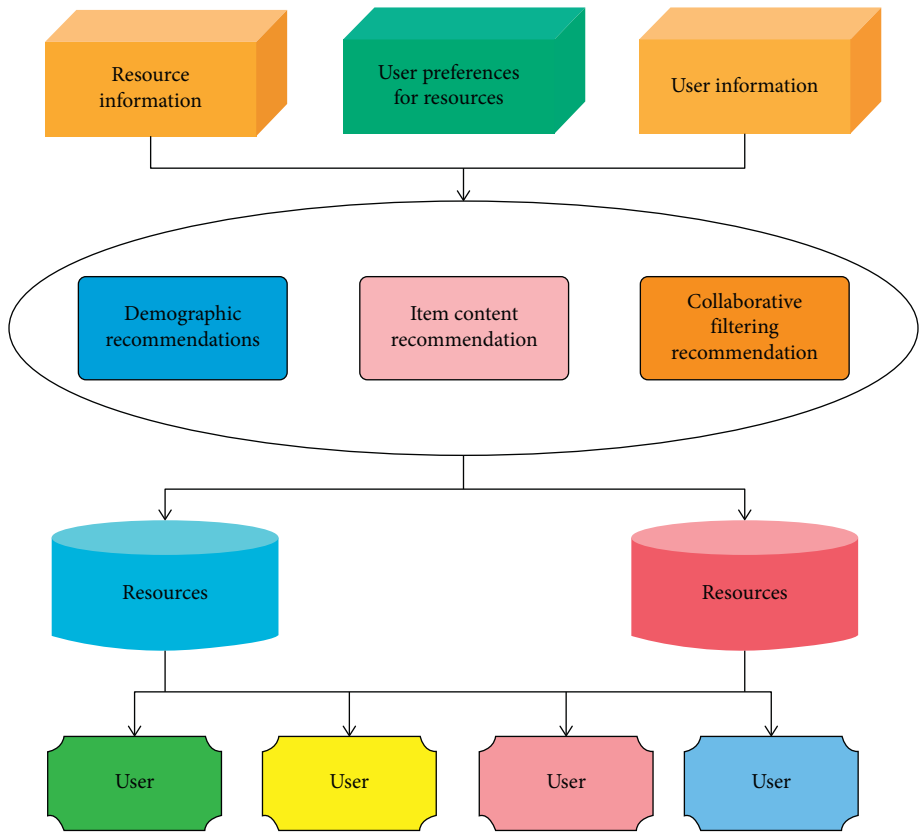

Figure 1: Architecture diagram of common recommendation system.

2.2. Personalized Recommendation under Big Data. A good recommendation algorithm can improve efficiency and serve the users, while a poor recommendation algorithm will produce various internal conflicts and the recommended information will not satisfy the users. The core of a personalized recommendation system is the recommendation algorithm, and among many recommendation algorithms, the collaborative filtering recommendation algorithm is the most researched and widely used recommendation algorithm.

Pardos et al. [21] proposed a matrix filling technique to fill the missing data with default values [21]. It is the process of processing a data source, transforming it into knowledge, and recommending it to the user. The effective fusion of different recommendation algorithms and recommendations is called the matrix filling technique. Zhu [22] uses an information-theoretic approach to measure the relevance between items and features and proposes a feature-weighted selection method to improve collaborative filtering algorithms to improve the accuracy and efficiency of recommendations [22]. Cui [23] proposed a method combining information games and Pearson correlation coefficients to improve the similarity accuracy of sparse data [23]. Singhal et al. [24] proposed using the singular value decomposition technique to reduce the dimensionality of feature vectors, reduce the time required to find nearest neighbors, and improve scaling performance based on item recommendations [24]. Sun et al. [25] proposed a method to add confidence values to the similarity calculation to improve accuracy [25].

According to the collaborative filtering algorithm, the personalized recommendation can predict which resources users may be interested in according to the historical data (exploration, scoring, etc.) and the user's community, so as to find the user's needs, increase user stickiness and loyalty, and improve user experience in a large amount of redundant information.

3. Main Methods of Constructing Personalized Educational Resources' Recommendation System

3.1. Similarity-Based Recommendation Method. A similarity-based method is the most representative and successful recommendation method in a recommendation system [26]. The main idea is that if some educational resources or users have the same behavior in the past, they will have similar behavior in the future, so as to predict the behavior that will occur according to the behavior that has occurred; that is, educational resources or users are implicitly cooperating with each other. The nontraditional search engine will make use of the data similarity-based indexing technology in the traditional search engine. Based on the recommendation algorithm, Figure 1 shows an example of the system architecture of a common personalized recommendation system.

Firstly, the algorithm based on user similarity collects the evaluation data of other users, especially those similar to the target user, and then predicts the preference characteristics

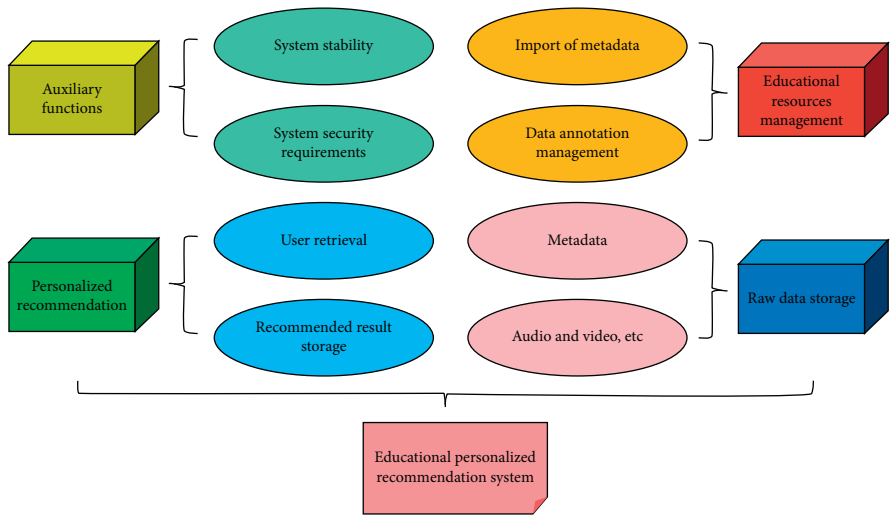

Figure 2: Personalized recommendation system in the process of education.

of the target user. According to the definition and theorem of attribute dependency, the dependency of class attributes relative to conditional attributes in the dataset is derived, so as to delete irrelevant attributes according to the calculation of attribute dependency [27]. Specific calculation formula of attribute dependency is as follows:

$$\gamma(C|A) = \frac{1}{|T|(m-1)} \sum_{i=1}^{n} \sum_{j=1}^{m} \frac{Tc_i A_j}{T}, \tag{1}$$

where $\gamma(C|A)$ is the attribute of A class dependence is C C and $|Tc_i A_j|$ is the number of samples.

By analyzing the user data of the alliance data resource trading platform, target users are identified as those who already use the platform, and identification methods are designed for potential users outside the alliance to prepare for the introduction of the alliance platform. The functional requirements of the personalized recommendation system for the education process are shown in Figure 2.

When big data is segmented and transported to different machines for processing (each Map corresponds to a machine node), its execution efficiency must be higher than that of a single machine, and the larger the data, the higher the efficiency ratio. HDFS stores super large files by taking data blocks as the basic unit. Each file can be divided into many blocks and stored on different disks, respectively, so that a single file can be larger than the capacity of any disk in the cluster and easy for system management [28]. Assuming that A is a discrete attribute with s different values, the calculation formula of the division information amount of the information gain obtained by dividing the sample set with A is as follows:

$$\text{split}(\text{T}) = \sum \frac{|T_i|}{T} \times \log_2 \left\{ P \frac{|T_i|}{T} \right\}. \tag{2}$$

Secondly, modern information extraction technology allows us to automatically extract the content or metadata information of educational resources, so we can compare the content of a given educational resource to calculate the similarity between the two resources. To eliminate the influence caused by different dimensions, this method is normalized as follows:

$$\text{x}' = \frac{x - \min(A)}{\max(A) - \min(A)}. \tag{3}$$

For explicit collection, through the filling in of students' basic personal information upon enrollment and the usual interactive survey of students, students are allowed to make in-depth heuristic inquiries about the knowledge they are interested in. For unified codification of shared and transactional data of alliance members, the data related to the alliance is effectively stored and managed through data processing, integration, transformation, and storage. After finding the nearest neighbors with the greatest similarity to the project, the target project is scored using the following reduction formula.

$$P(u,i) = \frac{\sum_{j \in \text{KNN}(i)} r_{ij}}{|\text{KNN}(i)|}, \tag{4}$$

where $|\text{KNN}(i)|$ is the number of items in the nearest neighbor set $\text{KNN}(i)$ of i.

Then, in the collaborative filtering algorithm based on items, the similarity between items is expressed as follows:

$$\text{sim}(i,j) = \cos(i,j) = \frac{\vec{i} \cdot \vec{j}}{|i||\vec{j}|}, \tag{5}$$

by collecting information about users and resources, processing this information using data mining-related techniques, so as to discover and analyze the intrinsic relationship between users and resources, and finally, using some recommendation strategy to select the most suitable resources for users to recommend.

Finally, in the recommendation system, the elements and dimensions of the system feature vector are first defined in advance by experts, and then all users or educational resources in the system are represented using the feature vector. In this way, the similarity between two users or educational resources can be obtained by calculating their

corresponding feature vectors. The system supports dynamic changes in database size or data volumes, such as regular maintenance of resources by administrators, absorption of high-quality resources, and deletion of low-quality resources. It also adopts modular design and layered architecture design, so that the system can be applied under different operating environments and customer needs. For potential target users outside the alliance, the data resource recommendation method is designed by RSS technology, and for target users already using the platform, the dichotomous network personalized recommendation method is designed, and the recommendation evaluation method is also designed. The recommendation evaluation is mainly used to evaluate the recommendation effect of the recommendation system and provide relevant feedback to facilitate the improvement of the recommendation algorithm.

3.2. Recommended Algorithm Data Storage Method. The traditional social recommendation algorithm only considers the impact of the social network relationship between users on the system from the perspective of users and assumes that the items in the system are independent [29]. Its services do not only focus on keyword search but also on how to analyze the massive search records generated every day and the search history of different users. The similarity between items i, j is the comprehensive similarity of their attribute characteristics, which can be expressed as

$$\operatorname{asim}(i,j) = \sum_{k=1}^{t} \frac{r_k}{1 + d\left(a_{ik} + a_{jk}\right)} = \sum_{k=1}^{t} \frac{r_k}{1 + \left|a_{ik} - a_{jk}\right|}, \quad (6)$$

where $r_k/1 + d(a_{ik}, a_{jk})$ is the similarity of items i, j in the attribute k.

However, information about the interrelationships between items in the system is also important because people will consider similar items or alternative items in some cases when choosing items. Traditional recommendation systems require explicit social network relationships between users. The data source can be imported directly into Elastic Search or Hbase, or one of the importing parties can subsequently perform data synchronization operations. The data storage and indexing module is shown in Figure 3.

The first is based on the content recommendation module; this module is relatively simple and computationally small, so the output data can be calculated in real time without saving. After the user submits the job with the command Hadoop jar, the JobClient instance uploads the job configuration information, jar file, environment variables, slice, and other related information to the distributed file system HDFS, and then JobHent notifies JobTracker through the RPC framework. The similarity between users u, v is the similarity of their combined features, which can be defined as follows:

$$\operatorname{csim}(u,v) = \sum_{k=1}^{s} \frac{l_k}{1 + d\left(c_{uk}, c_{vk}\right)} = \sum_{k=1}^{s} \frac{l_k}{1 + \left|c_{uk} - c_{vk}\right|}, \quad (7)$$

where $l_k/1 + d(c_{uk}, c_{vk})$ is the similarity of u, v users on the k feature.

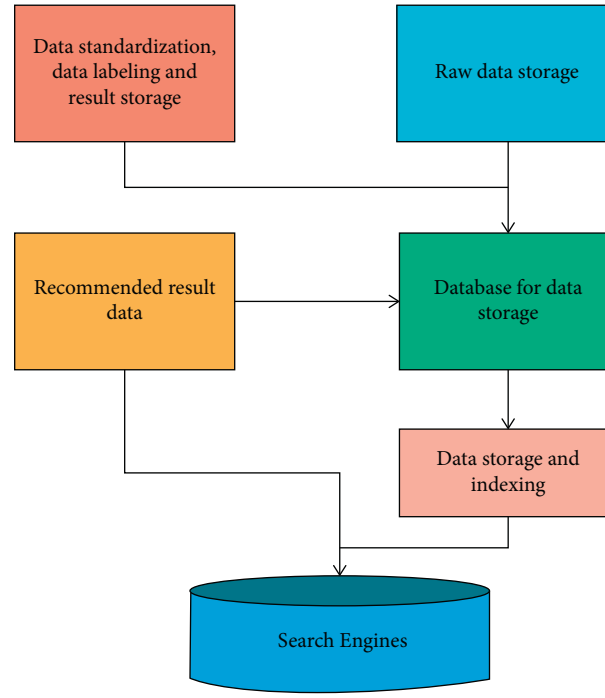

Figure 3: Data storage and indexing module.

The weight of the project i to the user u is defined as follows:

$$WT(u,i) = (1 - \alpha) + \alpha \frac{D_{ui}}{L_u}, \quad (8)$$

where D_{ui} D_{ui} is the time interval between visiting items i and u 's earliest visit to an item and L_u is the time span of using recommended system.

To ensure high availability and data fault tolerance in the Data Node, each block can be replicated to other server disks, with a default of 5, thus ensuring no data loss in case of the block, disk, or machine failure. Load the session logs from it to the data warehouse for offline analysis using big data analytics tools such as Hive and Pig.

Next is the user-based collaborative filtering recommendation module, which will calculate the user's K neighborhood and the degree of recommendation of teaching resources to the user based on the user's preference matrix, which will be calculated offline because of the large amount of calculation. The job scheduling module will initialize the job at the right time, that is, create a JobProgress object for the job to track the running status of the job, and JobProgress will create a TaskInProgress object for each Task to track the running status of each Task. This can reduce the probability of system downtime to a certain extent and further improve the stability and data tolerance of the system to cope with the increasing number of course teaching resources in the future. We back up system metadata files, while persisting file system metadata to local disk files and writing to a remotely mounted network file system. Generally, ETL (Extract, Transform, Load) operations are required on the data, even using data mining-related techniques. By introducing a temporal weight function in

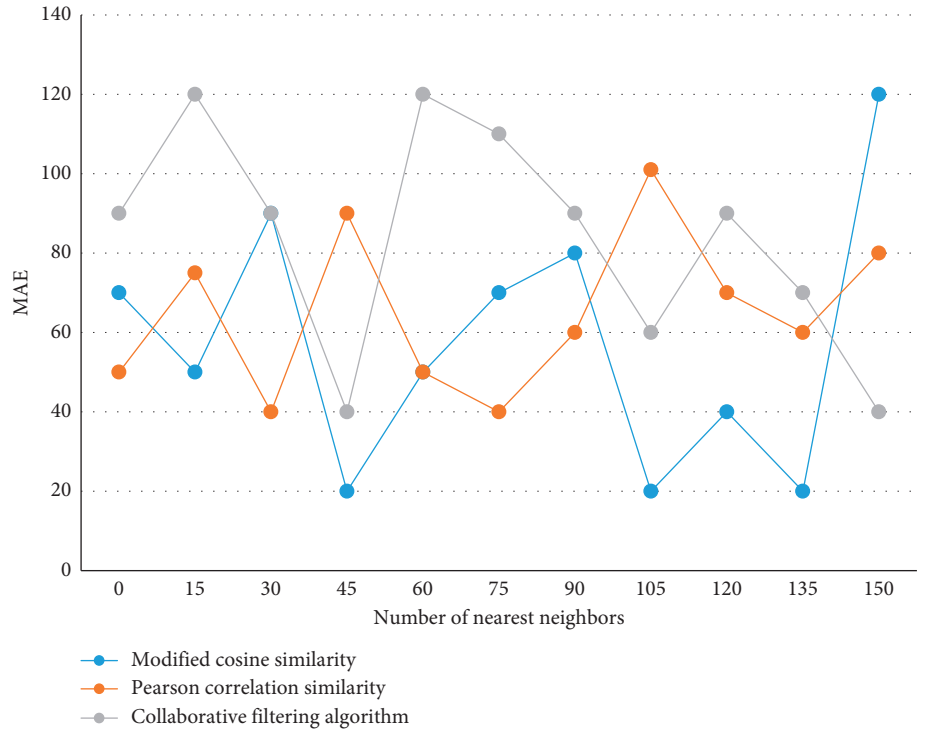

Figure 4: Comparison of similarity calculation methods in traditional recommendation algorithms.

the prediction scoring process, the new prediction equation is

$$P_{uj} = \overline{R_u} + \frac{\sum_{v \in L}\left(R_{vj} - \overline{R_v}\right)\mathrm{sim}(u,v) \cdot WT(u,i)}{\sum_{v \in L}\left(|\mathrm{sim}(u,v)WT(u,i)|\right)}, \tag{9}$$

where $\overline{R_u}$ $\overline{R_u}$ is the average score, R_{vj} is the scoring of item j, $\mathrm{sim}(u,v)$ is the similarity between users, and L is the nearest neighbor set.

When only one neighbor user scores an item, it is only related to this user's score, as shown in the following formula:

$$P_{ui} = \overline{R_u} + R_{vi} - R_v. \tag{10}$$

The last is based on the neural network recommendation module; when the user scores a resource, it will call the wood module on the home page recommendation neural network training, and the input feature value of the neural network is directly taken out from the database to get. The number of clicks students make using the education platform, the time they access the resources, the type of resources they access, exam records, and the time they spend doing questions are analyzed to train a student user model [30], for nonrelational massive data, such as user page stay practice, the number of clicks, learning behavior, and other massive data, by using Hadoop system in the HDFS (Distributed File Storage System) to the massive education big data storage operations. Once there are free resources, JobTracker will select a suitable task to use these resources according to a certain policy, which is done by the task scheduler. Teachers can carry out off-site synchronous interactive teaching through the big data platform and can also monitor each student's learning process and dynamically adjust the teaching content and pace according to the characteristics of students' learning behavior, tailoring high-quality personalized teaching.

4. Analysis of Personalized Recommendation Algorithm Based on Big Data

4.1. Analysis of Personalized Collaborative Filtering Recommendation Algorithm. The number of registered users on the Web is constantly increasing, and in the face of the complex structure of websites and the increasing number of large-scale users, recommendation algorithms will face great challenges in calculating the similarity between objects and finding the nearest neighbors of the target objects, and clustering can exactly remedy this problem. Three traditional collaborative filtering similarity measures, namely, cosine similarity, Pearson correlation similarity, and modified cosine similarity, are applied to the same platform for experiments, and the best similarity measure is selected based on the trend and applied to the collaborative filtering recommendation algorithm proposed in this paper to find the nearest neighbors of the target users. The results are shown in Figure 4.

The values of the three similarity calculations fluctuate with the gradual increase of the number of nearest neighbors. The algorithm in this paper is the largest when the number of neighbors is about 60, while the value of the Pearson correlation similarity has always been the smallest. It is inferred that applying this calculation method to the recommendation algorithm will improve the recommendation accuracy.

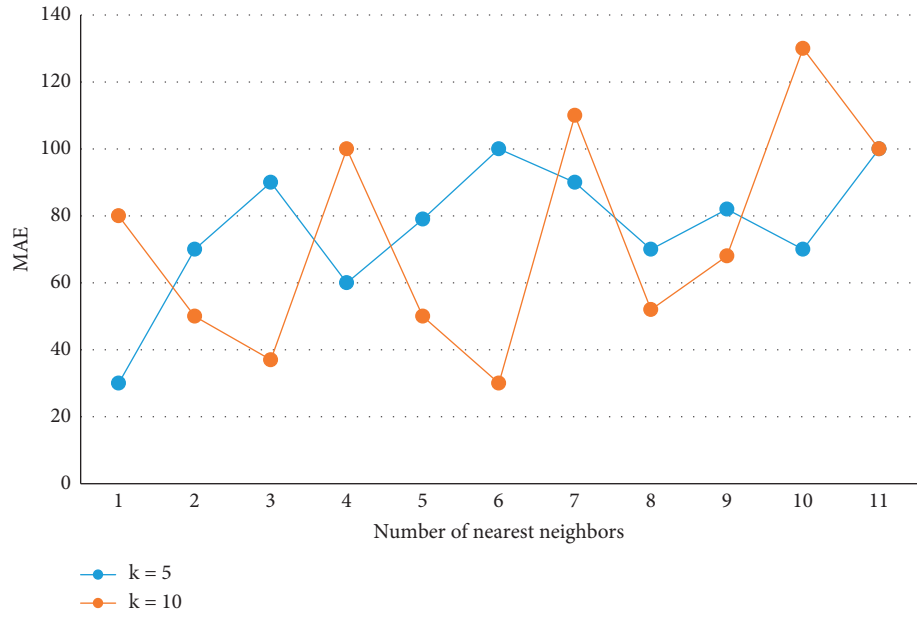

Figure 5: Comparison of recommendation accuracy with different cluster numbers.

The working mechanism of the collaborative filtering recommendation algorithm is to calculate user similarity based on user ratings of items, find nearest neighbors, and make recommendations to target users based on the nearest neighbors' ratings of the target items. That is, some features are extracted for each recommended object to represent this object, then the feature data of a user's past favorite (dislike) objects are used to learn this user's preferences, and finally, a set of objects with the greatest relevance is recommended for this user by comparing the user preferences obtained in the previous step with the features of the candidate objects. In order to verify the accuracy of for, $k = 5$, 10 is selected to compare the real face, while the number of neighbors is taken as the number of intervals between to, and the results are shown in Figure 5.

First, data mining and preprocessing methods are used to preprocess and model the data that can reflect users' purchasing habits or ratings so that they can be processed by recommendation algorithms to come up with quick conclusions. In the massive resource system, searching for resources is a more convenient way to obtain resources. As the number of users using the learning resource recommendation system increases, new users are gradually transformed into regular users. By analyzing users' search keywords, we can get some users' interest points. By the iterative method, the value of each clustering center is updated one by one until the best clustering result is obtained. Discovering frequent item sets based on support degree, we first scan the transactions to discover the number of occurrences of each item and build a candidate set. Then, the support degree is assumed in advance and all frequent item sets are calculated by an iterative approach. The optimal number of clusters is taken so that the number of nearest neighbors ranges from 0 to 150 with progressively increasing intervals, and the experimental results are shown in Figure 6.

Secondly, by calculating the distance between the target and the cluster centers of several clusters that have been determined, the cluster with the closest spatial distance, that is, the most similar cluster, is selected. The association rules are analyzed from the subset of frequent item sets through the preassumed confidence. Users are divided into different clusters according to their personal portrait information (gender, age, occupation, etc.). Users in the same cluster have high similarity (specifically, they may have the same or similar interest preferences). In each cluster, an "opinion leader" is generated by calculating the average evaluation of users on educational resources to represent the preferences of users for all items in the whole cluster. If the user is interested in what subject content, these subject words are used as the user's interest model.

Finally, based on the rating data information of K nearest neighbor users of the target user, the items not rated by the target user are predicted to be rated and the final recommendation results are generated. After the user's learning behavior database is gradually built up, the recommendation system will start the recommendation methods of collaborative filtering and association rules and finally realize the hybrid recommendation of three recommendation methods in parallel. If the buffer is written to a certain threshold value, it will start to partition into files, during which the data will be partitioned by the number of Reduces and sorted within the partition by the same key value and then written to the output partition file. In particular, the clustering center needs to be continuously adjusted to a suitable state through computation, and then other data objects are effectively classified, which involves a large amount of distance-based computation between data volumes in this process, thus making the clustering process take a lot of time and eventually affecting the rate of clustering.

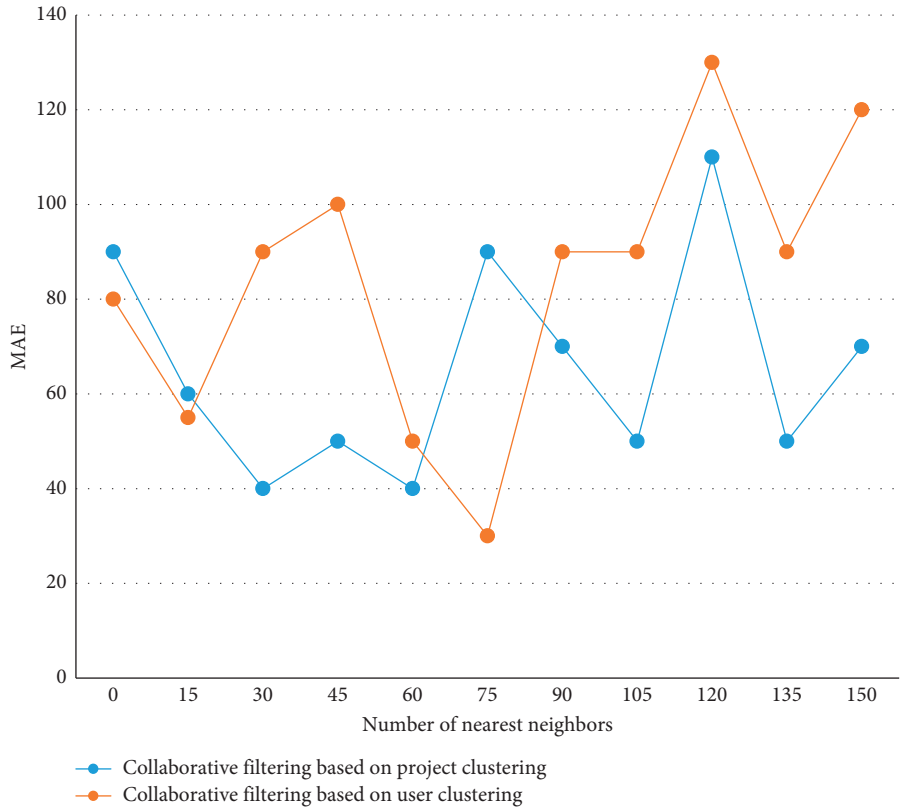

Figure 6: Comparison of recommendation quality of different recommendation algorithms.

4.2. Test and Analysis of Personalized Recommendation System. The recommendation process of the detailed page of teaching resources is somewhat similar to the search process of search engines, in that it calculates the result list that is closest to the user input and close to the user preference according to the user's input and extensive habits. In this dataset, the performance difference between social recommendation systems using explicit social network relationships and implicit social recommendation systems using implicit social network relationships is compared. However, the same user's rating on a project can also use this global difference to determine its relationship with the project, manage the server's hardware resource pool through the client, and then virtualize all the hardware resources in the resource pool to generate several independent virtual machines, so as to reduce the running burden of the system. By weighting the similarity of users in each cluster, this improved algorithm can be called the ICSL-WCF algorithm, and the comparison result with ICSL-CF is shown in Figure 7.

First, the top rankings are provided to the using users and switched to personalized recommendations after waiting until a certain amount of user data is collected. A penalty factor will be added to improve the user-based collaborative filtering algorithm together with the K-means clustering algorithm, and the evaluation results are shown in Tables 1 and 2.

The data is read into the Map function in parallel according to the chunking of the file in HDFS, and the Map extracts the (key, value) key-value pairs according to the actual requirements, sorts them, and submits them to the Reduce function. For image objects, we need to extract features such as color, texture, shape, and spatial relationship, while audio and video objects are generally extracted by deep learning methods for sound spectrum and video frames. This data is then used as input for the Reduce process, and the result is output to HDFS. Based on the relative preference matrix of each user, the clustering center is found. The number of clusters is selected as 10 and 20, and the contour coefficients are shown in Figure 8.

Secondly, for the information on different educational resources, it makes full use of the current resources such as teachers and experts in the school to label the resources in a corresponding way. As long as the user has a rating and can calculate its recommendation items, even if there are no brand new users, we can use the form of taking the closest user or popular average to supplement its rating and thus Slope open recommendation. This process can take full advantage of the distribution of computing resources of each node and parallel MapReduce processing, but this framework is a major problem that in the Reduce process requires all MapReduce written partition files through the network copy to the Reduce node and then the next step.

Finally, the prediction accuracy of the recommendation system implemented in this paper is statistically calculated by means of offline calculations. The method is based on the assumption that users are always interested in the most recently accessed information; i.e., data within the user's

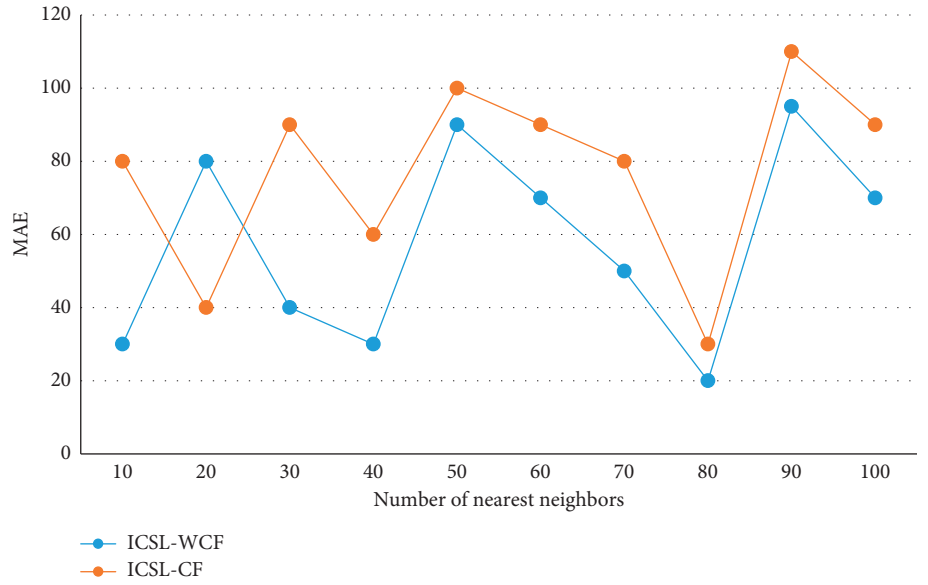

Figure 7: Comparison of algorithms.

Table 1: Comparison of accuracy before and after improvement.

User level	*S*1	*S*2	*S*3	*S*4
K-means accuracy	0.54	0.63	0.48	0.52
Comprehensive improvement accuracy	0.37	0.47	0.39	0.28
Relative improvement	0.48	0.51	0.38	0.47

Table 2: Comparison of recall rate before and after improvement.

User level	*S*1	*S*2	*S*3	*S*4
K-means accuracy	0.22	0.37	0.28	0.19
Comprehensive improvement accuracy	0.30	0.39	0.41	0.51
Relative improvement	0.49	0.51	0.44	0.39

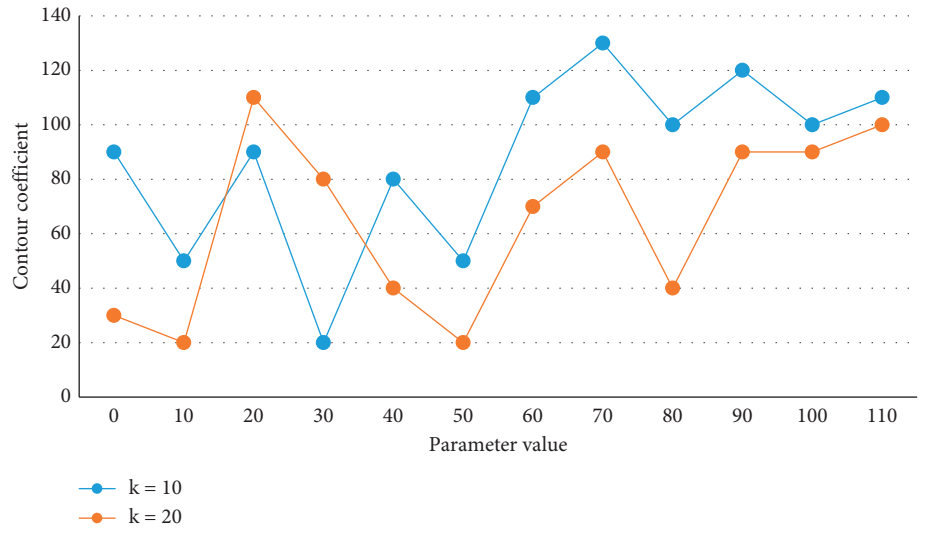

Figure 8: Comparison of contour coefficients of different cluster numbers.

most recent fixed time frame is always analyzed and modeled, ignoring all data prior to that time window. The validation process verifies the validity of the selected subset of features on a test dataset. In the data model of the recommender system, the data generated by the user during the use of the learning resources by the learner will be stored by creating and using the learning resources database. In different application domains, the focus of people on the attribute features is different, so the size of the contribution made by different attribute features in the final recommendation varies, and this weight is generally determined by the characteristics of the relevant domain or through expert opinion.

5. Conclusions

With the rapid growth of today's data volume, recommendation systems have become one of the most effective ways to solve the problem of "information overload". In the personalized recommendation system of educational resources, the user interest model is the foundation and core, and the research on the user interest model is increasing. With the rapid growth of Internet users and online information, the importance of recommendation systems is further strengthened and people's expectation of the recommendation result of recommendation system is further increased, so the recommendation accuracy of recommendation system must be improved continuously. In terms of students' self-learning, the web tracks the whole learning process of students to understand their learning methods and habits, personalities, and interests and to obtain relevant implicit data. However, data storage and nonstandardized descriptions increase the difficulty of data mining. This paper mainly designs and implements a personalized recommendation system for teaching resources, which can effectively solve the problems of a large amount of resource information, inaccurate resource allocation, scattered and difficult to share resources, duplicated resource organization, insufficient intelligence, and difficulties. It is a subsystem of the advanced computer network course faculty support system, and its main function is to provide a customized recommendation and faculty resource sharing platform. The personalized recommendation system based on big data meets functional and nonfunctional system design requirements, effectively helps solve the information overload problem, and recommends personalized educational resources in a timely manner. It effectively provides customized educational resources and supports and facilitates the promotion of education in China.

Data Availability

The dataset can be obtained from the corresponding author upon request.

Conflicts of Interest

The authors declare that they have no conflicts of interest.

Acknowledgments

This work received the First Class Course Project of Educational Technology.

References

[1] S. Dwivedi and V. Roshni, "Recommender system for big data in education," in *Proceedings of the E-learning & E-learning Technologies*, pp. 1–4, IEEE, Hyderabad, India, August 2017.

[2] R. Levesque, "Individualized education programs," *Practical Pointers*, vol. 1, no. 1, pp. 1418–1420, 2018.

[3] Y. Cheng and X. Bu, "Research on key technologies of personalized education resource recommendation system based on big data environment," *Journal of Physics: Conference Series*, vol. 1437, no. 1, Article ID 012024, 2020.

[4] C. Geng, J. Zhang, and L. Guan, "A recommendation method of teaching resources based on similarity and ALS," *Journal of Physics: Conference Series*, vol. 1865, no. 4, Article ID 042043, 2021.

[5] K. Villalba, S. C. Cuba, C. Deco, C. Bender, and F. J. García-Peñalvo, "A recommender system of open educational resources based on the purpose of learning," in *Proceedings of the Learning Technologies*, pp. 1–4, IEEE, La Plata, Argentina, October 2017.

[6] D. Seng, X. Chen, X. Fang, X. Zhang, and J. Chen, "Research on personalized recommendation of educational resources based on big data," *Educational Sciences: Theory and Practice*, vol. 18, no. 5, 2018.

[7] Y. V. Taratukhina, T. V. Bart, and V. V. Vlasov, "Machine learning models OF information recommendation system ON individualization OF education," *Educational Resources and Technology*, vol. 2, no. 2, pp. 7–14, 2019.

[8] F. Su, J. Tang, and Z. Zhang, "Research on college students' course selection recommendation model based on big data and cloud computing," *Journal of Physics: Conference Series*, vol. 1982, no. 1, Article ID 012203, 2021.

[9] L. M. Ang, F. L. Ge, and K. P. Seng, "Big educational data & analytics: survey, architecture and challenges," *IEEE Access*, vol. 8, no. 99, 1 page, 2020.

[10] S. R. Gandhi and J. Gheewala, "A survey on recommendation system with collaborative filtering using big data," in *Proceedings of the International Conference on Innovative Mechanisms for Industry Applications*, pp. 457–460, Bengaluru, India, February 2017.

[11] H. H. Syed, "Survey on recommendation system in big data analytics," *SSRN Electronic Journal*, vol. 6, no. 12, pp. 50–53, 2017.

[12] S. Cha, M. Y. Yi, and S. Youm, "Design and implementation of a big data evaluator recommendation system using deep learning methodology," *Applied Sciences*, vol. 10, no. 22, p. 8000, 2020.

[13] N. Singh, S. Tripathi, D. P. Singh, and P. Bhasker, "Recommendation systems in big data era," *International Journal of Innovative Technology and Exploring Engineering*, vol. 8, no. 12S3, pp. 80–85, 2019.

[14] A. Rahman and S. Dash, "Big data analysis for teacher recommendation using data mining techniques," *International Journal of Control Theory and Applications*, vol. 10, no. 18, pp. 95–105, 2017.

[15] C. K. Pereira, F. Campos, V. Ströele, and J. M. N. R. David, "BROAD-RSI - educational recommender system using social networks interactions and linked data," *Journal of Internet Services and Applications*, vol. 9, no. 1, p. 7, 2018.

[16] B. Gan and C. Zhang, "Design of personalized recommendation system for online learning resources based on improved collaborative filtering algorithm," *E3S Web of Conferences*, vol. 214, no. 3, Article ID 01051, 2020.
[17] H. Zheng, "Multi level recommendation system of college online learning resources based on multi intelligence algorithm," *Journal of Physics: Conference Series*, vol. 1873, no. 1, Article ID 012078, 2021.
[18] T. Saito and Y. Watanobe, "Learning path recommendation system for programming education based on neural networks," *International Journal of Distance Education Technologies*, vol. 18, no. 1, pp. 36–64, 2020.
[19] L. Ying and L. Boqin, "Application of transfer learning in task recommendation system," *Procedia Engineering*, vol. 174, no. Complete, pp. 518–523, 2017.
[20] L. Wu, "Collaborative filtering recommendation algorithm for MOOC resources based on deep learning," *Complexity*, vol. 2021, no. 46, 11 pages, Article ID 5555226, 2021.
[21] Z. A. Pardos, Z. Fan, and W. Jiang, "Connectionist recommendation in the wild: on the utility and scrutability of neural networks for personalized course guidance," *User Modeling and User-Adapted Interaction*, vol. 29, no. 2, pp. 487–525, 2019.
[22] W. Zhu, "Topic recommendation system using personalized fuzzy logic interest set," *Journal of Intelligent and Fuzzy Systems*, vol. 40, no. 2, pp. 1–11, 2020.
[23] Y. Cui, "Intelligent recommendation system based on mathematical modeling in personalized data mining," *Mathematical Problems in Engineering*, vol. 2021, no. 3, 11 pages, Article ID 6672036, 2021.
[24] A. Singhal, P. Sinha, and R. Pant, "Use of deep learning in modern recommendation system: a summary of recent works," *International Journal of Computer Application*, vol. 180, no. 7, pp. 17–22, 2017.
[25] G. Sun, T. Cui, G. Beydoun, and S. F. D. J. Chen, "Towards massive data and sparse data in adaptive micro open educational resource recommendation: a study on semantic knowledge base construction and cold start problem," *Sustainability*, vol. 9, no. 6, p. 898, 2017.
[26] L. Hui, H. Li, Z. Shu, Z. Zhong, and J. Cheng, "Intelligent learning system based on personalized recommendation technology," *Neural Computing & Applications*, vol. 31, pp. 4455–4462, 2018.
[27] L. Fang, L. A. Tuan, S. C. Hui, and L. Wu, "Personalized question recommendation for English grammar learning," *Expert Systems*, vol. 35, no. 2, Article ID e12244, 2018.
[28] C. K. Raghavendra, K. C. Srikantaiah, and K. R. Venugopal, "Personalized recommendation systems (pres): a comprehensive study and research issues," *International Journal of Modern Education and Computer Science*, vol. 10, no. 10, pp. 11–21, 2018.
[29] Z. Li and Y. Y. J. H. L. L. Yang, "Novel imidazole fluorescent poly(ionic liquid) nanoparticles for selective and sensitive determination of pyrogallol," *Talanta*, vol. 174, no. 11, pp. 198–205, 2017.
[30] G. Vincenti, A. Bucciero, and C. Carvalho, "E-learning E-education and online training," *Lecture Notes of the Institute for Computer Sciences Social Informatics & Telecommunications Engineering*, vol. 2014, 2014.

Hindawi
Computational Intelligence and Neuroscience
Volume 2022, Article ID 6868941, 9 pages
https://doi.org/10.1155/2022/6868941

Research Article

Reliability Analysis of a Functional Diagnostic Test for Primary Hyperaldosteronism Based on Data Analysis

Yan Wang and Jun Cai

Fuwai Hospital, Chinese Academy of Medical Sciences, Beijing 100037, China

Correspondence should be addressed to Jun Cai; 2021001645@poers.edu.pl

Received 12 May 2022; Accepted 27 May 2022; Published 27 June 2022

Academic Editor: Yaxiang Fan

Copyright © 2022 Yan Wang and Jun Cai. This is an open access article distributed under the Creative Commons Attribution License, which permits unrestricted use, distribution, and reproduction in any medium, provided the original work is properly cited.

Primary aldosteronism (PA) is one of the most common causes of secondary hypertension, with a prevalence of 12–20% in the hypertensive population. To determine the characteristic function of a fuzzy concept based on the epidemiological data, clinical manifestations, and auxiliary examinations of PA, the essence is to select a suitable domain and determine the affiliation of each element in the domain. The aldosterone/renin ratio was proposed to increase the detection rate of PA, which has the shortcoming of a high underdiagnosis rate when relying only on clinical manifestations. However, there is no unified standard for the diagnostic cut point, and there are differences in testing methods and diagnostic cut point values for different populations, which require different laboratories to establish appropriate cut points according to different regional populations to improve the diagnostic accuracy. In this article, we analyzed the reliability of functional diagnostic tests for PA based on data analysis and compared the sensitivity and specificity of different plasma aldosterone cut points for the diagnosis of PA in the 40 mg kibbutz test. The results showed that when post-saline PAC and post-cato PAC were used to confirm the diagnosis of proaldosterone, respectively, there was a similar subject working area under the curve between SSST and CCT, 0.89 and 0.78, respectively, with no significant difference in the area under the curve between the two ($p = 0.546$). Therefore, blood sodium and blood potassium have higher specificity and sensitivity than SUSPUP, but both are lower than ARR, and data analysis can be used as an auxiliary indicator for screening.

1. Introduction

PA is a syndrome characterized by hypertension with (or without) hypokalemia due to pathological changes in the adrenal cortex leading to the autocrine secretion of aldosterone, with high plasma aldosterone concentration and low renin as the main biochemical features [1]. PA is characterized by arterial hypertension, spontaneous hypokalemia, hyperkalemia, hyperaldosteronism, and reduced plasma renin activity [2]. With the economic and social development, the prevalence of hypertension is increasing year by year, and epidemiological surveys show that the prevalence of hypertension among adults in China is 31% [3]. It is known that the causes of hypertension include primary and secondary elevated blood pressure, and secondary causes include renal parenchymal, renal vascular, and adrenal and polyarteritis [4]. Substantial renal hypertension is mainly caused by primary or secondary renal lesions, the most common of which would be glomerulonephritis [5]. PA is not uncommon in hypertension, being 15% in severe hypertension (≥180/100 mm Hg) and up to 25% in resistant hypertension [6].

Screening for people at high risk of PA followed by confirmatory tests to clarify the diagnosis and finally typing of PA is an internationally accepted process for the diagnosis of PA [7]. The American College of Endocrinology PA guidelines recommend saline loading test, captopril test (CCT), oral sodium loading test, and fludrocortisone test as the four confirmatory tests for PA [8]. Numerous studies have shown a significantly increased risk of metabolic syndrome and cardiovascular disease in patients with PA compared to patients with essential hypertension [9]. The

risk to the organism is much higher than in patients with primary hypertension with the same disease duration and the same degree of blood pressure [10]. Data analysis is mainly a combination of a priori knowledge and available statistical data, using probabilities to predict things [11]. This method is a fundamental approach in statistical modeling and is widely used in medical fields such as oncology, pathology, and high-throughput histology [12]. In this study, we investigated the diagnostic value of data analysis on the reliability of functional diagnostic tests for PA and studied the sensitivity and specificity of different post-dose plasma aldosterone cut points for the diagnosis of PA to provide a more rational basis for clinical diagnosis.

The traditional reliability analysis method is based on the analysis of life data (time to failure) [13]. The statistical analysis of life data determines the type of life distribution of the product and based on that the reliability assessment, prediction, etc. of the product [14]. However, in our clinical work, we found that many patients with essential hypertension had a decrease in blood aldosterone levels <28% from baseline after oral administration of captopril, suggesting that the responsiveness to captopril is lower in national than in Western populations, making it difficult to identify hyporenin-active hypertension from PA in clinical practice based on the guideline-recommended blood aldosterone cut point values [15]. Therefore, as in all other endocrine diseases, functional diagnosis plays an important role in the diagnosis of PA and is the basis for localization and staging.

The innovative points of this study are as follows:

(1) This study uses the principles and methods of data analysis to select simple, rapid, and economical tests for the diagnosis of PA and identifies the most common subtypes of aldosteronism in PA.

(2) The study explores the optimal aldosterone level for CAPT diagnosis of PA by assessing the degree of suppression of blood aldosterone levels in patients with PA and essential hypertension by CCT and comparing them with normotensive volunteers.

(3) The SROC method and data analysis were used to evaluate the diagnostic results of IHA and ELISA, and it was found that the two statistical methods yielded similar conclusions, but the data analysis could yield the mean and confidence interval of sensitivity, specificity, and DOR, respectively, so that the data analysis was more reliable for the functional diagnostic test of PA.

The rest of the article is organized as follows: Section 2 imports the works related to the PA functional diagnostic test and data analysis. Section 3 sorts the PA screening method based on data analysis, and the method of Khyberton inhibition test, so that the readers of this article can have a more comprehensive understanding of the method of PA functional diagnostic test reliability based on data analysis. Section 4 is the core of the thesis, which completes the description of the application analysis of data analysis in PA diagnostic test reliability from two aspects: threshold effect detection analysis and statistical analysis of diagnostic test reliability. Section 5 summarizes the full work.

2. Related Works

2.1. PA Functional Diagnostic Test. At present, the diagnosis of PA is divided into three parts: first, screening diagnosis followed by the determination of diagnosis and then identification of various subtypes of PA for the selection of treatment. More and more studies have found that in addition to clinical manifestations such as hypertension and hypokalemia, PA can also cause serious damage to the heart, kidney, brain, and blood vessels of patients, and several domestic and international studies have shown that the proportion of cardiovascular disease is higher in patients with PA compared with primary hypertension. In addition, some patients may present with hypokalemia due to the long duration of the disease or after diuretics—weakness, numbness, muscle paralysis, and other discomforts—and target organ complications such as heart, brain, and kidney due to hypertension and high ALD levels.

Rege et al. found significant differences in the expression of genes in the globular and fascicular bands of the rat adrenal gland using gene microarrays, specific expression in the globular band of the rat adrenal gland by immunohistochemistry and other methods, and a close relationship with the expression of enzyme ketone synthase and enzyme ketone secretion [16]. Holler et al. found that some somatic cells in aldosterone adenoma are mutated, resulting in abnormalities in the genes encoding Na-KATPase and Ca2+ATPase that increase adrenal autocrine secretion of aldosterone leading to hypertension [17]. Fuss et al. determined the diagnosis of PA based on clinical presentation, confirmatory tests, and pathological examination [18]. Receiver operating characteristic (ROC) curves for diagnosing PA by ARR in different body positions were constructed and the best cut point for ARR screening of PA was selected according to the Youden's index. Zhang et al. found that during the follow-up of 2000 cases of intractable hypertension, about 13% of patients were confirmed to have PA and were those who could achieve clinically curable hypertension, suggesting that early diagnosis of PA can help to effectively control blood pressure and even end target organ damage caused by hypertension [19]. Freel and Connell considered the value of its application in the diagnosis of primary acid fixation, further assessing its sensitivity and specificity as a screening index by comparing it to the ARR ratio [20].

The probability that a patient with a specific disease has all the clinical manifestations and ancillary findings of this disease is almost small, and the diagnosis can only be made or excluded clinically based on the extent to which the patient's presentation matches all the manifestations. Therefore, the aim of this study was to further investigate the reliability of functional diagnostic tests for PA in a Chinese population by analyzing the data and correcting for relevant confounding factors.

2.2. Data Analysis. The clinical manifestations and ancillary findings of a disease are the sum of the results of a large sample of "all patients." The criteria for diagnosing PA is pathological diagnosis, but it is not required that all hypertensive patients undergo pathological biopsy, so a series of clinical diagnostic strategies are needed. The current diagnostic process of PA mainly includes a screening test, confirmatory test, and localized diagnosis, and this screening test can exclude the influence of other antihypertensive drugs in patients with newly diagnosed hypertension, which has a high diagnostic accuracy and helps to rationalize the use of drugs. However, the results of different studies suggest that the diagnostic efficacy of ADRR in PA screening is highly variable, and it is necessary to analyze the data on the diagnostic efficacy of ADRR in PA to clarify the role of ADRR in prodrug screening.

Gruber et al. used SAS 9.1 for statistical analysis and calculated the results of the study using data analysis, sensitivity, and specificity bivariate model analysis, respectively, and compared the calculated results of the two methods [21]. To assess the overall diagnostic value, Kersten et al. used data analysis for meta-analysis with effect indicators of total sensitivity, total specificity, total positive likelihood ratio, total negative likelihood ratio, diagnostic ratio, and the area under the working characteristic curve of the combined subjects [22]. Studies of Pitt and Byrd exploring the efficacy of ADRR screening for PA were included in the analysis, and two researchers independently extracted and analyzed the study data, which included general patient status and antihypertensive medication use [23]. Funder et al. concluded that reliability analysis through degraded information saved trial time and cost [24]. Reliability analysis based on performance degradation data is one of the solutions to the problem of reliability assessment of highly reliable and long-lived products. Pan et al. used chemiluminescence and data analysis to determine PAC and PRC of 200 hypertensive patients (including 67 patients with PA) in the prone and standing positions for 2 h, and 133 healthy volunteers in the standing position for 2 h, and calculated the ARR of different positions [25].

Therefore, the article explored the value of data analysis in the diagnosis of prodromal by exploring the predictors of prodromal and comparing their laboratory biochemical data in an attempt to construct a mathematical model using data analysis alone or in combination with traditional ARR methods.

3. Method of PA Functional Diagnostic Test Reliability Based on Data Analysis

3.1. PA Screening Method Based on Data Analysis. Cardiovascular diseases are included in the category of coronary atherosclerotic heart disease (coronary heart disease) and stroke [26]. Among them, coronary heart disease includes two types of stable angina pectoris and myocardial infarction [27]. Diagnostic criteria were used which developed by the Cardiovascular Disease Branch of the Chinese Medical Association [28]. A theoretical domain consisting of elements involving symptoms, laboratory tests, and imaging was selected and determined by reviewing the statistical literature related to PA [29]. The evaluation test diagnosed it as having the disease, and the false positive result put the subject under great mental stress. For the calculation of the above indicators, TPR and FPR were calculated and then logit transformations were applied to TPR and FPR with the following formulas:

$$\text{logit}(\text{TPR}) = \ln\left[\frac{\text{TPR}}{(1-\text{TPR})}\right], \tag{1}$$

$$\text{logit}(\text{FPR}) = \ln\left[\frac{\text{FPR}}{(1-\text{FPR})}\right]. \tag{2}$$

Add two variables D and S, and the expressions are as follows:

$$\text{D} = \text{logit}(\text{TPR}) - \text{logit}(\text{FPR}), \tag{3}$$

$$S = \text{logit}(\text{TPR}) + \text{logit}(\text{FPR}). \tag{4}$$

The ROC is commonly used in clinical practice to evaluate the ability of a test to detect disease [30]. Until the value of this screening test is fully investigated, it is not advisable to use it as a routine test for hypertensive patients, but it is supported that a reduction in potassium is not a necessary candidate for this screening test. The flow chart of the screening test is shown in Figure 1.

First, all patients were given a detailed medical history, recording gender, age, duration of hypertension, medications taken, and treatment history. Patients were required to collect fasting venous blood at least once during hospitalization and send it to the hospital laboratory to check liver and kidney function, blood electrolytes, and blood lipids. The statistical data and clinical experience were used to determine the weights and affiliation degree affiliation function of each element in the thesis domain. Cases with weights and art weight affiliation greater than or equal to the intercept are diagnosed as PA. The basic idea is to minimize the weighted sum of squared residuals, from which the parameters are solved. Suppose that the four cells of a, b, c, and d denote TPs, FPs, FNs, and TNs, respectively, and the weights, that is, the inverse of the variance, are noted as W, and the expressions are

$$\text{W} = [\text{var}(D)]^{-1} = \left(\frac{1}{a} + \frac{1}{b} + \frac{1}{c} + \frac{1}{d}\right)^{-1}. \tag{5}$$

The estimated AUC for CCT diagnosis of PA was 0.9 and the SSST was 0.6. The sample size ratio of patients with PA to patients with essential hypertension should be 3 : 1 in subjects with an ARR ratio greater than or equal to 2.0 ng-dl^{-1}/m IU-l^{-1}, and the area under the curve of false positive rate between 1 and 2 was calculated. Blood was collected at 8:00 a.m. on the morning of the test day in a resting, lying, fasting state. 50 mg of Kepone tablets (Sino-US Shanghai Squibb Pharmaceutical Co., Ltd.) was taken orally after blood collection, and blood was collected again at 10:00 a.m. 2 h later to measure plasma renin activity and angiotensin and aldosterone levels. The purpose was to differentiate from

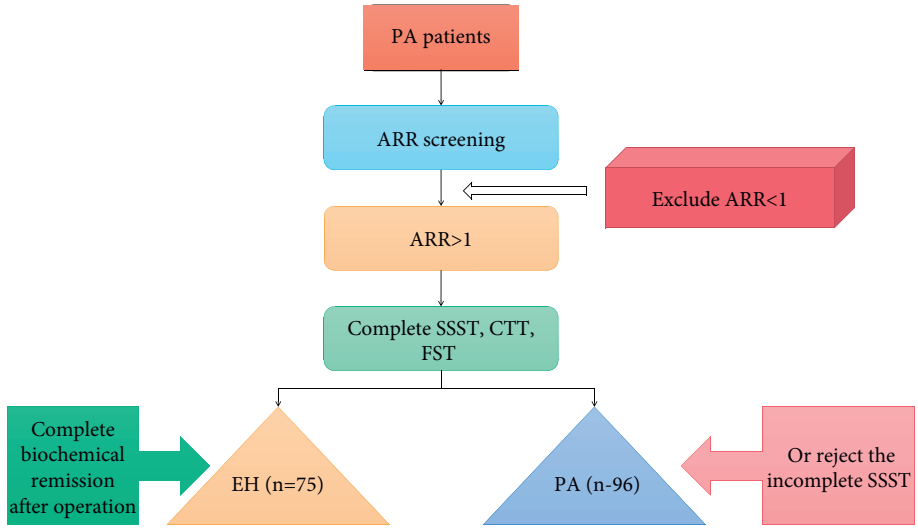

Figure 1: Research flow chart.

adrenal malignant tumor, and then use CAH for diagnosis, as shown in Figure 2.

Secondly, all hypertensive patients were asked to discontinue all types of antihypertensive drugs for at least 2 weeks before the test, and those who could not tolerate discontinuation could be given ion channel antagonists to control blood pressure. The blood specimens for PAC and PRC should be centrifuged within 2 h of collection and tested promptly. For the blood pressure test, the subject should rest calmly for 5 minutes or more and take a seated position with one sleeve removed to expose the forearm, so that the elbow is as close to the heart as possible. The mercury sphygmomanometer was selected and placed upright to zero the reading, then the sphygmomanometer cuff was wrapped around the upper arm close to the skin so that the lower edge of the cuff was approximately 2 fingers above the transverse elbow line, and the tightness was such that 1 finger could be reached.

Finally, the patients were asked to eat and drink normally before the test, and the day before the test, the patients were asked to accurately retain hourly urine, measure urine volume, and test urine potassium and urine sodium. All subjects began fasting after 10:00 pm the night before, and blood was drawn from the elbow at 8:00 pm the next day and sent to the hospital laboratory for biochemical, lipid, glycated hemoglobin, and fasting glucose measurements on a biochemical analyzer. In hypertensive patients, the basal recumbent ratio was measured, and in patients with renin after standing (tachypnea) excitation, the diagnosis of PA was made in combination with adrenal, post-surgical pathology, and follow-up results.

3.2. Method of the Captopril Inhibition Test. The Kepone inhibition test is one of the most widely used clinical tests to confirm the diagnosis of proaldosteronism. It is traditionally believed that the diagnosis of primary aldehyde should include three levels of screening, confirmation, and staging, and ARR is currently the preferred method recommended by national guidelines for the first level of primary aldehyde diagnosis [31]. In the early literature of pancreatic cancer diagnosis, it was noted that PET and EUS-FNAB techniques can improve the diagnosis of PDAC, but their effectiveness is often limited by the high cost and technical difficulty. The regression parameters A and B are derived from the five equations presented above, and then the regression equation for the SROC curve can be established using the following equation:

$$\mathrm{TPR} = \left[1 + e^{-A/(1-B)}\left(\frac{1-\mathrm{FPR}}{\mathrm{FPR}}\right)^{(1+B)/(1-B)}\right]. \tag{6}$$

Therefore, three confirmatory tests, SSST, CCT, and FST, were completed in the high-risk group for prodromal aldehyde, and the Kepone inhibition test was used as a reference standard to evaluate the diagnostic efficacy of SSST and CCT in the diagnosis of prodromal aldehyde and to finally determine the best diagnostic test for prodromal aldehyde. After the patients and their families gave their consent and signed the informed consent form, peripheral blood was collected from the prevalent patient, the father, and the mother for genomic DNA analysis. The genetic analysis process is shown in Figure 3.

First, gender (male/female), age (years), duration of hypertension (years), presence of hypokalemia, and medication use were recorded. Nonnormally distributed variables were expressed as medians (interquartile spacing), and the rank-sum test (U test) was used for comparison between groups. After fasting for at least 8 hours, patients were given 75 g of glucose powder dissolved in 250 ml of warm water orally in the early morning on an empty stomach, timed from the first sip and finished in 3–5 minutes, and blood glucose was measured on the forearm 2 hours after taking the glucose. TPR + FPR = 1 was a diagonal line, and on this diagonal line, the sensitivity and specificity were equal, that is, $S = 0$.

$$S = \mathrm{logit}(\mathrm{TPR}) + \mathrm{logit}(\mathrm{FPR}) = 0. \tag{7}$$

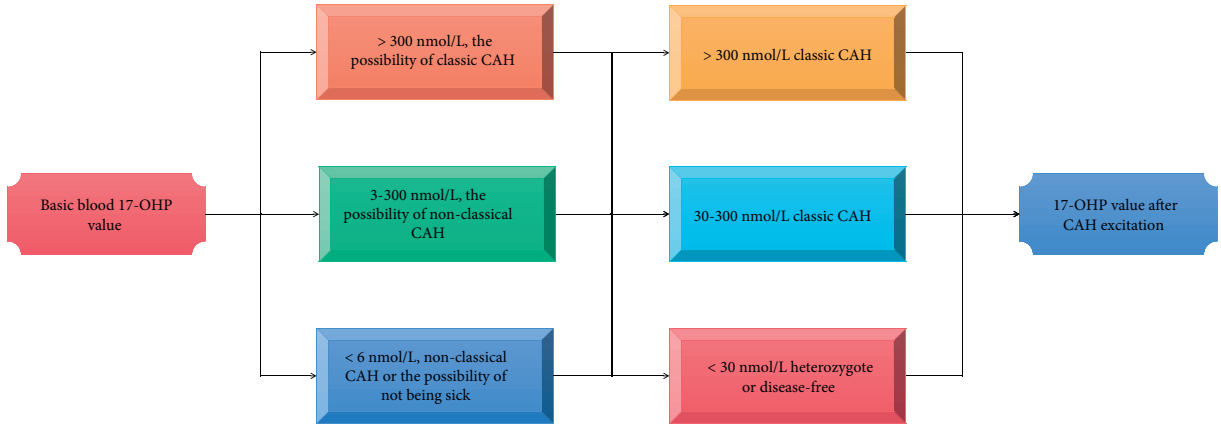

Figure 2: CAH diagnosis flow chart.

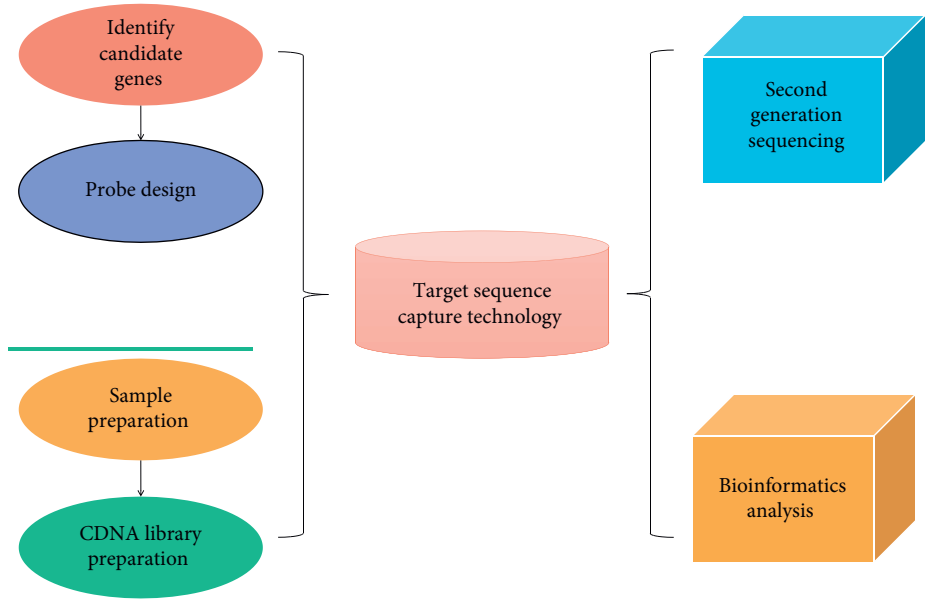

Figure 3: Gene analysis process.

Namely,

$$\text{logit}(\text{TPR}) = \text{logit}(\text{FPR}). \tag{8}$$

In the CTT experiment, plasma aldosterone and renin concentrations were measured in the prone position after the patient remained in the ambulatory position for at least 1 hour, and plasma aldosterone and renin concentrations were measured before the dose of 50 mg captopril at 8:00 a.m. Plasma aldosterone and plasma renin concentrations were measured again at 10:00 a.m. During the test, the patient was not allowed to lie down and eat. The standard error expression for TPR was:

$$\text{SE}(\text{TPR}) = \frac{\text{SE}(A)}{8[\cosh(A/4)]^2}. \tag{9}$$

Next, blood was drawn before the test and 2 h after oral administration of 20–45 mg of captopril, and PA and PRA were measured. Logistic regression analysis was used for risk factor analysis. $p < 0.04$ was defined as a statistically significant difference, and a two-sided test was used. At this time, the accuracy of the diagnostic test could be estimated by using statistical quantities, as shown in the following equation:

$$Z = \frac{\text{TPR}_1 - \text{TPR}_2}{\sqrt{\text{SE}^2(\text{TPR}_1) + \text{SE}^2(\text{TPR}_2)}}, \tag{10}$$

where Z is the normal deviation value; TPR_1 and TPR_2 are the diagnostic accuracy indexes to be compared; and $\text{SE}^2(\text{TPR}_1)$ and $\text{SE}^2(\text{TPR}_2)$ are the standard errors.

All subjects were required to complete blood biochemistry (electrolytes, liver function, renal function, etc.), plasma renin and aldosterone concentrations in the upright and prone positions, circadian rhythm of blood cortisol, 24-hour urinary cortisol and 24-hour urinary vanillyl amygdalin, saline loading or CCT, dexamethasone suppression test in some patients, and sex hormone testing. Under normal conditions, captopril inhibits angiotensin-converting enzyme, reduces angiotensin II production, and

suppresses aldosterone secretion even in the presence of high renin.

Finally, blood and 24-h urine were collected from both hypertensive patients and normal controls, and blood and urine electrolytes were measured by a fully automated biochemical analyzer. Clinical case data of suspected adrenal lesions were collected and used to evaluate the sensitivity and specificity of the diagnostic model of PA data analysis, using routine postoperative pathological findings as the gold standard. After screening the case data, the investigators independently extracted relevant information (e.g., patient characteristics, relevant indicators needed for various applications or calculations, etc.) and reconstructed these data into a 2×2 column table using a standard format. The angiotensin-converting enzyme inhibitors, angiotensin receptor blockers, and β receptor blockers for more than 2 weeks and diuretics or glycopyrrolate preparations for more than 4 weeks were discontinued prior to blood collection. The true positive rate, false positive rate, true negative rate, and false negative rate were calculated by a columnar table.

4. Application Analysis of Data Analysis in Reliability of the PA Diagnostic Test

4.1. Threshold Effect Detection and Analysis. Data analysis was used to assess statistical heterogeneity between studies, and no significant heterogeneity between studies was considered when $p \geq 0.03$. A fixed-effects model was selected for data analysis, and it was found that antihypertensive drug administration significantly affected the accuracy of the threshold effect assay. The results of two different immunological diagnostic tests, IHA and ELISA, were comprehensively evaluated using the threshold effect assay and bivariate model analysis of sensitivity and specificity in order to obtain more accurate conclusions and provide a basis for the selection of future screening methods for PA. The ROC curves of the confirmatory tests for the diagnosis of protoaldehyde and its subtypes are shown in Figure 4.

First, when using data analysis for PA screening, attention should also be paid to test method standardization and threshold setting, which varies in the literature reporting different body positions, blood collection times, etc. Threshold settings also vary. There are many ways to obtain comprehensive diagnostic test accuracy, but the more commonly used methods include comprehensive receiver operating characteristic analysis and bivariate model analysis for sensitivity and specificity. Plasma aldosterone levels do not follow a normal distribution, so they are expressed as the median of the data. Normally distributed data were expressed as mean ± standard deviation, and nonnormally distributed data were transformed for normality by taking natural logarithm values. Comparisons of plasma aldosterone levels between the proaldosterone and nonproaldosterone groups were performed by nonparametric tests. One-way ANOVA was used for comparisons between the two groups. Correlations between factors of normally distributed data were analyzed by correlation. Patients with a positive test should have an enhanced CT examination of the adrenal glands, and patients who are willing to undergo

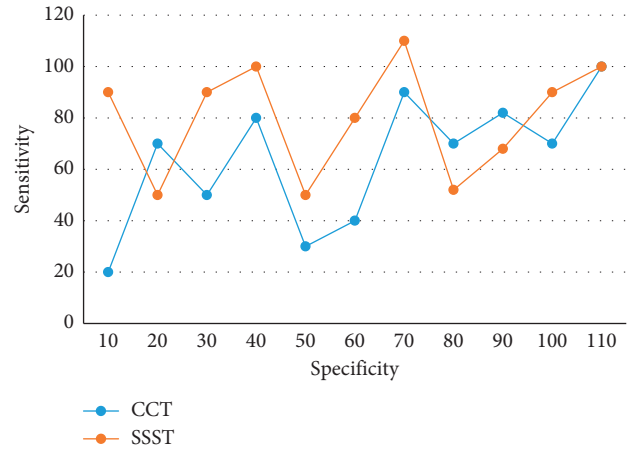

Figure 4: ROC curve of a diagnostic test for protoaldehyde and its subtypes.

adrenalectomy are recommended to have an adrenal vein (AVS) to identify the dominant side of aldosterone secretion. Almost all patients with PA showed different degrees of hypertension, except for the early PA patients who were found to have no hypertension during the health checkup, so the difference was statistically significant, and the 2-h postprandial blood glucose level was positively correlated with the standing aldosterone level, as shown in Figure 5.

Secondly, in the case of a certain test method, the higher the threshold setting, the lower the sensitivity and the higher the specificity. Acceleration equation and acceleration factor are two very important concepts in accelerated tests, which are called accelerated life equation in accelerated life test. True classification is defined as two mutually exclusive states, such as the presence or absence of disease, benign or malignant tumor, positive or negative test results, etc. For the determination of renin activity, two copies of the same sample are taken, one at 4°C to react directly with the antibody and the other at 37°C for a period of warming before reacting with the antibody. The concentration of angiotensin I in the two samples was measured separately, and the renin activity was obtained by dividing the concentration of angiotensin I in the 37°C sample by the concentration of angiotensin I in the 4°C sample by the incubation time. The sensitivity of standing ALD and ARR for the diagnosis of PA is slightly poorer, but the specificity is better, while the sensitivity of prone ALD and ARR for the diagnosis of PA is better, but the specificity is slightly poorer (Figure 6).

Finally, other confirmatory tests must be performed after the screening test to reduce the false positive rate. The true screening status is determined by the gold standard, which is a test that is completely different from the test being evaluated and whose results are recognized by all. Patients whose true status is higher than the initial screening cut point are further tested with a confirmatory test (intravenous saline test, or CCT, or fludrocortisone suppression test). Patients with a positive confirmatory test underwent enhanced CT of the adrenal glands and, in some cases, bilateral adrenal venous blood sampling. During this period, drugs with a low effect on this ratio, such as hydrazidiazide, prazosin, and

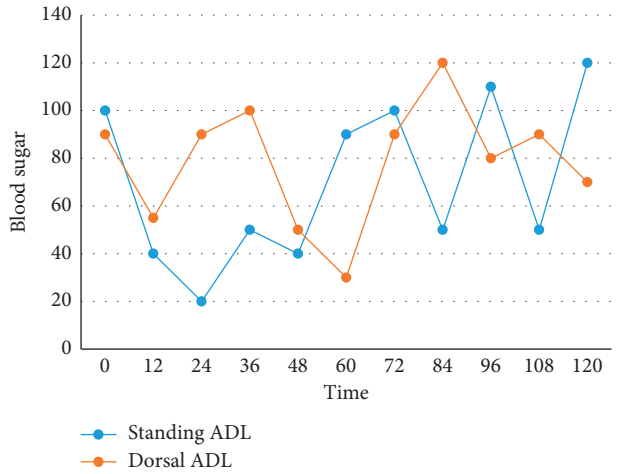

Figure 5: The correlation between blood glucose at 2 h after meal and ALD in upright and supine positions.

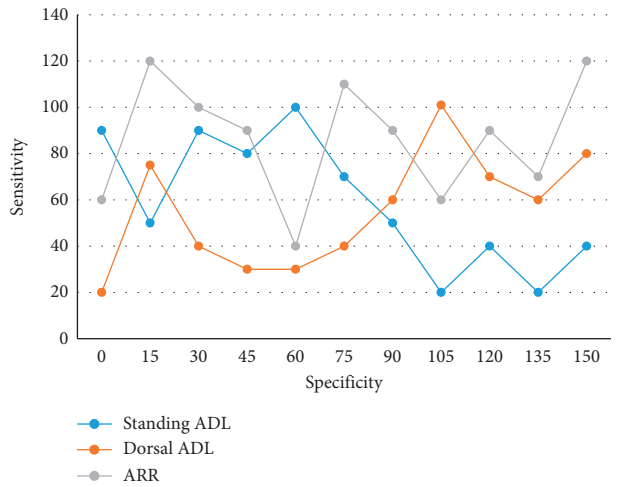

Figure 6: ROC curve of diagnostic PA drawn by ALD and ARR values in upright and supine positions.

verapamil extended-release agents, could be used as needed to control hypertension symptoms. The overall sensitivity, specificity, area under the curve, and diagnostic test advantage ratio were found to be 0.87 (95% CI 0.84–0.93), 0.93 (95% CI 0.95–0.98), 0.94, and 371.13, respectively, but heterogeneity was evident.

4.2. Statistical Analysis of Diagnostic Reliability. The purpose of diagnostic tests is to explore easy, quick, and cost-effective methods for early diagnosis, but their diagnostic value can be influenced by various factors, such as disease spectrum, gold standard, and outcome evaluators. The results of different studies suggest that the diagnostic efficacy of ADRR in PA screening is highly variable; there is also controversy over the need to discontinue medication in patients taking hypotensive drugs when measuring ADRR values. The clinical threshold for screening is generally set at 30, and a diagnosis of prodromalgia is confirmed if the patient's ARR is greater than 50. Therefore, it is necessary to analyze the data on the diagnostic efficacy of ADRR in PA to clarify the role of ADRR in proaldosterone screening. The septal thickness and left ventricular weight index of PA patients were higher than those of EH patients, with statistically significant differences, and there was a positive correlation between standing and lying ALD levels and septal thickness (see Figure 7).

First, threshold effects were assessed using Spearman's correlation coefficient, using I^2 values to assess heterogeneity between included studies ranging from 0% to 90%, with 0% indicating no heterogeneity and more than 40% indicating significant heterogeneity of included studies. Renin and aldosterone levels were influenced by a variety of conditions that were not uniformly controlled for in the study, including the use of antihypertensive medications, blood sample collection from outpatients or inpatients, timing of blood collection, body position during the trial, sodium and potassium intake, and menstrual cycle. Any new diagnostic technique or new diagnostic method formally applied in clinical practice needs to be evaluated for methodological quality and clinical applicability using scientific, standardized, and rigorous methods. A random-effects model was used when significant heterogeneity between studies was considered at $p < 0.06$. Deek's funnel plot was used for diagnostic tests to determine whether there was significant publication bias. Diagnostic accuracy was improved, thus guiding physicians to take correct and reasonable decisions for patients during clinical treatment. Patients had higher SUSPUP as well as SUSPPUP compared with patients with primary hypertension, with statistically significant differences, and the ROC curves of each index in PA screening are shown in Figure 8.

Second, the efficacy of PA screening for ADRR was assessed using the combined total sensitivity and total specificity, expressed as an 85% confidence interval. A dramatic increase in fluid volume can suppress blood aldosterone secretion to a large extent, while antihypertensive drugs have little effect on the results of this test. The design of the diagnostic test is unique, and its internal and external validity is susceptible to numerous factors.

The aldosterone levels were significantly higher in PA patients than in patients with essential hypertension, and the differences in blood and urine electrolytes were statistically significant. The blood potassium levels were lower in PA patients than in those with essential hypertension, while the blood sodium, urine sodium, and urine potassium levels were higher in PA patients than in those with essential hypertension. The comparison of the area under the curve of each index as well as the optimal cut point and sensitivity and specificity of each index are shown in Tables 1 and 2.

The diagnostic advantage ratio is the ratio of the positive likelihood ratio to the negative likelihood ratio and is the best indicator to evaluate the efficacy of a diagnostic test. In studies containing multiple PA subtypes, a higher APA ratio will result in a higher specificity and a lower sensitivity of the diagnostic cut point. Flawed trial design, inappropriate subject selection, poor trial execution, inappropriate data analysis, and poor interpretation of study results may lead to misestimation of trial accuracy, resulting in premature

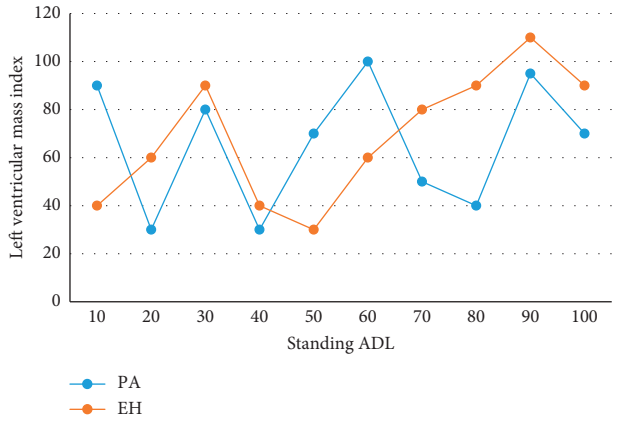

Figure 7: Comparison of ventricular septal thickness between PA and EH.

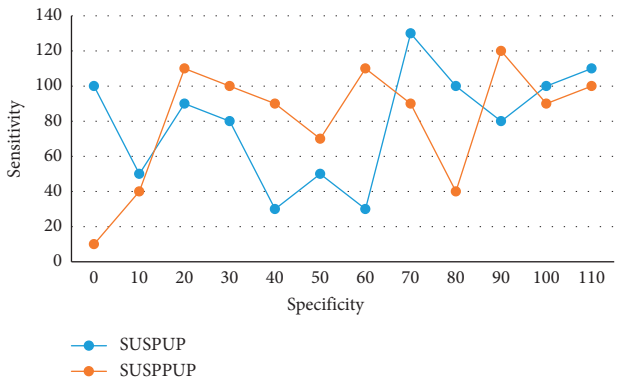

Figure 8: ROC curve of each index in PA screening.

Table 1: Comparison of the area under the curve of each index.

Index	ARR	Blood sodium/potassium	SUSPUP	SUSPPUP
AUC	0.876	0.782	0.694	0.578
SE	0.03	0.02	0.02	0.04
p value	<0.01	<0.01	<0.01	<0.01

Table 2: The best cutoff point, sensitivity, and specificity of each index.

	ARR	SP	SPP
Optimum tangent point	29.68	46.26	15.36
Sensibility	1.04	0.87	0.68
Specificity	0.897	0.765	0.695

application of immature diagnostic tests to clinical practice with harmful clinical consequences.

Finally, forest plots were used to indicate the sensitivity and specificity of all included studies. The mechanism could be the low level of aldosterone secretion and the weak autocrine capacity in patients with normal blood potassium. When post-saline PAC and post-cato PAC were used to confirm the diagnosis of prodromal, respectively, there was a similar area under the subject working curve between SSST and CCT, 0.89 and 0.78, respectively, with no significant difference in the area under the curve between the two ($p = 0.546$). Data analysis was used in the significant variable regression analysis to establish the scoring system predicting prodromal. The row variables of the column table reflect the true classification status of the patients, that is, the gold standard test results; while the column variables are the diagnostic results of the evaluated tests, noted as positive versus negative.

5. Conclusions

With the intensive study of PA, it is now believed that PA is a common cause of secondary hypertension, and its prevalence is about 6%–15% of hypertensive patients. Compared with typical UPA patients, patients with CT-negative unilateral PA have milder clinical symptoms, and an increased number of APCC is an important pathological feature. The diagnosis of PA is a complex process, especially in patients with mild clinical symptoms and no hypokalemia, and the diagnosis needs to be made by combining the results of multiple tests and comprehensive analysis to guide treatment. Therefore, this study proposes a data analysis-based reliability analysis of functional diagnostic tests for PA, incorporating proaldosterone cases, using data analysis to obtain eigenfunction coefficients, exploring new methods for proaldosterone screening and diagnosis, and conducting an in-depth study on the diagnostic reliability of medical mathematization. The combined use of data analysis would improve the reliability of test results, and data analysis-based reliability analysis of PA functional diagnostic tests is a more feasible option because it is safer and easier to implement. In conclusion, this study is a guideline for the screening of PA and provides a viable basis for the clinical development of plasma renin concentration screening for the disease.

Data Availability

The dataset can be accessed upon request.

Conflicts of Interest

The authors declare no conflicts of interest.

References

[1] H. Annie, A. Sumaiya, G. Ankur et al., "Performance of the aldosterone to renin ratio as a screening test for primary aldosteronism," *Journal of Clinical Endocrinology & Metabolism*, vol. 106, no. 8, pp. 2423–2435, 2021.

[2] R. Rusev, J. Matrozova, V. Vasilev, A. Elenkova, K. Kalinov, and S. Zacharieva, "Evaluation of a new diagnostic test for primary aldosteronism," *Journal of Hypertension*, vol. 39, no. Supplement 1, pp. e220–e221, 2021.

[3] N. Danforth, M. M. Orlando, F. C. Bartter, and N. Javadpour, "Renal changes in primary aldosteronism," *The Journal of Urology*, vol. 117, no. 2, pp. 140–144, 2019.

[4] K. Yamashita, M. Yatabe, Y. Seki et al., "Comparison of the shortened and standard saline infusion tests for primary aldosteronism diagnostics," *Hypertension Research*, vol. 43, no. 10, pp. 1113–1121, 2020.

[5] D. Ahmet, E. Henk, E. Ali et al., "Hypertension with primary aldosteronism is associated with increased carotid intima-media thickness and endothelial dysfunction," *Journal of Clinical Hypertension*, vol. 21, no. 7, pp. 932–941, 2021.

[6] G. P. Rossi, "Primary aldosteronism," *Journal of the American College of Cardiology*, vol. 74, no. 22, pp. 2799–2811, 2019.

[7] K. Azama, M. Okada, A. Yogi et al., "Adrenal venous sampling in patients with primary aldosteronism: which is the best evaluation method for laterality assessments?" *Open Journal of Radiology*, vol. 07, no. 04, pp. 219–227, 2017.

[8] S. H. Chen, P. Y. Luo, and Y. R. Yu, "The diagnostic value of captopril challenge test for primary aldosteronism," *Sichuan da xue xue bao. Yi xue ban*, vol. 52, no. 1, pp. 134–141, 2021.

[9] Y. M. Li, W. Wang, Q. R. Li et al., "Diagnostic efficiency of different screening indexes for primary aldosteronism," *Medical science edition*, vol. 51, no. 3, pp. 278–286, 2020.

[10] M. Adilijiang, Q. Luo, M. Wang et al., "Minor change of plasma renin activity during the saline infusion test provide an auxiliary diagnostic value for primary aldosteronism," *International Journal of Endocrinology*, vol. 2021, no. 58, 9 pages, Article ID 5757305, 2021.

[11] T. Dekkers, A. Prejbisz, L. Schultze Kool et al., "Adrenal vein sampling vs. CT scan to determine treatment in primary aldosteronism: an outcome-based randomised diagnostic trial," *European Urology Supplements*, vol. 16, no. 3, pp. e547–e548, 2017.

[12] H. Shen, Z. X. Xu, and Q. F. Li, "New advances in the diagnosis of primary aldosteronism," *Chronic Diseases and Translational Medicine*, vol. 6, no. 1, p. 1, 2020.

[13] J. Xu, Y. Yang, Y. Ling et al., "The association between eGFR and the aldosterone-to-renin ratio and its effect on screening for primary aldosteronism," *International Journal of Endocrinology*, vol. 2020, no. 5-6, 7 pages, Article ID 2639813, 2020.

[14] Z. Xu, J. Yang, J. Hu et al., "Primary aldosteronism in patients in China with recently detected hypertension," *Journal of the American College of Cardiology*, vol. 75, no. 16, pp. 1913–1922, 2020.

[15] M. Namba, K. Kikuchi, H. Komura et al., "Study on uric acid metabolism in patients with primary aldosteronism," *Folia Endocrinologica Japonica*, vol. 68, no. 1, pp. 51–61, 2019.

[16] J. Rege, A. F. Turcu, and W. E. Rainey, "Primary aldosteronism diagnostics: KCNJ5 mutations and hybrid steroid synthesis in aldosterone-producing adenomas," *Gland Surgery*, vol. 9, no. 1, pp. 3–13, 2020.

[17] F. Holler, D. A. Heinrich, C. Adolf et al., "Steroid profiling and immunohistochemistry for subtyping and outcome prediction in primary aldosteronism—a review," *Current Hypertension Reports*, vol. 21, no. 10, pp. 1–15, 2019.

[18] C. T. Fuss, K. Brohm, M. Kurlbaum et al., "Confirmatory testing of primary aldosteronism with saline infusion test and LC-MS/MS," *European Journal of Endocrinology*, vol. 184, no. 1, pp. 167–178, 2021.

[19] Y. Zhang, J. Tan, Q. Yang et al., "Primary aldosteronism concurrent with subclinical Cushing's syndrome: a case report and review of the literature," *Journal of Medical Case Reports*, vol. 14, no. 1, p. 32, 2020.

[20] E. M. Freel and J. M. Connell, "Primary aldosteronism: an update," *Hypertension*, vol. 69, no. 5, pp. 780-781, 2017.

[21] S. Gruber and F. Beuschlein, "Hypokalemia and the prevalence of primary aldosteronism," *Hormone and Metabolic Research*, vol. 52, no. 06, pp. 347–356, 2020.

[22] M. Kersten, K. Hancke, W. Janni, and K. Kraft, "Pregnancy induced Cushing's syndrome and primary aldosteronism: a case report," *BMC Pregnancy and Childbirth*, vol. 20, no. 1, p. 421, 2020.

[23] B. Pitt and J. B. Byrd, "Primary aldosteronism: new insights into its detection and cardiac involvement - ScienceDirect," *Journal of the American College of Cardiology: Cardiovascular Imaging*, vol. 13, no. 10, pp. 2160-2161, 2020.

[24] J. W. . Funder, "Primary aldosteronism," *Hypertension*, vol. 74, no. 3, pp. 458–466, 2019.

[25] C. T. Pan, C. S. Hung, and S. H. Sung, "[Abstract of a thesis] Evaluation of vascular dysfunction in primary aldosteronism using wave reflection analysis," *Straits Journal of Circulation Medicine*, vol. 1, no. 2S, pp. 170–172, 2019.

[26] A. Khler, A. L. Sarkis, D. A. Heinrich et al., "Renin, a marker for left ventricular hypertrophy, in primary aldosteronism: a cohort study," *European Journal of Endocrinology*, vol. 185, no. 5, pp. 663–672, 2021.

[27] W. Wang, Y. Li, Q. Li et al., "Developing a research database of primary aldosteronism: rationale and baseline characteristics," *BMC Endocrine Disorders*, vol. 21, no. 1, p. 137, 2021.

[28] M. Stowasser, A. Ahmed, Z. Guo et al., "Can screening and confirmatory testing in the management of patients with primary aldosteronism be improved?" *Hormone and Metabolic Research*, vol. 49, no. 12, pp. 915–921, 2017.

[29] M. Vivien, E. Deberles, R. Morello, A. Haddouche, D. Guenet, and Y. Reznik, "Evaluation of biochemical conditions allowing bypass of confirmatory testing in the workup of primary aldosteronism: a retrospective study in a French hypertensive population," *Hormone and Metabolic Research*, vol. 51, no. 03, pp. 172–177, 2019.

[30] K. Wang, J. Hu, J. Yang et al., "Development and validation of criteria for sparing confirmatory tests in diagnosing primary aldosteronism," *Journal of Clinical Endocrinology & Metabolism*, vol. 105, no. 7, Article ID dgaa282, 2020.

[31] B. Liu, J. Hu, Y. Song et al., "Seated saline suppression test is comparable with captopril challenge test for the diagnosis of primary aldosteronism: a prospective study," *Endocrine Practice*, vol. 27, no. 4, pp. 326–333, 2020.

Hindawi
Computational Intelligence and Neuroscience
Volume 2022, Article ID 4270295, 9 pages
https://doi.org/10.1155/2022/4270295

Research Article

A Micro Neural Network for Healthcare Sensor Data Stream Classification in Sustainable and Smart Cities

Jin Wu,[1,2] Le Sun,[1,2] Dandan Peng,[3] and Siuly Siuly[4]

[1]*Engineering Research Center of Digital Forensics, Ministry of Education, Nanjing University of Information Science and Technology, Nanjing, China*
[2]*Department of Jiangsu Collaborative Innovation Center of Atmospheric Environment and Equipment Technology (CICAEET), Nanjing University of Information Science and Technology, Nanjing 210044, China*
[3]*School of Computer Science and Network Engineering, Guangzhou University, Guangzhou, Guangdong, China*
[4]*Centre for Applied Informatics, College of Engineering and Science, Victoria University, Melbourne, Australia*

Correspondence should be addressed to Le Sun; 002813@nuist.edu.cn

Received 14 May 2022; Accepted 6 June 2022; Published 24 June 2022

Academic Editor: Yaxiang Fan

Copyright © 2022 Jin Wu et al. This is an open access article distributed under the Creative Commons Attribution License, which permits unrestricted use, distribution, and reproduction in any medium, provided the original work is properly cited.

A smart city is an intelligent space, in which large amounts of data are collected and analyzed using low-cost sensors and automatic algorithms. The application of artificial intelligence and Internet of Things (IoT) technologies in electronic health (E-health) can efficiently promote the development of sustainable and smart cities. The IoT sensors and intelligent algorithms enable the remote monitoring and analyzing of the healthcare data of patients, which reduces the medical and travel expenses in cities. Existing deep learning-based methods for healthcare sensor data classification have made great achievements. However, these methods take much time and storage space for model training and inference. They are difficult to be deployed in small devices to classify the physiological signal of patients in real time. To solve the above problems, this paper proposes a micro time series classification model called the micro neural network (MicroNN). The proposed model is micro enough to be deployed on tiny edge devices. MicroNN can be applied to long-term physiological signal monitoring based on edge computing devices. We conduct comprehensive experiments to evaluate the classification accuracy and computation complexity of MicroNN. Experiment results show that MicroNN performs better than the state-of-the-art methods. The accuracies on the two datasets (MIT-BIH-AR and INCART) are 98.4% and 98.1%, respectively. Finally, we present an application to show how MicroNN can improve the development of sustainable and smart cities.

1. Introduction

International Telecommunication Union (ITU) and the United Nations Economic Commission for Europe (UNECE) jointly put forward the construction scheme of a sustainable smart city [1, 2]. The scheme aims to use information technology to improve the level of people's living standards and increase the efficiency of urban services [3]. Problems, such as uneven distribution of medical resources and low efficiency of disease treatment, have gradually become prominent in urban construction [4, 5]. Many research works [6, 7] explore advanced Internet of Things (IoT) and artificial intelligence technologies to solve these problems to promote the development of urban intelligence and sustainability.

The rapid development of deep learning technology and the Internet of Medical Things (IoMT) has brought new opportunities and challenges to medical development in the construction of smart cities [3]. In recent years, some algorithms [6, 8] based on deep learning have been proposed to classify healthcare sensor data streams to solve the problem of medical problems in the process of urban development. Deep convolution neural network (CNN) [9] and deep recurrent neural network (RNN) [10] are two popular methods for classifying healthcare sensor data streams. The former is mainly represented by the one-dimensional convolutional neural network, which can extract the features of one-dimensional time series data [11]. The latter mainly serializes the neurons to process the serialized

data, so that the neurons among the hidden layers can be related to each other [10]. Most of the existing healthcare sensor data classification methods are improved based on the above two methods. However, these methods are difficult to deploy in edge devices because of their large time and space complexity [12].

To reduce the reasoning time and spatial complexity of the model, different lightweight neural network models are proposed in the literature [13, 14]. These methods can be divided into three scenarios: artificially designed lightweight neural network, neural network model compression algorithm, and automatic design of neural network structures [15]. In the first scenario, the model is made lightweight by reducing the number of parameters, for example, limiting the number of channels of features [16, 17], using decomposition convolution operation or $1 * 1$ convolution kernel [18], etc. However, the design process of this scenario needs a lot of time [19]. The second scenario mainly uses knowledge distillation [20] and network slimming [21] to compress the network model. Unfortunately, these methods often realize the lightweight of the model at the cost of sacrificing the performance of the model. The third scenario is to automatically design a neural network architecture to solve a specific task according to a certain search strategy [15, 22, 23]. When using the methods based on the above scenarios to classify healthcare sensor data streams, the accuracy of the models is not very high. It is mainly because these models do not consider how to distinguish classes with similar features [24, 25].

In contrast to the above methods, this paper proposes a novel model that ensures the classification accuracy of each class while ensuring the lightweight of the model, called MicroNN. Since RNN has the advantage of memory preservation for time series data, the architecture based on multilayered RNN [26] is used as the feature extractor of MicroNN. In addition, to improve the identification ability of MicroNN between classes with similar features [27], Kullback Leibler divergence (KL divergence) is introduced in this paper. Experiments show that the overall accuracy and the classification accuracy of each class using MicroNN exceed other work. Our main contributions are as follows:

(i) MicroNN model is composed of a microfeature extractor and some miniclassifiers.

(ii) MicroNN uses a method based on KL divergence to eliminate shared knowledge among classes.

(iii) We conduct comprehensive experiments based on time complexity and space complexity.

The rest of this paper is organized as follows: section 2 presents the related work, section 3 introduces the proposed model, section 4 shows the experiment, section 5 describes an application scenario of MicroNN, and section 6 summarizes this work.

2. Related Work

E-health has become a part of the development of sustainable and smart cities [2, 32]. With the mature development of deep learning and IoMT, healthcare sensor data stream classification based on edge computing has become possible [1, 33, 34]. It will effectively alleviate the uneven distribution of urban medical resources and further accelerate the intelligence development of cities.

Table 1: The space complexity comparison between MicroNN and state-of-the-art methods.

Work	Methods	Model size (MB)
Liu et al. [26]	CNN	39.5
Chen et al. [28]	CNN	32.9
Jun et al. [29]	LSTM	16.2
Saadatnejad et al. [30]	LSTM	15.4
Faust et al. [31]	Bi-LSTM	27.6
Ours	MicroNN	13.7

According to the survey [6], different diseases are bothering mankind, which seriously threaten human life and quality of life. Nowadays, how to detect and avoid related diseases as soon as possible has become a major issue in urban development [1, 35]. Therefore, disease diagnosis based on healthcare sensor data stream classification has become a hot research topic. Many pieces of research use traditional machine learning methods to classify healthcare sensor data streams, which rely heavily on the characteristics of manual design. Behadada and Chikh [36] proposed a method based on the fuzzy decision tree to improve the detection of arrhythmias. Nasiri et al. [37] designed a model based on the support vector machine and genetic algorithms to diagnose cardiac arrhythmia with relatively high accuracy. Bensujin and Hubert [38] raised a method by combining the K-means clustering algorithm and bacterial foraging optimization algorithm to examine the heart situation of a person. Sharipov [39] used principal component analysis to improve the cardiac diagnosis via ECG. Jadhav et al. [40] proposed static backpropagation algorithms and the momentum learning rule for diagnosing heart diseases.

At present, because of the excellent performance of deep learning technology in the fields of image classification and text recognition, more research works are trying to apply the deep learning model in the field of disease diagnosis. Liu et al. [26] developed a model based on a multiple-feature-branch convolutional neural network for checking the patient's abnormal heartbeat. Chen et al. [28] proposed a new end-to-end scheme using a convolutional neural network (CNN) for automated ECG analysis. Saadatnejad et al. [30] proposed multiple long-short term memory (LSTM) models to monitor the status of heart activity. Faust et al. [31] proposed a bidirectional LSTM for beat detection. Jun et al. [29] used a CNN model with more layers by transforming the healthcare sensor data into a two-dimensional gray image.

Our work is different from the above work. In Table 1, we compare MicroNN with the discussed methods in terms of space complexity. It can be found that the space complexity of the models discussed is relatively larger than MicroNN. It makes some models not widely used in portable devices or edge devices. Therefore, this paper not only considers the accuracy of the model but also further considers the space complexity of the model (Table 2).

Table 2: Meaning of the main notations.

Notation	Meaning
$X = \{x_1, x_2, \ldots, x_n\}$	The raw physiological information record, n is the length of the record.
$S_i = \{v_1, v_2, \ldots, v_r\}$	S_i refers to the i^{th} slice after being segmented.
$S_{i,j}$	$S_{i,j}$ represents the j^{th} point of i^{th} slice.
$F_i = \{e_1, e_2, \ldots, e_m\}$	The features after feature extractor.
$\mathrm{RNN}^{[1]}$, $\mathrm{RNN}^{[2]}$	$\mathrm{RNN}^{[1]}$ represents the collection of the RNN model at the first level, $\mathrm{RNN}^{[2]}$ represents the collection of the RNN model at the second level.
$X \sim P_X^{\mathrm{class}_i}$	It refers to the data distribution of each class.
W_1, W_2, and W_3	They are the weights of a miniclassifier.
$f_1, f_2, \ldots, f_n$	They are the output of the miniclassifier.
η , c , and π	They are all hyperparameters in the paper.

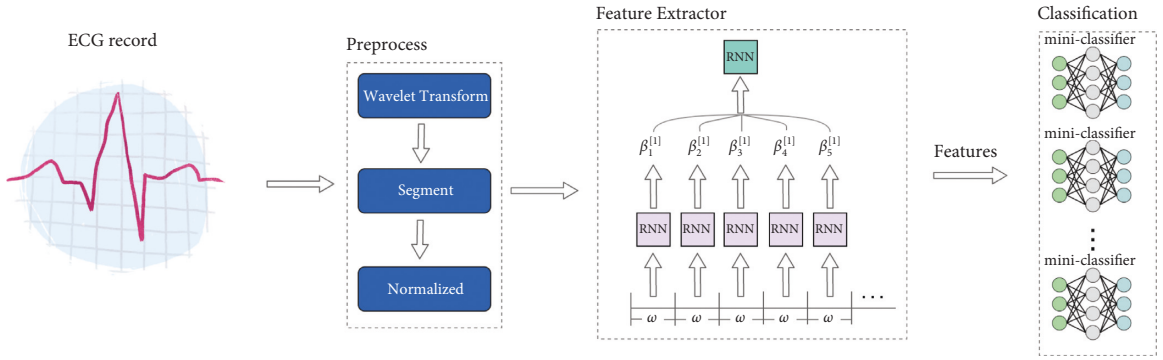

Figure 1: The workflow of MicroNN.

3. Our Proposed Model

3.1. System Overview. MicroNN mainly includes three parts: preprocessing model, microfeature extractor, and miniclassifiers. Figure 1 shows the overall architecture of MicroNN. Table 2 is an explanation of the notations used in the paper. The workflow of MicroNN is as follows: a physiological information record $X = \{x_1, x_2, \ldots, x_n\}$. The preprocessing model splits the record into slices with equal length n, and each slice refers to $S_i = \{v_1, v_2, \ldots, v_r\}$.

Then, the microfeature extractor is used to extract the features of S_i, $F_i = \{e_1, e_2, \ldots, e_m\}$. Finally, the feature F_i of S_i is input into each miniclassifier f_i to obtain the corresponding score. Hence, the label of heartbeat S_i is y, as shown in (1).

$$y = \mathrm{argmax}_i (f_1, f_2, \ldots, f_n). \tag{1}$$

3.2. Preprocessing Model. Physiological signals are mainly measured by some mobile edge devices. However, as physiological signals have the characteristics of low amplitude and low frequency, it is easy to be disturbed by noise in the acquisition process [39]. These noises mainly come from internal or external interference [36]. Therefore, the wavelet transform [41] is used to denoise the original signal in this paper. Firstly, the original data is decomposed into nine scales. Then, the wavelet coefficients of nine scales will be processed by threshold operation [41]. Finally, we reconstruct the original data by inverse wavelet transform. Figure 2 shows the changes in physiological signal records (such as ECG) before and after denoising. Secondly, each physiological signal record is segmented into slices based on the annotations provided by the standard file [42]. Each slice S_i was normalized, $S_{i,j} = S_{i,j}/\|S_i\|_2$, where $S_{i,j}$ represents the j **th** point of S_i and $\|S_i\|_2$ refers to the 2-norm of a heartbeat slice S_i.

3.3. Microfeature Extractor and Miniclassifiers. In the past, many research works used the convolutional neural network (CNN) as a feature extraction model. However, as CNN needs more computing and storage resources [26], it is difficult to deploy it in edge devices. Consider that the recurrent neural network (RNN) has a memory function in the processing of medical time series data and that its volume is smaller than that of the convolutional neural network [28]. Inspired by ShaRNN [43], this paper mainly adopts the collection of multilevel RNNs as the feature extractor (see Figure 1).

Firstly, it should be noted that we set the RNN collection with two levels. We set the slice data after preprocessing as $S_i = \{v_1, v_2, \ldots, v_r\}$, and we will divide it into some slices whose size is ω. S_i will generate n/ω slices, and we use A_k to represent each slice. Then, we set up an RNN model for each slice:

$$\beta_k^{[1]} = \mathrm{RNN}^{[1]}(A_k), \quad k \in \left[1, \frac{n}{\omega}\right]. \tag{2}$$

Here, $\mathrm{RNN}^{[1]}$ represents the RNN model of the first level, and $\beta_k^{[1]}$ refers to the output of $k^{\mathbf{th}}$ slice by $\mathrm{RNN}^{[1]}$. Therefore, we can get the result $[\beta_1^{[1]}, \beta_2^{[1]}, \ldots, \beta_{n/\omega}^{[1]}]$ after the training of RNNs collection of the first level.

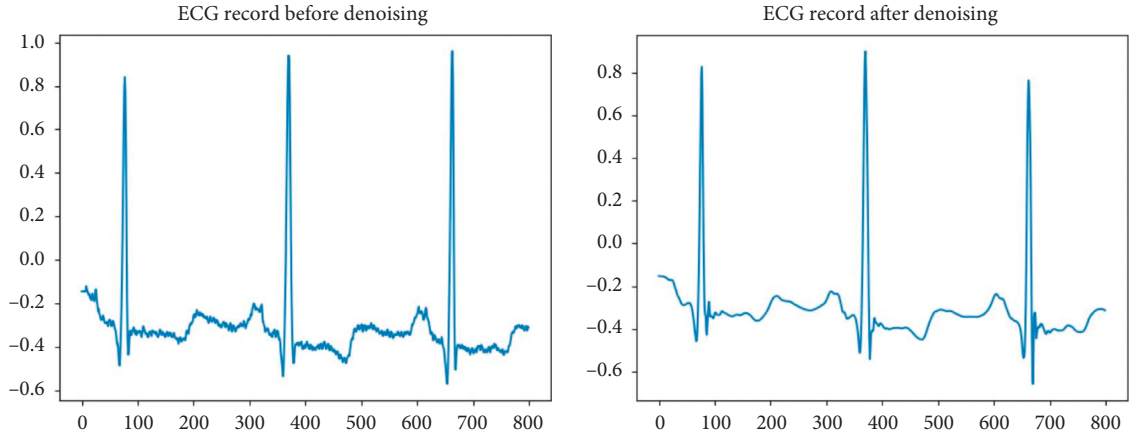

Figure 2: The changes in a physiological signal record represented by ECG before and after denoising. (a) ECG record before denoising. (b) ECG record after denoising.

In the next step, we feed the result into the RNN of the second level, and the output is

$$\beta^{[2]} = \mathrm{RNN}^{[2]}\left(\beta_1^{[1]}, \beta_2^{[1]}, \ldots, \beta_{n/\omega}^{[1]}\right), \quad y = \mathscr{F}\left(\beta^{[2]}\right), \tag{3}$$

where $\mathrm{RNN}^{[2]}$ represents the RNN model of the second level, $\mathscr{F}$ refers to the activation function, and y is the extracted feature. It should be noted that $\mathrm{RNN}^{[1]}$ or $\mathrm{RNN}^{[2]}$ can be any RNN model, such as RNN, LSTM, Bi-LSTM, GRU, and so on.

In the selection of a classifier for MicroNN, we adopt a per-class classification model. The model will establish a separate miniclassifier for each class of the task (see the part of classification in Figure 1). All miniclassifiers are connected with the feature extractor. In addition, to improve the performance of the classifier, we employ a loss function called one-class [24] in the training process:

$$\begin{aligned}\mathrm{loss} = {} & E_{X\sim P_X^{\mathrm{class}_i}}\left[-\log\left(\sigma\left(f_i(X)\right)\right)\right] + \eta \cdot E_{X\sim P_X^{\mathrm{class}_i}}\left\|\frac{\partial f_i(X)}{\partial X}\right\|_2^c \\ & + \pi \cdot \left\|\theta_i - \mu^*_{1:i-1}\right\|_2^2,\end{aligned} \tag{4}$$

where $X \sim P_X^{\mathrm{class}_i}$ refers to the data distribution of each class, σ is the activation function, and η, c, and π are all hyperparameters.

The first term in the loss function is negative log likelihood. Its purpose is to maximize the score of class_i during training. However, if there is no constraint to the negative log likelihood, it will lead to an unlimited increase in the score. Therefore, the second term, which is called H-reg, is applied in the loss function. It can reach a balance with the negative log likelihood. The structure of per-class classification is a multilayer perceptron with three layers, as shown in (5).

$$E_{X\sim P_X^{\mathrm{class}_i}}\left\|\frac{\partial f_i(X)}{\partial X}\right\|_2^c = E_{X\sim P_X^{\mathrm{class}_i}}\left\|\frac{\partial W_3 \cdot \left[\sigma\left(W_2 \cdot \sigma\left(W_1 \cdot X\right)\right)\right]}{\partial X}\right\|_2^c. \tag{5}$$

We can see that the derivation result of H-reg in the training process is related to the weight (W_1, W_2 and W_3). Therefore, H-reg can restrict the phenomenon of the unlimited growth of weight, which the negative log likelihood brings.

To make the parameters of classifiers between different classes in the same parameter space, the method uses the parameters from 1 to $i-1$ miniclassifiers to initialize the parameters of the i^{th} miniclassifier. Considering the existence of similar features between different classes, deep learning models have difficulty distinguishing classes in the process of training. During the testing stage, a method based on KL-divergence [44] is used to reduce the shared knowledge between classes, as described in the third term of the loss function. Assuming that there are T miniclassifiers in MicroNN, the calculation of shared knowledge among T miniclassifiers is as shown in (6).

$$\rho^*_{1:T} = \arg\min \sum_{i=1}^{T} \varphi_i \,\mathrm{KL}\left(P_i \| P_{1:T}\right), \tag{6}$$

where φ_i is the mixing ratio with $\sum_{i=1}^{T} \varphi_i = 1$, and P_i refers to the posterior parameter distribution of the i^{th} miniclassifier. The parameters of the i^{th} miniclassifier are updated by (7).

$$\vartheta_i^* = \vartheta_i - \tau \cdot \rho^*_{1:T}, \tag{7}$$

where τ is a hyperparameter.

4. Performance Analysis

The experiments are conducted on a computer with a GPU of Intel (R) Core (TM) i9-11900K and 64.00 GB memory. Experiments are done on two different ECG datasets to evaluate the performance of MicroNN. In the experiment, we divide each dataset into training sets, validation sets, and test sets, and their proportions are 6 : 2 : 2, respectively. To better evaluate the performance of the model, we mainly use precision (Pre), recall (Rec), and $F1$-score ($F1$) in the paper. Their relationship is as follows:

$$F1 = \frac{2 \cdot \mathrm{Pre} \cdot \mathrm{Rec}}{\mathrm{Pre} + \mathrm{Rec}}. \tag{8}$$

Table 3: The performance comparison between MicroNN and state-of-the-art methods based on MIT-BIH-AR.

Work	Overall ACC(%)	N (%)			S (%)			V (%)		
		PRE	REC	$F1$	PRE	REC	$F1$	PRE	REC	$F1$
MicroNN	98.4	99.0	99.2	99.1	95.1	93.3	94.2	96.5	97.3	96.8
Llamedo and Martinez [45]	78.0	99.1	78.0	87.3	41.0	76.0	53.3	88.0	83.0	85.4
De Chazal et al. [46]	81.9	99.2	86.9	92.6	38.5	75.9	51.1	81.9	77.7	80.0
He et al. [47]	95.1	97.6	97.5	97.6	59.4	83.8	69.5	90.2	80.4	85.0
Zhai and Tin [48]	97.6	98.5	97.6	98.0	74.0	76.8	75.4	92.4	93.8	93.1
Lee et al. [49]	98.1	99.6	97.4	98.5	77.6	91.5	84.0	86.0	89.2	87.6
Li et al. [50]	98.1	98.0	99.8	98.9	94.7	68.7	79.6	91.1	95.5	93.2
Niu et al. [51]	97.5	97.4	98.9	98.1	76.6	76.5	76.5	94.1	85.7	89.7

Table 4: The performance comparison between MicroNN and state-of-the-art methods based on INCART.

Work	Overall ACC(%)	N (%)			S (%)			V (%)		
		PRE	REC	$F1$	PRE	REC	$F1$	PRE	REC	$F1$
MicroNN	98.1	99.0	99.0	99.0	88.3	91.1	85.6	95.5	95.0	95.2
Merdjanovska and Rashkovska [52]	94.3	97.7	93.8	95.7	69.3	75.0	72.0	95.7	86.1	90.6
Bidias àMougoufan et al. [53]	81.9	97.7	95.9	96.8	61.8	80.8	70.0	60.9	69.1	64.7
Sun et al. [42]	99.7	99.7	100	99.8	60.8	90.2	72.7	99.0	94.2	96.5

4.1. Datasets Description. The details of the two datasets used in the experiment are as follows:

(1) MIT-BIH arrhythmia database (MIT-BIH-AR) includes the ECG record of 47 subjects studied by the BIH arrhythmia laboratory, and the sampling rate is 360 Hz. It contains 48 half-hour excerpts of two-channel ambulatory ECG recordings. In the experiment, we use the ECG record based on the MLII lead of MIT-BIH-AR. The full name of MIT-BIH is Massachusetts Institute of Technology, Beth Israel Hospital [42].

(2) St Petersburg INCART 12-lead arrhythmia database (INCART) consists of 75 annotated records from 32 humans, and the sampling rate is 257 Hz. Each record lasts for a half-hour and has the data of 12 standard leads. In the experiment, we use the ECG record based on the II lead of INCART.

4.2. Performance of MicroNN. At first, we compared the performance of MicroNN with existing methods at MIT-BIH-AR and INCART (see Tables 3 and 4). Micro has achieved good performance in ACC and $F1$. As can be seen from Table 3, the low accuracy of other methods is mainly because of the low $F1$ of class S. It is because class N and class S have many similar characteristics. The model is prone to recognition errors. However, MicroNN $'$s $F1$ in class S is much higher than other methods, which shows that MicroNN effectively reduces the shared knowledge among classes during training. Similarly, we can see from Table 4 that although the performance of MicroNN in classes N and V is not as good as partial work, MicroNN far exceeds other work in the classification of class S. It is mainly because that MicroNN can effectively solve the problem of the fuzzy boundary.

4.3. Measuring Time and Space Complexity of MicroNN. Table 2 compares the space complexity of MicroNN with other work, which shows that MicroNN is lightweight in terms of space complexity. In addition, we also measure the trend of training time and accuracy of MicroNN based on the change in the number of sample numbers in MIT-BIH-AR and INCART.

It can be seen from Figures 3 and 4 that the accuracy and training time of MicroNN increase with the increase of the number of instances of different datasets on the whole. In MIT-BIH-AR, when the number of instances reaches about 4000, the accuracy reaches 98.4% and tends to be stable. The training time is 23 seconds. For INCART, the number of instances reaches up to 4300 approximately, corresponding to the highest accuracy (98.1%), and the time of training is 27 seconds.

4.4. Threats to Validity. In the paper, threats to the validity of our proposed method are discussed from two perspectives: external validity and internal validity [14].

(1) Threats to internal validity: To prevent the occurrence of overfitting, we divide each dataset into a training set, validation set, and test set. We observed the change in classification accuracy based on different validation sets to check whether the classification model has overfitting.

(2) Threats to external validity: To verify the generalization of the model, we compared MicroNN on two different datasets. The experimental results show that the performance of MicroNN is better than other models.

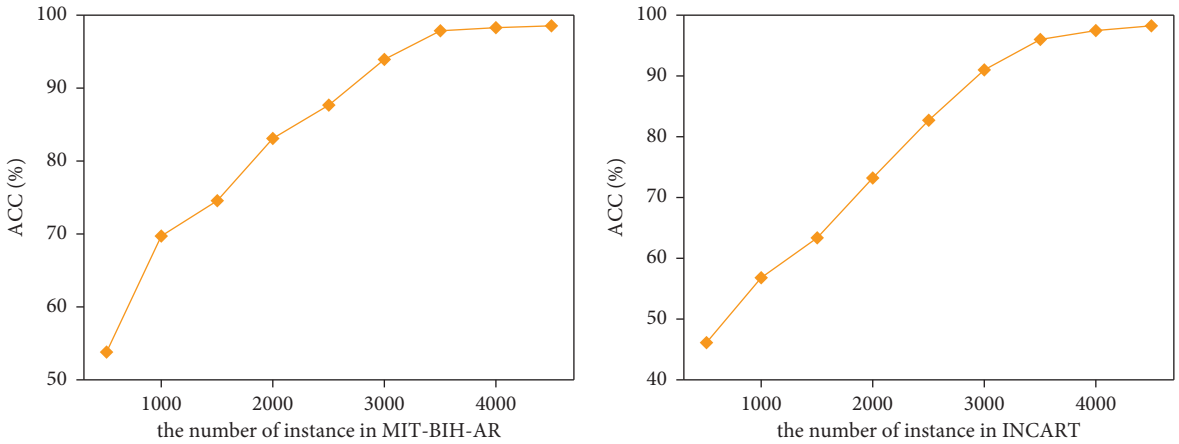

Figure 3: Accuracy with respect to the instance numbers in MIT-BIH-AR and INCART.

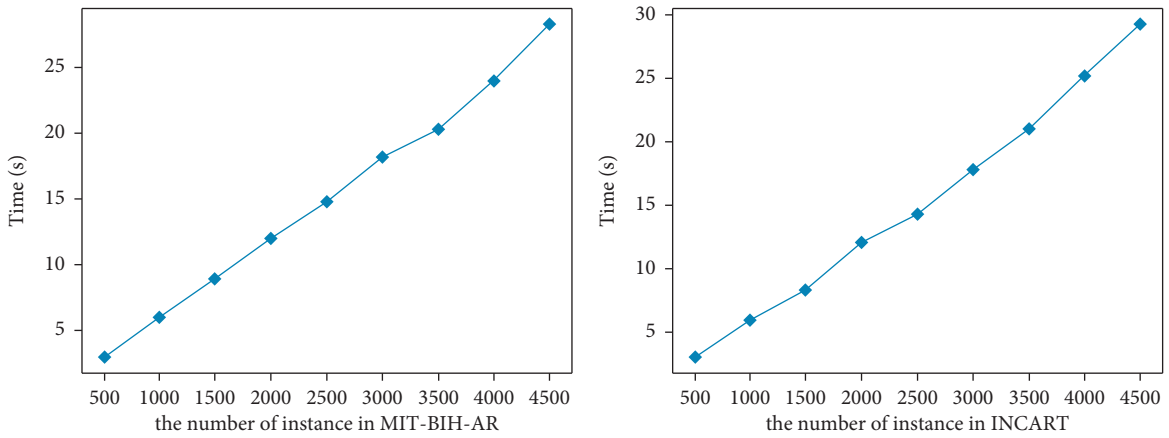

Figure 4: Time with respect to the instance numbers in MIT-BIH-AR and INCART.

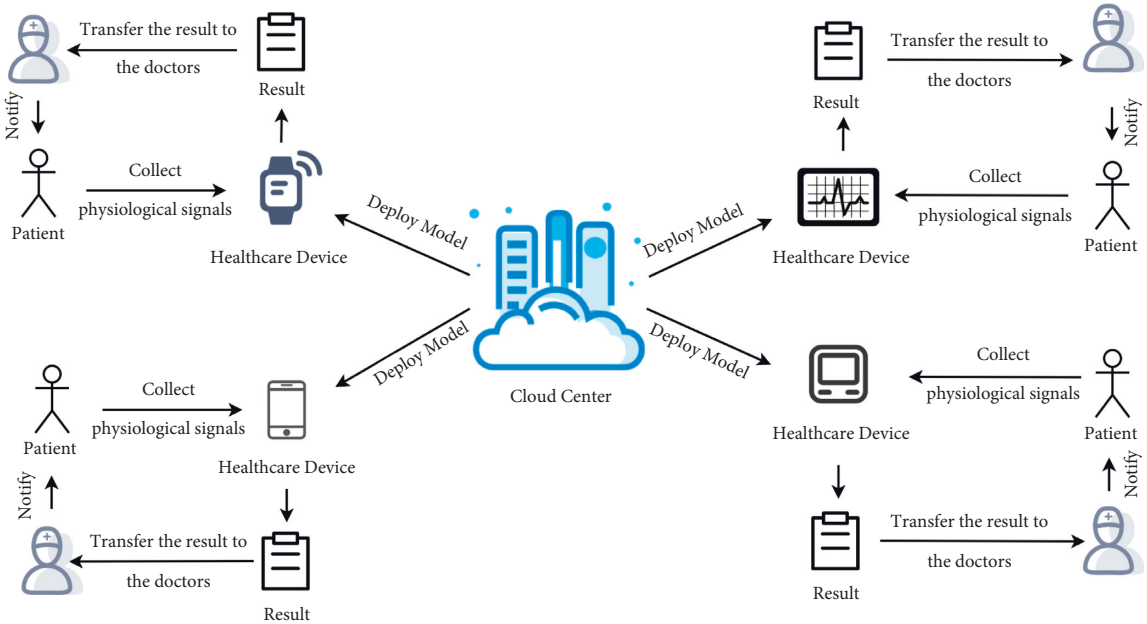

Figure 5: An application of MicroNN on the Internet of Medical Things based on edge computing.

5. An Engineering Application of MicroNN

Deep learning research on healthcare sensor data stream classification has attracted extensive attention [33, 54, 55]. However, we still face many challenges in the process of development. For example, the current urban medical resources are insufficient compared with the soaring urban population. The treatment efficiency cannot meet the needs of patients in time [4].

In this paper, we deploy MicroNN in edge devices to effectively improve the efficiency of medical treatment. Figure 5 shows an application example of MicroNN based on edge computing. Different healthcare devices have the function of classifying healthcare sensor data streams. The healthcare devices will classify the collected physiological signals of patients. Then, the results will be used to assist doctors in judging the condition of patients. Finally, the doctor will inform the patient of the specific situation. Therefore, MicroNN plays a certain role in promoting the development of sustainable and smart cities.

6. Conclusion and Future Work

In this paper, we propose a lightweight neural network model called MicroNN for classifying healthcare sensor data streams. It is composed of a microfeature extractor based on multiple recurrent neural networks (RNNs) and multiple miniclassifiers based on a full connection layer with three layers. At the same time, the method based on KL divergence is used to remove the shared knowledge among different classes to improve the performance of the model. In the experiment, we compared the accuracy, time complexity, and space complexity of the model with other models based on two different ECG datasets. MicroNN shows better performance than other works. In a word, MicroNN is a lightweight and efficient model. We will further improve the accuracy of MicroNN while ensuring the lightweight of the model and extend experiments on other healthcare sensor datasets.

Data Availability

The labeled datasets used to support the findings of this study are available from the corresponding author upon request.

Conflicts of Interest

No potential conflicts of interest were reported by the authors.

Acknowledgments

This work was partially supported by the Priority Academic Program Development of Jiangsu Higher Education Institutions.

References

[1] Z. Sang and K. Li, "ITU-T standardisation activities on smart sustainable cities," *IET smart cities*, vol. 1, no. 1, pp. 3–9, 2019.

[2] L. Sun, R. Zhou, and D. Peng, "Automatically building service-based systems with function relaxation," *IEEE Transactions on Cybernetics*, pp. 1–14, 2022.

[3] S. Heitlinger, N. Bryan-Kinns, and R. Comber, "The right to the sustainable smart city," in *Proceedings of the 2019 CHI Conference on Human Factors in Computing Systems*, pp. 1–13, ACM, New York, USA, May 2019.

[4] K. Okano, "Regional uneven distribution of healthcare resources related to medical imaging," *Journal of JART-English edition-*, vol. 7, pp. 18–27, 2021.

[5] Z. Qu, Z. Cheng, and W. Liu, "A novel quantum image steganography algorithm based on exploiting modification direction," *Multimedia Tools and Applications*, vol. 78, no. 7, pp. 7981–8001, 2019.

[6] Z. Ebrahimi, M. Loni, M. Daneshtalab, and A. Gharehbaghi, "A review on deep learning methods for ecg arrhythmia classification," *Expert Systems with Applications X*, vol. 7, Article ID 100033, 2020.

[7] L. Sun, Q. Yu, D. Peng, S. Subramani, and X. Wang, "Fogmed: a fog-based framework for disease prognosis based medical sensor data streams," *Computers, Materials & Continua*, vol. 66, no. 1, pp. 603–619, 2020.

[8] K. Wang, Y. Zhao, Q. Xiong et al., "Research on healthy anomaly detection model based on deep learning from multiple time-series physiological signals," *Scientific Programming*, vol. 2016, Article ID 5642856, 9 pages, 2016.

[9] T. Wen and Z. Zhang, "Deep convolution neural network and autoencoders-based unsupervised feature learning of eeg signals," *IEEE Access*, vol. 6, pp. 25399–25410, 2018.

[10] C. Zhang, G. Wang, J. Zhao, P. Gao, and J. Lin, "Patient-specific ECG classification based on recurrent neural networks and clustering technique," in *Proceedings of the 2017 13th IASTED International Conference on Biomedical Engineering (BioMed)*, pp. 63–67, IEEE, Innsbruck, Austria, February 2017.

[11] S. Harbola and V. Coors, "One dimensional convolutional neural network architectures for wind prediction," *Energy Conversion and Management*, vol. 195, pp. 70–75, 2019.

[12] Y. Mao, C. You, J. Zhang, K. Huang, and K. B. Letaief, "A survey on mobile edge computing: the communication perspective," *IEEE Communications Surveys & Tutorials*, vol. 19, no. 4, pp. 2322–2358, 2017.

[13] S. Roy, J. Li, B.-J. Choi, and Y. Bai, "A lightweight supervised intrusion detection mechanism for iot networks," *Future Generation Computer Systems*, vol. 127, pp. 276–285, 2022.

[14] L. Sun and J. Wu, "A scalable and transferable federated learning system for classifying healthcare sensor data," *IEEE Journal of Biomedical and Health Informatics*, 2022.

[15] Y. Zhou, S. Chen, Y. Wang, and W. Huan, "Review of research on lightweight convolutional neural networks," in *Proceedings of the 2020 IEEE 5th Information Technology and Mechatronics Engineering Conference (ITOEC)*, pp. 1713–1720, IEEE, Chongqing, China, June 2020.

[16] H.-Y. Chen and C.-Y. Su, "An enhanced hybrid mobilenet," in *Proceedings of the 2018 9th International Conference on Awareness Science and Technology (iCAST)*, pp. 308–312, IEEE, Taipei, Taiwan, September 2018.

[17] S. Huang, A. Liu, S. Zhang, T. Wang, and N. N Xiong, "BD-VTE: a novel baseline data based verifiable trust evaluation scheme for smart network systems," *IEEE transactions on network science and engineering*, vol. 8, no. 3, pp. 2087–2105, 2021.

[18] H. Liu, X. Mi, and Y. Li, "Smart deep learning based wind speed prediction model using wavelet packet decomposition, convolutional neural network and convolutional long short term memory network," *Energy Conversion and Management*, vol. 166, pp. 120–131, 2018.

[19] H. Park and Y. Kim, "Prediction of strength of reinforced lightweight soil using an artificial neural network," *Engineering Computations*, vol. 28, no. 5, pp. 600–615, 2011.

[20] J. Wang, W. Bao, L. Sun, X. Zhu, B. Cao, and P. S. Yu, "Private model compression via knowledge distillation," *Proceedings of the AAAI Conference on Artificial Intelligence*, vol. 33, no. 01, pp. 1190–1197, 2019.

[21] Z. Liu, J. Li, Z. Shen, G. Huang, S. Yan, and C. Zhang, "Learning efficient convolutional networks through network slimming," in *Proceedings of the IEEE international conference on computer vision*, pp. 2736–2744, IEEE, Venice, Italy, August 2017.

[22] J. Yin, W. Lo, S. Deng, Y. Li, Z. Wu, and N Xiong, "Colbar: a collaborative location-based regularization framework for QoS prediction," *Information Sciences*, vol. 265, pp. 68–84, 2014.

[23] Q. Yu and L. Sun, "LPClass: lightweight personalized sensor data classification in computational social systems," *IEEE Transactions on Computational Social Systems*, pp. 1–11, 2022.

[24] W. Hu, Q. Qin, M. Wang, J. Ma, and B. Liu, "Continual learning by using information of each class holistically," *Proceedings of the AAAI Conference on Artificial Intelligence*, vol. 35, no. 9, pp. 7797–7805, 2021.

[25] Z. Qu, H. Sun, and M. Zheng, "An efficient quantum image steganography protocol based on improved EMD algorithm [J]," *Quantum Information Processing*, vol. 20, no. 2, pp. 1–29, 2021.

[26] W. Liu, Q. Huang, S. Chang, H. Wang, and J. He, "Multiple-featurebranch convolutional neural network for myocardial infarction diagnosis using electrocardiogram," *Biomedical Signal Processing and Control*, vol. 45, pp. 22–32, 2018.

[27] M. A. Rodriguez and M. J. Egenhofer, "Determining semantic similarity among entity classes from different ontologies," *IEEE Transactions on Knowledge and Data Engineering*, vol. 15, no. 2, pp. 442–456, 2003.

[28] M. Chen, G. Wang, P. Xie et al., "Region aggregation network: improving convolutional neural network for ecg characteristic detection," in *Proceedings of the 2018 40th Annual International Conference of the IEEE Engineering in Medicine and Biology Society (EMBC)*, pp. 2559–2562, IEEE, Honolulu, HI, USA, July 2018.

[29] T. J. Jun, H. M. Nguyen, D. Kang, D. Kim, D. Kim, and Y.-H. Kim, "Ecg arrhythmia classification using a 2-d convolutional neural network," 2018, http://arxiv.org/abs/1804.06812.

[30] S. Saadatnejad, M. Oveisi, and M. Hashemi, "Lstm-based ecg classification for continuous monitoring on personal wearable devices," *IEEE journal of biomedical and health informatics*, vol. 24, no. 2, pp. 515–523, 2020.

[31] O. Faust, A. Shenfield, M. Kareem, T. R. San, H. Fujita, and U. R. Acharya, "Automated detection of atrial fibrillation using long short term memory network with rr interval signals," *Computers in Biology and Medicine*, vol. 102, pp. 327–335, 2018.

[32] Y. Wang, L. Sun, and S. Subramani, "Cab: classifying arrhythmias based on imbalanced sensor data," *KSII Transactions on Internet and Information Systems (TIIS)*, vol. 15, no. 7, pp. 2304–2320, 2021.

[33] W. J. Tan, X. Y. H. Lim, T. Lee, S. C. Wong, H. J. Koh, and D Yeo, "Enhancing the caregiving experience of family care partners in Singapore through an arts programme for persons with dementia: an exploratory study," *Aging & Mental Health*, pp. 1–7, 2021.

[34] Z. Qu, S. Chen, and X. Wang, "A secure controlled quantum image steganography algorithm[J]," *Quantum Information Processing*, vol. 19, no. 10, pp. 1–25, 2020.

[35] P. Lu, "A position self-adaptive method to detect fake access points," *Journal of Quantum Computing*, vol. 2, no. 2, p. 119, 2020.

[36] O. Behadada and M. A. Chikh, "An interpretable classifier for detection of cardiac arrhythmias by using the fuzzy decision tree," *Artificial Intelligence Research*, vol. 2, no. 3, pp. 45–58, 2013.

[37] J. A. Nasiri, M. Naghibzadeh, H. S. Yazdi, and B. Naghibzadeh, "Ecg arrhythmia classification with support vector machines and genetic algorithm," in *Proceedings of the 2009 Third UKSim European Symposium on Computer Modeling and Simulation*, pp. 187–192, IEEE, Athens, Greece, November 2009.

[38] C. Bensujin and C. Hubert, "Detection of st segment elevation myocardial infarction (stemi) using bacterial foraging optimization technique," *Int J Eng Technol*, vol. 6, no. 2, pp. 1212–1223, 2014.

[39] K. Sharipov, "International journal of advanced research in science," *engineering and technology*, vol. 27, p. 2979, 2020.

[40] S. M. Jadhav, S. L. Nalbalwar, and A. A. Ghatol, "Artificial neural network models based cardiac arrhythmia disease diagnosis from ecg signal data," *International Journal of Computer Applications*, vol. 44, no. 15, pp. 8–13, 2012.

[41] A. Arneodo, G. Grasseau, and M. Holschneider, "Wavelet transform of multifractals," *Physical Review Letters*, vol. 61, no. 20, p. 2281, 1988.

[42] L. Sun, Y. Wang, Z. Qu, and N. N. Xiong, "BeatClass: a sustainable ECG classification system in IoT-based eHealth," *IEEE Internet of Things Journal*, vol. 9, no. 10, pp. 7178–7195, 2022.

[43] D. K. Dennis, D. Acar, V. Mandikal et al., "Shallow rnns: a method for accurate time series classification on tiny devices," 2019.

[44] S. W. Lee, J. H. Kim, J. Jun, and J. W. Ha, "Overcoming catastrophic forgetting by incremental moment matching," *Advances in Neural Information Processing Systems*, p. 30, 2017.

[45] M. Llamedo and J. P. Mart´ınez, "Heartbeat classification using feature selection driven by database generalization criteria," *IEEE Transactions on Biomedical Engineering*, vol. 58, no. 3, pp. 616–625, 2011.

[46] P. De Chazal, M. O'Dwyer, and R. B. Reilly, "Automatic classification of heartbeats using ecg morphology and heartbeat interval features," *IEEE Transactions on Biomedical Engineering*, vol. 51, no. 7, pp. 1196–1206, 2004.

[47] J. He, J. Rong, L. Sun, H. Wang, and Y. Zhang, "An advanced two-step dnn-based framework for arrhythmia detection," *Advances in Knowledge Discovery and Data Mining*, vol. 12085, p. 422, 2020.

[48] X. Zhai and C. Tin, "Automated ecg classification using dual heartbeat coupling based on convolutional neural network," *IEEE Access*, vol. 6, pp. 27 465–527 472, 2018.

[49] M. Lee, T.-G. Song, and J.-H. Lee, "Heartbeat classification using local transform pattern feature and hybrid neural fuzzy-logic system based on self-organizing map," *Biomedical Signal Processing and Control*, vol. 57, Article ID 101690, 2020.

[50] Y. Li, Y. Pang, J. Wang, and X Li, "Patient-specific ECG classification by deeper CNN from generic to dedicated," *Neurocomputing*, vol. 314, pp. 336–346, 2018.

[51] J. Niu, Y. Tang, Z. Sun, and W Zhang, "Inter-patient ECG classification with symbolic representations and multi-perspective convolutional neural networks," *IEEE journal of biomedical and health informatics*, vol. 24, no. 5, pp. 1321–1332, 2020.

[52] E. Merdjanovska and A. Rashkovska, "Cross-database generalization of deep learning models for arrhythmia classification," in *Proceedings of the 2021 44th International Convention on Information, Communication and Electronic Technology (MIPRO)*, pp. 346–351, IEEE, Opatija, Croatia, September 2021.

[53] J. B. Bidias à Mougoufan, J. S. A. Eyebe Fouda, M. Tchuente, and W. Koepf, "Three-class ecg beat classification by ordinal entropies," *Biomedical Signal Processing and Control*, vol. 67, Article ID 102506, 2021.

[54] J. Guo and B. Li, "The application of medical artificial intelligence technology in rural areas of developing countries," *Health equity*, vol. 2, no. 1, pp. 174–181, 2018.

[55] M. Wu, L. Tan, and N. Xiong, "A structure fidelity approach for big data collection in wireless sensor networks," *Sensors*, vol. 15, no. 1, pp. 248–273, 2014.

Hindawi
Computational Intelligence and Neuroscience
Volume 2022, Article ID 4478978, 9 pages
https://doi.org/10.1155/2022/4478978

Research Article

Research on SLAM Road Sign Observation Based on Particle Filter

Yifan Wang and Xiaoyan Wang

School of Mechanical and Electrical Engineering, Xi'an University of Architecture and Technology, Xi'an 710055, China

Correspondence should be addressed to Yifan Wang; yifanwang1219@xauat.edu.cn

Received 16 May 2022; Accepted 28 May 2022; Published 20 June 2022

Academic Editor: Yaxiang Fan

Copyright © 2022 Yifan Wang and Xiaoyan Wang. This is an open access article distributed under the Creative Commons Attribution License, which permits unrestricted use, distribution, and reproduction in any medium, provided the original work is properly cited.

With the development of computer hardware technology, the real-time problem of visual target tracking algorithm increasingly depends on hardware solutions. The core problem of visual target tracking is how to enhance the robustness of tracking algorithm to various complex background environments and various interference factors. Aiming at overcoming the defect that the traditional SLAM (simultaneous localization and map building) algorithm based on EKF (extended Kalman filter) has a slow repair speed for environmental interference, a Monocular SLAM_WOCPF (Monocular vision SLAM based on weight optimization combined particle filter) algorithm is proposed. The weights of all particles are reoptimized in the particle set and they are combined with the tendency of particles to degenerate and deplete. In this way, the chance of self replication of low weight particles is increased, thus increasing the diversity of the whole sample. Furthermore, the improved PF (particle filter) algorithm is applied to solve the problem of road sign observation of mobile robots, so as to expand its application scope. The results show that the mean road sign errors of the Monocular SLAM_WOCPF algorithm in two noise environments are 0.332/m and 0.441/m. The conclusion shows that the Monocular SLAM_WOCPF road sign observation method proposed in this paper can effectively improve the matching success rate of visual road signs and improve the observation quality.

1. Introduction

Human feeling and processing information is an important field of artificial intelligence research and application. Human perception of the external world is mainly obtained through sensory organs such as vision, touch, hearing, and smell, and about 80% of the information is obtained through visual organs [1]. When the mobile robot is running, various sensors installed on the mobile robot will sense the surrounding environment in real time; collect relevant data; and, according to this information, judge the road conditions around the mobile robot, the number and direction of pedestrians, the number and direction of mobile robots, and other information. In the process of SLAM (simultaneous localization and map building), some sensors need to be used as data measurement and acquisition tools. Computers can process image and video data by simulating human visual mechanism and accomplish tasks such as image classification and target detection and tracking, which makes the research of computer vision an important part of intelligent driving system.

With the development of robots toward intelligence, the research significance of robot autonomy is becoming more and more important [2]. Among robots, the autonomous navigation of mobile robot in unknown environment fully reflects the autonomy of robot. PF (particle filter) is a Monte Carlo method. Its basic idea is to update the robot's position distribution by using new observation data [3]. Recently, PF has become the core method to solve robot problems with higher dimensions (such as SLAM). Zhang et al. used Rao-Blackwellized PF to effectively estimate the robot path and related maps [4]. Sola et al. introduced fading factor in the process of updating covariance of unscented KF (Kalman filtering) and applied it to integrated navigation, which improved the robustness of integrated navigation system when the state changed suddenly [5]. Miao and Li put forward the resampling method to solve the problem of particle degradation, which stimulated the research upsurge of PF [6]. At present, there are still many problems to be

solved in PF algorithm, such as the lack of particle diversity. EKF (extended Kalman filter) can realize the optimal estimation of nonlinear system state by observing the input and output data of the system.

The sensors of the robot should take into account various tasks as much as possible, and cameras are undoubtedly an ideal choice. With their rich information and low price, cameras have attracted more and more attention in robot positioning and mapping. The development of machine vision can be applied to the working environment that is harmful to human health or the environment with high risk [2]. On the other hand, it also improves the safety of people's lives and property and is conducive to improving people's quality of life. As the target tracking and filtering technology is widely used, it is closely related to national defense construction and people's daily life. In recent years, the research in related fields has also been paid attention to by the relevant state departments. Therefore, it has a profound realistic background to study target tracking in the field of nonlinear estimation and the application of PF in road sign observation.

2. Related Work

2.1. Development Status of Mobile Robots. SLAM problem of mobile robot includes the determination of its own pose information and the acquisition and processing of external environment information. When moving in an unknown environment, the robot uses its own sensors to calculate its own position information and detect unknown road signs around it. With the realization of industrialization and informatization in the 21st century, robot technology has been further developed and improved.

Nasir et al. get feedback information through trial and error iteration between robot and environment to optimize the strategy [7]. It does not depend on the environmental model and prior knowledge, and it has the characteristics of autonomous learning and online learning. It has gradually become the research hotspot of robot path planning in unstructured environment. Jin-Chun and Shin-Dug put forward a hierarchical learning method based on selection. In the first layer, Q-learning algorithm is used to train the basic behaviors of sports, and in the second layer, these basic behaviors are coordinated to solve the planning tasks. Simulation results show that this algorithm can be well applied to path planning in unknown environment [8]. Yun-Won et al. use Monocular RGB vision sensor to build a double-layer reinforcement learning network structure, which can achieve a good obstacle avoidance effect and lay a good foundation for the realization of path planning [9]. Silva et al. obtained the optimal parameters by optimizing the strategy parameters [10].

On the basis of Li et al.'s traditional genetic algorithm, an improved genetic algorithm is proposed, which uses serial number coding and genetic operators suitable for this coding mechanism. At the same time, more new mutation operators, insertion operators, and deletion operators are added, which improves the optimal preservation strategy, finally improves the running speed of the algorithm, and enhances the obstacle avoidance ability in the search process [11]. Jia et al. proposed an idea of RRT (rapid-exploring random tree) algorithm and rolling path planning to guide mobile robots to avoid obstacles online [12]. Sun et al. proposed a path planning method for high degree-of-freedom articulated mobile robot with fast random search tree. To realize the path planning in high-dimensional space, it first describes a robot theme selected according to the complexity of the path and then selects the robot joints involved, that is, the path planning with adaptive dimensions of configuration space and sampling [13]. Fang et al. proposed an improved path planning method for mobile robots based on the traditional bee colony algorithm. This method combines artificial bee colony algorithm as a local search process and uses evolutionary programming algorithm to refine the feasible path found by a set of local solutions, thereby improving the accuracy of the algorithm and shortening the search time [14].

2.2. Overview of PF Research. The core idea of PF algorithm is to use a group of particle sets with different weights to represent the prior density function, then calculate the likelihood of each particle, and finally fuse the prior value data of each particle and the newly obtained likelihood data, so as to obtain an approximate particle set that can describe the posterior density function of the estimated state.

In just a few decades, the application scope of PF has been continuously expanded, such as in the fields of economics, traffic control, wireless signal processing, and military. PF is playing a huge role.

Chen et al. solved the problem of particle degradation by adding resampling process. The basic idea of resampling is to copy the particles with high weights in the resampling stage to achieve the purpose of suppressing the increase of the number of particles with low weights [15]. A new PF algorithm of particle swarm optimization simulated annealing proposed by Zhu et al. overcomes the difficulty of sampling in high-dimensional space [16] Algorithm 1. Vallivaara et al. designed a real-time PF tracking algorithm with distributed parallel PF tracking function according to the data concurrency characteristics inside PF, which was proved to meet the time constraints of hard real-time systems [17]. Yang et al. proposed using unscented KF as a proposed distribution function for sampling particles [18]; In the related research on multitarget tracking estimation, Gil Aparicio et al. pointed out that the application of PF in multitarget tracking requires not only accurate modeling technologies such as new targets, disappearances, false alarms, false alarms, and over reporting, but also complex and variable technologies such as multisensor information fusion [19].

In the real world, people's life scenes and problems are mostly nonlinear, so linear filtering is far less widely used than nonlinear filtering. KF is the best estimation under linear Gaussian model. Moratuwage et al. argued that KF is only a special case of Bayesian filtering. Bayesian filtering provides the best research idea for state estimation of dynamic systems [20]. Do et al. combined target tracking with deep learning, applied target tracking to computer vision

tracking, and expanded the application range of target tracking [21].

3. Research Method

3.1. Motion Model of Mobile Robot. The mobile robot is generally a highly nonlinear system, so it is difficult to accurately model the robot. Generally, the simplified approximate model is established. However, the error will be introduced into the approximate model, which is called model noise, and the sensor observation will also produce error, which is called observation noise. For the convenience of research, all noises are assumed to be Gaussian white noises in this paper.

There are many kinds of mobile robots, which can be divided into indoor mobile robots and outdoor mobile robots according to the working environment. Usually, the constraints can be classified into complete constraints and non-holonomic constraints. The complete constraints limit only the spatial position of the controlled object or both the spatial position and the motion speed, so they are called geometric constraints, while the non-holonomic constraints are constraints on the motion speed of the system and cannot be converted into spatial position constraints through integration. Simply put, they are non-integrable velocity constraints.

In this paper, the path tracking problem of mobile robot is described as taking an effective control decision and designing an appropriate control algorithm with the cooperation of a certain navigation system, so that the mobile robot moves in the plane rectangular coordinate system according to the curve planned beforehand, which is called the path tracking problem of mobile robot.

In the research of tracking control of mobile robots, it is generally assumed that the wheels of mobile robots touch the ground in a point way, satisfying the assumption that there is only pure rolling at the contact point [16], but no longitudinal sliding or lateral sliding. That is to say, this non-holonomic constraint is ideal, and it strictly satisfies the mathematical definition of non-holonomic constraint. If the mobile robot moves on a plane, then the rectangular coordinate system XOY can be set as the global coordinate system, as shown in Figure 1.

From Figure 1, aiming at the point P, the discrete kinematics model of the mobile robot can be obtained by using analytical method and coordinate operation, and its expression is as follows:

$$\begin{bmatrix} x_p(k+1) \\ y_p(k+1) \\ \theta_p(k+1) \end{bmatrix} = \begin{bmatrix} x_p(k) \\ y_p(k) \\ \theta_p(k) \end{bmatrix} + \Delta T \begin{bmatrix} \cos\theta_p(k) \\ \sin\theta_p(k) \\ 0 \end{bmatrix} \begin{bmatrix} v_p(k) \\ w_p(k) \end{bmatrix}, \quad (1)$$

where ΔT is the sampling time, the control input of the mobile robot is $u_p(k) = [v_p(k), w(k)]^T$, and its state vector is $q(k) = [x_p(k), y_p(k), \theta_p(k)]^T$.

In this module, an algorithm is designed to find the best reference signal, and the reference signal is selected as the robot's expected heading angle and the road surface curvature in front. The third module is the feedback controller, which takes the reference signal and the actual pose of the robot as the controller inputs, calculates the appropriate control quantity according to a certain control method, and sends it to the fourth module. The fourth module is the final control object mobile robot, that is, the mechanical realization part of the control quantity. For simplicity, only the wheel load of the mobile robot when it is stationary or moving in a straight line at a uniform speed is considered here. The load diagram of the driving wheel and universal wheel of the mobile robot is shown in Figure 2.

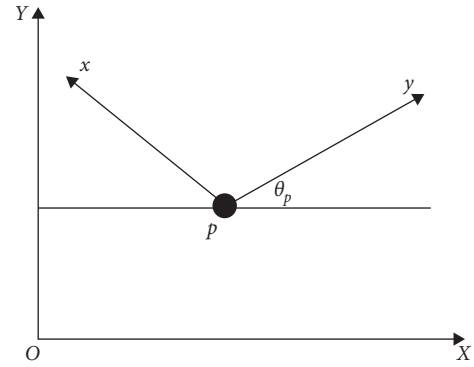

Figure 1: Motion diagram of mobile robot.

Assuming that the wheels are rigid wheels (with the elastic deformation being negligible) and the center of mass of the mobile robot is on the longitudinal axis of symmetry, according to the principle of force balance, we can obtain the vertical load on the driving wheel and the universal wheel as follows:

$$F_f = \frac{Mgl_b}{l_a + l_b}, \qquad F_l = F_r \frac{Mgl_a}{2(l_a + l_b)}. \quad (2)$$

Among them, c is the center of mass of the mobile robot; F_f is the reaction force of the universal wheel on the ground; F_t, F_f is the reaction to the force of the driving wheel on the ground; M is the total mass of the mobile robot; l_a is the horizontal distance from the universal wheel to the center of mass c; l_b is the horizontal distance from the axis of the two driving wheels to the center of mass c; and g is the gravitational acceleration.

Since the world coordinates of each characteristic road sign are constant, (x_i, y_i) is used to represent the coordinates of the ith characteristic road sign B_i, and $(x_c(k), y_c(k))$ is the coordinates of the center point of the mobile robot at time k, so the observation model is as follows:

$$z(k) = \begin{bmatrix} r(k) \\ \beta(k) \end{bmatrix} = \begin{bmatrix} \sqrt{(x_i - x_c(k))^2 + (y_i - y_c(k))^2} \\ \tan^{-1}\dfrac{y_i - y_c(k)}{x_i - x_c(k)} - \phi + \dfrac{\pi}{2} \end{bmatrix} + v(k). \quad (3)$$

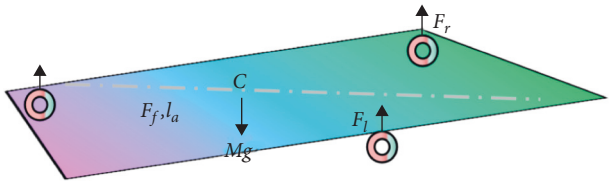

Figure 2: Schematic diagram of wheel load.

Similar to the state model, where the vector $v(k)$ is the observed noise data, it is also set as a 0-vector, and its covariance is set as $R(k)$.

3.2. Monocular Visual SLAM Road Sign Observation

3.2.1. SLAM Model Description. The mobile robot uses the structured map information to constantly calibrate its own position to realize accurate positioning, or to realize accurate map construction when the current position is known by a high-precision hardware sensor system. Because SLAM mainly solves robot pose estimation and environmental feature location estimation, the modeling and positioning algorithms in the field of mobile robot navigation mainly adopt probability algorithm, and EKF, PF, and other methods are the most classic and commonly used online SLAM solutions.

Because EKF algorithm is unique in dealing with uncertain information, it has been in the mainstream position in the research of robot synchronous positioning and map construction. However, in recent years, in order to maintain the uncertainty between robots and features and between features, many researches have been devoted to reducing the computational scale of EKF algorithm. However, with the continuous increase of the number of environmental features, the computational resources are still inevitably exhausted. At the same time, EKF algorithm assumes that the state noise and the observation noise are uncorrelated white noise, but this assumption is very ideal, and more consideration should be given to colored noise when dealing with practical problems.

The appearance of PF algorithm solves the problem of state estimation of nonlinear and non-Gaussian systems. It helps to solve a large number of probability problems in solving SLAM problems and samples variables to approximate the probability with a large number of sampling distributions.

SLAM problem involves the estimation of its own position and the construction of external continuous environment map. In the research process, we usually use state vector x_k to represent the posture state vector of mobile robot at k time, m_j to represent the position state vector of the jth environmental characteristic road sign, u_k to represent the input control quantity exerted on the robot at k time, and z_k to represent the observation of the sensor equipped by the robot at k time.

Based on the Bayesian formula and the motion process of robot being Markov process, $p(x_k, m|z_{1k}, u_{1k})$ can be simplified into the following formula:

$$p(x_k, m|z_{1k}, u_{1k}) \propto p(z_k|x_k, m) \int p(x_k|x_{k-1}, u_k) \\ p(x_{k-1}, m|z_{1k-1}, u_{1k-1}) dx_{k-1}. \tag{4}$$

The general model of SLAM problem can be obtained from (4).

3.2.2. Road Sign Observation Realization. PF is a recursive Bayesian filtering algorithm based on Monte Carlo thought [11]. Based on the theorem of large numbers in probability and statistics theory, this method uses computer simulation technology to solve some problems that are difficult to solve directly. Monte Carlo methods randomly simulate a certain distribution through a series of sampling points. On the basis of a large number of experiments, the probability of random events is infinitely close to the frequency (Algorithm 1).

The basic idea of PF is to estimate $p(x_t|z_t, u_t)$ with some samples or particles $\{x_t^{(i)}\}$. $x_t^{(i)}$ is the ith sample among M samples, and M is the size of PF.

After repeating the above process several times, except for one or a few particles, the weight of other particles is approximately zero. This phenomenon is called particle degradation, and it is also an obvious problem in sequence importance sampling. It wastes a lot of computing resources on most particles whose contribution to state estimation is almost zero. Through the analysis, it can be seen that with the iterative operation of the filtering process, the variance of particle weight will increase continuously.

PF can be used in any state space description system. Its core lies in constructing a posterior probability density function, which needs to reflect the real probability distribution. By sampling the constructed posterior probability function, we can approximate the sampling process from the real distribution [13].

Let $\{x_{0:k}^i, w_k^i\}_{i=1}^N$ be the particles sampled from the posterior probability density function and their corresponding weights, and the weights of the particles satisfy $\sum_i w_k^i = 1$. With the above-mentioned series of particle pairs, the posterior probability density of the system can be expressed by the following formula:

$$p(X_k|Z_k) \approx \sum_{i=1}^{N} w_k^i \delta(X_k - X_k^i). \tag{5}$$

In the formula, the solution process of posterior probability density function is transformed from integral to algebraic summation problem, and the calculation process is simplified. Take solving the statistics of function $f(x)$ as an example, and the following formula is its expected expression:

$$E(f(x)) = \int f(x) p(X_k|Z_k) dx = \sum_{i=1}^{N} w_k^i f(x_k^i). \tag{6}$$

PF tracking is a robust visual target tracking algorithm, which can effectively solve the problems of nonlinear state and non-Gaussian noise distribution in visual target tracking and can simultaneously track various state changes of visual

(1) Initialize random M particles.
(2) Find the motion model of each particle.
(3) For each particle, predict the observed value, and then calculate the weight according to the observed value.
(4) Resampling. Reselect the particles that best explain the observations according to the weights.

Algorithm 1: PF algorithm.

target, without any requirement for the motion state of visual platform, and it has achieved good results in practical application. With the in-depth study of PF tracking, effectively solving these problems is of great significance to further improve the robustness of PF tracking algorithm and expand its application scope.

In order to reduce the loss of low-weight particles in each filtering, this section introduces a new algorithm, Monocular SLAM_WOCPF (Monocular vision SLAM based on weight optimization combined particle filter) algorithm.

The basic idea is to first calculate the particle swarm weight $\{w_k^i, i = 0, \cdots, N\}$ through important weights; then take the average value $\overline{w}_k$ of the particle swarm weight; then carry out appropriate optimization and combination operation on $\overline{w}_k, w_k'\overline{w}_k, w_k'$; and then get a new particle set $\{x_k^i, \psi_k^i\}_{i=1}^N$.

The specific formula is as follows:

$$\begin{aligned} \overline{w}_k &= \frac{\sum_{i=1}^N w_k^i}{N}, \\ \psi_k^i &= \frac{K-1}{K} w_k^i + \frac{\overline{w}_k}{K}, \end{aligned} \tag{7}$$

where $K\,(1 \le K \le +\infty)$ is the scaling factor. Under the effect of weight optimization and combination algorithm, the weight of the original low-weight particles is improved, so that more particles participate in the reproduction in the resampling process.

Under the condition of camera motion, the influence of camera translation on motion detection should usually be considered. Some methods first achieve the registration of consecutive images by motion estimation and then detect the motion by frame difference or optical flow [19]. In this work, the visual saliency map based on dynamic features is regarded as a global suggested distribution for PF tracking. For simplicity, this work uses frame difference method to detect the motion in the scene as MSM (Motion Saliency Map).

$$\mathrm{MSM} = \left| I_k - I_{k-1} \right|, \tag{8}$$

where I_k represents the image at the k time.

Set S_{t-1}, robot control quantity u_t, and observation quantity z_t are used to find set S_t. Firstly, each particle in the set S_{t-1} is used to generate an estimate of the pose of the robot at time t:

$$s_t^{(i)} \sim p\left(s_t | u_t, s_{t-1}^{(i)}\right). \tag{9}$$

The weights required for resampling the robot path particles are calculated as follows:

$$w_t^{(i)} \propto \frac{p\left(s^{t,(i)} | z^t, u^t, n^t\right)}{p\left(s^{t,(i)} | z^{t-1}, u^t, n^{t-1}\right)}. \tag{10}$$

In this paper, we need to match the road sign information detected at the current moment with the road sign information in the state vector according to the feature matching algorithm, so as to determine the stable and repeatable road sign points existing at the current moment. That is, each iteration only needs to extract one data item from the observation data set.

Map feature estimation is represented by $\{u^1, p^1, \cdots, u^M, p^M\}$. u^i, p^i represent the Gaussian mean and variance of the ith map feature, respectively. When the robot is moving, if a landmark feature in the map is detected at a certain moment, the following formula is adopted to update the feature. If no new landmark feature is detected, the mean and variance are equal to the values of the previous moment.

$$\begin{aligned} u_{k+1}^i &= u_k^i + K_{k+1}^i \left[z_{k+1}^i - h\left(u_k^i\right) \right], \\ p_{k+1}^i &= p_k^i + K_{k+1}^i S_{k+1}^i \left(K_{k+1}^i\right)^T. \end{aligned} \tag{11}$$

To facilitate understanding, Figure 3 shows the algorithm flow of Monocular SLAM_WOCPF.

The implementation process of the algorithm is as follows:

(1) Initialize. Determine the initial state value and covariance matrix of the mobile robot system, and sample the first 10 samples from the initial distribution.
(2) Forecast. Based on the motion model of the robot, the pose of the robot at $k + 1$ time is predicted by the control input.
(3) Data association. The observed value at $k + 1$ time is obtained and correlated with the estimated observed value of each particle at the time. These correlation processes are independent of each other.
(4) Get the suggested distribution. Based on the observed values of each particle, the mean and variance of each particle's pose estimation are calculated, and a Gaussian distribution function is constructed with the mean and variance as the importance probability density function to be calculated.
(5) Robot path estimation. The algorithm estimates the path of the robot and calculates the particle set used to characterize the posterior probability distribution of the robot at $k + 1$ time.

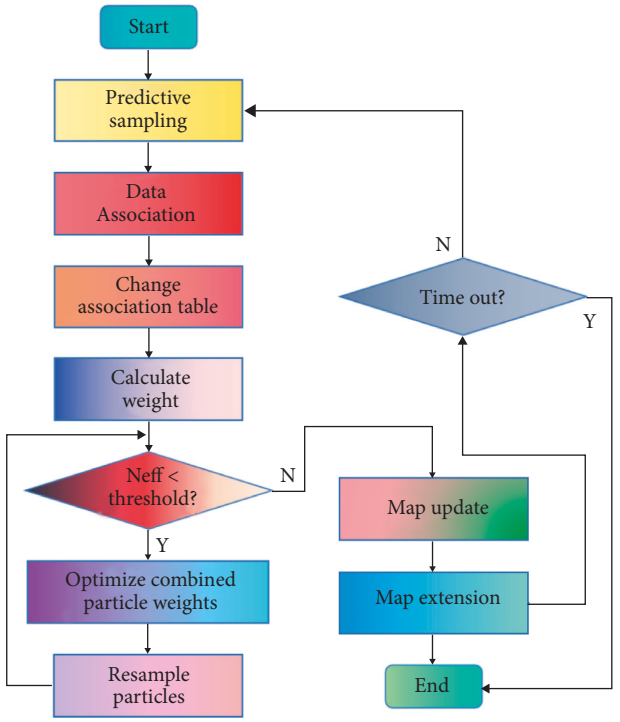

Figure 3: The flowchart of Monocular SLAM_WOCPF algorithm.

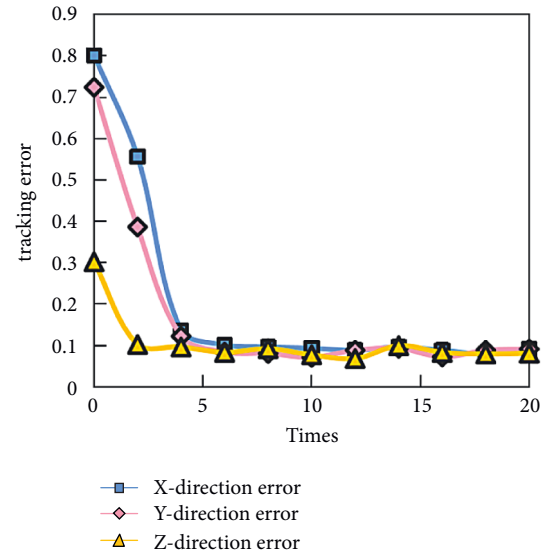

Figure 4: The change of position and angle tracking error with iteration number based on KF.

4. Result Analysis

Under the Matlab simulation environment, the motion and observation of the mobile robot are simulated by using the above-mentioned motion model and observation model, and the simulation of the mobile robot Monocular SLAM_WOCPF is realized.

The output of KF is represented by y_e. Both process excitation noise β and measurement noise γ are bounded, their values can only be within a certain range, and they are independent of each other. By combining iterative learning control with KF, KF iterative learning control system can give full play to the advantages of iterative learning control.

In practical engineering applications, the system can be stabilized with fewer iterations, which is conducive to improving the real-time performance of the control system. However, if the algorithm converges slowly, it will not only fail to achieve the real-time control of the system, but also affect the tracking accuracy, so it is very unfavorable for the real-time tracking control of mobile robot. The number of iterations is set to 20, the sampling time is 0.002 s, and the given time for each iteration is 2 s. The simulation results are shown in Figure 4.

It can be seen that the control system can stabilize quickly, and the tracking error is small. Therefore, it can be inferred that after adding KF, although there are interference terms β and noise terms γ, the control performance of the system does not deteriorate. In practical applications, KF has been widely used in various practical systems, which is of great significance to improve the control system's resistance to external disturbances.

For any input, the fuzzy controller should give appropriate control output, which is called completeness. The requirement of fuzzy control completeness for rule base is that at least one applicable rule should be ensured for any input. From the analysis of kinematics model, it is concluded that there is a coupling relationship between the velocity and angular velocity of the mobile robot.

The reason why the speed of the mobile robot is affected by the difference of heading angle and the bending degree of the road ahead is that, in the final analysis, the mechanical constraint of angular velocity should be considered. The tracking effect diagram in Figure 5 and the error diagram in Figure 6 can be obtained by simulating the described model.

It can be seen that the tracking error of the algorithm used in this paper is reduced, which is closer to the real state value. The reason is that the basic PF algorithm resamples to reduce the number of effective particles, and the particles selected by resampling are highly concentrated on a few heavyweight particles.

This optimization process ensures the diversity of particle population and changes the PF algorithm's practice of directly discarding low-weight particles. At the same time, in the process of moving to the best individual, the decrease of the distance between individuals leads to the increase of relative attraction. In this paper, the improved algorithm introduces a decreasing function to guide the movement of individuals, so as to avoid falling into the situation of inability to converge.

The increase of the number of particles will make up for the lack of diversity of particles to a certain extent, making very small or even almost no improvement in the accuracy of the improved algorithm after the number of particles reaches a certain level. In addition, for the same algorithm, the increase of particle number will increase the viscosity of the algorithm. To compare the simulation results more

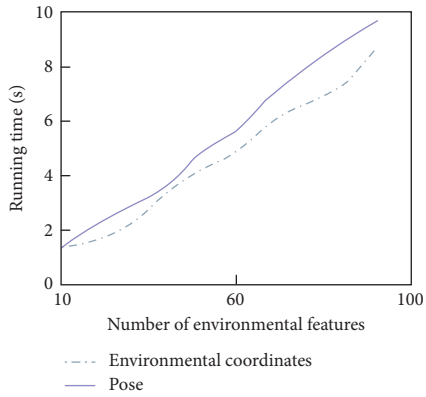

Figure 5: Tracking effect comparison.

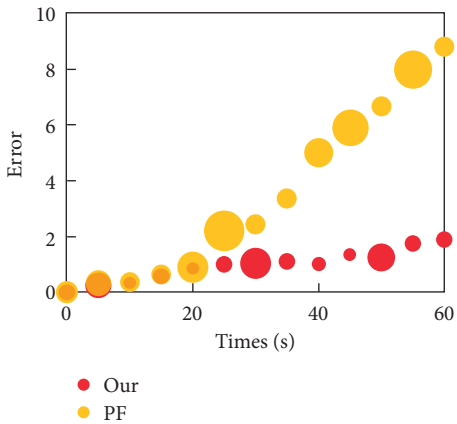

Figure 6: Error distribution comparison.

intuitively, Table 1 and Figure 7 list the average execution time of each algorithm and RMSE (Root Mean Squared Error) average in digital form.

It can be seen intuitively that the accuracy of Monocular SLAM_WOCPF algorithm is better than that of EKF_SLAM algorithm under the same particle number and the algorithm complexity is equivalent. With the increase of the number of particles, the increasing trend of precision slows down.

There are two reasons for this phenomenon: one is that PF algorithm itself has the characteristic that the accuracy changes gently after the number of particles reaches a certain level; the other is that the increase of the number of particles makes up for the deficiency of the diversity of particles, which makes more particles participate in the replication and estimation, which directly leads to weakening the weight optimization combination effect.

Therefore, the Monocular SLAM_WOCPF algorithm can increase the diversity of particle sets, delay the process of particle depletion, and slightly improve the estimation accuracy without affecting the computational complexity.

Simulating the characteristics of human visual tracking, the visual saliency area is defined as the global recommendation distribution of PF, and it is organically combined with the local recommendation distribution. When the target is caught up, the target is tracked in the local recommendation distribution, and when the target is lost, the target is searched in the global recommendation distribution. In the experiment, this tracking algorithm is compared with PF tracking, Kalman PF tracking, and unscented PF tracking. The results show that the tracking algorithm proposed in this paper not only inherits the superior local tracking ability of the traditional PF, but also can search and locate the target in the global scope as quickly as people, thus adapting to the rapid movement and large-scale transfer of the target.

In order to make the above statement more convincing, we compare the robot estimation errors of the EKF-SLAM algorithm, the algorithm in [14], and the Monocular SLAM_WOCPF algorithm. The results are shown in Figure 8.

It is not difficult to find that the estimation error of the Monocular SLAM_WOCPF algorithm is obviously lower than that of the EKF-SLAM algorithm and not higher than that of [14] algorithm. Therefore, the accuracy of Monocular SLAM_WOCPF algorithm in robot pose positioning and map building is obviously higher than that of EKF-SLAM algorithm, and its pose positioning accuracy is obviously higher than that of [14]. The Monocular SLAM_WOCPF algorithm is practical and effective.

In order to avoid the randomness caused by noise, the noise environment is changed now. The EKF-SLAM algorithm, the algorithm in [14], and the Monocular SLAM_WOCPF algorithm are carried out in two different observation noise environments, and the process noise is the same as $\sigma_v = 0.2$ m/s, $\sigma_G = 4^\circ$. Every simulation is conducted with 20 Monte Carlo experiments, and the results are shown in Table 2.

It can be seen that in any noise environment, the accuracy of pose estimation of Monocular SLAM_WOCPF algorithm is the best compared with the other two algorithms, and the average road sign errors of the Monocular SLAM_WOCPF algorithm in the two noise environments are 0.332/m and 0.441/m, respectively, which are obviously less than those of the other algorithms.

Fundamentally, this is because the weight optimization combination introduced in Monocular SLAM_WOCPF can improve the particle distribution; the rotation factor and movement factor can make the particle set approach the real robot pose state more quickly; and at the same time, rotation factor and movement factor can improve the problem of particle degradation and dilution in the algorithm, making the estimation result more stable and accurate.

Given the initial pose and expected path of the mobile robot, if the initial position is outside the trackable area of the expected path, a temporary path needs to be planned first, and the whole path formed by the connection of the temporary path and the expected path is regarded as the track to be tracked by the mobile robot. Clamping slots are arranged at the sides of both ends of the load adjustable layer to realize the longitudinal position adjustment of the weight block, and the weight block can also realize the lateral position adjustment through the clamping slots on the baffle. Therefore, that lay can adjust the position of the weight block

Table 1: Statistical comparison of simulation results of two algorithms.

Algorithm	Particle number	Average execution time (s)	Estimated path RMSE average (m)	Estimate RMSE average of map (m)
EKF_SLAM	10	50.21	2.0367	2.8814
	20	123.36	1.5531	2.2417
	30	233.68	1.2347	1.8249
	40	268.7	1.0326	1.6271
Monocular SLAM_WOCPF	10	51.03	1.8824	2.6035
	20	124.66	1.4023	2.0513
	30	235.08	1.1827	1.7322
	40	265.19	1.0138	1.4369

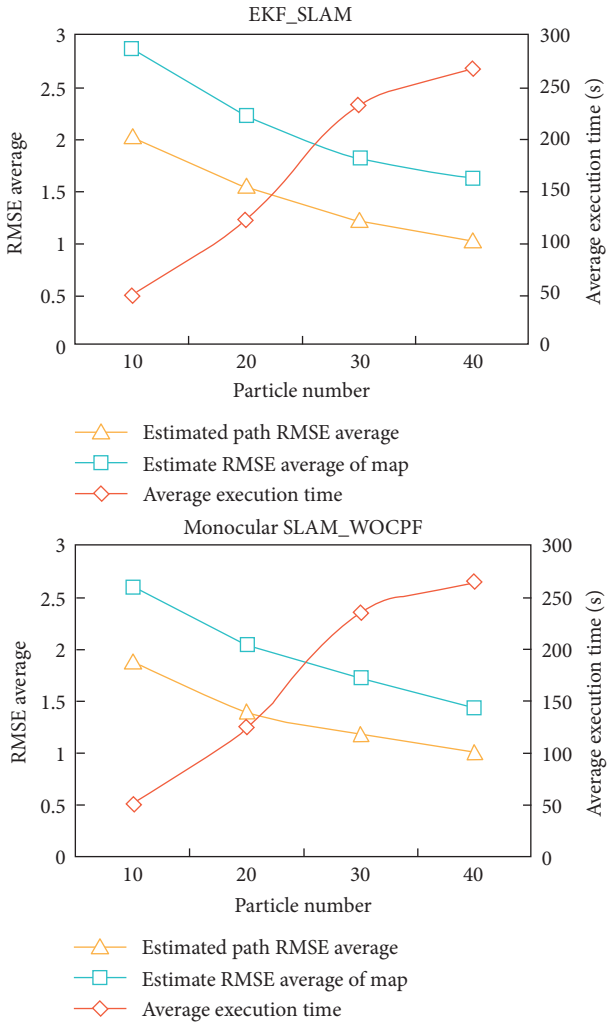

Figure 7: Comparison curve of simulation results of two algorithms.

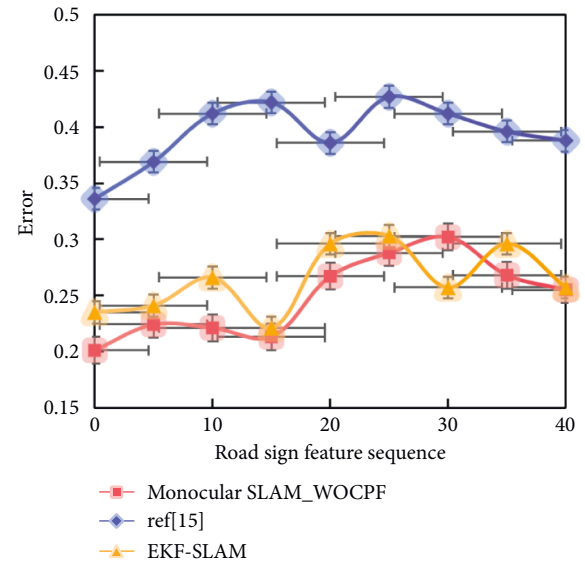

Figure 8: Road sign estimation error.

Table 2: Estimation accuracy of each algorithm in two noisy environments.

Algorithm	$\sigma_r = 0.2$ m/s, $\sigma_\theta = 2°$		$\sigma_r = 0.4$ m/s, $\sigma_\theta = 4°$	
	Mean pose error (m)	Mean road sign error (m)	Mean pose error (m)	Mean road sign error (m)
EKF_SLAM	0.436	0.374	0.589	0.501
Reference [14]	0.723	0.445	0.869	0.664
Fast Monocular SLAM_WOCPF	0.174	0.332	0.208	0.441

in a large range on a two-dimensional plane. In addition, it can be changed by adjusting the height of the aluminum alloy support column between the robot chassis and the load adjustable layer.

Once all the states reach the sliding mode surface, the system will no longer be sensitive to parameter changes and external disturbances and only keep moving in the sliding mode. By combining the moment calculation method with the adaptive method, we can make full use of the known information of the mobile robot, thus improving the control performance of the system. However, the method of calculating moment has great dependence on the accuracy of the dynamic model of mobile robot. With the expanding application range of mobile robots, the working environment and tasks of mobile robots will become more complicated. It is necessary to consider how to extend the path planning of a single robot to the path planning of multiple robots. In addition, future robots may have to perform other tasks while planning their paths.

5. Conclusion

Visual target tracking is an important research direction in the field of computer vision, and robustness is the premise of practical application of visual target tracking algorithm. PF is a new filtering estimation algorithm which is widely used in nonlinear and non-Gaussian random systems. Compared with other nonlinear filtering algorithms, it is more practical. In this paper, an improved algorithm based on the traditional EKF-SLAM algorithm is proposed. Through the observation of the characteristic road signs by the mobile robot at the previous moment, combined with the system input, the position of these road signs relative to the robot at the next moment is predicted. The SLAM simulation experiment proves that the Monocular SLAM_WOCPF algorithm has the best estimation accuracy for robot pose and signpost characteristics compared with other algorithms under the same noise condition.

Data Availability

The dataset can be accessed upon request.

Conflicts of Interest

The authors declare no conflicts of interest.

References

[1] S.-Y. Hwang and J.-B. Song, "Monocular vision-based SLAM in indoor environment using corner, lamp, and door features from upward-looking camera," *IEEE Transactions on Industrial Electronics*, vol. 58, no. 10, pp. 4804–4812, 2011.

[2] A. M. Santana and A. A. D. Medeiros, "A line-based approach to SLAM using monocular vision," *IEEE Latin America Transactions*, vol. 9, no. 3, pp. 231–239, 2011.

[3] M. N. A. Bakar and A. R. M. Saad, "A monocular vision-based specific person detection system for mobile robot applications," *Procedia Engineering*, vol. 41, pp. 22–31, 2012.

[4] X. Z. Zhang, A. B. Rad, and Y. K. Wong, "A virtual range finder based on monocular vision system in simultaneous localization and mapping," *IFAC Proceedings Volumes*, vol. 41, no. 2, pp. 2336–2341, 2008.

[5] J. Solà, T. Vidal-Calleja, J. Civera, and J. M. M. Montiel, "Impact of landmark parametrization on monocular EKF-SLAM with points and lines," *International Journal of Computer Vision*, vol. 97, no. 3, pp. 339–368, 2012.

[6] C. Miao and J. Li, "Autonomous landing of small unmanned aerial rotorcraft based on monocular vision in GPS-denied area," *Acta Automatica Sinica*, vol. 1, p. 6, 2015.

[7] A. K. Nasir, A. Hsino, H. Roth, and K. Hartmann, "Aerial robot localization using ground robot tracking - towards cooperative SLAM," *IFAC Proceedings Volumes*, vol. 46, no. 19, pp. 313–318, 2013.

[8] P. Jin-Chun and K. Shin-Dug, "Adaptive monocular visual–inertial SLAM for real-time augmented reality applications in mobile devices," *Sensors*, vol. 17, no. 11, Article ID 2567, 2017.

[9] C. Yun-Won, K. Kee-Koo, L. Soo-In, J. W. Choi, and S. G. Lee, "Multi-robot mapping using omnidirectional-vision SLAM based on fisheye images," *ETRI Journal*, vol. 36, no. 6, pp. 913–923, 2014.

[10] A. Silva, R. Mendonça, and P. Santana, "Monocular trail detection and tracking aided by visual SLAM for small unmanned aerial vehicles," *Journal of Intelligent and Robotic Systems*, vol. 97, no. 3-4, pp. 531–551, 2019.

[11] Y. Li, J. Zhang, and S. Li, "STMVO: biologically inspired monocular visual odometry," *Neural Computing & Applications*, vol. 29, no. 6, pp. 215–225, 2016.

[12] B. Jia, R. Liu, and M. Zhu, "Real-time obstacle detection with motion features using monocular vision," *The Visual Computer*, vol. 31, no. 3, pp. 281–293, 2015.

[13] T. Sun, Y. Liu, Y. Wang, and Z. Xiao, "An improved monocular visual-inertial navigation system," *IEEE Sensors Journal*, vol. 8, no. 99, 1 page, 2020.

[14] B. Fang, G. Mei, X. Yuan, L. Z. Wang, and J. Wang, "Visual SLAM for robot navigation in healthcare facility," *Pattern Recognition*, vol. 113, no. 12, Article ID 107822, 2021.

[15] L. Chen, A. Yang, H. Hu, and W. Naeem, "RBPF-MSIS: toward rao-blackwellized particle filter SLAM for autonomous underwater vehicle with slow mechanical scanning imaging sonar," *IEEE Systems Journal*, vol. 14, no. 99, pp. 1–12, 2019.

[16] D. Zhu, X. Sun, S. Liu, and P. Guo, "A SLAM method to improve the safety performance of mine robot," *Safety Science*, vol. 120, pp. 422–427, 2019.

[17] I. Vallivaara, K. Poikselkä, A. Kemppainen, and J. Röning, "Quadtree-based ancestry tree maps for 2D scattered data SLAM," *Advanced Robotics*, vol. 32, no. 5, pp. 215–230, 2018.

[18] X. Yang, Y. Xiao, Y. Y. Ma, and F. Tittel, "A miniaturized QEPAS trace gas sensor with a 3D-printed acoustic detection module," *Sensors*, vol. 17, no. 8, p. 1750, 2017.

[19] A. Gil Aparicio, O. Reinoso, L. Paya, and M. Ballesta, "Assessing the influence in the parameters of a Rao-Blackwellised particle filter to solve the SLAM problem," *IEEE Latin America Transactions*, vol. 6, no. 1, pp. 18–27, 2008.

[20] D. Moratuwage, D. Wang, A. Rao, N. Senarathne, and H. Wang, "RFS collaborative multivehicle SLAM: SLAM in dynamic high-clutter environments," *IEEE Robotics and Automation Magazine*, vol. 21, no. 2, pp. 53–59, 2014.

[21] H. N. Do, M. Jadaliha, M. Temel, and J. Choi, "Fully Bayesian field slam using Gaussian Markov random fields," *Asian Journal of Control*, vol. 18, no. 4, pp. 1175–1188, 2016.

Hindawi
Computational Intelligence and Neuroscience
Volume 2022, Article ID 2041592, 12 pages
https://doi.org/10.1155/2022/2041592

Research Article

Exploration of Joint Optimization and Visualization of Inventory Transportation in Agricultural Logistics Based on Ant Colony Algorithm

Bo Dong, Manzhen Duan, and Yinfeng Li

College of Civil and Architectural Engineering, North China University of Science and Technology, Tangshan, Hebei 063210, China

Correspondence should be addressed to Bo Dong; dongbo@ncst.edu.cn

Received 16 May 2022; Accepted 31 May 2022; Published 15 June 2022

Academic Editor: Yaxiang Fan

Copyright © 2022 Bo Dong et al. This is an open access article distributed under the Creative Commons Attribution License, which permits unrestricted use, distribution, and reproduction in any medium, provided the original work is properly cited.

The problem of joint optimization of inventory and transportation in agricultural logistics and distribution is a typical logistics problem, but agricultural logistics and distribution also have their own characteristics, such as uneven distribution of outlets, complex road conditions, very many outlets, a single order with few goods but high frequency of ordering, centralized distribution, and unified channels. To promote the sustainable development of the economy, it is necessary to save energy and reduce emissions, and eventually enter a new era of "low consumption, low pollution, and low emissions." Modern logistics vehicle-scheduling process is complex and changeable, and the existing mathematical methods are not perfect in solving this problem, lacking scientific theory as a guide. The joint optimization problem introduces the inventory change factor on the basis of periodic vehicle path optimization and optimizes the inventory decision and path planning in an integrated manner. As a system to support the logistics industry, the visualized logistics information system is capable of video viewing and querying logistics information. In order to reduce gas emissions and save costs, it is necessary to optimize the transportation link, and the focus of optimization is the route optimization of distribution vehicles. Ant colony algorithm (ACA) is an emerging search and optimization technique, which emerged from the research of ACA. In this study, we study the joint optimization and visualization of inventory transportation in agricultural logistics based on ACA. In addition, the experimental results show that the inventory cost/total cost of improved ACA is 0.006 when the unit mileage transportation cost is 10, and the IBM ILOG CPLEX is 0.031, which is reduced by 0.0025, that is to say, in the case of high inventory cost per unit product, the use of improved ACA can lead to a significant reduction in inventory costs. Therefore, it can realize the whole process of control, traceability, and dynamic optimization to ensure the timeliness of emergency finished food security and provide real-time information for decision-making in command as well.

1. Introduction

China's agricultural products are not only rich in resources but also rank steadily among the top in the world in terms of production, but the problem of agricultural logistics has been plaguing agricultural players [1]. The so-called logistics refers to the flow process of material materials in physical form from the place of supply to the place of consumption in social reproduction [2]. Through the study and application of optimal scheduling of logistics transport vehicles, it is possible to improve the economic efficiency of logistics and achieve scientific logistics [3]. In the process of logistics distribution, to reduce resource consumption, it is necessary to start from the distribution path, which is the main basis and ultimate goal of sustainable development [4]. Agricultural product logistics and distribution are the end of frustrated agricultural product logistics, connecting agricultural product logistics centers with the final sales outlets such as various farmers' markets and supermarkets [5]. At the same time, with the development of information technology and the changing needs of e-commerce consumers, e-commerce merchants more urgently need third-party logistics to provide personalized and specialized logistics services [6]. Both merchants and consumers want to visualize the entire logistics service

process to improve logistics efficiency, reduce logistics costs, and thus, better meet the needs of consumers [7].

The consumption level of the population has gradually increased, the structure of the agricultural industry has gradually made adjustments, and the circulation and production of fresh agricultural products have gradually increased every year [8]. Therefore, more stringent requirements are put forward for the quality and the safety of products [9]. To improve the operational efficiency of the railroad transport industry, reduce costs and enhance service quality, and achieve industrial upgrading, the active development of modern logistics services is the way to go, and the use of computer technology to realize the informationization of logistics is one of the important means [10]. On the one hand, the rapid development of computers promotes the continuous development of optimization methods, on the other hand, it also makes the engineering optimization problems become larger and larger, and the nature of the optimization objective function becomes more and more complex [11]. How to use scientific and effective methods to optimize inventory transportation to improve the economic efficiency of enterprises under the condition of satisfying the diversified needs of customers is an important issue of concern and research focus in the field of logistics today [12].

Chinese logistics enterprises want to grasp the pulse of the future era and become the world market leader, understand the industry competition, win market exclusivity, and seize market opportunities in order to stand firm in this big market economy [13]. In solving multiobjective optimization problems, since the objectives are often in conflict with each other, there is often no constraint that can satisfy all constraints [14]. Instead, there is a set of Pareto optimal solutions [15]. Therefore, the ACA is introduced into this problem to provide technical measures to build an integrated logistics system, establish a modern scheduling and command system, develop an intelligent transportation system, and carry out modern e-commerce with the help of process simulation technology, in view of the comprehensive, complex, and uncertain characteristics of joint optimization and visualization of inventory transportation in agricultural logistics.

The innovative points of this study are as follows:

(1) Considering the influence of freshness input on freshness level and quantitative loss, the functional relationship between freshness and quantitative loss is portrayed.

(2) Considering the cost of vehicles, such as fixed cost, refrigeration cost, transportation cost, penalty cost, cargo damage cost, and setting the goal of distribution as the total cost minimization, an optimization model is constructed, i.e., the joint optimization model of inventory transportation based on ACA.

(3) To conduct a joint optimization study, inventory level and distribution path are affected by market demand, product deterioration rate, and other factors at the same time, and the cost-minimization path can be planned according to the demand node location and distribution volume.

The research framework of this study contains five major parts, which are organized as follows.

The first part of this study introduces the research background and significance, and then introduces the main work of this study. The second part introduces the work related to the joint optimization and visualization of inventory transportation in agricultural logistics, and the development of an e-commerce platform based on ACA for logistics transportation optimization. In the third part, the establishment of ACA-based inventory and transportation optimization model and the establishment of ACA-based inventory and transportation visualization platform are explained, so that the readers of this study can have a more comprehensive understanding of the idea of ACA-based inventory and transportation optimization and visualization in agricultural logistics. The fourth part is the core of the thesis, which describes the application analysis of ACA in the joint optimization and visualization of inventory transportation in agricultural logistics from two aspects, namely, the improvement of ACA analysis and the improvement of the process analysis of ACA for agricultural logistics. The last part of the thesis is the summary of the full work.

2. Related Work

2.1. Joint Optimization and Visualization of Inventory Transportation in Agricultural Product Logistics. "Logistics" is an emerging science, and the results of this concept are first used in the Second World War in the United States military logistics supply and achieved success; after, the war has attracted the attention of the economic community and developed. Agricultural product logistics usually covers postproduction processing, storage, transportation, and distribution, etc. Through the coordination and cooperation of producers, warehouses, logistics enterprises, retailers, and other subjects, agricultural products enter the field of consumption and finally realize the value added of agricultural products. For the actual situation of logistics application, providing the optimal path information for logistics distribution management platform and distributors is also a necessary means to improve the efficiency of logistics delivery.

Liu realizes the procurement and distribution of customer products through a single vehicle, uses two stacks for the purpose of product transit in the warehouse, and finally solves the vehicle path problem by an improved branch delimitation method [16]. Teschemacher and Reinhart proposed an ant colony system combined with a forbidden search algorithm to solve heterogeneous vehicle path problems with time windows and multiple products, introducing a strategy of two pheromones to accelerate the learning process of ants [17]. Lu et al. performed the solution by a forbidden search algorithm, in which the execution

frequencies of insertion and exchange operations are linked to the neighborhood solution set, following the principle of dynamic adjustment [18]. Wang studied the effect of temperature changes in the quality of frozen vegetables, etc., during cold chain logistics distribution, providing a corresponding theoretical basis for reducing the losses in the distribution process of agricultural products [19]. The Xiong design column generation method solves the vehicle distribution problem for larger demand conditions, where the pricing problem is determined by a local search algorithm [20].

The joint inventory-transport optimization problem is an organic combination of inventory decision and path planning, which extends the joint inventory-transport optimization problem that belongs to a spatial decision. By taking inventory management, which is a temporal decision, as a prerequisite for joint inventory-transportation optimization, the joint optimization problem solution is also spatiotemporal in nature. In logistics visualization, storage and warehousing of materials are one of the main activities in logistics visualization. Based on the integration of geographic information and supply and demand information in logistics visualization, a more suitable location for the storage of goods is selected, which saves logistics costs.

2.2. Optimization of Logistics Transportation Based on ACA. Logistics transportation is an important part of the logistics system, and the optimal scheduling of logistics transportation vehicles is a key part of logistics system optimization and an indispensable and important part of e-commerce activities. The ACA adopts a positive feedback parallel autocatalytic mechanism, which has the advantages of strong robustness, excellent distributed computing mechanism and is easy to combine with other methods, and has demonstrated its excellent performance and great development potential in many complex combinatorial optimization problems.

Zhou proposed an improved ACA combining a stochastic algorithm and a local search algorithm to solve the distribution vehicle-scheduling problem [21]. Yang et al. proposed the idea of multiple ant colonies to solve the vehicle path problem with time windows, where one ant colony is used to optimize the number of distribution vehicles and another ant colony is used to optimize the total distribution distance [22]. Zhao et al. provided a combined general criterion using heuristics. Since the introduction of heuristics has received better results for the improvement of the performance of global optimization methods, finding better heuristics with more generality is a more researched development direction, especially in metaheuristic algorithms [23]. Liang proposed a saving ACA to solve the vehicle path problem, and the algorithm proposed the probability of attractiveness based on the saving value and then introduced the attractiveness into the state transfer probability [24]. Pei proposed a hypercube framework ant colony optimization algorithm, which restricts the pheromone between 0 and 1 and improves the pheromone update rule [25].

A variety of artificial intelligence algorithms such as evolutionary algorithm, particle swarm optimization, and ant colony algorithm are widely used in machine learning, process control, economic prediction, engineering optimization, and other fields. How to apply these methods to solve complex multiobjective optimization problems with multiple constraints has become a hot topic of research in this field. In the field of customer-centric logistics services, ACA is an indispensable tool by which the provision of integrated and comprehensive logistics management services can be carried out. Using this tool, resource integration can be maximized. Using this means well, it is possible to increase the social and economic benefits well.

3. Joint Optimization and Visualization of Inventory Transportation in Agricultural Product Logistics Based on ACA

3.1. Establishment of Joint Optimization Model of Inventory Transportation Based on ACA. The agricultural logistics system is a continuous and complete chain composed of several "nodes," including agricultural producers, buyers, distributors, retailers, logistics distribution and storage enterprises, and other logistics entities [26]. The transportation process is carried out between the various nodes and facilitates the downstream flow of agricultural products [27]. After inputting the relevant information, the system is allowed to prioritize the distribution and the results are shown in the data flow diagram in Figure 1.

First, the penalty function is established. The common feature of the penalty cost is that the more the vehicle arrival time deviates from the constraint time window, the higher its penalty cost. Therefore, we assume that the penalty cost linearly increases to simplify the problem. Using Baidu Telematics technology, we call the API interface of the Baidu service to obtain the information on driving route, driving distance and duration between distribution centers and retail merchants, and retail merchants and retail merchants, and write them into the basic information database. The information is initialized (including the number of ants, the amount of information, the maximum number of iterations, etc.), and the initial number of iterations is set to 1. The improved ACA process is illustrated in Figure 2 below.

According to the vehicle loading status, it is divided into the full-load problem and non-full-load problem. Full-load problem means that the freight volume is greater than the capacity of one vehicle, and multiple transport vehicles are required to complete all tasks [28]. Freshness loss and volume loss of fresh agricultural products simultaneously occur, i.e., after a period of time, fresh agricultural products no longer have the initial freshness. For example, water loss from vegetables and fruits, or waste from poor customer-picking behavior can impair product freshness [29]. Therefore, the integration of production, supply, and marketing directly omits the intermediate links and establishes a direct link between producers and retailers by establishing a logistics and warehousing enterprise. This performance evaluation can be used to measure the variation

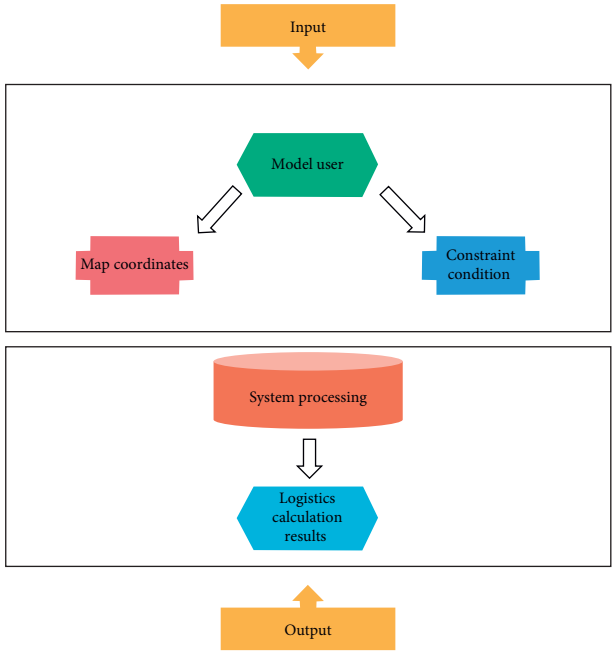

Figure 1: Data flow diagram.

of the distance between adjacent solutions on the resulting Pareto frontier, which is defined as follows:

$$S = \frac{1}{n-1}\sum_{i=1}^{n}\left(\overline{d} - d_i\right)^2. \tag{1}$$

Among them,

$$d_i = \min_j\left(f_1{}^i(x) - f_1{}^j(x) + f_2{}^i(x) - f_2{}^j(x)\right). \tag{2}$$

n—number of vectors, $\overline{d}$—distance average, and S—distance.

Next is the definition of the parameter that each delivery vehicle cannot exceed its rated capacity at one time. In order to improve the utilization of vehicles, the number of vehicles used is minimized through scheduling, while meeting the delivery tasks, and finally minimizing the total cost of vehicle operation. The delivery area is first optimally divided, and then, the delivery routes within the area are optimized. In each step of the path construction, ants follow a probabilistic behavioral selection rule called the random proportion rule to decide which city they will move to next. The probability that an ant located in the current city will choose as the next city is as follows:

$$\begin{cases} p_{ij}^k = \dfrac{\left[\tau_{ij}(t)^\alpha\right]\left[\eta_{ij}\right]^\beta}{\sum_{t\in N_i^k}\left[\tau_{ij}(t)^\alpha\right]\left[\eta_{ij}\right]^\beta}, & j \in N_i^k, \\ 0, \ j \notin N_i^k. \end{cases} \tag{3}$$

k—ant, i—current city, j—next city, and N_i^k—feasible neighborhood that can be directly reached.

The next city to be visited is selected based on the state transfer probability and the taboo table changes accordingly [30]. The pheromone that goes to each path changes and an update of the amount of information is required, and if the maximum number of iterations is satisfied, the program is exited, and if not, it returns and continues iterating until the number of iterations is satisfied. The pheromone on all edges is reduced by a fixed size value, and then, each ant adds pheromone to the edge it passes through. This fixed size pheromone is as follows:

$$\tau_{ij} \longleftarrow (1-\rho)\tau_{ij}, \quad \forall (i,j) \notin L. \tag{4}$$

ρ—evaporation rate of pheromone.

According to the transport task that is divided into pure loading problem, pure unloading problem, and loading and unloading mixed problem, the so-called loading and unloading mixed problem is the vehicle in transit during both loading and unloading. On the electronic map, information related to agricultural products (such as retail outlet locations and administrative information) is superimposed. Graphical representation presents a global display effect, convenient for agricultural products business personnel to carry out macroanalysis and decision-making. The volume of cargo transportation tasks is generally larger than one half of the vehicle capacity, or the collection and delivery points of each task are relatively scattered. At this time, the goods are difficult to mix, and the vehicle completes a task and then empties to the next task collection point to complete the next task. After completing the pheromone evaporation step, all ants release pheromones on the side through which it passes the following:

$$\tau_{ij} \longleftarrow \tau_{ij} + \sum_{k=1}^{m} \nabla\tau_{ij}{}^k, \quad \forall (i,j) \notin L. \tag{5}$$

$\nabla\tau_{ij}{}^k$—the amount of pheromone released by the k first ant to its passing edge.

Finally, since the operation of each logistics truck is independent, in order to ensure the "first-come-first-served" scheduling rule of the service, a dynamic time series needs to be established to represent the time series of the boxes available at each depot. When the delivery starts, the Android vehicle terminal calls the remote service interface to read the delivery task information of the associated delivery vehicle, such as delivery serial number, merchant order number, merchant address information, and the total number of goods. In the process of making the delivery, we also have to consider the sorting system in distributing varieties and the balance of the transport vehicle operation. Therefore, each freight task has its own collection point and delivery point, and the vehicle departs from the yard, goes to the collection point of a certain task, loads the goods after transporting to its delivery point to unload that is loading and unloading mixed, and returns to the yard after completing all tasks.

3.2. Establishment of Visualization Platform of Inventory Transportation Based on ACA. The main components of the visualized finished grain logistics information system include vehicle terminals, communication, and video monitoring center. In transit visualization is mainly to be able to

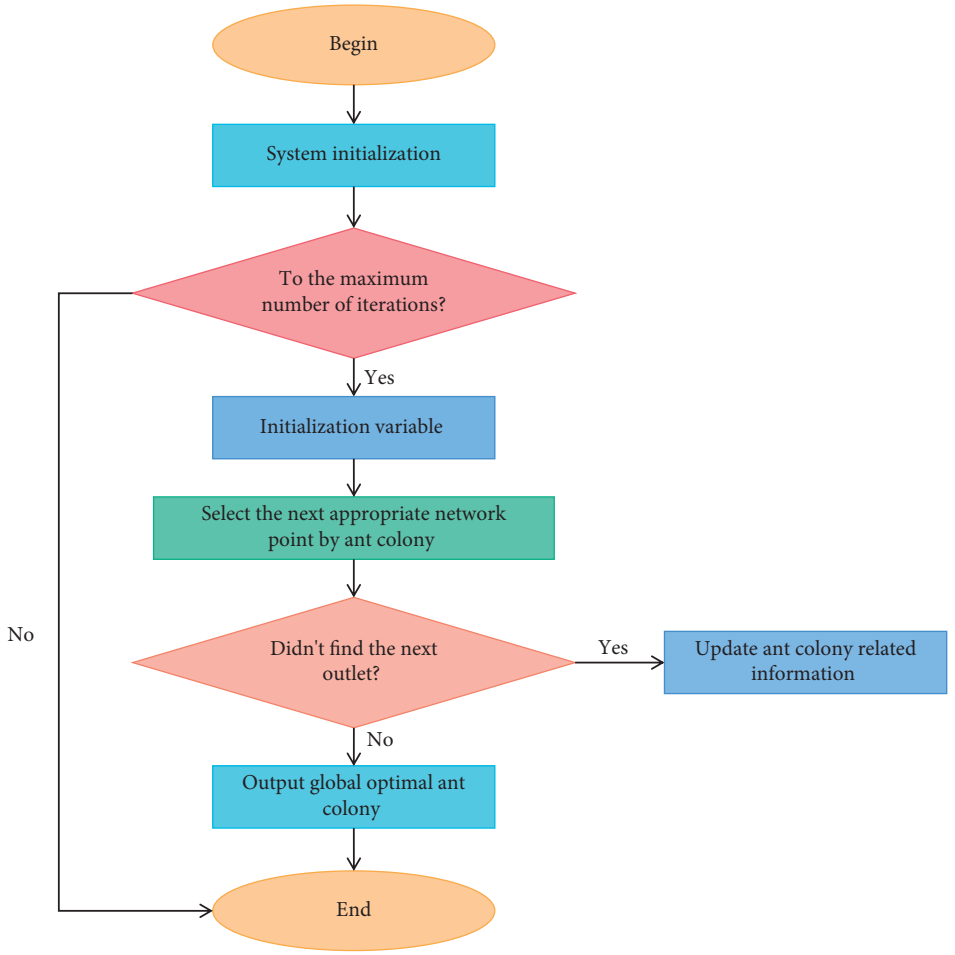

Figure 2: Flowchart of improved ACA.

monitor the vehicle's operation status and operation route in the control center. Open-source framework technology is used. The main framework technologies include the following: JSF2, Spring3.0, and JPA. The platform is designed with a three-tier architecture, as shown in Figure 3 below.

First is the display layer, which is used to visualize the data information of the finished grain logistics information system, and clearly shows the business process between the event occurrence and the event completion. We visualize the relationship between data, and the main application technology is the front-end display technology, such as JSP, HTML, and Flash technology. The visualization functions in this project include real-time visualization and monitoring of logistics in holding warehouses, real-time visualization and monitoring of remote logistics, management of refrigerated vehicles, and real-time monitoring of refrigerated vehicles. The distance between the collection point and the distribution center cannot be a straight-line distance (Euclidean distance), according to its actual road conditions is an available formula to calculate the distance between these two points, and the vast majority of roads will be in this mode as follows:

$$d_i = |x_i - x| + |y_i - y|. \tag{6}$$

Transportation lines and warehouses constitute a logistics network in the logistics system, and warehouses are the nodes of the network, which need to determine the routes according to the nodes and then form the transportation and distribution network. Using a continuous ACA, it first performs a global search of the solution space using a genetic algorithm. Then, ACA is used to locally optimize the results obtained by taking the farthest demand point from the depot as the seed point of the route. The next insertion point is the one with the smallest insertion value according to the nearest-neighbor insertion method. Finally, the generalized savings formula is used to determine the insertion position with the largest savings value, and the selection and insertion steps are repeated. When the path can no longer be expanded, another route is created. The algorithm generally uses the error sum-of-squares criterion function as the clustering criterion function, and the error sum-of-squares criterion function is defined as follows:

$$J_c = \sum_{i=1}^{k} \sum_{p \in C_i} \|p - M_i\|^2. \tag{7}$$

p—sample point and M_i—average value of data.

Next is the functional layer: it is mainly the 6 functional modules of the system, including business functions and

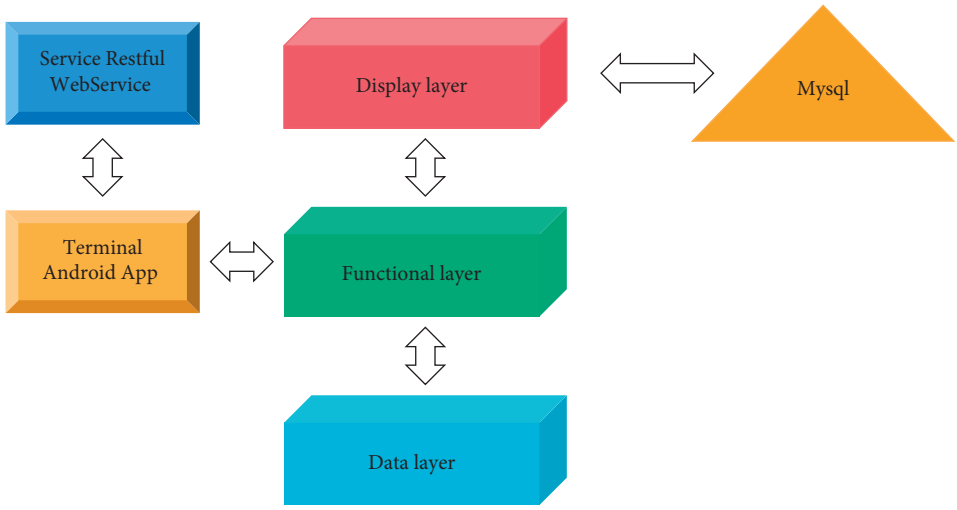

Figure 3: Multilayer architecture technology of the system.

system setting functions, business functions constitute the thematic framework of the system, and auxiliary functions are used for system setting, etc., which cooperate to complete the realization of the main functions. To realize the visualization function of the system, it is necessary to equip video collection equipment and sensor nodes in key links to collect information in real time. The sparsity of the feasible region is usually measured by the ratio of the feasible region to the whole search space. At the same time, the intensity of the variation of the constraint on the boundary of the feasible region is also greatly related to the determination of the penalty term. In order to meet the supply and demand transportation and distribution needs and ensure economic efficiency, it is necessary to set up a reasonable number of warehouses or other facilities in the identified area, and determine the size and location of each facility and the logistics connections existing between the facilities, etc. The facility location model can better solve these problems. Based on such adjustment rules, the advantage of the local optimal path is appropriately weakened, and the algorithm converges to the local optimal solution by effectively avoiding the information on the local optimal path that is far too large. The space composed of all points on the decision space by the mapping of the objective function is called the objective function space. Its feasible domain is described by the following equation:

$$D_f = \left\{ F \in \left[f_1(x), f_2(x), \ldots, f_q(x) \right]^T, \quad X \in D_x \right\}. \tag{8}$$

n—n dimension decision variable, x—decision vector, and $F(x)$—target vector.

The decision space refers to the space composed of all the parameters of the objective function that meet the constraint conditions as follows:

$$D_x = \{ \mathrm{X} \in \mathrm{R}^n | g_u(x) \geq 0, h_v(x) = 0 \}. \tag{9}$$

Finally, there is the data layer; the system database table is constructed, including the spatial database and the attribute database; and the data can be added, deleted, changed, and checked. After the data are stored, the picture can be investigated by inquiry, and the monitor can also monitor the status of frozen food at that time. A logistics company has to set up D logistics transit points, and it is necessary to consider that these transit points can cover a certain area, and the number of customers at each transit point should be approximately the same level. Using a uniform constant as a posteriori function, this cannot achieve the purpose of distinguishing the superiority from the inferiority. In this study, the dominance factor of CLS will be considered in the heuristic function, and the heuristic information is calculated as follows:

$$\eta_{(j,b)} = \frac{1 + \mathrm{CLS}_{jb}.D}{N}. \tag{10}$$

N—the number of ALS.

At the beginning of the iteration, the pheromone concentration on all paths is set to the upper pheromone limit, which helps to increase the search ability of the algorithm at the beginning and avoid the phenomenon that the initial convergence ability of the algorithm is constrained by the small initial pheromone and the large influence of the posterior factor. The topological nature of the surface corresponding to the objective function, such as under the same constraints, linear or convex function, is easier to solve than the irregular function. The logistics nodes such as warehouse, vehicle dispatching, and demand destination need to be marked on the electronic map with specific geographical locations. The emergency monitoring also needs to obtain various data collected from the vehicle terminals from the system database, including distance, road level, road condition video, and other vehicles and road conditions.

4. Application Analysis of ACA in Joint Optimization and Visualization of Inventory and Transportation in Agricultural Product Logistics

4.1. Improved ACA Analysis. The ACA can be used to solve TDP and VRP problems and many other problems, and is very scalable.

First, we read the set of orders to be delivered on a certain day for agricultural products and obtain the basic information of the associated agricultural products retail outlets, such as number, latitude, and longitude. The retail outlets of agricultural products are equivalent to cities in ACA. From the perspective of logistics cost, we analyze how the research algorithm weighs the relationship between transportation volume and inventory volume, and give the check-and-balance relationship curve between inventory level and transportation mileage, as shown in Figure 4.

The problem model mainly involves a procurement network consisting of several farmers' cooperatives and a super logistics center to fully reduce inventory and transportation costs under the premise of meeting the procurement needs of the logistics center. Due to the asymmetry of market information and the special characteristics of fresh produce, in order to reduce the transaction risk, it is necessary to carefully find cooperative enterprises and supervise the completion of the performance, and if there are too many upstream and downstream partners or the updated information is not timely, it is necessary to pay higher transaction costs. To further test the performance of the algorithm, the study cites the sets of S12T4, S20T21, and S50T21 arithmetic cases and compares the results of the algorithm in this chapter with those of the hybrid genetic algorithm, and the computational results are shown in Table 1.

It should be emphasized that the main purpose of introducing artificial ants is to allow these ants to find some better routes between the corresponding the two nodes, and by better routes, we mean those routes that choose a node that is closest and takes the shortest time. Replacing a vehicle with an artificial ant to serve a customer point returns to the distribution center when the next customer point to be served would cause the total amount of the shipment to exceed the car's capacity or cause the distance to exceed the maximum distance traveled at one time. Indicating that this vehicle completes this transport, the vehicle then departs to serve the remaining customers until all customer points have been served at one time. The acceleration ratio trend graph for the parallel ACA experiment is shown in Figure 5.

Second, the global optimal ratio of vehicle loading to vehicle capacity, the global optimal ratio of individual vehicle loading to vehicle capacity, and the default individual vehicle loading to vehicle capacity are set. Unlike the simple path-planning problem, the model takes into account conditions such as product demand and inventory of each product in the logistics center, in addition to the transportation distance. The length of the path determines the probability size of the ants in choosing the next node and the concentration of pheromones left between two nodes. In order to keep a balance between "exploration" and "utilization" and to avoid stagnation while the algorithm has a strong search capability, the adaptive ACA uses adaptive pseudorandom rate selection rules. Due to a large amount of cargo for each task, each vehicle can only go to one task, in which case, the vehicle returns to the yard after loading or unloading directly from the yard to the task point. Let the pheromone parameter = 1, heuristic factor = 5, and information evaporation factor = 3, the adaptive ACA path simulation diagram is obtained, as shown in Figure 6.

Table 1: Comparison of algorithm results.

Example	S12T4	S20T21	S50T21
Algorithms in this chapter	19.172	27.172	32.241
Hybrid genetic algorithm	15.263	19.761	22.654

Finally, the suitable outlet is one of the next outlets set reachable by the ant's current outlet, and the cargo volume of this outlet is less than the remaining load volume of the ant. To increase the vehicle full-load rate, the logistics center purchases products in each procurement period by LTL transport, i.e., a single vehicle visits each cooperative in sequence and without considering the maximum load of the transport vehicle. However, due to the excessive growth of pheromones on some edges, this strategy may lead to a stagnation phenomenon where all ants search for the same path, and although the paths on which these edges are located may be better, they are often not the optimal ones. Therefore, penalties are considered for deviations from customer requirements, and customer losses due to deliveries outside the service time window are included in the penalty cost. The volume of freight task is small compared with the vehicle capacity, which generally means less than one-half of the vehicle capacity, and some tasks have concentrated collection and delivery points. We consider that one vehicle needs to load and unload goods at multiple assembly points. In order to achieve the above purpose, the goods can be mixed and loaded first, and then unloaded at several corresponding delivery points.

4.2. Process Analysis of Improving ACA in Agricultural Product Logistics. In the discrete space optimization problem, the travel of ants is achieved by jumping on the set of points in the discrete solution space, i.e., moving directly from one node to another node in the solution space. The distribution customers are mostly retailers, which belong to the end of the supply chain and are responsible for the sales of agricultural products. In the case of multiple yards, the transportation vehicles depart from multiple yards to perform tasks at multiple task points, which is the general transportation problem in operations research. Therefore, the improved ACA defines an activity range for the ants, which can only be within the radius of the ants, in order to increase the search range of the algorithm; as the number of iterations increases, the range of random perturbations can be linearly reduced to enhance the local convergence ability of the algorithm.

First, it is necessary to check whether there are goods placed on top of the exit tables of the 10 lanes and also to check the backlog signs of the transports to see whether the transports are in a waiting state. Similar to real ants that leave pheromones on the road, these electronic ants convert the information they collect, i.e., the speed and congestion of the route into electronic codes that are left on the road they pass. The existing pheromones on the road start to

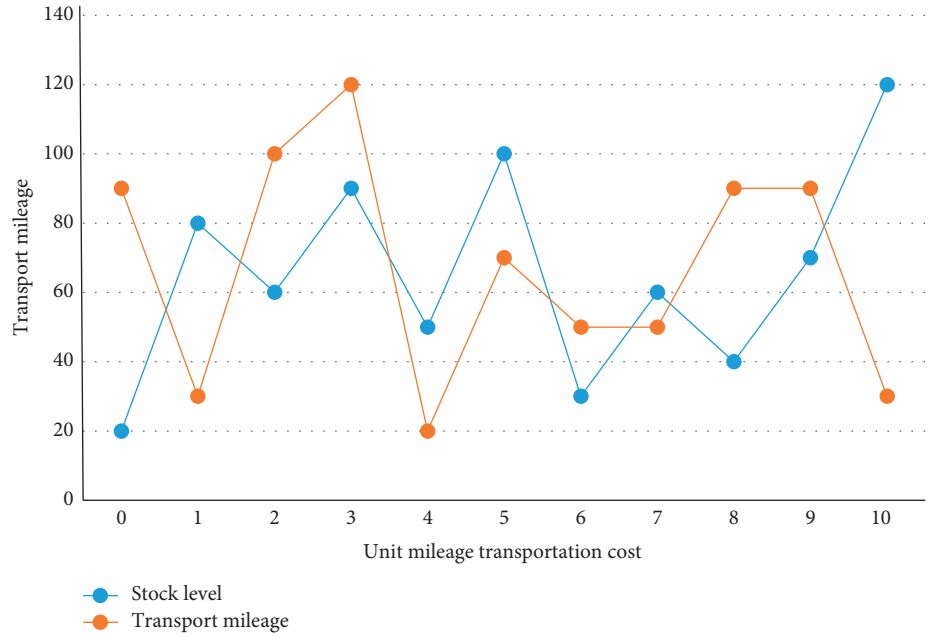

Figure 4: Relationship between inventory level and transportation mileage.

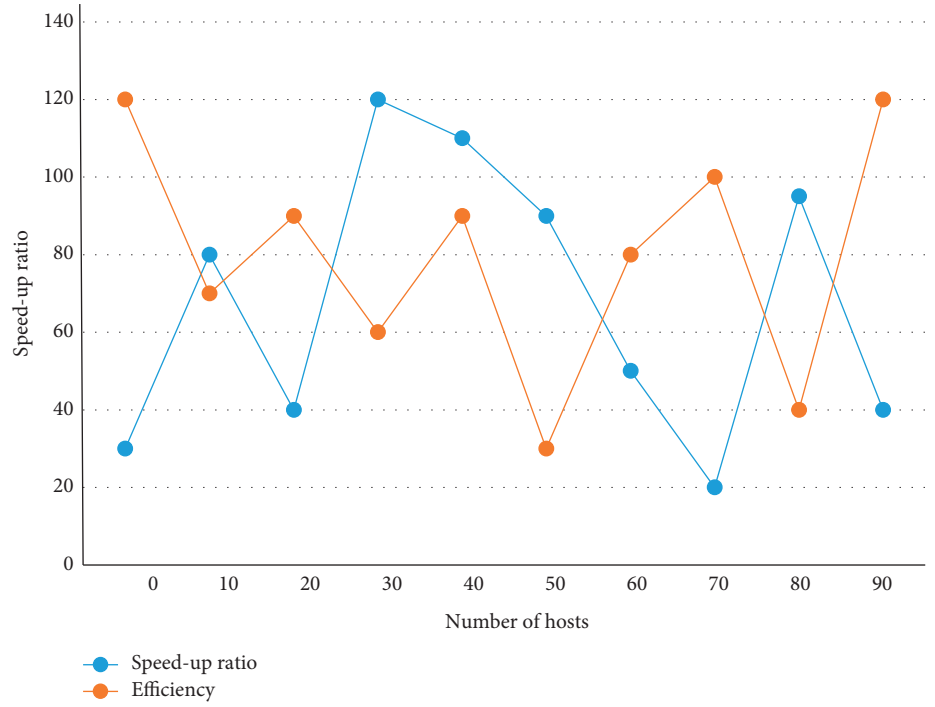

Figure 5: Trend diagram of acceleration ratio of parallel ACA experiment.

"evaporate," i.e., decrease, in proportion to a fixed parameter: each ant then adds new pheromones to the road it passes. The constraints of the problem are expressed in the form of states, and special operators are designed so that the solutions represented by the states remain viable during the search process. Since the update of the pheromone directly affects the selection probability, if the update of the pheromone is made more diverse, the selection of paths will be diversified. Therefore, the simulation results of the apriori algorithm, SVM algorithm, and improved ACA are compared, as shown in Figure 7 below.

Next, the information obtained in the first step is stored inside the D_s sequence. Based on the data inside the T_S sequence and the cargo priority Y_s sequence, the cargo priority size of these 10 lanes is found. For the dense distribution near the optimal point, using the local strategy can

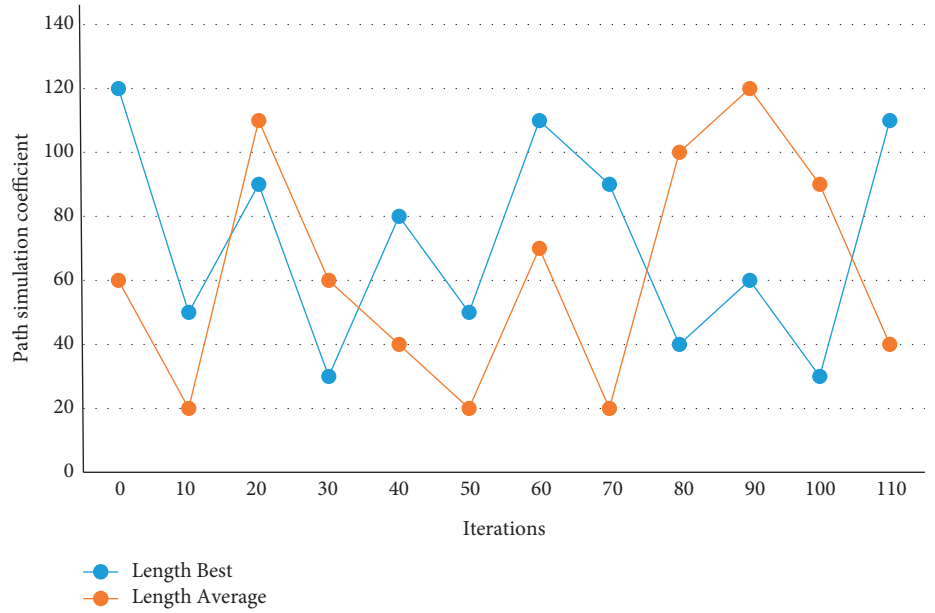

Figure 6: Adaptive ACA path simulation diagram.

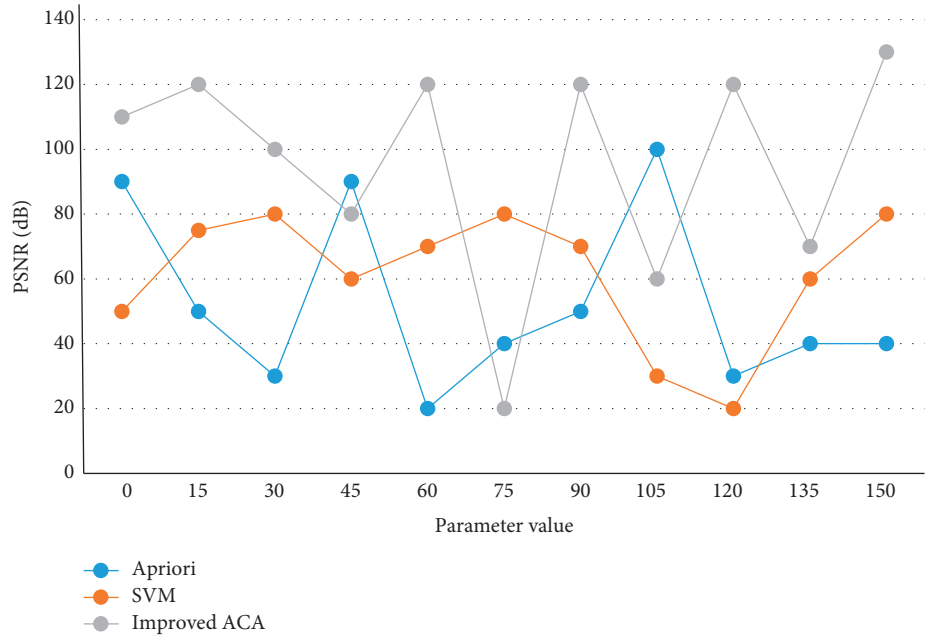

Figure 7: Simulation comparison of three different algorithms.

search only the subregion where the optimal point is located, which will be more effective and fast to search for the new minimum value. For the yard, logistics information technology allows freight forwarders to quickly and comprehensively grasp the nature, quantity, and flow of LTL cargo, so as to develop a reasonable loading and unloading operation plan, to better implement the principle of "sitting over the main, landing as a supplement." At the same time, as the key facilities distribution information in the visualized grain logistics information system, such as finished grain storage warehouses, vehicle dispatching centers and finished grain demand destinations are indispensable databases for spatial query and route planning analysis, and are also the basic attributes of the finished grain logistics information system. Therefore, the improved ant algorithm applied to the path scheduling of conveying trolleys can find out the shortest path, and after the shortest path encounters the phenomenon of blockage, it can promptly discover and bypass this blockage break to find another suboptimal route. To further illustrate the effect of considering inventory on

Table 2: Optimization results of one-to-many distribution model.

	IBM ILOG CPLEX	Improved ACA
H	6	10
Optimal solution	1425	3461
Inventory costs/total cost	271/8815	52/8900

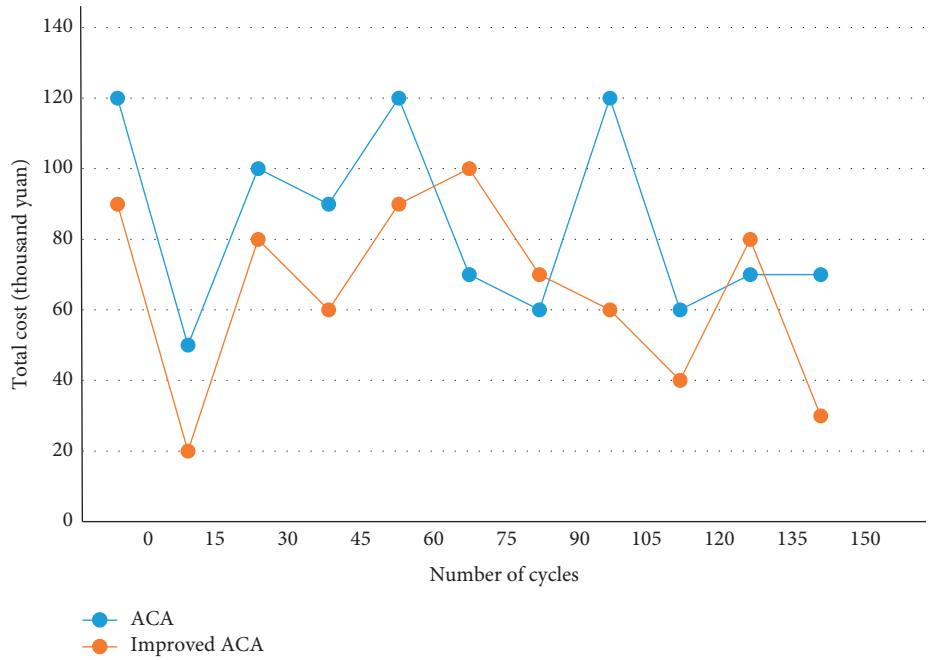

Figure 8: Comparison chart of total cost convergence.

path planning in a finite cycle, let the transportation cost per unit mile be 10, the algorithm is optimized by IBM ILOG CPLEX and improved ACA, respectively, and the results are shown in Table 2.

The inventory cost/total cost of the improved ACA is 0.006 for a unit mile transportation cost of 10, compared with 0.031 for IBM ILOG CPLEX, a reduction of 0.0025, i.e., it shows that the inventory cost can be significantly reduced by using the improved ACA in the case of high inventory cost per unit of product.

The problem is solved with the basic ACA and the improved ACA, respectively, and run in the MATLAB environment to obtain a comparison graph of the total cost convergence of agricultural logistics distribution, as shown in Figure 8.

Finally, the two lanes with the highest priority are obtained, and they are prioritized for transport pickup. We make the network signal propagate along the line with the highest degree of electronic pheromone reinforcement. By using a positive feedback mechanism to enhance the attractiveness of paths with ant paths to ants in subsequent iterations, the elite ant system additionally enhances the strength of information on contemporary optimal paths. However, because of this, the algorithm is prone to stagnation after a certain number of iterations and does not continue to explore other new solutions. Therefore, the ants deliver to the customer point from the yard and then return to the yard to form a delivery route after the delivery is completed, and all the delivery routes are added together to form a complete delivery route. The constraints are not considered in the coding process, and the solution abandonment is decided by checking the feasibility of the solution in the search process.

5. Conclusions

The development of modern logistics technology and the widespread use of the automated three-dimensional warehouse, resulting in an automated three-dimensional warehouse in the joint optimization of inventory transportation and scheduling problems, have become the bottleneck in modern logistics technology that has yet to be solved. The modern economy is a more important part of modern logistics, the development of modern logistics to improve the country's economy, optimize the system configuration, save time costs, etc. is of great significance. In addition, the traditional information system of finished grain cannot meet the needs of users, and the visualization of the information system is getting more and more attention. The ACA can complete the construction of a global solution by local solution with the help of positive and negative feedback function; in addition, it can prevent the algorithm from entering the local optimal mode with the help of negative feedback function. Therefore, in this study, based on the

analysis of the current development of China's agricultural logistics system, the research focuses on the inventory and transportation aspects to improve the comprehensive decision-making level, and proposes the joint optimization of inventory and transportation with the "efficiency backward" relationship. This study introduces ACA into logistics vehicle scheduling and explores the joint optimization of inventory and transportation of transportation vehicles by using ACA to pursue the optimal solution with the lowest total cost and the greatest total benefit of the transportation system. Therefore, the study of joint optimization and visualization of inventory transportation in agricultural logistics based on ACA takes into account the constraints closer to the reality and has the advantages of simplicity, intuition, easy-to-understand, and easy-to-design algorithms to solve and strengthen expandability.

Data Availability

The dataset can be accessed upon request.

Conflicts of Interest

The authors declare no conflicts of interest.

Acknowledgments

This work received funding from the Hebei Social Science Fund Project "Comprehensive Transportation Low-Carbon Development Mode and Management System Research in Hebei Province" (Project No. HB19GL021).

References

[1] X. Yang, Z. Zhang, and Y. Wu, "Research on joint distribution route optimization of cold-chain logistics for fresh agricultural products," *Journal of Physics: Conference Series*, vol. 1624, no. 4, Article ID 042032, 2020.

[2] H. Wang, Z. Liu, and Y. Liang, "Research on the three-in-one model of agricultural products E-commerce logistics under the combination of resource saving and blockchain technology," *IOP Conference Series: Materials Science and Engineering*, vol. 677, no. 3, Article ID 032111, 2019.

[3] M. Li and Y. Zhang, "A bibliometric and visualization review analysis of agricultural ecosystem services research," *Low Carbon Economy*, vol. 13, no. 1, p. 16, 2022.

[4] L. Liu, H. Wang, and S. Xing, "Optimization of distribution planning for agricultural products in logistics based on degree of maturity," *Computers and Electronics in Agriculture*, vol. 160, pp. 1–7, 2019.

[5] B. Li and H. Hu, "Logistics model based on agricultural product transportation," *Agro Food Industry Hi-Tech*, vol. 28, no. 1, pp. 3370–3373, 2017.

[6] I. Tanaino, O. Yugrina, and L. Zharikova, "Routing of freight transportation in logistics of agriculture," *IOP Conference Series: Earth and Environmental Science*, vol. 403, no. 1, Article ID 012192, 2019.

[7] Z. Fu, Y. Yan, and Q. Guo, "Risk transfer mechanism and control in logistics of fresh agriculture product supply chain," *Xinan Jiaotong Daxue Xuebao/Journal of Southwest Jiaotong University*, vol. 53, no. 3, pp. 654–660, 2018.

[8] A. V. Paraskevov and V. I. Loiko, "The use of indicators of traffic in the logistics of agricultural holdings related to the transportation of agricultural products," *Polythematic Online Scientific Journal of Kuban State Agrarian University*, vol. 163, pp. 213–227, 2020.

[9] M. Yaziz, "Inventory, warehousing and transportation management impacts towards logistics performance in supply chain management MF mohamad," *Journal of Supply Chain Management*, vol. 7, no. 6, p. 296, 2020.

[10] M. Grazia Speranza, "Trends in transportation and logistics," *European Journal of Operational Research*, vol. 264, no. 3, pp. 830–836, 2018.

[11] D. G. Mogale, A. Dolgui, R. Kandhway, S. K. Kumar, and M. K. Tiwari, "A multi-period inventory transportation model for tactical planning of food grain supply chain," *Computers & Industrial Engineering*, vol. 110, pp. 379–394, 2017.

[12] M. Deyi and Z. Xiaoqian, "Stochastic programming for the optimization of transportation-inventory strategy," *Industrial Engineering and Management Systems*, vol. 16, no. 1, pp. 44–51, 2017.

[13] R. Ding and P. Ren, "The Logistics Performance Evaluation index System in the Transportation Industry Based on Big Data," in *Proceedings of the 2018 IEEE 3rd International Conference on Big Data Analysis (ICBDA)*, pp. 33–37, IEEE, Shanghai, China, March 2018.

[14] J. Jiang, N. Yu, J. Ye, and B. Wei, "Vehicle logistics path optimization based on ant colony and particle hybrid algorithm," *Journal of Physics: Conference Series*, vol. 1865, no. 4, Article ID 042086, 2021.

[15] X. Tian, L. Liu, S. Liu, Z. Du, and M. Pang, "Path planning of mobile robot based on improved ant colony algorithm for logistics," *Mathematical Biosciences and Engineering*, vol. 18, no. 4, pp. 3034–3045, 2021.

[16] W. Liu, "Route optimization for last-mile distribution of rural E-commerce logistics based on ant colony optimization," *IEEE Access*, vol. 8, no. 99, p. 1, 2020.

[17] U. Teschemacher and G. Reinhart, "Ant colony optimization algorithms to enable dynamic milkrun logistics," *Procedia CIRP*, vol. 63, pp. 762–767, 2017.

[18] F. Lu, W. Feng, M. Gao, H. Bi, and S. Wang, "The fourth-party logistics routing problem using ant colony system-improved grey wolf optimization," *Journal of Advanced Transportation*, vol. 2020, no. 4, 15 pages, Article ID 8831746, 2020.

[19] Y. Wang, "Research on inventory path optimization of VMI large logistics enterprises based on ant colony algorithm," *Journal of Intelligent and Fuzzy Systems*, vol. 4, no. 1, pp. 1–11, 2021.

[20] H. Xiong, "Research on cold chain logistics distribution route based on ant colony optimization algorithm," *Discrete Dynamics in Nature and Society*, vol. 2021, Article ID 6623563, 2021.

[21] Z. Zhou, "Logistics distribution route optimization algorithm based on improved ant colony algorithm of gray wolf optimizer," *Computer Science and Application*, vol. 11, no. 4, pp. 892–901, 2021.

[22] Y. Yang, G. Zhang, and M. Du, "Research on seafood logistics path based on ant colony optimization algorithm," *Journal of Coastal Research*, vol. 108, 2020.

[23] B. Zhao, H. Gui, H. Li, and J. Xue, "Cold chain logistics path optimization via improved multi-objective ant colony algorithm," *IEEE Access*, vol. 8, Article ID 142977, 2020.

[24] K. Liang, "Research on marine port logistics transportation system based on ant colony algorithm," *Journal of Coastal Research*, vol. 115, p. 64, 2020.

[25] L. Peijing, "Logistics transportation route for agricultural products based on an improved ant colony algorithm," *Agro Food Industry Hi-Tech*, vol. 28, no. 1, pp. 1876–1880, 2017.
[26] F. Xue and T. Dong, "Research on the logistics robot task allocation method based on improved ant colony algorithm," *International Journal of Wireless and Mobile Computing*, vol. 14, no. 4, pp. 307–311, 2018.
[27] G. Zhang, "Solving route optimisation problem in logistics distribution through an improved ant colony optimisation algorithm," *International Journal of Services Operations and Informatics*, vol. 8, no. 3, p. 218, 2017.
[28] J. Wang, "Research on the optimization of path information in the process of logistics distribution by improved ant colony algorithm," *Italian Journal of Pure and Applied Mathematics*, no. 41, pp. 343–352, 2019.
[29] D. Seng, Q. Wang, and X. Fang, "Application and analysis of logistics distribution routing based on ant colony algorithm," *Revista de la Facultad de Ingenieria*, vol. 32, no. 3, pp. 423–431, 2017.
[30] M. Shang, "Research on optimal scheduling of logistics vehicle based on improved ant colony algorithm," *Journal of Critical Care*, vol. 42, no. 2, pp. 679–683, 2017.

Hindawi
Computational Intelligence and Neuroscience
Volume 2022, Article ID 8646463, 9 pages
https://doi.org/10.1155/2022/8646463

Research Article

Research on the Construction of English Autonomous Learning Model Based on Computer Network-Assisted Instruction

Mijuan Tian, Rong Fu, and Qianjun Tang

School of Educational Sciences, Leshan Normal University, Leshan, Sichuan 614000, China

Correspondence should be addressed to Mijuan Tian; tianmj@lsnu.edu.cn

Received 12 May 2022; Accepted 1 June 2022; Published 15 June 2022

Academic Editor: Yaxiang Fan

Copyright © 2022 Mijuan Tian et al. This is an open access article distributed under the Creative Commons Attribution License, which permits unrestricted use, distribution, and reproduction in any medium, provided the original work is properly cited.

As a supplement to traditional teaching methods, computer-assisted teaching methods can reflect modern educational concepts, such as creating student-led, teacher-led environments. The goal of college English education is to enable them to communicate effectively in English in their future academic, work, and social interactions, while also developing students' self-learning skills. Chinese society improves overall cultural competence and adapts to the needs of international communication. Self-directed learning is not static and will increase or decrease with time, discipline, and conditions and is an evolving process. Understanding learning, taking responsibility for one's own learning, and learning how to learn are all beneficial. Students abound in school life and even throughout their lives. In this paper, we try to propose a computer-based method for constructing an independent English learning model based on a practical study of computer network technology for the development of self-learning ability of non-English majors in a university. This paper uses comparative analysis techniques to compare traditional paper-and-pencil examinations and computer-based online evaluations and analyzes the effects of each. The survey showed that 81% of the students preferred the computer-based assessment. Therefore, the focus of this research is to strengthen the oral English training in college and create an authentic English learning environment for students to really feel the standard English pronunciation, intonation, and knowledge of grammar, listening, reading, writing, and translation.

1. Introduction

In the context of the rapid growth in the number of college students in China and the relatively limited educational resources, the existing single-class teaching model was improved and a computer and new teaching model was developed [1]. With the support of modern information technology, especially network technology, English education is developing in the direction of personalized learning and self-study which is not limited by time and place [2]. Traditional teaching methods centered on teachers, classrooms, and books can no longer meet the needs of the information society [3]. Modern educational technology, represented by network-based computer-assisted education, is having a profound impact on education [4]. At the same time, all kinds of latest information on the Internet and constantly updated educational models are affecting traditional education, and both students and teachers are overwhelmed by rich educational resources [5].

In the era of knowledge and information explosion, individual learning ability is a key factor for sustainable development [6]. Assistive teaching methods such as computers play an important role in teaching English listening, reading, writing, and translation [7]. Teachers teach English through multimedia and other supplementary teaching resources. Teaching content is presented in a three-dimensional combination of images, sound, animation, and text, which changes the traditional teaching methods and significantly improves teaching efficiency [8]. Allowing learners to learn independently through the Internet has become an important means to cultivate students' comprehensive quality [9]. The quality of students has also changed significantly, with students becoming more individualized and the traditional elite education not

interconnecting with the needs of students [10]. In the context of web-assisted teaching, teachers and students inevitably fall into the confusing stage of "how to teach and how to learn" [11]. This has put forward higher demands on the audiovisual learning and teaching of English for college students. The independent learning mode of English based on computer network-assisted teaching allows students to learn anytime and anywhere, choose the materials that suit their needs, and should be able to complete listening and speaking training that cannot be done in traditional classrooms, including recording, comprehension, and student learning. It can test the teacher's teaching and learning at any time, urge students to study actively, and quickly improve practical skills such as English listening and speaking ability.

Creating a computer-assisted teaching system and using the system for educational services can save time for after-school tutors [12]. It can also help students to solve problems in the process of learning computer courses, and the theoretical base tests in the assistive teaching system can help students to integrate the learning effect of the classroom [13]. At a deeper level, teachers and researchers are finding and applying various new pedagogical concepts for teaching university English courses under informational conditions, which significantly increases the efficiency of informational-based physical devices [4]. Computer-supported college English education can apply modern technology to education, realize the perfect combination of information technology and classroom education, effectively improve college English education, and play a positive role in promoting the reform of college English education [14]. Among them, expert system is a model of artificial intelligence, which has successfully penetrated into various fields from theoretical research to practical application, from general thinking to professional knowledge application, and has created great social and economic benefits.

The innovations of this paper are as follows:

(1) This system combines teaching evaluation with autonomous learning, strengthens the contact and interaction between teachers and students, and better realizes the purpose of assisting teaching.

(2) Using this model, learners can no longer study completely according to the traditional teaching mode and can arrange their own study flexibly and independently, which can be said to be a complete change of the traditional learning form.

(3) The system uses an expert system to analyze all students in a specific group (e.g., multiple classes, universities, etc.), allowing the system to provide better education.

The research framework of this paper consists of five parts, which are arranged as follows:

The first part of this paper introduces the research background and significance, and then introduces the main work of this paper. The second part introduces the work related to English autonomous learning mode and computer network-assisted teaching. The third part combs the main construction steps of the expert system and the knowledge representation methods of English autonomous learning model, so that the readers of this paper can have a more comprehensive understanding of the construction of autonomous learning model. The fourth part is the core of the paper. It describes the analysis of students' autonomous learning system from two aspects: BP neural network and implicit knowledge base analysis based on computer network. The last part of the paper is the work summary of the full text.

2. Related Work

2.1. English Autonomous Learning Model. Using the Internet to acquire knowledge has become an important means of human learning. It allows students who want to learn anytime and anywhere to improve learning efficiency and reduce learning costs. Interactive computer-aided teaching system provides a platform for teachers and students to interact and communicate, facilitates teachers' course instruction, and improves the efficiency of problem solving. It provides a whole new level of modern education and promotes a major new leap in education technology, education system, and education methods. Therefore, how to develop information technology and how to use it more effectively in education has become a matter of concern.

At the same time, Cassady et al. have done a lot of empirical research in combination with theoretical research and developed and built a number of self-learning application centers or platforms, with good results [15]. Mandad et al. propose an integrated technique designed to improve their self-directed learning and self-confidence, and to develop cultural literacy for social development and international exchange [16]. Alotumi adopts network transmission mode, all data are provided through the existing network, and educational content is provided in the form of web page [17]. Chunlin argues that modern information technology should provide new ways of teaching and learning, so that English teaching and learning can move toward autonomy [18]. Lolita et al. have built a computer-assisted instruction system by using the computer laboratory teaching network to establish an environment where students can actively participate in learning [19]. As a comprehensive technology that uses computer as a medium and realizes teaching activities through computer programs, it occupies an important position in the educational circles at home and abroad.

It is necessary to fully apply modern educational technology to college English professors and self-study teachers to further personalize the English teaching model so that all national reform projects can be carried out successfully in an information-based environment.

2.2. Computer Network-Assisted Instruction. The history of computer-assisted English education is divided into behaviorism and communicative constructivism. The basic theory of computer-assisted English teaching is the cornerstone of further research on computer-assisted English teaching based on constructivism. Internet provides a large

number of shared learning resources for students, which not only meets their English learning needs, but also breaks the boundaries of English teaching time and space, and helps to improve the overall level of English education.

Gao and Jin used artificial intelligence-driven natural language processing techniques to extract, compute, and predict features of articles, which can be classified according to their grammar, usage, structure, style, composition, development, lexical complexity, and inter-word relationships [20]. Aghajani and Amnzadeh developed a new "information modeling" approach. Candidate models are provided by a computer, while emotional selection and human-computer cooperation are performed by a human, so that complex learning can effectively construct satisfactory information models [21]. He provided several supporting features for teacher education and student writing, such as a rich library of configurable questions, exercises, student profile tracking and management, and writing ability diagnosis [22]. As a study of theoretical approaches, Djordjevic and Blagojevic proposed the theory of intelligent transformation of information knowledge, full information theory, and general logic theory [23]. Xie introduced the concept of personalization into traditional computer education systems, enabling the system to teach students according to their cognitive abilities, interest characteristics, etc. [24].

Computer network-assisted training mode allows teachers to create online courses on the platform, while learners choose courses to study independently and learn course content independently. Informatization talents can ensure the normal operation of social order by making maximum use of educational informatization resources, and establishing and improving informatization laws and regulations and informatization policies. Therefore, it is necessary to further study some new technologies that can be applied to college English teaching in order to further promote the reform of College English teaching.

3. Construction of English Autonomous Learning Model Based on Network Teaching

3.1. Main Construction Steps of Expert System. Learners learn independently through the use of web technologies and web-based learning resources, and instructors create learning contexts and build web-based platforms to accomplish the corresponding teaching tasks [25]. Fuzzy assessment and fuzzy reasoning are good methods for assessing students because there are no clear criteria for assessing their behavior. The weighting factor $w_i\,(i = 1, 2, \ldots, n)$ is the weighting coefficient of the sub-condition A_i, its value must be given by domain experts, and it satisfies the normalization condition:

$$\sum_{i=1}^{n} W_i = 1. \tag{1}$$

Experts systematically promote educational reform, expand subject knowledge, strengthen skill training, and enlighten and promote learners' thinking. Their functions not only relate to their own value, but also directly affect their position and effect in the educational process. The expert system structure is shown in Figure 1.

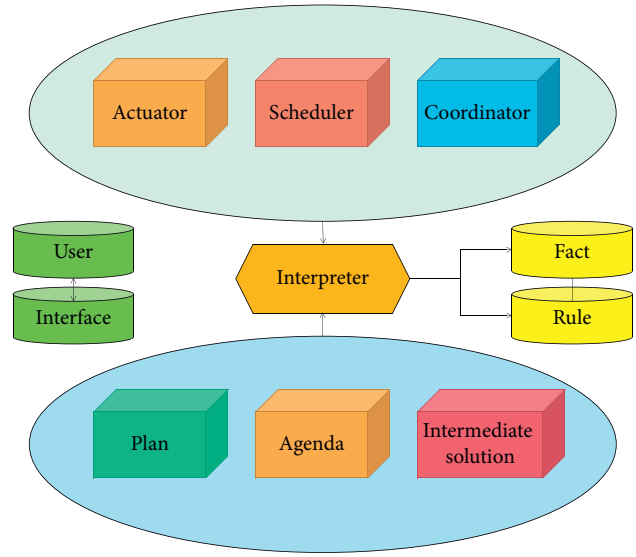

Figure 1: Structure of expert system.

First, make a detailed investigation and careful analysis of user needs, and then focus on the application problems to be solved. Task stage is a process in which learners clarify the content of new learning tasks and analyze their relevant conditions and factors according to their existing knowledge system. Let the credibility of each sub-condition A_i be $\mathrm{CF}(A_i)$, and the credibility of combined evidence is calculated by the following formula:

$$\mathrm{CF}(A_i) = \sum_{i=1}^{n} w_i \times \mathrm{CF}(A_i). \tag{2}$$

In the computer course-assisted teaching system, students will be able to log in to the system through a browser and register as users to perform corresponding operations, such as browsing course-related information, submitting questions and checking the status of answers through the web browser, taking online tests and viewing statistics, and viewing and submitting assignments. For the P th sample, the output error E_P of the network is

$$E_P = \frac{1}{2}\sum_{i=0}^{n-1}\left(tP_j - o_{P_j}^{(l)}\right)^2. \tag{3}$$

Using a Web browser as the integrated client, integrating the core and functionality of the system into the server and implementing it is the core of the model, and if a Web browser is installed, the client can use it. Assuming that the cost of adding a WME is the average value of the WME added to each α memory, there are

$$M_n = \frac{1}{n+1}\sum_{m=0}^{n} M_{m,n}. \tag{4}$$

It is a method of constructing and simulating display system by using object-oriented information modeling concepts, such as classes, relationships, attributes,

encapsulation, inheritance, polymorphism, and other mechanisms. The B/S structure achieves powerful functions that previously required complex dedicated software, reduces development costs, and builds a new software system [26]. This structure has become the preferred architecture of reference software today. The three-tier structure system is shown in Figure 2.

Secondly, under the current technological conditions, a large amount of domestic and foreign materials are consulted to collect, summarize, and organize domain knowledge, and appropriate methods are selected for knowledge acquisition, such as manual knowledge acquisition, semi-automatic knowledge acquisition, and fully automatic knowledge acquisition. The goal-setting and planning stage is the process in which learners determine learning goals and learning plans and use learning strategies according to the teaching requirements and standards [27]. The processed result data are then transmitted to the client side, and finally, the client completes the processing and display of the data. The administrator and teacher can manage the module in the background, and the server runs the relevant program module to process the request after receiving it. This protects the data of the object from malicious or unintentional modification by other objects, provides the underlying guarantee for data security, and allows the module to be extended when the requirements change. Therefore, the overhead of deleting a WME is one more than the overhead of adding a WME to find the β memory. And the overhead of finding β memory at this point is

$$R_{m,n} = \sum_{i=m}^{n} a \circ \prod_{j=1}^{i} a_j p_j (a_m = 1). \tag{5}$$

Finally, collect and reorganize the formalized knowledge, including the separation of knowledge base and fact base, knowledge representation, the realization of reasoning mechanism, and man-machine interaction, so as to make it consistent with the characteristics of the problem requiring solution. The strategy execution stage is a process in which learners learn and produce results according to the selected learning strategies [28]. It starts from the teaching objectives and flexibly designs and adjusts the teaching scheme according to the situation of different students. It is a kind of simulation of teachers' computer behavior. According to the requirements of teaching objectives and combined with the cognitive level of learners, it dynamically selects appropriate teaching contents from the Teaching Library. When using the object-oriented method to design a software system, we must first distinguish the types of things in the real world, analyze their properties and functions, and then abstract them into entities and classes that are meaningful in the computer virtual world.

3.2. Knowledge Representation of English Autonomous Learning Model. In an expert system, knowledge representation refers to the strategy of representing human knowledge into data structures and system control structures that can be processed by machines. With the use of computer and network in English teaching, students can learn independently and individually according to their interests, needs, tasks, and cognitive styles, thus breaking through the time and space limitations of traditional teaching mode and building an infinite and open teaching space. In the case that the nodes of the hidden layer can be set freely according to the need, the three-layer forward neural network can realize any continuous function with any approximation, and let the output of the layer neuron from the layer l neuron j to the layer $l + 1$ neuron under P samples be

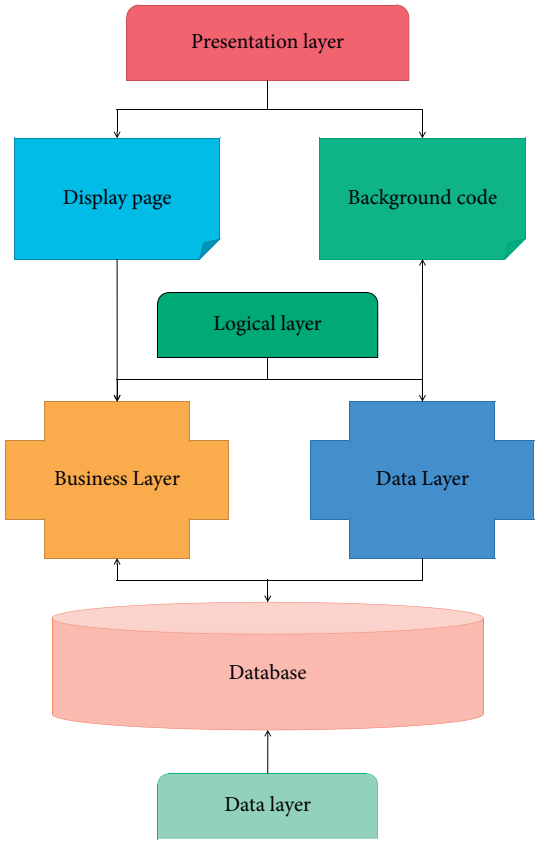

Figure 2: Three-layer structure system.

$$f(x) = \frac{1}{1 + e^{(-x)}}. \tag{6}$$

Knowledge representation is student-centered, and teachers are teaching designers and instructors. It refers to that teachers send the produced teaching videos to students by using micro-classes before class, so that students can carry out extracurricular self-study and master the classroom content in advance. The data flow design of knowledge representation method is shown in Figure 3.

First of all, in the process of building and using an expert system, it is necessary to continuously expand and improve the knowledge in the knowledge base, and whether the knowledge representation is easy to modify and expand knowledge is directly related to the success of the expert system. In the goal-setting stage, learners analyze the learning task, judge their own abilities, envision the learning

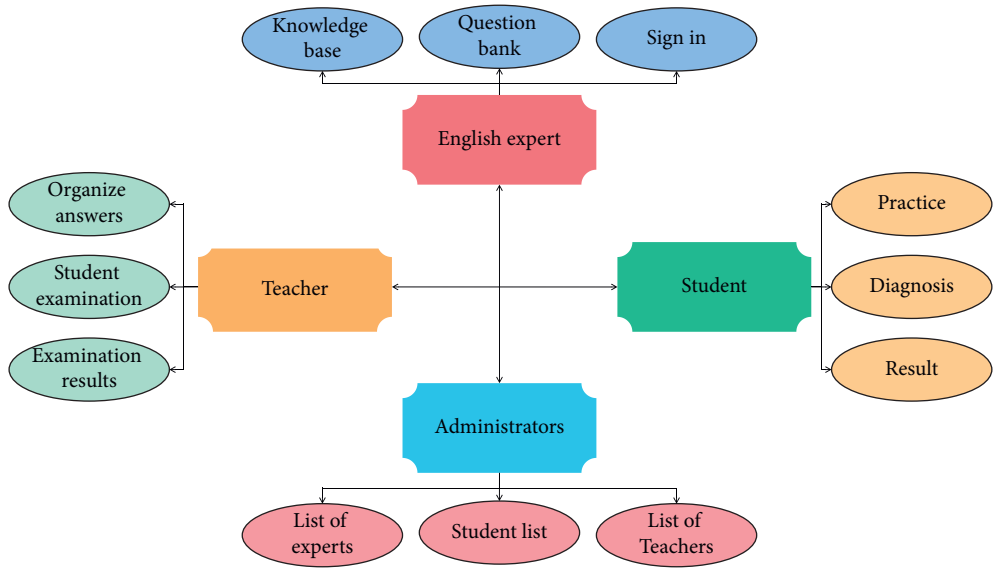

Figure 3: Data flow design.

outcome, and then determine the learning goal based on the combination of these aspects [29]. The number of nodes in the hidden layer of the three-layer network is not chosen arbitrarily, in this system, the number of nodes in the input and output layers can be determined, and the number of nodes in the hidden layer l can be given according to the empirical formula.

$$l = \sqrt{m+n} + a, \quad a \in \{1, 2, \ldots, 10\}. \tag{7}$$

As far as the full review is concerned, the breadth of memory is infinite and forgetting is relatively slow. So, modeling the forgetting law of memory, the Ebbinghaus forgetting curve can be obtained as

$$S(t) = \frac{1}{1+V_t}. \tag{8}$$

From the perspective of administrators, teachers, and students, dynamic web technologies are used to transfer information between the client, server, and database for login, logout, browsing, viewing, searching, and testing, as well as for backend management of teachers and administrators. The administrator can manage the teacher user information through this module, and teacher users can access the system backend through the teacher management login screen after the administrator adds teacher user information. In addition to studying the representation of uncertain and imprecise knowledge, imprecise reasoning methods are also explored. Compute the output of each neuron in the implicit layer and output layer of the network:

$$O_{Pj}^{l} = fi\left(\sum_{j} w_{ji}^{l} O_{i}^{l-1} - \theta_{j}^{1}\right). \tag{9}$$

Secondly, using concise and consistent knowledge representation methods, the knowledge represented by complex representation methods is difficult to understand. The function of students' personality reasoning is to evaluate students' learning effect, diagnose problems in learning, and evaluate their cognitive ability through students' learning process. Students are able to easily request learning services from the web, and the entire service delivery process requires no human intervention. The formulas for correction weights and thresholds are as follows:

$$w_{ji}^{l}(n+1) = w_{ji}^{l}(n) + \eta\delta_{Pj}^{l} o_{Pi}^{1-l} \partial\left(w_{ji}^{l}(n) - w_{ji}^{l}(n-1)\right). \tag{10}$$

Aided review systems are a combination of automatic review and manual review by the teacher, which is done through online annotations, where the teacher selects the original essay with errors and adds tips and suggestions for improvement. In current repository construction practice, the construction of a large repository often involves the integration of several smaller repositories or even fragmented resources.

Finally, the representation should be clear and unambiguous. A clear and unambiguous knowledge representation helps experts understand and directly debug the knowledge in the expert system. The knowledge representation provides code reusability, so that previously designed classes with similar functionality can be masked and expanded in the inherited subclasses without changing the original code, thus making the original code largely reusable. After the integration is completed, the resource base will become a large network with a complex topology. The English language learners who use this university English teaching resource library are likely to face an extremely complex user interface.

4. Systematic Analysis of Students' Autonomous Learning

4.1. BP Neural Network Analysis. Judging the mastery of students' knowledge points is actually the fault diagnosis of

students' knowledge points. The most used and effective in the field of fault diagnosis is the forward multilayer network. Because this kind of network adopts BP algorithm in the process of learning and training, this network is also called BP network. At the same time, there are still some problems in autonomous learning under the network environment, such as backward concept, ignoring design, not focusing on effect, single content, and poor sharing. Therefore, these problems are fully considered in the construction of pattern design. Lamp is a combination of LAMP is a combination of MySQL, Apache, and Linux open-source software, commonly used to build dynamic websites or servers, often used together and highly compatible with each other. Together, they therefore form a powerful web application platform. A detailed comparison of the three is shown in Figure 4.

First, the adjacent layers in the network are connected by interconnection, there is no connection between neurons in the same layer, and there is no direct connection between the output layer and the input layer. It is a mode of operation in which the server receives requests from the browser, then gets the data from the database, runs the processing on the server, and returns the results to the browser. When the student user registers, the information entered by the user will be verified by setting the verification from operation, such as QQ number can only be in numeric format and special format of e-mail address. The information entered by the student user can only be written to the database if it passes the verification; otherwise, the system will give a prompt and need to re-enter. When generating random numbers, the system automatically compares the newly generated random numbers with the existing random numbers, and if it is found to be equal to the existing random numbers, the newly generated random numbers will be discarded and generated again to ensure that all random numbers are not the same. The fuzzy output variables of the system have the reliability of the conclusion and the confidence level is propagated sequentially. Figure 5 shows the uncertainty of the following two fuzzy quantifiers.

Secondly, the number of samples required for network training depends on the complexity of the input-output nonlinear mapping relationship; the more complex the mapping relationship is, the more noise the samples contain, the larger the number of samples required to ensure a certain mapping accuracy, and the larger the network size. The core part of the system function is concentrated on the server, and the main application part is concentrated on the client with web browser, which makes the development and maintenance of the system simpler. The task of the teaching strategy reasoner is to select appropriate learning resources and teaching methods for students through corresponding reasoning algorithms based on the personalized information provided by the student model. Through the theoretical self-test and data statistics module in the system, students can take online tests after learning the theoretical knowledge, through which they can know their knowledge mastery, and after the tests, they can record the results and view the results and histogram, so that they can understand their learning situation in time. Therefore, the independent learning platform must be an Internet-based system that makes full

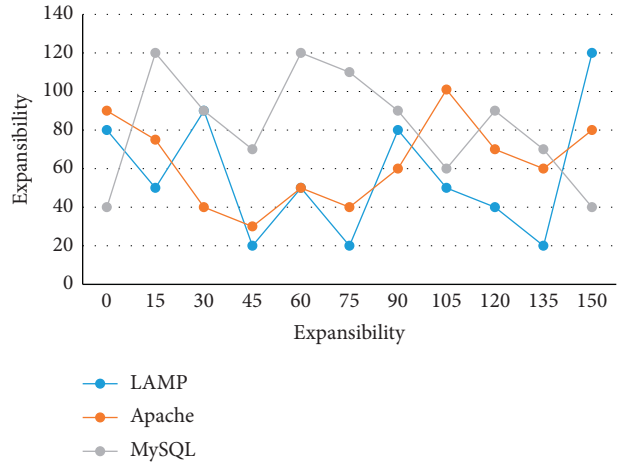

Figure 4: Comparison of two main platforms of web development.

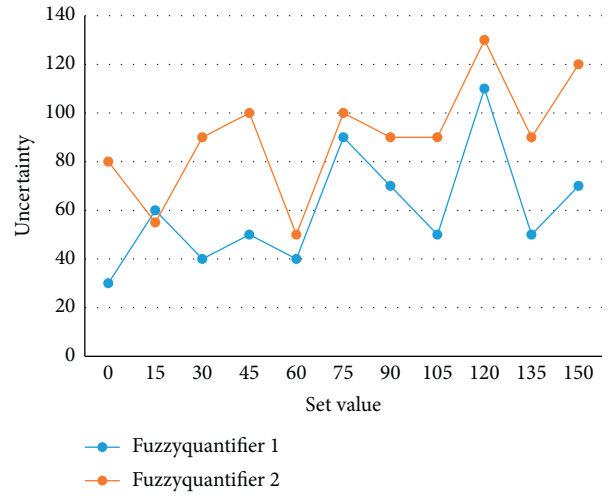

Figure 5: Uncertainty comparison of different quantifiers.

use of computer technology to make the learning content rich and vivid, and is designed to be modularized for easy maintenance and expansion in the future. The database is designed to record the test results of students, and the design is shown in Table 1.

Finally, under the condition that the hidden layer nodes can be freely set as required, any continuous function with arbitrary approximation can be realized by using three-layer feedforward neural network. Any computer that can be connected to the Internet network can access services and operate various applications, which does not need to be installed and maintained, and has good scalability at the same time. Essay class, composition class, stores students' writing, and practice information are as shown in Table 2.

Through the update record function in the server behavior, the information is updated, the function of changing the student user data is realized, and the updated information is returned to the main page of the system. The control information of the next learning plan given systematically, such as controlling the teaching content, the

Table 1: Test record.

Listing	Student-ID	Last time	Count	Grade
Type	Int	Data time	Int	Int
Can it be blank	N	N	N	N
Meaning	Student	Last test time	Number of tests	Total test score

Table 2: Data storage design—essay composition classes and attributes.

Attribute name	Title	Status	Creator
Attribute type	String	String	User
Explain	Title, null allowed	Writing state	Writing students

difficulty of controlling the teaching process, and the next teaching strategy, aims to make the teaching content information be presented according to different students' levels and needs under the control of the system.

4.2. Analysis of Implicit Knowledge Base Based on Computer Network. The survey shows that about 79% of students believe that web-based assisted instruction is only some common learning aids such as ppt used by teachers during class, and their understanding of web-based assisted instruction is too narrow. However, many autonomous learning modules for college English viewing, listening, and speaking are poorly understood. In the implicit knowledge base, the sufficiency measure and necessity measure are defined as the form of possibility ratio. Domain experts do not need to provide accurate probability estimation, but only provide possibility ratio. The process of developing a self-learning implicit knowledge base in a network environment is summarized according to the general rules of software design and development education.

First, according to the knowledge provided by the domain experts, the English knowledge was divided into 20 knowledge points, the English experts added questions for these 20 knowledge points as the test bank of the sample database, and the questions were selected to be representative. According to the characteristics of online learning, the content of each teaching unit and the logical relationship between the units were designed and scripted according to the constructivist learning theory. Therefore, importing formatted files allows the system administrator to manage the system user information in bulk, and the system administrator can update the user information in the system by uploading files with the user information or export the user information in the system to files. The system can record the last 20 test scores of students, and the statistical interface is shown in Figure 6.

Second, training and test samples are selected from this library, and when the network is well trained, students take questions from it for self-testing. Since the information on the Internet is mixed, students can easily devote their time and energy to information that is not related to the learning content. Therefore, teachers should provide online self-study for students, recognize the content, provide effective guidance on learning strategies, etc., and check the effectiveness

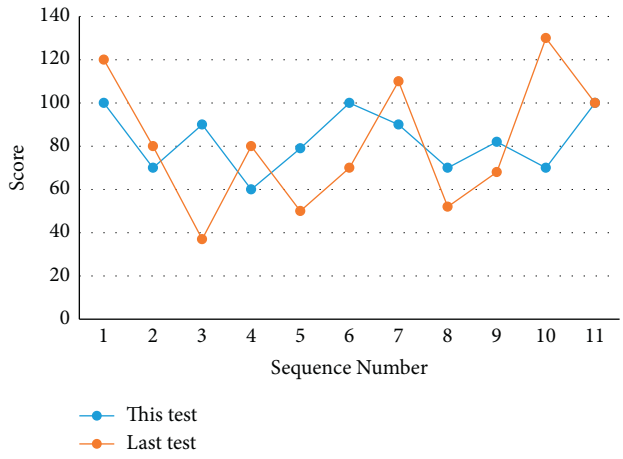

Figure 6: Data statistics interface.

of students' self-study. Through the interconnection of special equipment, it realizes the sharing of different types of educational resources files within the campus network segment, ensures the security, unity, and scalability of the educational resources file transfer system, and improves the management-level resources of various types of educational resources. The core is the function that can be used to determine whether data exist on a socket or whether data can be written. A comparative analysis method was used to experimentally compare traditional paper-and-pencil tests with computerized online assessments and analyze the impact of each, and the comparative results are shown in Figure 7.

The results show that both groups basically meet the requirements of the syllabus, but the effect of system controlled learning in the computer test group is better than that in the traditional test. However, 81% of students prefer computer evaluation. The comparison between the learning ability value given by the system and the written test score is shown in Figure 8.

Therefore, the learning ability value given by the system is basically consistent with the final test result, which shows that the student model established by the system is basically reasonable.

Finally, the set of weighted coefficients and the set of thresholds are obtained after the conversion of the topics

Figure 7: Comparison between paper-and-pen test and computer online evaluation.

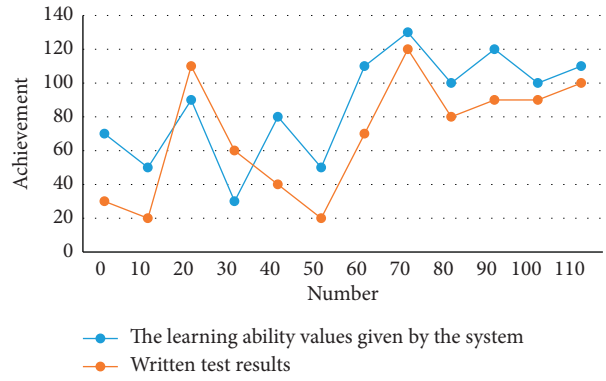

Figure 8: Comparison between the learning ability value given by the system and the written test score.

and rule tables provided by the domain experts to the learning in the form of internal codes, and the knowledge base stores the knowledge about the network structure, the composition of the weights, etc. There are database and its application system to store data efficiently and to meet user information requirements and processing requirements. This knowledge base can effectively prevent the application from being in blocking mode or entering a blocking state when the socket is in blocking mode. After the student selects a course and enters the diagnostic test phase, the system shall give the student the competency test questions for that level according to the level selected. Upon completion of the submission, the system should provide timely feedback and evaluation, and suggest appropriate adjustments to the level selected by the student.

5. Conclusion

Independent learning in the network environment is the new development direction of lifelong learning, and it gradually develops into an excellent educational environment parallel to the classroom. How to integrate different types of computer teaching resources into English classroom education, realize the sharing of high-quality English teaching resources, and stimulate students' interest in learning is the perfect education for the four major abilities of listening. The integration of oral, reading, and writing in English education and the change of traditional classroom teaching methods are the main goals of the current reform of English education in universities. In this paper, we analyze the problems of the current educational status and the limitations of the existing system by combining the current situation of teaching and research of domestic and foreign auxiliary education systems with the background of actual computer-based teaching and self-learning English based on computer networks supporting teaching methods. The article combines the practical application requirements, a detailed analysis of the system through the implicit knowledge base based on BP neural networks and computer networks, and the techniques of expert systems, the main construction steps, and the learning model of self-study knowledge representation of English. The teacher of computer-assisted design English teaching can fully utilize the technology of computers to create real-life scenarios for students in this authentic language learning environment, where students can perform semantic construction of knowledge in the classroom with bilateral stimulation of both visual and audio.

Data Availability

The dataset can be accessed upon request.

Conflicts of Interest

The authors declare that there are no conflicts of interest.

References

[1] J. Ying, "How to improve the autonomous learning ability of students in higher vocational colleges with multimedia-assisted instruction," *Agro Food Industry Hi-Tech*, vol. 28, no. 1, pp. 467–470, 2017.

[2] X. Hu, "Computer-assisted English teaching model in academic writing: a case study of three-stage development," *Overseas English*, vol. 20, no. 3, 2020.

[3] G. Min, "The application of computer assisted English teaching model in college English teaching," *Agro Food Industry Hi-Tech*, vol. 28, no. 1, pp. 745–748, 2017.

[4] L. Zuo, "Computer network assisted test of spoken English," *Computer Systems Science and Engineering*, vol. 34, no. 6, pp. 319–323, 2019.

[5] P. Kang, "A study of college English autonomous learning model based on computer and network," *IOP Conference Series: Materials Science and Engineering*, vol. 750, no. 1, Article ID 012031, 2020.

[6] L. Wang, "Study on the optimization application of computer assisted instruction in college art teaching," *Revista de la Facultad de Ingenieria*, vol. 32, no. 12, pp. 479–485, 2017.

[7] Q. Zheng, T. Chen, and D. Kong, "An empirical study on context awareness integrated mobile assisted instruction and the factors," *Eurasia Journal of Mathematics, Science and Technology Education*, vol. 13, no. 6, pp. 1737–1747, 2017.

[8] Q. Liu, "On the instruction design of the course business English writing based on blended learning model," *Review of Educational Theory*, vol. 4, no. 4, p. 24, 2021.
[9] Y. Du, "Study on cultivating college Students English autonomous learning ability under the flipped classroom model," *English Language Teaching*, vol. 13, no. 6, p. 13, 2020.
[10] K. O. Jeong, "Developing efl learners' communicative competence through multimedia-assisted language learning," *Journal of Theoretical and Applied Information Technology*, vol. 96, no. 5, pp. 1367–1376, 2018.
[11] H. Li and J. Ji, "Analysis of English listening obstacles based on computer assisted instruction," *Computer-Aided Design and Applications*, vol. 18, no. S4, pp. 130–140, 2021.
[12] J. Simarmata, T. Limbong, E. Napitupulu et al., "Learning application of multimedia-based-computer network using computer assisted instruction method," *International Journal of Engineering & Technology*, vol. 7, no. 2.13, p. 341, 2018.
[13] Y. Widiawati, "Designing and building exercise model of technical English vocabularies using call (computer assisted language learning)," *Lingua: Journal of Languages and Culture*, vol. 4, no. 2, p. 1, 2017.
[14] D. Ratnaningsih, F. Nofandii, D. Purba, and D. Wiratno, "The influence of computer assisted language learning (call) to improve English speaking skills," *Research, Society and Development*, vol. 8, no. 10, Article ID e438101413, 2019.
[15] J. C. Cassady, L. L. Smith, and C. L. Thomas, "Supporting emergent literacy for English language learners with computer-assisted instruction," *Journal of Research in Reading*, vol. 41, pp. 1–20, 2018.
[16] R. Manda, H. Nurlaila, and W. B. Indri, "Development of web-based computer-assisted language learning in English intensive course," *IOP Conference Series: Materials Science and Engineering*, vol. 180, Article ID 012291, 2017.
[17] M. Alotumi, "The effect of computer-assisted language learning project (CALLP) on Yemeni EFL student teachers' perceived TPACK self-efficacy," *International Journal of Research in English Education*, vol. 5, no. 4, pp. 14–40, 2020.
[18] Y. Chunlin, "How peer review affects Chinese adult college students' English writing acquisition in a computer assisted online learning environment," *Journal of Physics: Conference Series*, vol. 1176, no. 2, Article ID 22044, 2019.
[19] Y. Lolita, E. Boeriswati, and N. Lustyantie, "The impact of computer assisted language learning (CALL) use of English vocabulary enhancement," *Linguistic, English Education and Art (LEEA) Journal*, vol. 4, no. 1, pp. 206–221, 2020.
[20] J. C. Gao and M. H. Jin, "An analysis of college students' autonomous English learning ability under the network environment," *Literature & Art Studies: English version*, vol. 8, no. 1, p. 9, 2018.
[21] M. Aghajani and H. Amanzadeh, "Computer-assisted language learning in reading comprehension by using visual mnemonics A case study of Iranian EFL learners," *International Journal of Applied Linguistics & English Literature*, vol. 7, no. 1, p. 130, 2017.
[22] H. He, H. Yan, and W. Liu, "Intelligent teaching ability of contemporary college talents based on BP neural network and fuzzy mathematical model," *Journal of Intelligent and Fuzzy Systems*, vol. 39, no. 4, pp. 4913–4923, 2020.
[23] J. Djordjevic and S. Blagojevic, "Project-based learning in computer-assisted language learning: an example from legal English," *Nasledje, Kragujevac*, vol. 14, no. 36, pp. 247–259, 2017.
[24] G. Xie, "An instructional model of online synchronous instruction--A case study of college English course for college students," *Frontier of educational research: Chinese and English version*, vol. 10, no. 3, p. 8, 2020.
[25] C. C. Sheng, N. Idris, N. Idris, D. L. E. Fu, D. L. E. Fu, and M. M. Yusof, "Developing a computer assisted summary writing learning model," *International Journal of Learning and Teaching*, vol. 4, pp. 94–101, 2018.
[26] X. Cui and X. Wang, "Research on the online college English teaching mode from the perspective of autonomous learning," *Journal of Contemporary Educational Research*, vol. 5, no. 11, pp. 114–117, 2021.
[27] B. Yi, "Analysis on ESP theory-based college English autonomous learning," *Revista de la Facultad de Ingenieria*, vol. 32, no. 15, pp. 693–697, 2017.
[28] M. K. Kim, J. W. Mckenna, and Y. Park, "The use of computer-assisted instruction to improve the reading comprehension of students with learning disabilities," *Remedial and Special Education*, vol. 38, Article ID 074193251769339, 2017.
[29] H. Idris, N. Nurhayati, and S. Satriani, "Developing computer-assisted instruction multimedia for educational technology course of coastal area students," *IOP Conference Series: Earth and Environmental Science*, vol. 156, no. 1, Article ID 012049, 9 pages, 2018.

Hindawi
Computational Intelligence and Neuroscience
Volume 2022, Article ID 5354326, 10 pages
https://doi.org/10.1155/2022/5354326

Research Article

DSM and Optimization of Multihop Smart Grid Based on Genetic Algorithm

Qi Zhu, Yingliang Li, and Jiuxu Song

School of Electronic Engineering, Xi'an Shiyou University, Xi'an 710065, China

Correspondence should be addressed to Qi Zhu; qzhu@xsyu.edu.cn

Received 12 May 2022; Accepted 27 May 2022; Published 10 June 2022

Academic Editor: Yaxiang Fan

Copyright © 2022 Qi Zhu et al. This is an open access article distributed under the Creative Commons Attribution License, which permits unrestricted use, distribution, and reproduction in any medium, provided the original work is properly cited.

Multihop smart grid is built on the basis of an integrated and high-speed communication network. Through the application of advanced sensing and measurement technology, equipment technology, control method, and advanced decision support system technology, the goal of reliable, safe, economic, efficient, environment-friendly, and safe use of the power grid is realized. In order to solve the problem of excessive demand for power supply, new energy power generation and demand response are proposed. According to the above background, the demand side economic scheduling problem is a complex optimization problem, which is difficult to be solved by ordinary algorithms. The adaptive global search algorithm based on a genetic algorithm can better solve complex optimization problems. The genetic algorithm proposed in this paper can effectively manage a large number of controllable loads in the selected area. The algorithm minimizes the cost and peak to the average ratio by changing the load. Home users can arrange their maximum load when the price is low. The peak load of residential buildings decreased from 98.5 kw/h to 90 kw/h, and the peak load decreased by about 7.53%. Through appropriate load dispatching, users minimize the daily electricity charge, which is reduced from 1352 yuan to 1245 yuan per day, and the daily electricity charge is reduced by about 7.25%. In addition, the advanced measurement, communication, and control means under the framework of the smart grid also play a key role in promoting all aspects of demand side management (DSM).

1. Introduction

Smart grid technology in intelligent buildings is a technology that uses two-way transmission of information and power. Then, it creates an advanced energy transmission network, which has the characteristics of automation and distribution. Multihop smart grid is built on the basis of an integrated and high-speed communication network. Through the application of advanced sensing and measurement technology, equipment technology, control method, and advanced decision support system technology, the goal of reliable, safe, economic, efficient, environment-friendly, and safe use of the power grid is realized [1, 2]. In order to solve the problem of excessive demand for power supply, new energy power generation and demand response are proposed. In order to improve household energy efficiency, demand side intelligent power dispatching has become a hot topic in the research of multihop smart grids. DSM plays the role of a control unit in the smart grid. It is a process used to balance the energy demand and supply between users and energy providers [3, 4]. This balance is achieved by combining energy management and reliable communication. The purpose of this is to establish a real-time and effective connection between users and energy suppliers. On the premise of maintaining the comprehensive service level of electric energy, adopt reasonable distribution and regulation methods to reduce the total consumption and load level of electric energy so as to achieve the purpose of reasonable distribution of electric energy, improving load curve, improving power supply efficiency and level, and promoting the coordinated development of sustainable economy, energy, environment, and other factors. In the current research, in order to improve the system performance of wireless communication networks in a multihop smart grid

system and make it more reliable and safe, a variety of wireless multihop network architectures have been applied to the multihop smart grid [5].

According to the above background, the demand-side economic scheduling problem is a complex optimization problem that is difficult to be solved by ordinary algorithms. The adaptive global search algorithm based on the genetic algorithm in this paper can better solve complex optimization problems. Then, the genetic algorithm is used to select the most discriminating features and reduce the computational complexity [6]. This algorithm can not only detect more discriminating features and save computing time but also improve the classification accuracy of the classifier to some extent [7]. The purpose of the genetic algorithm is to make the final load curve as close as possible to the target load curve and realize the goal of the DSM strategy [8, 9]. If the goal of DSM is to reduce the electricity bill, the target load curve will be the price of electricity in the electricity market. A genetic algorithm provides an approximately optimal solution to a given problem, and it has the potential to solve such complex problems. Therefore, this paper uses a genetic algorithm to improve the scheduling algorithm to solve the cost optimization problem.

Combined with the DSM in the smart grid system and the rate optimization of wireless multihop network in the smart grid system, it brings benefits to users and further improves the performance of the whole network. DSM strategy includes DSM controller, which is used to calculate the user side energy-saving control method of smart grid based on genetic algorithm. User side intelligent controller is used to disconnect or connect different types of loads [10]. The DSM controller takes the target load curve as the input and calculates the load to be transferred to meet the target load consumption [11]. The algorithm is flexible and completely independent of the standard used to generate the target load curve. Comprehensively monitor the power load of users, advocate the use of smart appliances and vigorously develop energy storage equipment, and encourage the generation of distributed green energy to go online. In addition, the advanced measurement, communication, and control means under the framework of the smart grid also play a key role in promoting all aspects of DSM. In this paper, I put forward the following innovations. The specific contents are as follows:

(1) This paper constructs a multihop smart grid structure model. As the DSM structure model of multihop smart grid is based on a genetic algorithm, it is necessary to monitor and analyze a set of key indicators to reflect the credit situation of power customers. Therefore, it is an important link to establish a scientific credit evaluation index of power customers.

(2) In this paper, the DSM system in the smart grid is constructed. In this paper, a multihop smart grid DSM system is constructed based on a genetic algorithm. The goal of DSM can maximize the use of renewable energy resources, improve economic benefits, and reduce the use of electric energy from the main distribution network, that is, reduce peak load demand.

The overall structure of this paper consists of five parts. The first chapter introduces the background and significance of DSM in multihop smart grids. The second chapter mainly describes the related work of DSM in multihop smart grids at home and abroad. Chapter 3 constructs the DSM system model of the smart grid. The fourth chapter carries out the experiment and analyzes the results. The fifth chapter is a summary of the full text.

2. Related Work of DSM in Multihop Smart Grid at Home and Abroad

Chen et al. put forward that the demand side should be considered as the classification of consumer electrical appliances. In order to get a more perfect electricity consumption model, consider adding a distributed generation model on the demand side, in which the distributed generation model can supply part of users' demand through independent power generation and make better use of resources [12]. Yao et al. put forward the interruptible load model of demand side appliances, which can dispatch household appliances better and increase the elasticity of the demand side [13]. Arun and Selvan designed a scheduling framework for residential energy consumption in a real-time pricing environment. This framework tries to achieve an ideal trade-off between minimizing the electricity cost and minimizing the waiting time for each household appliance to run, and the ultimate goal is to reduce the electricity cost and peak-to-average ratio [14]. Liang et al. put forward that the main purpose of DSM technology is to reduce the peak load demand and operating cost of the system. Although power companies can provide incentives to their customers and indirectly control the load through customer load grouping, most of the methods used do not consider independent criteria and objectives [15]. Zhu et al. proposed a traffic scheduling algorithm based on instrument data acquisition in building LAN. This method can effectively avoid interference between data communication devices, realize efficient traffic scheduling and data transmission, and finally meet the requirements of smart grid applications [16]. Wang et al. developed a realistic model to calculate the price of smart grid in order to reduce users' expenses, in which a convergent distributed algorithm was introduced and an estimate of production cost was provided according to actual demand changes [17]. Jabash and Jasper considered the access of distributed generation model but did not classify household appliances and only uniformly dispatch household appliances. After the addition of distributed generation, there may be residual power after meeting the needs of users, so the access of the municipal power model is considered [18]. Xu et al. proposed to consider the access of municipal power model and distributed model and the classification of household appliances, which reduced the power consumption cost of users but did not consider the user comfort, and there will be new power consumption peaks and valleys [19]. Fernandez et al. proposed and studied a DSM system

based on real-time information and proposed a centralized scheme and game theory method to reduce the power generation cost and peak-to-average ratio of the smart grid [20]. Scarabaggio et al. proposed that in smart grid, DSM strategy needs to deal with a large number of various types of controllable loads. In addition, the load can last for several hours. Therefore, the strategy should be able to handle all possible control of various controllable load durations [21].

This paper mainly studies the problems of DSM and rate optimization under information transmission in multihop smart grid systems. In this paper, the DSM of multihop smart grid is studied based on a genetic algorithm. This strategy is based on load transfer technology and can handle a large number of various types of equipment. The design and analysis of a multihop smart grid need basic insight into the influence of grid topology and big data integrated network control, as well as the complex interaction between physical layer and network layer, including supporting communication, information, network, and computing system. DSM emphasizes obtaining direct economic benefits on the basis of improving the efficiency of electricity consumption. It is an operational activity, which not only seeks efficiency but also pursues efficiency. In the operation process of electric power companies, on the premise of obtaining the permitted power-saving income, it is necessary to adopt the market means of encouragement to promote users to actively save energy and electricity. The simulation research is carried out on the user side of the smart grid in residential areas with various loads. The DSM strategy suitable for smart grids in the future is simply explained, the mathematical load transfer technology is formulated, the DSM strategy based on a genetic algorithm is put forward, and the simulation results are given. If large users have a large demand for electricity load, they can report it to the power grid company in advance. The power grid company can make preparations in advance, reasonably dispatch the power generation, respond to the peak load in time, reduce the reserve capacity of the whole power grid, increase the load rate of running generators, and improve the generator efficiency.

3. DSM System Model of Smart Grid

3.1. Proposal of Genetic Algorithm. As a classical optimization algorithm, a genetic algorithm is usually used to solve various optimization problems. Aiming at the optimization objective model in this paper, genetic algorithm mainly has the following four characteristics.

(i) Selection operation: select 90% of chromosomes through a roulette selection algorithm. Excellent individuals are retained, and poor individuals are also given some living space to avoid falling into local optimization.

(ii) Crossover operation generates a random number and compares it with crossover probability. Cross operation shall be carried out if conditions are met.

(iii) Mutation operation generates random numbers and compares the mutation probability. The mutation operation shall be carried out if the conditions are met.

(iv) Elite selection operation sorts the fitness and selects 10% to insert into the population. In the iterative process, the number of chromosomes of the population is the same as that of the initial population.

The proposed DSM strategy realizes that the actual power consumption curve of each transfer device at the moment of connection is as close as possible to the target power consumption curve. A genetic algorithm describes a set of attributes as a specific pattern and returns it, which is the predicted value of the input features, and the output values can be discrete or continuous. The learning of discrete values is called classification, while a genetic algorithm makes decisions by performing a series of tests [22, 23]. Therefore, the input features selected by the genetic algorithm are used to classify different electrical appliances. Genetic algorithm advances and new populations are generated from contemporary populations through remains algorithm: single-point crossover and binary mutation. A large crossover rate ensures faster convergence of solutions, and a very large mutation rate may lead to loss of good solutions inherited from the previous generation and prevent premature convergence of algorithms. The main steps of the genetic algorithm are shown in Figure 1.

Peak cutting and valley filling technologies are mathematically expressed as follows:

$$\sum_{t=1}^{N} \left(P_L(kT)\right) - P_o(kT)^2, \tag{1}$$

where $P_o(kT)$ is the target consumption curve of kT under time; $P_L(kT)$ is the actual consumption curve of kT under time.

This minimization problem is subject to the following limitations:

$$X_{nikT} > 0. \tag{2}$$

The number of devices transferred in a one-time step cannot be greater than the number of devices controllable in the current time step.

$$\sum_{kT=1}^{N} X_{nikT} > \text{Ctrlable}(i), \tag{3}$$

where $\text{Ctrlable}(i)$ is the controllable number of n type equipment in time step i.

The characteristics of demand-side management problems, for example, the connection time of equipment can only be delayed but not advanced, which can be expressed as follows:

$$X_{nikT} = 0. \tag{4}$$

Options specify the maximum allowable delay time of all devices and the number of possible time steps to which devices can be transferred.

After the completion of the genetic algorithm, the calculation results are reflected on each planning line in the

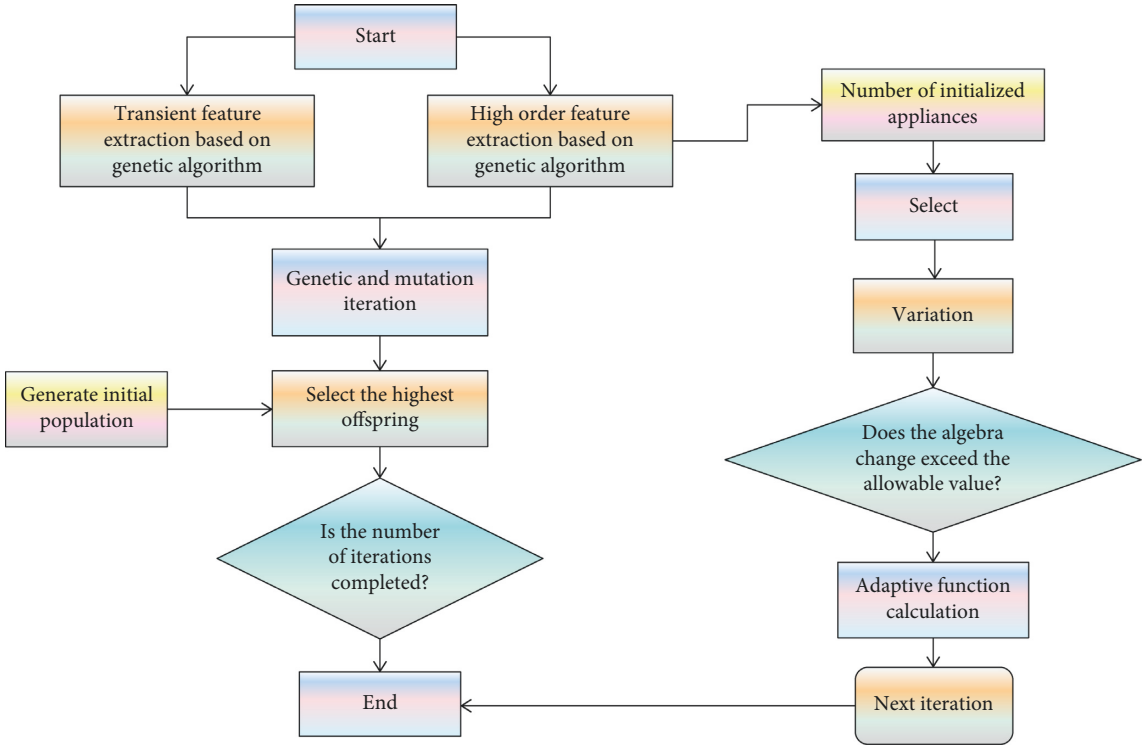

Figure 1: Flow chart of genetic algorithm.

form of pheromone, which is a part of the initial pheromone strength of the genetic algorithm. The other part is the pheromone constant given by the genetic algorithm according to the specific scale of the problem. These two parts are the initial pheromone of the genetic algorithm. Then, the pheromone update model updates the pheromone intensity. Under the smart grid based on a genetic algorithm, a more comprehensive and reasonable TOU price policy will be implemented, which can promote energy conservation and consumption reduction. Comprehensively implement the real-time electricity price system in all power consumption fields and inform power users of the electricity price in time so that users can choose their own power consumption mode according to their own needs and combined with the actual electricity price, so as to realize users' active load regulation and peak shifting and valley filling [24].

3.2. Demand Side Management System Model of Smart Grid. As the structural model of the multihop smart grid DSM system is based on a genetic algorithm, it is necessary to monitor and analyze a group of key indicators to reflect the credit situation of power customers. Therefore, the establishment of scientific power customer credit evaluation indicators is an important link in the establishment of the customer credit evaluation model [25, 26]. Through the benefit analysis of the example, it is found that under the premise of reasonable DSM, there will be better economic benefits and environmental protection benefits for power generation enterprises, power users, power grid enterprises, and the whole society. Scientific and reasonable real-time electricity price systems and information give users a great right of choice. Users can choose an efficient power consumption mode according to their own needs, actively mobilize users to participate in power distribution and dispatching, and realize the function of load peak shifting and valley filling. The composition of the current peak and valley electricity price and the change of the daily service cost policy cannot accurately reflect the current peak and valley electricity price. It is suggested to promote a flexible electricity price policy reflecting the power supply and consumption cost in different time periods. According to the actual statistical data of the customer service center of the power supply bureau, based on a large number of analysis and research, this paper constructs the power customer credit evaluation index system according to the following principles.

(i) Guiding principle.

In order to evaluate the credit of electric power customers, it is necessary to select the change of index characteristics to be ahead of time so as to sensitively reflect the problems existing in the credit of electric power customers and the development trend of the problems.

(ii) Principle of completeness.

When analyzing the reasons why power customers do not pay the electricity bill, we should collect information such as the background, development process, and consequences of the phenomenon of nonpayment of electricity bills as comprehensively and systematically as possible.

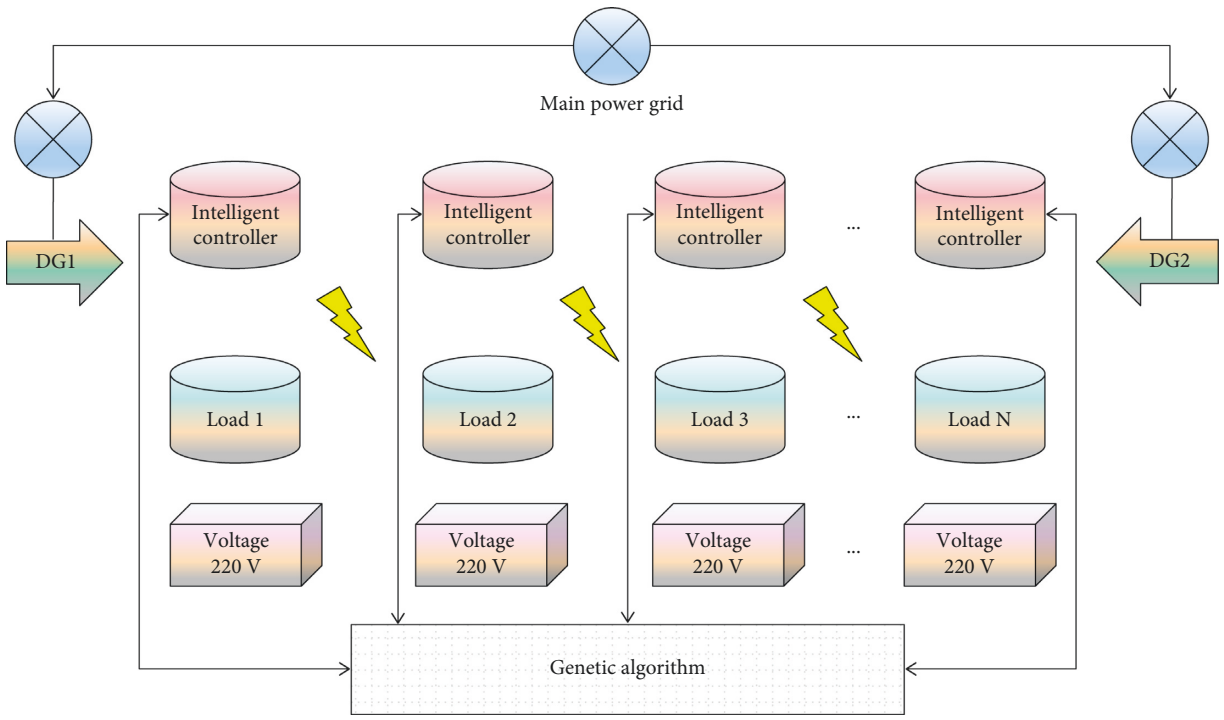

Figure 2: Structure model of multi-hop smart grid.

(iii) Principle of proximate cause.

The index design is determined according to the nature and characteristics of the reasons that lead to electricity customers not paying electricity bills on time. Different reasons for electricity customers not paying electricity bills have different properties and characteristics.

(iv) The principle of combining qualitative and quantitative analysis.

In the credit evaluation of electric power customers, adopting different evaluation indexes according to the characteristics of different evaluation contents can more accurately reflect the current situation and trend of electric power customers' credit. The goal of the genetic algorithm in this paper is to maximize the classification performance and minimize the number of features. The individual is the binary sequence of extracted feature vectors, and its size is equal to the dimension of features. The structural model diagram of the multihop smart grid DSM system based on genetic algorithm described in this paper is shown in Figure 2.

The output power of the generator set is affected by wind speed, and the approximate expression of the relationship between power and wind speed is as follows:

$$p_{WV}^{t}(v) = P_n \frac{v^t - v_i}{v_r - v_i}, v_i < v^t < v_r, \tag{5}$$

where P_{WV}^{T} is the output power of the system at t; v_i is the cut in and cut out wind speed; v^t is the actual wind speed at t time; v_r is the rated wind speed; P_n is the rated power.

Power generation is determined by the current light, external temperature, and temperature coefficient

$$P_{PV}^{t} = P_{stc} \frac{G^t}{G_{stc}}, \tag{6}$$

where P_{PV}^{t} is the output power of the system at t time; G^t is the light intensity at t time; $P_{stc}G_{stc}$ is the active power and light intensity under standard test conditions.

The traditional nonintrusive electrical monitoring method uses Fisher discriminant analysis to select features, and its objective function is as follows:

$$J = (\mu_1 - \mu_2)^2 \otimes \frac{1}{\sigma_1^2 + \sigma_2^2}, \tag{7}$$

where $J = [J_1, J_2, \ldots\ldots, J_L]^T$, L are the total number of parameters; $\mu_1, \mu_2, \sigma_1, \sigma_2$ is the mean and variance of two different eigenvectors, respectively; $\otimes$ represents Hadamard product.

Active power P

$$P = \frac{1}{T} \int_0^T ui \, dt = \sum_{i=1}^{\infty} V_i I_i \cos \theta_i, \tag{8}$$

where V is the voltage; I is current; θ is the included angle; The subscript i is the i dimensional component of voltage or current.

Reactive power Q

$$Q = \sum_{i=1}^{\infty} V_i I_i \sin \theta_i. \tag{9}$$

Power factor angle θ

$$\theta = \operatorname{arctg}\left(\frac{P}{Q}\right). \tag{10}$$

Current distortion rate ITHD

$$\mathrm{ITHD} = \frac{1}{I_l\sqrt{\sum_{i=2}^{\infty} I_h^2}}, \tag{11}$$

where I_l is the fundamental current; I_h is the ratio of total harmonic current effective value to fundamental current.

It can be transferred to an appropriate time step by a genetic algorithm according to its importance. From the analysis of the results obtained from the genetic algorithm, it can be known that after DSM, the daily maximum load can be reduced, the daily minimum load can be increased, and the peak-valley difference can be reduced, which can play a role in shifting the peak and filling the valley. After selecting the individual with the highest fitness, it can carry out gene crossover and mutation operations on the population. Establish the cost compensation mechanism and incentive mechanism of DSM. Research and establish new energy demand side special management funds suitable for the development of smart grid, make up for the cost of power grid enterprises to carry out power DSM, strive to break the power grid enterprises' pursuit of power sales interests, reform the assessment system, and increase incentives for power grid enterprises to take the leading force to deeply carry out power DSM.

3.3. Constructing DSM System in Smart Grid. DSM includes technologies and policies aimed at balancing daily energy consumption. Compared with the management scheme of adding new generator sets and other power suppliers, DSM is not only to increase the supplied energy but also to control the consumption form by using energy management technology. The most important goal of DSM is to reduce the peak value. In this paper, a multihop smart grid DSM system is constructed based on a genetic algorithm. The goal of DSM can maximize the use of renewable energy resources, improve economic benefits, and reduce the use of electric energy from the main distribution network, that is, reduce peak load demand. Multihop smart grid managers design the target load curve through the target of DSM system. Smart grid provides two-way interactive marketing technology and mechanism support, which makes the implementation of DSM naturally transition from the past government behavior and policy orientation to the market mechanism. In the past, due to the lack of advanced measurement and communication means, it was impossible to give convincing information on income sharing and investment return of DSM measures, which was effectively solved in the smart grid era. The front-end management software of DSM can realize remote power consumption information data collection and remote power distribution fault diagnosis according to user requirements.

The common technologies of DSM in smart grids are as follows.

(i) Increase nonpeak load

When the production cost in off-peak hours is lower than that in peak hours, this promotes energy consumption in off-peak hours. Various incentives, such as discounts, can encourage consumers to change their consumption habits.

(ii) Strategic power saving

Strategic power saving mainly reduces the periodic consumption of energy by reducing the waste of energy so as to improve the efficiency of energy consumption. The program includes a variety of incentives, mainly for technological change.

(iii) Strategic load growth

Strategic load growth increases periodic energy consumption. Power suppliers achieve this goal by deploying intelligent systems, node equipment, and more competitive energy.

(iv) Elastic modeling

This strategy is more flexible and needs modeling to be carried out according to the needs of consumers at every moment. By installing load-limiting devices, this strategy will limit consumers' energy use for certain periods of time without affecting the actual and safety conditions.

The software system supports various channel modes, Chinese information, centralized and remote reading of electricity consumption information of multifunction meters, parameter setting and correction, data sharing of demand-side user terminals, real-time copying of abnormal data analysis of terminals, fault event information recording, etc. DSM system emphasizes the establishment of a partnership between power companies and users. It is required to establish a very harmonious cooperative feeling between power companies and users so as to share risks and gain benefits for the benefit of power supply and electricity consumption. The system can also automatically analyze and judge the historical operation data of power users and remind the power demand side operation management personnel to make relevant inspections by voice, curve, report form, etc, for users who may steal electricity and leak electricity, so as to improve the efficiency of power supply reliability analysis of distribution branches and on-site power dispute handling by operators.

4. Experimental Results and Analysis

4.1. Experimental Analysis. The genetic algorithm is applied to the power demand dispatching management of a residential building in a community of a city. The building has more than 1000 controllable basic household appliances with different rated power in 6 different types. Generally speaking, the residential load has the characteristics of low power consumption and small duty cycle. Different types of household appliances and their rated power are shown in Table 1.

It can be seen from Table 1 that among different types of household appliances, water heaters account for the highest energy consumption, followed by air conditioners,

Table 1: Rated power of different types of household appliances in residential areas.

Equipment name	Energy consumption (kWh)	Quantity
Electric fan	0.07	135
Heater	4	136
Television	0.2	135
Microwave oven	2	135
Computer	0.6	67
Air conditioner	2.6	205

microwave ovens, computers, televisions, and finally, electric fans. Therefore, adopting reasonable optimization methods and adjusting the basic functions and structure of China's power, demand side can greatly improve the power supply and distribution capacity of the power grid, achieve energy conservation and consumption reduction, and promote the construction of a smart grid.

The load curve after load reduction by the genetic algorithm is shown in Figure 3.

As can be seen from Figure 3, the shape of the daily load curve has been obviously improved after the load is reduced by the genetic algorithm. From 20:30 to 22:30, the unplanned load was obviously reduced from 285 MW to 273 MW, effectively reducing the peak-valley difference, achieving the effect of demand-side management and improving the economy of power system operation.

After the real-time sales price is implemented, the daily maximum load appears at 20:30, and it is assumed that the maximum load that intelligent equipment can cut at each moment is predicted, as shown in Figure 4.

As can be seen from Figure 4, 7:00 a.m. to 9:00 a.m. and 17:00 p.m. to 19:00 p.m. are the peak periods of people's travel, and electric vehicles are in use, so the standby capacity is small. From 11:00 to 13:00 noon, a small number of car owners will go home for dinner, and the standby capacity is slightly reduced compared with working hours. At night, because the electric vehicle has been running during the day, the remaining power is not much, so the standby capacity will be much less than the working hours.

Calculate the load index of the active load curve before and after the adjustment of the real-time sales price model, as shown in Table 2.

It can be seen from Table 2 that after users adjust the load according to the real-time sales price, the load curve has changed significantly, the maximum load decreases, the minimum load increases, the peak-valley difference decreases, and the effect of shifting peak and filling valley is obvious, and the load tends to be stable, which can guide users to use electricity reasonably and optimize resource allocation.

Assume the relationship function between the compensation price and the load reduction of intelligent equipment, and the intelligent parameters of each node are shown in Table 3.

As can be seen from Table 3, the intelligent equipment compensation electricity price model program is called at 20:30, 21:00, and 21:30, respectively, [qzi, qz] = Zhen (30, 21, 0.5, [0120.80.900.60.600.60.80100) $P >$

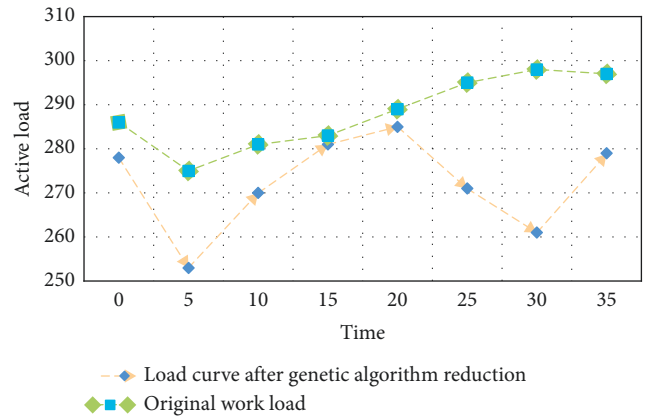

Figure 3: Load curve after genetic algorithm reduction.

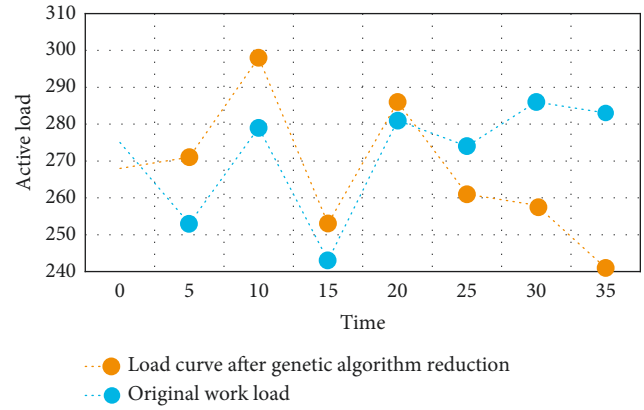

Figure 4: Maximum load after genetic algorithm reduction.

[01.9400.5520.9706.02002.3401.88000.55001.22000.5500.7600.8800.8677058555. Actively promote the establishment of a new mechanism for unified planning, unified approval, and coordinated development of smart grid and distributed energy, as well as the market access mechanism, exit and stop operation boundary conditions of distributed energy, and promote the healthy and orderly development of distributed energy. Establish a scientific and reasonable electricity price system and form a comprehensive electricity price selected by users of the power supply according to the four periods of peak, peak, flat, and valley. According to the seasonal load requirements, some energy-saving and consumption-reducing electricity price incentives are formulated to reduce unnecessary power waste.

The running results of multihop smart grid scheduling using machine learning algorithm, ant colony algorithm, particle swarm optimization algorithm, and genetic algorithm in this paper are shown in Figures 5–7.

It can be seen from Figures 5–7 that the genetic algorithm proposed in this paper can effectively manage a large number of controllable loads in the selected area. The algorithm minimizes the cost and peak to the average ratio by changing the load. Home users can arrange their maximum load when the price is low. The peak load of residential buildings decreased from 98.5 kw/h to 90 kw/h, and the peak

Table 2: Comparison of load indicators before and after real-time sales price model adjustment.

	Daily maximum load (MW)	Daily minimum load (MW)	Peak valley difference (MW)	Daily average load (MW)	Daily load rate (%)
Before adjustment	309.8948	244.3473	65.5471	277.2354	89.4612
After adjustment	301.2984	253.4577	47.8406	277.2347	92.0133

Table 3: Parameters of intelligent equipment.

Node number	Actual reduced load of chemical equipment			Default rate	Duration
	20:30	21:00	21:30		
1	1.931	1.942	1.961	0.35	2
2	0.551	0.553	0.571	0.26	2
3	0.972	0.971	0.992	0.21	0.7

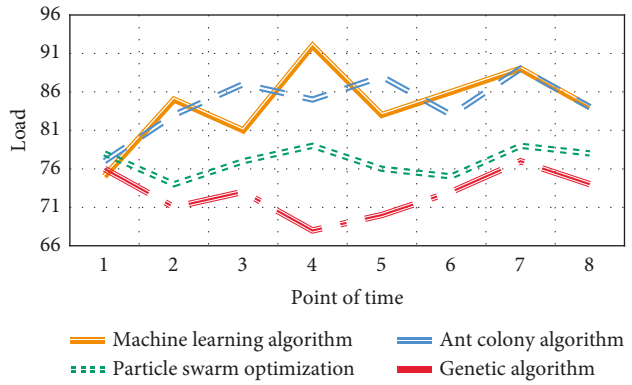

Figure 5: Comparison of daily power consumption of residential buildings before and after planning.

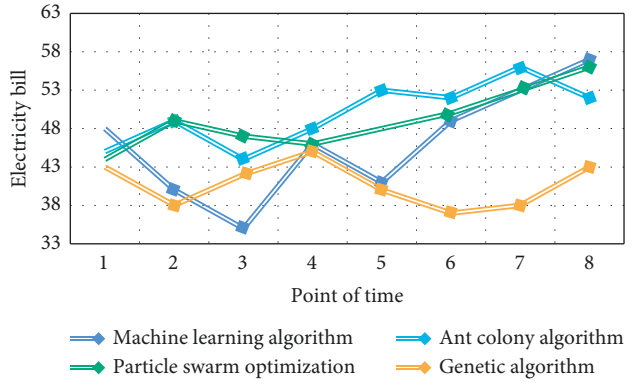

Figure 6: Daily electricity consumption of residential buildings before and after planning.

load decreased by about 7.53%. Through appropriate load dispatching, users minimize the daily electricity charge, which is reduced from 1352 yuan to 1245 yuan per day, and the daily electricity charge is reduced by about 7.25%.

4.2. Empirical Conclusion. The ultimate goal of DSM is to improve the power consumption efficiency of customers' power terminals. However, in the design process of DSM

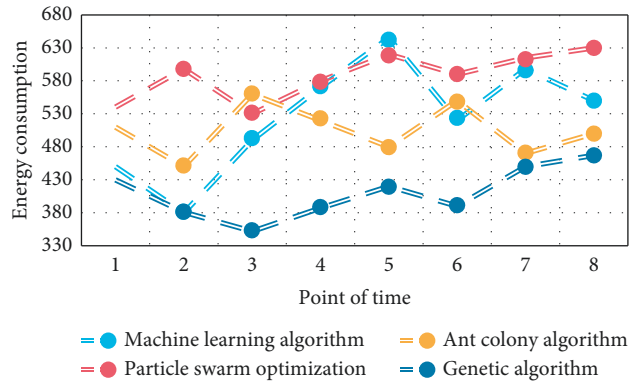

Figure 7: Comparison of energy consumption of residential buildings before and after planning.

mode, users must actively participate and discuss the power supply mode and structure of DSM. In this paper, the genetic algorithm has been compared with other algorithms many times, and finally, it is concluded that the method in this paper is the most advantageous in the DSM of multihop smart grid. Because of the change of load type and capacity of the power demand side, the imperfect function of DSM technology, and other factors, it is difficult for power grid demand side dispatching to achieve the functions of supply and demand balance, energy saving, and safety, and there are some disadvantages such as increased power loss and high unit power production cost. From the analysis of the results obtained from the genetic algorithm, it can be known that after DSM, the daily maximum load can be reduced, the daily minimum load can be increased, and the peak-valley difference can be reduced, which can play a role in shifting the peak and filling the valley. It can also guide users to use electricity reasonably, optimize resource allocation, achieve the effect of energy saving, improve the economy and stability of power system operation, and finally achieve the purpose of DSM.

Based on a genetic algorithm, the real-time monitoring of power load is the basic guarantee for the construction of an intelligent DSM system. In the process of system construction, higher requirements are put forward for the

metering system of power terminals. It is required that the metering system must have the function of real-time power load demand communication with the DSM system and obtain dynamic power grid parameters and load through the corresponding monitoring instruments. Using a genetic algorithm to carry out multiobjective optimization planning successfully solves the multiobjective, nonlinear, and discrete optimization problems in power grid planning and can simultaneously generate several optimization planning schemes in which each objective can be realized in different degrees, thus coordinating the conflicts among objectives and obtaining satisfactory results, which shows that this method is feasible.

5. Conclusions

The construction of an electric power company not only involves the huge economic benefits of users but also involves the economic development of the electric power system. This paper focuses on the application of multihop smart grid DSM based on a genetic algorithm. In the integrated model of DSM in this paper, through the genetic algorithm, firstly, the load response technology is established to dynamically adjust the load demand through the adjustment and change of real-time sales price. The smart grid has an advanced metering system and communication system, which provides conditions for load response technology. The control center can monitor the system operating parameters in real-time and transmit the real-time sales price to users. The genetic algorithm proposed in this paper can effectively manage a large number of controllable loads in the selected area. The algorithm minimizes the cost and peak to the average ratio by changing the load. Home users can arrange their maximum load when the price is low. The peak load of residential buildings decreased from 98.5 kw/h to 90 kw/h, and the peak load decreased by about 7.53%. Through appropriate load dispatching, users minimize the daily electricity charge, which is reduced from 1352 yuan to 1245 yuan per day, and the daily electricity charge is reduced by about 7.25%. The establishment of a reasonable management system, a scientific electricity price system, and an integrated monitoring system with a high level of automation through genetic algorithm can improve China's existing DSM system, achieve the purpose of peak load shifting and valley filling, energy conservation, and consumption reduction, and promote the construction of intelligent power demand side system and the sustainable development of power resources.

Data Availability

The dataset can be obtained from the corresponding author upon request.

Conflicts of Interest

The authors declare no conflicts of interest.

Acknowledgments

This work received Scientific Research Program Funded by Shaanxi Provincial Education Department (program no. 21JK0843).

References

[1] G. R. Aghajani, H. A. Shayanfar, and H. Shayeghi, "Demand side management in a smart micro-grid in the presence of renewable generation and demand response," *Energy*, vol. 126, no. may1, pp. 622–637, 2017.

[2] R. Tang, S. Wang, and H. Li, "Game theory based interactive demand side management responding to dynamic pricing in price-based demand response of smart grids," *Applied Energy*, vol. 250, no. 1, pp. 118–130, 2019.

[3] C. Li, X. Yu, W. Yu, and G. J. Chen, "Efficient computation for sparse load shifting in demand side management," *IEEE Transactions on Smart Grid*, vol. 8, no. 1, pp. 250–261, 2017.

[4] J. Nadeem, J. Sakeena, A. Wadood et al., "A hybrid genetic wind driven heuristic optimization algorithm for DSM in smart grid[J]," *Energies*, vol. 10, no. 3, pp. 1–27, 2017.

[5] R.-S. Liu and Y.-F. Hsu, "A scalable and robust approach to demand side management for smart grids with uncertain renewable power generation and bi-directional energy trading," *International Journal of Electrical Power & Energy Systems*, vol. 97, pp. 396–407, 2018.

[6] J. Lizana, D. Friedrich, R. Renaldi, and R. Chacartegui, "Energy flexible building through smart demand-side management and latent heat storage," *Applied Energy*, vol. 230, pp. 471–485, 2018.

[7] R. G. Babu, V. Amudha, C. Chellaswamy, and K. Senthil Kumar, "Retracted article," *Building Simulation*, vol. 15, no. 9, p. 1703, 2022.

[8] Al-S. Mohammed, M. Anbar, T. C. Wan, and Z. Alqattan, "Energy efficient multi-hop path in wireless sensor networks using an enhanced genetic algorithm - ScienceDirect[J]," *Information Sciences*, vol. 500, pp. 259–273, 2019.

[9] I. Erdin and R. Achar, "Multipin optimization method for placement of decoupling capacitors using a genetic algorithm," *IEEE Transactions on Electromagnetic Compatibility*, vol. 60, no. 6, pp. 1662–1669, 2018.

[10] J. L. Gonzalez, P. K. Jo, A. Reza, and M. S. Bakir, "Flexible interconnect design using a mechanically-focused, multiobjective genetic algorithm[J]," *Journal of Microelectromechanical Systems*, vol. 27, pp. 1–9, 2018.

[11] E. Bradford, A. M. Schweidtmann, and A. Lapkin, "Efficient multiobjective optimization employing Gaussian processes, spectral sampling and a genetic algorithm[J]," *Journal of Global Optimization*, vol. 71, no. 2, pp. 1–33, 2018.

[12] W. H. Chen, P. H. Wu, and Y. L. Lin, "Performance optimization of thermoelectric generators designed by multiobjective genetic algorithm[J]," *IET Renewable Power Generation*, vol. 209, pp. 211–223, 2018.

[13] E. Yao, P. Samadi, V. W. S. Wong, and R. Schober, "Residential demand side management under high penetration of rooftop photovoltaic units," *IEEE Transactions on Smart Grid*, vol. 7, no. 3, pp. 1597–1608, 2016.

[14] S. L. Arun and M. P. Selvan, "Intelligent residential energy management system for dynamic demand response in smart buildings[J]," *IEEE Systems Journal*, vol. 12, pp. 1–12, 2017.

[15] Y. Liang, F. Liu, C. Wang, and S. Mei, "Distributed demand-side energy management scheme in residential smart grids: An ordinal state-based potential game approach," *Energy Efficiency*, vol. 206, pp. 991–1008, 2017.

[16] H. Zhu, Y. Gao, Y. Hou, and L. Tao, "Multi-time slots real-time pricing strategy with power fluctuation caused by operating continuity of smart home appliances," *Engineering Applications of Artificial Intelligence*, vol. 71, pp. 166–174, 2018.

[17] Y. Wang, W. Yang, and T. Liu, "Appliances considered demand response optimisation for smart grid," *IET Generation, Transmission & Distribution*, vol. 11, no. 4, pp. 856–864, 2017.

[18] S. Jabash and J. Jasper, "MANFIS based SMART home energy management system to support SMART grid[J]," *Peer-to-Peer Networking and Applications*, vol. 13, no. 6, pp. 2177–2188, 2020.

[19] Z. Xu, Y. Gao, M. Hussain, and P. Cheng, "Demand side management for smart grid based on smart home appliances with renewable energy sources and an energy storage system," *Mathematical Problems in Engineering*, vol. 2020, pp. 1–20, Article ID 9545439, 2020.

[20] E. Fernandez, M. J. Hossain, and M. S. H. Nizami, "Game-theoretic approach to demand-side energy management for a smart neighbourhood in Sydney incorporating renewable resources," *Applied Energy*, vol. 232, pp. 245–257, 2018.

[21] P. Scarabaggio, S. Grammatico, R. Carli, and M. Dotoli, "Distributed DSM with stochastic wind power forecasting[J]," *IEEE Transactions on Control Systems Technology*, no. 99, pp. 1–16, 2021.

[22] K. Hrknen, L. Hannola, and O. Pyrhnen, "Advancing the smart city objectives of electric demand management and new services to residents by home automation—learnings from a case[J]," *Energy Efficiency*, vol. 15, no. 5, pp. 1–13, 2022.

[23] L. Bhamidi and S. Sivasubramani, "Optimal planning and operational strategy of a residential microgrid with demand side management," *IEEE Systems Journal*, vol. 14, no. 2, pp. 2624–2632, 2020.

[24] N. Sana, W. Yang, M. Guo, K. H. van Dam, and X. Wang, "Energy DSM within micro-grid networks enhanced by blockchain[J]," *Mathematical Problems in Engineering*, vol. 228, pp. 1385–1398, 2018.

[25] A. Mehdizadeh and N. Taghizadegan, "Robust optimisation approach for bidding strategy of renewable generation-based microgrid under demand side management," *IET Renewable Power Generation*, vol. 11, no. 11, pp. 1446–1455, 2017.

[26] R. S. Kumar, L. P. Raghav, D. K. Raju, and A. R. Singh, "Intelligent demand side management for optimal energy scheduling of grid connected microgrids," *Applied Energy*, vol. 285, no. march, pp. 116435–116449, 2021.

Hindawi
Computational Intelligence and Neuroscience
Volume 2022, Article ID 9773452, 9 pages
https://doi.org/10.1155/2022/9773452

Research Article

Construction of English and American Literature Corpus Based on Machine Learning Algorithm

Qian Dai

School of Foreign Languages, Henan Polytechnic University, Jiaozuo 454003, Henan Province, China

Correspondence should be addressed to Qian Dai; daiqian88@hpu.edu.cn

Received 7 May 2022; Accepted 20 May 2022; Published 2 June 2022

Academic Editor: Yaxiang Fan

Copyright © 2022 Qian Dai. This is an open access article distributed under the Creative Commons Attribution License, which permits unrestricted use, distribution, and reproduction in any medium, provided the original work is properly cited.

In China, the application of corpus in language teaching, especially in English and American literature teaching, is still in the preliminary research stage, and there are various shortcomings, which have not been paid due attention by front-line educators. Constructing English and American literature corpus according to certain principles can effectively promote English and American literature teaching. The research of this paper is devoted to how to automatically build a corpus of English and American literature. In the process of keyword extraction, key phrases and keywords are effectively combined. The similarity between atomic events is calculated by the TextRank algorithm, and then the first N sentences with high similarity are selected and sorted. Based on ML (machine learning) text classification method, a combined classifier based on SVM (support vector machine) and NB (Naive Bayes) is proposed. The experimental results show that, from the point of view of accuracy and recall, the classification effect of the combined algorithm proposed in this paper is the best among the three methods. The best classification results of accuracy, recall, and F value are 0.87, 0.9, and 0.89, respectively. Experimental results show that this method can quickly, accurately, and persistently obtain high-quality bilingual mixed web pages.

1. Introduction

In recent years, English and American literature has been paid more and more attention as a professional course to improve the humanistic quality and basic language skills of English majors. English and American literature course plays a very important role in the training plan of English majors in colleges and universities in China. Reading and analyzing a certain number of British and American literary works can improve students' basic language skills and humanistic quality and enhance their understanding of western literature and culture. As the course of English and American literature involves historical and cultural background, literary history, appreciation of original works, and literary theory and its contents are complex, it is inevitable that there will be a phenomenon of "cramming, ordering, and passing by" in the teaching process, and learners lack interest and initiative in learning. To understand British and American culture, it is more important to improve and cultivate students' autonomous learning ability, cultivate their literary appreciation and aesthetic sensitivity, and promote the cultivation of humanistic quality as a whole.

With the wide application of statistical methods, large-scale corpus has become an indispensable basic resource in the field of natural language processing. Natural language processing technologies developed based on statistical methods include hidden Markov model, maximum entropy model, Bayesian method, SVM (support vector machine), and other mining methods, which can be compared with this paper [1–3]. Based on this assumption, pages in different languages on the network have similar document structures, such as titles and paragraphs, if their contents are comparable. Stasak et al. proposed a comparable text mining method based on statistical information on word frequency distribution, which is independent of the construction language [4]. Meng et al. translated the words in the source language pages through a bilingual dictionary, then used these words to construct a query, and retrieved the first N (fixed value) related documents from the acquired target language page set [5]. Hassanpour and Langlotz crawled the

monolingual culture through the designated website and adopted a method similar to Talvensaari to obtain a comparable corpus [6]. Sun and Du adopted the improved minimum editing distance algorithm and achieved good results in the experiment [7]. The above methods, with the help of machine translation and cross-language retrieval technology, have achieved certain results in obtaining comparable pages. However, at present, there are few researches on English and American literature corpus retrieval technology, and there are no referential results.

Corpus usually refers to the language materials collected for language research and stored in electronic form. It is a basic resource that is collected from naturally occurring written or spoken language samples, scientifically selected and marked, has an appropriate scale, and can reflect and record the actual use of language. Many corpora have been established in China in recent years, but most of them are used for linguistic research, grammar research, dictionary compilation, textbook compilation, or research in a specific field [8]. The corpus of three sources of English and American literary and cultural context is quite different from other existing corpora. In the past, the materials in the corpus were collected and sorted out manually. Today, due to the use of advanced computer technology, the efficiency and scale of corpus construction have been greatly improved, laying a solid foundation for corpus construction and wider application. At present, the construction of English and American literature corpus in China mainly focuses on the research of alignment technology and application technology. In recent years, the systematic construction of English and American literature corpus has gradually increased. The significance of this paper lies in learning the technical achievements of predecessors and exploring the construction process of English and American literature corpus through actual programming so as to apply what we have learned.

2. Related Work

2.1. Overview of ML Theory. In recent years, ML (machine learning) algorithm has received unprecedented attention and has been widely used in personalized recommendation, speech recognition, spam filtering, face detection, protein structure prediction, vehicle control, and medical diagnosis.

Liu et al. used the data parallel strategy to split a large data set into several small data sets for parallel local clustering and synchronously generated a global clustering center after the local clustering was finished [9]. The experimental results show that the parallel clustering algorithm has a short time cost in the process of large-scale data clustering. Huang et al. found through theoretical analysis of the modified classical ML algorithm that the new algorithm is not an approximate solution of the original algorithm, but an exact solution, and the distributed implementation technology can have linear scalability with the increase of cluster scale [10]. Babu and Suresh proposed a parallel logistic regression algorithm based on the Spark platform [11]. In this study, the data sets that are reused in logistic regression are cached in memory by the Spark platform, and the parameters are optimized by distributed computing gradient descent. Ajitha et al. distributed data and linear algebra operations in a number of cluster nodes for parallel execution, and at the same time, the main operations were mapped into the parallel computation of matrix multiplication based on the principle of data locality by using multithread architecture in cluster nodes [12]. The experimental results show that the implementation of parallel algorithm based on hybrid architecture is faster than the simple implementation.

Zhong et al. proposed an online learning algorithm for SVM, which is used to deal with the classification problem of gradually providing input data in sequence [13]. The algorithm is faster, uses fewer support vectors, and has better generalization ability. Yuvaraj et al. put forward a fast, numerically stable, and robust incremental SVM learning method [14]. Abualhaija et al. put forward a feature selection method for classification based on SVM. The accuracy of the SVM classification algorithm is related to the number of features and the size of data sets, so selecting features of data before classification is beneficial to improve the classification accuracy [15]. However, the feature selection method is also very important, and the features selected by different feature selection methods are very different. Tsai and Chang put forward an algorithm to build a decision tree classifier. This algorithm runs in a distributed environment and is suitable for large data sets and streaming data. Compared with serial decision trees, this method can improve the efficiency on the premise of approximate accuracy error [16].

2.2. Research Corpus. The application fields of natural processing mainly include automatic question answering system, machine translation, speech recognition, document summarization, and document classification. With the popularity of electronic devices and the growth of the World Wide Web, the corpus has been expanding in scale. At first, the corpus had little content, and the capacity of words was very small, which basically did not reach more than one million words, and it was all based on the research of English in various countries' linguistics. Researchers found and constructed random models from the speech corpus, which made it possible to realize the speech recognition function.

Dattner extracts the key information in the source language document and then queries it through the information retrieval system after translation. In order to improve the alignment effect, the retrieval results are filtered [17]. Knight constructs a corresponding URL(Uniform resource locator), and if there is such a URL, it is used as a candidate web page pair. After manual evaluation of the web pages obtained by this system, the accuracy rate is nearly 90%, and the obtained English texts are 137 M and 117 M [18]. Mori et al. marked the reference information and text type of the text, divided the text chapters, paragraphs, and sentence boundaries, automatically aligned the sentences in the original text and the translated text, and then corrected them manually [19]. Charles made a more in-depth study on the structural similarity of parallel web pages, adding more features to eliminate the nonparallel web page pairs among

the candidate parallel web pages. When manually evaluating about 400 pairs of Chinese-English parallel web pages, about 3,500 pairs of Chinese-English parallel web pages were obtained, with an accuracy rate of 98% and a recall rate of 61% [20].

Mereu carried out various types of searches, including searches based on words, word frequencies, and sentence patterns. The Chinese-Japanese subdatabases in this English-American literature corpus are aligned at the segment level [21]. Ozn people put forward a feature that can automatically discover the parallel web page pairs named by the authors of the current site and then obtain the candidate parallel web page pairs. This method does not need to define language-related string sets in advance [22].

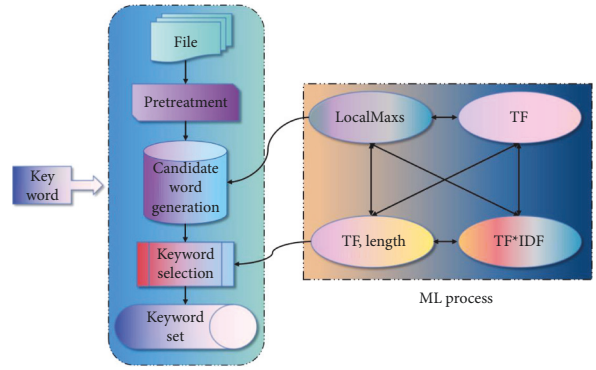

Figure 1: Keyword extraction process.

3. Research Method

3.1. Corpus Extraction. The corpus of English and American literature courses is designed to provide sufficient information sources for English and American literature teachers and learners so as to help improve the teaching effect of English and American literature courses and learners' interest in learning and enhance learners' comprehensive quality and appreciation ability. The principle of corpus construction should be based on meeting the teaching objectives of British and American courses. Therefore, when constructing the corpus, according to the needs of this part of learners, the knowledge can be concentrated and systematized, and all relevant contents not covered in the class can be included in the corpus to meet the needs of learners. According to this theory, we decided to adhere to the principle of student-centered and teacher-led and highlight the elements of environmental design, meaning construction, and interactive learning to build a literary corpus.

The construction of literary corpus should highlight literariness, embody teaching content, emphasize the literary knowledge of English and American literature from background to original works, and avoid taking the public as the object and taking the examination as the guide. Literary corpus needs to be prominent, systematic, centralized, and interactive. For example, for students majoring in English language and literature, they should not only master the knowledge of English and American literature in an all-round way, but also know the background knowledge of English and American culture in literary works. This kind of corpus-based literature teaching can not only provide rich and authentic language patterns for language and literature learners but also make it easier for teachers to guide students to conduct in-depth study and further research because of the multidimensional, integrated, and interactive nature of computers and the powerful functions of software.

In this paper, keywords are extracted from source language documents and translated and used for information retrieval to retrieve target language documents related to translated keywords. This process is equivalent to indirectly using the extracted keywords for information retrieval. Automatic keyword extraction provides convenience for quick browsing and application of these resources. The existing keyword extraction methods can be roughly divided into two types: supervised and unsupervised.

This paper presents a keyword extraction method based on multiword expression and related word ranking. In order to make the extracted keywords more suitable for retrieval, this method pays more attention to the construction of candidate phrases and combines key phrases with keywords. Figure 1 describes the overall process of keyword extraction in this paper.

It mainly includes three modules: preprocessing, candidate set construction, and keyword selection. Because of the characteristics of English texts, it is necessary to analyze the source language documents first, then construct the candidate sets of phrases and single words respectively, sort the candidate words, and finally select the candidate words with the highest weight as the keyword set.

Text diagram is a formal model to describe the relationship between texts. It is a diagram structure in which some feature items in a text are vertices, and the relationship between features is edges. The graph-based sorting algorithm applied in the field of natural language processing is called TextRank.

The general TextRank model can be expressed as a weighted directed graph $G = (V, E)$, which consists of a set of points V and an edge set E. The weight of the edge between two vertices (i, j) in the graph is noted as w_{ij}.

For a given vertex V_i, $\mathrm{In}(V_i)$ is expressed as the set of points pointing to that point, and $\mathrm{Out}(V_i)$ is the set of points that the V_i point points to other points, as shown in the following formula (1):

$$WS(V_i) = (1-d) + d * \sum_{V_j \in In(V_i)} \frac{w_{ji}}{\sum_{V_k \in \mathrm{Out}(V_j)} w_{jk}} WS(V_j). \tag{1}$$

w_{ji} represents the similarity of two sentences, $WS(V_j)$ represents the weight of the last iteration J, and the whole formula is an iterative process.

For bilingual parallel resource pairs, a character in language S_1 is related to a random number of characters in another language S_2, and these random numbers are not only independent of each other but also in accord with normal distribution. The model of normal distribution is determined by the median c and variance s^2. Define the

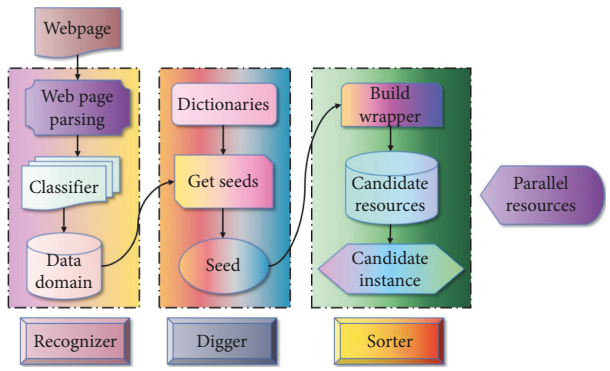

Figure 2: System flow of automatic construction of English and American literature corpus on mixed web pages.

following formula to calculate the length-based measure δ to meet the expected value of 0 and the normal distribution with variance of 1.

$$\delta = \frac{l_2 - l_1 c}{\sqrt{l_1 s^2}}, \tag{2}$$

where l_1, l_2 denote the length of sentences S_1, S_2 (i.e., the total number of words).

From the above, it can be seen that the construction process of candidate phrases and candidate single words is independent of each other, and the phrases and single words have different characteristics, so the correlation ranking process is also carried out separately.

3.2. Automatic Acquisition of Parallel Resources in English and American Literary Corpora. In the field of machine translation, bilingual parallel corpus has been widely concerned by researchers in recent years. British-American literary corpus can also be used to improve learning efficiency in bilingual teaching, and linguists can study the development trend of language and characters. Therefore, the corpus of English and American literature is a very good research direction. Particularly in bilingual mixed web pages, parallel resources always appear in similar or even identical layout. Based on this phenomenon, this section proposes a completely adaptive method to mine parallel resources.

In order to obtain parallel resource pairs from the web data domain, we should first cut the text into continuous segments according to the language and other pieces of information, then mine a few typical parallel text segment pairs based on the length model, alignment model, and symbol features, and use them as seeds for the next task. Once the wrapper is built, more potential parallel resources can be obtained by positive expression matching (i.e., the parallel resources are abandoned because they do not conform to the length model or the alignment model when the seed mining task is performed).

When constructing the multiview semantic tree database, an important goal is to keep the compatibility between the grammar tree and the semantic tree, which involves the transmission of empty components. After the transmission, the transmitted components semantically act as predicates that have no direct jurisdiction with them; in other words, they involve either verbs parallel to the current verbs or verbs that govern the current verbs. We name these two kinds of transmission as semantic role transmission within verbs and semantic role transmission between verbs, and they can be used in combination.

The method in this chapter can be applied to mixed web pages described by any language pair; that is, it can be used to obtain parallel resources between any language pairs. The fundamental reason is that this method does not need any expert knowledge related to language, domain, and so on. Figure 2 shows the system flow of automatic construction of English and American literature corpus.

In the abstract of the page, many translations of unknown words are embedded in an English sentence; that is, they contain interfering words. If all the components of an unknown word can be translated by a bilingual dictionary, the translation combination query will be conducted. The cooccurrence model makes use of the number of cooccurrence words of unknown words and their candidate translations in page abstracts, and the specific definition is shown in formula (3):

$$\mathrm{Fre}\left(E_i^*\right) = \frac{f\left(E_i^*\right)}{\max_{j\in[1,n]}\left(f\left(E_i^*\right)\right) + 1}, \tag{3}$$

where $f(E_i^*)$ is the cooccurrence times of candidate translations and unlisted words and n is the number of candidate translations.

Map document D through vector space to get the weight information of word items, and the expression form of document D is converted into $D = \{T_1, W_1; T_1, W_1; \ldots; T_n, W_n\}$, where W_n represents the weight of each word item. At this point, we can get the vector expression form of document D, abbreviated as $D = D(W_1, W_2, \ldots, W_n)$.

In the vector space model, the content correlation degree $S(D_1, D_2)$ between two documents D_1, D_2 is usually expressed by the cosine of the angle between vectors, and the formula (4) is

$$S\left(D_1, D_2\right) = \cos\theta = \frac{\sum_{i=1}^{n} W_{1i} \times W_{2i}}{\sqrt{\left(\sum_{i=1}^{n} W_{1i}^2 \times W_{2i}^2\right)}}. \tag{4}$$

As all events have obvious event elements such as time, place, and people, most of the features are named entities. These feature items are converted into vector form, and the content similarity is calculated by formula (4). Finally, the similarity of texts is measured by summing the time similarity and the content similarity.

3.3. Text Classification. There are many kinds of textbooks for English and American literature courses. In order to provide learners with more reference range, when constructing corpus, we should expand the scope of material selection, make use of the superior resources of the Internet at present, and establish hyperlinks of literary background and literary criticism. In addition to using various resources

to collect the necessary cultural background and literary knowledge materials for English and American literature teaching, we should also set up tracking corpus to form a complete corpus system so as to help teach workers to grasp the characteristics and overall picture of language learners' learning as a whole.

Text classification is to determine the classification of all unknown documents according to the predetermined topic categories so as to realize the objective processing of texts and achieve the goal of improving the accuracy of classification. As a tool for processing information, it perfectly presents efficient classification algorithms and accurate query results in the field of information retrieval. Text classification can generally be divided into single label and multilabel. The single label means that an article belongs to only one category, while multilabel means that an article may belong to both one category and multiple categories at the same time. This topic only involves the task of single label text classification.

Literary corpus can be used to study literature, especially the style of writers. The unique computer retrieval and statistical technology can accurately count the word frequency, word length, and sentence length of a writer's works, which can reflect the writer's writing style and literary background in a certain period. ML refers to the method of feature extraction based on the idea of word frequency, and classification algorithms such as SVM, K-nearest neighbor method, and NB (Naive Bayes) method are used to classify texts. Every word in English is connected by spaces, so its word segmentation can be completed by using spaces.

From the perspective of system workflow, the system workflow in the prototype of text classification demonstration is as follows:

(1) The training text is segmented, and stop words are removed to obtain the initial text feature information.

(2) Complete the text representation operation to obtain the text feature vector for the training of the classifier.

(3) Classify the text; that is, first classify the text with SVM classifier, and then classify the text with NB classifier for the second time so as to get the classification result.

(4) Evaluate the final result of system classification and determine the classification effect of system prototype.

From this, it can be concluded that the process framework of the system prototype is shown in Figure 3.

In the traditional text classification technology, according to the research of related scholars, the SVM algorithm and NB algorithm have good classification effects and have been widely used in the field of text classification. Based on the statistical learning theory, SVM avoids the problem of infinite samples in traditional classification algorithms and has good generalization performance and obvious advantages in accuracy. At present, it has been successfully applied in the field of pattern recognition.

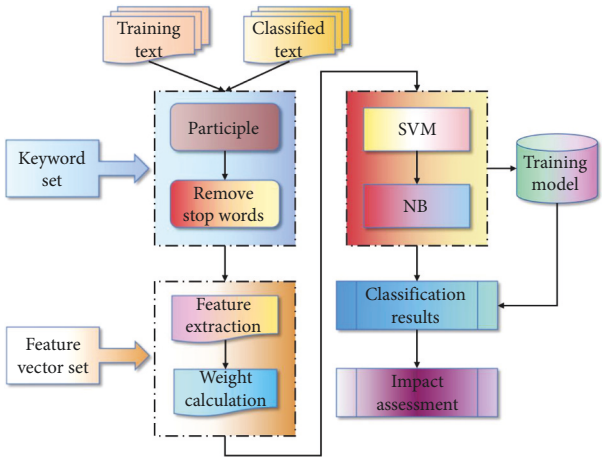

Figure 3: Text classification framework flowchart.

The excellent performance of SVM in nonlinear cases is largely due to its different inner product kernel functions. So far, there are three main types of kernel functions that are most used:

Linear kernel function:

$$K(x_i, x_j) = x_i \cdot x_j. \tag{5}$$

Polynomial kernel function:

$$K(x_i, x_j) = \left[(x_i \cdot x_j) + 1\right]^q. \tag{6}$$

The polynomial classifier of order q is obtained from the formula.

Radial basis kernel function:

$$K(x_i, x_j) = \exp\left(-\gamma \left\| x_i - x_j \right\|^2\right). \tag{7}$$

In this experiment, the radial basis function is chosen because it can also perform well for nonlinear mapping, and the complexity of the model depends on the number of parameters, which is small, so the model is not complicated, which is beneficial to text classification.

NB classifier is a classifier based on the Bayesian learning method and a classification method based on probability. Assuming that there are m classes $C_1, C_2, \ldots, C_m$, given the unknown text d, Bayesian classification will give the highest posterior probability of determining the class C_i for the text d, that is, maximizing $P(C_i|d)$. According to the Bayes theorem,

$$P(C_i|d) = \frac{P(d \mid C_i) \times P(C_i)}{P(d)}. \tag{8}$$

Obviously, $P(d)$ is a constant for all classes, so we just need to maximize $P(d|C_i) \times P(C_i)$. To avoid $P(C_i) = 0$, Laplace probability estimation is adopted as follows:

$$P(C_i) = \frac{1 + |C_i|}{m + |D|}. \tag{9}$$

$|C_i|$ is the number of texts contained in category C_i, $|D|$ is the total number of texts in the training set, and $P(d|C_i)$ is

Table 1: Experimental result.

Experimental project	Precision (%)	Recall %)	F value(%)
Experiment 1	24.13	28.66	26.87
Experiment 2	18.11	23.17	20.56
Experiment 3	34.32	44.05	38.29
Experiment 4	32.65	41.36	36.55

simply calculated by the probability of each attribute appearing in category C_i.

Calculate the maximum posterior probability by the above formula:

$$y = \arg\max_{c_k} P(Y = c_k) \prod_{j=1}^{n} P\left(X^{(j)} = x^{(j)} | Y = c_k\right). \quad (10)$$

When the calculated probability value of the category to which the document x belongs is the largest, it belongs to the category c_k.

NB model has obvious advantages, its theoretical basis is classical mathematical theory, and its classification efficiency is stable. It is especially suitable for small-scale data and can solve the problem of multilabel classification. It can also be widely used in text classification, and its algorithm is simple and can be used when data is missing. There are a lot of hypothetical models in the field of ML, so the classification results may be biased due to the selection of prior models. At the same time, it is sensitive to the expression of input data.

4. Result Analysis

In this paper, NTCIR corpus is used for estimation and testing. NTCIR is a cross-language information retrieval conference dedicated to Asian languages, which provides the basic corpus of consulting retrieval and natural language processing, including a large number of Chinese news corpora. Select 500 articles from NTCIR Chinese corpus (all highly related or related to a certain topic) as the experimental corpus. In order to facilitate the evaluation of the results, these 500 corpora are manually labeled, and no more than 15 keywords are labeled for each document as a comparison standard by correcting and supplementing the corresponding topic keywords of each document.

The remaining 200 corpora are used as test corpora to test the performance of the keyword extraction method in this paper.

The following four groups of experiments were designed:

(1) Only keywords being extracted.

(2) Only keyword group extraction being carried out.

(3) Appropriate combination of keywords and keyword phrases.

(4) Similar to Experiment 3, except that word segmentation is not corrected.

The experimental results are shown in Table 1.

As can be seen from Table 1, the results of extracting only keywords or key phrases are not ideal. The combination of keywords and key phrases used in the text is more effective. And after the word segmentation result is optimized through the extraction process, the keyword extraction result is improved by nearly 2%, which shows that the merging process is quite meaningful.

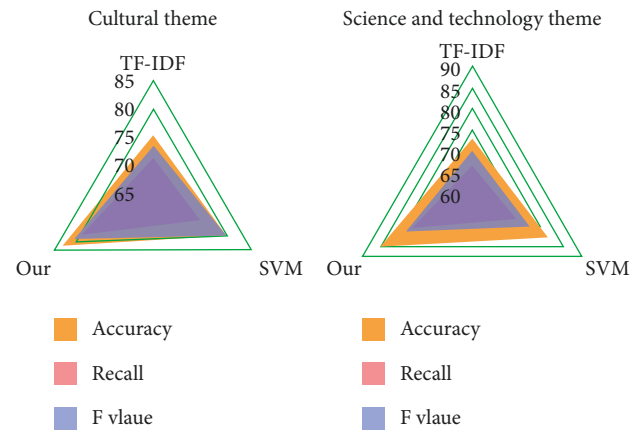

Figure 4: Comparison of topic sentence extraction effects under different methods.

Table 2: Performance comparison results of parallel literature resource acquisition systems in Britain and America.

System name	Precision (%)	Recall (%)	F value (%)
Reference [18]	71.66	85.02	77.89
Reference [20]	73.63	85.11	78.96
This paper system	82.24	89.65	85.47

In order to verify the effectiveness of this method, the TF-IDF method, SVM, and this method are used for comparative experiments. The performance of this method is verified by comparing the extraction results of the three methods. The experimental results are shown in Figure 4.

The experimental results show that the method in this paper has obviously improved on three evaluation indexes. The extraction effect of the TF-IDF method is the worst compared with the other two methods. The reason is that the nonevent sentences are not considered, which leads to a decrease in efficiency. Besides the characteristics of sentences themselves, the thematic relevance and semantic relevance between sentences and titles are also considered. Compared with the SVM method, the extraction effect of this method is still improved, which is mainly due to the comprehensive consideration of the correlation between events and the identification of the authenticity of event sentences.

This paper is a system based on candidate parallel resources filtering. This system also builds wrappers based on character surface features and then defines a sorting method based on length, bilingual dictionary, and translation model, which sorts all candidate resources, and the last one is noise data. Table 2 shows the performance comparison results of English and American literature parallel resource acquisition systems.

As can be seen from Table 2, the quality of English and American literature corpus obtained by the method proposed in this section has been greatly improved, and the recall rate has also been slightly improved. According to statistics, the accuracy rate of parallel resources obtained by

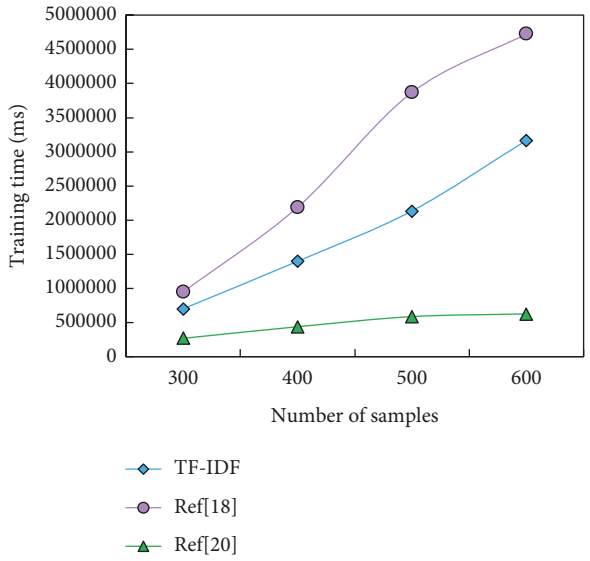

Figure 5: Time-consuming situation of training stage under different sample numbers.

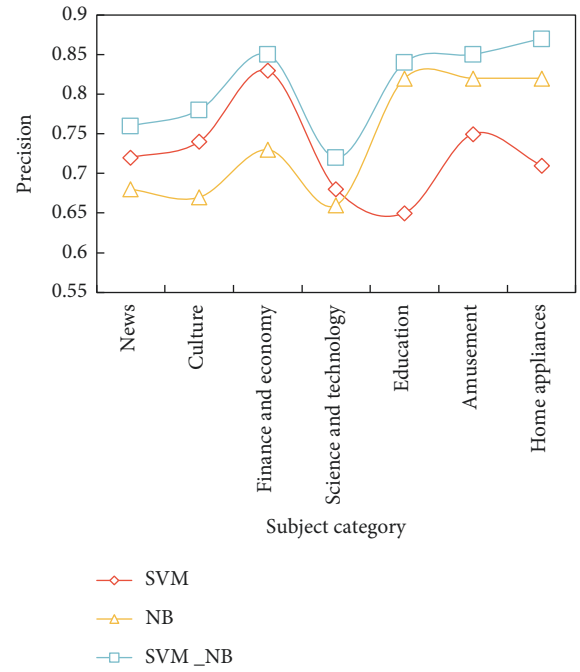

Figure 6: Precision of three classification methods.

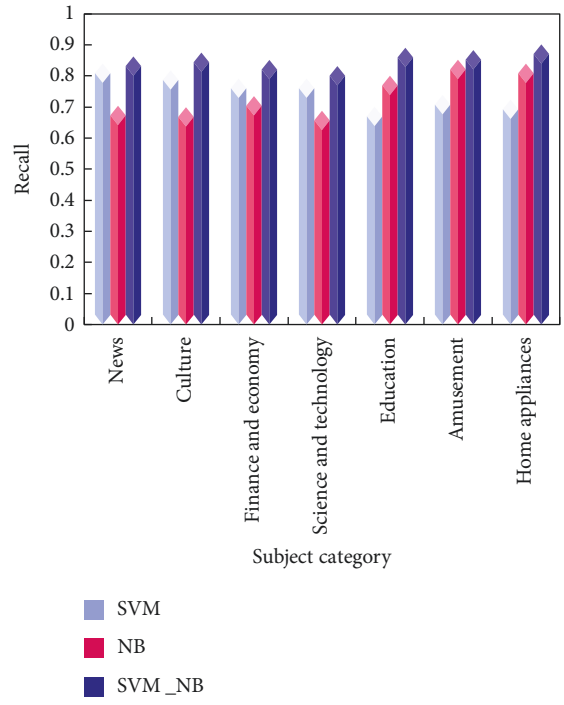

Figure 7: Recall rate of three classification methods.

the system of [18] is only 71.66%, except for a few errors caused by improper text segmentation, and most other noises are introduced by high-quality templates themselves. The accuracy of this system is 82.24%. Compared with other systems, it is about 8%. Compared with the system of [18], the F value of the system of [20] has been improved to some extent.

Once the system identifies a wrapper as a nonquality type, it ignores its acquired parallel resources, but the ignored resources still contain parallel resources [18]. This system does not consider the quality of wrappers but takes all the resources acquired by wrappers as candidates, thus slightly improving the recall rate.

For the second classification problem, a balanced number of samples is used for model training and text classification prediction; that is, the number of training samples and test samples is the same, and the number of samples in each category is the same. The TF-IDF text representation model of the corpus itself is a large and sparse matrix, which is linearly separable, so it is more suitable to use linear kernel function, and it does not need high-dimensional mapping. However, after the corpus is represented by reference [18] text and reference [20] text, the dimensions of the document model are greatly reduced, and the correctness of this inference is also verified by experiments. Figure 5 shows the classification accuracy when the number of training samples and test samples is 300.

When matching, define the sequence length of the longest word in the dictionary for segmentation. On this basis, match it with the words in the dictionary. After the first word is cut out, repeat the remaining sequence according to the above method. However, due to the complexity of Chinese, the segmentation results obtained by the forward maximum matching algorithm are often not ideal, while the application of the reverse maximum matching algorithm will get a better segmentation result.

Test the classification effect of the combination classifier, that is, test SVM_NB, the combination classifier of SVM and NB, respectively. The classification details are shown in Figures 6–8.

On the whole, the recall rate of the three classification methods is slightly higher than the accuracy rate, and the SVM algorithm is better than the NB algorithm. The

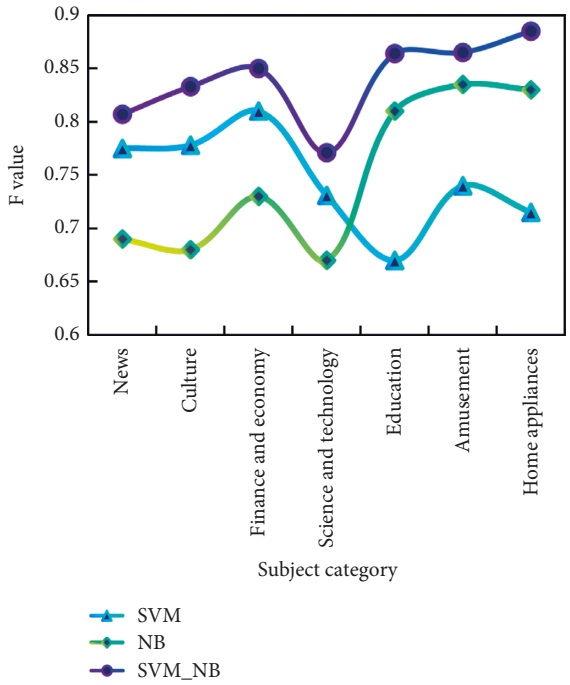

Figure 8: F values of three classification methods.

combination algorithm of SVM and NB is the best among the three, showing good accuracy and precision in both precision and recall.

At the same time, it is noted that when the SVM classifier is used to classify the small categories in the category of "Science and Technology," the precision rate and recall rate are lower than those of the large categories. The classifier is also effective in classifying small classes.

It is concluded that the combined classifier combines the advantages of two classical classifiers and shows a very good classification effect when the text content is relatively independent. In terms of accuracy and recall, the classification effect of the combined algorithm proposed in this paper is the best among the three methods, and the best classification results of accuracy, recall, and F value are 0.87, 0.9, and 0.89, respectively.

5. Conclusion

In China, the application of corpus to teaching is still in its infancy. In this paper, the verification of bilingual mixed web pages is regarded as an effective classification problem, and the feature data based on length, translation degree of overlapping words, and word frequency are collected to train an effective classifier. In the process of extraction, we make full use of the characteristics of the web page itself, parts of speech, and other features, estimate the combination of key phrases and keywords through experiments, and achieve good keyword extraction results. A combined classifier of SVM and NB is constructed, and classification experiments are carried out on text corpora in different fields. The precision, recall, and F value of the proposed combined algorithm are 0.87, 0.9, and 0.89, respectively, and good classification results are achieved. There are still some areas to be improved in our English and American literature corpus; for example, the amount of information and retrieval methods need to be expanded and updated.

Data Availability

The data set can be obtained from the author upon request.

Conflicts of Interest

The author declares no conflicts of interest.

References

[1] W. Zheng, Y. Qian, and H. Lu, "Text categorization based on regularization extreme learning machine," *Neural Computing & Applications*, vol. 22, no. 3-4, pp. 447–456, 2013.

[2] R. Deotale, S. Rawat, V. Vijayarajan, and V. B. Surya Prasath, "POCASUM: policy categorizer and summarizer based on text mining and machine learning," *Soft Computing*, vol. 25, no. 14, pp. 9365–9375, 2021.

[3] H. Wang, J. He, X. Zhang, and S. Liu, "A short text classification method based on N -g," *Chinese Journal of Electronics*, vol. 29, no. 2, pp. 248–254, 2020.

[4] B. Stasak, J. Epps, and R. Goecke, "Automatic depression classification based on affective read sentences: o," *Speech Communication*, vol. 115, pp. 1–14, 2019.

[5] J. Meng, H. Lin, and Y. Li, "Knowledge transfer based on feature representation mapping for text classification," *Expert Systems with Applications*, vol. 38, no. 8, pp. 10562–10567, 2011.

[6] S. Hassanpour and C. P. Langlotz, "Predicting high imaging utilization based on initial radiology reports," *Academic Radiology*, vol. 23, no. 1, pp. 84–89, 2016.

[7] N. Sun and C. Du, "News text classification method and simulation based on the hybrid deep learning model," *Complexity*, vol. 2021, no. 5, 11 pages, Article ID 8064579, 2021.

[8] W. Wang and A. Feng, "Self-information loss compensation learning for machine-generated text detection," *Mathematical Problems in Engineering*, vol. 2021, no. 1, 7 pages, Article ID 6669468, 2021.

[9] C. L. Liu, W.-H. Hsaio, C.-H. Lee, and T.-H. Chang, "Semi-supervised text classification with universum learning," *IEEE Transactions on Cybernetics*, vol. 46, no. 2, pp. 462–473, 2016.

[10] P. Huang, G. Wang, and S. Qin, "A novel learning approach to multiple tasks based on boosting methodology," *Pattern Recognition Letters*, vol. 31, no. 12, pp. 1693–1700, 2010.

[11] G. S. Babu and S. Suresh, "Meta-cognitive RBF network and its projection based learning algorithm for classification problems," *Applied Soft Computing*, vol. 13, no. 1, pp. 654–666, 2013.

[12] P. Ajitha, A. Sivasangari, R. I. Rajkumar, and S. Poonguzhali, "Design of text sentiment analysis tool using feature extraction based on fusing machine learning algorithms," *Journal of Intelligent and Fuzzy Systems*, vol. 40, no. 1, pp. 1–9, 2020.

[13] M. Zhong, M. Georgiopoulos, and G. C. Anagnostopoulos, "A k-norm pruning algorithm for decision tree classifiers based on error rate estimation," *Machine Learning*, vol. 71, no. 1, pp. 55–88, 2008.

[14] N. Yuvaraj, K. Srihari, G. Dhiman et al., "Nature-inspired-based approach for automated cyberbullying classification on

multimedia social networking," *Mathematical Problems in Engineering*, vol. 2021, Article ID 6644652, 12 pages, 2021.

[15] S. Abualhaija, C. Arora, M. Sabetzadeh, L. C. Briand, and M. Traynor, "Automated demarcation of requirements in textual specifications: a machine learning-based approach," *Empirical Software Engineering*, vol. 25, no. 6, pp. 1–44, 2020.

[16] C.-F. Tsai and C.-W. Chang, "SVOIS: support vector oriented instance selection for text classification," *Information Systems*, vol. 38, no. 8, pp. 1070–1083, 2013.

[17] E. Dattner, "Florent perek: argument structure in usage-based construction grammar: experimental and corpus-based perspectives. Constructional approaches to language 17," *Cognitive Linguistics*, vol. 29, no. 2, pp. 363–369, 2018.

[18] D. Knight, "Multimodality and active listenership: a corpus approach," *Discourse Studies*, vol. 15, no. 5, pp. 649–651, 2013.

[19] Y. Mori, H. Yamane, Y. Ushiku, and T. Harada, "How narratives move your mind: a corpus of shared-character stories for connecting emotional flow and interestingness," *Information Processing & Management*, vol. 56, no. 5, pp. 1865–1879, 2019.

[20] M. Charles, ""Proper vocabulary and juicy collocations": EAP students evaluate do-it-yourself corpus-building", *English for Specific Purposes*, vol. 31, no. 2, pp. 93–102, 2012.

[21] L. Mereu, "Argument structure in usage-based construction grammar," *Linguistics*, vol. 53, no. 6, pp. 1433–1441, 2015.

[22] G. Ozn, M. Ayafor, M. Green, and S. Fitzgerald, "The spoken corpus of Cameroon Pidgin English," *World Englishes*, vol. 36, no. 3, pp. 427–447, 2017.